AD-A008 584

TAKE-OFF AND LANDING

Advisory Group for Aerospace Research and Development
Paris, France

January 1975

AD-A008584

REPORT DOCUMENTATION PAGE

1. Recipient's Reference	2. Originator's Reference	3. Further Reference	4. Security Classification of Document
	AGARD-CP-160		UNCLASSIFIED

5. Originator Advisory Group for Aerospace Research and Development
North Atlantic Treaty Organization
7 rue Ancelle, 92200 Neuilly sur Seine, France

6. Title Take-off and Landing

7. Presented at 44th Meeting of the AGARD Flight Mechanics Panel held in Edinburgh, UK, on 1–4 April 1974.

8. Author(s)	9. Date
Various	January 1975
10. Author's Address	**11. Pages**
Various	312

12. Distribution Statement This document is distributed in accordance with AGARD policies and regulations, which are outlined on the Outside Back Covers of all AGARD publications.

13. Keywords/Descriptors

Takeoff	Fighter aircraft	Flight Control
Landing	Supersonic transports	Display devices
High lift devices	Aerodynamic stability	

14. UDC 629.73.077.2:629.73.085:
533.6.015

15. Abstract

Twenty-two papers are contained in this Proceedings. The first three papers, from a session on aircraft design optimization, review high lift aerodynamics and take-off and landing design considerations of fighter aircraft and a supersonic transport. Three papers were presented at a session on energy management. Aircraft stability and control characteristics are discussed in seven papers, two of which report on direct force control applications. Five papers, from a session on guidance, include considerations of ground-based guidance systems and pilots' displays. The final session on operational aspects had four papers.

NORTH ATLANTIC TREATY ORGANIZATION

ADVISORY GROUP FOR AEROSPACE RESEARCH AND DEVELOPMENT

(ORGANISATION DU TRAITE DE L'ATLANTIQUE NORD)

AGARD Conference Proceedings No.160

TAKE-OFF AND LANDING

Papers presented at the 44th Meeting of the Flight Mechanics Panel of AGARD
held in Edinburgh, UK on 1–4 April 1974.

THE MISSION OF AGARD

The mission of AGARD is to bring together the leading personalities of the NATO nations in the fields of science and technology relating to aerospace for the following purposes:

- Exchanging of scientific and technical information;
- Continuously stimulating advances in the aerospace sciences relevant to strengthening the common defence posture;
- Improving the co-operation among member nations in aerospace research and development;
- Providing scientific and technical advice and assistance to the North Atlantic Military Committee in the field of aerospace research and development;
- Rendering scientific and technical assistance, as requested, to other NATO bodies and to member nations in connection with research and development problems in the aerospace field;
- Providing assistance to member nations for the purpose of increasing their scientific and technical potential;
- Recommending effective ways for the member nations to use their research and development capabilities for the common benefit of the NATO community.

The highest authority within AGARD is the National Delegates Board consisting of officially appointed senior representatives from each member nation. The mission of AGARD is carried out through the Panels which are composed of experts appointed by the National Delegates, the Consultant and Exchange Program and the Aerospace Applications Studies Program. The results of AGARD work are reported to the member nations and the NATO Authorities through the AGARD series of publications of which this is one.

Participation in AGARD activities is by invitation only and is normally limited to citizens of the NATO nations.

Published January 1975

629.73.077.2:629.73.085:533.6.015

Printed by Technical Editing and Reproduction Ltd
Harford House, 7–9 Charlotte St, London, W1P 1HD

PREFACE AND EVALUATION

The process of take-off and landing is inherent in all flight operations, but it has been treated, generally, as a necessary subset of the primary mission application. For some years attention to the take-off and landing phase has focused on VTOL and V/STOL operations. Not since 1963 had the Flight Mechanics Panel explicitly addressed the subject of landing or take-off of conventional aircraft. Consequently, the Panel felt it would be useful to take a fresh look at the problem area, particularly at the tradeoffs involved in design and operations important to the process of take-off and landing and of specific interest to the flight mechanics disciplines and concerns.

The operational functions involved in take-off and landing are a demanding combination of technology and human skills. Increasingly, the optimization of this operation is impacting total mission performance. Whatever function is to be performed, whether weapon delivery, aerial combat, logistics support or civil airlift, the importance of improving the qualities of the approach and landing manoeuvre is clear. For the most part take-off is not a problem. Only for a short period of climb-out are the constraints significant and even there the options for solutions are available. However, in the landing manoeuvre the fundamental concern for safety in the transition from steady airborne operation to a satisfactory landing continues to present a challenge. To this we now add the concern for effective utilization of the terminal facilities, the impact of operations on the environment, the imposition of "presence" on the neighbors of the airport and the unpredictable phenomena associated with more operations in a smaller airspace. All of these considerations can occur in a variety of atmospheric conditions.

The Flight Mechanics Panel has a role in giving thorough consideration to trades involved in the application of fundamental design disciplines. The Panel is concerned with understanding the factors which influence system options and which promote harmony between the vehicle and the operator. This Symposium offered the opportunity to develop a beneficial exchange of views.

The Symposium did not surface any new topics but it highlighted some points quite clearly and called for alertness to new opportunities, as follows:

- The precision with which an aircraft flight path can be controlled under unfavorable conditions is extremely important. Encouragement was given in the new control technologies.
- Direct lift control (DLC) and direct side force control (DSFC) provide significant alternatives in permitting precise corrections at very low altitudes. These concepts offer promise of substantial improvement in the pilot's ability to make corrections.
- The desire to incorporate such control techniques to reduce airspace use and help accomplish steeper approach paths is clearly apparent; it is envisioned that special systems are needed to reduce pilot workload.
- The need for steeper approaches and new techniques for reducing noise exposure near the terminal area, or vulnerability to hostile action outside the airfield, was addressed by several techniques which deserve continued exploitation, including two-segment, continuously decelerating and low power dynamic approaches.
- Pilot workload, stress levels and the need for "natural" cues brought forth considerable discussion on the need for better displays.
- The incorporation of DLC and other configuration variables specifically for improved landing performance was cited as appropriate for control configured vehicle (CCV) designs.
- For designs which do not lend themselves to fully automated landing systems the man/machine relationship and pilot workload were noted to be very important; the life scientist (psychologist) and the pilot should be brought more completely into the design process.
- With or without the fully automatic mechanization the fundamental techniques of control harmonization, direct force systems, improved operational techniques, and more predictable pilotage commands will continue to challenge flight mechanics research.

L.P.GREENE
Member
Flight Mechanics Panel

J.BUHRMAN
Member
Flight Mechanics Panel

O.H.GERLACH
Member
Flight Mechanics Panel

CONTENTS

HIGH-LIFT AERODYNAMICS - TRENDS, TRADES, AND OPTIONS

Richard J. Margason
Aeronautical Engineer
and
Harry L. Morgan, Jr.
Aeronautical Engineer
NASA Langley Research Center
Hampton, Virginia, 23665, U.S.A.

SUMMARY

Throughout the history of aviation, there has been a steady trend toward the utilization of higher maximum lift coefficient as aircraft size and cruise velocities have increased. These trends have generated a need for trades between cruise performance and take-off, climb, and landing performance. Through the years, the application of high-lift technology to new aircraft developments has been led by wind-tunnel research.

In an effort to improve methods for development of high-lift capabilties, theoretical methods for the analysis of the two-dimensional characteristics of flap systems have been described and compared with experimental data. The need to extend these methods to adequately describe flow separation effects has been noted. Further, methods for three-dimensional analysis have also been described.

At the present time, operational airplanes have utilized most of the mechanical-flap developments demonstrated in wind tunnels. Further increases in maximum lift coefficient will require the utilization of engine thrust for powered lift. Four powered-lift concepts have been described to outline some of the options currently being developed. Two jet-flap theories have been described which provide analytical methods for estimation of the three-dimensional aerodynamic high-lift performance characteristics of powered-lift systems. While these latter methods provide a useful beginning, further refinement is needed to make them useful for estimating powered-lift performance.

SYMBOLS

b	wing span, m (ft)
c	wing chord, m (ft)
c_d	section-drag coefficient, Section drag/(qc)
c_ℓ	section-lift coefficient, Section lift/(qc)
c_m	section pitching-moment coefficient, Section pitching moment/(qc)
c_p	pressure coefficient, $(p_{local} - p)/q$
C_D	drag coefficient, Drag/(qS)
C_L	lift coefficient, Lift/(qS)
$C_{L,max}$	maximum lift coefficient
C_m	pitching-moment coefficient, Pitching moment/(qSc)
C_N	normal-force coefficient, Normal force/(qS)
C_μ	thrust coefficient, Thrust/(qS)
q	dynamic pressure, N/m^2 (lbf/ft^2)
p	static pressure, N/m^2 (lbf/ft^2)
S	wing area, m^2 (ft^2)
T	thrust, N (lb)
V	velocity, knots
W	aircraft weight, N (lb)
x,z	airfoil abscissa, ordinate, cm (in.)
α	angle of attack, deg
δ_f	flap deflection, deg
θ	jet-deflection angle with respect to the wing chord plane, deg

1. INTRODUCTION

Requirements of high-performance aircraft dictate a variety of lifting conditions throughout the flight regime (Ref. 1). In cruise, there is a requirement for good efficiency (high lift-to-drag ratio) or for high-speed capabilities (increased wing sweep and/or thinner airfoils). During take-off, the high-lift coefficient which is required to reduce the take-off velocity (shorter ground run) is constrained by the need for high lift-to-drag ratios to permit adequate climb. During approach and landing, considerably higher lift coefficients are often needed to reduce approach speeds and the resultant landing ground roll.

These many requirements have, through the years (Fig. 1), been satisfied by increased maximum lift coefficients for take-off, climb, and landing operations on new high-performance airplanes (Ref. 2). These increases have been made possible by wind-tunnel developments. During most of this time (Fig. 2), these high-lift developments have utilized flaps for high trailing-edge camber; and, in many cases where the leading edge is loaded, additional leading-edge camber is needed. These high-camber shapes have been achieved using multiple-element trailing-edge flaps and leading-edge slats.

Using the definition of lift coefficient $\left[V \sim \sqrt{\frac{W/S}{C_L}}\right]$, it is noted in Figure 3 that the airplane minimum flight velocity is proportional to the square root of the ratio of wing loading divided by maximum lift coefficient. Most of the current aircraft operate at approach lift coefficients of 1.5 to 1.8. As high-performance aircraft are developed for higher wing loadings, the present approach speeds and resultant field lengths can only be maintained through the use of higher maximum lift coefficients. Large lift increases (Fig. 1) are most readily available using higher thrust-to-weight ratios in the form of powered lift (Ref. 3).

The primary purpose of this paper will be to review the recent developments in the design of high-lift devices and estimation of their performance characteristics. First, two different two-dimensional computational methods will be described for application to airfoils and to multiple-element high-lift flaps. Then, results of these methods will be related to three-dimensional wing planforms. Finally, some methods for analyzing three-dimensional powered-lift concepts will be discussed.

2. TWO-DIMENSIONAL ANALYSIS

2.1 Viscous-flow, high-lift flap analytical methods

The essential elements of the NASA/Lockheed-Georgia two-dimensional high-lift flap computer program (Ref. 4) are shown in Figure 4. Depicted by the sketch in the figure is a single-slotted flap having flow around the two airfoil elements and through the slot forward of the flap. The first step in computing the single-slotted flap characteristics is to obtain the potential-flow solution for the flow around each of the airfoil elements in proximity of the other. From the data obtained, the basic boundary layer for each airfoil element is computed and combined with results from the slot-flow analysis to obtain the confluent boundary layer over the downstream element, which is the flow interaction between the basic airfoil shape to produce a new equivalent airfoil shape. The normal and axial forces and the pitching moment are computed by integrating the pressure-distribution data. This procedure is repeated until a convergence in the value of normal force is obtained. It has been found that the results from this two-dimensional program agree well with available two-dimensional data on flapped airfoils.

An application of the NASA/Lockheed-Georgia program is shown in Figure 5 and reported in Reference 5. The experimental data were obtained from Reference 6 from a gap optimization investigation using a single-slotted flap having a 10° drooped nose and a flap deflection of 30°. The flap was moved with respect to the airfoil in order to vary the gap as is indicated in the sketch. The two-dimensional lift coefficient is presented as a function of the flap gap in percent of the basic wing chord. The symbols indicate the experimental data at an angle of attack of 0°. This angle of attack was selected for the comparison because the analytical prediction cannot account for separation effects and is only valid up to that point where separation occurs on the wing. The analytical results obtained from the method of Reference 4 are shown by two curves; the inviscid prediction from potential flow is shown as the solid curve and the viscous prediction as the dashed curve. The inviscid prediction does not give an optimum gap setting; rather it indicates that the maximum lift for this flap configuration at 0° angle of attack would occur for zero gap, which is not in agreement with previous experience. The viscous prediction indicates that the optimum gap is about 2 percent c, which is in agreement with the experimental data. This prediction shows promise that the analytical procedures will provide valuable guidance in optimizing flap configurations.

An additional correlation of program results with experimentally derived data is provided in Figure 6. The three-element NACA 23012 airfoil (Ref. 7) used here is composed of a leading-edge slat plus a single-slotted trailing-edge flap. The correlation for the normal-force and pitching-moment coefficients (Fig. 6(a)) shows good agreement between the viscous theory and the experimental data in the range of angle of attack where there is no flow separation apparent. As noted in the reference source, the force data are corrected for tunnel wall effects in such a direction as to reduce the overall pressure level. The pressure data remain in an uncorrected form (Fig. 6(b)). If such a correction were made, it probably would account for the minor difference shown in the two pressure distributions. These data can be considered fairly typical of the correlations currently obtained by the present method as well as by the methods described in References 8 and 9. These comparisons definitely illustrate the need to improve the present methods to properly account for flow separation. In addition, it should be noted that there are very few two-dimensional high-lift slotted-flap airfoil pressure data available for comparison with these theories.

2.2 Inviscid, inverse airfoil design method

Another analytical method for airfoil design has been defined in References 10 and 11 to obtain high maximum lift coefficients for single- or multiple-element airfoils. This method is useful for design of leading-edge slats and/or trailing-edge flap elements. The method first determines the separation-free

pressure distribution at maximum lift and, then, based on this pressure distribution, determines the airfoil coordinates for an incompressible-inviscid flow. The resultant airfoil is then evaluated in the NASA/Lockheed-Georgia two-dimensional high-lift flap program to determine the effects of viscosity on the design pressure distributions. A comparison of theory and experiment from Reference 12 is presented in Figure 7 for angles of attack of 3.4° and 12.2°. These results are typical of those observed over this range of angles of attack. The agreement between the theory and experiment is good except for the pressures measured at an angle of attack of 3.4° on the lower surface near the leading edge where the experimental data indicate the formation of a separation bubble with downstream reattachment of the flow.

3. THREE-DIMENSIONAL ANALYSIS

Current subsonic three-dimensional analytical methods are usually based on potential methods and are suitable only for inviscid flow. At the present time, solutions for viscous three-dimensional flow are not available even though there is research under way to develop three-dimensional boundary-layer methods suitable for wings. However, an empirical method is presented which can be used to estimate stall characteristics of straight-wing aircraft.

As an illustration of present three-dimensional analytical methods, two procedures will be used with data obtained from tests of a general aviation configuration (Fig. 8) which utilized a recently developed airfoil. This configuration had an unswept, untapered, aspect-ratio-9.0 wing with 2° of washout at the tips. The airfoil and its section characteristics are presented in Figure 9. The correlation of the two-dimensional pressure distributions obtained from theory (Ref. 4) and experiment (Ref. 13) at an angle of attack of 4.17° is presented in Figure 9(a). The same excellent agreement (Fig. 9(b)) between experimental and theoretical two-dimensional lift, drag, and pitching moment was obtained for the angles of attack where trailing-edge boundary-layer separation was not present. The three-dimensional experimental data (Ref. 14) are presented in Figure 10 along with results from two three-dimensional analytical methods (Refs. 15 and 16).

One analytical method (Ref. 16) utilizes a vortex-lattice (see lower right portion of Fig. 10) which is paneled on a planar surface with zero thickness to represent the wing-body configuration. The method represents a simple extension of lifting-line theory and requires very little computer storage or time for its solution. The solid curve on Figure 10 shows excellent agreement in the range of angle of attack having a linear lift-curve slope (unseparated flow). The drag coefficient due to lift was computed and found to agree well with the experimental data when it was combined with the experimental profile-drag coefficient obtained at zero lift coefficient. Analytical methods are available to estimate profile drag; however, they were not used for this correlation. The pitching-moment coefficient correlation is not particularly good.

A more sophisticated three-dimensional method (Ref. 15) adds source panels on the surface of the wing and body to represent thickness while leaving a modified vortex lattice on the wing chord plane. Using this method (see dashed curve in Fig. 10), there is a modest overprediction of lift coefficient at a given angle of attack, even though the linear portion of the lift-curve slope shows excellent agreement. For drag and pitching-moment coefficients, the slopes are predicted accurately, even though the levels are somewhat low.

Evaluation of these results indicates that the addition of thickness to an inviscid method causes an overprediction of lift coefficient. Experience with the previously discussed two-dimensional viscous method indicates that this overprediction would be corrected by the addition of a viscous boundary-layer representation which would reduce the effective wing camber near the trailing edge. This effect would reduce lift coefficient and increase pitching-moment coefficient. Another deficiency is that neither method gives any indication of flow separation. Again, this requires development of adequate three-dimensional boundary-layer methods.

At the present time, there is an empirical method available (Ref. 17) for estimating the characteristics of straight-wing aircraft approaching stall. These characteristics are obtained with a computer program which utilizes lifting-line theory and available data for the wing section characteristics. The effectiveness of this method is illustrated in Figure 11 for the previously described general aviation configuration (Fig. 8) where both theoretical and experimental two-dimensional input data were used. While there were minor differences between the sets of section input data for drag and pitching-moment coefficients, the differences in lift coefficient were more striking. The poor results obtained using the theoretical two-dimensional data, which did not account for separation effects, are quite apparent. In contrast, the good agreement obtained using the experimental two-dimensional data indicates the importance of an accurate representation of the stall characteristics for the utilization of the method of Reference 17. The analytical method outlined in Reference 17 computes the wing, not wing-body, pitching moment. To obtain the wing-body pitching moment presented in Figure 11, the computed wing pitching moment and the experimentally measured body pitching moment were summed.

4. POWERED-LIFT AERODYNAMICS

4.1 Effect of high lift on landing performance

Some information on the landing performance of high-lift systems is presented in Figure 12. The variation of lift coefficient with angle of attack for two types of high-lift systems is shown on the left-hand plot of Figure 12. The bottom curve represents the present state of the art for mechanical flaps, and the top curve is for the same mechanical flaps with discrete leading-edge blowing. Mechanical flap systems can attain maximum lift coefficients as high as 3.5. With this level of maximum lift coefficient, the maximum usable lift coefficient of approximately 2.0 (indicated by the circle symbols) can be maintained in the landing approach. The calculated usable lift was based on the present-day rules for civil transports which use a 1.3 speed margin between the stall speed (maximum lift capability) and the approach speed. The right-hand plot of Figure 12 presents the variation of lift coefficient with velocity for wing loadings of 3.83 kN/m^2 (80 lb/ft^2) and 5.75 kN/m^2 (120 lb/ft^2). Also given in this plot is the field length that goes with the velocities when they are considered to be approach velocities. It can be seen

from the data that, for a lift coefficient of 2.0 in the approach as indicated for the mechanical flap, the level flight approach speed is in the neighborhood of 138 knots with a corresponding field length greater than 1.5 km (5000 ft) for a wing loading of 5.75 kN/m^2 (120 lb/ft^2). However, if this same lift capability is used on an airplane with a low wing loading, such as 3.83 kN/m^2 (80 lb/ft^2), the approach speed can be reduced to about 115 knots and field length can be reduced to about 1.2 km (4000 ft). If leading-edge blowing or discrete boundary-layer control is used at the leading edge of a mechanical-flap system in such a way that it is not appreciably affected by the engine power level and if the present ground rules for speed margins apply, an approach lift coefficient of 2.5 and the higher wing-loading field length of 1.2 km (4000 ft) can be attained. For the lower wing loading, the speed can be reduced to about 90 knots with a corresponding reduction in field length to 0.80 km (2500 ft). If performance levels much higher than that shown for the flaps plus leading-edge blowing are desired, use of powered lift will be required.

4.2 Powered-lift concepts

Powered-lift concepts develop circulation lift that is proportional to the installed thrust-weight ratio of the aircraft and depend on the efflux from the power source to develop a large portion of this additional lift. Some high-lift concepts that might be considered are shown in Figure 13. The high-lift configurations shown in the upper portion of Figure 13 have internally blown flap systems in which air is taken from the engines and ducted through the wing and out to slots across the wing span. These configurations require that the engines have a relatively high pressure ratio to pump air efficiently through these ducts. The sketch at the upper right of Figure 13 shows a conventional jet flap which could be installed on such an airplane for which this ducted air is blown out of slots over a simple trailing-edge flap system. A considerable increase in lift capability of conventional transport configurations can be obtained with the jet flap. An augmentor-wing, high-lift system which also might be used on this airplane is illustrated at the upper left of Figure 13. This augmentor wing not only uses the air that is blown out of the slot, but the flap itself is essentially an ejector which entrains some of the free-stream air into the flap system to augment the jet thrust. With this augmentation, the efficiency of the flap is improved at very low speeds; however, the mechanical complexity is increased.

Systems that depend on the external flow of the efflux from the wing are shown in the middle portion of Figure 13. This type of system takes advantage of very high-bypass-ratio engines that have low noise levels and represent simple applications of the jet-flap principle. The sketch at the middle left of Figure 13 shows an externally blown flap system with a double-slotted flap which is deflected behind the engine so that the air flows through the slots and induces circulation lift over the wing. Another externally blown flap concept is shown at the middle right of Figure 13 where the engine nacelle is mounted on the wing upper surface, and its efflux blows over the flaps as a thick Coanda jet across a portion of the wing span. This concept utilizes the wing to shield the ground from direct engine-exhaust noise so that a lower flyover-noise level is possible.

4.3 Powered-lift analysis

Almost all of the development of these powered-lift concepts have been based on wind-tunnel research which has achieved the maximum lift coefficients illustrated in Figure 1. Recently, several efforts were undertaken to develop analytical methods for the analysis of powered-lift aerodynamic performance. For these methods, Spence's two-dimensional jet-flap theory (Ref. 18) has been extended to three dimensions (Refs. 19 and 20). A comparison of experimental data (Ref. 21) with calculated results using the method developed by Lissaman (Ref. 19) is presented in Figure 14. Other comparisons are presented in Reference 22. One application (Fig. 15) of particular interest involved an externally blown flap configuration whose experimental performance was calculated by the theories. For input to these computations, detailed measurements of the mixed free stream and propulsion flow at the wing trailing edge were made with a three-velocity-component hot-film anemometer. As described in detail in Reference 22, these velocities were integrated to provide the experimental variations of momentum and deflection as a function of spanwise location. These data were then used in the methods of References 19 and 20 to calculate the lift coefficient performance. These results (Fig. 15) indicate that significant progress is being made to predict the performance of powered-lift concepts. This work also demonstrates that further development of the methods is needed to define how the propulsion flow interacts with the free stream between the engine exit and the wing trailing edge to analytically determine its trailing-edge momentum and deflection angle.

5. CONCLUDING REMARKS

This paper has shown that throughout the history of aviation there has been a steady trend toward the utilization of higher maximum lift coefficients as aircraft size and cruise velocities have increased. As a direct result, the wing loading (W/S) and the thrust-weight ratio (T/W) have increased. These trends have generated a need for trades between cruise performance and take-off, climb, and landing performance. Through the years, the application of high-lift technology to new aircraft developments has been led by wind-tunnel research. In an effort to further improve high-lift capabilities, theoretical methods for optimization of multiple-element flap systems are being developed. The theoretical methods for the analysis of the two-dimensional characteristics of flap systems have been described and compared with experimental data. The need to extend these methods to adequately describe flow-separation effects has been noted. Further, methods for three-dimensional analysis have also been described.

At the present time, operational airplanes have utilized most of the mechanical-flap developments demonstrated in wind tunnels. Further increases in maximum lift coefficient will require the utilization of engine thrust for powered lift. Four powered-lift concepts have been described to outline some of the options currently being developed. Two jet-flap theories have been described which provide analytical methods for estimation of the three-dimensional aerodynamic high-lift performance characteristics of powered-lift systems. While these latter methods provide a useful beginning, further refinement is needed to make them useful for estimating powered-lift performance.

6. REFERENCES

1. Loftin, L. K., Jr. — Transport Aircraft - 1980 and Beyond. 2nd Intersociety Conference on Transportation (Denver, Colorado), 1973

2. Hammond, A. D. — High-Lift Aerodynamics. Proceedings of Conference on Vehicle Technology for Civil Aviation, NASA SP-292, 1971, pp. 15-26

3. Hoad, D. R. — Comparison of Aerodynamic Performance of Several STOL Concepts. Proceedings of Conference on STOL Technology, NASA SP-320, 1972, pp. 111-119

4. Stevens, W. A.; Goradia, S. H.; Braden, J. A. — A Mathematical Model for Two-Dimensional Multi-Component Airfoils in Viscous Flow. NASA CR 1843, 1971

5. Stevens, W. A.; Goradia, S. H.; Braden, J. A.; Morgan, H. L. — Mathematical Model for Two-Dimensional Multi-Component Airfoils in Viscous Flow. AIAA Paper 72-2, 10th Aerospace Sciences Meeting (San Diego, California), 1972

6. Foster, D. N.; Irwin, H. P. A. H.; Williams, B. R. — The Two-Dimensional Flow Around a Slotted Flap. R & M No. 3681, British A.R.C., 1971

7. Harris, T. A.; Lowry, J. G. — Pressure Distribution Over an NACA 23012 Airfoil With a Fixed Slot and a Slotted Flap. NACA Rep. 732, 1942

8. Callaghan, J. G.; Beatty, T. D. — A Theoretical Method for the Analysis and Design of Multi-Element Airfoils. AIAA Paper 72-3, 10th Aerospace Sciences Meeting (San Diego, California), 1972

9. Bhateley, I. C.; Bradley, R. G. — A Simplified Mathematical Model for the Analysis of Multi-Element Airfoils Near Stall. AGARD Conference Preprint No. 102 on Fluid Dynamics of Aircraft Stalling, 1972, pp. 12-1 - 12-12

10. Liebeck, R. H.; Ormsbee, A. I. — Optimization of Airfoils for Maximum Lift. Journal of Aircraft, Vol. 5, September-October 1970, pp. 409-415

11. Ormsbee, A. I.; Chen, A. W. — Multiple-Element Airfoils Optimized for Maximum Lift Coefficient. AIAA Journal, Vol. 10, No. 12, December 1972, pp. 1620-1624

12. Bingham, G. J.; Chen, A. W. — Low-Speed Aerodynamic Characteristics of an Airfoil Optimized for Maximum Lift Coefficient. NASA TN D-7071, 1972

13. McGhee, R. J.; Beasley, W. G. — Low-Speed Aerodynamic Characteristics of a 17-Percent-Thick Airfoil Section Designed for General Aviation Applications. NASA TN D-7428, 1972

14. Crane, H. L.; McGhee, R. J. — Applications of Advanced Aerodynamics Technology of Light Aircraft. SAE Paper No. 730318, Business Aircraft Meeting (Wichita, Kansas), 1973

15. Rubbert, P. E.; Saaris, G. R.; Scholey, M. B.; Standen, N. M.; Wallace, R. E. — A General Method for Determining the Aerodynamic Characteristics of Fan-in-Wing Configurations. U.S. Army Aviation Materiel Labs. Tech. Rep. 67-61A, Vol. I - Theory and Application, 1967

16. Margason, R. J.; Lamar, J. E. — Vortex Lattice FORTRAN Program for Estimating Subsonic Aerodynamic Characteristics of Complex Panforms. NASA TN D-6142, 1971

17. McVeigh, M. A.; Kisielowski, E. — A Design Summary of Stall Characteristics of Straight Wing Aircraft. NASA CR 1646, 1971

18. Spence, D. A. — The Lift Coefficient of a Thin Jet-Flapped Wing. Proceedings of the Royal Society, Series A, No. 1212, Vol. 238, 1956, pp. 46-58

19. Lissaman, P. B. S. — Analysis of High-Aspect-Ratio Jet-Flap Wings of Arbitrary Geometry. NASA CR 2179, 1973

20. Shen, C. C.; Lopez, M. L.; Wasson, N. F. — A Jet-Wing Lifting-Surface Theory Using Elementary Vortex Distributions. AIAA Paper 73-652, 6th Fluid & Plasma Dynamics Conference (Palm Springs, California), 1973

21. Williams, J.; Butler, S. F. J.; Wood, M. N. — The Aerodynamics of Jet Flaps. Proceedings of Advances in Aeronautical Sciences, Vol. 4, 2nd International Conference of the Aeronautical Sciences (Zurich, Switzerland), September 1960, Pergamon Press, 1962, pp. 619-656 (Also available R & M 3304, British A.R.C., 1973)

22. Kardas, G. E. — Analysis of an Externally Blown Flap High-Lift System Using a Jet-Flap-Wing Theory. M.S. Thesis, George Washington University, May 1973

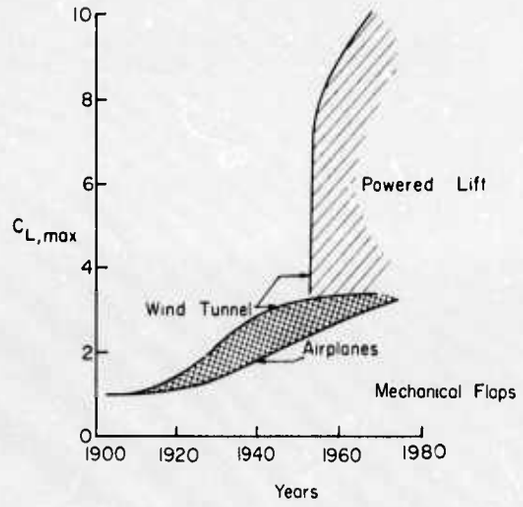

Figure 1. - Trend for maximum lift coefficient capabilities.

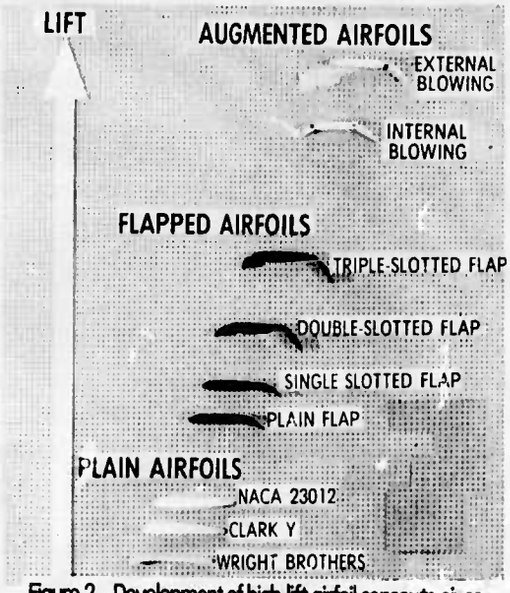

Figure 2. - Development of high-lift airfoil concepts since the Wright Brothers.

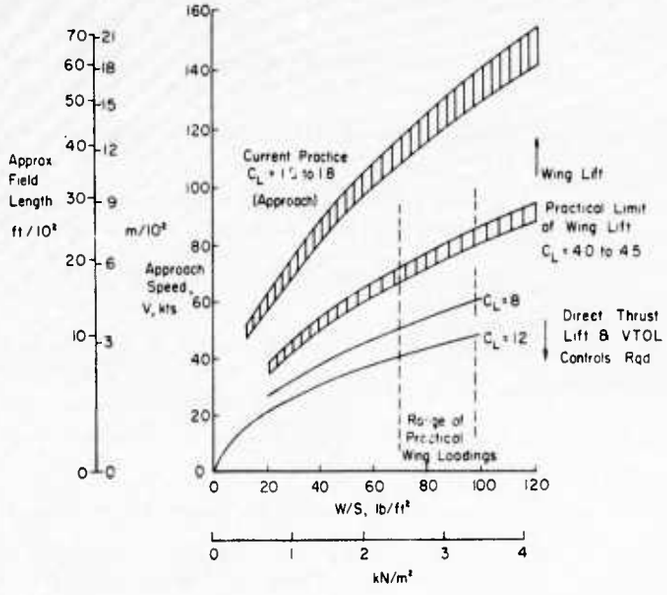

Figure 3. - Takeoff and landing requirements for various wing loadings.

- POTENTIAL-FLOW SOLUTION
- BASIC BOUNDARY LAYER
- SLOT-FLOW ANALYSIS
- CONFLUENT BOUNDARY LAYERS
- COMBINED SOLUTION

Figure 4. - Computational sequences of NASA/Lockheed-Georgia two-dimensional multi-element viscous-flow airfoil program.

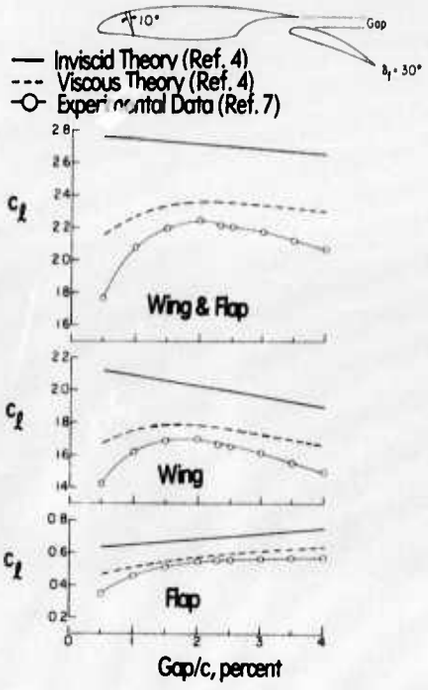

Figure 5. - Gap optimization results from 10°-drooped nose airfoil with slotted flap.

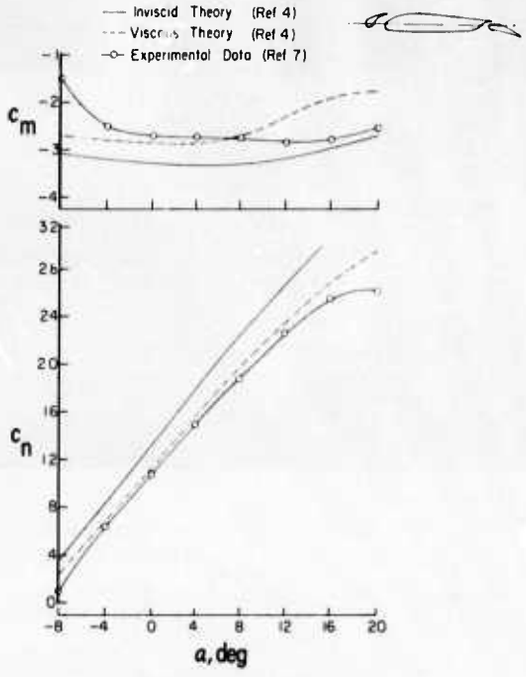

(a) Normal force and pitching moment

Figure 6. - Comparison of two-dimensional theoretical and experimental three-component NACA 23012 airfoil.

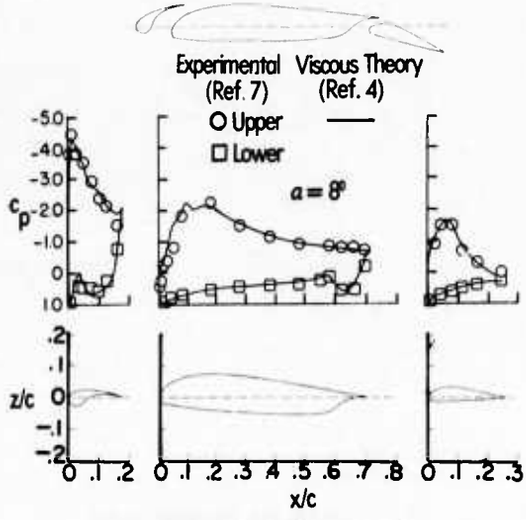

(b) Pressure distribution at $\alpha = 8°$

Figure 6. - Concluded.

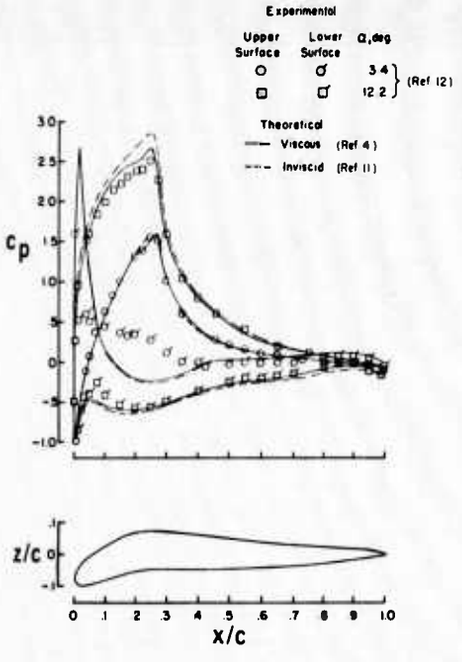

Figure 7. - Comparison of two-dimensional theoretical and experimental results for an airfoil optimized for maximum lift.

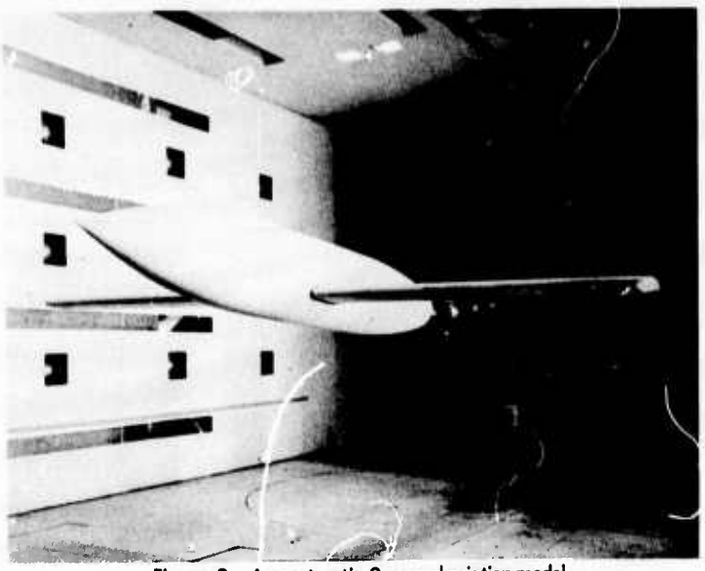

Figure 8. - Aspect-ratio-9 general aviation model.

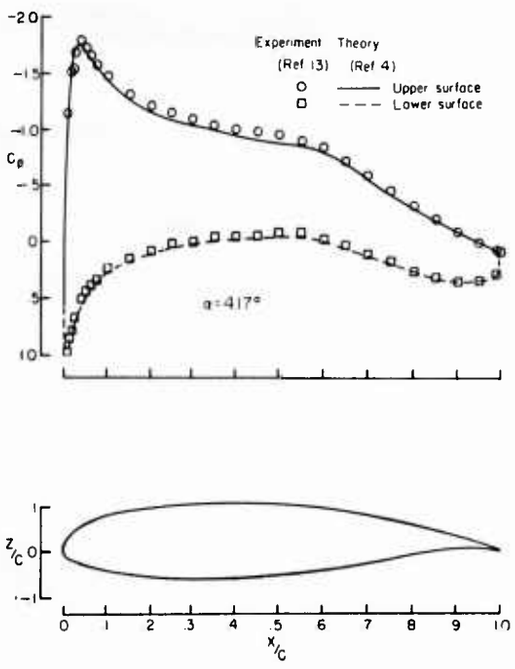

(a) Pressure distribution at $\alpha = 4.17°$

Figure 9. - Comparison of two-dimensional theoretical and experimental results for improved 17-percent-thick general aviation airfoil.

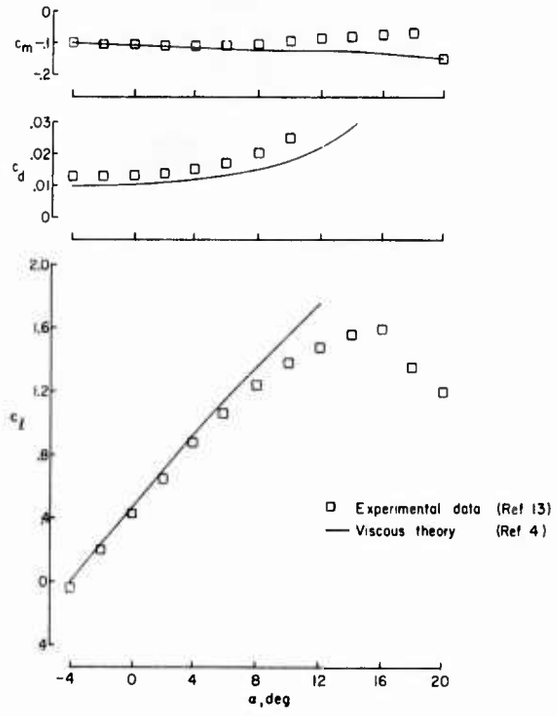

(b) Lift, drag, and pitching moment

Figure 9. - Concluded.

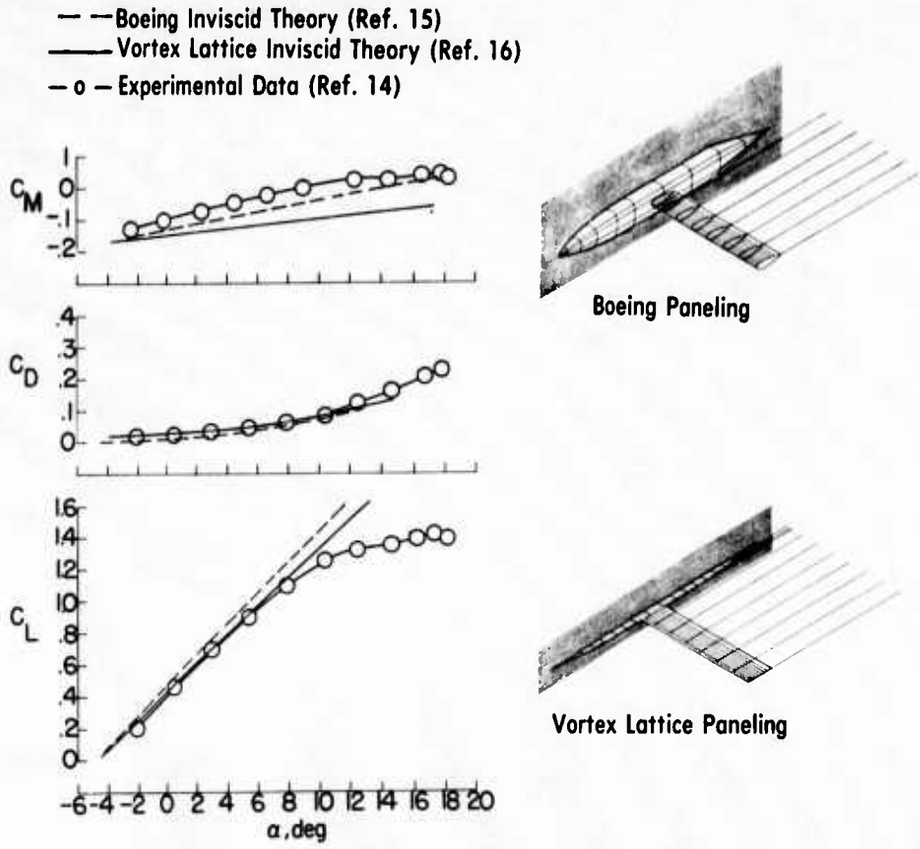

Figure 10. - Comparison of three-dimensional inviscid theoretical and experimental data for general aviation model.

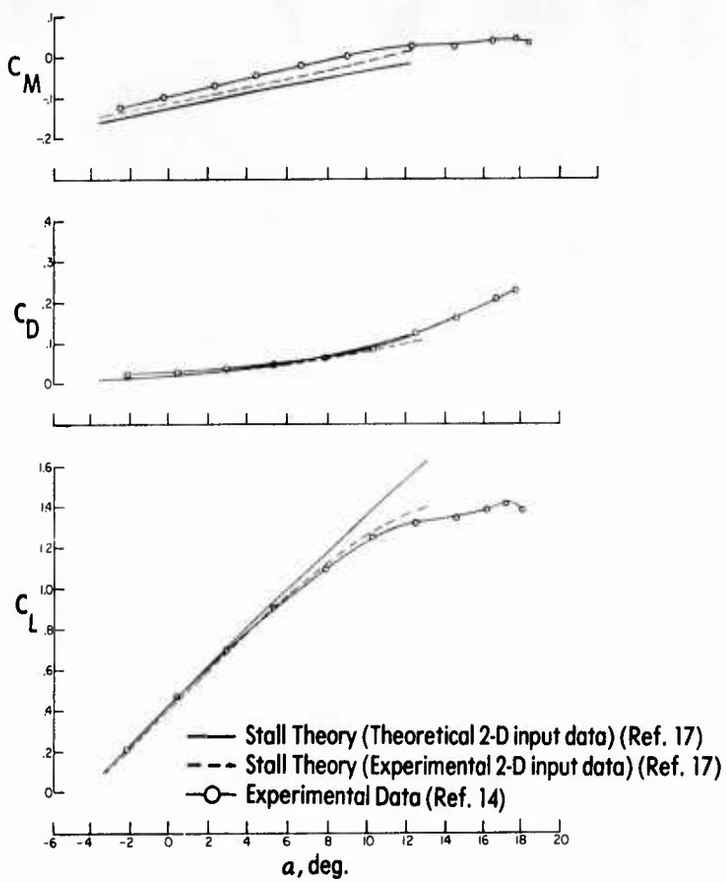

Figure 11. - Comparison of three-dimensional viscous stall theoretical and experimental data for general aviation model.

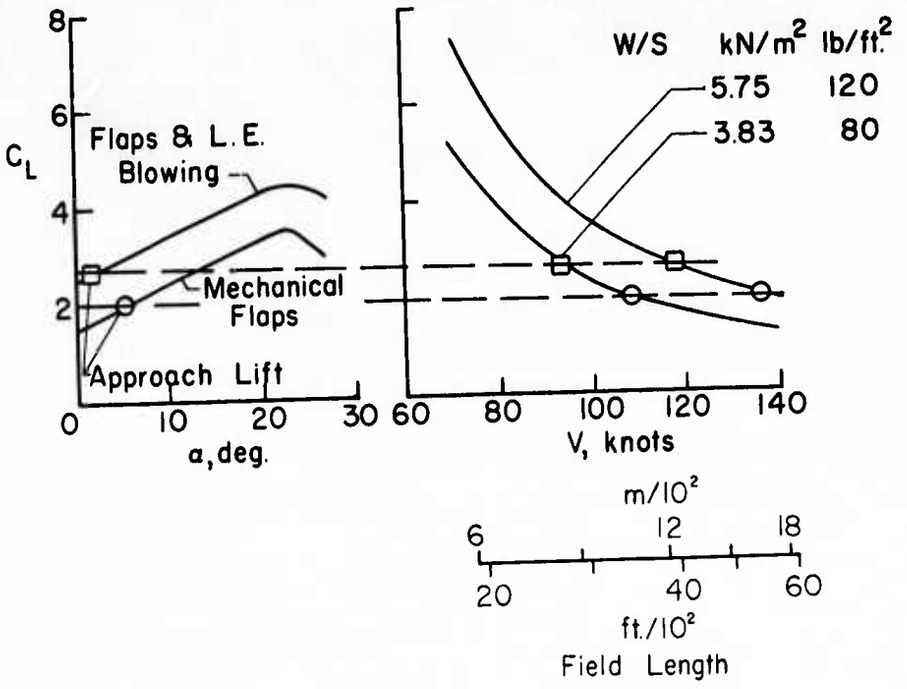

Figure 12. - Landing performance of high-lift systems.

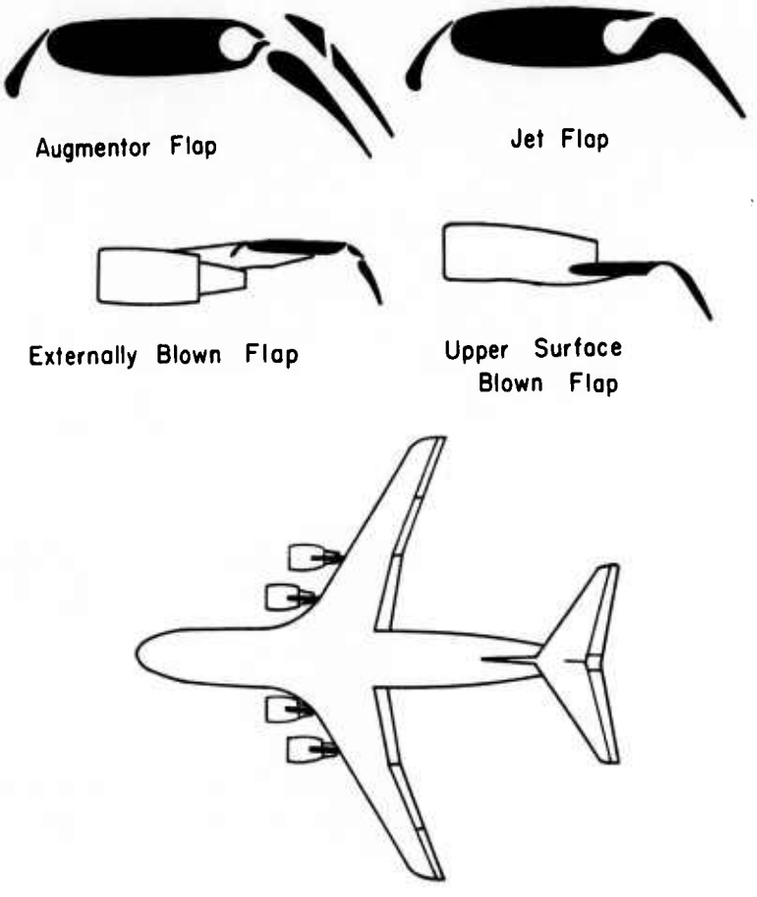

Figure 13. - Propulsive-lift-flap concepts.

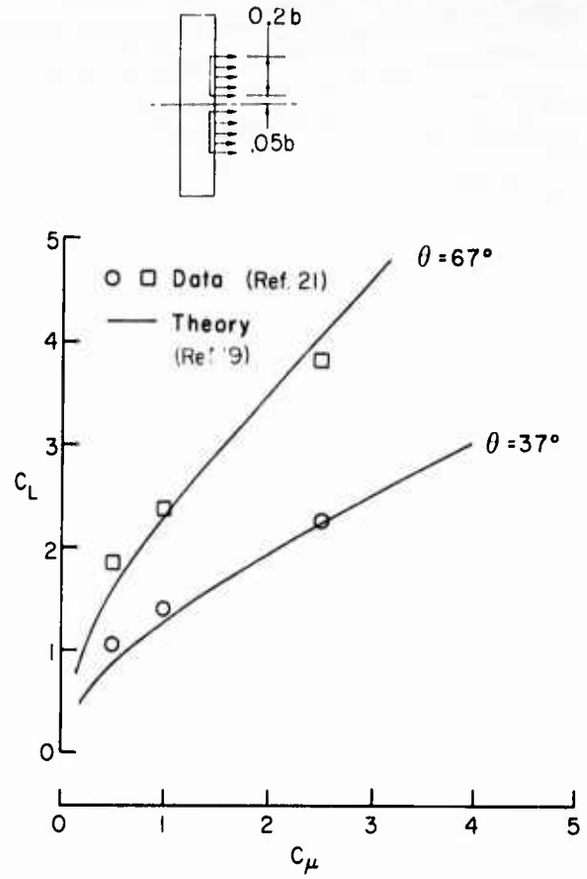

Figure 14. - Comparison of three-dimensional jet-flap theoretical and experimental data for an aspect-ratio-6 wing with partial span blowing

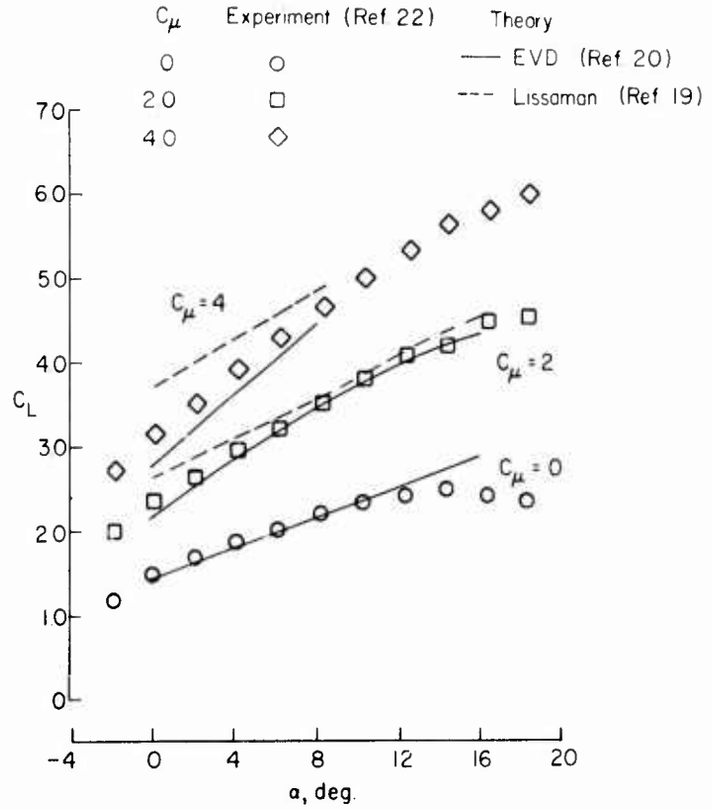

Figure 15. - Comparison of three-dimensional jet-flap theoretical and experimental data for an externally blown flap model.

COMPATIBILITY OF TAKE-OFF AND LANDING WITH MISSION AND MANOEUVRE PERFORMANCE REQUIREMENTS FOR FIGHTER AIRCRAFT

by

Dieter REICH and Josef WIMBAUER
Messerschmitt-Bölkow-Blohm GmbH
Unternehmensbereich Flugzeuge
8 München 80
Postfach 80 11 60
Germany

SUMMARY

By means of an aircraft synthesis programme the effect of engine cycle, thrust to weight ratio, and wing parameter combination on field and flight performance has been investigated.
Using different lift systems and ground deceleration devices the conditions are shown under which a matching of flight and field performance is economically feasable.

INTRODUCTION

There are two major operational tasks for fighter aircraft. Each of them require various, sometimes contradicting capabilities:Payload/Range performance is essential for Close Air Support/ Interdiction type missions, manoeuverability is required for Air Superiority/Air Defence tasks. A summary of parameters which effect mission, manoeuvre,and field performance is shown in Fig. 1.

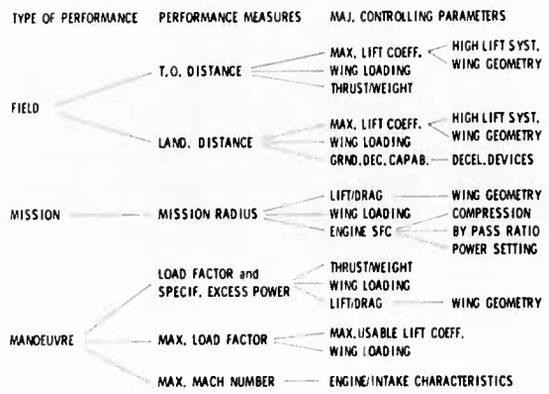

Fig. 1 PERFORMANCE ASSESSMENTS

ENGINE / INTAKE	HIGH BPR PITOT	HIGH BPR 2 WEDGE INTAKE	LOW BPR 2 WEDGE INTAKE
DESIGN MISSION RADIUS	150 n. m.	150 n. m.	90 → 150 n. m.
HIGH LIFT DEVICES	2 - SLOTTED FLAPS + SLATS AND PLAIN FLAPS	2 - SLOTTED FLAPS + SLATS	2 - SLOTTED FLAPS + SLATS
ASPECT RATIO, WING SWEEP	3.0/45° 4.5/37.5°	3.0 / 45°	3.0 / 45°
WING LOADING LB / FT^2	55 → 100	55 → 100	55 → 100
(THRUST/WEIGHT)$_{INSTALLED}$*	.76 → 1.6	.76 → 1.6	.6 → 1.1
DECELERATION DEVICES	BRAKES ONLY, DRAG CHUTE, THRUST REVERSER		
ALTERNATE MISSION PERF.	LO-LO-LO MISSION WITH EXTERN. TANKS AND 4 x 1000 LB PAY LOAD		

* Sea Level Static

Fig. 2 RANGE OF VARIATION

Wing loading and thrust to weight ratio affect most frequently aircraft performance. A high wing loading, for example, penalizes take-off and landing performance, on the other hand it is beneficial to cruise performance. A high thrust to weight ratio is favourable for take-off and manoeuvre performance. Due to lower power setting, however, high thrust to weight ratios penalize payload/range performance rather severely. Other parameters such as aspect ratio, wing sweep, engine cycle etc. have similar effects on field and flight performance. Since all these parameters influence not only aircraft performance but aircraft weight at the same time, the effect must be investigated simultaneously. This can be done most efficiently and most consistently by means of an aircraft synthesis programme (Ref. 1).

1. RANGE OF VARIATION

For three different engine/intake configurations thrust to weight ratio and wing loading were varied. Each combination represents an aircraft designed to meet a specified mission radius. Plain flaps and an alternate aspect ratio/wing sweep combination were investigated for the high bypass ratio engine/pitot intake configuration only (Fig. 2). All landing distances were computed using different ground deceleration devices. In addition,alternate mission performance has been calculated based on a low altitude mission profile.

2. GROUND RULES AND BASIC ASSUMPTIONS

Base Design

All aircraft synthesized for this study are considered to be derivatives from one base design shown in Fig. 3. This configuration is a single seat, fixed wing, supersonic fighter in the 20 000 LB-weight-class. A moderate wing loading and an appropriate choice of wing and intake location guarantee weapon cariing capability and good manoeuverability. There were no high speed manoeuvering devices built in. The aircraft synthesis takes into account all primary and secondary scaling effects and represents adequately the preliminary design process with all the major disciplines involved.

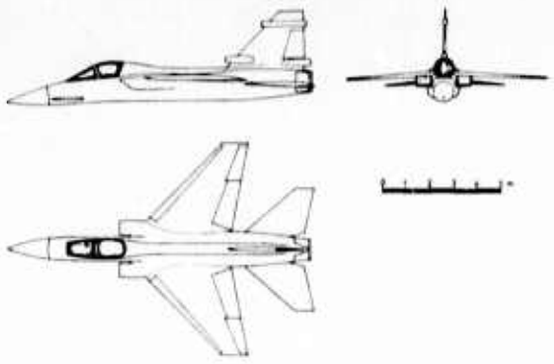

Fig. 3 BASE DESIGN

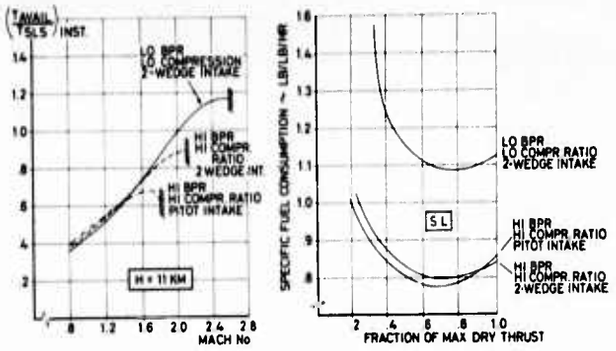

Fig. 4 MAX. REHEAT THRUST AND SFC COMPARISON

Engine Performance

In order to show the effect of engine cycle, two engines of the same state of technology were compared: a high bypass ratio (BPR = 1.3), high compression ratio engine and a low bypass ratio engine (BPR = .3), low compression ratio engine. The high BPR-engine was designed for low fuel consumption at max. dry thrust setting and high subsonic Mach numbers. The low BPR, low compression ratio engine was designed for low specific fuel consumption at max. reheat condition and supersonic Mach numbers. Some characteristic performance data are presented in Fig. 4. All data are installed values, assuming a variable double wedge intake for both engines. In comparison, data for the high BPR/pitot intake combination are shown.

Manoeuverability

There are several possibilities to describe or measure manoeuverability performance. For a high speed interceptor one would measure manoeuverability at low g-conditions in terms of climb acceleration time or specific excess power (Fig. 5). For air superiority fighters operating at high subsonic speeds, specific excess power at low and high load factors is an appropriate measure for manoeuverability. For self defence capability, maximum load factor or maximum turn rate respectively seems to be a good measure for manoeuvre performance (Ref. 2). In this study manoeuverability is defined in terms of specific excess power (as shown in Fig. 5) at specified Mach number, altitude, and load factor conditions.

SPECIFIC EXCESS POWER (SEP) = $\frac{\text{THRUST - DRAG}}{\text{WEIGHT}}$ x VELOCITY [FT/SEC]

ENERGY HEIGHT (E_H) = $H + \frac{\text{A/C MASS}}{2}$ x VELOCITY^2 [FT]

COMBAT TIME = $\frac{E_{H2} - E_{H1}}{SEP}$ [SEC]

Fig. 5 SPECIFIC EXCESS POWER AND ENERGY HEIGHT

TAKE-OFF	
RUNWAY ALTITUDE	SL
AMBIENT TEMP.	ISA + 15° C
OBSTACLE HEIGHT	50 FT
SAFETY FACT. FOR T.O. VELOCITY	1.1 x V_{STALL}
SAFETY FACT. FOR SPEED AT OBST.	1.2 x V_{STALL}
ROLLING FRICTION COEFF.	.025
TAKE OFF WEIGHT	1.3 x T.O. GROSS WEIGHT

LANDING	
RUNWAY ALTITUDE	SL
AMBIENT TEMP.	ISA + 15° C
OBSTACLE HEIGHT	50 FT
SAFETY FACT. FOR APPR. SPEED	1.1 x V_{STALL}
RATE OF SINK	10 FT/SEC
BRAKE CAPACITY	.45
WHEEL BRAKING	1 SEC AFTER T.D.
CHUTE DRAG AREA	150 FT^2
CHUTE ACTUATION DELAY	3 SEC
REVERSE THRUST	55% OF MAX. DRY THRUST
REVERSE THRUST ACTUATION DELAY	2 SEC
LAND. WEIGHT	T.O.G.W. - 90% FUEL

Fig. 6 TAKE-OFF AND LANDING GROUND RULES

Take-off and Landing

Fig. 6 summarizes the ground rules and basic assumptions used for take-off and landing calculation. It has to be noted that take-off distances are computed using a take-off weight which is 30 percent higher than the take-off gross weight for the design mission described below. This is to account for off-design operational payload carriing capability. In addition, it has to be mentioned that the terms wing loading and thrust to weight ratio used in this study are based on design mission take-off gross weight and not on the 30 percent overload condition.

Mission Profiles

Fig. 7 describes design mission and alternate mission profiles. The design mission was used to determine the amount of internal fuel. It is an air superiority type profile which contains elements of loiter, optimum cruise, and combat manoeuvering with maximum reheat. In order to account for the difference in combat performance of aircraft with different thrust to weight ratios, a gain of energy height was used instead of a fixed combat time requirement (Fig. 5) to estimate combat fuel allowance (Ref. 3).

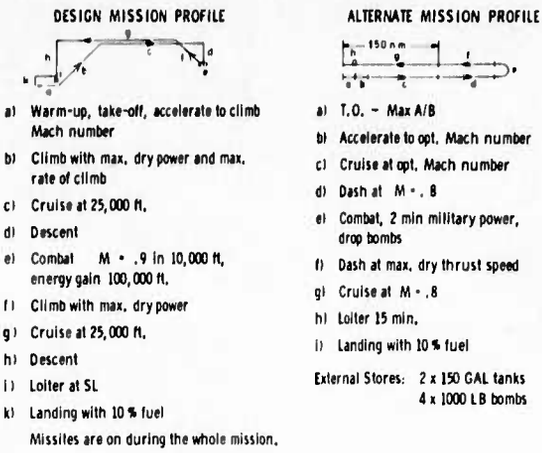

Fig. 7 MISSION PROFILES

3. ASYMPTOTIC THRUST TO WEIGHT RATIO

Wing loading and thrust to weight - as mentioned earlier - are the driving parameters with respect to vehicle performance and size. It could be expected, as indicated in Ref. 2, that there is a feasibility limit for extreme combinations of thrust to weight ratio and wing loading. Fig. 8 shows three diagrams where take-off gross weight is plotted against thrust to weight ratio for two extreme wing loadings. Each curve represents a serie of aircraft, designed for a mission radius of 150 n.m., for which the take-off gross weight is given as a function of thrust to weight ratio and wing loading. The first two diagrams differ by the selection of sweep angle and aspect ratio while wing taper ratio is held constant. Due to a higher structural weight for higher aspect ratio wings, take-off gross weight shows a stronger progressiveness especially for the lower wing loadings. A design iteration divergence can be expected at a thrust to weight ratio of about 1.6. For the low bypass ratio, low compression

Fig. 8 THRUST/WEIGHT RATIO AND WING LOADING LIMITS

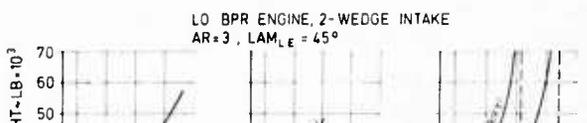

Fig. 9 ASYMPTOTIC THRUST/WEIGHT RATIO VERSUS MISSION RADIUS

ratio engine asymptotic thrust to weight ratios can be assumed at about 1.0 for the low wing loading, and 1.3 for the high wing loading. The main reason for the low asymptotic thrust to weight ratios in the latter case is the fact that for higher thrust to weight ratios the power setting during cruise flight becomes rather low, thus specific fuel consumption increases more rapidely compared with the high bypass ratio engine (Fig. 4). The penalizing effect is quite significant at high thrust to weight ratios. As shown in Fig. 9 a similar problem arises when the design mission radius is increased.

4. PERFORMANCE COMPATIBILITY

Any combination of wing loading and thrust to weight ratio stands for one aircraft design as shown in the previous figures. When substituting thrust to weight ratio by vehicle flight and field performance - which can be achieved with this thrust to weight ratio at a specified wing loading and take-off gross weight - a diagram as presented in Fig. 10, can be drawn. It shows in a schematic manner take-off gross weight as a function of wing loading for any combination of flight and field performance requirements. There is one line, for example, representing a subsonic high load factor turn requirements in terms of specific excess power at a specified Mach number, altitude, and load-factor condition, going from the upper right to the lower left corner of the diagram. This tendency indicates, that for high load factors (which means high lift coefficient and high induced drag) the use of a larger wing (lower wing loading) in spite of its higher structural weight results in a lower take-off gross weight. On the other hand a vehicle which is designed for a low load factor supersonic requirement benefits from a higher wing loading (smaller wing) because of the smaller zero lift drag (wave drag). A third line, designated

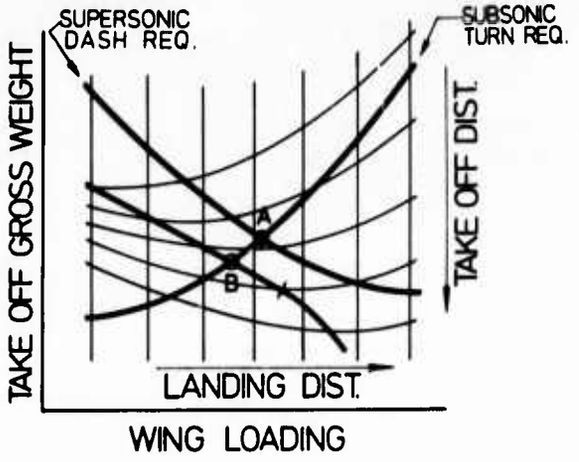

Fig. 10 MATCHING (SCHEMATIC)

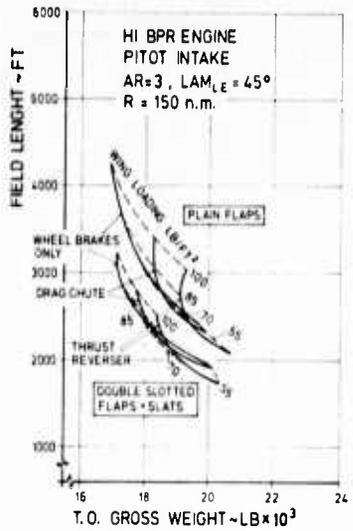

Fig. 11 FLAP SYSTEM - DECELERATION DEVICES EFFECTIVENESS

as "minimum-weight-field-performance" is a curve, connecting values of different field performance which can be achieved at minimum take-off gross weight. The upper part of the curve combines merely the points where take-off and landing distances are equal. The lower part of the "minimum-weight-field-length" curve represents the field length, where take-off does not match landing distance, because minimum weight for a given take-off distance is achieved at a wing loading smaller than required for matching field performance.

Performance matching is achieved at an intersection of at least two requirement lines. For example: subsonic turn performance matches supersonic dash performance at A, subsonic turn requirement matches "minimum weight field length" at B. There is, however, no compatibility of supersonic dash performance and "minimum weight field length".

Fig. 11 shows the effect of high lift and ground deceleration devices on achievable field length and take-off gross weight. The solid lines indicate "minimum weight field lengths" for different deceleration devices. It can be seen how each of the different deceleration devices has its own area of application; so does the thrust reverser at low wing loadings (low approach speeds), the drag chute at moderate wing loadings, and brakes only at high wing loadings.

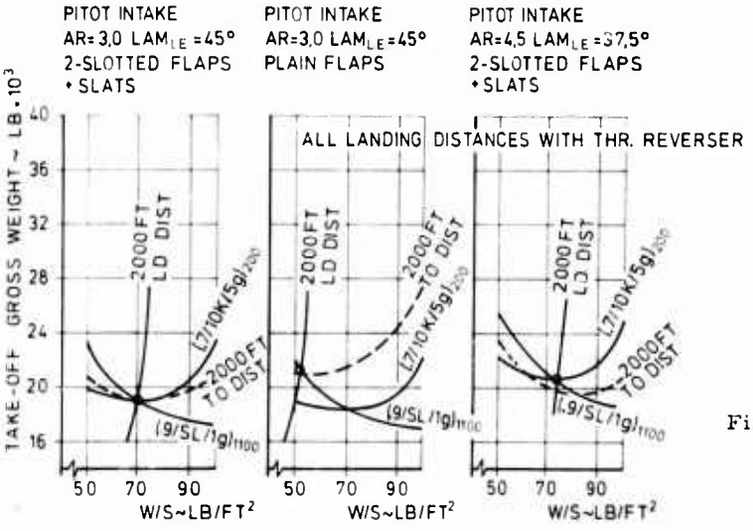

Fig. 12 MATCHING REQUIREMENTS, R = 150 n.m.

Fig. 12 presents the principles of matching for a sample set of requirements. These are:

a) 2000 FT field length,
b) SEP = 200 FT/S at Mach = .7, Alt. = 10 000 FT, Load factor = 5.,
c) SEP = 1 100 FT/S at Mach = .9, Alt. = Sea level, Load factor = 1.

It happens that all requirements size the aircraft simultaneously (left diagram). Utilizing the lighter plain flap lift system, the lack of lift is compensated by a reduction in wing loading, the Mach = .7 turn performance requirement is exceeded, the take-off gross weight, however, higher than for the

previous case. Switching to a higher aspect ratio the minimum weight is achieved at a higher wing loading (due to better flap efficiency) compared with the first case. The take-off gross weight, however, increases because of a structural weight penalty for the higher aspect ratio wing.

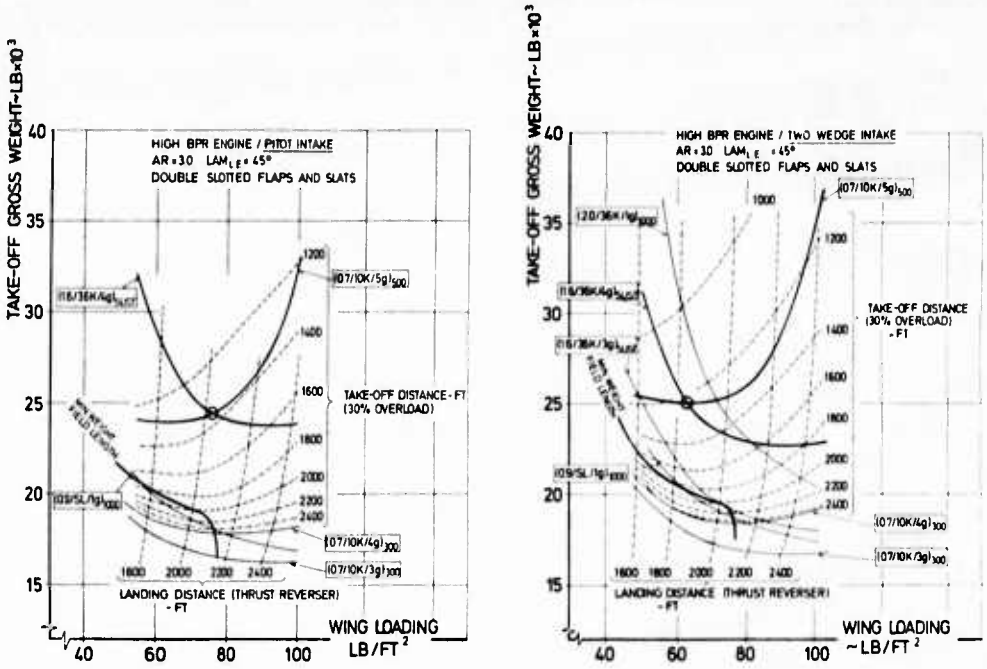

Fig. 13 SUBSONIC VERSUS SUPERSONIC MANOEUVRE REQUIREMENTS, R = 150 n.m.

A trade between subsonic and supersonic manoeuvre capability is shown in Fig. 13 for two different intakes. The minimum take-off gross weight to meet a Mach = .7 subsonic and a Mach = 1.6 supersonic turn requirement is achieved at a lower wing loading for the double wedge intake than for a pitot intake aircraft. Take-off gross weight, however, is still higher because the weight penalty for a double wedge intake offsets the advantage of better supersonic performance.

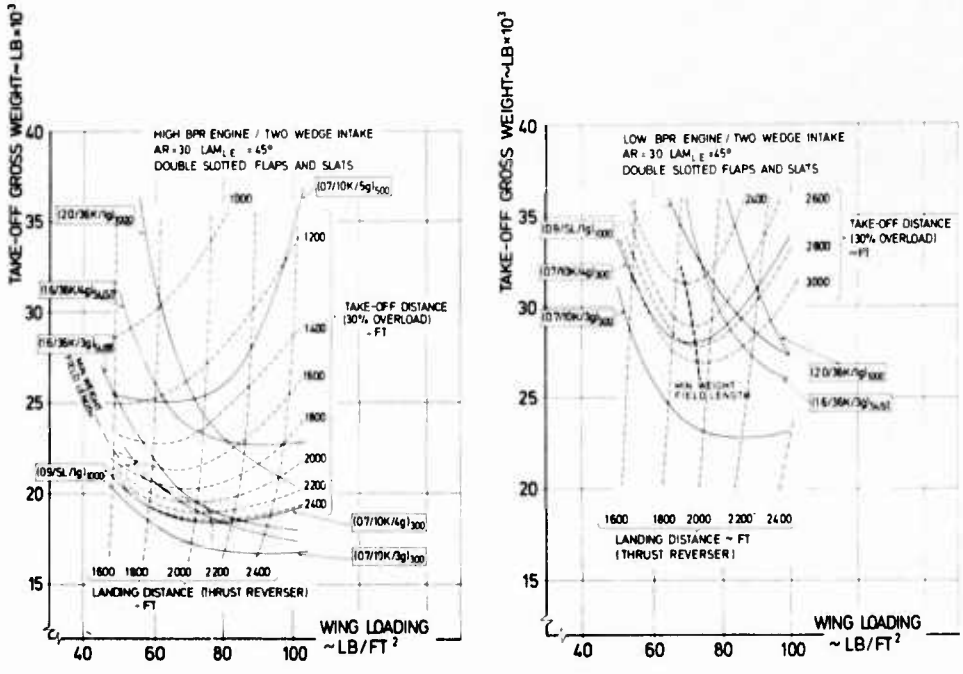

Fig. 14 EFFECT OF ENGINE PERFORMANCE, R = 150 n.m.

The effect of engine characteristics is shown in Fig. 14. To maintain the same performance levels, take-off gross weights for the low BPR-engine are much higher and more sensitive to a change in wing loading than the high BPR-engine.

An indication how alternate mission performance is affected by thrust to weight ratio and wing loading is given in Fig. 15. The strong performance degradation (at constant design mission radius) with increasing thrust to weight ratio is caused by the fact, that in contrast to the design mission - where about 40 percent of fuel is consumed during combat - almost the entire alternate mission is flown at a low power setting, thus penalyzing engine specific fuel consumption significantly.

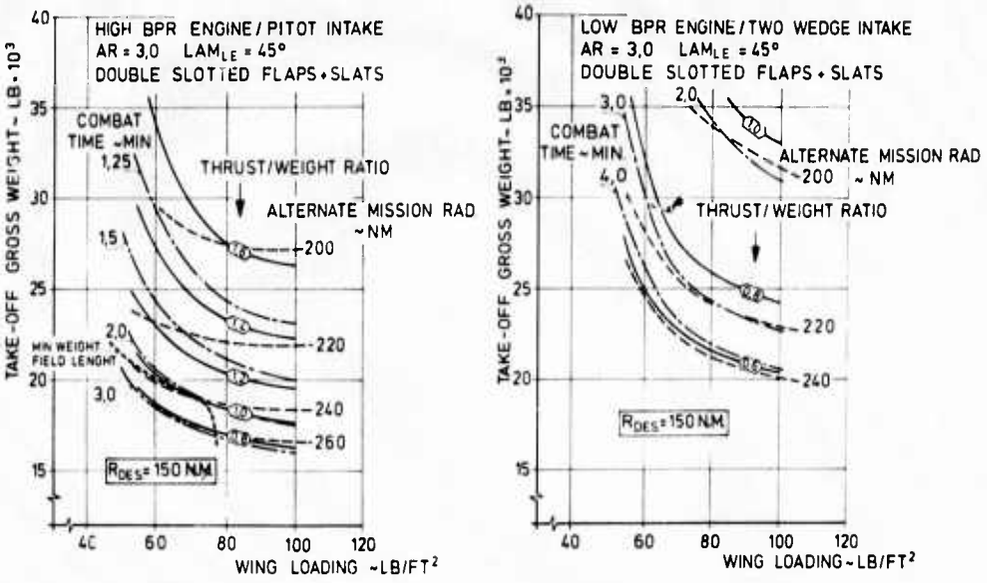

Fig. 15 ALTERNATE MISSION PERFORMANCE

Fig. 16 finally, illustrates in two examples the conditions under which a matching of flight and field performance is feasable. In order to show the effect of the two major parameters in one diagram, thrust to weight ratio was plotted against wing loading. The left diagram is applicable to double slotted flaps and slats, the right one is valid for plain flaps. Lines of "minimum weight field length" are shown for three different ground deceleration devices. Manoeuvre performance is represented by specific excess power at the following conditions:

a) M = 1.6, Alt. = 36 KFT, Load factor = 1
b) M = .7, Alt. = 10 KFT, Load factor = 4

Neglecting the different slopes between "minimum weight field length" and the lines of constant turn performance, maximum manoeuvre performance can be matched with a field length requirement of about 2 000 FT for aircraft using double slotted flaps and thrust reverser. Utilizing plain flaps only, compatibility is achieved for field lengths of about 2 400 FT at a slightly higher thrust to weight ratio.

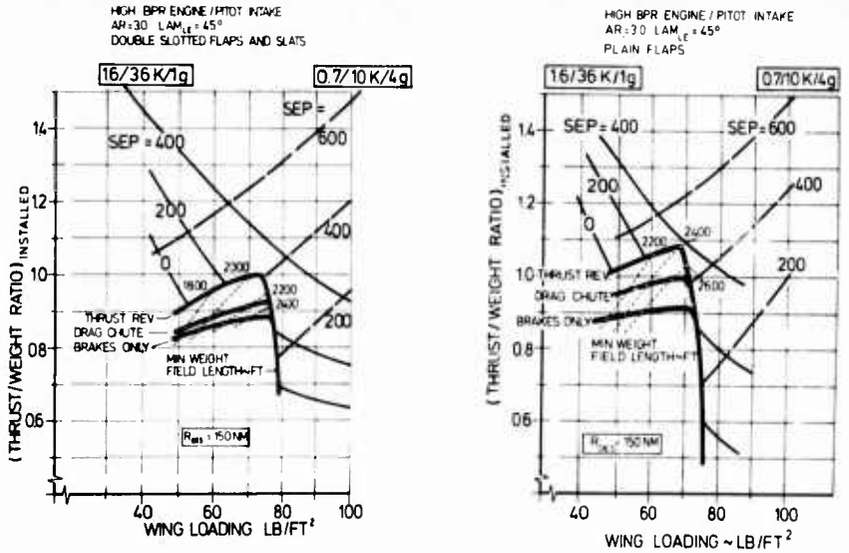

Fig. 16 PERFORMANCE COMPATIBILITY

5. CONCLUSIONS

- Only high bypass ratio, high compression ratio engines, and moderate thrust/weight ratios seem to satisfy economically the demand for small field lengths, good manoeuverability (up to Mach numbers of about 2.0), and transportation capability at the same time. The best combination of thrust to weight ratio and wing loading, for which field and manoeuvre performance can be matched, depends on the maximum lift coefficient provided by high lift devices. Compatibility for fixed wing aircraft can be achieved at thrust to weight ratios of about 1.1, when using plain flaps and thrust reverser. Utilizing double slotted flaps the thrust to weight ratio decreases to about 1.0. For high aspect ratio or variable geometry aircraft this value would even be lower.

- There is an asymptotic thrust to weight ratio for fighter aircraft depending on design mission profile, design mission radius, engine SFC, wing loading,and wing shape. This asymptotic behaviour limits the level of achievable field and manoeuvre performance. Due to higher SFC's at lower power settings these limitations become crucial for aircraft using low bypass ratio, low compression ratio engines.

6. REFERENCES

1. Herbst, W.B., and Ross, H.: Application of Computer Aided Design Programs for the Management of Fighter Development Projects. AIAA Paper No. 70 - 364
2. Herbst, W.B., and Krogull, B.: Design for Air Combat. AIAA Paper No. 72 - 749
3. Ross, H.G., and Frenzl, W.: Design Features for Air Combat. AGARD Symposium on Aircraft Design Integration and Optimization, Florence, Oct. 1973

CRITERES GENERAUX POUR LA DEFINITION AU DECOLLAGE ET A L'ATTERRISSAGE D'UN AVION NON LIMITE EN PORTANCE

par

C. PELAGATTI, Ingénieur,
Direction des Etudes Toulouse,
AEROSPATIALE, 316 route de Bayonne
31 053 TOULOUSE CEDEX - FRANCE.

et

T. MARKHAM, Ingénieur,
Bureau Aérodynamique
British Aircraft Corporation
Filton House, BRISTOL, ENGLAND.

SOMMAIRE

Nous avons considéré pour l'exposé ci-après, un avion à voilure élancée "non limité en portance". Nous décrivons d'abord le processus qui, à partir d'une nouvelle configuration, a conduit à de nouvelles caractéristiques aérodynamiques et à de nouveaux réglements de Certification. L'optimisation des caractéristiques aux basses vitesses est ensuite développée en prenant l'exemple de CONCORDE.

1. INTRODUCTION

Un grand nombre de facteurs doivent être pris en compte pour le calcul des performances à l'atterrissage et au décollage d'une nouvelle génération d'avions de transport à voilure élancée, dont les caractéristiques diffèrent sensiblement de celles des avions subsoniques actuels.
Il est nécessaire non seulement de bien connaître et d'interpréter ces caractéristiques aérodynamiques nouvelles tant sur le plan du pilotage que des performances, mais aussi de s'assurer que l'effet de tout changement significatif par rapport aux caractéristiques classiques est bien reflété dans les réglements de certification. Une fois la configuration générale choisie et son effet probable sur les réglements de certification déduit, l'optimisation des performances pour l'ensemble de la mission pourra alors se poursuivre.
Ce processus qui, à partir de formes aérodynamiques inhabituelles, a conduit à des caractéristiques aérodynamiques nouvelles, conduisant à leur tour à une modification des réglements et des procédures d'essais en vol, sera décrit en prenant l'exemple de CONCORDE.
Les nouveaux réglements auxquels nous nous réfererons sont les réglements TSS proposés par les Autorités de Certification franco-britanniques. Inévitablement les avionneurs estiment que certaines exigences contenues dans les réglements sont trop sévères, et le fait de s'y référer ne doit pas être considéré comme indiquant un accord complet !

2. COMPARAISON ENTRE LES CARACTERISTIQUES AERODYNAMIQUES AUX BASSES VITESSES D'UN AVION CLASSIQUE ET D'UN AVION A VOILURE ELANCEE.

Ayant choisi une voilure élancée principalement à cause des possibilités offertes pour l'optimisation des performances en croisière supersonique, il est nécessaire de considérer les différences qui en découlent aux basses vitesses par rapport à une voilure classique. Elles résultent directement du faible allongement de la voilure, qui entraîne :
(i) un gradient de portance plus faible et une incidence plus élevée pour une portance donnée. La figure 1 compare les deux types d'avion, et l'on peut noter l'absence de décrochage classique pour l'avion à voilure élancée.
(ii) La combinaison d'une forte flèche et d'une faible épaisseur relative conduit à une séparation de l'écoulement aérodynamique par rapport au profil, le long du bord d'attaque. Bien que ce type d'écoulement n'apparaisse pas sur une voilure à flèche modérée, il constitue une forme stable d'écoulement sur une voilure élancée (Figure 2) et, initialement considéré avec une certaine suspicion, il est maintenant bien accepté. La figure 1 montre le gain de portance qu'il procure par rapport à l'écoulement attaché au profil et la figure 3 montre la dégradation qui en résulte dans l'évolution du moment de tangage.
(iii) La combinaison d'un faible allongement et d'un écoulement séparé du profil conduit à une traînée induite élevée ; la configuration lisse, sans volets, conduit également à une faible traînée à portance nulle. Ces deux caractéristiques entraînent une vitesse de finesse maximale suffisamment élevée pour qu'on soit amené à utiliser opérationnellement l'avion au second régime.

Nous examinerons d'abord l'impact de ces nouvelles caractéristiques aérodynamiques sur le pilotage aux basses vitesses.

3. EVOLUTION DES CARACTERISTIQUES DE PILOTAGE AUX BASSES VITESSES D'UN AVION A VOILURE ELANCEE.

L'augmentation de l'incidence se traduit d'abord par une dégradation progressive de la stabilité statique longitudinale, ainsi que nous l'avons montré sur la figure 3.
Comme les performances au décollage imposent un centrage assez arrière, il en résulte assez rapidement une instabilité longitudinale qu'il est nécessaire de corriger : nous verrons plus loin les moyens utilisés dans le cas de l'avion TSS CONCORDE.
- le contrôle transversal ne subit pas d'abord de dégradations notables quand l'incidence augmente, la stabilité de route conservant une valeur suffisante ainsi qu'il est indiqué sur la figure 4.

La situation que nous venons de décrire se dégrade toutefois quand on atteint une incidence plus élevée où se produisent des pertes partielles de portance sur les bords de fuite, dues à la dégénérescence des tourbillons d'apex : il apparaît alors un "pitch up" d'amplitude limitée (sur CONCORDE, il se traduit par une variation de braquage d'équilibre des gouvernes d'environ 3 degrés), mais suivi d'une dégradation de la stabilité statique telle qu'elle pourrait conduire à plus long terme à une perte de contrôle longitudinal.

Le contrôle transversal se dégrade également par suite notamment de la perte de stabilité de route qui intervient au voisinage de l'incidence de "pitch up" ; il devient difficile, puis impossible, au volant seul, quand l'instabilité de route entraîne la divergence du dérapage, ainsi que l'ont montré des essais sur simulateur.
Nous devons ajouter que l'efficacité des différentes gouvernes reste suffisante pour équilibrer statiquement l'avion jusqu'à des incidences très élevées (Cf. figure 5), et qu'elle permet des récupérations très faciles à des incidences plus modérées, ainsi que l'ont montré les essais en vol.
Il est donc nécessaire de limiter le domaine de vol de l'avion vers les basses vitesses ou les grandes incidences avant que n'apparaissent des difficultés de contrôle trop importantes. Ainsi il nous a paru raisonnable sur l'avion prototype CONCORDE 001 de ne pas aller délibérément jusqu'au "pitch up", bien que des essais sur simulateur aient montré que le contrôle restait encore possible au delà. La vitesse minimale V_{MIN} peut alors être démontrée en vol à facteur de charge unité, et nous confondrons dans la suite de l'exposé les deux concepts de vitesse minimale ou d'incidence maximale dans les configurations symétriques de l'avion.

4. CRITERES D'IDENTIFICATION DE LA VITESSE MINIMALE

Nous allons maintenant examiner les critères auxquels il est nécessaire de satisfaire pour l'identification de cette vitesse minimale, par analogie avec les avions subsoniques actuels.
Sur ces derniers, certaines limites sont habituellement fournies par un comportement naturel : c'est, par exemple, l'apparition du buffeting qui signale la sortie du domaine autorisé vers les basses vitesses, et l'abattée au décrochage qui caractérise la vitesse de décrochage V_S.
Sur un avion à voilure élancée, il est nécessaire de matérialiser ces limites par des moyens artificiels, s'il n'existe jusqu'à la vitesse minimale démontrée en vol aucun phénomène naturel susceptible d'éveiller l'attention du pilote.
Outre un système classique d'avertissement de sortie du domaine autorisé, tel qu'un vibreur de manche, un second niveau d'alarme doit être fourni pour satisfaire pleinement aux exigences de certification. Cette alarme inmanquable, calée au voisinage de l'incidence maximale, doit satisfaire aux objectifs suivants :
- elle doit opérer suffisamment à l'avance par rapport à l'incidence maximale, dans des conditions dynamiques, pour permettre à l'équipage d'observer cette limitation sans habileté exceptionnelle et suffisamment près de l'incidence maximale pour ne pas être une gêne durant les opérations normales, et certaines manoeuvres d'évitement,
- elle doit être suffisamment puissante pour être perçue dans tous les cas,
- elle doit être directive si l'action corrective à prendre par l'équipage n'est pas évidente.

Nous verrons plus loin les solutions retenues pour l'avion TSS CONCORDE.

5. MARGES REGLEMENTAIRES ENTRE V_{MIN} ET VITESSE OPERATIONNELLE A L'APPROCHE.

Les marges suivantes ont été imposées dans les réglements TSS pour un avion supersonique qui possèderait à l'approche des caractéristiques de maintien de vitesse comparables à celles des avions subsoniques actuels.

(i) $V_{MIN}\ 1\ g \leq V_{REF}/1{,}3$, la poussée affichée étant égale à la poussée nécessaire pour maintenir une approche stabilisée avec un angle de descente stabilisé n'excédant pas 3 degrés,

(ii) $V_{MIN}\ 1\ g \leq V_{REF}/1{,}25$, la poussée affichée n'excédant pas la poussée minimale autorisée pour l'approche finale jusqu'en seuil de piste, V_{REF} étant la vitesse minimale autorisée dans la configuration approche tous moteurs en fonctionnement.

Ces marges apparaissent comme sensiblement plus sévères que celles imposées aux avions classiques, puisque par exemple les réglements BCAR et les conditions spéciales franco-allemandes (A 300 B) admettent une chute de 6 % de la vitesse entre le début de l'abattée et l'instant où la vitesse minimale est obtenue : ainsi la plupart des avions subsoniques actuels satisfont à ce réglement avec une marge entre la vitesse minimale démontrée en vol moteurs réduits V_{MSC} et la vitesse objectif au seuil de piste V_{TT} telle que : $V_{TT} = 1{,}3\ V_{MSO} \sim 1{,}22\ V_{MIN}\ 1\ g$.
On peut noter en outre que la poussée nécessaire durant toute l'approche et jusqu'au voisinage du sol, reste relativement élevée pour un avion à voilure élancée et que dans cette configuration de poussée la plus fréquente, qui est celle de l'approche stabilisée sous 3° de pente, les marges exigées par rapport à la vitesse minimale démontrée en vol $V_{MIN}\ 1\ g$ se trouvent encore accrues.
Toutefois, si un standard de maintien de vitesse amélioré peut être démontré (variabilité à 3 σ au seuil de piste inférieure à 10 Kts environ), une certaine relaxation par rapport aux exigences précédentes est admise :

(i) $V_{MIN}\ 1\ g \leq V_{REF}\ /\ 1{,}25$ à la poussée d'approche

(ii) $V_{MIN}\ 1\ g \leq V_{REF}\ /\ 1{,}2$ à la poussée réduite.

Ce standard de maintien de vitesse amélioré peut être obtenu par l'utilisation d'une automanette.
Comme il sera vu plus loin, les vitesses au décollage sont moins dimmensionnées par le pilotage que par les performances.

6. CONSEQUENCES DANS LA CONCEPTION DE L'AVION.

A titre d'exemple, nous décrirons ci-après les solutions retenues pour satisfaire à ces exigences dans le cas du TSS CONCORDE, ainsi que leur expérimentation en vol sur l'avion CONCORDE prototype 001.

6.1. L'instabilité statique naturelle a été corrigée par un déroulement du trim de profondeur en fonction de l'incidence qui rétablit une stabilité en effort positive (Cf. figure 6). Toutefois, pour des raisons de sécurité, il est nécessaire de limiter la vitesse de déroulement du trim : ce "trim d'incidence" est donc insuffisant en cas d'approche dynamique rapide des grandes incidences.
Pour couvrir ce dernier cas et en addition au système d'augmentation de stabilité utilisé dans le domaine normal, nous avons développé un superstabilisateur actif aux grandes incidences pour des variations rapides d'assiette ou de vitesse, et dont le schéma de principe est représenté sur la figure 7. Ce dispositif permet de restituer des efforts de manoeuvre corrects aux basses vitesses ; il limite le taux de variation d'incidence à une valeur telle que, le pilote ayant entamé une manoeuvre d'évitement qui entraîne le déclenchement de l'alarme inmanquable à un facteur de charge de l'ordre de 1,5 g en virage à $\phi = 45°$, il lui soit possible de récupérer son avion sans habileté exceptionnelle et sans dépasser l'incidence maximale démontrée en vol. Cette manoeuvre est en effet considérée comme une manoeuvre enveloppe pour un avion tel que CONCORDE.

Il convient de noter que la plupart des fonctionnements intempestifs de ce dispositif n'affectent pas l'avion, si ce dernier se trouve dans une condition de vol stabilisée et qu'il est prévu une inhibition lors de la rotation au décollage.

6.2. Comme il n'y a pas dégradation notable du contrôle transversal jusqu'à α MAX, les dispositifs d'augmentation de stabilité définis dans le domaine normal restent suffisants : ils comportent une coordination gauchissement direction qui permet de limiter aux basses vitesses la valeur maximale de dérapage obtenue lors de manoeuvres en roulis de grande amplitude.

6.3. Avertissements et alarmes associés aux grandes incidences. Ils consistent en :

- un vibreur de manche dont le déclenchement est calé par rapport à la limite autorisée d'incidence en utilisation normale,
- une alarme dite "immanquable" constituée par un pulseur de manche (stick-wobbler) à effet directif, introduisant des à-coups à piquer à la fréquence de 3 Hz tant que le pilote tire sur le manche et l'empêchant de dépasser la limite absolue d'incidence.

Son déclenchement est commandé soit à l'incidence maximale pour une approche quasi statique des grandes incidences, soit à une incidence inférieure au cours d'une approche dynamique, l'avance introduite étant proportionnelle au taux de variation d'incidence.
Cette dernière alarme n'est active que si le pilote exerce une action à tirer : elle est inhibée dès qu'il exerce une action à piquer, de manière à ne pas gêner la manoeuvre de récupération. Son déclenchement intempestif n'entraîne pas de mouvement de gouverne dans une condition de vol où l'avion est trimmé ; elle est en outre inhibée lors de la rotation au décollage.

6.4. Nous traiterons maintenant brièvement de l'aspect sécurité lié à l'utilisation de ces "boîtes noires".

Les objectifs de sécurité à satisfaire sont fixés de manière à obtenir un niveau de sécurité au moins égal à celui des avions existants. Pour y satisfaire, on doit s'assurer :
- que leur fonctionnement opérationnel est satisfaisant pour l'ensemble des configurations de l'avion,
- que la plupart des pannes, et en particulier des fonctionnements intempestifs, ne conduisent pas à des situations critiques,
- que les pannes ou les combinaisons de pannes qui pourront avoir des conséquences catastrophiques, soient rendues extrêmement improbables.

Ces objectifs conditionnent le choix des principes, ainsi que le niveau d'autosurveillance et de redondance à prendre en compte pour la réalisation des systèmes.

6.5. Expérimentation en vol sur CONCORDE prototype 001.

Un total de 11 vols a été consacré par les constructeurs tant à l'exploration quasi statique jusqu'à une incidence de 23,5°, qu'à l'expérimentation des dispositifs précédemments décrits. Outre quelques vols préparatoires, on doit ajouter au total précédent quatre vols d'évaluation par les Services Officiels franco-britanniques. Ces vols ont permis de confirmer :
- qu'il n'existe pas d'avertissement naturel (buffeting par exemple) dans l'ensemble du domaine exploré,
- que jusqu'à l'incidence maximale explorée, la manoeuvrabilité reste excellente et tout particulièrement en tangage, ce qui assure des récupérations très faciles, sans même utiliser toute la course en profondeur à piquer,
- que la stabilité dynamique reste très satisfaisante jusqu'à l'incidence maximale explorée, avec les systèmes d'augmentation de stabilité en fonctionnement,
- que la stabilité statique naturelle est franchement négative au centrage arrière, mais que le trim d'incidence restitue une stabilité en efforts positive.

Une légère anomalie aérodynamique se traduisant par une petite discontinuité d'équilibre longitudinal associée à une lente divergence de dérapage, a été observée, mais seulement en associant à une incidence voisine de l'incidence maximale un dérapage d'au moins 8 degrés.

Une incidence maximale de 21 degrés étant suffisante pour démontrer les marges réglementaires par rapport aux vitesses de référence choisies pour l'avion prototype, le déclenchement de l'alarme (pulseur de manche) a donc été calé à cette valeur en fonctionnement statique.
L'ensemble des dispositifs anti hautes incidences procure alors une protection qui a été reconnue efficace par toutes les Autorités de Certification françaises, britanniques et américaines qui l'ont expérimentée : car, d'après le jugement des pilotes, il s'oppose à toute sortie du domaine normal avec une autorité, voire une brutalité proportionnelle à l'aveuglement du pilote qui tenterait de s'en éloigner.

7. CONSEQUENCES DES CARACTERISTIQUES D'UNE VOILURE ELANCEE SUR LES PERFORMANCES.

Les caractéristiques citées au paragraphe 2 ci-dessus, ont essentiellement deux conséquences :

(i) Etant donné que les caractéristiques de traînée induite sont plus sévères, la finesse sera faible et bien plus affectée par les erreurs de vitesse que celle d'un avion à réaction subsonique.
(ii) On doit s'attendre à ce que la combinaison d'une traînée à portance nulle inférieure à la normale, et d'une traînée induite supérieure à la normale, entraîne une instabilité de vitesse, et rende plus difficile le maintien précis de la vitesse.

La figure 8 représente les caractéristiques de gradient en fonction de la vitesse d'un avion à voilure élancée et d'un avion à réaction courant, chacune étant ajustée pour satisfaire aux exigences actuelles des BCAR au second segment pour un quadriréacteur avec un moteur en panne, c'est à dire l'obtention d'un gradient de 3 % à V_2.
Elle montre clairement que toute réduction de vitesse entraîne une détérioration des performances plus importante dans le cas d'une voilure élancée. Une telle détérioration pourrait affecter non seulement le gradient dans le deuxième segment, mais aussi la distance de décollage nécessaire.
Ces considérations nous ont, depuis longtemps, conduit à admettre que des modifications réglementaires seraient nécessaires. Naturellement, les discussions ont porté sur leur forme et leur sévérité.

8. FORME DES NOUVEAUX REGLEMENTS.

8.1. Exigences de gradient

Comme la nécessité de modifier les réglements provient surtout de l'aggravation des caractéristiques de traînée, les nouveaux réglements ne devraient pas être basés arbitrairement sur, par exemple, les caractéristiques connues du CONCORDE actuel, mais ils devraient être applicables de façon générale. Par exemple,

une amélioration de la traînée devrait avoir deux répercussions : premièrement l'amélioration directe, et ensuite l'assouplissement des exigences de gradient. De plus, pour que les nouveaux réglements soient défendables, ils devraient également être équivalents aux exigences actuelles lorsqu'ils sont appliqués aux avions actuels.
Trois façons de prendre en compte ces influences de manière rationnelle ont été considérées :

(i) démontrer un gradient = a + b $\frac{K' D}{W}$
où $\frac{K' D}{W}$ est le rapport entre la traînée induite par la portance et la masse.

(ii) démontrer un gradient réduit dans le cas d'une erreur de vitesse donnée : x % gradient à V_2 - y kt, où V_2 est la vitesse de montée prévue avec pannes de réacteur. Par exemple, une règle simple, que nous avons suggérée et défendue, et que nous considérons toujours comme appropriée dans le cas du deuxième segment, serait la suivante : (voir figure 8)
- démontrer un gradient de 2 % à V_2 - 10 Kts.

(iii) satisfaire à un gradient réduit lors d'un virage à une inclinaison donnée : x % gradient à V_2 lors d'un virage coordonné à Ø° d'inclinaison, à poussée symétrique.

Ces trois méthodes, ayant comme point de départ commun la forme de la polaire, avaient chacune leur défenseurs, mais le choix définitif des Services Officiels s'est porté sur la troisième méthode.
On peut dire ici que, malgré une grande méfiance de la part de nos pilotes et de nous-mêmes, les essais en vol délicats exigés pour réaliser des virages stabilisés avec un moteur en panne et un trim latéral particulier, se sont déroulés de manière assez satisfaisante. Nos premiers calculs nous avaient laissé croire que la traînée d'équilibrage minimale était obtenue à dérapage nul plutôt que dans un virage coordonné (effort latéral nul). Les essais ont confirmé cette hypothèse et ont donné des résultats remarquablement homogènes. Ainsi nos craintes sur la possibilité d'obtenir des résultats de vol exploitables à l'aide de cette méthode, n'étaient pas justifiées, mais il faut dire que ce succès est en grande partie dû à la quantité importante d'essais en vol et d'analyses supplémentaires effectués. On peut donc considérer que les exigences de gradient en virage couvrent les erreurs de vitesse normales. Les erreurs grossières de vitesses, c'est à dire celles qui mènent à un gradient nul sur la figure 8, ont été traitées différemment en prenant une certaine marge entre V_2 et V_{ZRC}, vitesse où la pente est nulle. Cette dernière exigence est entièrement nouvelle et non pas une adaptation d'une exigence figurant déjà dans les BCAR ou FAR.

8.2. Distance de décollage

Les réglements classiques BCAR sont maintenus, mais pour couvrir le cas d'un avion à voilure élancée dont le maintien de la vitesse serait difficile, et (ou) les qualités de vol médiocres, un certain nombre de cas d'erreur ont été ajoutés.
Ces cas prennent en considération des décollages prématurés et tardifs, pour lesquels il est demandé de ne pas excéder la longueur de piste prévue et de démontrer la pente nette de trajectoire exigée.

8.3. Masse maximale d'atterrissage

La forme des réglements est analogue à celle discutée au paragraphe 8.1. ci-dessus. Cependant, en plus des exigences de gradient avec tous moteurs et un moteur en panne dans la configuration atterrissage, il y a maintenant une exigence sur le gradient (de descente) dans le cas d'une approche continuée avec deux moteurs en panne.
Il est juste d'observer que bien qu'une telle exigence ne figure pas dans les BCAR, les caractéristiques des quadriréacteurs actuels certifiés suivant l'exigence de montée avec un seul réacteur en panne, leur permettent de suivre une trajectoire de glide de 3° et de réaliser une approche en sécurité, avec deux réacteurs en panne.

8.4. Distance d'atterrissage

A l'exception de la définition différente des vitesses de référence d'atterrissage (voir paragraphe 5), les réglements TSS sont presque identiques aux BCAR.

8.5. Passage des obstacles

Encore une fois, la sensibilité à une erreur de vitesse doit être prise en compte, et l'on a choisi un abattement de la pente brute à la pente nette basé sur la réduction de gradient de montée pour un angle d'inclinaison donné.

9. SEVERITE DES NOUVEAUX REGLEMENTS

La sévérité des nouveaux réglements est basée de façon générale sur la considération des caractéristiques de l'avion pendant la montée sur le deuxième segment et les conclusions sont ensuite étendues aux autres régimes.
L'expérience acquise sur CONCORDE lors des essais en vol et au simulateur, a démontré que, du fait de la combinaison de bonnes qualités de vol et d'excellentes informations d'assiette, le contrôle de la vitesse est au moins aussi bon que sur les avions à réaction actuels.
En particulier, des décollages satisfaisants et répétitifs peuvent être réalisés, non seulement en visant une vitesse V_2 au dessus de l'obstacle, mais aussi en visant cette vitesse et une assiette donnée. Ainsi, depuis la première action à tirer à V_R et à l'assiette de roulage, le pilote peut contrôler les augmentations d'assiette de manière à ce que V_2 soit obtenue à l'assiette θ 2.
Ce contrôle satisfaisant de la vitesse a permis de baser les réglements sur des caractéristiques de maintien de vitesse similaires à celles des avions actuels.
Après avoir considéré toutes les preuves disponibles, et après de nombreuses discussions, les Services Officiels ont décidé que l'exigence pour le deuxième segment serait : à V_2, 3 % de pente à démontrer en vol rectiligne (c'est à dire idem BCAR), et, en plus, un gradient de 2 % à démontrer en virage à 18° d'inclinaison.
Pour un avion à voilure élancée, l'exigence enveloppe est, comme prévu, celle relative au virage à 18° qui pour CONCORDE est équivalente à un gradient d'environ 4 % en vol rectiligne (Figure 9).
Cette exigence conduit à des gradients meilleurs que ceux des avions actuels pour toutes les erreurs de vitesse ; nous pensons qu'elle est encore conservatrice, et nous estimons pouvoir obtenir une certaine relaxation lorsque nous aurons acquis davantage d'expérience sur CONCORDE.
D'une manière générale, cette philosophie a été étendue aux autres conditions de vol, en réduisant de 1 % le gradient exigé par rapport aux valeurs figurant dans les BCAR, mais en demandant la démonstration en virage

à 18° d'inclinaison ; les règles qui en résultent sont présentées sous forme simplifiée au tableau 1.

10. COMPROMIS DANS L'OPTIMISATION DES PERFORMANCES.

10.1. Généralités

Nous supposerons ici que les aspects principaux d'un nouveau projet sont issus de la définition de la mission, et que l'optimisation des performances au décollage et à l'atterrissage doit être réalisée compte-tenu des contraintes imposées par l'ensemble de la mission.
Dans le cas de CONCORDE, ceci signifie que l'avion doit être capable de décoller à une masse voisine de la masse maximale d'un aérodrome situé à 12 000 pieds au dessus du niveau de la mer, et que l'avion doit pouvoir atterrir sur une distance de 8 400 pieds.
Les raisons du paradoxe apparent que représente une piste d'atterrissage bien plus courte, sont doubles :
- d'une part sur les grands aéroports, la piste d'atterrissage équipée de l'ILS est normalement plus courte que celle qui est réservée principalement aux décollages,
- d'autre part, sur les aéroports moins importants, la piste sera plus courte de toute façon, et tandis que la masse à l'atterrissage ne peut varier que très peu, la masse au décollage sera bien inférieure à la masse maximale pour les missions à faibles rayons d'action.

10.2. Atterrissage

Pour une masse donnée, et une réglementation donnée, la distance d'atterrissage est fonction de :

(i) la vitesse d'approche
(ii) l'arrondi avant impact
(iii) l'efficacité des dispositifs de freinage.

Dans l'ensemble, comme pour la plupart des avions actuels, les deux facteurs prédominants pour les performances d'atterrissage sont la vitesse d'approche, et le coefficient de frottement des pneus.
Les caractéristiques de frottement des pneus peuvent être traitées séparément et ne diffèrent pas de celles des autres avions.
L'obtention de la vitesse d'atterrissage la plus faible possible entraîne des considérations différentes de celles qui ont été prises en compte précédemment :

(i) L'absence de portance maximale conduit à choisir les vitesses de référence en fonction de V_{MIN} comme nous l'avons déjà dit plus haut.
(ii) L'absence d'empennage horizontal et le positionnement des gouvernes de profondeur au bord de fuite de la voilure, ne permettent pas l'utilisation de dispositifs d'hypersustentation tels que volets, non plus qu'une optimisation à grande échelle pour le choix de la géométrie de ces volets.
On peut étudier divers dispositifs pour augmenter la portance équilibrée :
- empennage "canard"
- empennages arrières (associés à des volets)
- onglets articulés.
Mais sur le CONCORDE au moins, aucun de ces dispositifs ne s'est révélé avantageux compte-tenu de sa masse et de sa complexité. L'optimisation pour l'atterrissage et pour d'autres raisons, consiste alors dans le choix détaillé de la forme en plan, de la cambrure et de la surface de la voilure ; elle nous a conduit à augmenter la surface alaire très tôt dans le projet ($7\frac{1}{2}$ %) et à augmenter la surface des bouts d'aile (réduction de la flèche du bord d'attaque du saumon d'aile) lors du passage du prototype à la présérie.
Des considérations de masse et d'encombrement conduisent à définir un train d'atterrissage de longueur minimale. Le cas dimensionnant étant un impact de la partie arrière du fuselage, la masse a été minimisée en choisissant la longueur du train principal de manière à obtenir une garde au sol réduite pour le fuselage arrière et les nacelles, mais en les protégeant par un amortisseur souple muni d'une roue (figure 10).

10.3. Décollage

Les performances en montée des avions à réaction subsoniques actuels ne dépendant que peu de leur vitesse, la vitesse de franchissement de l'obstacle choisie avec panne de moteur, est normalement la vitesse minimale admissible ($1{,}2\ V_S$), afin d'obtenir la longueur de piste la plus courte.
En général, c'est l'inverse qui se produit pour les avions à voilure élancée, cette vitesse étant choisie pour satisfaire aux exigences de performance de montée, tandis que l'exigence de pilotage n'est pas critique. S'il devenait nécessaire de décoller court à poids léger, les exigences de qualités de vol pourraient alors redevenir prédominantes. Cependant, pour CONCORDE, à la fois V_{MIN} et la garde au sol ont été dimensionnés par le cas d'atterrissage, les exigences étant moins sévères au décollage.
Les exigences de gradient de montée ont décidé de la configuration décollage, puisque, à poussée donnée, elles définissent la finesse nécessaire. L'amélioration la plus évidente qu'il est possible d'appliquer sur un avion volant au second régime, est la réduction du coefficient de portance. Dans le cas d'une géométrie fixe, ceci entraîne immédiatement une augmentation de la vitesse au décollage et de la longueur de piste nécessaire, ainsi que des inquiétudes sur la tenue des pneus.
L'augmentation de surface alaire augmentera la masse de la voilure et la traînée de frottement du revêtement, et si la définition initiale était proche de l'optimum pour les performances de la mission, il sera très difficile d'améliorer le rendement aérodynamique de la voilure, de manière à compenser son augmentation de masse.
De même, l'autre option consistant à diminuer la traînée au décollage par augmentation de l'envergure de voilure, rend la voilure moins élancée et entraînera presque certainement une dégradation des performances pour l'ensemble de la mission.
Rappelons que les exigences au décollage ont été en grande partie à l'origine des deux modifications apportées à la définition de la voilure (augmentation d'échelle de $7\frac{1}{2}$ %, suivie d'une augmentation de la surface du bout d'aile) mentionnées au paragraphe précédent.

10.4. Résumé de l'optimisation

Nous pensons que dans l'ensemble, bien que les sensibilités soient assez différentes, notre message est le même que celui qu'apporte tout nouveau projet depuis des années : pour faire décoller un avion et le ramener en sécurité au sol, il doit posséder une envergure et une surface alaire un peu plus importante que celles qui seraient nécessaires pour la mission aérienne seule.

COMPARAISON DES CARACTERISTIQUES DE PORTANCE
LIFT CURVES COMPARISON

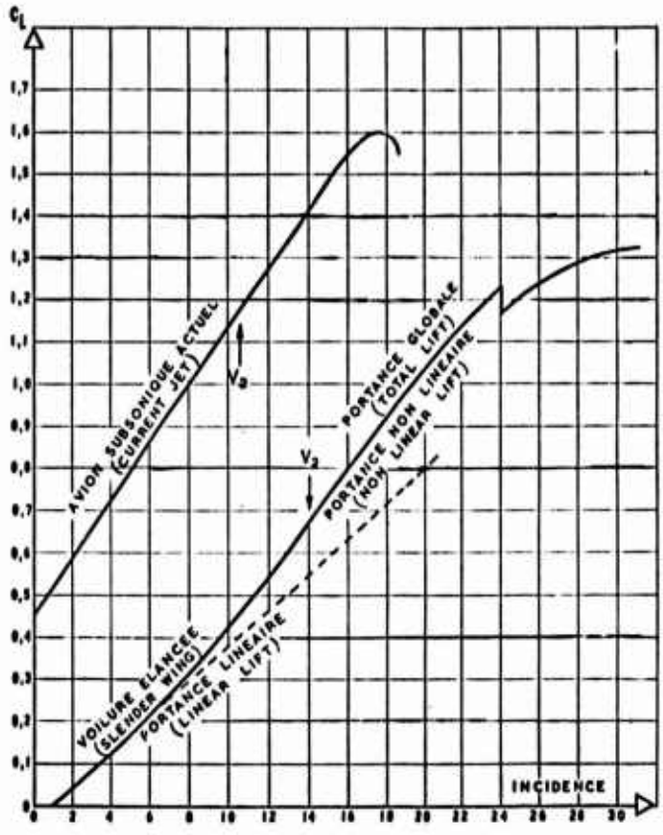

Figure 1

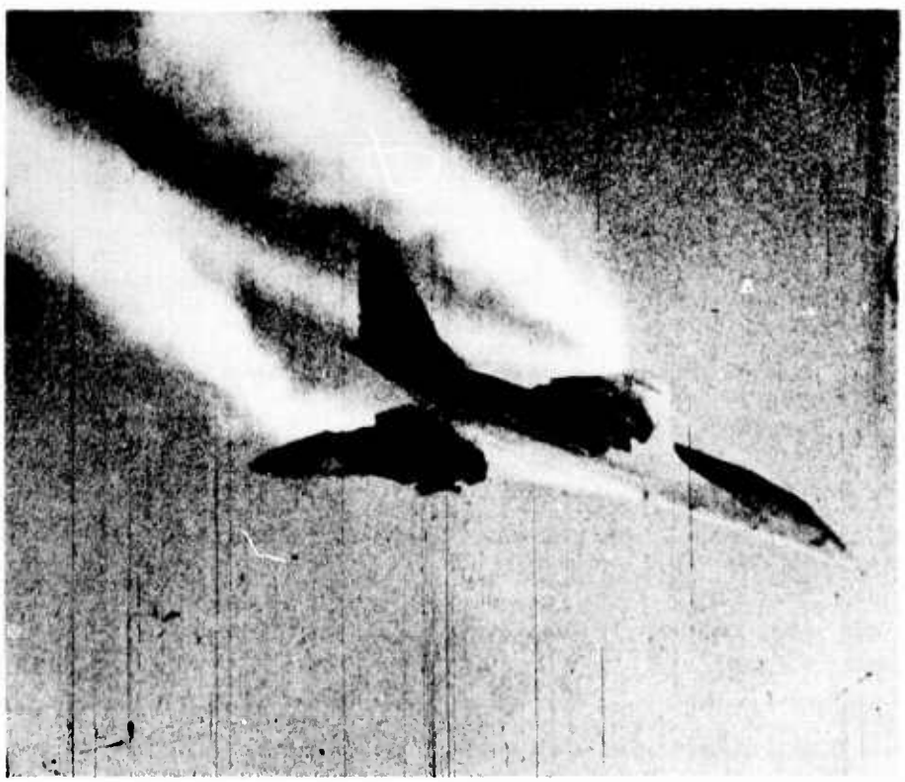

Figure 2

COMPARAISON DES CARACTERISTIQUES DE MOMENT DE TANGAGE
PITCHING MOMENT CURVES COMPARISON

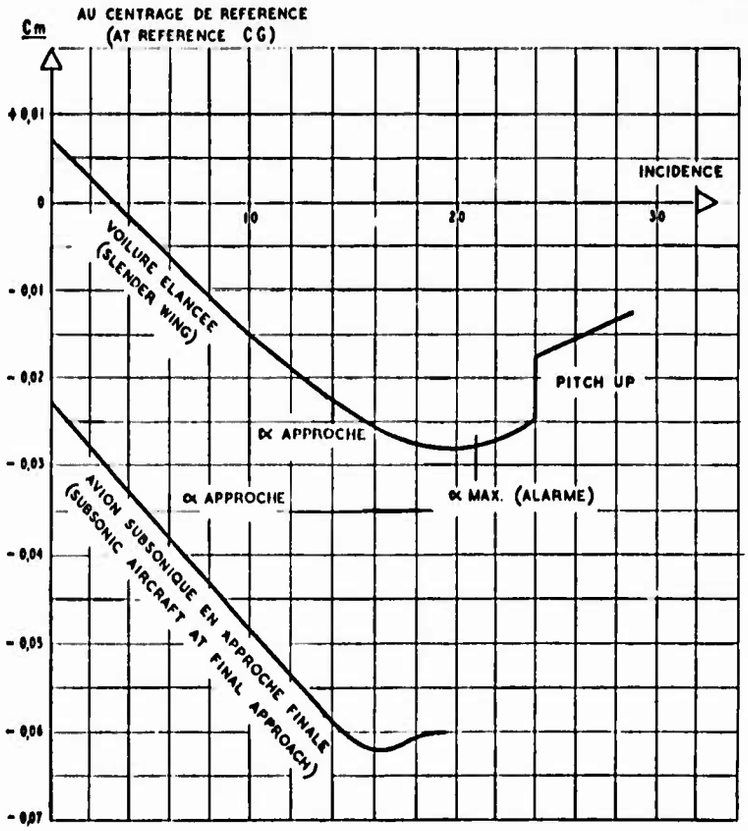

Figure 3

STABILITE DE ROUTE (AXES AVION)
WEATHERCOCK STABILITY (BODY AXES)

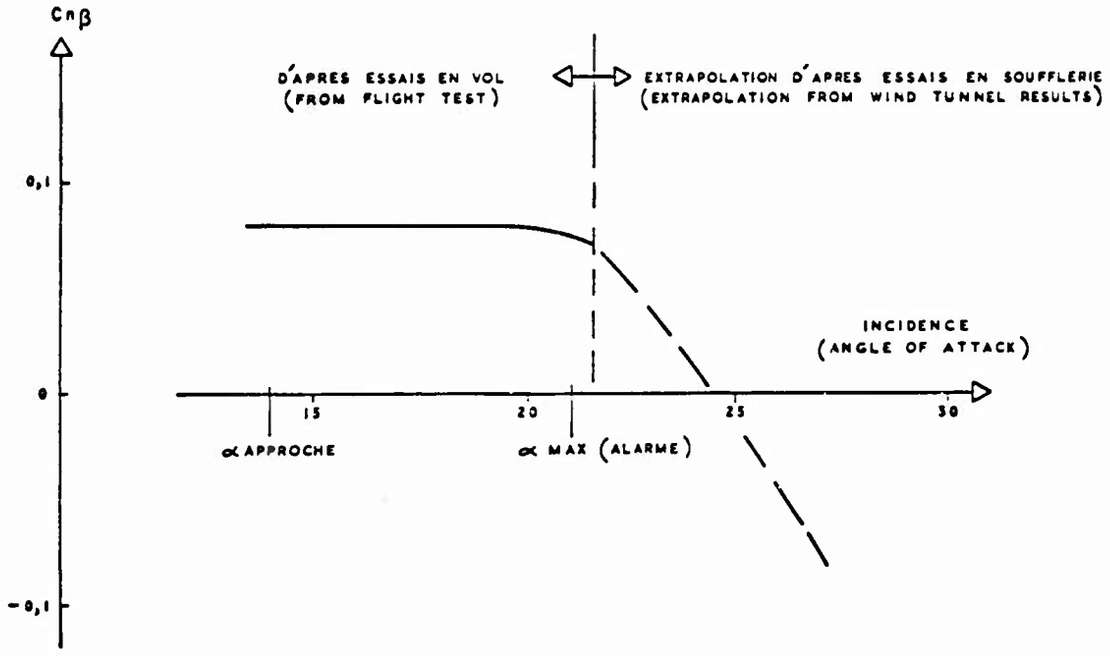

Figure 4

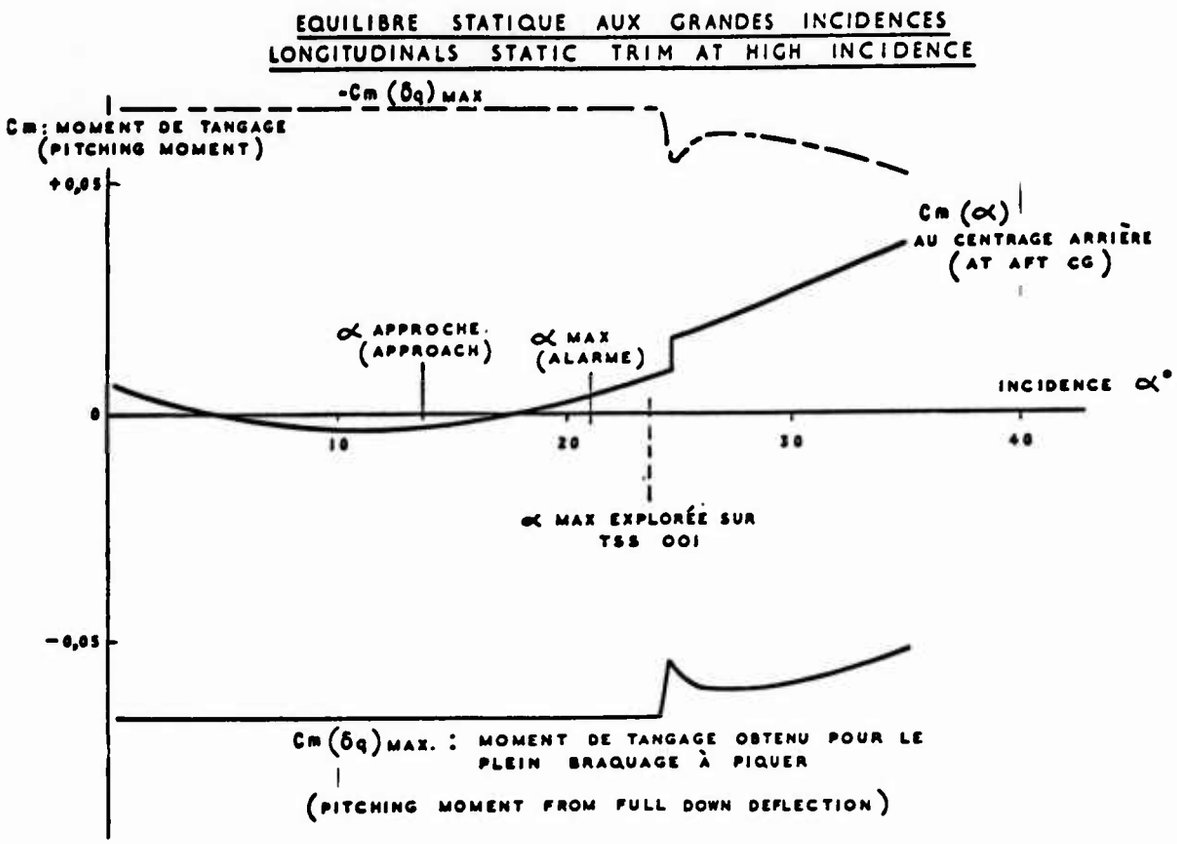

Figure 5

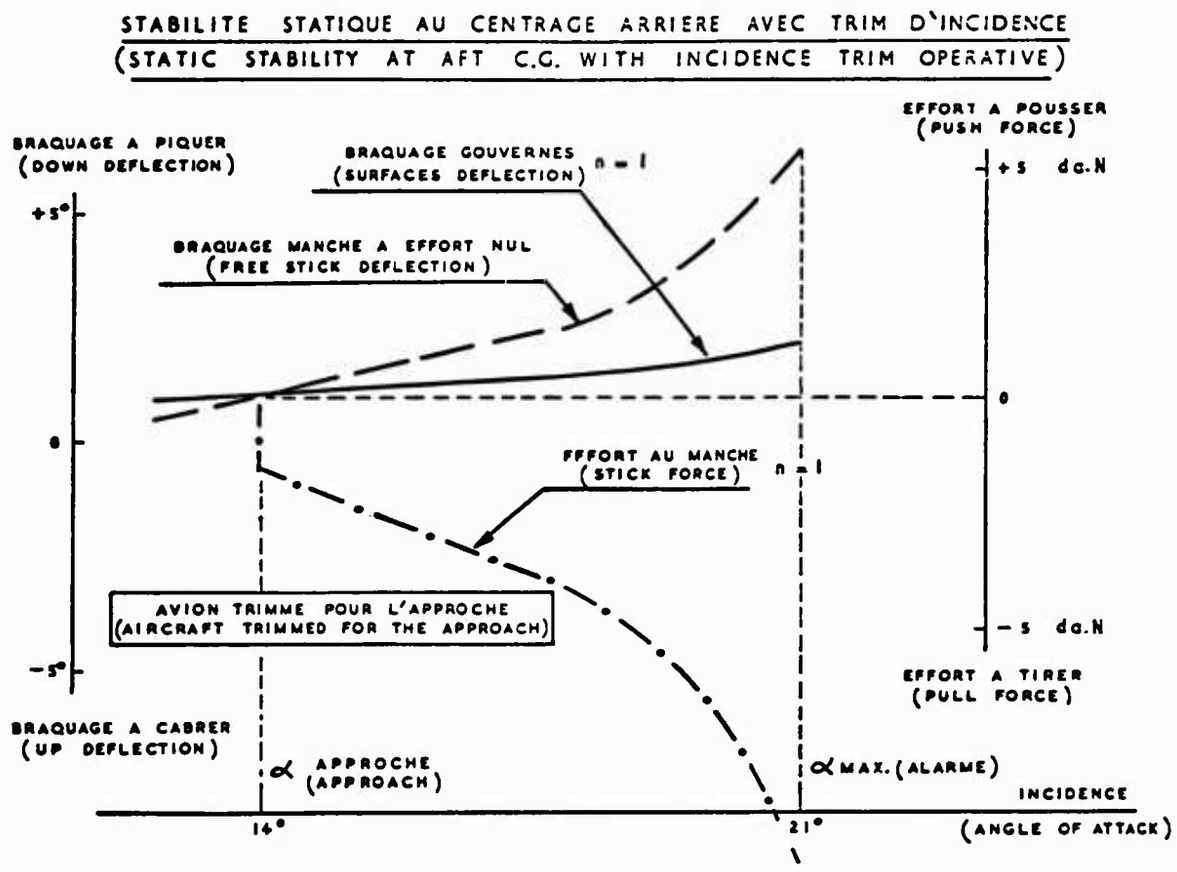

Figure 6

SCHEMA DE PRINCIPE DU SUPERSTABILISATEUR
BLOCK DIAGRAM OF THE SUPERSTABILISER

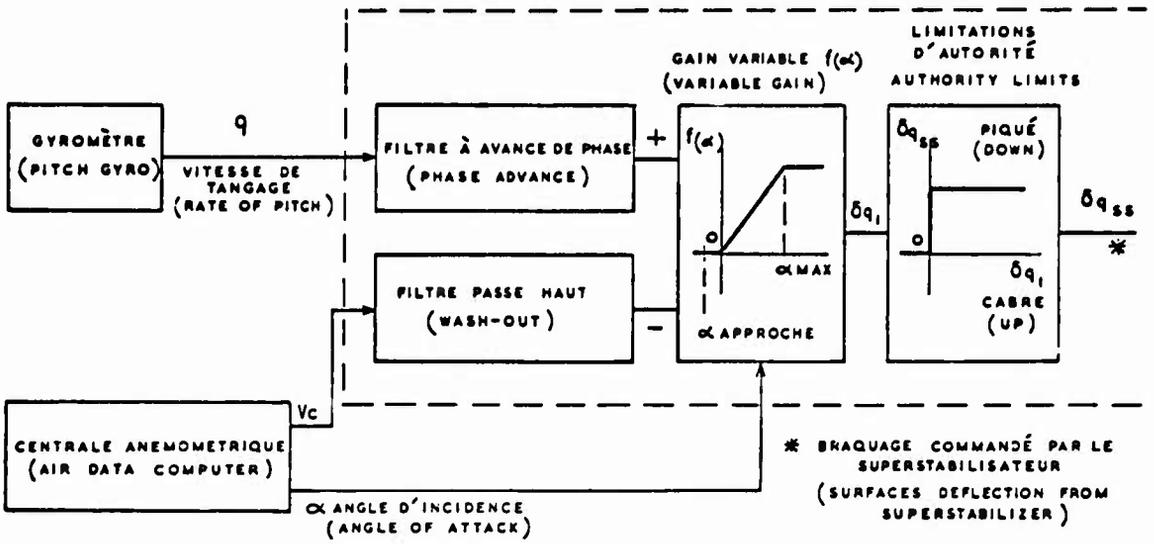

NOTA: IL EXISTE 2 VOIES DE COMMANDES SÉPARÉES POUR LES ÉLEVONS INTERNES D'UNE PART POUR LES ELEVONS EXTERNES ET MEDIANS D'AUTRE PART

NOTE: THERE ARE TWO SEPARATE SIGNALLING CHANNELS THE ONE FOR INNER ELEVONS THE OTHER FOR THE MID AND OUTER ELEVONS

$$\delta q_{ss} = \left\{ \left[\frac{1 + aTs}{1 + Ts} \right] q - \left[\frac{b\,Ts}{1 + Ts} \right] Vc \right\} f(\alpha)$$

Figure 7

COMPARAISON DES PENTES
GRADIENT COMPARISON

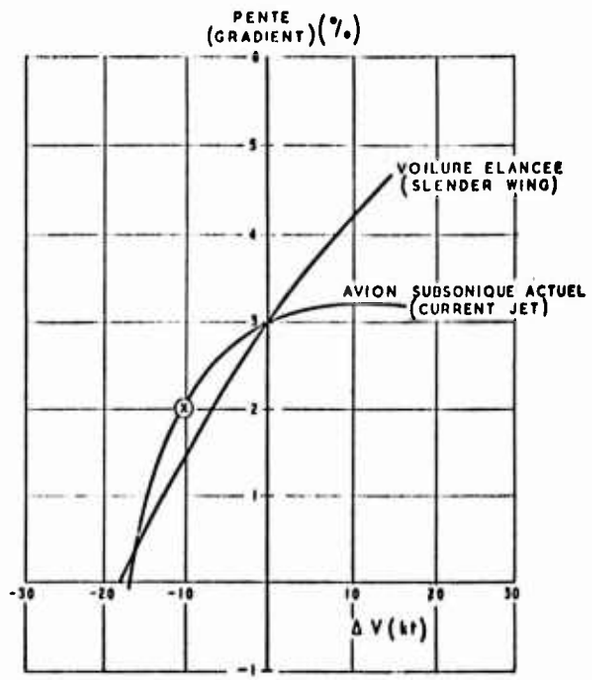

TYPICAL V_2 CURRENT 170 Kts.
TYPICAL V_2 SLENDER 210 Kts.

Figure 8

COMPARAISON DES PENTES
GRADIENT COMPARISON

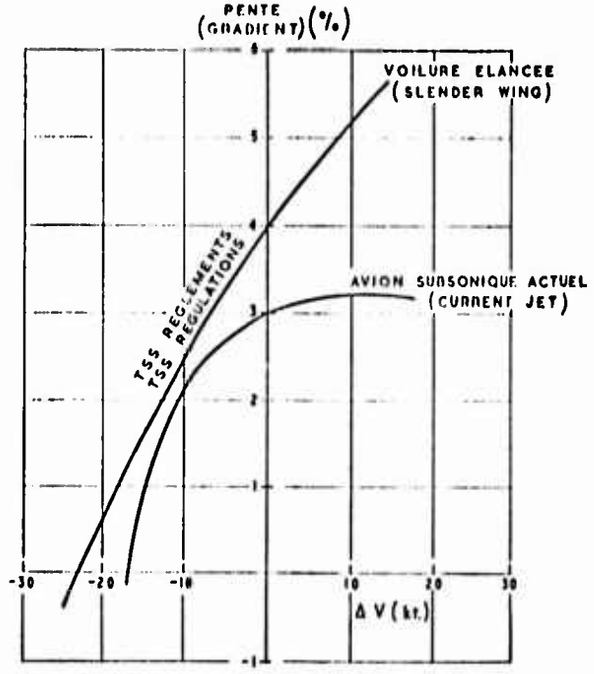

TYPICAL V_2 CURRENT 170 Kts.
TYPICAL V_2 SLENDER 210 Kts.

Figure 9

Figure 10

TSS n° 2 - GRADIENT DE MONTEE AU DECOLLAGE

CAS	CONDITIONS DE VOL	MOTEURS	REGIME	EXIGENCE	GRADIENT APPROX. VOL RECTILIGNE
1	Vitesse de décollage train sorti	3	Décollage avec réchauffe	γ = 1,5 %	1,5 %
2	Vitesse de montée sur tous moteurs train rentré	4	"	$V_3 \geq 1,2\ V_{ZRC}$	8,5
3	Vitesse de montée un moteur coupé, train rentré	3	"	$V_2 \geq 1,125\ V_{ZRC}$	4,0
4	"	3	"	$\gamma \geq$ 2 % Avec 18° d'assiette	4,0
5	Décollage final train rentré	3	Maximum continu	$\gamma \geq$ 0,7 % Avec 18° d'assiette	2,5

TSS n° 2 - LONGUEUR DE DECOLLAGE

CAS	CONDITIONS DE VOL	MOTEURS	FACTEURS
1	Distance jusqu'à 35 ft avec tous moteurs	4	1,15
2	Distance balancée sur piste sèche (longueur accélération arrêt = longueur décollage jusqu'à 35 ft)	3	1,00
3	Distance balancée sur piste mouillée (longueur accélération arrêt égale longueur décollage jusqu'à 15 ft)	3	1,00
4	Rotation avancée de 3 secondes	4	1,00
5	Rotation prématurée à 0,95 V_R	3	1,00
6	Rotation retardée de 3 secondes	4	1,00
7	Taux de rotation de tous moteurs en fonctionnement	3	1,00

TSS n° 2 - GRADIENTS DE MONTEE A L'ATTERRISSAGE

CAS	CONDITIONS DE VOL	MOTEURS	REGIME	EXIGENCE	GRADIENT APPROX. VOL RECTILIGNE.
1	Montée en configuration atterrissage train sorti, vitesse $\geq V_{TTO}$	4	Poussée obtenue au bout de 8 s	$\gamma \geq$ 2,2 % Avec 18° d'assiette	4,2
2	Approche interrompue	3	Décollage	$\gamma \geq$ 1,7 % Avec 18° d'assiette	3,7
3	Approche continue	2	Poussée obtenue au bout de 8 s.	$\gamma \geq$ - 4 % Avec 18° d'assiette	- 2,0

TABLEAU 1

TERMINAL AREA CONSIDERATIONS FOR AN ADVANCED CTOL TRANSPORT AIRCRAFT

by

Mark B. Sussman
Renton, Washington, U.S.A.
The Boeing Commercial Airplane Company
P.O. Box 3707
Seattle, Washington 98124

SUMMARY

Projected future conditions at large urban airports were used to identify design objectives for a long-haul, advanced transport airplane introduced for operation in the mid-1980s. Operating constraints associated with airport congestion and aircraft noise and emissions were of central interest. In addition, some of the interaction of these constraints with aircraft fuel usage were identified. The study allowed for advanced aircraft design features consistent with the future operating period.

A baseline 200 passenger airplane design was modified to comply with design requirements imposed by terminal area constraints. Specific design changes included: modification of engine arrangement; wing planform; drag and spoiler surfaces; secondary power systems; brake and landing gear characteristics; and the aircraft avionics. These changes, based on exploratory design estimates and allowing for technology advance, were judged to enable the airplane to: reduce wake turbulence; handle steeper descent paths with fewer limitations due to engine characteristics; reduce runway occupancy times; improve community noise contours; and reduce the total engine emittants deposited in the terminal area.

The penalties to airplane performance and operating cost associated with improving the terminal area characteristics of the airplane were assessed. Finally, key research problems requiring solution in order to validate the assumed advanced airplane technology were identified.

INTRODUCTION

This paper contains results of exploratory design studies directed to future advanced, CTOL, subsonic transport aircraft.

The objective of the studies was: (1) to identify design opportunities to help solve potential noise, emission, and congestion problems in the terminal area portion of aircraft flight for the 1980-2000 time period; and (2) to determine the required research and technology. This study followed a previous industry/NASA program entitled the "ATT" or Advanced Transport Technology program (ref. 1). That program emphasized various advanced technology airplane features, including use of super-critical airfoil technology to increase subsonic airplane cruise speed. A subsequent criticism was that the advantages of increased cruise speed might, in fact, not be realized on future aircraft because of bottlenecks and problems in the airport terminal area. This led to the current study, with emphasis on improved aircraft characteristics in and around principal airports (referred to in short as terminal-compatibility).

To determine desirable design features, current airplane noise impact, airplane arrival and departure rates, and urban area air quality were forecast to the year 2000 for example airports. Improved airplane capabilities were then postulated and the effects evaluated quantitatively. The burden of terminal compatibility for study purposes was placed on the airplane. Possible ground-based solutions were not studied. Three specific airports, J. F. Kennedy, O'Hare, and Los Angeles International, were considered to lend realism to the projections.

The feasibility of achieving the desirable capabilities was examined by designing airplanes with the needed features. Changes to weight, performance, and economics were assessed. As a final step, the airplane technology development which had been found to be critical to the desired improvement was identified, and the research and development programs necessary to achieve them were defined.

Near the end of these studies, considerable interest developed in the characteristics of aircraft fuel usage. Although a detailed evaluation could not be undertaken, it was clear that many of the design considerations relating to terminal compatibility affected fuel conservation. This paper treats, in a preliminary way, certain of these.

DESIGN REQUIREMENTS

Projected future airport conditions served to identify design requirements and objectives for the advanced transport. Figure 1 is typical of the results of these projections. Considerably more detail can be found in reference 2.

The left side of Figure 1 shows average busy-hour delay plotted against year. These data were developed on the basis of an analytical model which simulates runway operations representative of existing and projected airport traffic. The predicted runway rates depend upon a number of operational parameters such as the separation requirements assumed between two aircraft on approach. The model is also sensitive to such other airplane design parameters as: braking capability of the airplane; speed at which runway turnoff is made; the accuracy in time with which the airplane can be assumed to position itself at a given point in space; approach speed of the airplane; and others.

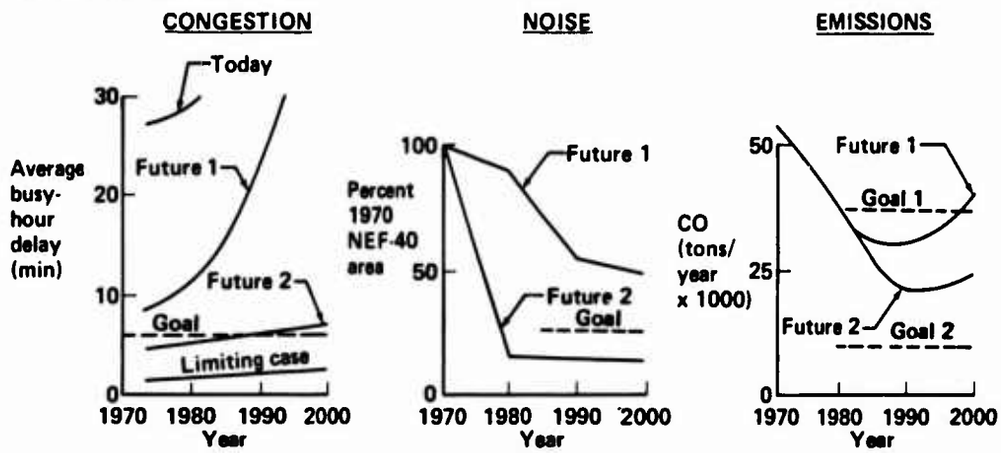

Figure 1. Airport Projections

Numerous cases were studied considering a matrix of parameters. The figure illustrates the results for four specific sets of assumed parameters. The sets range from a baseline "do-nothing" technology level representing today's conditions to a "limiting-case" situation which represents nearly ideal conditions for every design parameter. The results indicated that in today's operations under IFR conditions, the average busy-hour delay (for the airport considered) would be on the order of 28 minutes. The curve also shows that under the impact of additional traffic, such delay would grow exponentially. If technology improvements are made to the airplane and to the air traffic control system, such that reduced aircraft separation distances can be safely achieved, and, in conjunction with this, increased deceleration rates and increased turnoff velocities can be achieved on the ground, then a major jump can be made in terms of reducing average busy-hour delay (see curve labeled "Future 1"). Similarly, even more advanced projections of aircraft separation and runway operations parameters could eventually reduce delay levels down below the 6-minute delay goal set for the purpose of the study.

Similar projections were developed for noise and emissions. Based upon these projections, aircraft characteristics desirable for future terminal area operations were then established.

Figures 2, 3, and 4 summarize the desirable airplane characteristics in terms of three terminal area components: approach-landing operations, ground operations, and takeoff operations. Figure 2 gives an indication of pertinent approach parameters (shown in parentheses) as they currently exist at a typical large urban airport. For example, on approach we see separation requirements between aircraft on the order of 3 to 5 miles, the latter being required behind large jumbo jets. Typical approach paths are 3°. The approach speeds average about 135 knots. Typical source noise levels for the aircraft are on the order of FAR Part 36 although there is considerable variation, with some of the early turbojet aircraft exceeding these noise levels by 10 to 15 EPNdB. Similarly, "airframe" noise levels (that is, the noise level of the airplane with the engine propulsive noise removed) approaches 8 to 12 EPNdB below FAR Part 36.

In contrast to these values, improved values (boxed) are shown which, based on the results summarized in figure 1, would enable the terminal compatibility goals to be essentially achieved. Thus, for instance, to improve congestion, calculations showed that maintaining 1 to 2 miles separation during final approach together with approach speed reductions to about 120 knots and the other indicated changes would achieve the required operations rates. Other desirable characteristics included reduction of airplane source noise levels, increased approach glidepath slopes, and improved knowledge of where the airplane is enabling relaxation of the requirement for 5000-foot spacing for independent parallel runway operations while maintaining safety.

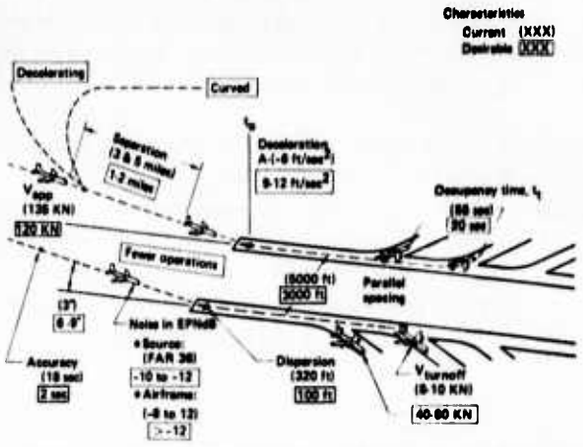

Figure 2. Airplane Characteristics–Approach/Landing Operations

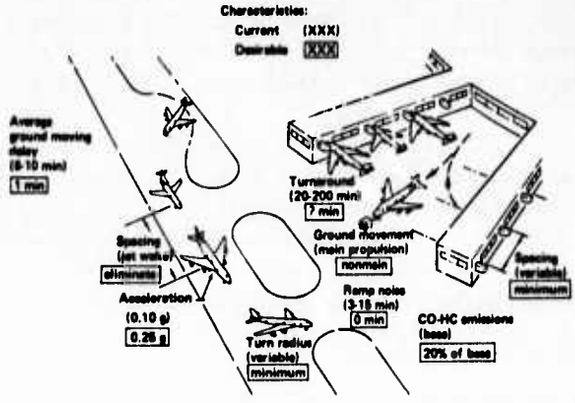

Figure 3. Airplane Characteristics–Ground Operations

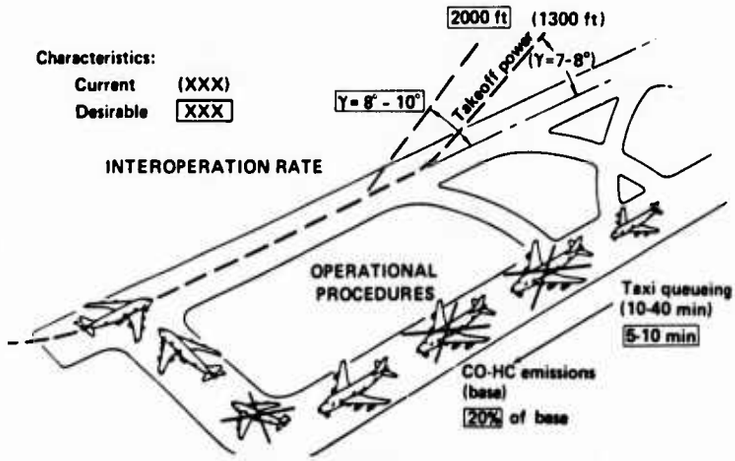

Figure 4. Airplane Characteristics–Takeoff Operations

Similarly, in reviewing airplane ground operations a number of desirable characteristics were projected (fig. 3). Among these was a need for taxi operation of the airplane without utilizing the main engines. This was deemed desirable from the point of view of airplane ground emissions. Direct landing-gear-wheel-drive substitutes for the inefficient propulsive thrust developed at low power by the main engines. Additional benefits might be improved ground operations through elimination of main engine jet blast. In and around the gates, self-powered taxi capability by the airplane might help turnaround times by removing the dependence of the airplane on ground tugs for backing out of the gates.

An additional design feature identified as desirable by various airport personnel was some "invention" enabling reduced gate time and space. Many major airports today are restricted in their capacity to provide gates to the number of operating aircraft.

A similar assessment of takeoff and climb operations is shown in Figure 4. In terms of takeoff operations, it was deemed desirable that the airplane be able to achieve steeper climbout angles than current aircraft achieve, as a means of reducing airport noise impact. Current average aircraft climbout gradients are on the order of 7° to 8°. Based on the noise studies, higher climbout gradients, perhaps on the order of 8° to 10° were sought. In addition, it should be noted that some of the aircraft design features discussed in conjunction with approach operations also contribute to improved takeoff operations. This occurs since high runway demand is currently accommodated by a combination of holding patterns for approach and queueing lines for takeoff. Decreased ground emissions can be associated with improvements to the latter.

SPECIFIC DESIGN CONSIDERATIONS

Having established appropriate design criteria, the terminal-compatible airplane was then configured by modification of a previously configured baseline design. This was achieved in the following way:

- Alternate design concepts capable of satisfying the design objectives were evaluated.
- A preliminary airplane drawing was then developed and analyzed for configuration acceptability in terms of weight and balance, structural soundness, controllability, aerodynamic drag, and propulsion characteristics.
- The airplane was then re-sized to provide the required range and payload.

Since the principal output of the overall study was an identification of critical research and technology areas, the airplane designs served primarily as a tool whereby the appropriate research and technology might be identified. The designs accordingly do not necessarily represent optimum designs. Again the reader is referred to reference 2 for further detail.

Figure 5 gives an overview of the major design changes several of which subsequently will be individually described in more detail. A major change from the three-engine baseline to a four-engine terminal-compatible (TAC) airplane provided flexibility for positioning the outboard engines near the wing tip as a potential method of tip vortex control. Tip vortex control was also the motivation for the mechanical device shown at the trailing edge of the outboard wing position. Increased aspect ratio for the wing accompanied by an area increase of some 300 square feet improved the low-speed aerodynamics enabling reduced airplane noise impact on the community. Another change was the incorporation of large drag brakes which deploy from the aft fuselage. This change was motivated by the requirement for achieving steep descents for the purpose of noise abatement on approach.

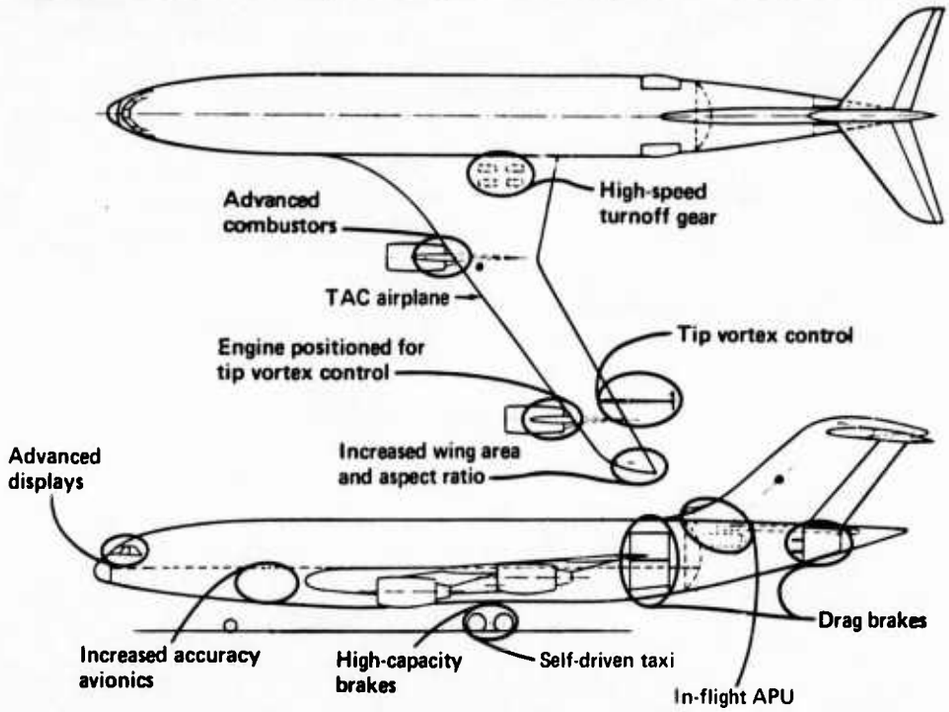

Figure 5. Design Changes for Terminal Compatibility

Changes assumed made to the engines included an advanced combustor to improve engine emissions. A smaller change involved a slight modification of the engine cycle toward reduced overall pressure ratio, again for the purpose of emission reduction.

Incorporation of a "powered-wheel" device for low-speed taxi required increasing the size (relative to the baseline airplane) of the auxiliary power unit to drive the wheel. The APU size was further increased to provide an in-flight capability for driving all the auxiliary power systems of the TAC airplane. For reasons which will be discussed, this latter design modification was made to reduce the steep descent drag requirement and to effect additional noise reduction through the ability to realize lower throttle settings for the airplane on approach.

Further design changes made to the airplane included increasing the braking material in each of the landing gear wheels in order to provide the capability for high-speed deceleration without compromising brake life. The landing gear, including both the main gear and the nose gear, were reviewed for structural soundness to accomplish the high-speed turnoffs which were deemed desirable for improved congestion reasons.

A number of modifications were made to the airplane avionic system in several areas as shown in the figure. Improved displays were incorporated to enable the pilot to perform desirable operational procedures such as steep descents, passenger-tolerated high-deceleration rates, and high-speed turnoffs. These advanced displays were deemed necessary in order that pilot workload be kept to levels consistent with current airplane operations. Beyond that, the navigation and guidance system of the airplane was also upgraded to provide (in conjunction with ground-based ATC equipment) an increased positional accuracy.

Wing Trailing Vortex (Wake Turbulence) Modifications

The basic motivation to establish a design change to control aircraft wake turbulence is shown in Figure 6. This figure shows runway acceptance rate plotted against aircraft in-air separation distance while parametrically varying outer marker delivery accuracy. Typically, in today's operations this knowledge is established to an accuracy of within 18 seconds; in-air separation rules require between 3- and 5-mile distances depending upon airplane size. The curve illustrates the potential doubling of runway operations if in-air separation levels can be reduced and simultaneously the time-wise knowledge of where the airplane is can be increased.

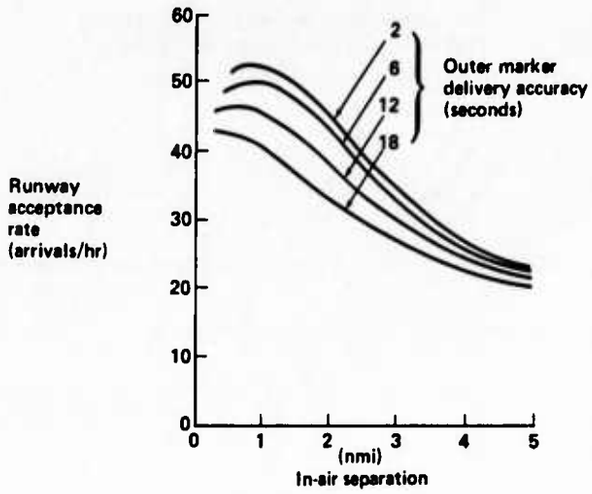

Figure 6. Tip Vortex Design Motivation

It is important to note that the technology for evaluating and controlling wake turbulence is still limited in terms of defining specific design approaches. In arriving at the selected approach, discussions were held with representatives of the NASA to establish the technical work which has been recently initiated in various branches of that agency. This analysis and testing had encompassed a number of design approaches for wake-turbulence control. These included: injecting large masses of air directly into the wing vortex; utilizing some kind of blockage device trailed behind the wing which would protrude directly into the tip vortex; redesigning the lift distribution on the wing in a spanwise direction to distribute rather than concentrate the tip vortex; and other approaches such as various end plates, vortex generators, or other devices installed directly in the wing tip area in the hope of modifying and breaking up the tip vortex.

As a result of this work and also on the basis of other studies, a number of design criteria were established. These criteria recognized the need for tip vortex control for both takeoff and approach operations. They required that improvements to congestion avoid adverse impact to the noise and emissions problem (the other elements of terminal-area compatibility). More specific criteria were established in some cases as a result of the NASA studies where, for example, it was shown that the approach utilizing mass injection required relatively large rates of air. Also, relating to the various proposed drag devices, operational requirements imposed the constraint that if such devices are deployed during approach they must be capable of rapid retraction in the event of an airplane go-around.

Of the various design approaches studied by the NASA, several were rejected for the purpose of this study on the basis of the limited data available. These included many of the proposed wing-tip modifications. Based on the early data, these tended to modify the tip vortex in the near-field region of the wing trailing edge, but this effect was generally shown to be local in nature and, in fact, the tip vortex often re-formed downstream shortly thereafter. The idea of aerodynamically designing the wing to provide more optimally distributed spanwise loading is an attractive one; however, no data were yet available to provide an indication of the effectiveness of such an approach or the possible penalties. Similar comments hold for proposals to introduce variations in flap and aileron deployment in the hope of promoting tip-vortex instability.

Of the various NASA studies, qualitative model data in the form of flow visualization studies indicated that large amounts of air injected directly into the wing vortex did provide some measure of vortex dissipation. Similarly, the flow visualization studies indicated promise for some kind of blockage device which would be deployed from the trailing edge of the wing and positioned in the path of the tip vortex. It was on the basis of these studies that the design approach utilized for the TAC airplane was selected.

In fact, to achieve a solution for both takeoff and approach, two vortex dissipation methods were adopted. The reasoning was this. The requirements for massive amounts of air injection into the tip vortex could be accommodated by locating the primary propulsion engine out near the wing tip. This solution was satisfactory for takeoff where high levels of thrust are normally desirable and achieved anyway. However, high levels of thrust are not compatible with the various approach requirements including noise levels. Similarly, the utilization of a blockage or drag device deployed from the trailing edge of the wing appeared suitable for approach operations and, in fact, for steep descents the airplane was in need of additional drag anyway. However, such a device would not be suitable for takeoff operations where additional drag would require oversizing of the engine and considerable penalties would be incurred.

Thus, the design approach adopted for this study (see fig. 7) was to select a four-engine-on-the-wing arrangement and to reposition an outboard engine near the wing tip, although the specific location could not be evaluated because of lack of data. Operation at full throttle of this engine was assumed to control tip vortices during takeoff. During approach with the engines throttled back and presumably ineffective to control the tip vortex, deployment of the mechanical vortex dissipator device would be used.

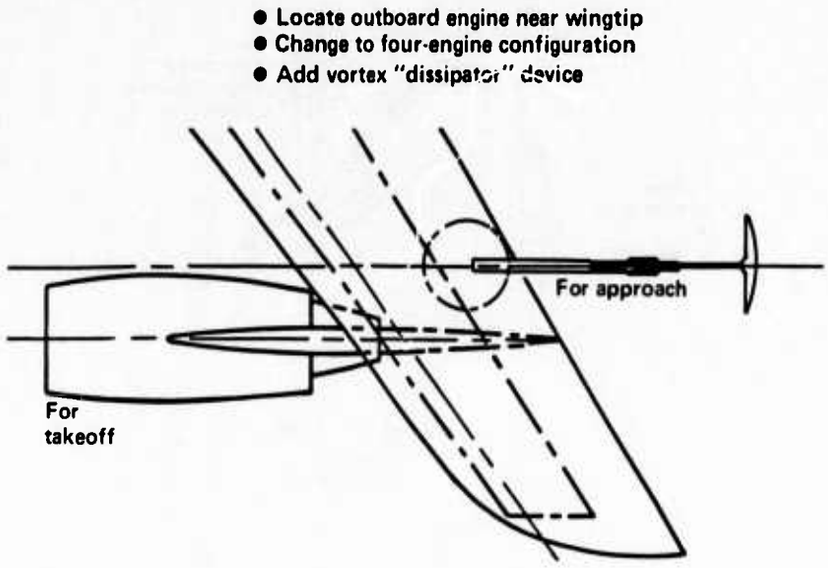

Figure 7. Tip Vortex Design Considerations

The design approach incurred several penalties which included weight increases associated with moving the outboard engine from a normal spanwise location of 70% span to a tip-vortex control location which was estimated to be on the order of 85% to 100% span. Additional penalties are incurred as a result of increased vertical tail size to control engine-out conditions. The mechanical dissipator device and its actuation and assembly also add weight. Some additional drag was charged to the installation including the drag associated with enlarged vertical tail and fairings for the vortex dissipator. Potential aerodynamic drag penalties associated with integrating the outboard nacelle with the high-aspect ratio wing also exist. These latter penalties, however, could not be assessed without wind-tunnel data and were not incorporated into the analyses of the TAC airplane. Some penalty is paid in terms of increased noise on a 3° approach because of the increased engine throttle setting required to compensate for the vortex-dissipator drag when the device is deployed.

It is emphasized that because of the lack of detailed design data, there are a number of unknowns involved in the design approach adopted. These include: the effectiveness of the vortex control measures; selection of engine position; and vortex dissipator position and sizing. Questions exist concerning the potential flutter problems if the spanwise location of the outboard engine is required to exceed a certain distance. Results of a limited study conducted within the current investigation indicated that large flutter penalties could be avoided provided the outboard engine was located inboard of a 90% spanwise location. For the TAC airplane, an 85% spanwise location was selected. It is not known, of course, whether this is consistent with the required vortex control.

Steep Descent Capability

The basic motivation for providing the TAC airplane with steep descent capability concerned reduced approach noise. Studies showed continual (although at reduced rate) improvement in reducing the 90 EPNdB approach noise contour-centerline-closure as the upper segment glideslope is increased to 9°.

Calculations showed that the baseline airplane would accelerate on a 9° approach path if additional drag is not available. This requirement to develop additional drag placed an increased emphasis on reducing the airplane approach thrust to the absolute minimum level. Two constraints were identified which can limit the minimum practicable thrust setting:

1) Maintaining sufficient thrust so that, in the event of an airplane go-around, the time required to recover full thrust is compatible with airplane safety;

2) Maintaining sufficient engine thrust so that all auxiliary systems taking power from the main engines (e.g., bleed air for aircraft anti-icing) can be properly operated.

Figure 8a indicates some of the considerations relating to minimum engine thrust levels. The figure shows estimates of engine acceleration times for throttle excursions from initially low thrust levels. Curves are shown for a contemporary engine and for an advanced engine studied in reference 3. That investigation showed that engine design changes could be introduced which would improve the time required to achieve 95% of full thrust from some lower thrust typical of a 6° steep descent power setting. This required modifications to the fuel control logic and the schedule for the variable compressor stator vanes. These changes were judged to halve the acceleration time and furthermore were assessed to introduce no weight, cost, or noise degradation. If required, further engine response improvement could be obtained by introducing variable turbine area. This change, together with the others, would

enable a 1-second engine response time as shown in the figure. However, the variable turbine geometry does incur considerable weight and complexity penalties and would be used only if the slightly improved response time were deemed critical. As a result of the reference 3 study, it was assumed that no constraint on minimum thrust setting would exist due to engine acceleration requirements.

Figure 8b reflects the results of recent Boeing studies related to the capability of existing airplanes to execute a 6°/3° two-segment steep descent. As the figure suggests, a relatively high minimum throttle setting was identified as necessary to supply adequate engine bleed air for airplane anti-icing. One approach to removing this restriction and any potential others of like kind was to relieve the main engines from the burden of supplying power for all auxiliary systems. This was achieved, by the somewhat arbitrary decision to provide an in-flight auxiliary power unit (APU) capability. As discussed subsequently, this required upgrading the baseline APU unit to two, independent, larger units.

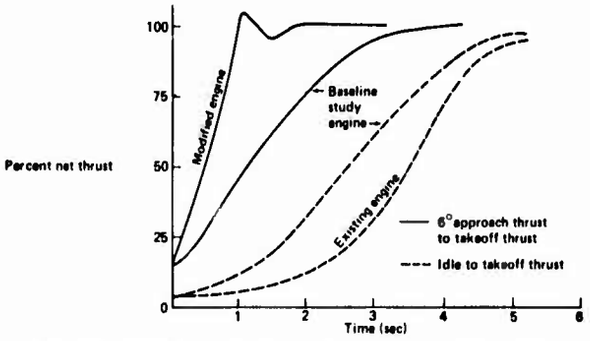

Figure 8a. Engine Acceleration Characteristics (From Ref 3)

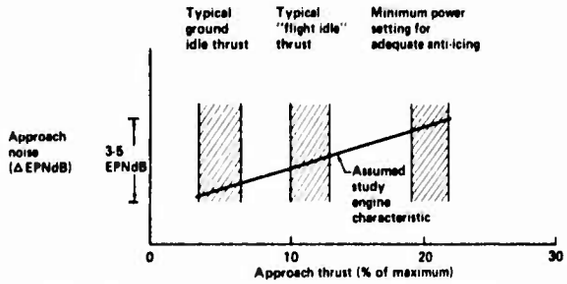

Figure 8b. Low Power Setting Engine Characteristics

Several design options were available to effect the drag increase required for the steep approach including increasing the drag-brake area available on the wing surface, utilizing in-flight thrust reversing, or finding other airplane areas from which drag surfaces might be deployed. In assessing the various options available, wing speedbrakes were ruled out because of their anticipated tendency to aggravate wing buffet. In-flight thrust reversers, although perhaps a promising approach, were not adopted because of the potential increase in noise. This could not be assessed accurately. However, at some airports, the tendency already exists towards reducing the use of thrust reversers even during ground roll because of the community noise impact.

The design criteria established to guide the steep descent airplane design modifications included the following. The design goal was to provide the airplane with the capability to handle a 9°/3° two-segment landing approach. A transition from the upper glideslope to a current 3° glideslope was fixed at 500-foot altitude consistent with pilot comments made during recent flight tests of existing aircraft during noise-abatement approaches. The use of a two-segment approach reduces the community area noise without fears of adversely affecting aircraft safety by increasing the descent rate close to the ground which would be a consequence of a straight-in steep glideslope approach. For simplification, all calculations were made assuming a constant speed, fixed configuration (landing flaps, gear down). Additional design criteria were established which required sufficient speed and flightpath control capability to handle unanticipated glideslope errors and shearing tailwinds.

The design approach adopted to obtain the necessary drag consisted of utilizing deployable aerodynamic drag brakes configured at the aft end of the airplane fuselage. Figure 9 gives an indication of the thrust required on a 9°/3° two-segment approach. Aerodynamic drag (shaded region) is required on the 9° upper glideslope to maintain nonaccelerating flight as the "thrust required" falls below the engine minimum thrust limit. Additional drag is required as margin for speed and path control and in order to land in a shearing tailwind. In sum, as the shaded area of the figure shows, additional drag, approximately equal to the low-speed drag of the airplane in level flight, must be added to implement the 9° glideslope.

1. Fuselage drag brakes

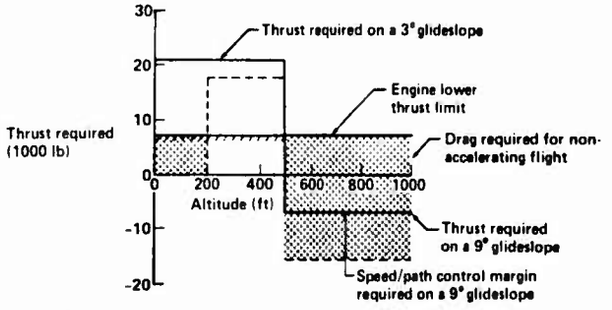

2. Remove minimum thrust constraint due to anti-icing: offload secondary power, requirements from main engine to in-flight APU

3. Avionics capability

Figure 9. Steep Descent Design Considerations

Again, considerable design risk and uncertainty exist with respect to the proposed airplane modifications. These include a lack of knowledge concerning aerodynamic flow interference of the deployed drag panels with respect to the empennage surfaces. Similarly, the fail-safe operation of such drag panels has not been considered but is, of course, an important consideration. Study is required to determine the complexity of integrating the drag device with the airplane flight control system. Although preliminary conceptual designs were established for the drag-device mechanization, questions exist concerning potential interference of this mechanization with the pressurized fuselage structure. Finally, concern exists over the impact on airplane airframe noise, i.e., nonpropulsive noise, which is expected to increase as a result of the deployed aerodynamic drag panels. Insufficient data exist to make an estimate of the potential airframe noise penalty which might be realized relative to the overall noise improvement achieved through the steep approach path.

Low-Speed Aerodynamic Improvements

Two separate reasons to modify the low-speed aerodynamics of the basic ATT airplane were identified. First, studies showed that contingent on the wake turbulence improvement, runway acceptance rate can be improved by about 30% provided approach speeds could be reduced from the 135 knot baseline approach speed. This enables reduced ground rollout times following touchdown and reduces runway occupancy time. The second reason for improving low-speed aerodynamics was takeoff noise. Previous calculations had established that the baseline airplane relative to the study goal of 15 EPNdB below FAR Part 36 was: fairly close for sideline noise; several EPNdB above for approach noise; but on the order of 6 to 8 EPNdB above the goal for takeoff noise.

It was concluded to be reasonable to reduce takeoff noise by providing the airplane with improved climbout gradients. This capability could then be used to provide either increased height above the community as a noise buffer or to reduce the thrust necessary to maintain the required climb gradient under thrust cutback operation. Several design options existed to achieve the objectives of reduced approach speed and the improved takeoff-climb gradients. These included: additional engine thrust, increased flap area, increased wing area, and improved low-speed lift-to-drag.

Several design criteria were established to guide the low-speed aerodynamic design changes. One ground rule was to retain Mach 0.9 cruise capability for the advanced technology airplane. In addition, it was estimated that an increase in height of about 500 feet over the community at the noise takeoff measuring station would accomplish the required noise reduction. A 120-knot approach speed was specified based upon runway rate considerations.

In reviewing various design options, increased engine thrust and increased flap capability were ruled out since neither were able to achieve both the approach speed and takeoff noise goal by themselves. Increased wing area had been studied previously during the ATT study and was shown to be uneconomical if utilized alone. Changes to wing sweep and thickness, although potentially useful, were not adopted in order that cruise Mach number would not be compromised.

Thus, the design approach selected for the TAC airplane was to employ a higher-aspect ratio wing. As shown in Figure 10, increased aspect ratio had the advantage not only of improving the climbout gradient, because of its improvement to low-speed aerodynamic performance, but also reduced approach speeds. The data shown, developed in a brief design study, indicated that an aspect ratio on the order of 9.0 would accomplish the design goals.

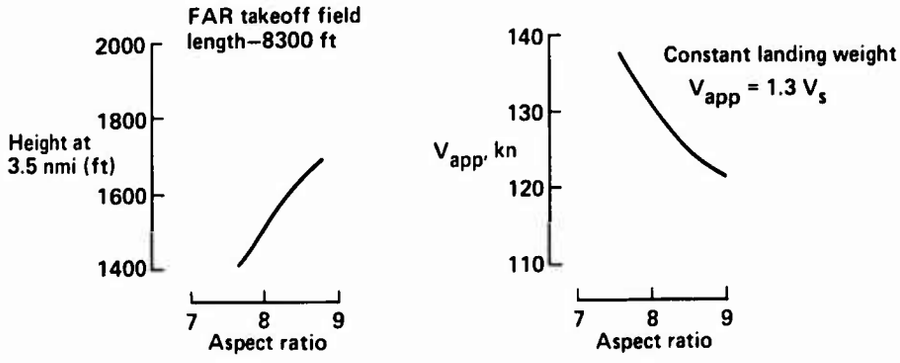

Figure 10. Low-Speed Aerodynamic Design Considerations

There are several design-risk areas associated with the modifications proposed. These include potential low-speed pitch-up tendencies due to the aspect ratio 9, 36.5° sweep wing. Some evidence exists that separation on the outboard portion of the wing may be difficult to control. Secondly, the question of successful aerodynamic integration of the high-bypass ratio engine at an outboard spanwise location on a high-aspect ratio (i.e., small chord) wing may be difficult to achieve without undue penalties. The aspect ratio 9 wing in combination with high-bypass ratio engines is not a configuration for which considerable previous design experience exists.

Powered Wheel/Secondary Power System Modifications

One way to decrease the quantity of undesirable airplane-engine emissions in the terminal area is to decrease the fraction of the time during which the engines are running. This was made possible in the TAC airplane by putting motors on the airplane's wheels, powered from the auxiliary power unit (APU), so that the main engines could be shut off during taxi operation. This has a large effect on the emission of carbon monoxide and unburned hydrocarbons, since they are mainly produced by the low-thrust, low-efficiency engine settings characterized by taxi operations. Secondary advantages of powered wheels include lower total fuel consumption and elimination of the need for tugs to back airplanes away from gates.

Since the APU power must be increased to power the wheels in addition to supplying the normal airplane loads, it was decided for reasons independent of emission reduction to integrate the larger APU into the airborne secondary power system (in the baseline airplane, the APU was only used on the ground). This caused a substantially larger APU size requirement but removed the burden of supplying anti-icing power from the main engines, allowing lower power settings during descent, giving less noise and less auxiliary drag requirements as noted previously. Figure 11 illustrates the APU sizing data. It is emphasized that the in-flight APU use is not an essential part of the powered-wheel concept; alternative anti-icing means may be preferable for some airplane configurations.

Redundant power requirements were met by using two APUs to supply all anti-icing power, all on-the-ground power, and the bulk of the in-flight power, with electrical generators and hydraulic pumps on the two inboard engines supplying additional channels of safety-of-flight essential loads. Electrical and hydraulic power lines from the outboard engines (placed near the wing tips in the TAC airplane for tip-vortex control) were eliminated, and outboard engine pneumatic ducting reduced to the size needed for starting air to the outboard engines. The APUs required sea-level ratings of 1800 horsepower each; this capacity was set by the anti-icing requirement as seen in the figure.

The powered wheels were required to move the airplane at 15 knots forward and 5 knots backward. Typical resistance forces at these speeds are 2% of gross weight, giving a power requirement of 66 horsepower for each of four driven wheels (at least four of the eight main gear wheels must be driven, for reasons of mechanical symmetry). Hydraulic motors were chosen to drive the wheels because of their lower weight and volume relative to electric and pneumatic motors.

The highest torque requirement occurs at zero speed, rather than maximum speed. This is due to the deformation of the tires of a parked airplane persisting for several revolutions under cold conditions, requiring a large breakaway force. Allowance of 6% of gross weight for this effect plus 2% for ramp slope covers essentially all situations. If the wheel motors were sized for this torque at low speed, then run at the maximum speed required without a change in gearing, excessive power would be required. A mechanical gear shifting mechanism was provided for load matching; alternatives include multiple motors switched in and out, and variable supply pressure.

The wheel drive mechanism must be disconnected during landing and takeoff and engaged smoothly during taxi (prior to shutting off the main engines after landing) and at rest. Mechanically engaging and disengaging a pinion with the wheel-ring gear was chosen over various clutches as leaving the minimum inertia attached to the wheel, an important factor during landing spinup.

Reversing is by external valving of the flow to the hydraulic motor, to avoid further mechanical complexity at the wheel. Mounting of the wheel-drive mechanism within the wheel along with the brakes requires considerable redesign of the wheel. A combination of increased tire diameter, lower tire-aspect-ratio, and greater wheel assembly width is necessary to accommodate the mechanism. The wheel configuration was changed so that both brake maintenance and tire changing are still easy.

Each of the design choices concerning the wheel-drive mechanism was somewhat arbitrary; other combinations might prove to be feasible also. However, the weight penalties and wheel configuration problems of the approach chosen were judged typical. The need for considerable improvement to APU reliability before an in-flight application as described above was identified as a major research and development requirement.

Other Design Changes

Each of the design changes noted in Figure 5 have been assessed in a manner similar to the four example changes described above. The reader is referred to reference 2 for this information.

SUMMARY AIRPLANE CHARACTERISTICS

Figure 12 gives a summary comparison of the principal size, geometry, performance, and noise characteristics of both the baseline and terminal-compatible aircraft. Both designs were sized for the same 200 passenger/3000-nautical-mile range mission. Whereas the baseline engine was sized to achieve the required field length, the TAC engine was sized to be consistent with the climbout gradient required by the previously mentioned takeoff noise objective. Moreover, the baseline airplane wing was sized to provide a minimum gross weight airplane whereas the TAC wing size was set by the 120-knot approach-speed requirement.

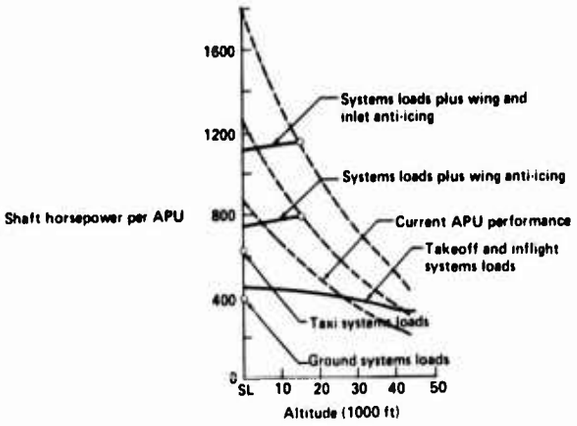

Figure 11. APU Sizing Considerations

Characteristic	Baseline	TAC
M_{cruise}	0.90	0.90
TOGW (lb)	302,200	311,000
OEW (lb)	159,200	172,630
Wing area (ft^2)	2300	2570
Sweep (deg)	36.5	36.5
Aspect ratio	7.6	9.0
Engine/number	ATSA4/3	ATSA4/4
Thrust per engine, sea level static, (lb)	31,100	23,200
Acoustic treatment	2R/1S	2R/1S
TOFL (ft)	8300	8300
Approach speed (kn)	135	120

3000 nmi range
40,000 lb payload

Figure 12. Study Airplanes–Summary Characteristics

In comparing the two aircraft, for fixed cruise Mach number and fixed payload/range, minimum takeoff gross weight serves as a figure of merit in assessing aircraft efficiency. It is seen that in these terms the TAC airplane incurs a 3% penalty as a result of the combined features added to improve terminal area operations. This penalty must be judged against the estimated improvements in congestion, noise, and emissions which the design modifications were intended to achieve. These improvements are considered in the next several figures. Moreover, for the purposes of the present paper, some discussion is given relative to impact on the aircraft fuel usage characteristics.

Figure 13 gives an indication of the airborne delay assessed by the simulation method as a function of the runway operations rate for both the baseline and TAC aircraft. These calculations, for one of the study airports indicate that for required traffic levels much beyond 20 movements per hour, the baseline aircraft would be unable to hold delay levels to the 6-minute goal of the study. The TAC airplane was assessed to achieve this goal at nearly double the flow rate. It should be noted, however, that even with a fleet of aircraft of TAC capability, projections for the three study airports determined substantially saturated conditions for two of the particular airports considered.

Figure 14 depicts the impact on fuel usage of both the design and assumed operational characteristics of the TAC and baseline airplanes. If both aircraft operate under minimum delay conditions, then for a 1000-nautical-mile trip, the TAC airplane saves slightly more than 1% of the block fuel. This savings results largely from the improved range factor achieved by the higher aspect ratio wing (although the design of the wing was selected for noise, not fuel-economy reasons). However, if the TAC features added to improve congestion prove effective, then elimination of "holding" type delays would yield a nearly 10% advantage in fuel use for the TAC airplane.

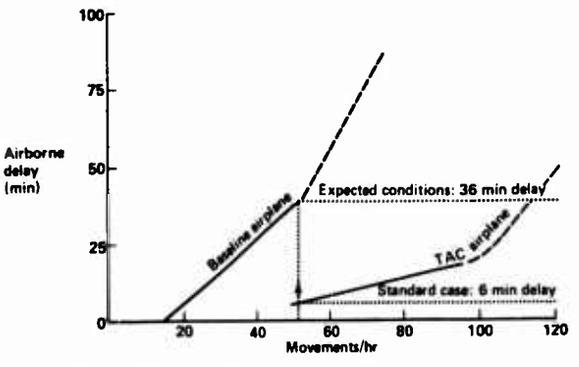

Figure 13. Delay Characteristics of Study Airplanes

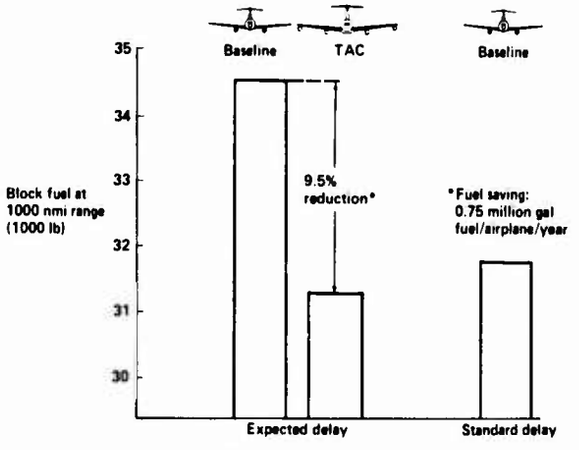

Figure 14. Effect of Delay on Block Fuel

Figure 15 shows a comparison in terms of relative 90 EPNdB noise footprint areas for the two study airplanes. For this plot, neither "airframe" (i.e., nonpropulsive) nor the so-called engine "core" noise have been included for lack of sufficient data. An important point of the figure is the interplay between heavy noise attenuation systems and airplane flightpath capability. Whereas the baseline airplane design had utilized two inlet rings and one fan duct splitter treated with acoustic material, the TAC airplane design concentrated on improved climbout gradients and steep descent paths. The figure shows a comparison with both aircraft either heavily treated or with peripheral treatment only. It is seen that the heavily treated baseline airplane during a 3° approach produces about the same 90-EPNdB area as a heavily treated TAC airplane during a 9°/3° approach. Basically, the reduced source noise levels are already approaching 90 EPNdB and thus path variations have no effect.

The 9°/3° two-segment approach is, however, highly effective in reducing 90-EPNdB approach area for peripherally treated engines. Figure 15 shows this to be on the order of an 80% reduction in approach area.

During takeoff the peripherally treated TAC airplane provides almost the same 90-EPNdB takeoff noise contour as the heavily treated baseline. This is explained by the fact that, for takeoff, at altitudes of 2000-3000 feet, say, the high-frequency engine noise components–those reduced by noise treatment–are attenuated substantially below the low-frequency noise by atmospheric absorption. The result of this comparison is to show the attractiveness of peripherally treated engines if used in conjunction with innate airplane noise-abatement flightpath capability.

Figure 16 illustrates the typical conflict between energy requirements and environmental quality (in this case aircraft noise). As shown in the figure, the use of increasing levels of acoustic treatment carries with it successively increased block fuel penalties. The curve has a significant knee in it which is associated ultimately with losses due to a large number of acoustically treated inlet rings and fan duct splitters. It is seen that the higher levels of fuel penalty can approach increments of 10 to 12% relative to a nontreated installation. This fuel loss is of particular interest in relation to the previous discussion showing that noise reduction achieved by improved flight path capability can be made equivalent to that achieved by acoustic treatment. However, in the latter case, the drain on fuel energy can be significant whereas lesser penalties have been assessed for the first method.

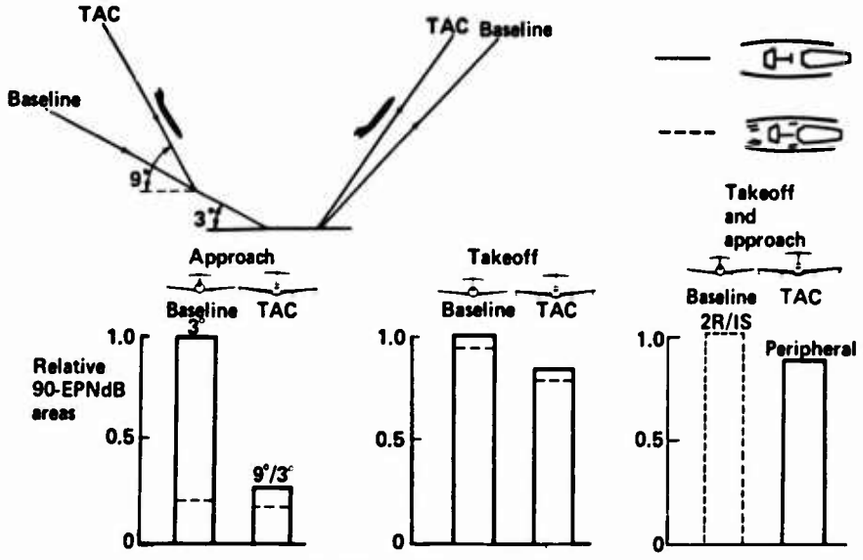

Figure 15. Effects of Treatment VS Flightpath

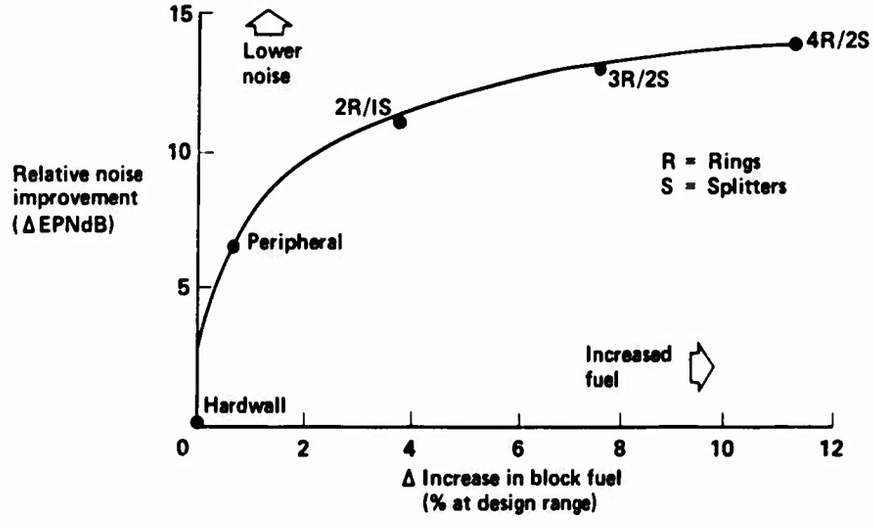

Figure 16. Noise VS Fuel Usage Trends

Turning to aircraft emissions, Figure 17 illustrates the interplay, for carbon monoxide, between the various design approaches to reduce the total number of pounds produced during a given landing-takeoff cycle. These approaches include: combustor improvement; improvements to ground congestion; and use of a powered wheel. As shown in the figure, the various control approaches just mentioned are completely independent and thus different options can be used to achieve a given level of pollutant per landing-takeoff cycle.

The figure indicates the situation for today's aircraft with relatively high emission indices, conventional ground taxi and landing-takeoff times defined in accordance with the U.S. Environmental Protection Agency (EPA) standard. The advanced, baseline airplane is projected to achieve a 50% improvement in pollutant emitted due to advanced combustor design concepts. The TAC

airplane retaining the advanced combustor but also making use of its "powered wheel" design and its congestion-reducing capabilities is estimated to achieve an additional 30% improvement. Similar trends were projected for hydrocarbon emissions. Oxides of nitrogen, however, were shown to be controllable only by engine design since only a small percentage of the total landing-takeoff emissions is produced during ground operation.

Figure 18 indicates that the powered wheel can also be beneficial from a fuel-usage viewpoint. The number of pounds used during a given landing-takeoff cycle is shown for: (1) varying ground operating time, and (2) powered wheel capability or not. If the EPA standard ground operating times are used, the powered wheel offers savings on the order of 1% of block fuel. Only half this savings would be achieved if ground operating times reflected no inflation due to delays.

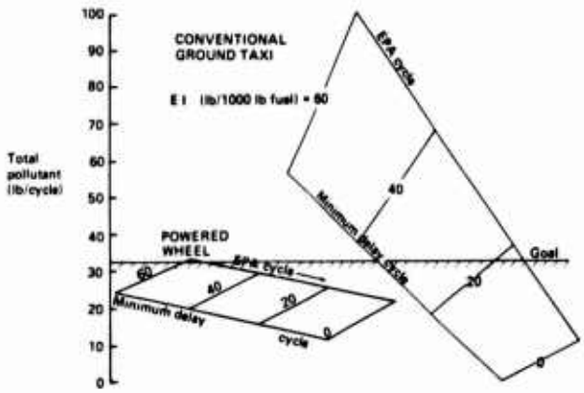

Figure 17. Design Impact on Carbon Monoxide Emissions

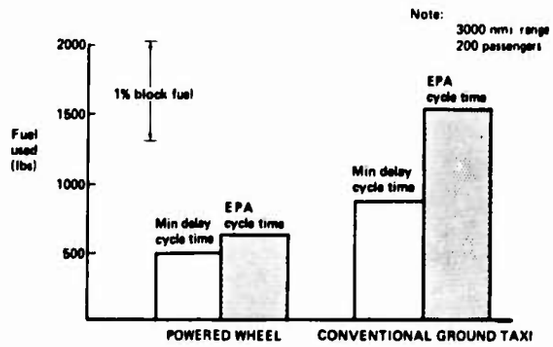

Figure 18. Fuel Usage for Ground Operations

This paper has addressed airplane design for airport terminal area operations. The effect on fuel usage of the design changes made for improvement to congestion, noise and emissions was considered. However, the question—what potential exists for specific design changes addressing fuel improvement for takeoff and landing—was not specifically considered in the present study. Nevertheless, for completeness, the following considerations are offered.

The data of Figure 19 are based upon calculations made for existing Boeing aircraft and show potential incremental improvements for both terminal area and cruise operations, if special care is taken to adopt specific fuel-saving schedules rather than the more general-purpose flight manual schedules typical of airline practice. The improved paths considered are not totally optimized; nevertheless, they represent typical obtainable improvements after considering varying aircraft attitudes, configurations, and speeds. For example, the climb-improvement increments shown reflect adoption of a more nearly optimum climb speed. (The choice for a specific case is affected by such other considerations as takeoff gross weight, air temperature, and initial cruise conditions.) Nevertheless, the data serve to provide an indication of the magnitude of potential fuel savings to be expected from a detailed optimization analysis. It might be inferred from the data that, from the standpoint of operational usage, the departure and arrival portions of a typical commercial transport already reflect fairly close to optimum fuel usage.

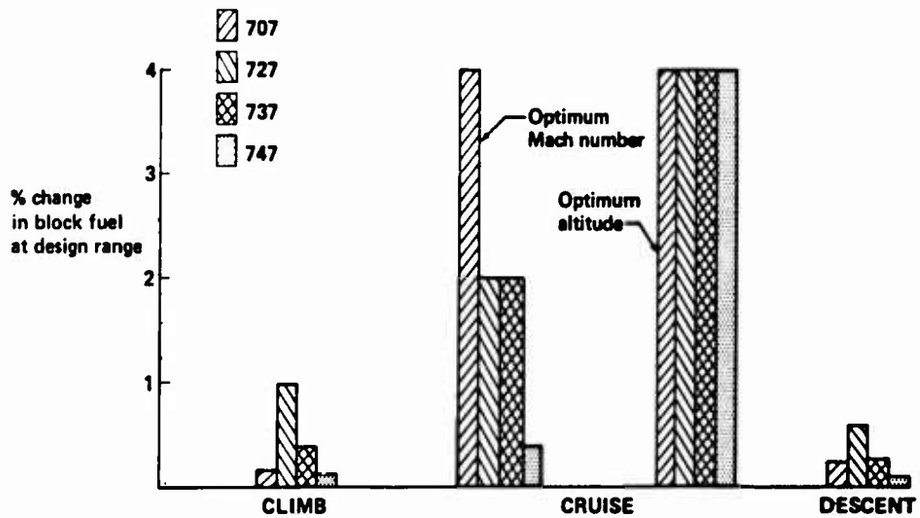

Figure 19. Fuel Savings Potential by Operational Considerations—Typical

CONCLUDING REMARKS

A broad study has been completed which, for given assumptions, projected future, unconstrained air traffic growth and the potential impact on airplane and airport compatibility. Particular emphasis was placed on congestion, noise, and emissions. Aircraft were configured in the course of the study to help understand the role of proposed design modifications. Sufficient detail was developed to satisfactorily identify limiting aeronautical research and technology areas. Principal conclusions are summarized below.

- With respect to air-transport congestion:
  The results showed that, if no corrective steps are taken, major urban airports face considerable peak-hour delay if the forecast travel demand is to be handled. One way to improve this situation is to upgrade runway usage efficiency by increasing runway operation rates. A principal obstacle to this goal is the required separation distance between aircraft dictated by wing-tip vortex (wake turbulence) constraints. Design approaches to reduce tip vortex impact are currently under investigation but no effective control method has yet been demonstrated. One potential approach, air injection using the engine-jet exhaust, was evaluated with respect to airplane design implications. This approach, when supplemented by other airplane modifications to enable more rapid removal of aircraft from the runway and permit more parallel runway use, can improve runway operations rates by 100% to 150% for a fleet of like-equipped aircraft. The proposed design solution of increased runway usage efficiency still contains major questions. Foremost among these are safety and ground handling of the increased number of airplanes.

- With respect to community noise:
  The current study showed potential noise improvement due to modifications of the airplane takeoff and descent flightpath. A 5- to 7-EPNdB improvement at the FAR Part 36 takeoff noise station was obtained relative to the baseline airplane. This was achieved by improved low-speed aerodynamics using a higher aspect ratio wing. This aerodynamic improvement also provided 2- to 3-EPNdB reduction on approach; however, this was offset by an independent design modification adopted to improve wake turbulence.

  Noise-abatement steep approach capability required large, innovative, deployable-drag brakes (together with advanced navigation, guidance and cockpit display avionics). A $9^{\circ}/3^{\circ}$ two-segment approach showed an 80% approach-noise-contour-area reduction if used in conjunction with a peripherally treated engine nacelle. However, no substantial benefit was assessed for steep approaches if used in conjunction with a heavily treated engine installation. Furthermore, with only peripheral treatment, but with the improved takeoff and approach path capability, the study airplane 90-EPNdB area was equivalent to the baseline airplane with extensive acoustic treatment. No attempt was made in this study to establish or evaluate optimized noise-abatement flightpaths.

- With respect to engine emissions:
  Aircraft emissions today constitute a very small percentage of the total overall pollution question; even within the immediate airport vicinity, emission sources today are about evenly divided between aircraft and automobiles. An assessment of satisfactory emission levels of future aircraft engines is hampered, however, by lack of ability to relate such levels accurately to ambient air-quality standards. Ignoring the question of air quality, several means to reduce aircraft engine emissions have been studied, including: improved combustor technology; aircraft taxi operations using a powered wheel; and, projections of reduced ground delay. Relative to an existing current wide-body airplane, an advanced airplane taking advantage of all of these would, during a given landing/takeoff cycle, show reductions of 80% for CO, 90% for HC, and 80% for NO_X.

  Combustor improvements for new, advanced engines have been estimated by the engine manufacturers in informal discussions to incur negligible weight, performance, or cost penalties. Under these conditions the powered-wheel device, which incurs a modest penalty of less than 1% TOGW, is nevertheless noncompetitive. Study estimates show, however, that a 10% increased engine cost could cause a net effect on operating cost equivalent to that of the powered wheel.

  Importantly, the powered wheel offers potential design flexibility which may prove convenient to control NO_X emissions. This occurs as follows. Many projected combustor advancements reduce NO_X emissions at the expense of increasing CO and HC, and vice-versa. This study has shown that the powered wheel, while ineffective in controlling NO_X, is quite effective in reducing CO and HC tonnages. Thus the powered wheel and advanced combustor might be properly regarded as complementary rather than competitive design approaches, allowing the latter to be biased in favor of NO_X control.

- With respect to airplane fuel usage:
  Substantial interaction exists between airplane design modifications directed toward improved terminal area operations and those which affect overall fuel usage. Although fuel usage was not a primary consideration in the current study, some preliminary points can be made:

  1) Aircraft design modifications directed toward improved runway operating efficiency could, if the projected delay improvements are realized, simultaneously improve fuel usage by 10%.

2) The use of extensive acoustic treatment to effect noise reduction carries with it penalties to fuel usage on the order of several percent of block fuel or more. An alternate, less fuel-expensive approach, shown to provide equivalent 90 EPNdB noise contour impact, may be found in providing improved airplane takeoff and descent paths.

3) Selection of a higher-aspect-ratio wing to reduce noise through improved departure flightpaths led to a significant block fuel savings due to improved cruise range factor. This result suggests that, were fuel efficiency to be the sole design objective, considerable opportunity might exist for innovative design thought.

4) Use of the powered wheel, besides effecting carbon monoxide and hydrocarbon emissions improvement, also could contribute to improved fuel economy on the order of 1/2% to 1% of block fuel.

The improved airplane qualities considered in this study are rational projections. However, it is important to note that implicit in these projections is the assumption of extensive research effort followed by sufficient development to demonstrate technology readiness. Figure 20 summarizes those technology areas found most critical to achieving improved terminal area compatibility. Reasons for identifying the problem areas shown included: large calculated benefits if effective design solutions could be achieved, and insufficient existing technical base to assess potential benefits.

Both of the above reasons were judged sufficient to recommend active research programs in all of the critical technology areas. Moreover, the reader is cautioned that in the absence of R&D expenditure, the projected improvements shown in this paper have little likelihood of realization.

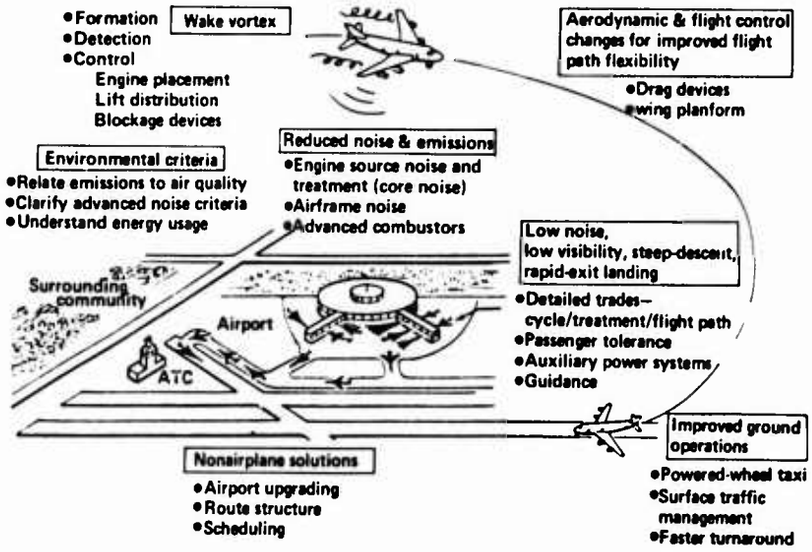

Figure 20. Terminal Compatibility Key Research

REFERENCES

1. NASA contract NAS1-10703, Final Report, "Study of the Application of Advanced Technologies to Long-Range Transport Aircraft," The Boeing Company, May 1972.

2. NASA CR-132367, "Advanced Subsonic Long-Haul Transport Terminal Area Compatibility Study," volume 1, The Boeing Company, February 1974.

3. NASA CR-121243, "Studies for Determining Rapid Thrust Response Requirements and Techniques for Use in a Long-Range Transport Aircraft," Newirth, D. M. and Ferguson, W. W., August 1973.

ACKNOWLEDGEMENT

Considerable portions of the material presented were developed under contract with the NASA Langley Research Center, Langley Field, Virginia, Contract NAS 1-12018, A. R. Heath, Jr., contract monitor. In addition, the author is pleased to acknowledge the dedicated efforts of the following Boeing engineers: L. A. Irish, C. W. Miller, A. R. Mulally, J. K. Murakami, H. Segal and A. Stutz.

PERFORMANCES DE FREINAGE

par Georges LEBLANC
Service Technique Aéronautique, Paris, Fr.

Résumé

Les distances de freinage lors d'un atterrissage ou lors d'un décollage abandonné dépendent des vitesses permises par les dispositifs hypersustentateurs et de l'énergie cinétique pouvant être abordée par les systèmes de freinage selon le coefficient de frottement disponible pneu-piste.

Ce dernier aspect n'a pas fait l'objet d'études aussi poussées que celles entreprises pour améliorer l'aérodynamique de l'avion. En plus de l'intérêt évident sur les performances,il est nécessaire de déterminer les marges de sécurité qu'il convient de prendre sur les distances de freinage pour différents états de la piste.

Dans ce papier, l'auteur propose, pour parvenir à une prédiction des distances de freinage, un schéma compréhensif du phénomène de glissance sur piste mouillée basé sur le modèle des trois zones de GROUGH. Les résultats d'essais obtenus sur CARAVELLE confirment que le modèle est satisfaisant et qu'il peut conduire à la prédiction des distances de freinage.

Enfin l'auteur porte dans ses conclusions l'accent sur la nécessité de poursuivre des études pour diminuer les risques d'accident sur les avions de transport.

BRAKING PERFORMANCES

Abstract

During Landing or aborted take-off, the braking distances are depending on the speed allowed by night lift devices and on the Kinetic energy which must be absorbed by the braking systems according to the available friction coefficient of tyre runway. Studies on this last point has not yet been so deepened as aerodynamic studies. Beside obvious interest for performances, it is necessary to know how to determine the safety margins which have to be taken on braking distances according to actual conditions of the runway.

In this paper, the author suggests for the prediction of braking distance a comprehensive schema of friction phenomena on wet runway according the three zone's GROUCH model. The test results obtained with CARAVELLE Aircraft confirm that the proposed model is correct and that il can give a satisfactory prediction of the braking distance.

At last the author puts in his conclusions the emphasis on the need to pursue studies in order to alleviate risks of accidents on the transport aircraft.

---

1 - INTRODUCTION

Les performances de freinage lors de l'atterrissage ou lors d'un décollage abandonné n'ont pas fait l'objet d'études aussi poussées que les performances en vol, peut être parce que cette partie est moins rentable, ou parce que, à tort, elle ne fait pas appel aux mêmes spécialistes aéronautiques. Pourtant il semble bien établi, et tous les pilotes interrogés le confirment, que la phase du freinage peut devenir hasardeuse dans certaines conditions défavorables de piste, de vent ou de vitesses pratiquées à l'impact.

Les nouveaux avions de combat ou de transport à grande capacité d'un prix élevé, exigent maintenant que les distances d'arrêt, et par conséquent les longueurs de piste nécessaires, ne soient plus le fait du hasard mais qu'elles puissent être reproductibles et que leurs méthodes de prédiction soient définies pour différentes conditions de vitesses d'impact, de vent, d'état de la piste.

Le but de ce papier est d'apporter certaines remarques sur les méthodes de prédiction des distances dans le cas ou le freinage n'est pas limité par les freins, mais par les caractéristiques du contact pneu-piste. Ces remarques ont pu être faites à la suite des essais de GLISSANCE effectués sur un avion Caravelle équipé d'un dispositif SPAD sur 4 terrains différents (3 pistes en béton, 1 en asphalte).

Bien du travail analytique et bien des essais ont été entrepris par des chercheurs principalement aux USA et au Royaume Uni pour expliquer les phénomènes de frottement et pour développer des méthodes de prédiction des distances de freinage. Le problème du freinage pneu-piste apparaît bien plus compliqué que le problème des performances liées à l'aérodynamique de l'avion ; des facteurs tels que la flexibilité du pneu, le dessin de la bande de roulement et la rugosité de la surface du revêtement rendant toute approche purement analytique pratiquement insoluble, s'il n'est pas faits d'hypothèses simplificatrices basées sur des résultats d'essais.

Ce papier s'inspire largement des études américaines et britanniques et particulièrement de l'étude théorique de M. Walter B. HORNE et de l'ensemble des importants travaux de son équipe.

2 - PARAMETRE INTERVENANT DANS LE FROTTEMENT PNEU-PISTE

2.1 - Le coefficient de frottement

Par définition le coefficient de frottement μ est le rapport entre la force horizontale Fx développée dans l'aire de contact pneu-sol et la force verticale Fy appliquée sur cette aire de contact. Il apparaît que pour un avion le coefficient de frottement à prendre en considération est celui pour lequel la force verticale représente la somme des composantes verticales sur les roues principales freinantes, du poids de l'avion, de la portance et des forces verticales d'inertie introduites par l'avion et le profil de la piste.

Il est aussi utilisé un coefficient de frottement généralisé μ_G pour lequel la force globale (poids - portance) est supposée appliquée sur les roues principales.

La connaissance du coefficient de frottement généralisé instantanné, et des forces verticales permet de calculer la distance de freinage D. En négligeant les forces d'inertie "avion - piste", cette distance est représentée par la relation approchée suivante :

$$D = -\int_{0}^{V} \frac{m.V.dV}{\mu_G (mg - R_z) + R_x + F_r}$$

dans cette relation

V = vitesse de l'avion en m/s

m = masse en Kg

g = accélération de la pesanteur = 9,81 m/s^2

Rz = portance en N

Rx = traînée en N

Fr = poussée reverse des réacteurs en N.

2.2 - Paramètre intervenant dans le frottement pneu-piste

Le frottement ou le coefficient de frottement généralisé longitudinal dépend de 17 paramètres indépendants :

- piste (6) : texture ou forme, η_p viscosité, E_p élasticité, H hauteur d'eau, η_e viscosité eau, ρ_e masse volumique de l'eau.
- pneu (8) : texture ou forme initiale, usure, R rayon, η_c viscosité caoutchouc, Ec élasticité équivalente de la bande de roulement, ρ_c masse volumique du caoutchouc, T température, Cp chaleur spécifique.
- véhicule (3) : Fz force résultante verticale, V vitesse, ω R vitesse tangentielle de la roue non déformée (ce paramètre tient compte du couple de freinage appliqué) R est le rayon du pneu.

Il est facile de comprendre que les conditions d'essais doivent mentionner ces paramètres. Heureusement un certain nombre de ces paramètres sont des constantes, et l'analyse dimensionnelle montre qu'un groupement judicieux permet dediminuer de façon utilisable les paramètres sans dimensions les plus influents.

2.3 - Paramètres les plus influents

Il est habituel de considérer les paramètres suivants comme les plus influents sur le frottement :

- le glissement s défini par $s = \frac{V - \omega R}{V}$. La figure 1 donne l'allure classique du coefficient de frottement avec le glissement tous les autres paramètres étant constants. Il serait illusoire de comparer des résultats d'essais différents si ce paramètre n'était pas connu, ou mieux s'il n'était pas maintenu constant. Les dispositifs "anti-patinage" donnant une loi moyenne du glissement doivent être utilisés pour rendre les distances de freinage reproductibles.
- La texture de la piste semble intervenir sous deux formes : (a) la macrotexture, ou irrégularités visibles, définie généralement par une hauteur moyenne de sable fin ou de graisse recouvrant toutes les aspérités. La macrotexture est responsable du frottement d'hystérésis, du frottement d'abrasion (tearing), de l'écoulement de l'eau sous l'empreinte du penu. (b) la microtexture, irrégularités inférieures au 1/10 de millimètre, dont l'effet moins évident semble porter principalement sur le frottement d'adhésion, origine profonde du frottement. Les distances de freinage sont grandement influencées par la texture de la piste. Il est nécessaire de faire intervenir ce paramètre dans la prédiction des distances de freinage.
- La hauteur d'eau réduite H.V., dont l'effet se fait surtout sentir pour des valeurs de H inférieures à la

macrotexture et pour des valeurs suffisantes permettant l'hydroplanage. Le paramètre HV est l'écriture simplifiée du Nombre de Reynolds global Rg dans le début de la zone de contact réel pneu piste :

$$Rg = (H.V.)\ \frac{\rho_e}{\eta_e}$$

- La vitesse réduite du pneu $\frac{V}{P}$ qui marque l'influence de la vitesse seule est l'écriture simplifiée du nombre de Sommerfeld So :

$$So = \eta_e \cdot V / P.R$$

- Le rapport de pression dynamique $\frac{\rho_e . V^2}{2P}$. L'influence de ce rapport commence à se faire sentir sous l'empreinte du pneu à des vitesses très inférieures à la vitesse d'hydroplannage.

- L'aire du contact réduite : $\frac{Fz}{P.R^2}$, ou déflexion réduite du pneu, qui est pratiquement proportionnelle au rapport $\frac{AO}{R^2}$, AO étant l'aire apparente de l'empreinte pneu - sol.

Le frottement peut être représenté à l'aide de ces 6 paramètres réduits, faisant intervenir les paramètres indépendants : V, ω.R, ρ_e, η_e, H, P, R, Fz, texture piste, lorsqu'il est négligé l'effet des paramètres liés au caoutchouc, c'est-à-dire l'énergie dissipée par hystérésis, et l'effet propre du pneumatique lequel est considéré comme un élément constant. Les résultats ne sont donc valables que pour une qualité donnée de pneumatique. Les prédictions seraient à faire pour un avion donné avec les différents types de pneus prévus en utilisation.

3 - RAPPEL SOMMAIRE DES PRINCIPES DES DIFFERENTS SYSTEMES D'ANTI-PATINAGE

La fonction primaire d'un système anti-patinage est de diminuer la pression des freins lorsque le pneu a tendance à se bloquer, c'est-à-dire lorsque sa décélération angulaire devient supérieure (en valeur absolue) à une valeur estimée limite. Les différents systèmes existants peuvent être approximativement schématisés par 4 principes de base.

3.1 - Le système à pression tout ou rien

La pression de freinage est supprimée dès que la décélération atteint une valeur constante prédéterminée ou seuil.

3.2 - Le système à pression modulée à seuil prédéterminé

Dans ce système, la pression de freinage est une fonction de l'écart mesuré entre la décélération actuelle et le seuil prédéterminé.

3.3 - Le système à pression modulée et seuil variable

Le seuil est variable pour tenir compte des variations du coefficient de frottement disponible selon l'état de la piste (sèche ou mouillée). Le principe de ce système diffère du précédent dans ce sens que le seuil est déterminé soit comme une fonction de la vitesse, soit d'une façon telle que la variation de l'écart de la décélération (entre décélération actuelle et seuil) reste proportionnelle à la variation de la pression de freinage.

3.4 - Le système à taux de glissement constant ou ajustable

La pression de freinage est régulée de façon à ce que le taux de glissement mesuré à bord de l'avion soit constant ou soit tel que le coefficient de frottement ou de décélération de l'avion soit au maximum de la courbe $\mu = f(s)$ ou $dV/dt = f(s)$. C'est ce dernier système qui a été utilisé lors des essais de glissance sur la Caravelle, il est désigné par le sigle SPAD.

4 - LES 3 REGIMES DE FONCTIONNEMENT D'UN PNEU SUR PISTE MOUILLEE

Les premiers résultats disponibles des essais de glissance sur Caravelle ont fait l'objet de diverses théories de synthèse basées sur des modèles différents pour expliquer les dispersions apparentes dans ces résultats. Il est apparu à ce stade de l'étude qu'un modèle basé sur celui proposé par GOUGH en 1959 permettrait une meilleure synthèse des résultats, puis une compréhension physique probable du frottement d'un pneu sur piste mouillée.

La figure 2 représente le modèle adopté, dans lequel l'interface entre le pneu et le sol est décomposé en 3 zones arbitrairement distinctes :

Une zone I d'écoulement dynamique, une zone II d'écoulement laminaire, et une zone III de contact "pseudo-sec". Dans cette dernière zone le pneu est en contact partiel avec la piste et maintient prisonnière une certaine quantité d'eau dans laquelle se développe une pression visqueuse proportionnelle à la vitesse. Pratiquement la zone III est la seule donnant naissance au frottement par adhésion, abrasion et par hystérésis.

Une étude théorique basée sur ce concept des trois zones successives permet de montrer que suivant la hauteur d'eau et la vitesse, il existe 3 régimes distincts de fonctionnement comme illustré sur la figure 3. Ce sont :

(a) régime A : aux vitesses faibles et hauteur d'eau faible, seule la zone de contact "pseudo sec" existe. Le contact est partiellement sec selon la grandeur (H -gp), gp étant une dimension figurant la macrotexture et H étant généralement inférieure à gp. La partie restante mouillée dans l'empreinte, à adhérence négligeable développe une pression visqueuse proportionnelle à la vitesse. Ces considérations montrent que le coefficient de frottement peut être exprimée sous la forme approchée suivante :

$$\mu = \mu_s - K_1 . H.V$$

μ_s est le coefficient de frottement sur la piste sèche à la vitesse considérée V.

K1 est un ceofficient tenant compte de la macrotexture, de la forme du granulé et de la porosité de la piste. La figure 4 donne l'évolution du coefficient de frottement μ à iso vitesse V en régime A pour la Caravelle sur le terrain de Brétigny.

(b) régime B : pour une valeur donnée de HV, à iso vitesse $\frac{V}{P}$, la hauteur critique hc, définie par un nombre de Reynolds critique tel que :

$$Rc = \frac{\rho_e}{\eta_e} V. hc$$

devient égale à la hauteur d'eau H. A cet instant un écoulement visqueux apparaît (zone II) et la partie avant de l'empreinte se soulève. Ce cas de fonctionnement transitoire doit vraisemblablement être fugitif, il correspond à la figure 3 A-B. Dès l'instant où la vitesse augmente, la hauteur critique hc diminue, la zone II se déplace vers l'arrière de l'empreinte et la zone I apparaît immédiatement. Un bourrelet frontal se développe. La hauteur ha du point A extrémité avant de l'empreinte augmente avec la vitesse, puis diminue ensuite.

Le rapport ha/H est une fonction du paramètre : $\frac{\rho_e . V^2}{2p.}$

La ligne de séparation entre les régimes de fonctionnement A et B présentée sur la figure 4 est définie par la relation approximative suivante :

$$H^2 = K2. \frac{\eta_e}{\rho_e} . \frac{R}{V}$$

K2 est un coefficient combiné dépendant de la forme et de l'usure du pneu et de la texture de la piste. Ainsi à vitesse $\frac{V}{P}$ constante en régime B, ha/H et hc sont déterminés, la forme géométrique de l'empreinte et par conséquent la zone de contact "pseudo-sec" sont elles-mêmes bien déterminées. Le coefficient de frottement devient donc pratiquement indépendant de la hauteur H.

(c) régime C : ou régime d'hydroplanage ou d'écoulement dynamique pur. Lorsque la hauteur d'eau le permet, et pour une valeur de $\frac{\rho_e . V^2}{2P}$ supérieure à la valeur de 1,45 environ (selon la forme du pneu), la zone II d'écoulement visqueux et la zone III de contact "pseudo-sec" peuvent disparaître, le pneu hydroplane. La hauteur d'eau H nécessaire pour qu'un tel phénomène se réalise à la vitesse minimale de $Vp = \sqrt{\frac{2p}{\rho_e . Cz}}$, avec Cz $\approx$ 0,70, serait théoriquement trop grande pour être rencontrée fréquemment en utilisation, par contre, pour des vitesses supérieures la hauteur d'eau nécessaire à l'hydroplanage diminue, et le phénomène peut être observé. Le régime C de fonctionnement en hydroplanage n'a pas été obtenu lors des essais effectués sur l'avion Caravelle. A titre d'illustration, la zone possible de ce régime a été portée sur la figure 5 pour le cas particulier du terrain de Brétigny. L'augmentation des zones I et II par pression visqueuse et pression dynamique diminue la zone III de contact"pseudo-sec", pratiquement seule zone génératrice du coefficient de frottement.

5 - PREDICTION DES DISTANCES DE FREINAGE

La présentation assez habituelle des résultats donnée par la figure 5 ne doit pas être retenue pour la prédiction des distances de freinage. Il doit lui être préféré la représentation $\mu = f(H.V, \frac{V}{P})$ ou $\mu = f(HV, \frac{Vpo}{P})$ pour les vitesses correspondant aux régimes de fonctionnement A et B comme illustré sur la figure 6 et la représentation $\mu = f(\frac{H}{R}, \frac{\rho_e . V^2}{2p})$ pour les vitesses correspondant aux régimes de fonctionnement B et C.

Dans ces conditions les prédictions des distances de freinage sur un terrain donné deviennent accessibles grâce à la connaissance des réseaux préétablis pour ce terrain et pour l'avion considéré, des courbes $\mu = f(HV, \frac{V}{p}, \frac{\rho_e . V^2}{2P}, \frac{H}{R})$. Il est alors possible de calculer la distance de freinage d'après la relation donnée au § 2.1.

Il est cependant préférable, semble-t-il, et aussi précis d'établir directement des réseaux de courbes donnant $\frac{D}{m.V^2} = f(HV, \frac{V}{P}, \frac{\rho_e . V^2}{2p}, \frac{H}{R})$ sans passer par l'intermédiaire du coefficient de frottement. En effet la prédiction des distances de freinage ne peut être faite que si la loi de pilotage est fixée, c'est-à-dire que si la vitesse d'impact est proportionnelle à la racine carrée de la masse et si l'incidence au sol est maintenue identique, soit les paramètres sans dimensions constants* :

* Dans ces relations les nouveaux paramètres introduits sont ceux liés à l'avion et à l'air : ρ_a la masse volumique de l'air, S : surface de référence de l'avion, et m : masse de l'avion (en plus de mg).

$\frac{\rho_a . S V^2}{m.g}$, $\frac{S}{R^2}$, et le paramètre $\frac{V}{P} . g . R^2$, $\frac{\rho_a}{7e}$ déjà inclus sous la forme du paramète $\frac{V}{P}$ à des constantes près.

La distance de freinage réduite $\frac{D}{m.V2}$, écriture simplifiée de $\frac{D}{m.V^2} . (\rho_a . S^{3/2} . g)$ est alors représentée par des paramètres identiques à ceux de μ. Les figures 7 et 10 donnent les résultats sur 4 terrains différents. Il peut y être reconnu l'influence des deux régimes de fonctionnement A et B et l'importance de l'effet de macrotexture. Le meilleur terrain du point de vue freinage est celui à revêtement d'asphalte poreux à gros granulé. La figure 11 permet de comparer les quatre terrains à la même vitesse de début de freinage de 45 m/s (87,5 Kt).

REMARQUES :

(1) Le modèle proposé ci-dessus a pour but de permettre le développement d'une méthode simplifiée de prédiction des distances de freinage d'après diverses mesures portant principalement sur la texture en particulier en développant des véhicules spéciaux.

(2) La hauteur d'eau intervenant dans la détermination du coefficient de frottement comme cela a été vu en 4 (a) doit inclure l'eau logée dans les aspérités du revêtement de la piste, c'est pourquoi il semble que la mesure de la hauteur d'eau par sonde à neutrons* , telle qu'elle a été faite lors de ces essais, soit préférable.

(3) La figure 12 donne les résultats des distances d'arrêt du véhicule DBV * * de la NASA. La comparaison de ces résultats avec ceux de la figure précédente 11 montre que le rapport des distances de freinage entre le cas mouillé et le cas sec pour l'avion et pour le véhicule varie approximativement de façon identique d'un terrain à un autre, mais que le DBV classe Roissy meilleur que Bricy alors que pour la Caravelle c'est pratiquement le cas inverse. Dès que la vitesse de début de freinage de l'avion varie, la comparaison immédiate des résultats montre les dispersions importantes.

"Une relation universelle entre l'indication fournie par un véhicule de mesure de frottement et les performances d'un avion n'a pas encore émergée. Il est peu vraisemblable qu'une telle relation soit trouvée". Cette réflexion pertinente peut cependant être prise en défaut si l'on s'assure (par exemple sur le DBV) que la vitesse de début de freinage soit représentative de celle de l'avion. Enfin, le développement d'une méthode transcription des performances ne peut être valablement mené qu'à l'aide d'un véhicule d'essais sur lequel on peut effectuer un grand nombre d'essais sur différents revêtements.

6 - CONSIDERATIONS SUR LE FROTTEMENT LATERAL

Le frottement latéral disponible n'est pas habituellement examiné pour un avion sous l'aspect des performances de freinage à l'atterrissage, car il n'intervient pas directement, comme le frottement longitudinal, dans la détermination des distances de freinage. Cependant, il doit être pris en considération pour les deux raisons essentielles suivantes :

(a) Contrôle latéral au sol, roues libres en cas de panne soudaine d'un moteur au décollage (VMCG).

(b) Contrôle latéral au sol, roues freinées, par vent de travers.

Dans le cas (a), pour les avions à trains principaux arrières, à VMCG les gouvernes aérodynamiques seules doivent être capables d'assurer le contrôle directionnel de l'avion, mais le couple de lacet exigé des gouvernes sera d'autant plus faible que le dérapage introduit par le couple de lacet dû aux moteurs engendrera un couple important de lacet opposé dû au frottement latéral des pneus sur le sol. D'après des essais récents, il semble que le déport maxi latéral observé, définissant VMCG, soit lié à la variation de cap au moment de la panne de moteur ; il apparaît donc que la condition de piste mouillée devient un critère important dans la justification de VMCG.

Le frottement latéral roues libres par son influence sur VMCG contribuerait ainsi sur les avions de transport à définir les performances au décollage.

Dans le cas (b) lors du freinage à l'atterrissage ou en accélération - arrêt, le frottement latéral doit permettre de maintenir l'avion sur la piste par vent de travers. Tout le long de la trajectoire, il doit exister un frottement latéral disponible suffisant pour compenser les forces aérodynamiques latérales. Il est possible que ce frottement, pour certaines conditions de piste, soit obtenu pour un glissement inférieur à celui donnant le frottement longitudinal maximal. Les règles de sécurité voudraient que dans ce cas il y ait réduction du glissement, donc une certaine dégradation des distances de freinage.

Le frottement latéral roues freinées par son influence sur la sécurité contribuerait ainsi, sur tous les types d'avion, à définir les performances d'atterrissage et d'accélération - arrêt

La figure 1 donne l'allure typique du coefficient de frottement latéral disponible pour un angle constant de dérapage (ou dérive).

---

* La sonde à neutrons mesure pratiquement le volume d'eau contenu par unité de surface.

* * Véhicule développé par la NASA, mesurant la distance d'arrêt, deux roues diagonales bloquées, les deux autres libres, à partir de V = 60 MPH.

7 - CONCLUSIONS

- Les résultats disponibles des études de freinage menés aux U.S.A. et au Royaume Uni ont permis de mieux comprendre les phénomènes liés au frottement et de développer des méthodes d'essais destinés à prédire les distances de freinage des avion.

- Les essais effectués sur l'avion Caravelle ont montré qu'un modèle basé sur celui de GOUGH des trois zones de contact était satisfaisant pour interpréter les résultats. Il semble qu'il y ait trois régimes distincts de fonctionnement d'un pneu sur piste mouillée : un régime où toute l'empreinte du pneu est en contact "pseudo-sec" avec la piste, un régime où la partie avant de l'empreinte est séparée du sol par un écoulement dynamique suivi d'un écoulement laminaire, et un régime d'hydroplanage.

Le régime d'hydroplanage n'a pas été atteint lors des essais sur Caravelle.

- Les connaissances actuelles en matière de frottement, et les résultats d'essais ne sont pas encore suffisants pour prédire de façon simple et satisfaisante les distances de freinage. Une prudence est nécessaire avant d'élaborer des principes, des consignes, voire des règlements relatifs au freinage des avions.

- Des recherches théoriques doivent être menées en relation avec les spécialistes de l'aéronautique pour étudier les causes profondes de l'adhésion, paramètre fondamental du frottement, les autres paramètres intervenant généralement comme agents réducteurs du frottement.

- Des essais sur avions, sur véhicules spéciaux d'études ou sur maquettes doivent être développés pour déterminer l'influence des caractéristiques des pneus (mélange, forme, dessins de la bande, usure), de la texture de la piste, et de la nature des contaminants.

- Les performances au sol de freinage des avions n'ont pas été examinées dans le passé avec autant de moyens que ceux mis à la disposition des performances traditionnelles en vol. Les statistiques d'accidents dûs aux caractéristiques propres des avions (navigabilité) montrent que la phase du freinage est parmi les plus critiques. Les pilotes interrogés reconnaissent que cette phase de freinage est la plus hasardeuse, eut égard du nombre d'accidents évités. Pour aider au développement du moyen de transport aérien, il devient impératif de créer une juste balance entre les études menées pour les performances traditionnelles en vol et les performances de freinage.

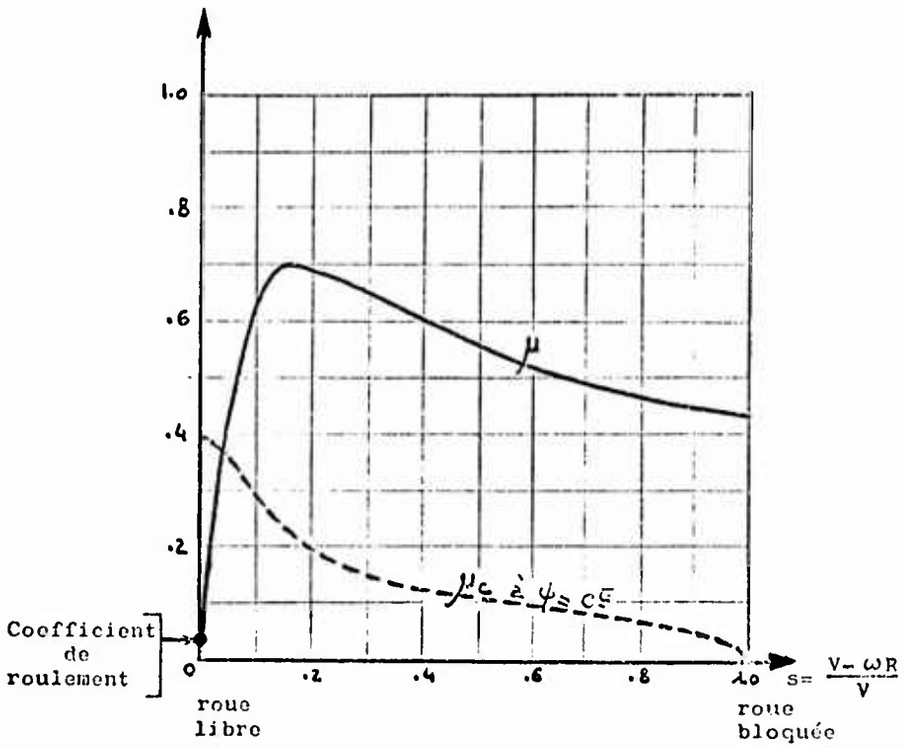

μ et μ_c sont des coefficients liés à la direction du véhicule et non au plan de symétrie de la roue

Fig.1 Allure typique du coefficient de frottement longitudinal μ latéral disponible μ_c avec le glissement s

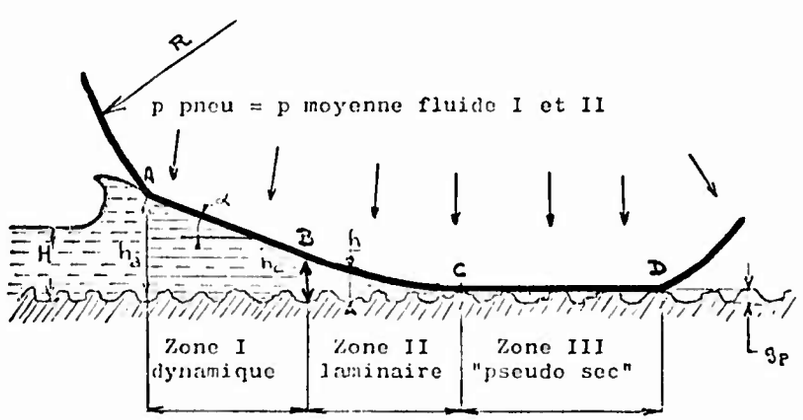

$$\frac{H}{h_a} = f\left(\frac{H}{R}, \frac{\varrho_e \cdot V^2}{2p}\right)$$

$$h_c^2 \simeq K_2 \cdot \frac{\eta_e \cdot R}{\varrho_e \cdot V}$$

zone I → $\alpha = K_3 \cdot \frac{2p}{\varrho_e \cdot V^2}$

zone II → $\alpha = K_4 \cdot \frac{h^2 \cdot p}{R \cdot \eta_e \cdot V}$

avec: η_e = viscosité de l'eau

ϱ_e = masse volumique de l'eau

Fig.2 Modèle des 3 zones de Gough

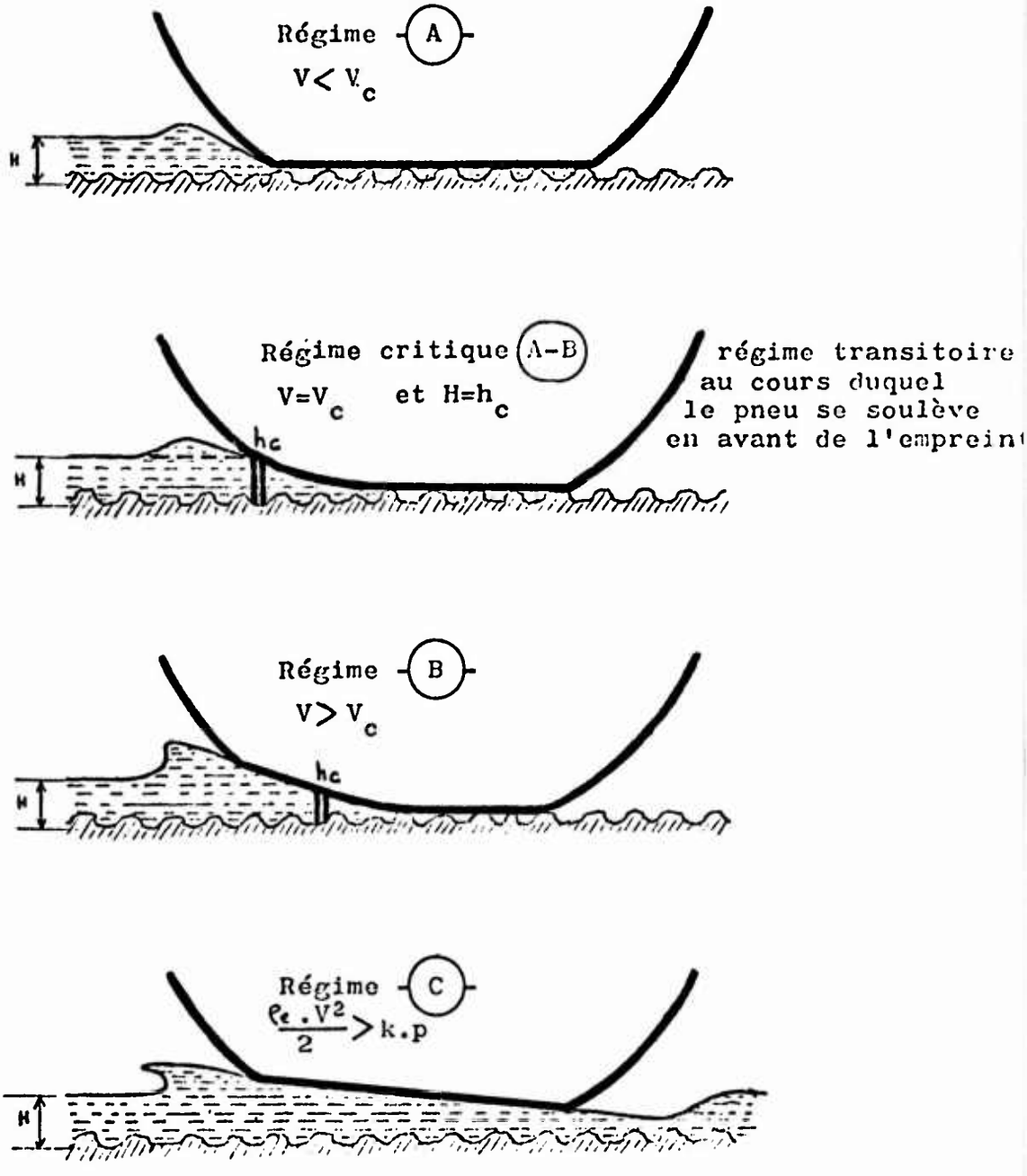

Fig.3 Les trois régimes de fonctionnement d'un pneu sur piste mouillée

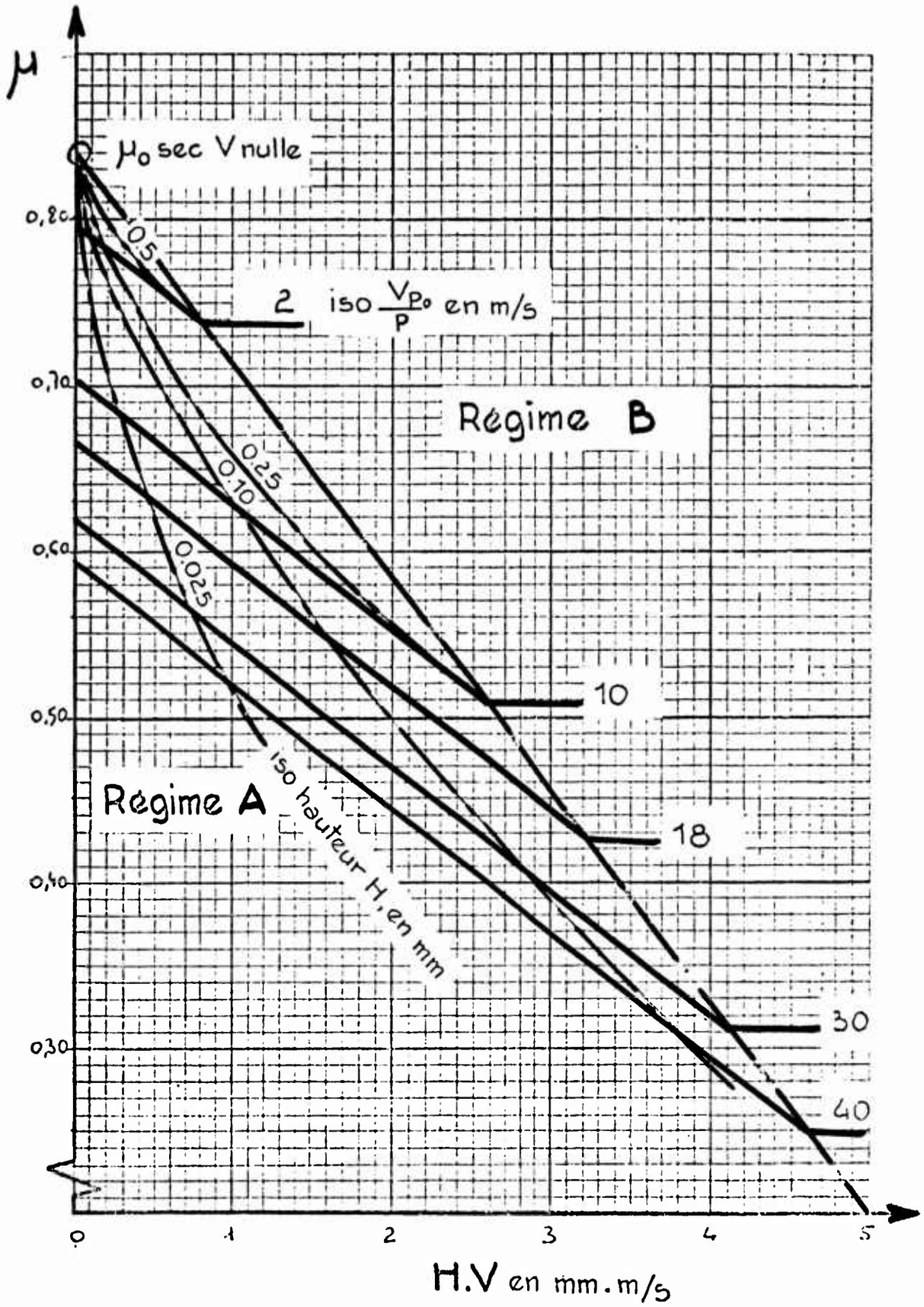

Fig.4 Essais de freinage – Piste de Brétigny. Caravelle n° 116, équipée du SPAD masse moyenne: 36 000 kg

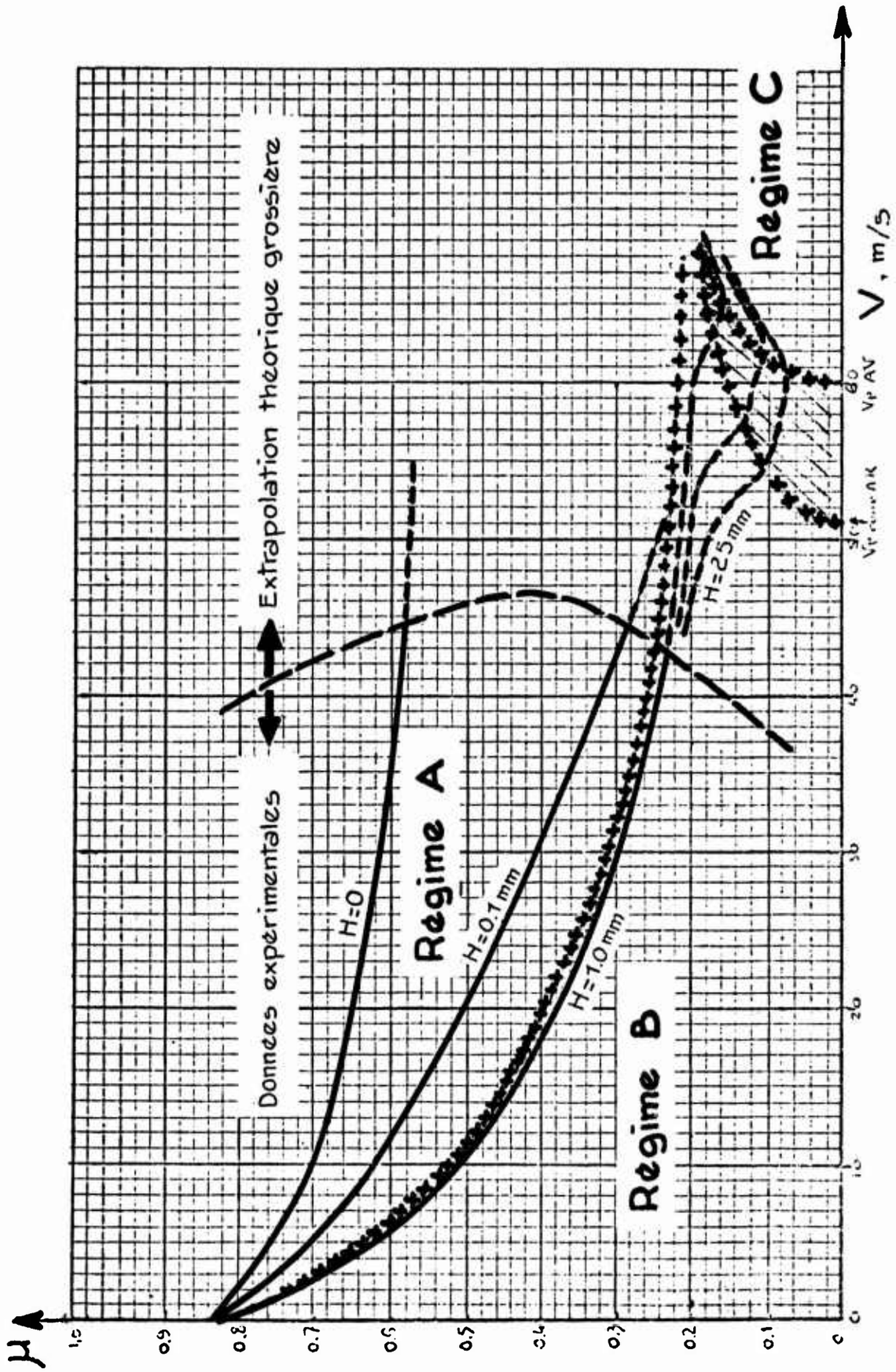

Fig.5 Essais de freinage – Piste de Brétigny. Caravelle n° 116, équipée du SPAD – masse moyenne: 36 000 kg

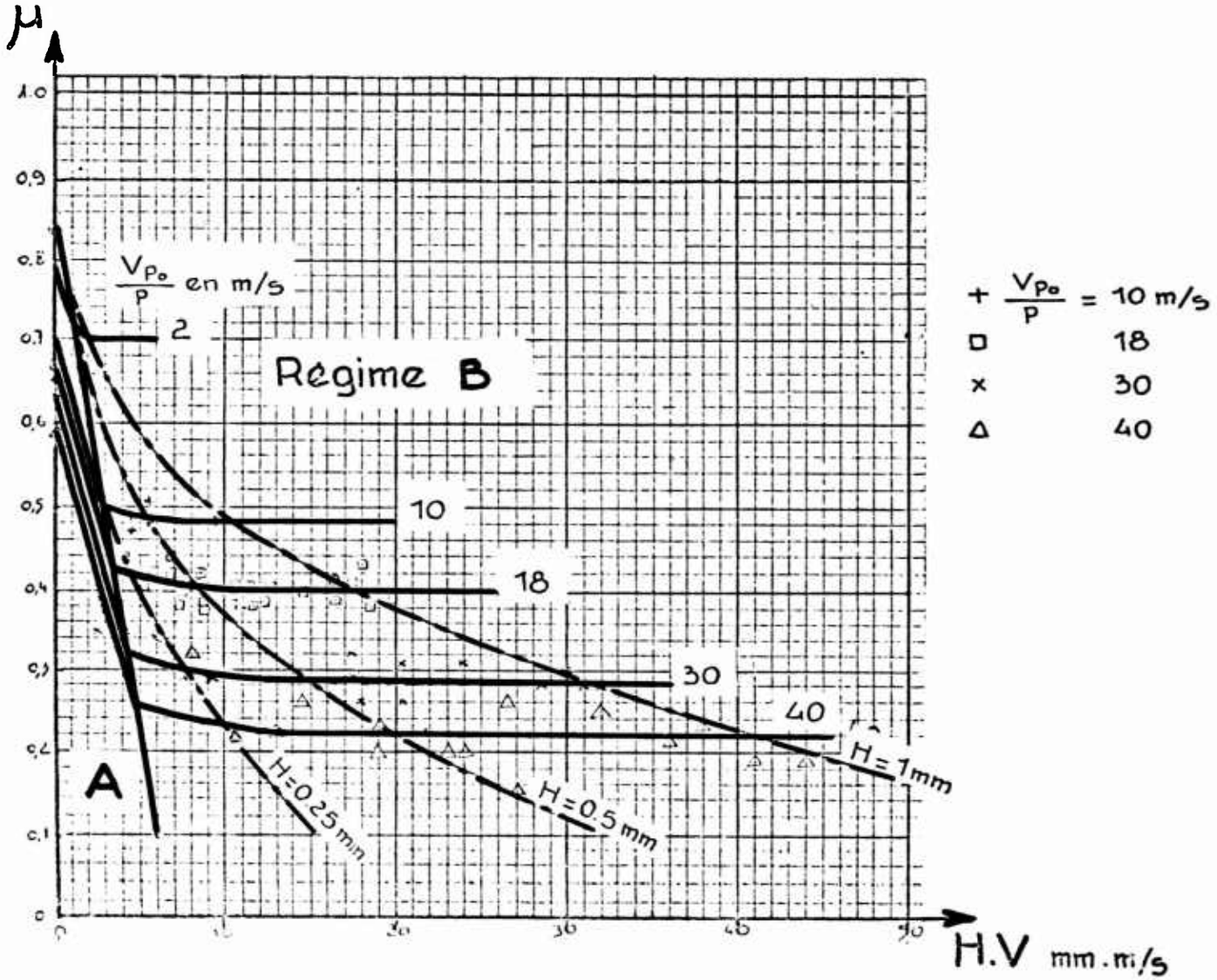

Fig.6 Essais de freinage — Piste de Brétigny. Caravelle n° 116, équipée du SPAD — masse moyenne: 36 000 kg

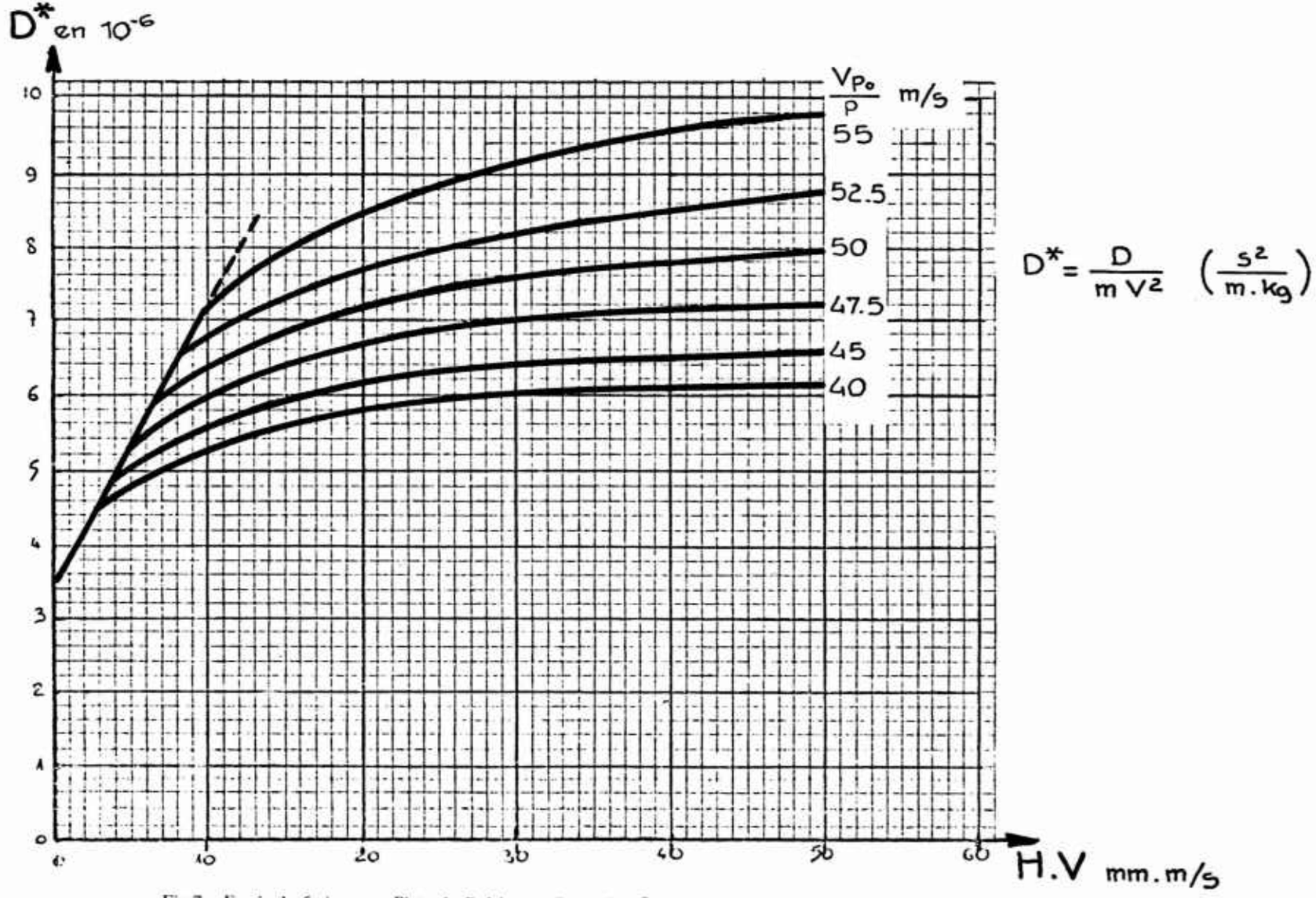

Fig.7 Essais de freinage – Piste de Brétigny. Caravelle n° 116, équipée du SPAD – masse moyenne: 36 000 kg

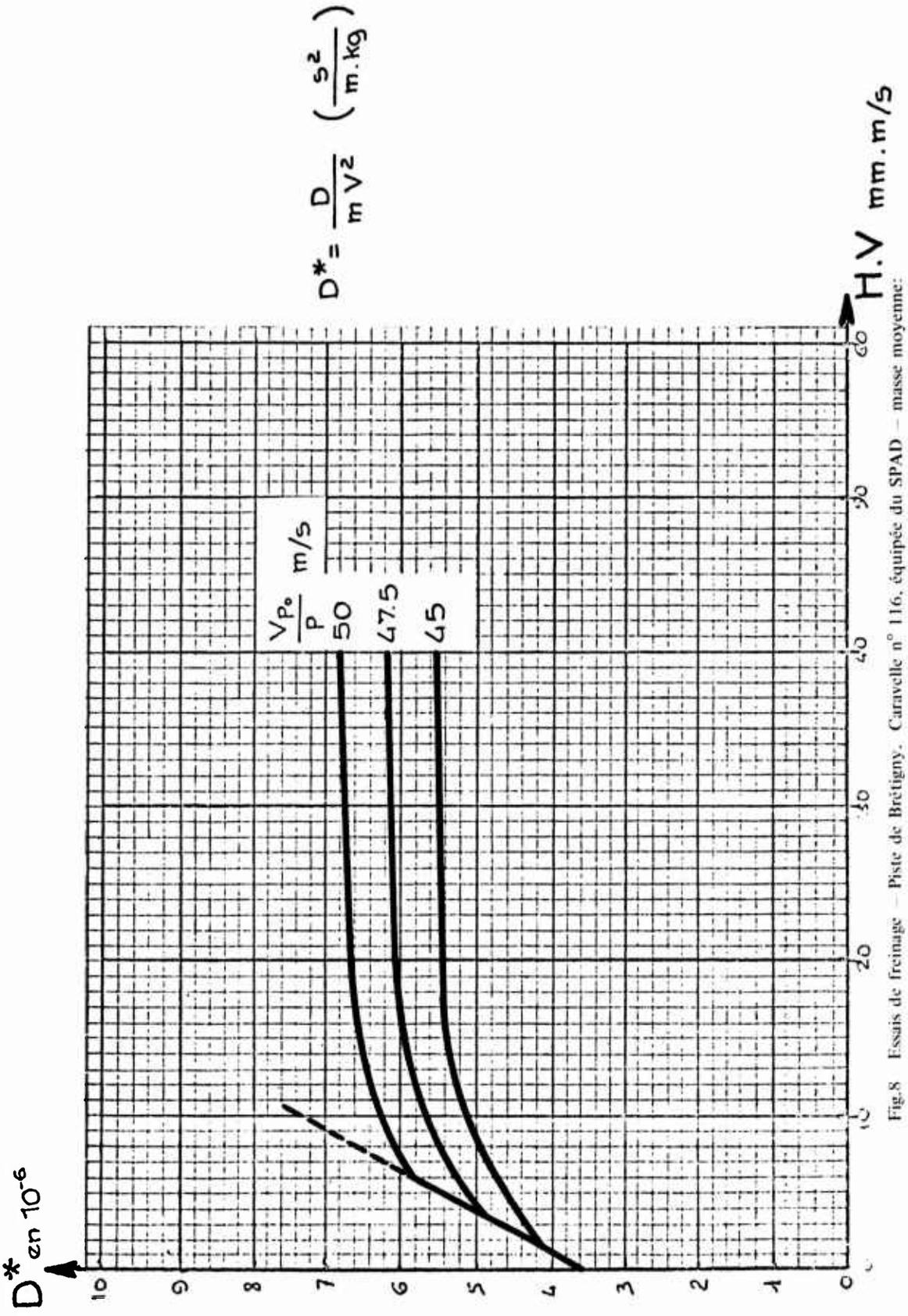

Fig.8 Essais de freinage – Piste de Brétigny. Caravelle n° 116, équipée du SPAD – masse moyenne: 36 000 kg

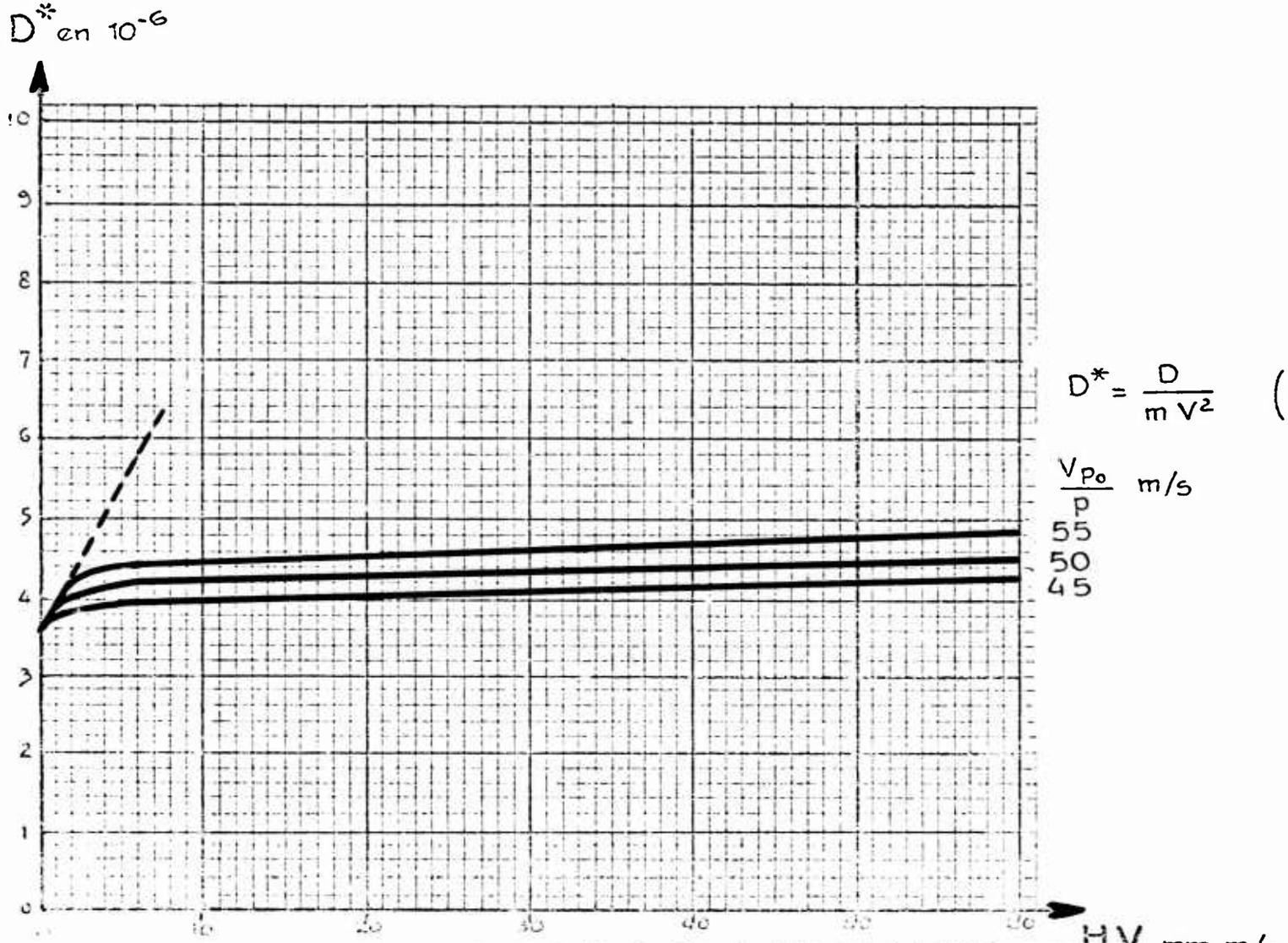

Fig.9 Essais de freinage – Piste de Saint-Nazaire. Caravelle n° 116, équipée du SPAD – masse moyenne 36 000 kg

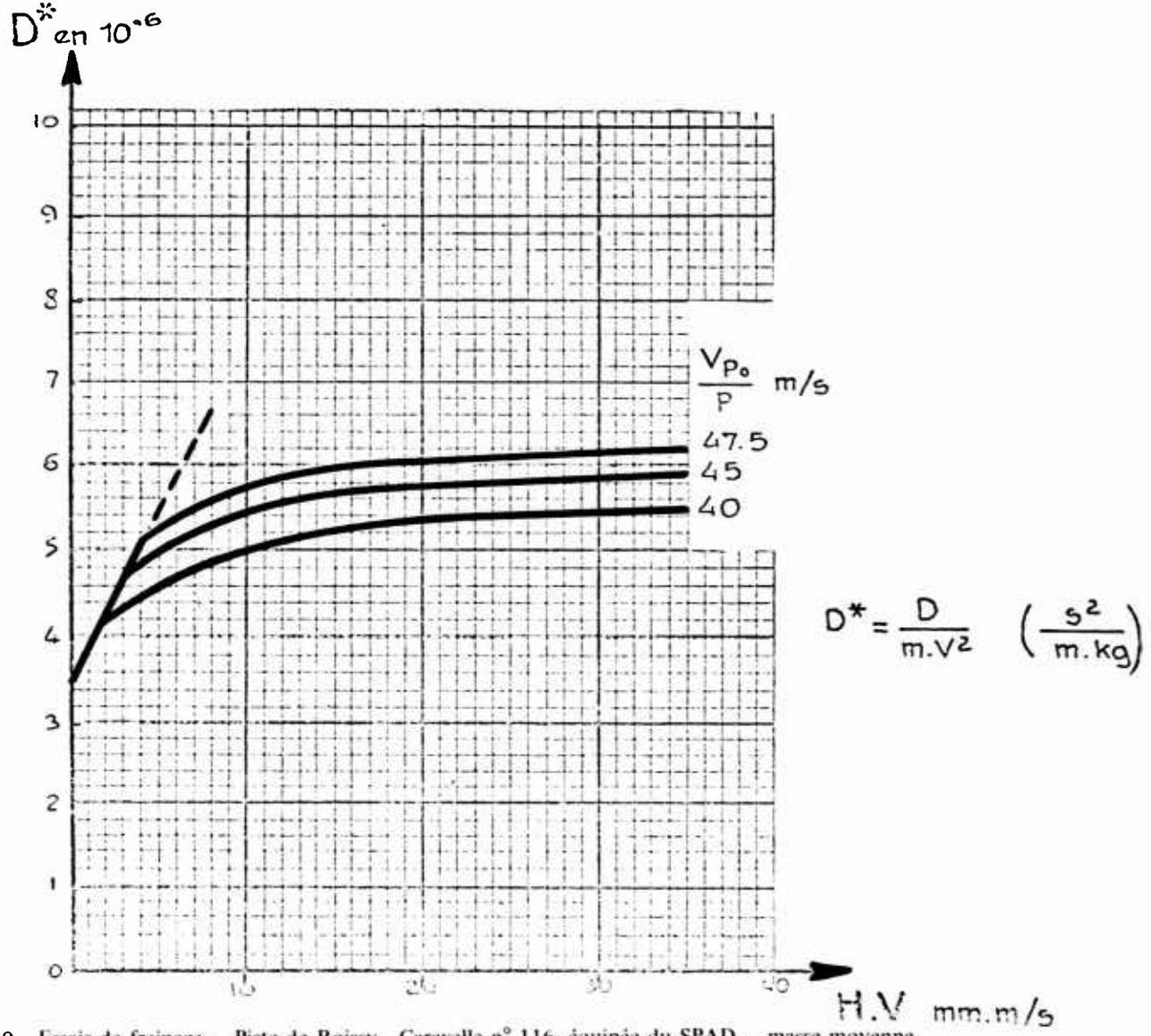

Fig.10 Essais de freinage – Piste de Roissy. Caravelle n° 116, équipée du SPAD – masse moyenne 36 000 kg

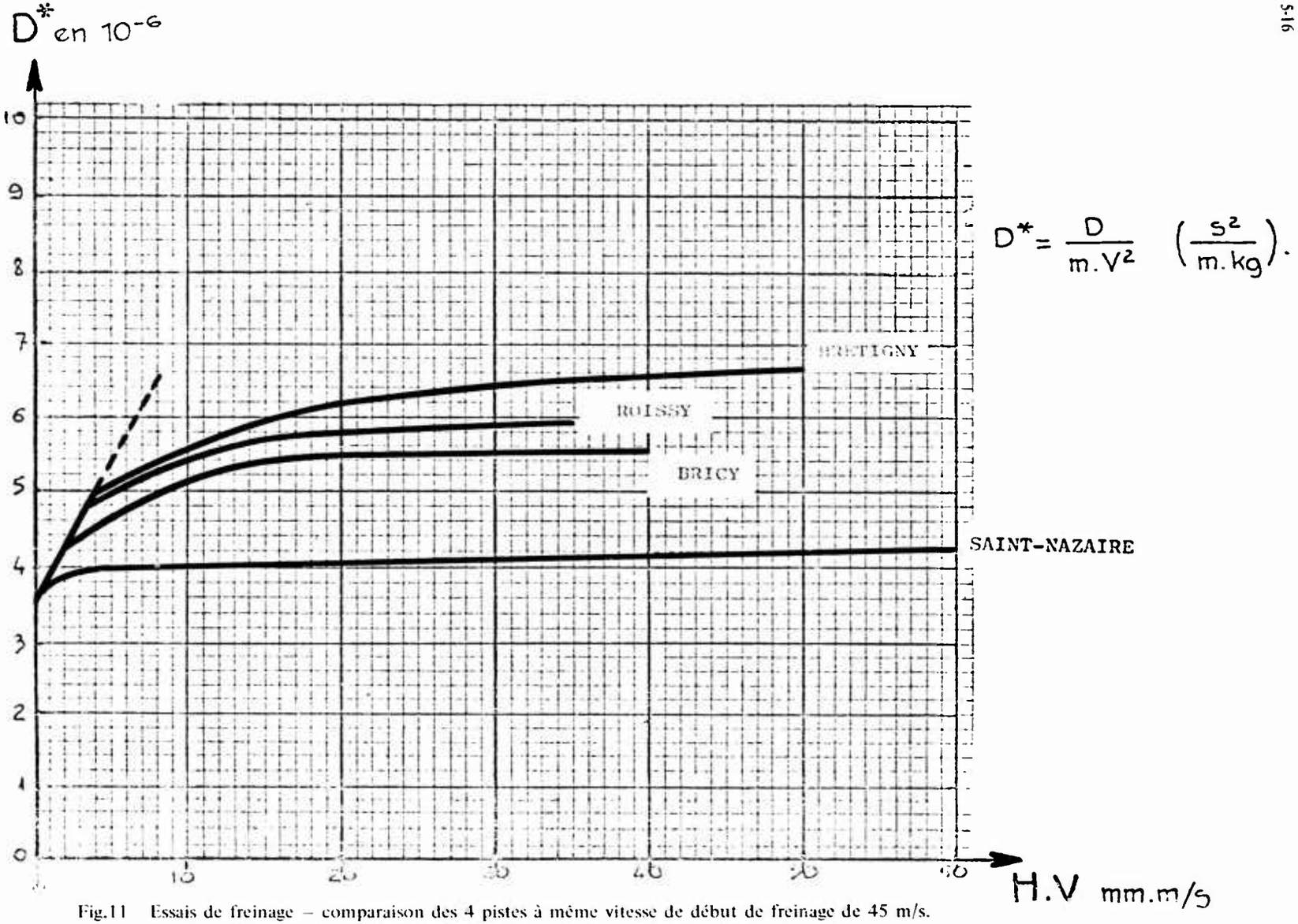

Fig.11 Essais de freinage – comparaison des 4 pistes à même vitesse de début de freinage de 45 m/s.
Caravelle n° 116, équipée du SPAD – masse moyenne 36 000 kg

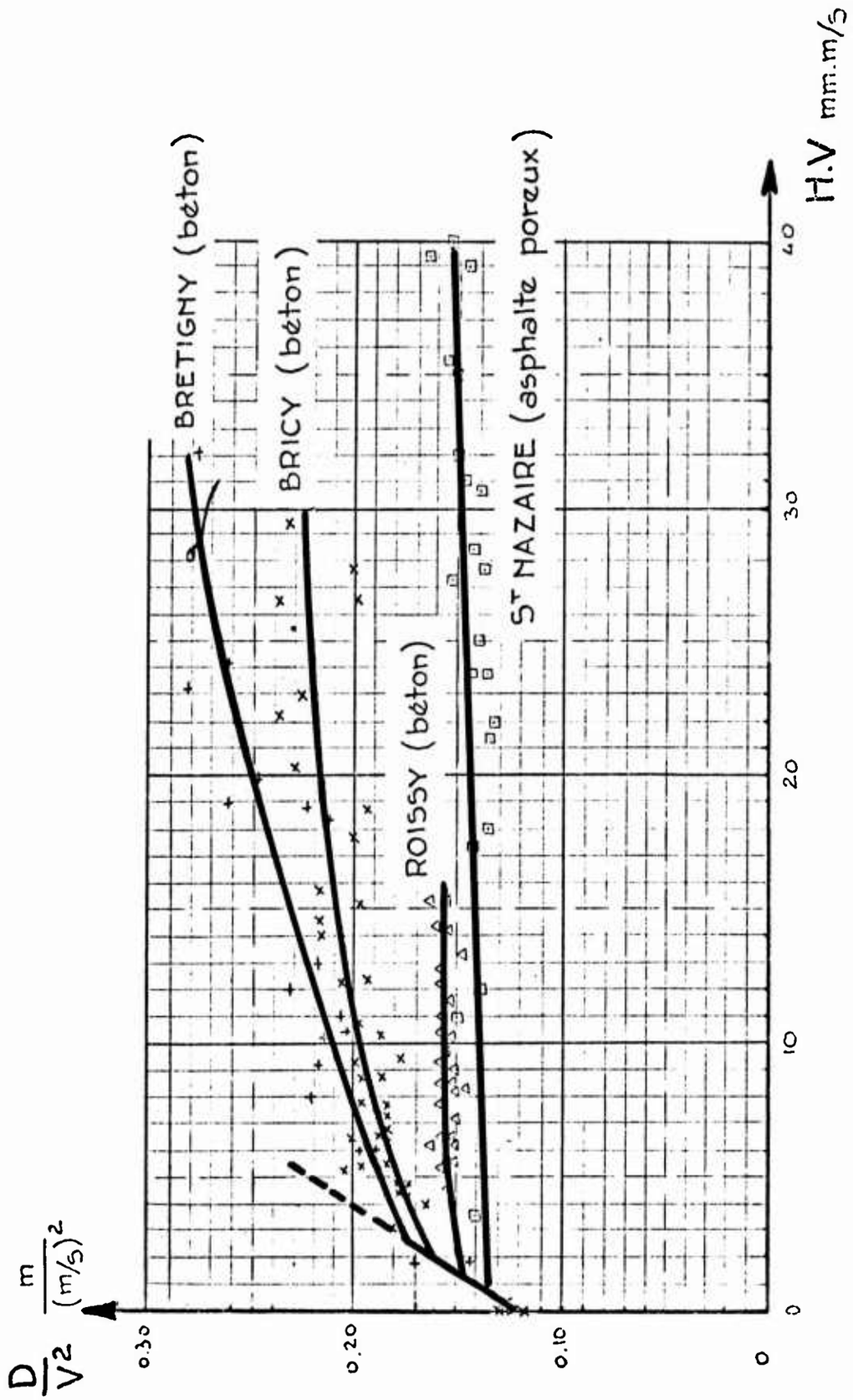

Fig.12 Essais de freinage – distances d'arrêt du DBV. Vitesse de début de freinage: 60 mph, sur les 4 pistes utilisées par la Caravelle n° 116

TRADEOFF PARAMETERS OF ALTERNATIVE TAKEOFF AND LANDING AIDS

by

Kennerly H. Digges
Chief, Mechanical Branch
AF Flight Dynamics Laboratory
Wright-Patterson Air Force Base, Ohio 45433

SUMMARY

The various aids for reducing takeoff and landing distance are discussed. The launch aids include rocket assist, catapults and powered lift. The landing aids include reversed turbojet thrust, parachutes and wheel brakes. New technology aimed at reducing the weight or increasing the performance of landing aids is indicated. The ways in which stopping distance is affected by variations in parameters such as lift coefficient, drag coefficient, reversed thrust, landing velocity and runway friction coefficient are shown.

LIST OF SYMBOLS

C_D = drag coefficient

C_{Do} = drag coefficient for a parachute based on nominal area

ΔC_{Do} = change in drag coefficient due to parachute

C_j = thrust coefficient

C_L = lift coefficient

D = drag, lb_f

D_o = nominal parachute diameter, ft

F_A = nose gear retarding force, lb_f

F_B = main gear retarding force, lb_f

FG = sea level static thrust, lb_f

Fmg = main gear load, lb_f

F_n = algebraic sum of the horizontal forces, lb_f

Fnw = nose gear load, lb_f

g = acceleration equal to 32.2 ft/sec^2

g_o = gravitational constant, ft/sec^2

L = lift, lb_f

l = distance between points on aircraft as defined in Figure 1, ft

LSD = braking distance, ft

M_{aero} = aircraft aerodynamic moment, $ft\text{-}lb_f$

M_b = maximum brake torque, $ft\text{-}lb_f$

q = dynamic pressure, lb_f/ft^2

r = radius, ft

S = wing area, ft^2

S_o = parachute area based on nominal diameter, ft^2

T = aircraft thrust, lb_f

TR = reversed thrust, lb_f

$\dot{V}$ = aircraft horizontal acceleration, ft/sec^2

V = aircraft horizontal velocity, ft/sec, knots

V_{co} = thrust reverser cut-off velocity, ft/sec

W = aircraft gross weight, lb_m

GREEK LETTERS

β = aircraft approach angle, degrees

δ_F = flap deflection, degrees

η_b = braking effectiveness

η_t = thrust reverser efficiency

μ = friction coefficient

μ_a = maximum available braking coefficient

μ_b = braking coefficient

μ_R = rolling friction

ρ = air density, lb_m/ft^3

ω = wheel angular velocity — free rolling, rad/sec

ω_b = wheel angular velocity — braked, rad/sec

SUBSCRIPTS

i = initial or design condition

o = nominal parachute area

t = condition at beginning of landing

s = condition at end of landing

INTRODUCTION

Takeoffs and landings are necessary "evils" of aircraft operation. The takeoff and landing operation is a high contributor to aircraft accidents, and is the source of weight penalties for equipment which is often useless during flight. Yet, every successful mission begins with a takeoff and ends with a landing. Indeed, the takeoff and landing performance of an aircraft becomes a critical consideration during bad weather, and during operations from bases with sub-standard runways. These conditions may exert a large influence on the design of STOL aircraft.

A variety of equipment may be used to aid the aircraft in reducing the takeoff and landing distance. Examples are: conventional wheels and brakes, parachutes and drag devices, thrust reversers, ground installed arresting gear, catapults and various types of propulsion assistance for takeoff. A study of the effectiveness of these devices requires consideration of the forces and moments exerted on an aircraft during terminal operation.

PHYSICS OF TAKEOFF AND LANDING

The forces and moments on an aircraft with conventional landing gear are shown in Figure 1, and defined in the List of Symbols. Newton's second law, applied to pure horizontal translation, gives:

$$\frac{W}{g_o}\ \dot{V} = Fn \tag{1}$$

Fn is defined as the sum of all forces acting in the horizontal direction. In Figure 1,

$$Fn = T - (D + F_B + F_A) \tag{2}$$

The value of Fn is generally dependent on a number of variables including velocity. However, in order to gain an insight into the problem, it is instructive to examine the relationship between velocity and distance for constant values of Fn.

Figure 2 is a plot derived from the well-known relationship:

$$\dot{V} = g_o\ (F_{n/W}) \tag{3}$$

The ratio (Fn/W) provides the acceleration or deceleration level in g's. The curve for a constant g level shows the distance required to decelerate from a given touchdown velocity to zero. Alternatively, it shows the distance required to accelerate from zero to a given takeoff velocity.

The curves show that touchdown and takeoff velocity affect ground roll distance significantly. Reductions in takeoff and landing velocity reduce the roll distance and also result in large reductions in thrust and braking force requirements during ground run. The force, Fn, may be made up of a variety of components which originate from a number of sources. The way in which Fn varies will be developed in the sections to follow.

LAUNCHING AIDS

Equations 1, 2 and 3 provide a basis for assessing the physics of takeoff. Referring to Equation (2), the terms in parentheses are aerodynamic drag and tire friction terms which, on the whole, tend to increase with velocity. The thrust also varies velocity. However, as a first approximation, it may be considered constant. For short, high acceleration takeoffs, the thrust term is much larger than the drag terms and the velocity dependence is less pronounced. Constant values of Fn/W may be used in Equation (3) to estimate takeoff distance when the velocity dependence of (Fn/W) may be ignored.

An examination of Figure 2 gives an insight into the takeoff problem. Consider, for example, an aircraft with a required takeoff velocity of 150 knots, and assume it has accelerating force to weight ratio (Fn/W) of 0.3. Figure 2 shows that the resulting takeoff distance is 3200 ft. Consider next, the options for reducing this takeoff distance to 2000 ft. Three options for reducing the takeoff distance are: (1) increase the thrust, (2) reduce the takeoff velocity, and (3) some combination of one and two.

The required thrust increase may be estimated from Figure 2. The figure shows that a net thrust to weight ratio of .5 would be required to uniformly accelerate the aircraft to 150 knots within a distance of 2000 ft. This additional thrust may be provided by increasing the installed power. Alternatively, it may be added through the use of launching aids such as catapults of rocket thrusters.

The selection between these two launching aids is primarily a matter of economics. Catapults have high procurement and installation costs but relatively low operating costs. Thrusters, on the other hand, have relatively low installation costs but high operating costs. For a limited number of launches from a base not normally equipped with a catapult, thrusters are more cost effective. As the number of launches from a given installation increases, the catapult installation becomes more cost effective.

The option to reduce takeoff velocity requires that takeoff lift must be developed at the reduced velocity. In the example, for a constant (Fn/W) of 0.3, the reduced velocity for a 2000 ft takeoff distance is 120 knots. This 20% takeoff velocity reduction could be achieved by a 56% increase in the wing area, lift coefficient, or the product of the two.

The combination of power and lift to reduce takeoff velocity and distance has been the subject of a number of studies in recent years. Five concepts for powered lift which have been proposed are shown in Figure 3. These concepts are:

(1) Vectored Thrust with Mechanical Flaps (VT/MF), studied in Reference (1)

(2) Externally Blown Jet Flaps (EBJF), studied in Reference (1); applied by McDonnell-Douglas on the AMST prototype

(3) Internally Blown Jet Flaps (IBJF), studied in Reference (1)

(4) Augmentor Wing (AW), experimentally studied by de Havilland; applied by de Havilland and Boeing on the C-8

(5) Upper Surface Blown Flap (USBF), applied by Boeing on the AMST prototype

Figure 4 shows untrimmed C_D and C_L (including propulsive forces) as measured in the wind tunnel for all five systems (1). The net C_L advantage for these systems is in the range of 1.5 to 2.0, which is the same range as required by the example. It is premature at this stage to select a single powered lift concept for takeoff assistance. A parametric design of a STOL Transport using Vectored Thrust with Mechanical Flaps (VT/MF) is shown in Figure 5 (1). Equal takeoff gross weight countours are shown plotted on the T/W vs W/S plane. Lines of 2000 ft landing and takeoff distances are also shown as functions of T/W and W/S. In addition, the wing loading which provided enough internal fuel tank volume to fly 3600 nautical miles at zero payload influenced the design point.

The tradeoff parameters for aircraft installed takeoff aids are extremely sensitive to the total mission requirements of the aircraft. The reader is referred to Reference (1) for an in-depth study of alternative powered lift systems for an advanced STOL transport.

GROUND ARRESTERS

Ground arresters are routinely used to aid aircraft landing on carriers. They are frequently used to arrest fighter aircraft on slippery runways and may be used as emergency overrun arresters for all aircraft. Important parameters in ground arrester design are: (1) the aircraft speed and weight, (2) the desired stopping distance and (3) the level of the decelerating force. Referring again to Figure 2, the relationship between aircraft engagment speed and stopping distance for various deceleration levels is shown. The deceleration is related to the ratio of decelerating force to aircraft weight as shown in Equation (3). Aircraft of significantly different weights, but similar landing velocities, require different levels of force to produce the same g level of deceleration. Consequently, if a ground-installed arrester is to service a variety of aircraft, its force level should be adjustable.

Other major design considerations for ground-installed arrester systems are the means for transmitting the force to the aircraft and methods for minimizing initial shock. There are relatively few places on the aircraft which will withstand the high loads which can be produced by arrester systems. The time-honored method of engaging the barrier is by the use of a tail hook which is attached to the main structure of the aircraft. The tail hook is dropped from the aircraft and engages an arrester cable which is stretched across the runway. Shock is minimized through the use of nylon lines between the arrester cable and the energy absorber. For aircraft without tail hooks, it is desirable to engage the main gear, or to distribute the load to various points in the aircraft through the use of netting.

The relationship between aircraft engagement speed and deceleration force to aircraft weight ratio is given in the Summary Figure 16. In this instance, a constant runout distance of 1000 ft was assumed.

CHARACTERISTICS OF AIRCRAFT-INSTALLED BRAKING DEVICES

The landing involves four phases as shown in Figure 6. These phases are approach, flare, transition and braking. The total landing distance includes the transition and braking distance. The transition distance includes the time period before the braking devices come into full deployment. For the purposes of the discussion to follow, only the braking distance will be considered.

Many of the decelerating forces which act during the landing roll are velocity-dependent. Typical examples of how the deceleration forces on a jet aircraft vary with velocity are given in Figure 7. The figure shows that the reversed thrust from a turbojet engine varies only slightly with velocity. For a propeller aircraft, reversed propellers would show a pronounced decrease in thrust with velocity. Parachutes, speed brakes and aircraft drag produce forces which vary with velocity as predicted by the equation:

$$D = C_D \frac{\rho}{2g_o} V^2 \qquad (4)$$

The wheel braking force, on the other hand, increases with decreasing velocity. The wheel braking force is the product of the braking coefficient and the load on the main gear:

$$F_B = \mu_b F_{mg} \qquad (5)$$

When the runway is dry, the braking coefficient, μb, is relatively insensitive to velocity. However, the force on the main gear is highly sensitive to velocity. This force increases with decreasing forward speed; that is, more and more of the aircraft weight is supported by the main gear as the vehicle slows down during ground roll.

An examination of Figure 7 shows that drag chutes are very effective at high velocity where the wheel brakes are ineffective. The forces produced by aircraft drag and the fuselage speed brake are much smaller than the parachute drag or wheel braking forces. However, they can become significant on slippery runways when the wheel braking force is reduced. The thrust force is effective down to low velocities. However, it must be terminated at some cut-off velocity due to problems which will be discussed later. Consequently, wheel braking is the only force which can be effectively employed at low velocities.

In the sections to follow, the parameters which influence the design of the various aircraft installed decelerators are discussed. Where applicable, advanced or emerging technology is indicated. In most cases, weight reduction is the objective of the emerging technology.

REVERSED THRUST

Since power is available from the engines during the landing condition, this power can be used in generating reversed thrust. Thrust reversal is accomplished by the deployment of surfaces which block the exhaust stream and change its direction of flow.

The reverser effectiveness is measured by the ratio of reversed thrust to forward thrust TR/FG and is defined by:

$$\eta_t = TR/FG \tag{6}$$

Theoretically, reverser effectiveness up to 1.0 is possible and values in excess of 0.8 have been achieved. However, high values of reverser effectiveness at low forward flight speeds tend to cause impingement and/or attachment of the exhaust gases on the engine cowling and/or fuselage. This effect also results in re-ingestion of exhaust gases, into the engine inlet. These factors are undesirable because they cause excessive heating of components and engine surge. As a consequence, it is desirable that reverse thrust not be used at low speeds. Typical values of thrust reverser effectiveness and cut-off speed are given in Table 1(2).

Although thrust reversers are very effective during landing, their weight and complexity have made them difficult to justify on high performance military aircraft. In order to make them more attractive, a thrust reverser which could provide in-flight thrust vectoring as well as landing roll thrust reversal has been suggested (2). Representative weights for this type of thrust reverser are given in Figure 8. The lower curve in Figure 8 is representative of conventional thrust reverser weight.

PARACHUTES

Landing drag chutes are a very effective means of reducing landing distance. As shown in Figure 7, the drag chute is particularly effective at high speed.

The drag force developed by the chute is given by the relation:

$$D_{chute} = C_{Do}\, q\, So \tag{7}$$

Based on the aircraft reference area, the increase in aircraft drag coefficient is:

$$\Delta C_{Do} = C_{Do} \frac{So}{S_{REF}} \tag{8}$$

where S_{REF} is generally the wing area.

The values C_D and S_o are based on, D_o, the "nominal diameter" of the parachute. Ref (3) defines nominal diameter as follows:

"The computed diameter designation of any design canopy which is equal to the diameter of a circle having the same total area as the total area of the drag-producing surface, which includes all openings in the drag-producing surface, such as slots and vents."

Two types of drag chutes are currently used by the US. They are the Ribbon and the Ring Slot chutes. Their general characteristics are listed in Table 2. Both of these chutes produce low opening shock and are similar in geometric proportions and drag production. As will be shown later, the ring slot parachute has a significant weight advantage.

The affect of parachute diameter on the weight is plotted in Figure 9. The weights shown are for lightweight construction which is generally satisfactory for parachutes deployed below 200 knots. The weight includes the parachute and its lines, but not the aircraft structure for attaching, housing and deploying the drag chute.

The affect of advanced technology on reducing parachute weight is also shown in Figure 9. The lower line in Figure 9 represents a 1955 technology ribbon-type parachute. The middle line represents a nylon ring slot parachute of improved design. The upper line projects the weight saving for a ring-slot parachute made from an advanced technology fiber. Experimental chutes made from this material have achieved a 50% weight reduction as compared to a nylon chute of similar design. This improved technology is expected to be available by 1975.

WHEEL BRAKING – DRY RUNWAYS

As shown in Figure 7, wheel braking is most effective at low speeds. However, the braking force is dependent on a number of factors other than velocity.

Five factors limit the ability of brakes to stop the airplane. These factors are the braking friction available between the tire and the runway, the torque capacity of the brake, the kinetic energy capacity of the brake, the antiskid effectiveness in combination with pilot technique, and finally, the force on the main gear.

Consider, first, the coefficient of friction on a dry runway. A tire undergoing free rolling develops a rolling coefficient of friction (μ_R). Factors which influence the rolling friction coefficient are summarized in Table 3 and examples of experimental data are plotted in Figure 10(4).

As the brakes are applied, the rolling tire is slowed down and it begins slipping relative to the surface on which it is rolling. The braking coefficient, μ, is dependent on the slip ratio. As shown in Figure 11, the slip ratio is defined as the slip velocity ($\omega - \omega_b$) written as a fraction of the free-rolling wheel angular velocity (ω). A slip ratio of 0 corresponds to a free-rolling wheel and a value of 1.0 to a locked wheel. A typical variation of μ with slip ratio is shown in Figure 11.

With brake application, the coefficient of friction rises from its free-rolling value. With the application of sufficiently high brake torque, the friction coefficient reaches its maximum value. Further increases in brake torque will then result in an unstable condition, since further increases in slip will cause the wheel to decelerate to a locked condition. The available coefficient of friction at the condition of incipient skidding is called μ_a. Because of the instability which occurs at μ_a, it is desirable to control the brake torque so that the developed friction is some value below the maximum. The actual level of coefficient developed is called μ_b. The braking efficiency is defined as:

$$\eta_b = \mu_b/\mu_a \tag{9}$$

The parameter η_b may be considered as a measure of the effectiveness of the antiskid system or of the pilot technique for brake usage. An indication of the importance of this parameter is given in Figure 17, and will be discussed later.

It should be noted that the curve shown in Figure 11 may vary greatly with velocity, runway texture, runway contamination, tire characteristics and other factors. A number of experimental studies have been conducted to determine how various factors influence μ on dry runways. Table 4 summarizes the experimental results reported in References 5 and 6.

The maximum braking force which can be developed may be limited by the maximum brake torque rather than the tire friction. The maximum brake torque which can be developed for a given brake pressure is a function of wheel speed and brake temperature. The maximum brake torque, M_b, may be related to the retarding force, F_B, by the expression:

$$F_B = M_b/r \tag{10}$$

In Equation 10, r is the rolling radius of the tire. Brakes are generally designed to produce a maximum retarding force equal to 30 to 50% of the airplane weight. For brakes designed to the 30% level, the maximum braking deceleration which could be developed would be .3g, regardless of the friction coefficient of the runway. Recent trends have been toward brakes with higher torque capacities.

It is also possible for brakes to be energy-limited. Absorbing excessive energy without allowing the brake to cool can result in a fade in the torque capacity as well as overheating of the brake components. The most dramatic recent technology advancement in brakes has been the use of carbon and beryllium to achieve the necessary energy capacity at a significant weight reduction. Figure 12 shows a weight comparison between conventional steel brakes and advanced brakes using beryllium or carbon. The comparison shows a brake weight advantage in the order of 40% for the advanced materials.

The final factor which influences wheel braking force is the vertical force on the main gear. Referring to Figure 1, it is evident that the force on the main gear, Fmg, may be determined by taking moments about the nose gear. The result is:

$$Fmg = \frac{1}{\ell_{xmg}} \left[M_{aero} + \ell_{xCG} \cdot (W - L) + \ell_{zCG} \cdot \left(D - T + \frac{W}{go} \cdot \dot{V}\right)\right] \tag{11}$$

The manner in which Fmg contributes to aircraft deceleration may be shown by applying Newton's second law in the horizontal direction.

$$Fn = T - (D + \mu_b Fmg + \mu_R Fnw) \tag{12}$$

A conclusion which can be drawn from Equation (12) is that positive terms tend to increase braking distance while negative terms tend to reduce it. For effective wheel braking, it is desirable for the term ($\mu b \cdot$ Fmg) to become large). Consequently, the manner in which the main gear is loaded during the braking distance influences the decelerating force developed by the brakes.

Referring next to Equation (11), the terms which influence the force on the main gear may be examined. Positive terms in Equation (11) increase main gear load while negative terms cause a reduction in main gear load. For the purposes of this discussion, the linear dimensions in Figure 1 and Equation (11) are constants. A summary of the effect of the variable terms on main gear load (Equation 11) and on braking distance (Equation 12) is given in Table 5.

A plus sign in Table 5 indicates a beneficial effect while a minus sign represents a detrimental effect. It is evident from the data presented in Table 5 that effective braking is enhanced by devices which decrease lift and increase drag during the landing run. Spoilers act in this manner. Flaps also act to increase drag, but their main function is to increase lift which is detrimental to braking. Zalovcik (7) examined the tradeoffs associated with the use of flaps, spoilers, and elevators during landing. Typical results of his study are shown in Table 6.

Table 6 summarizes how the contribution of drag, moment and lift change when elevators are raised, flaps are extended, or spoilers are raised. A plus sign indicates the contribution increases deceleration. The contribution of spoilers is beneficial to both the drag term and the Fmg term. These devices act to increase drag and decrease lift without major changes in the aerodynamic moment.

With regard to flaps, the increase in drag is offset to some extent by the increase in lift. The increase in lift reduces the wheel braking force available. However, on wet or slippery runways, the drag force developed by the flaps may exceed the braking force which can be developed by the wheels. Consequently, a flaps-down landing would provide minimum stopping distance at low values of μ_a while flaps-up would provide minimum stopping distance at high values of μ_a. Zalovcik found that flaps-down resulted in minimum stopping when:

$$\mu_a = \frac{1}{\eta_b} \frac{\Delta C_D}{\Delta C_L} \tag{13}$$

Raising elevators provides an upward rotation to the nose of the aircraft. This rotation increases the drag and the load on the main gear. Both of these factors tend to reduce stopping distance. Illustrations of the effect of elevators and flaps on main gear loads are shown in Figure 13. The condition of flaps-up and elevator-down gives the highest load on the gear and results in the shortest stopping distance on dry runways. With flaps-down, the elevator is less effective, and lift generated by the flaps, greatly reduces the load on the main gear.

From a practical standpoint, there are a number of factors which mitigate against using the minimum distance solution of flaps retracted and elevators up during braking. The first is economics; that is, the use of available drag is the cheapest way of stopping an aircraft. Consequently, flaps-down landing is more economically attractive. The second is control; that is, the ability to control an aircraft at the optimum nose-high attitude becomes considerably more difficult than in the nose-down condition. Moreover, loading of the nose gear is beneficial in providing steering and lateral control. Positive nose wheel control is particularly critical on a slippery runway.

The influence of flaps and elevators is of course highly configuration-sensitive. A number of configurations are described in Reference 5, along with the stopping distance associated with various control techniques. From a stopping distance standpoint, techniques which develop maximum drag with negative lift, such as spoilers, are desirable.

WHEEL BRAKING – CONTAMINATED RUNWAYS

The primary result of contaminated runways is a reduction in the available friction coefficient. This reduced friction has an influence on both the braking coefficient μ, and side or cornering friction coefficient. As a consequence, braking is less effective and skidding occurs at lower magnitudes of side force.

Considerable effort has been expended on developing and evaluating runway surfaces which retain high friction coefficients when wet. The results of some of these studies are reported in Reference 8.

Typical test results of aircraft braking tests on various surfaces are shown in Figure 14. These tests verify the benefit of pavement grooving for wet runway traction. Grooved pavements are in service on a number of runways in the US. A more recent approach to improved pavements has been the coarse, open textured pavement which has been tested both in the UK and US. This pavement has the high friction when wet and has the benefit of being more economical to apply, particularly when resurfacing of the existing pavement is required.

The effect of tire tread design and aircraft velocity on the coefficient of friction is presented in Figure 15. These test results show that the circumferential ribbed tires which are now in wide use provide significantly better traction than the older diamond or dimple tread tires.

An estimate of the additional improvement which might be expected by cross-grooving the tire tread is shown by the dashed line in Figure 15. The difficulty with cross-grooving is its detrimental effect on the strength of the tire tread. At the present time, cross-grooved tires have been tested for traction but have not been developed to the point where they possess adequate tread retention characteristics. It is anticipated that these improved traction tires will be developed by the 1975 time period.

CONCLUSIONS

A summary of the relative magnitudes of deceleration forces produced by various sources is shown in Figure 16(7). Referring to Figure 16, the cross-hatched area around the symbol † shows the range of the force level at touchdown. A similar cross-hatched area is shown around the symbol S to represent the force level at rest. The mean deceleration force falls somewhere between these two variables.

The effect of various decelerators on stopping distance is shown in Figure 17(7). In this case, stopping distance is plotted against the maximum available braking coefficient μ_a for braking efficiencies, η_b, of 1.0 and 0.5. The figures show that reversed thrust is particularly valuable in reducing stopping distance on slippery runways. For this study, it was assumed that reversed thrust was applied until the aircraft reached zero forward velocity.

A comparison of the graph for $\eta_b = 1.0$ with the graph for $\eta_b = 0.5$ gives an insight into the importance of the brake control system in reducing stopping distance. Antiskid systems are designed to function in the pitot technique and/or range between the braking effectiveness shown in the two plots.

Figure 18 summarizes a parametric variation of the factors which influence landing distance for a fighter aircraft (2). The base condition for this parametric analysis is a normal braked landing on a dry, hard surfaced runway without drag chutes or reversed thrust. This base point design is designated by the Subscript i. The base conditions at the design point i are:

$C_{Di} = .098$	$LSD_i = 3{,}042$ ft
$\mu i = .3$	$W = 11{,}500$ lb
$C_{Li} = .17$	$V_{co} = 40$ knots
$Vi = 150$ knots	$\eta_t = .5$

The curve shows that a change in landing velocity has a pronounced influence on stopping distance. For example, a 10% change in landing velocity results in a corresponding 10% change in landing distance. Similar results were obtained earlier in this paper when reference was made to Figure 2.

The application of thrust reversers is also a very effective means of reducing stopping distance. Development of a reversed thrust equal to 20% of the gross weight would reduce the stopping distance by 40%. To gain this same improvement using wheel braking, it would require an increase in μ by a factor of 1.8. Using drag to gain the same improvement would require an increase in C_D by a factor of 5.82. This could be done by providing a drag chute whose area is approximately equal to the wing area.

Figure 16 also shows the detrimental effects that increases in C_L have on aircraft stopping distance. For the example discussed earlier, the increase in C_L which was required for reducing the takeoff distance would be detrimental if it existed during landing roll. Tradeoffs between devices which increase both lift and drag can be compared by determining the net effect of increase in drag vs the increase in lift. At the same time, the weight charts presented in Reference (2) and in the text of this paper provide a comparative indication of the weight penalties of alternatives such as drag chutes and thrust reversers.

Considerable advanced technology aimed at reducing the weight and increasing the effectiveness of deceleration aids is currently under development. Any future aircraft design should take advantage of these developments when selecting between alternative takeoff and landing aids.

LIST OF REFERENCES

1. "STOL Tactical Aircraft Investigation", AFFDL-TR-73-21, May 1973

2. "Methods for Evaluating the Effectiveness and Weight of Aircraft Deceleration Devices", H. Greiner & J. H. Hilbig, Technical Report ASB 68-13, June 1968

3. "Performance of, and Design Criteria for Deployment of Aerodynamic Deceleration", ASD TR 61-579, December 1963

4. "Rolling Resistance and Carcass Life of Tires Operating at High Deflections", P. Skele, AFFDL-TR-70-138, February 1972

5. "Mechanical Properties of Pneumatic Tires with Special Reference to Modern Aircraft Tires", Smiley & Horne, NASA TR R-64, 1960

6. "Influence of Tire Tread Pattern and Runway Surface Condition on Braking Friction and Rolling Resistance of a Modern Aircraft Tire", Horne & Leland, NASA TN D-1376, September 1962

7. "Ground Deceleration and Stopping of Large Aircraft", Zalovcik, AGARD Report 231, October 1949

8. "Pavement Grooving and Traction Studies", NASA SP-5073, Conference at Langley Research Center, November 1968

TABLE 1 – THRUST REVERSER CHARACTERISTICS

A/C TYPE	THRUST REVERSER EFFECTIVENESS	CUTOFF SPEED (KNOTS)
Commercial Turbojet	.4	50
Commercial Fanjet	.6	20
Military	.6	20

Ref (2)

TABLE 2 – DECELERATION CHUTES

CANOPY TYPE	C_{Do}	OPENING SHOCK FACTOR
Ribbon	.45 to .55	1.00
Ring Slot	.45 to .65	1.05

Ref (3)

TABLE 3 – FACTORS WHICH INFLUENCE ROLLING FRICTION

Deflection	Increases
Vertical Load	Decreases (With Deflection Constant)
Velocity	Increases
Tire Pressure	Decreases (With Deflection Constant)
Tire Temperature	Slight Decrease

Ref (4)

TABLE 4 – FACTORS WHICH INFLUENCE BRAKING FRICTION ON DRY RUNWAYS

FACTOR	EFFECT ON μ_b
Vertical Load	Decrease
Velocity	None
Tread Compound	Slight
Tire Construction	Slight
Tire Inflation	Slight Decrease
Tire Temperature	Slight Decrease

TABLE 5 – FACTORS WHICH INFLUENCE DECELERATION FORCE ON MAIN GEAR

TERM	EFFECT ON Fmg	EFFECT ON DECELERATION
Aero moment	+	Indeterminate
L	–	–
D	+	+
Reversed Thrust	+	+

TABLE 6 – EFFECT OF AIRCRAFT DRAG DEVICES ON DECELERATION & FORCE ON MAIN GEAR

	DRAG	NET WHEEL LOAD		
	Drag	Aero Moment	–Lift	Net Influence on Deceleration
Raising elevators	+	+	+	+
Extending flaps	+	+ or –*	–	+ or –**
Raising spoilers	+	+ or –*	+	+

* depends on configuration

** minus above some value of μ_a

Ref (7)

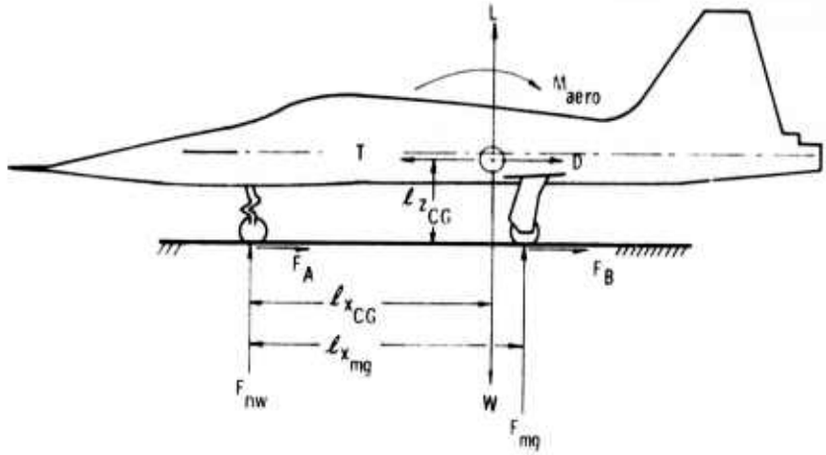

FIGURE 1. FORCES AND MOMENTS FOR GROUND OPERATIONS

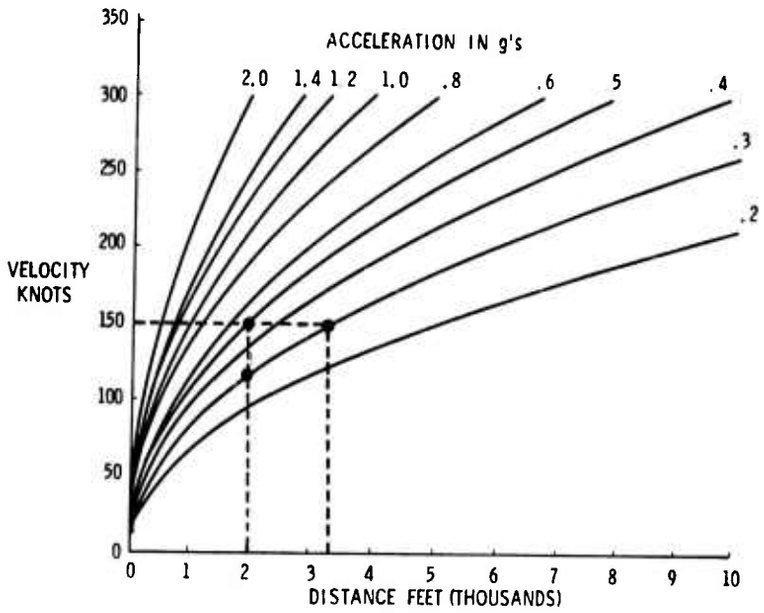

FIGURE 2. DISTANCE vs VELOCITY FOR CONSTANT ACCELERATION

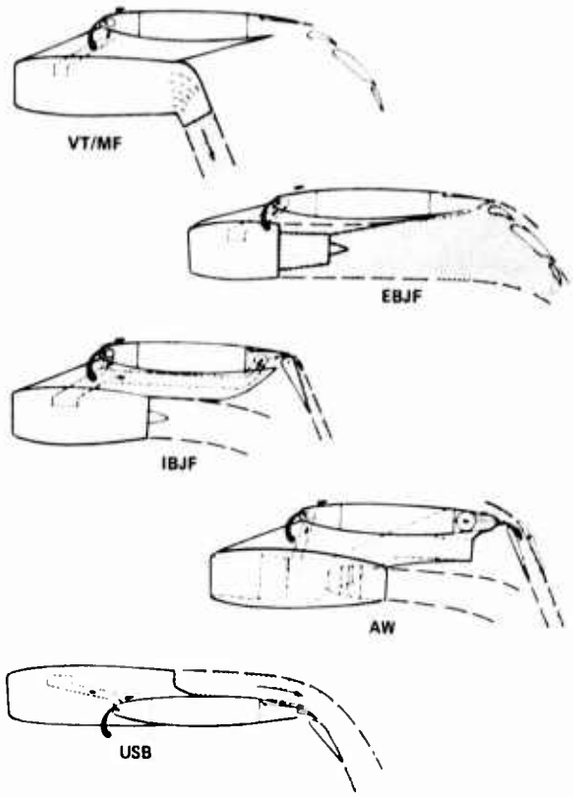

FIGURE 3 POWERED LIFT STOL CONCEPTS

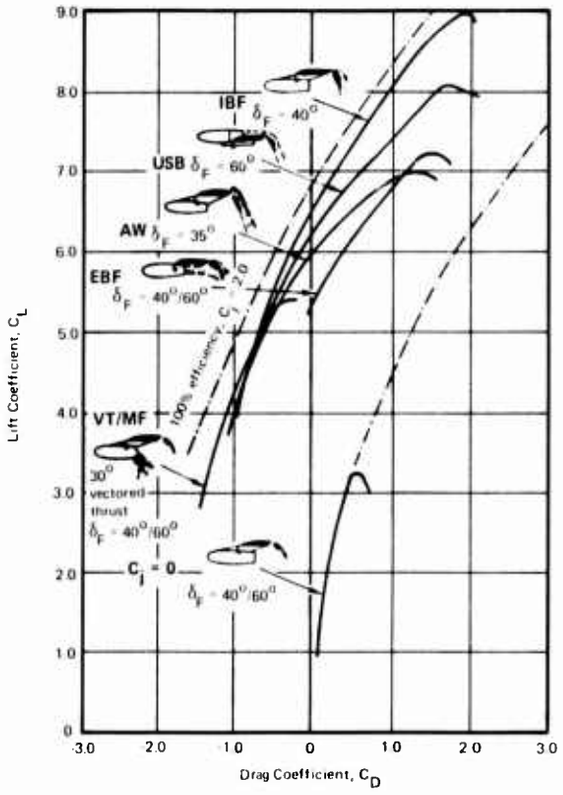

FIGURE 4 DRAG POLARS FOR POWERED-LIFT CONCEPTS

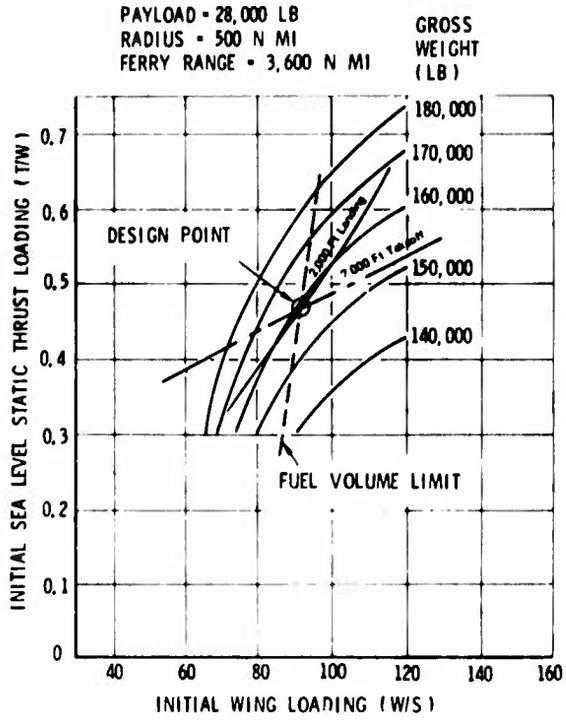

FIGURE 5 PARAMETRIC DESIGN STOL TRANSPORT

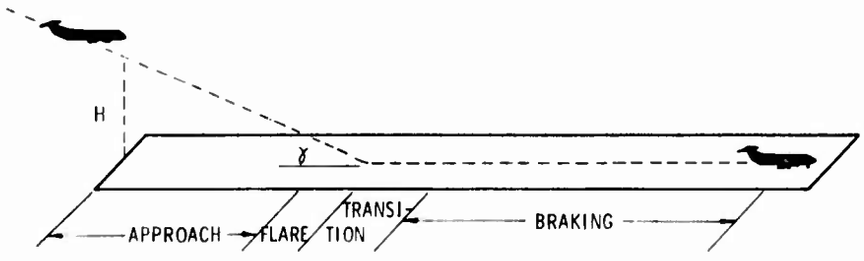

FIGURE 6. LANDING SEGMENTS

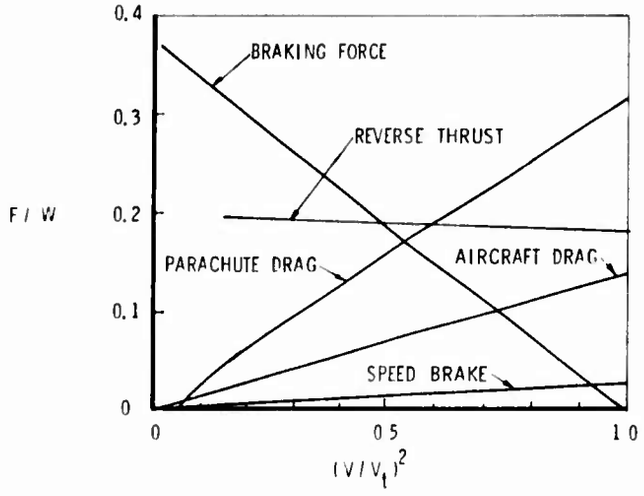

FIGURE 7. VELOCITY DEPENDENCE OF DECELERATION FORCES

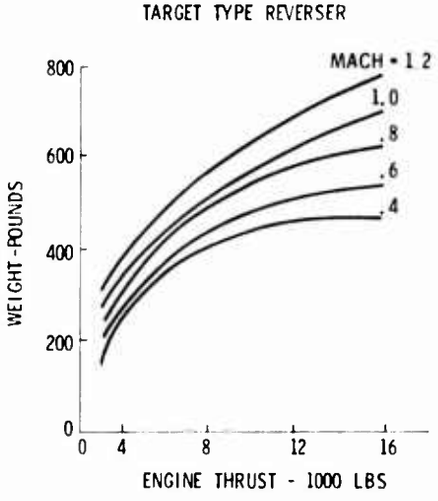

FIGURE 8 WEIGHT OF THRUST REVERSERS

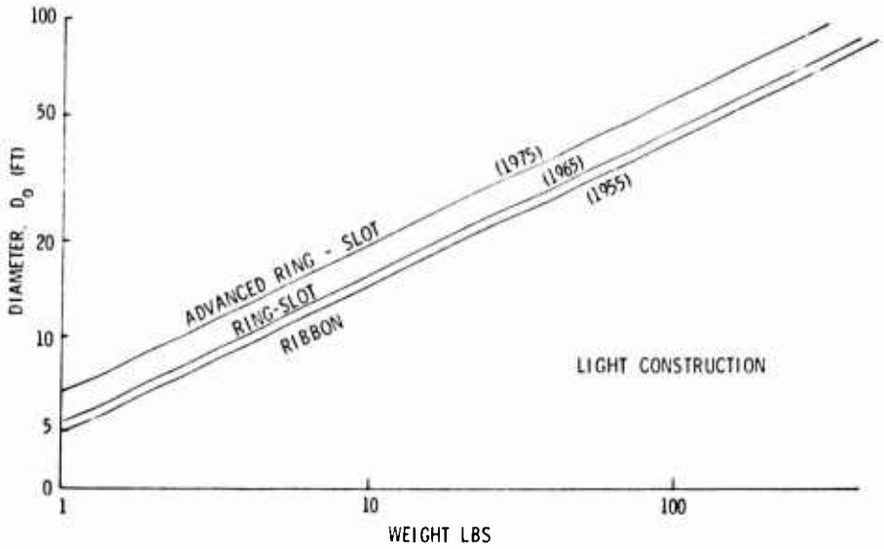

FIGURE 9. PARACHUTE WEIGHT vs DIAMETER

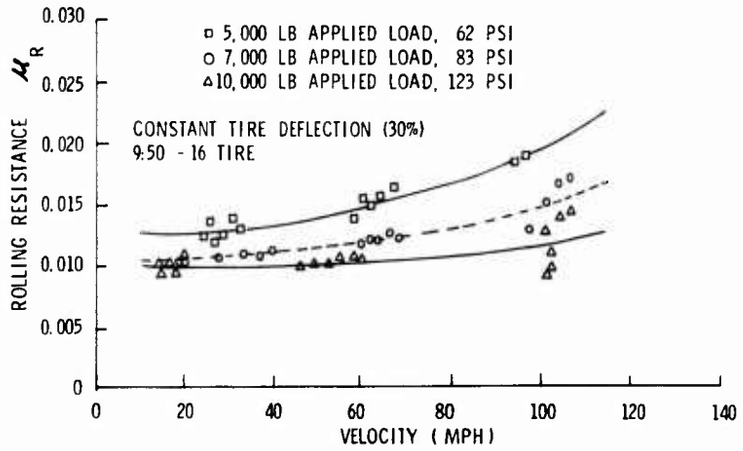

FIGURE 10. ROLLING FRICTION VS VELOCITY

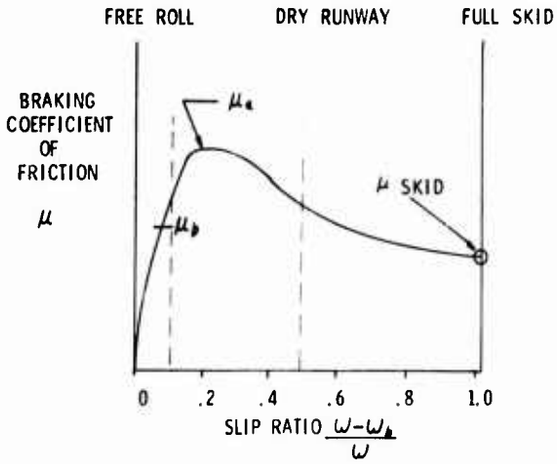

FIGURE 11 BRAKING FRICTION vs SLIP RATIO

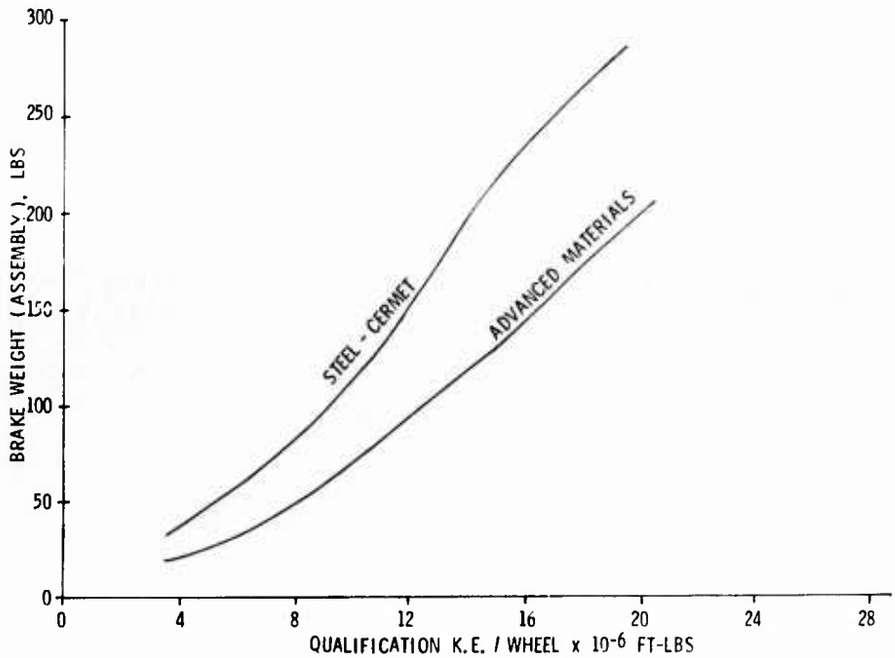

FIGURF 12. WEIGHT OF BRAKE vs KINETIC ENERGY CAPACITY

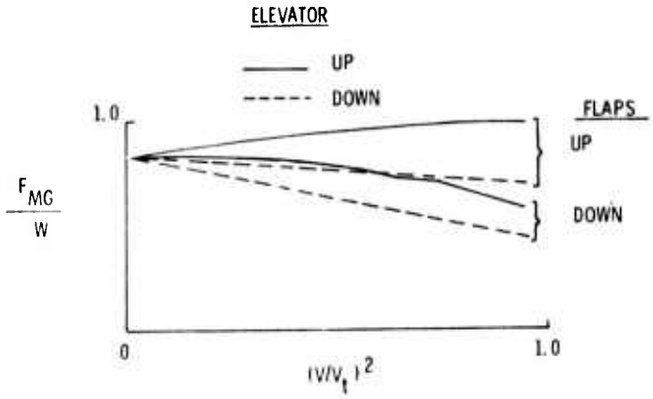

FIGURE 13. EFFECT OF FLAPS & ELEVATORS ON MAIN GEAR LOADS

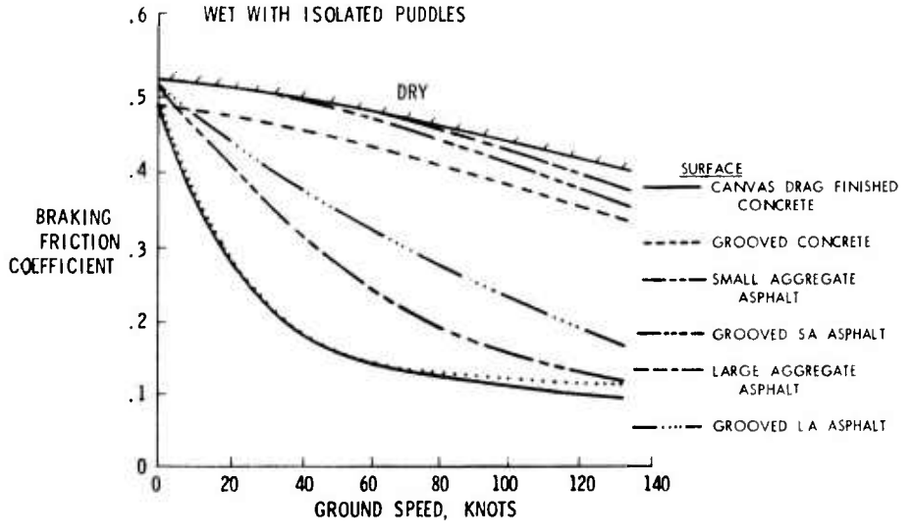

FIGURE 14 FRICTION OF RUNWAY SURFACES

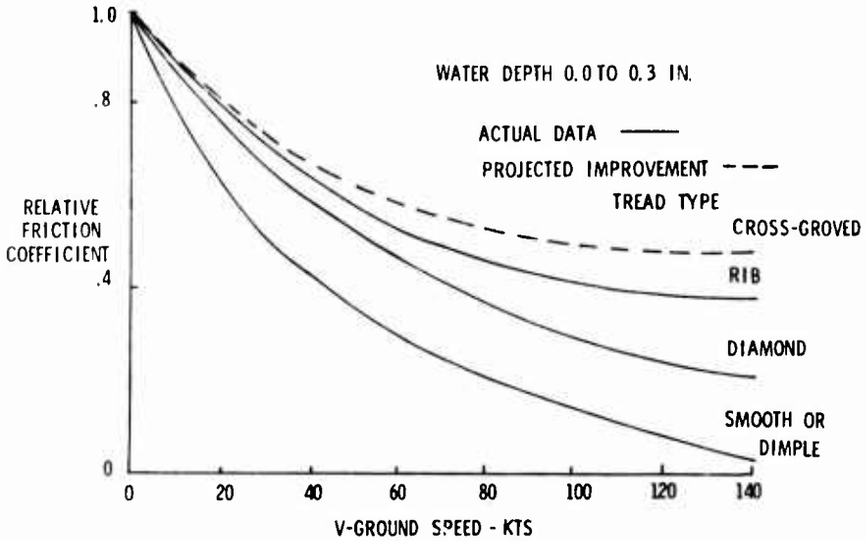

FIGURE 15. EFFECT OF TREAD AND VELOCITY ON WET RUNWAY TRACTION

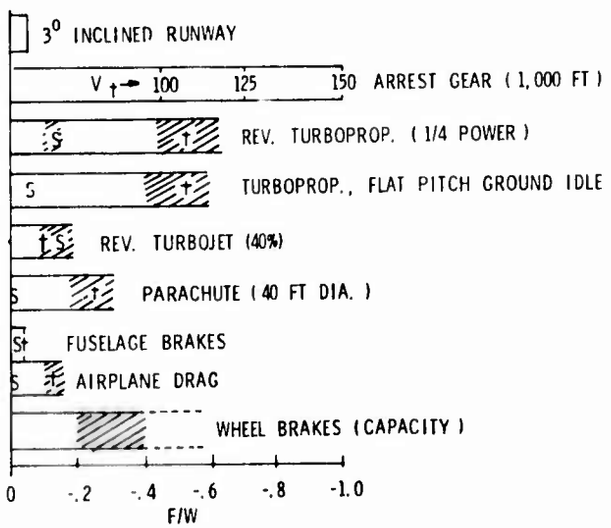

FIGURE 16. APPROXIMATE MAGNITUDE OF DECELERATION FORCES

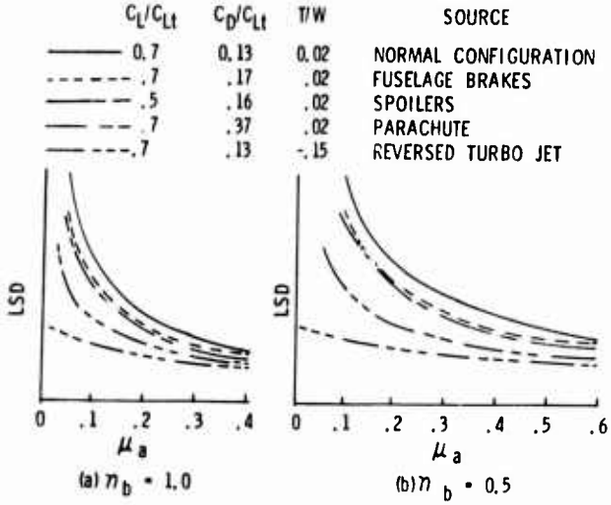

FIGURE 17. STOPPING DISTANCE AS AFFECTED BY VARIOUS SOURCES OF DECELERATION

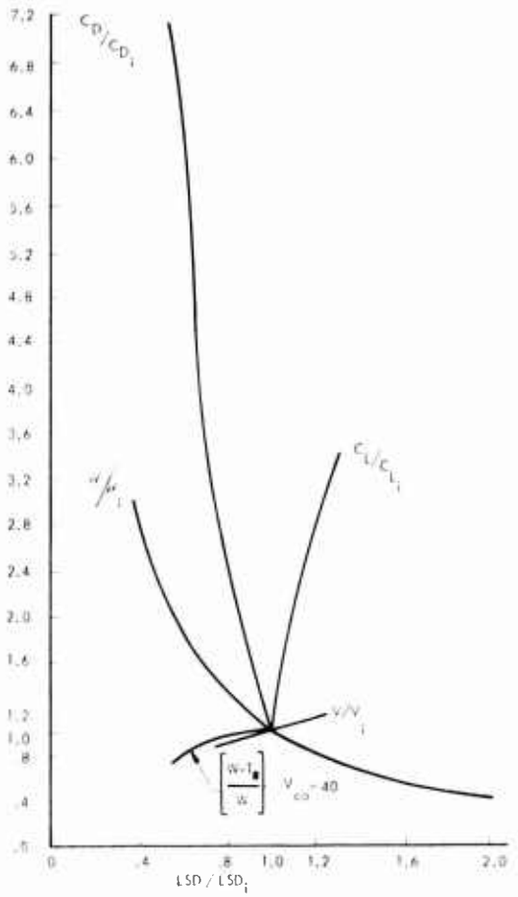

FIGURE 18 SENSITIVITY OF LANDING DISTANCE TO VARIOUS PARAMETERS

A TECHNIQUE FOR ANALYSING THE LANDING MANOEUVRE

R F A KEATING, ROYAL AIRCRAFT ESTABLISHMENT, BEDFORD, ENGLAND.

SUMMARY

Recent RAE studies of steep gradient aviation have highlighted the need to find the underlying piloting strategy of landings. A graphic presentation of landing records is put forward which, it is hoped, will assist in the solution to this problem. By expressing the pilot's longitudinal control activity as equivalent speed and climb rate demands, it is possible to plot simultaneously the aircraft motion and the control strategy against the performance chart as a reference grid. By suitable choice of axis scaling, the aircraft's response to simple control input traces out simple geometric patterns such as circular arcs.

Examples are given of flight data, principally of the HS 125 in normal, steep and two segment approaches. Power margins and target speeds are discussed for these examples.

LIST OF SYMBOLS

C_L	lift coefficient
C_D	drag coefficient
D	drag } relative to flight path
L	lift } relative to flight path
g	acceleration due to gravity
$\dot{H}$	rate of climb, time differential of height (normal units are feet per minute)
V	airspeed, usually in knots
T	thrust of engines
α	angle of incidence
γ	flight path angle
η	angle of elevator
θ	angle of pitch attitude

SUFFICES

e	equilibrium condition
0	initial condition
D	demanded condition
a	a typical condition

ABBREVIATIONS

EAS	equivalent air speed
IAS	indicated air speed (uncorrected)
ASI	air speed indicator
VASI	visual approach slope indicator
ROD	rate of descent usually in feet per minute
RPM	revolutions per minute of engine
FLT 123	flight number 123
FLT 12345	landing 45 of flight number 123

SPECIAL SPEEDS

V_{TD}	target touchdown speed
V_{AT}	target threshold speed
V_{APP}	target approach speed
V_S	stalling speed from aerodynamic measurements

1 INTRODUCTION

RAE are currently investigating steep gradient aviation using a prop-jet transport aircraft, an executive jet and, later this year, a large jet airliner. The object of the programme is not only to collate statistics and pilot opinions but to derive and record suitable control strategies for steep gradient approaches. With nearly 2000 landings already completed the analysis presents a problem. 'Spot values' such as, maximum g in the flare are easy enough to handle statistically and do provide some useful data. But the crucial problem of the analysis is to find representative 'good' landings and identify the underlying piloting strategy. This problem can only be solved by studying and understanding the complete combination of pilot, controls and response of the aircraft to control inputs. There are two fundamentally different ways in which one might expect the aircraft to be controlled during the landing manoeuvre. One is to visualize the pilot as a continuously operating automatic controller, closing a relatively tight feed-back loop. The other is to view the operation as an essentially open-loop, ie as a precognitive, wherein the pilot uses relatively infrequent (in extreme, only one) simple step type inputs or programmed control sequences which experience has taught him leads to the desired end result. Of these concepts, the former would have the attraction of having available for analysis a rigorous theoretical framework, that of automatic control theory. Although modelling the human pilot as a servo-controller has led to useful results in many areas of aircraft control, notably when the tracking of moving targets has been involved, the analysis of manual landing control has so far defied this approach. This is perhaps an indication that the pilot controls the preparatory phase and even part of the flare in open-loop fashion. However strongly intuition may attract one to this view, the systematic study of open-loop control has

always been frustrated by lack of a suitable theoretical concept. Traditionally the analysis of such situations has been restricted simply to visual inspection of flight records without any coordinating principles.

In this paper a method of graphically presenting landing records is given which it is hoped will materially assist in this purpose. By expressing the pilot's longitudinal control activity as equivalent speed and climb rate demands it is shown to be possible to plot simultaneously the actual aircraft motion and the control strategy against the performance chart as a reference grid. The interpretation and analysis of the data presented in this form is further aided by the fact that, if a particular scaling is chosen, the open-loop response to simple control inputs traces out simple geometrical patterns such as circular arcs.

Examples will be given of flight data principally of the HS 125 in normal steep and two-segment approaches.

2 PRESENTATION OF DATA

Although the technique put forward in this paper is simple to use numerically, a number of unfamiliar concepts are involved. These concepts are discussed in this section and then tested experimentally for a controls-fixed phugoid, which it is suggested is the principal response made relevant to flares, before dealing with real landings.

2.1 PERFORMANCE CHARTS AND EQUILIBRIUM STATES

The essence of the proposed method of landing control analysis rests on the observation that it is possible to map the time history of a landing manoeuvre onto the $\dot{H}$ - V plane, ie in the plane in which aircraft performance data are also presented. By suitable simplifying assumptions it is also possible to present in the same diagram the pilot's control activity in terms of equivalent performance demands.

A typical performance chart is shown in Fig 1, where steady state flight path angle γ is plotted against airspeed, with incidence α and throttle setting as parameters. In addition a number of conditions of special relevance to landing control are indicated, namely :

i. the boundary for stick-shaker operation

ii. the target threshold speed V_{AT} (here, $V_{AT} = 1.3\ V_s$)

iii. the 3° glide slope

iv. the approach speed, which equals V_{AT} + 10 knots in this case

v. the target touchdown speed V_{TD} usually V_{AT} - 10 knots.

In practice the numerical data will be influenced by such parameters as aircraft weight, altitude and outside air temperature. Each point in this chart uniquely defines an equilibrium flight condition which will establish itself for a given control setting, ie for a given combination of throttle and elevator angle. The latter control parameter is here represented by the equivalent angle of incidence α. One advantage of this device is that it removes CG position as a variable. Hence we can interpret each point on this chart either as an actual equilibrium flight condition $\dot{H}_e$, V_e or as a demanded flight condition $\dot{H}_D$, V_D defined by the associated control state (α, throttle).

If at a given instant in time the actual flight state and the control demand state coincide the aircraft is in steady equilibrium and will remain in this condition, ie it will continue on the existing glide path angle γ_0 and at the existing speed V_0. If the controls are moved away from this equilibrium state there will now exist a difference between the actual flight state and the demanded equilibrium state. The flight condition cannot remain steady and the aircraft will try to acquire the new demanded state. In the next section we shall show that the natural aircraft response to such a demand - ignoring the short period pitching mode as a closed inner loop - takes effect via the phugoid mode and that the response can be mapped onto the $\dot{H}$ - V plane as the simplest possible geometric shape, namely a circle. This feature will be utilised as the central principle for the analysis or synthesis of landing flare manoeuvres.

2.2 RESPONSE TO DISTURBANCES FROM EQUILIBRIUM

Ignoring the pitch oscillation as an inner loop by restricting the discussion to medium and long term response, the aircraft longitudinal motion is defined by the two equations[1]

$$m\dot{V} = T \cos \alpha - D - mg \sin \gamma \qquad (1)$$

$$mV\dot{\gamma} = T \sin \alpha + L - mg \cos \gamma \quad . \qquad (2)$$

In steady flight with $\dot{V} = \dot{\gamma} = 0$ we obtain equilibrium from

$$0 = T_e \cos \alpha_e - D_e - mg \sin \gamma_e \qquad (3)$$

$$0 = T_e \sin \alpha_e + L_e - mg \cos \gamma_e \quad . \qquad (4)$$

Subtracting (3) and (4) from (1) and (2) and linearizing for small displacements and restricting the analysis to small γ, we obtain the differential equations

$$\dot{V} = g(\gamma_e - \gamma) - (D_e/m)(2\Delta V/V_e)$$

$$V\dot{\gamma} = (L_e/m)(2\Delta V/V_e)$$

where $\Delta V = V - V_e$. Substituting $\dot{H} = V\gamma$ and $L_e/m \doteq g$ we get

$$\dot{V} = (g/V_e)(\dot{H}_e - \dot{H}) - 2(g/V_e)(C_D/C_L)(V - V_e) \qquad (5)$$

$$\ddot{H} = 2(g/V_e)(V - V_e) \quad . \qquad (6)$$

These equations define the small perturbation response in $\dot{H}$ and V of the aircraft disturbed from an equilibrium state (V_e, $\dot{H}_e$). This equilibrium state is of course identical to the demanded flight state V_D and γ_D defined in the previous section. The solution of equations (5)-(6) is the phugoid, ie a periodic and normally damped oscillation in $\dot{H}$ and V. The amplitude of $\dot{H}$ is equal to $\sqrt{2}$ times that of V, and $\dot{H}$ lags V by approximately 1/4 period as shown in Fig 2. This mode maps onto the $\dot{H}$ - V plane as a spiral centred on $\dot{H}_e$, V_e as the equilibrium state if the scale are so chosen that units in $(\dot{H}/\sqrt{2})$ and (V) are equal. If in equation (5) the drag terms are ignored, the result simplifies to an undamped sinusoid which projects as a circle in the $\dot{H}$ - V plane. In the application to the analysis of the landing flare manoeuvre we shall find that one is only interested in response corresponding to less than 1/4 of a phugoid period. If the method is used for a qualitative analysis, the circle can then be taken as an adequate approximation to the spiral and hence to the true response. For more accurate work and/or when dealing with an exceptionally well damped phugoid a portion of the relevant spiral ought to be used.

We have already seen in section 2.1 that it is possible to plot in the $\dot{H}$ - V plane the actual aircraft motion state $\dot{H}$, V and by regarding elevator (or incidence) and throttle position as the equilibrium performance $\dot{H}_e$, V_e, we can show equivalent control demands also. We shall represent the former by the symbol ● and the latter by the symbol ✖. It is obvious that if the demand ✖ and actual state ● coincide the aircraft is in steady equilibrium flight and will remain so until disturbed. The time history collapses into a point. However if at any instant in time, control demands do not coincide with the actual flight state - say as a result of the pilot's elevator or throttle movements - the aircraft will respond in such a way that the response follows a spiral in the $\dot{H}$ - V plane, the initial flight state $\dot{H}_0$. V_0 forming the initial condition of the spiral which centres on the demanded state $\dot{H}_D$, V_D.

2.3 RESPONSE TO CONTROL DEMANDS

We shall now consider the effects of some basic control inputs.

i. Elevator control. We have indicated that elevator control can be equated with a demanded incidence α and this in turn equates with a speed demand V_D. Fig 3a illustrates the case when the aircraft was originally in equilibrium flight at $\dot{H}_0$, V_0 and the pilot now applies a step demand in aft elevator, ie a demand for a speed reduction to V_D. An approximation to the aircraft response is obtained by drawing a circle centred on $\dot{H}_D$, V_D as the new equilibrium state and passing through $\dot{H}_0$, V_0 the initial flight path state. We observe that, as expected the initial response is an increase in climb rate which then leads to a speed reduction. It will be noted that the speed demand (strictly α demand) also involves a small change in $\dot{H}_D$ since we must follow a locus of constant throttle in the performance chart, Fig 1.

ii. Throttle control. The throttle controls vertical velocity as an equilibrium state and the response to a throttle reduction will therefore appear as in Fig 3b, ie as an initial speed reduction followed by an increase in sink rate or a reduction in climb rate.

iii. Simultaneous throttle and elevator control. If the two control demands considered above are combined the response in Fig 3c results, combining of course the features of the responses considered individually above.

One of the disadvantages of this presentation is that by plotting $\dot{H}$ against V, time has been lost as a parameter, which may be reintroduced by marking a time scale against the motion trace. In this context it is useful to consider that equal time intervals are associated with equal rotation angles and that a full revolution clearly corresponds to a full phugoid period or 90° to 1/4 phugoid period. The phugoid period itself will be a function of airspeed and a very crude approximation[2] is to take the airspeed in miles per hour and divide by five to obtain the period in seconds.

So far we have considered simple step demands in control and it was shown that these lead to responses which map particularly simply in the $\dot{H}$ - V plane, ideally to sections of a circle. We shall also be interested in situations when control is changed continuously, ie the general case when both $\dot{H}_e$ and $\dot{V}_e$ are themselves functions of time and trace out a line in the $\dot{H}$ - V plane. The concepts developed can still be used if we build the response in a step-by-step procedure, say for example at intervals of one second. Fig 4 gives an example for an aircraft with a phugoid of 30 second period, when one second corresponds to 12° rotation, damping being allowed for by the use of right-angled triangles instead of arcs. It is quite obvious that when control is changed continuously the present method becomes less attractive than in situations where the pilot applies control in a few discrete steps.

It should be noted that this method is equally suitable for synthesis and analysis of landing manoeuvres. It can be used to identify pilot control strategy in actual landings and judge their usefulness and efficiency. On the other hand it can be used to derive theoretically control strategies which lead to a desired result.

2.4 RESPONSE TO GUSTS

The aircraft motion is not only changed by the pilot's control activity, but it may also be affected by gusts and wind shears. It would be interesting to see how gusts will affect the trajectory of aircraft motion in the $\dot{H}$ - V plane. So far we have noted that the trajectory in the $\dot{H}$ - V plane of the aircraft flight state affected only by pilot control is continuous and progressive. Steps in control applied lead only to step

slope changes in aircraft response, ie discontinuous slopes. Gusts on the other hand appear as jumps in the aircraft state locus and are therefore easy to recognise.

A sudden fore and aft gust will change the airspeed by an equivalent amount and if pilot control is not changed at the same time we get a response as illustrated in Fig 5a. Wind shear can be represented similarly as a change in the fore and aft wind component, normally of course as a reduction of airspeed.

The representation of vertical gusts requires some caution as the result depends on the chosen reference frame. In flight testing we will normally derive flight path angle γ and hence $\dot{H}$ from measurements of α and θ. The flight path angle so derived is thus related to the air and not to space. (The answer would obviously be different if $\dot{H}$ were measured directly with reference to the ground, say from a radio altimeter or by kine-theodolites). In the former case an up-gust would cause an apparent dive and the response would then appear as in Fig 5b. The demanded state would here remain unchanged. In a space oriented reference frame, on the other hand, the equilibrium response to an upgust would be an increase in climb rate, the gust would cause an apparent change in demand.

2.5 FLIGHT RESULTS

The method advanced in this paper is intended primarily to assist in the analysis of flight records of landing manoeuvres. Above we have shown by theoretical argument that aircraft response and control inputs can be uniquely related in this presentation. To demonstrate that the ideas developed there do in fact conform to real life, in Fig 6 two manoeuvres recorded on the HS 125 are presented. One is a phugoid which is seen to trace out the expected spiral converging on $\dot{H}_e = 0$ and $V_e = 114.5$ knots as the equilibrium condition. The other is a response to a step elevator (incidence or speed demand) demand which again is seen to trace out the initial portion of the spiral. It will be noted that this manoeuvre was rather extreme as the demanded incidence was beyond the stick shaker limit throughout. The aim of that particular manoeuvre was to find the limiting response which would give a period of near-level flight. This represents the hardest flare possible at the most extreme throttle setting and as expected lies at lower speeds than the target threshold speed V_{AT}.

3 ANALYSIS OF LANDINGS

The method outlined above has been developed in the course of a programme of flight tests dedicated to the exploration of steep approach landing techniques. The aircraft used for the work discussed here is the HS 125, an executive-type two-engined jet. The same aircraft was also simulated on the Aero Flight simulator at Bedford and occasionally reference will be made to experience gained in this exercise. Three different landing techniques were tried, steep approaches from about 7° terminated by a single flare, normal approaches and finally two segment flares from a steep initial approach. Some of the results from these tests will now be discussed.

3.1 STEEP APPROACHES, HS 125

The programme of flying at RAE Bedford has shown that, contrary to initial doubts, the HS 125 can be safely landed from a steep gradient approach. Tests were first made to establish the steepest glideslope that could be achieved in steady flight with idle thrust. This turned out to be about 9°. Then the pilot was asked to find the steepest practical glide slope which allowed speed to be comfortably controlled and the aircraft to be landed without unusual skill. From this test a 7° glide path was selected as the steepest feasible approach and a number of landings were made from a 7° glide path defined by VASI (visual approach slope indicator) guidance[3]. Fig 7 shows the results from seven landings of one flight in the programme as the envelope of all data including part of the glide path. The trace of one particular landing is shown in detail. The envelope of data showed touchdown speeds in excess of 105 knots compared with a target threshold speed V_{AT} of about 110 knots EAS. The approach values of airspeed and vertical velocity fall into a region roughly circular in form (phugoid mode) less than 5 knots in diameter centred on a speed lower than 120 knots (V_{AT} + 10). Presumably this reflects instrument errors, position errors, etc.

One landing is analysed more fully in Fig 8a with points plotted at one second intervals. The dots indicate the actual motion in terms of $\dot{H}$ versus speed and the crosses represent the corresponding control inputs expressed as equivalent speed and $\dot{H}$ demands. Although in this particular example the locii of these demanded flight states moved progressively from right to left, in general it was found necessary to number the points to keep track of the fluctuations especially in incidence. On the glide path the motion locus and demanded locus form an incoherent jumble of points and it is difficult to uniquely define the start of flare. However the point labelled '1' representing a distinct reduction of throttle is taken as an indication of preparing to flare. Using the stick only for the rest of the landing the motion traces approximately a straight line on the $\dot{H}$ - V plane rather than the circular arc expected from a step demand of incidence. This is of course due to the fact that the stick and hence speed demand is moved progressively during the manoeuvre. A curve constructed by drawing segments of one second (≡ 12°) centred at the appropriate control inputs is seen to give a good reproduction of the original measured motion plot, provided allowance is made for damping (ie spiral is used rather than circle). The touchdown speed in this landing was 105 knots against a target of 100 knots and from this envelope of data it is seen that all landings in this group terminated with excess velocity. It seems worth speculating what changes in the technique would be required to reduce the touchdown speed to the value achieved in normal approaches, ie V_{AT} - 10 knots = 100 knots, in the interest of constraining the ground run and avoiding 'floating'. In Fig 8b flare manoeuvres are synthesised which would bring the aircraft to the desired touchdown condition, 100 knots, from approaches on 3°, 5° and 7° glide slope. The same initial approach speed is assumed in each case. The landing manoeuvre is divided into two stages, first speed is bled off without changing the glide path and when the appropriate point is reached a flare is initiated by elevator controlling incidence in the same form as previously measured. In the case of a 7° approach, speeds in the flare are thereby lowered by 6 knots. It is apparent that - other than starting from an appropriately lower approach speed in the first place - this is the only strategy which will produce touchdown at the desired speed. One may in fact ask the question why the pilot did not do this as he was free to do so, being given an entirely free hand in briefing. The calculation of Fig 8b gives the answer. In each case the manoeuvre is initiated by a thrust reduction to the level chosen by the pilot in the actual flight case. This is apparently the lowest throttle setting that the pilot was prepared to use since further

reductions to full idle would bring the engine into a regime of poor response say for overshoot needs and also there would be no margins for further control if the need arose. (It may be noted that in fact full idling thrust is only marginally lower so that the actual overall performance is not too strongly affected by this limitation). We see now from Fig 8b that on the 7° slope the available deceleration is so poor that the manoeuvre has to be initiated at 620 feet altitude so that speed is sufficiently reduced for a flare starting from 120 feet to bring the aircraft to the desired touchdown. This situation rapidly improves with the less steep approaches because now substantially more deceleration is obtained upon throttle closure. As a result the manoeuvre may be initiated at a much more realistic altitude, namely at 210 feet from a 5° approach and at 96 feet from a 3° approach. Note that the peak incidence required for these hypothetical manoeuvres corresponds to a demanded speed 4½ knots lower than the touchdown speed, ie 95½ knots and that a further increase in incidence by 1° would have triggered the stick shaker! Incidence margins are important in this situation and what appears superficially to be a perfectly satisfactory technique clearly needs further study.

3.2 NORMAL 3° APPROACHES AND LANDINGS

Fig 9 shows the results from a sample of 14 normal landings from a 3° approach again represented as a data envelope. These landings were made before the steep approach trials. One notes clearly substantial differences from the steep approach data. The area representing glide slope holding is larger as seen by the 'head' of the envelope but this is attributed to the wider pilot sample used. The 'body' of the envelope slopes a good deal less than with the 7° approaches. Generally there is greater speed variability. In Fig 10a, one landing is shown in detail and is seen to trace out a locus approximating a straight line. This is quite different from what would be expected if the pilot had followed the strategy which he declared he would use on the occasion of some simulator tests of the same aircraft. There he stated that he would first reduce airspeed and then initiate the flare. The control action as represented by the three groups of demand loci, suggests a flare made up of three distinct steps and an approximate reconstruction is shown in Fig 10b which clearly will approximate to the true flight record. The height calculated from this construction for flare initiation is 98 feet compared to height actually measured in flight of 90 feet. Had this pilot followed his declared strategy a height of 231 feet would have been required for this speed reduction phase and an additional 32 feet for the flare, taking the actual throttle setting used in flight. In the real flight case at 50 feet altitude, speed was reduced by only 3 knots. If power is reduced at flare preparation to the lower value used in the steep approaches as in the calculated example for 3° glideslope in Fig 8b, total flare height would be reduced to 96 feet.

The motion locus in Fig 10a indicates a degree of scatter which can be attributed to measurement inaccuracies, gusts and short period transients, and similar inaccuracies may occur in the loci of equivalent control demand. (They are derived from measurements of α, and θ). A much more instructive picture is obtained if one considers the motion locus and the input demands together to get a better appreciation of the broader control strategy.

3.3 TWO SEGMENT APPROACHES

Two examples are given in Fig 11 of two segment approaches. The steep segment of 7° inclination is intersecting a 3° beam at a height of 220 feet. The pilot was completely free to choose his own technique. In the first example, flight 21407, the manoeuvre was not continued to touchdown, the interest being centred on the transition between the segments. This is basically a flare without any overshooting of the 3° beam. Six seconds after flare initiation, power was increased and speed stabilized after another 4 seconds on the shallower glide slope, 9 knots below the initial approach speed. With an autothrottle available a different story may emerge but in manual operation it seems expedient to accept a reduced speed in the second segment, as demonstrated in this example. Other significant data relevant to this flight are: peak normal acceleration 0.11 g, the 3° glide slope was acquired at 150 feet height.

The second example from the same flight was made by deliberately maintaining power constant to demonstrate the effect of either a later power demand or slow engine response. This landing was completed to touchdown. Beginning with 130 knots ASI the transition is similar to that of the previous example but on the 3° glide slope, speed then falls at a rate of somewhat less than 1 knot per second, arriving at the threshold with the correct speed. During the course of this flight weight decreased and as a result, for the same procedure, speed decreased too rapidly and overshoots were initiated.

The third example shown in Fig 11 was obtained with a Hunter aircraft (a single engined jet fighter) on a two segment guidance system starting with a 6° initial slope intersecting a 3° slope at 100 feet altitude. In fact the 3° glide slope was of little practical value, as it was generated by a VASI located too far to the left of the runway for close pilot guidance.

The procedure is to use the first colour change of the VASI beams defining the 3° slope as a warning of the approaching change of glide slope. The next change is used as a signal to flare, heading for the glide path origin which must be clearly marked, finally flaring to touchdown within 1000 feet of the glide path origin. The approach speed used is V_{AT} + 10 knots and the transition and initial flare is made at the throttle setting appropriate to the steep glide path. As Fig 11 shows 15 knots of speed is lost which allows the pilot a margin of control to close the throttle before touchdown. Pilot opinion of this form of landing from a steep gradient approach is more favourable than a single flare procedure and this technique is being investigated further.

4 CONCLUSIONS

A method of data presentation has been proposed which allows three different aspects of landing control to be shown and correlated. In a reference frame of V as the abscissa and H as the ordinate it is possible to present

i. the steady state performance

ii. the actual time history of a landing manoeuvre

iii. the pilot's control strategy in terms of equivalent demands in airspeed (elevator or incidence) and vertical velocity (throttle).

By choosing scales such that ($\dot{H}/\sqrt{2}$) and V are plotted in equal units, the aircraft response to step demands in either control traces out simple geometric patterns as a trajectory and this property can be used to rationalize analysis as well as for the synthesis of landing manoeuvres.

The method has been applied to the discussion of some flight results obtained in trials of normal and steep approaches. For the latter, both single flare and two-segment techniques have been examined. Various significant aspects have been identified as subjects for further investigation, especially power margins and target speeds.

REFERENCES

1 H H B M Thomas. A study of the longitudinal behaviour of an aircraft at near-stall and post-stall conditions.
International AGARD CP 17. Stability and control Parts 1 and 2, selected papers from the AGARD Flight Mechanics Panel Specialists Meeting, Cambridge, September 1966.

2 C D Perkins, R E Hage. Airplane performance stability and control.
John Wiley & Sons, New York (1949).

3 Anon. ICAO Aerodrome manual. Annex 14.

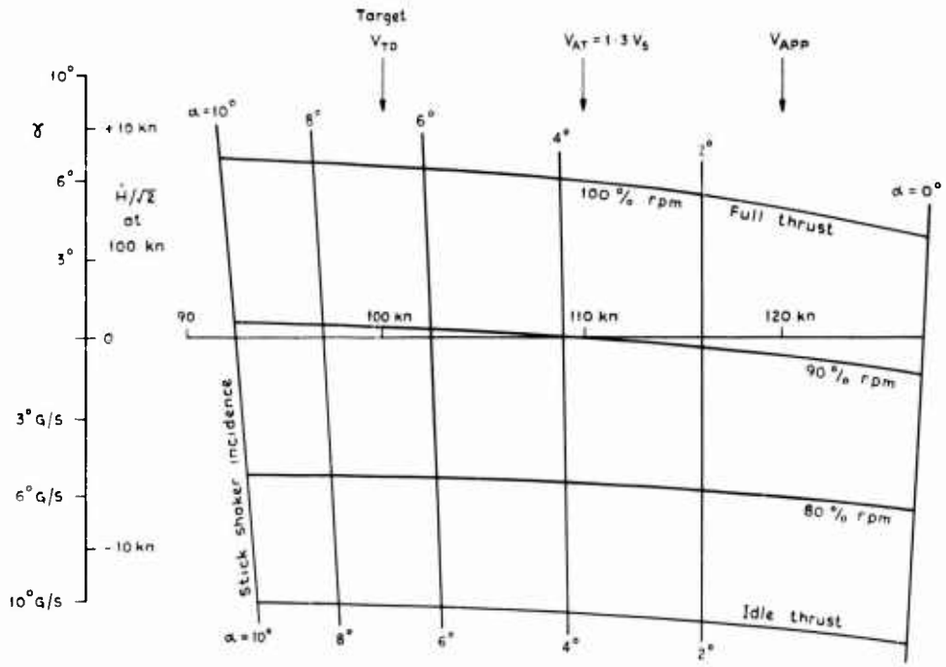

Fig.1 Performance chart of HS 125 aircraft

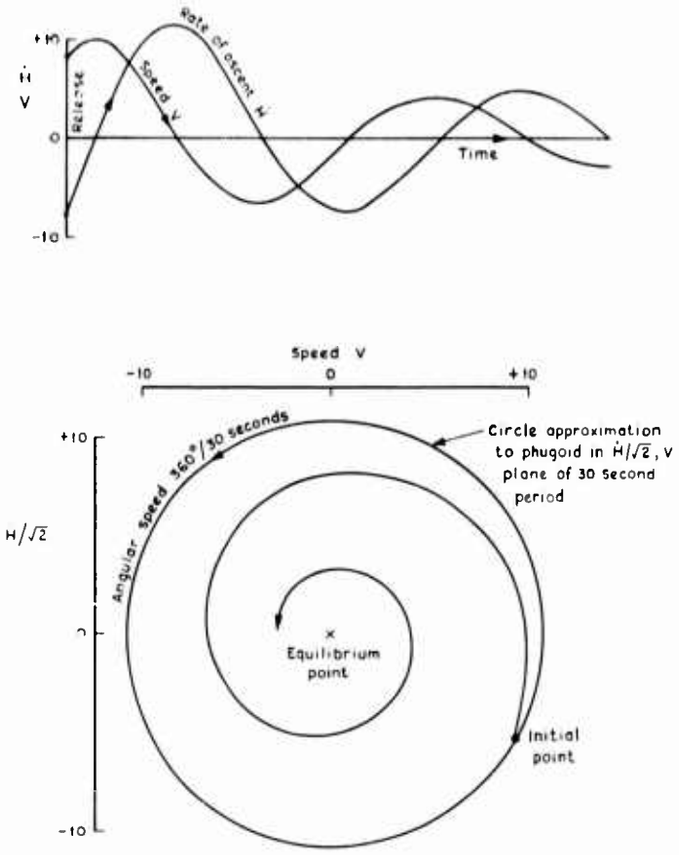

Fig.2 The phugoid projected on to the Ḣ-V plane

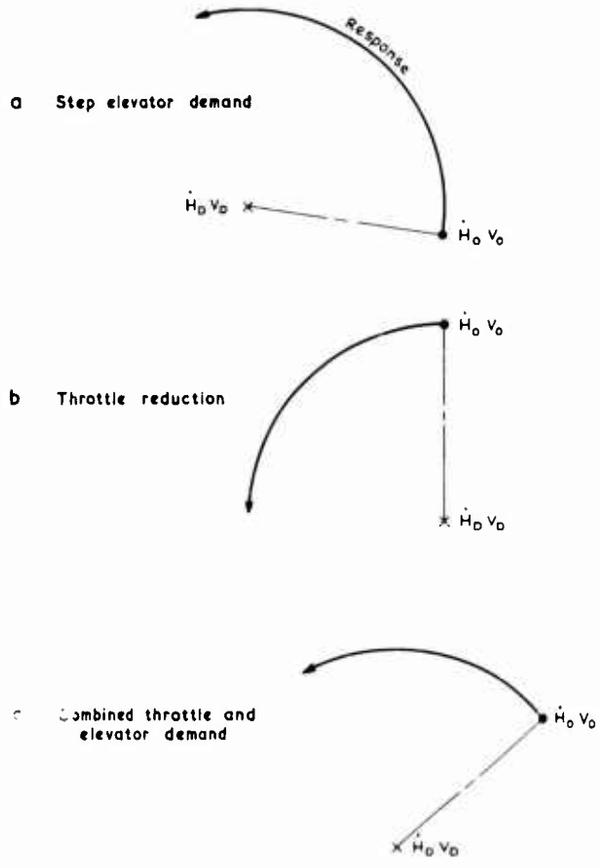

Fig.3(a)–(c) Response to control demands

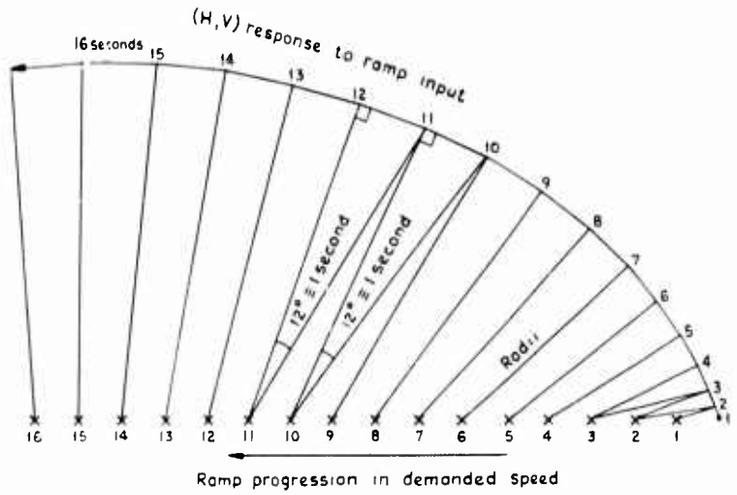

Fig.4 Step by step construction of response to continually varying control demand

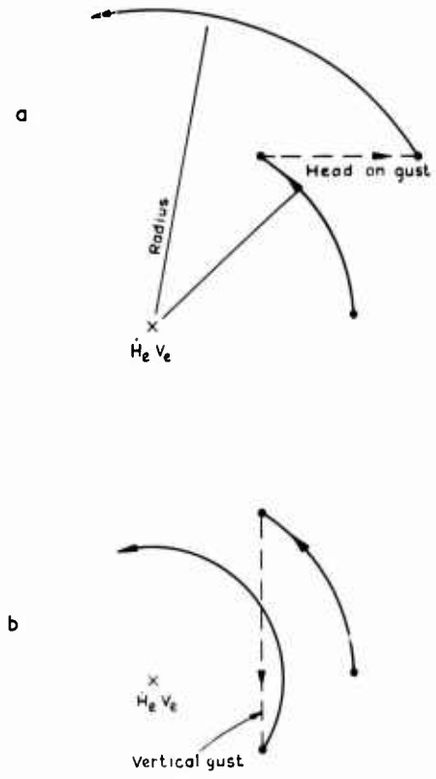

Fig.5 Response to gusts in $\dot{H}$-V plane

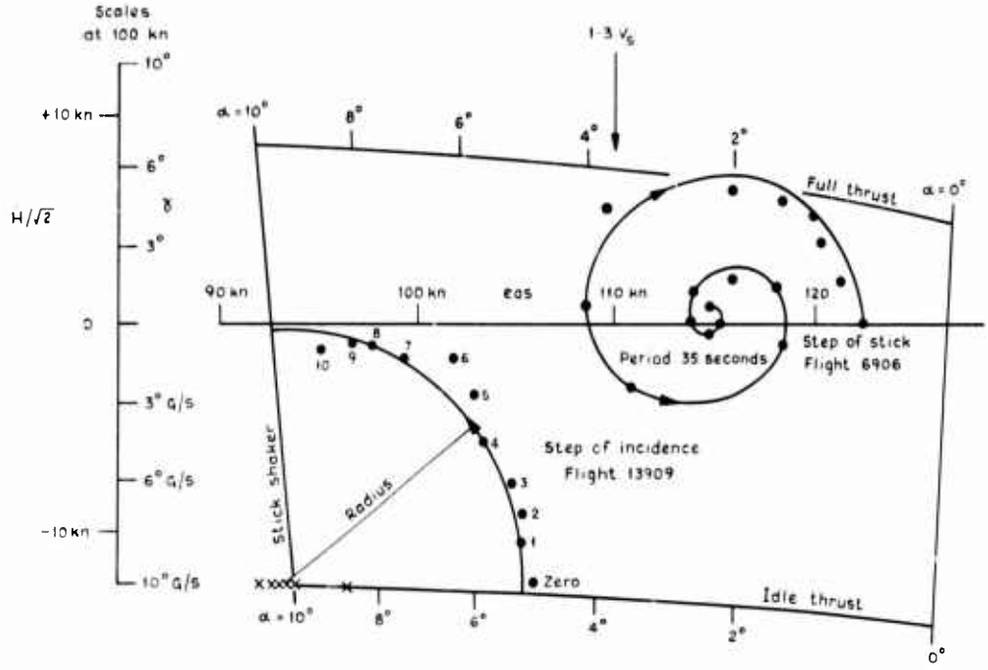

Fig.6 Flight results of a phugoid and an elevator step demand plotted in the $\dot{H}$-V plane

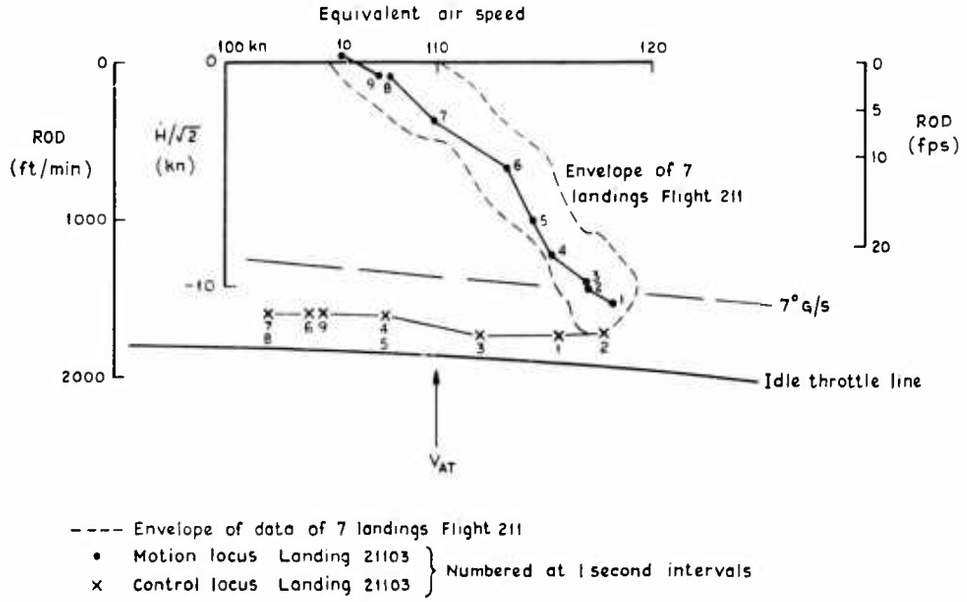

Fig.7 Flight results from steep approaches: 7° glide slope

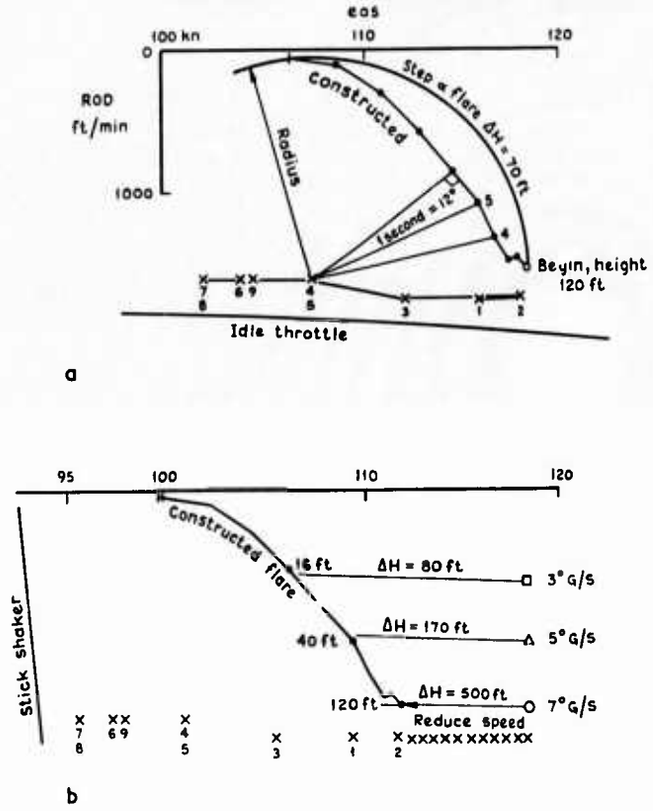

Fig.8(a) & (b) Control strategy required to achieve the desired touchdown speed from various glide slopes

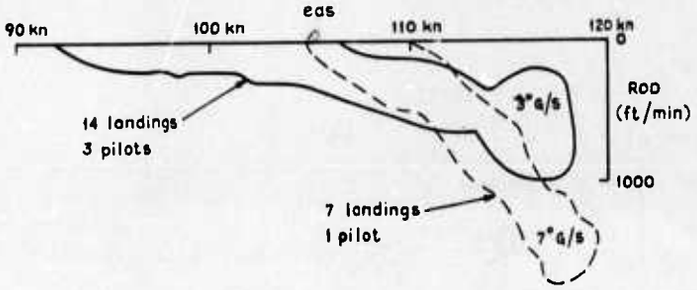

Fig.9 Normal landings compared to steep approaches

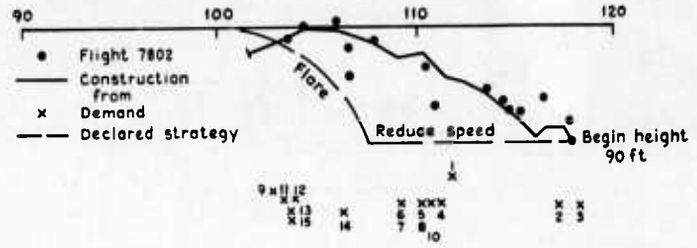

Fig.10(a) Reconstruction of normal landing

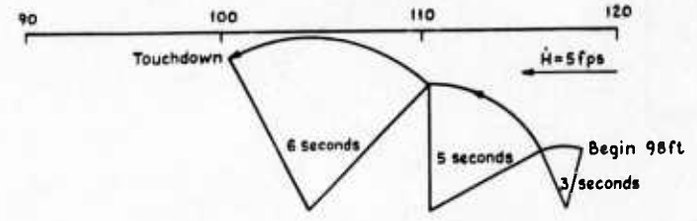

Fig.10(b) Reconstruction of flare using 3 steps of elevator demand

Fig.9 & 10 Flight results and constructions of normal landings. 3° glide slope

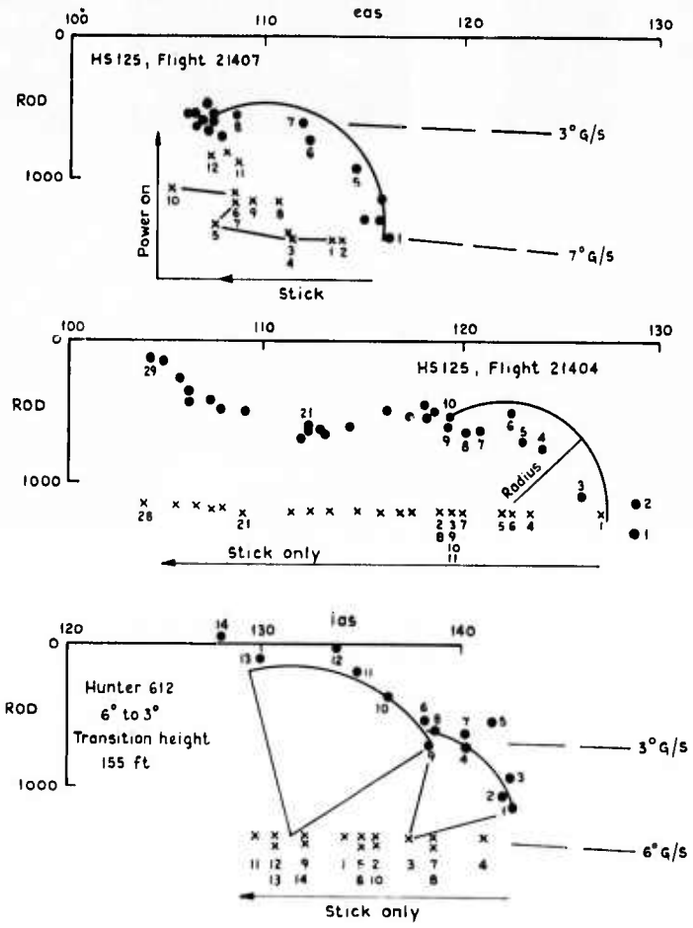

Fig.11 Flight results from 2 segment approaches

STABILITY AND CONTROL HARMONY IN APPROACH AND LANDING

Seth B. Anderson
Assistant for Interagency Programs
Ames Research Center, NASA, Moffett Field, Calif. 94035

SUMMARY

A review of the factors which affect stability and control harmony in approach and landing has been made to obtain a clearer understanding of the proper relationship, the trade-offs involved, and to show how limits in stability and control harmony are established for advanced aircraft. Factors which influence stability and control harmony include the longitudinal short period response of the aircraft and the level of several pitch control characteristics including control power, control sensitivity, and control feel. At low stability levels for advanced aircraft, less conventional control techniques such as DLC are needed to improve harmony and some form of stability augmentation must be provided to improve precession of flight path control and reduce pilot work load.

INTRODUCTION

A proper relationship must exist between the degree of stability present and the amount of control available for satisfactory operation of an aircraft throughout its flight envelope. Stability and control are said to be in harmony when an aircraft can be operated to meet its design performance specifications with the desired precision of flight-path control and minimum pilot effort. Aircraft that inherently have large stability require large amounts of control for harmony with an adverse effect on performance.

Stability and control harmony was significant even in the early days of flight. Historic aircraft that exemplify the importance of stability and control harmony are shown in figure 1. In an excellent summary of the history of the development of stability and control technology (ref. 1), it was noted that the early Otto Lilienthal gliders were designed to have positive static-longitudinal stability, but were seriously lacking in pitch control (provided by movement of the pilot's body). Because of the lack of stability and control harmony, Lilienthal was killed in an accident when his glider was upset by a gust. The Wright Brothers, on the other hand, deemphasized the requirement for static stability, as evidenced by their tail-first designs, but partially overcame the lack of harmony by providing sufficient control power. They learned to fly their unstable aircraft by sacrificing precision of control and tolerating high pilot workload. In a letter of 1909 (long after their initial flights), it was stated: "The difficulty in handling our machine is due to the rudder (horizontal tail) being in front, which makes it hard to keep on a level course. If you want to climb, you must first give the front rudder a larger angle, but immediately the machine begins to rise you must reverse the rudder and give a smaller angle. The machine is always in unstable equilibrium. I do not think it necessary to lengthen the machine but to simply put the rudder behind instead of before." The early aircraft of the Wright Brothers was in a sense an early control-configured vehicle (CCV) without, of course, the benefit of a stability control augmentation system (SCAS).

Recently, increased attention has been focused on stability and control harmony in the design of high performance aircraft such as the SST. These aircraft must be more concerned with obtaining proper stability and control harmony than conventional aircraft because a mismatch of stability and control can have a very serious effect on performance. Stability and control harmony is particularly important in approach and landing because stability and control tend to deteriorate at low speeds and the greatest demand is placed on controlling the aircraft. Although harmony is needed for all axes, the longitudinal (pitch) axis is usually the most critical because acquiring and tracking the glide slope and adjusting pitch attitude for touchdown must be done precisely in the presence of wind shear, gusty air, and adverse ground effects. A definition of stability and control harmony requirements for approach and landing is complicated because many interrelated factors affect the precision of control obtainable.

The handling qualities military specifications for conventional aircraft (ref. 2) do not relate the amount of control power needed to the stability. Only lower limits are specified for both stability and control and there is no direct attempt to treat stability and control harmony.

This paper reviews longitudinal stability and control harmony in approach and landing to obtain a clearer understanding of the proper relationship, the tradeoffs involved, and to show how limits in stability and control harmony are established for advanced aircraft. Areas of interest include the degree of negative stability allowable and the associated control requirements for a carrier fighter aircraft and an SST aircraft.

RESULTS AND DISCUSSION

In the following discussion, the factors that influence stability and control harmony in approach and landing are reviewed first – in a general sense, to show how the level of stability expressed by aircraft dynamic response relates to pilot opinion and workload, and the interrelationship of various control characteristics. With this background then specific harmony problems of the two types of aircraft are addressed.

Factors That Influence Stability and Control Harmony

Longitudinal short-period dynamics: Advanced aircraft such as the supersonic transport are expected to be designed to have low levels of angle-of-attack stability, M_α. Consequently, their short-period dynamic stability will be weak. Many studies have examined the effect of reduced stability on precision of flight-path control. The data in figure 2 summarize pilot comments of the effects of variations in dynamic stability with damping. This information (ref. 3), obtained in a modern (Jet Star) airborne flight simulator, is typical of results obtained in other studies.

Pilot comments indicate that the aircraft is most pleasant to fly when stability levels are neither too high nor too low and sufficient damping is available. As stability is decreased it becomes more difficult to trim the aircraft to a given speed or attitude, and pitch response divergences require continuous pilot concentration to avoid complete upset. Increased damping helps to reduce the magnitude of the excursions, and even unstable modes are considered safe, but not desirable, provided there is sufficient damping.

The manner in which the pilot rating varies with the stability parameter for various levels of damping is shown in figure 3. Note that pilot opinion deteriorates before zero stability is reached regardless of the amount of damping present. The problem arises because

the response of the aircraft is too sluggish at low frequencies, making it difficult for the pilot to start and stop pitch attitude changes with the desired precision because of his inability to predict the final response. At low stability, complaints of lack of damping persist no matter how much damping is available. The fact is simply that the pilot is unable to obtain the desired aircraft response with an acceptable pilot workload. In the landing approach task, the effects of low stability appear as undesired airspeed or angle-of-attack excursions.

A stability level that is too high is also undesirable because of the tendency of the aircraft to oscillate in pitch at frequencies too fast for the pilot to damp adequately. In addition, large stability requires large control power to trim and maneuver the aircraft up to $C_{L_{max}}$ – a condition that affects the performance aspect of stability and control harmony.

Effect of stability margins on tail size: One of the primary benefits in terms of performance gains in relaxing static stability margins is that less horizontal tail area is needed to balance the wing-fuselage pitching moments. A specific example for a large aircraft (B-52, ref. 4) is shown in figure 4 where the required horizontal tail area is plotted as a function of c.g. location for the landing condition. Curves for trimming the wing-fuselage pitching moment and for maneuvering are included. Both the trim and maneuvering moment requirements are sized (largest) for the flaps-down configuration. Also shown is the manner in which neutral point and maneuver point varies with tail area and c.g. position. The neutral point is defined as the c.g. location where the stick force and stick position gradient with airspeed are zero; the maneuver point is where the stick force per g gradient is zero at constant airspeed.

Note that, for the B-52 aircraft, minimum horizontal tail size occurs at a c.g. location of approximately 34%, where the tail load changes to an up load for more rearward c.g. locations. This is approximately 5% aft of the neutral point but ahead of the maneuver point. For comparison, the baseline horizontal tail area for 5% inherent stability is also shown. For the B-52 aircraft, it is calculated that the reduced tail size would save approximately 4000 lb (8,880 N) in structural weight, which, along with reduced drag, would improve performance considerably. The negative static stability would, of course, require a SCAS to improve handling deficiencies (harmony).

Pitch control power: Longitudinal control characteristics play an important part in achieving stability and control harmony in approach and landing. To understand the control requirements, the various uses of pitch control are addressed first. Pitch control in approach and landing is used primarily to (1) maneuver the aircraft on the flight path and flare for landing, (2) trim out the moments when speed changes are made and maintain a given attitude or speed when power, flaps, gear, etc., are changed, and (3) adjust pitch attitude to compensate for gusts, wind shear, ground effect, recirculation, or other disturbances.

The amount of control (control power) required for each of the foregoing varies for the following reasons: First, maneuvering control requirements depend directly on how rapidly the aircraft must be rotated for the most critical task. For example, the landing flare is made gradually (less angular acceleration) for a large supersonic transport aircraft in a shallow approach compared to a STOL aircraft in a steep approach. Second, the pitch trim requirements will vary, depending on the aircraft concept. For example, the trim moments due to changes in engine power, forward speed, flap deflection, etc., are markedly different for a tilt-wing STOL aircraft than for a delta-wing supersonic transport. Third, the control required to offset pitch attitude changes induced by turbulence, wind shear, and downwash changes are also configuration-dependent. Finally, the effects due to ground proximity differ depending on the aerodynamic configuration (wing aspect ratio) and lift coefficient at touchdown. Changes in lift and pitching moment are more pronounced for low-wing aircraft and at high values of lift coefficient.

Effect of control sensitivity: Control sensitivity also influences the pilot's impression of the response of the aircraft. If too low (large control travel for a given pitch acceleration), the aircraft will appear sluggish, while excessively high sensitivity can lead to overcontrolling tendencies. Optimum sensitivity depends on the amount of pitch damping, the level of stability, and the pilot's task. Improvements in flight-path control for the low stability levels are expected to result from optimizing control sensitivity. Early studies (1966, ref. 5) of the effect of control sensitivity on pilot rating in landing approach for various levels of static stability are illustrated in figure 5 for stable and unstable short period frequencies. These results show two points: (1) optimum control sensitivity was approximately 0.3 rad/sec^2/in. and (2) over the short period frequency range considered, the level of stability had only a small effect on optimum values of control sensitivity. In these studies conducted on an airborne simulator, satisfactory pilot ratings were obtained even with negative stability values. In a later study (ref. 6), the results (fig. 6) show the need for proportional increases in control sensitivity, with increases in short period frequency. In these tests, pilots were allowed to select a desirable control sensitivity for each configuration (short period frequency). The tests were not carried far enough to ascertain if increases in control sensitivity would be beneficial for negative stability values. The pilot comments tended to illustrate the point, however, that total control power available can become a critical factor in controlling pitch divergences. Although pilot preference for lower sensitivities was evident in keeping with the loose response dynamics at the lower frequencies, they complained about hitting the forward stick stop and "almost losing it, once it got upset," when not enough control power was available, regardless of the selected control sensitivity.

Effect of control feel: A further point in connection with improving aircraft response at low stability levels is that of control feel. The effect of changing control feel on pilot rating in the region where poor handling qualities exist is illustrated in figure 7. These data (ref. 3) are for a test case of good pitch damping but negative static stability. Pilot rating was not highly sensitive to variations in the control feel parameter (pitch angular acceleration per unit stick force). As the parameter is increased, the aircraft becomes too responsive and upset problems prevail. At the other extreme, the aircraft is too sluggish, and the pilot has difficulty controlling fast enough to provide the amount of compensation (lead) necessary for the unstable conditions. Generally, the best value of the feel parameter was approximately 0.3 deg/sec^2/lb and, so long as control power available was not a limiting factor, the pilot ratings were in an acceptable, but not satisfactory, range for the negative stability region.

From the foregoing, since pitch control requirements depend on many interrelated factors, it is not possible to generalize on control harmony for all stability levels. The individual requirements for each type aircraft must be examined in detail to select control characteristics appropriate to the aircraft's dynamic behavior, keeping in mind the desire for the least performance penalty.

Considerations for Carrier Aircraft

One of the more demanding tasks which illustrates the importance of stability and control harmony is that of the approach and landing on an aircraft carrier. High precision approach and touchdown is stressed because of the small landing area and the need to account for the ship's motions in rough seas. In addition, control requirements for touchdown differ from conventional landings in that the aircraft is not flared for touchdown. The carrier approach and landing is a precision control task where the pilot usually uses pitch control to make altitude adjustments. The stability and control harmony requirements for the carrier approach task can be examined by the short-period response.

Effect of short-period dynamics: It was noted previously that the pilot's impression of aircraft response depends on the short-period frequency, ω_n and pitch damping. In addition, studies have shown that in the approach and landing task the change in normal acceleration per unit change in angle of attack, N_{z_α} is a parameter that influences the pilot's impression of flight-path control. The need for the proper relationship of these parameters is reflected by the summary of pilot comments in figure 8. This information was obtained in piloted simulation studies (ref. 7) for the carrier approach task in which the pilot is concerned about intercepting and tracking a 4° flight path. As last minute changes in flight-path control become difficult because of the slow response of the aircraft at low stability levels, the pilot may be unable to simultaneously adjust his sink rate at touchdown and his touchdown point. As noted in the figure, upper and lower boundaries exist within which the pilot can perform the task to his satisfaction. In the middle area, his comments would reflect "good harmony between pitch and meatball (flight-path) response." At the reduced stability levels (lower frequencies), the pilot tends to overdrive or undercorrect the aircraft, and he must fly with greater anticipation of the final response. When N_{z_α} values fall below approximately 3 g/rad, flight-path adjustments are difficult to achieve by pitching the aircraft to change wing lift. Further improvements in flight-path control must be made by thrust modulation, thrust vectoring, or by direct lift control (DLC).

Effect of DLC: An example that illustrates some unique control problems in carrier approach landings for an advanced aircraft (F-14, ref. 8) is shown in figure 9 in terms of the variation of pilot rating with static margin for several control modes. Two points are evident from these tests conducted on a piloted 6° motion simulator: (1) pilot rating deteriorated relatively slowly with a decrease in static margin and (2) regardless of static margin, a completely satisfactory rating could be only obtained with DLC. Part of the reason for better pilot rating with DLC is that, by using DLC, the undesirable short period dynamics were not excited as much. In effect, the use of DLC tends to uncouple control from stability. Requirements for quick flight-path response were accentuated by the pitching and heaving motions of the aircraft carrier in simulating rough seas. Even with the wing swept forward on the F-14 (normal for landing), a large pitch rotation was required to achieve the desired "g" value in correcting for a low flight-path position that created cockpit visibility problems at the required approach speed. When DLC was used, "low" flight-path corrections could be made with less nose-up aircraft pitch attitude change. Slightly better pilot ratings were obtained using a separate (thumb-wheel) controller, since g and pitch attitude could be adjusted independently.

Considerations for SST Aircraft

For the SST aircraft, it is well known that the optimum configuration arrangement for good supersonic cruise L/D tends to place the engine nacelles far aft on the wing. This could create severe longitudinal balance problems which would increase structural weight and aerodynamic drag if conventional static margins were used. In addition, since the center of pressure moves aft going to supersonic flight speeds, the resultant increase in longitudinal static stability produces a large penalty in trim drag. Because of the foregoing, supersonic transport aircraft will operate with the c.g. located far aft of that commonly accepted for conventional subsonic jet transports. As noted previously, as the static margin is decreased to zero, less tail area is needed since the inherent stability of the aircraft need not be overcome when maneuvering or changing trim. Control during the approach and landing flare is complicated by the sluggish response due to the high-pitch inertia associated with the long slender fuselage configuration and the low short period frequency. These conditions result in unique requirements for achieving stability and control harmony.

Effect of lift loss due to control deflection: Early studies (see, e.g., ref. 9) predicted increased control problems for the supersonic transport, depending on the design, because of the initial reversal in flight-path response following a pitch control input. This effect (illustrated in fig. 10 in terms of a time history of altitude change) is caused by the instantaneous lift loss due to pitch control deflection before the aircraft rotates to a higher angle of attack. The loss of total lift, which can be relatively large for short-coupled configurations, tends to decrease the precision of flight-path control and therefore degrade stability and control harmony.

The pilot's impression of aircraft response to this adverse lift loss is reflected in terms of "time to crossover" (i.e., the delay in altitude change) in figure 11 for an advanced supersonic transport configuration. The data indicate a rapid deterioration in pilot rating with an increase in crossover time. The low N_{z_α} for the SST tends to prolong the sinking effect and the net effect is that the flight-path-angle response deteriorates. In fact, the more the pilot attempts to "hurry up" pitch response, the greater is the altitude loss.

Control power requirements: Studies have been made to determine the minimum amount of control required to land an SST in keeping with the desire to minimize performance loss. The flare control requirements are the most demanding because of a nose-down trim change due to ground effect and the adverse lift loss due to control deflection previously discussed. The relationship between control power required and lift loss due to control deflection is shown in figure 12. The control power boundary selected for supersonic transport configurations was established from piloted simulator tests (ref. 10) and shows that considerably less pitch control power is needed when lift loss due to pitch control deflection is low. Comparison of data for current conventional transports shows a smaller lift loss and a wide scatter in control power available for a nearly constant value of $\Delta(L/W)$. The reason for the large spread in control requirements for the various conventional aircraft is due in part to the different c.g. ranges over which they are designed to operate. Note that the double-delta (L-2000) configuration would be judged unacceptable by this criterion and even the B-70 and Concorde SST would appear marginal, although this is not borne out by pilot opinion. In fact, although the Concorde SST inherently has a large negative $\Delta(L/W)$, it is not flown in a manner that requires large positive pitch angular accelerations when approaching the ground. Comments from pilots point out that satisfactory touchdowns can be achieved for the Concorde with zero pitch attitude change since a nose-up pitch attitude is normal in landing approach for this aircraft. The nose-down trim change due to ground effect must be counteracted, of course, by increased back-pressure on the control to avoid a hard touchdown. When the pilot desires to make a very soft landing, only a 0.5 to 1.0° change in pitch attitude is needed. One must be careful, therefore, in generalizing on the applicability of a control power boundary to all types of aircraft since additional factors other than lift loss due to control deflection must be considered.

Effect of minimum control power on touchdown performance: From the control boundary in figure 12, these data indicate that very low pitch control power may be acceptable for low values of $\Delta(L/W)$. Although reduced control power is desirable from a structural weight standpoint, the tradeoff in reducing control power can be reflected in terms of touchdown performance. Figure 13 indicates a general deterioration in touchdown performance as pitch control power is reduced. Although the maximum acceptable sink rate of 6 fps (1.83 m/sec) could be obtained with relatively low control power, it should be appreciated that this represents a minimum below which structural damage to the aircraft could occur. Also two additional conditions must be fulfilled for very low control power to be acceptable: (1) little or no lift loss due to pitch control deflection is necessary and (2) no stability must be overcome in maneuvering (proper stability and control harmony).

Effect of approach speed: The difficulty of obtaining satisfactory pitch control power to harmonize with various stability levels depends, to a large degree, on the value of approach speed (and C_L) selected. The trend is, of course, to reduce approach speed in the interest of improving field performance. Two effects are associated with a reduction in approach speed: (1) decreased dynamic pressure directly reduces pitch control power available and (2) increased C_L (for a constant g) results in larger pitching moment and lift changes in ground effect (more adverse ground effect). The effects of changing airspeed on the control requirements for a conventional subsonic jet transport and an advanced supersonic transport design are shown in figures 14 and 15. Of interest are such factors as the degree of static stability, trim changes due to ground proximity, and control required to flare (maneuver). These data illustrate two significant points for the conventional transport: (1) available control power is appreciably reduced by pitching moment changes in ground effect and (2) airspeed decreases such as usually occur in the flare seriously erode the available control power. Maneuvering requirements represent a much smaller percentage of the total control power required. The data in figure 15 for a supersonic transport aircraft show several pronounced differences. Because the aircraft is operated without a positive static margin, changes in control power with speed are considerably smaller; in fact, instability (pitch up) at the lower speeds results in a greater margin in control available for maneuvering. Ground effect is more pronounced for the supersonic transport configuration and dominates the need for pitch control power. This effect is accentuated if the pilot delays making a correction for the nose-down pitch change due to ground effect since, as previously noted, it is not possible to "speed up" the nominally sluggish response of the high inertia SST before touchdown.

Acceptable limits of instability: As previously noted, operation with negative static longitudinal stability is possible for limited (emergency) operation and the question arises as to the limits of instability for minimum safe operation. The degree of instability permissible depends on many interrelated factors, including the type of aircraft, mission, task, degree of turbulence, ground effect, backside of thrust-required curve, pitch damping, etc.

The results of piloted simulator studies of a version of the SST are given in figure 16, in terms of pilot rating versus c.g. position, including the effect of SAS. These data indicate that with SAS off, there is a rapid degradation in pilot rating with rearward c.g. movement. Operation at c.g. locations aft of the maneuver point would be considered unsafe because of the extremely high pilot workload. With the type of SAS used in these tests (rate command, attitude hold), the aircraft could be flown acceptably for c.g. positions past the maneuver point. The tracking performance for these unstable conditions is given in figure 17, which shows flight-path error as a function of c.g. position. Without the use of SAS, flight-path tracking deteriorates rapidly for c.g. positions aft of the maneuver point. Although not shown here, pilot workload increases considerably from indications of throttle and control movements.

Other parameters that relate to pilot opinion in controlling an unstable aircraft are time to double velocity error, T_{2_V}, and time to double angle of attack T_{2_α}. The results of a SST simulation study show (fig. 18) that unsafe operations would be expected for times to double velocity error of less than 10 seconds. Note that in the approach speed range for this SST configuration, operation is on the back side of the power required curve, which in itself can contribute to a speed instability problem (without use of autothrottle). In these tests, back-side operation results in a rather long time constant (approximately 50 sec) and would be difficult for the pilot to detect and would be considered of secondary importance to his workload and performance problems.

Of concern to the pilot also in landing approach is the divergence in angle of attack. Several studies have been conducted to establish safe operational limits for the Concorde class supersonic transport using T_{2_α} to indicate acceptable instability limits under conditions that represent a multiple (SAS) failure case. Figure 19 shows pilot rating versus T_{2_α} from tests on a airborne (in-flight) simulator (ref. 11) and flight tests of the Concorde aircraft. The rapid deterioration in pilot rating occurs because the pilot must devote his attention to attitude control. Note that periods greater than approximately 6 sec showed no significant improvement in pilot rating nor was a satisfactory pilot rating ever obtained for this condition (no SAS).

A more detailed study of instability boundaries for airworthiness considerations of the Concorde class supersonic transport is contained in a NASA-Ames study (ref. 12) conducted on a piloted six-degree-of-freedom motion simulator. The results are in general agreement with the T_{2_α} trends previously mentioned. In these tests, pitch control sensitivity was varied to provide closer harmony with stability. Although a systematic variation of pitch control sensitivity was not made, the few points checked did not show significant improvement in pilot rating. In effect, the pilot did not set the limits in controlling the pitch divergences by inability to adjust the aircraft response to produce a given α or speed change, but rather by the increase in pilot workload that accompanied the increases in instability. Even large increases (five times normal) in pitch damping did not satisfactorily improve pilot opinion since, in the tests conducted, it created an insidious delay in divergence.

CONCLUSIONS

From the study that has been made to identify factors which influence longitudinal stability and control harmony is approach and landing, the following conclusions have been reached:

1. Stability and control harmony exists when aircraft response is such that flight path adjustments can be precisely made with low pilot work load which will achieve the desired sink rate at touchdown, and the smallest overall penalty on aircraft performance.

2. Large stability margins require large values of control power for harmony in order to provide trim and maneuver capability throughout the angle of attack range up to $C_{L_{max}}$. Since large horizontal tail size is needed to provide large control power, the increased structural weight and aerodynamic drag have adverse effect on performance.

3. Relaxing static stability margins to obtain improved overall aircraft performance results in sluggish short period dynamic response, a condition for which it is difficult to provide harmony regardless of the amount of control available. The pilot is unable to start and stop pitch attitude changes with the desired precision because of his inability to predict the final response.

4. For the selected level of stability in approach and landing, particular attention must be given to obtain satisfactory longitudinal control characteristics in terms of control power, control sensitivity, and control feel to achieve harmony.

5. Because pitch control requirements depend on many interrelated factors, it is not possible to generalize on control harmony for all stability levels. The individual requirements for each type aircraft must be examined in detail to select control power, sensitivity and feel appropriate to the aircraft's dynamic behavior, with the desire for the least performance penalty in mind.

6. Stability and control harmony is of special importance in approach and landing aboard a carrier because of the increased precision required to land on a small area and to account for the ship's motion in rough seas. When these aircraft require low static stability to achieve design performance goals, unconventional control techniques such as DLC can be used to advantage with the nominally poor (sluggish) pitch dynamics associated with low stability margins.

7. Achieving stability and control harmony for SST aircraft is more complicated due to the sluggish pitch response, high pitch inertia, and low short period frequency. In achieving good harmony, attention must be given to the effect of lift loss due to control deflection and the minimum amount of control power commensurate with obtaining the desired sink rate at touchdown.

8. The effect of reducing approach speed is less deleterious for advanced SST aircraft compared to conventional transports because control loss is less and more maneuverability is retained. The lift and moment changes due to ground effect dominate the control requirements for all types of transport aircraft regardless of the stability margin.

9. Operation with negative static longitudinal stability is possible for limited (emergency) operation with less than optimum harmony. The degree of instability permissible depends on many interrelated factors including the task, turbulence intensity, ground effect characteristics, pitch damping, etc. Parameters which relate to pilot opinion in controlling an unstable aircraft in approach and landing are time to double velocity error and time to double angle of attack.

REFERENCES

1. Perkins, Courtland D.: The Development of Airplane Stability and Control Technology. AIAA Paper 69-1137, Oct. 1969.

2. Anon: Military Specification-Flying Qualities of Piloted Airplanes. MIL-F-8785 (ASG), Aug. 1969.

3. Rediess, Herman A., *et al.*: Recent Flight Test Results on Minimum Longitudinal Handling Qualities for Transport Aircraft. Presented at the FAUSST VIII Meeting, Washington, D.C., Jan. 1971.

4. Anon: Compatibility of Maneuver Load Control and Relaxed Static Stability. AFFDL-TR-71-183, Jan. 1972.

5. Eney, John A.: Comparative Flight Evaluation of Longitudinal Handling Qualities in Carrier Approach. Princeton University, Rep. 777, May 1966.

6. Miller, G. E. and Seckel, E.: Flight Evaluation of the Effects of Short Period Frequency and Normal Acceleration Response in Carrier Approach. Princeton University, Rep. 882, Nov. 1969.

7. Bihrle, William Jr.: Aircraft Characteristics That Influence the Longitudinal Handling Qualities During a Carrier Approach. AIAA Paper 69-894, Aug. 1969.

8. Stevens, Victor C. *et al.*: Preliminary Results of a Piloted Simulatory Study of Carrier Landing Approaches. NASA TM X-62,080, July 1971.

9. Kehrer, William T.: Longitudinal Stability and Control of Large Supersonic Aircraft at Low Speeds. ICAS Paper 64-586, Aug. 1964.

10. Kehrer, William T.: Handling Qualities Criteria for Supersonic Transport. AGARD-CP-106, Sept. 1971.

11. Wasserman, Richard and Mitchell, John F.: In-Flight Simulation of Minimum Longitudinal Stability for Large Delta-Wing Transports in Landing Approach and Touchdown. AFFDL-TR-72-143, Feb. 1973.

12. Snyder, C. T. *et al.*: Motion Simulator Study of Longitudinal Stability Requirements for Large Delta-Wing Transport Airplanes During Approach and Landing with Stability Augmentation Systems Failed. NASA TM X-62,200, Dec. 1972.

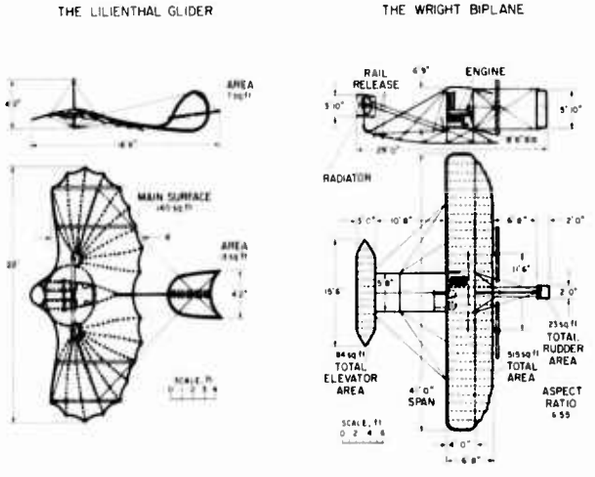

Fig. 1 Historic aircraft.

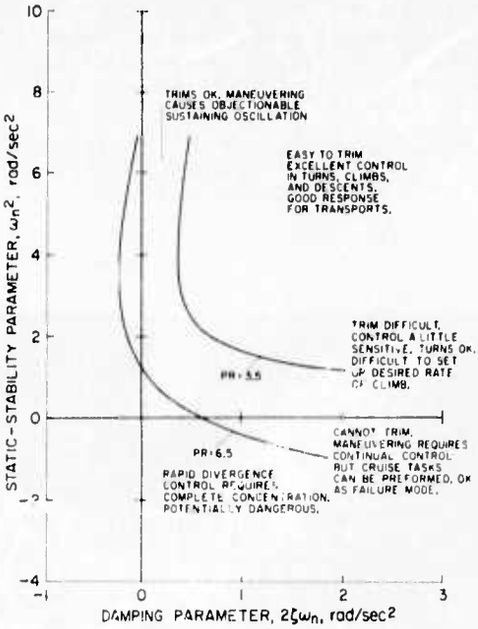

Fig. 2 Summary of pilot comments on dynamic stability, (ref. 3).

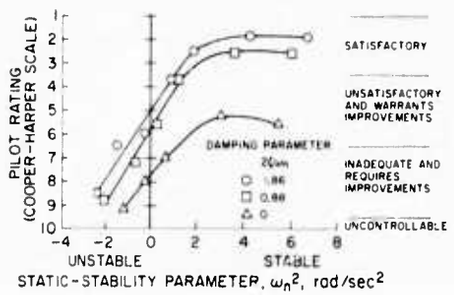

Fig. 3 Average pilot ratings as a function of static stability for three damping levels (ref. 3).

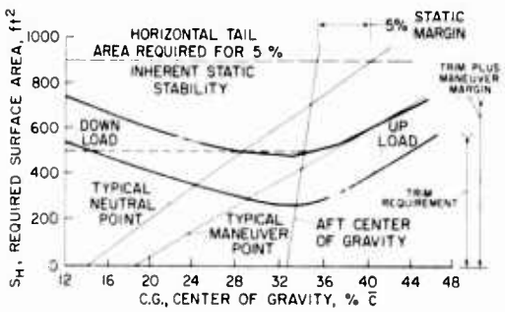

Fig. 4 B-52 Longitudinal control surface area required (ref. 4).

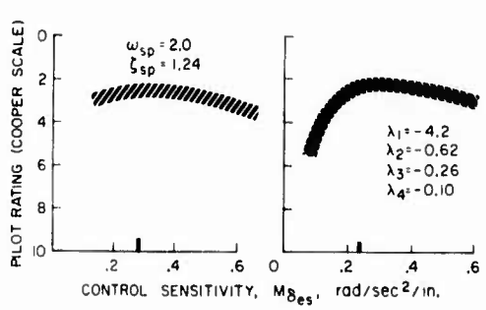

Fig. 5 Pilot rating vs. control sensitivity – light to moderate turbulence (ref. 5).

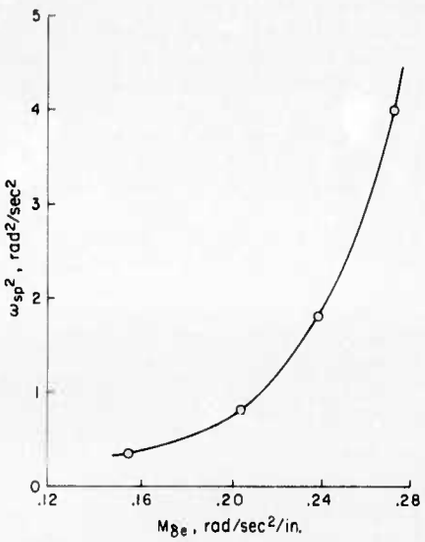

Fig. 6 Pilot selected control sensitivity (ref. 6).

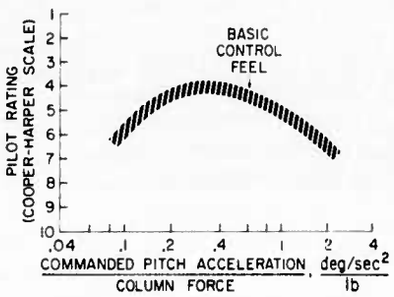

Fig. 7 Typical pilot rating of the effect of control feel on handling qualities. $\omega_n^2 \approx -0.23$; $2\zeta\omega_n \approx 1.86$. (ref. 3)

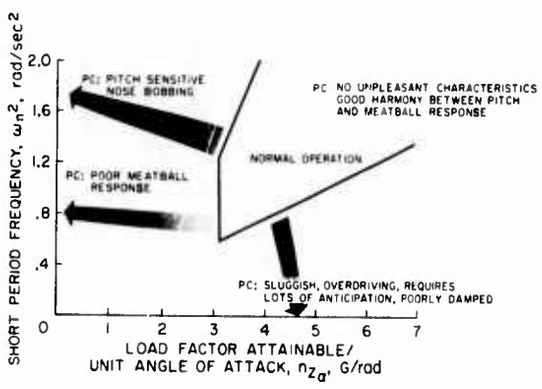

Fig. 8 Carrier landing longitudinal requirement and corresponding pilot comments (PC) (ref. 7).

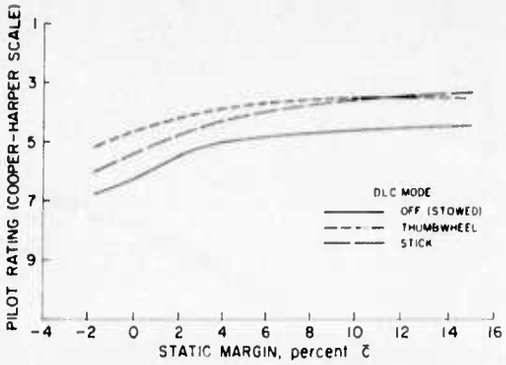

Fig. 9 Effect of DLC mode on pilot rating as a function of static margin. Carrier approaches, F-14 aircraft (ref. 8).

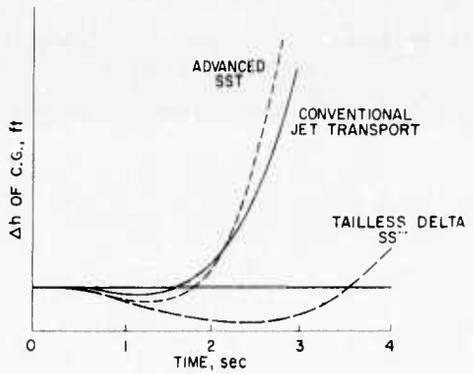

Fig. 10 Comparison of airplane response during abrupt flare maneuver.

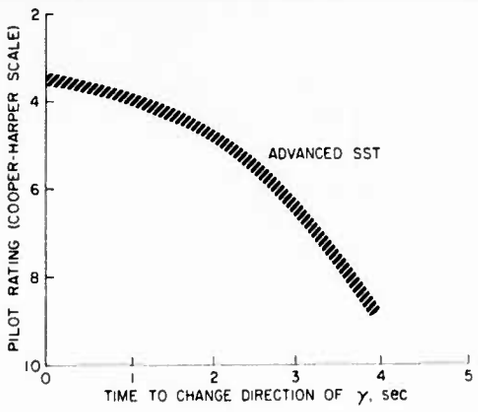

Fig. 11 Effect of crossover time on pilot rating.

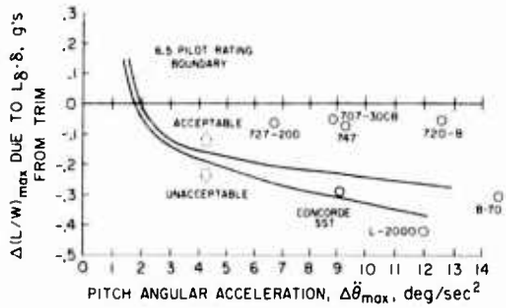

Fig. 12 Pitch control power criteria, $\Delta\Theta_{max}$ (from trim).

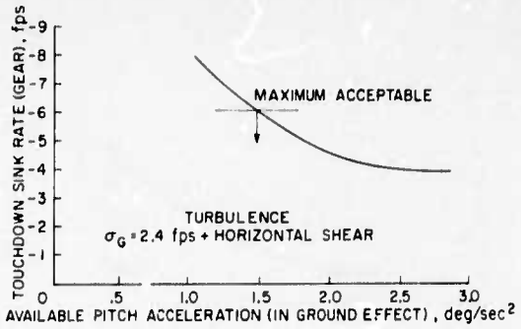

Fig. 13 Effect of control power on touchdown sink rate.

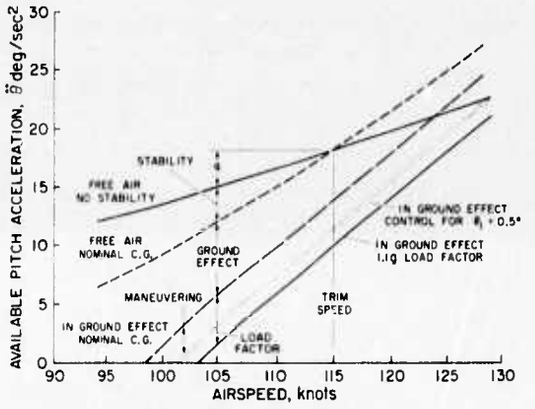

Fig. 14 Effect of airspeed on control power characteristics -- conventional jet transport.

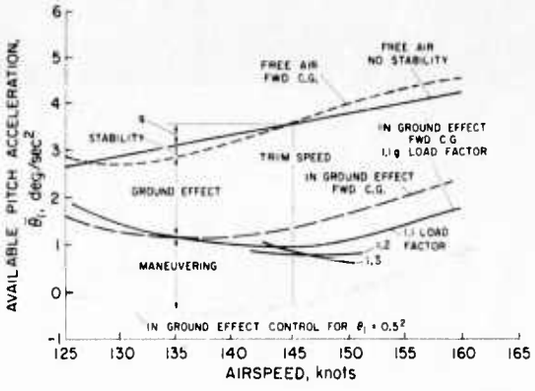

Fig. 15 Effect of airspeed on control power characteristics for advanced SST aircraft.

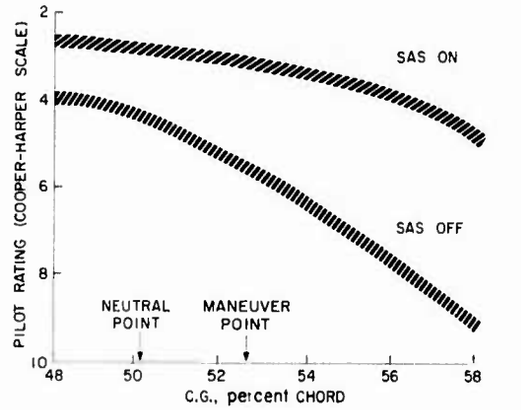

Fig. 16 Effect of SAS on c.g. limits -- advanced SST.

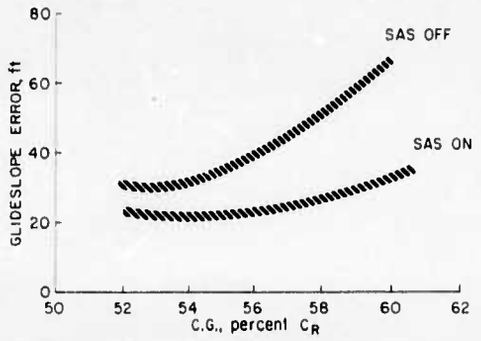

Fig. 17 Variation of glide slope error with c.g. position — advanced SST.

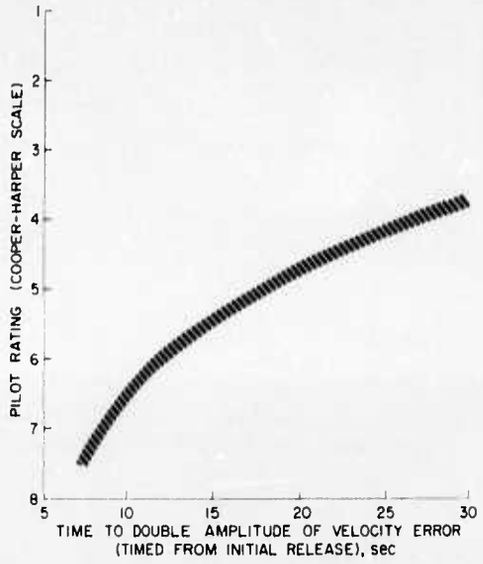

Fig. 18 Effect of time to double velocity error on pilot rating — advanced SST.

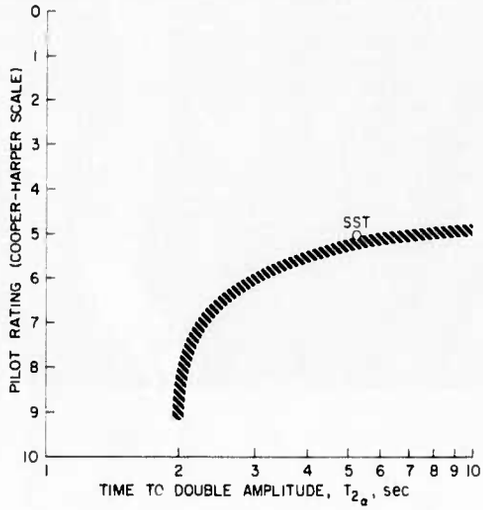

Fig. 19 Pilot rating vs. time to double amplitude.

THE INFLUENCE OF STOL LONGITUDINAL HANDLING QUALITIES ON PILOTS' OPINIONS

by

K-H. Doetsch, Jr.
National Aeronautical Establishment
National Research Council of Canada
Ottawa, Ontario, Canada. K1A 0R6

SUMMARY

Consideration is given to some of the factors which distinguish the longitudinal handling qualities of STOL aircraft from those of the CTOL class and to the influence of these differences on pilots' opinions. The effects of wind, wind-shear, trim speed, thrust vector inclination, speed coupling, pitch characteristics and of using different control technique options on flight-path control are discussed briefly. In-flight evaluations of variations in some of these parameters provided a basis for assessing their relative importance to the pilot when he was faced with a demanding instrument approach task.

Control of pitch proved to be central to the overall flight-path control task and the more easily and precisely the pilot could modulate pitch, the more adverse the speed coupling effects he was prepared to tolerate. For the typical unaugmented stability characteristics of the STOL class of aircraft exhibiting small modal separation, the handling qualities were governed by the overall responses to control and disturbance inputs rather than by the location of individual roots of the characteristic equation. This was true even for reasonable short-period characteristics when the stiffness and total damping of the short-term mode was derived to a large extent from the derivative, Z_w. Atmospheric turbulence, wind and wind shear often affected the control task significantly during the steep, low-speed approaches evaluated.

LIST OF SYMBOLS

g	Acceleration constant due to gravity, ft/sec^2
h, $\dot{h}$	Perturbations in height and rate of change of height, ft, ft/sec
M	Pitching acceleration, rad/sec^2/unit subscript
q	Perturbation in rate of pitch, rad/sec
s	Laplace's transform variable 1/sec
u, w	Perturbations in linear velocities along X and Z axes, ft/sec
U, W	Linear velocities along X and Z axes, ft/sec
X, Y, Z	(i) Principal axis system
	(ii) Linear accelerations along axes, ft/sec^2/unit subscript
α	Perturbation in angle of attack
γ_o	Ground referenced glide slope
δe	Pitching moment controller
δe_p	Pilot's elevator control displacement
δT	Pilot's thrust control displacement
ζ	Damping ratio of a second-order linear system
θ	Perturbation in pitch attitude, rad
λ_h	Zero of Eq (1), 1/sec
ω	Undamped natural frequency of a second-order mode, rad/sec

Subscripts

A	Apparent
o	(i) Fixed operating point, (ii) Ground referenced quantity
SP	Short period
ss	Steady state
W	Wind

1.0 INTRODUCTION

The trend towards increased airspeeds during the landing approach, after a steady rise to the plateau utilized for current conventional jet transports, took a deliberate and marked reversal for the STOL class of aircraft where it no longer remained a prerequisite that the lift be generated almost exclusively by aerodynamic means. The first flight tests of this type of aircraft showed, however, that the relaxation of many of the classical aerodynamic constraints not only influenced the trajectories that could

be achieved but also led, if not to undesirable, then at least to unusual handling qualities. It is the purpose of this paper to discuss the influence of some of these characteristics on pilots' opinions.

In the longitudinal plane the most readily apparent differences occur in the control of pitch and flight path. It often becomes difficult to control precisely the pitching moment of unaugmented STOL aircraft because of their decreased short-period stiffness and/or damping and because the phugoid mode may become excited more easily through an increase in its frequency without a commensurate increase in its damping. For aircraft without stability augmentation, the natural separation between the short-period and phugoid modes is diminished and must be re-established either by the pilot or by a stability augmentation system before satisfactory flight path control can be achieved. Moreover, flight path control through pitch attitude variations becomes less effective because the relationship between pitch and the resulting normal acceleration, to which most professional, or high as opposed to low speed, pilots have become accustomed, changes markedly with reduced trim speed even before consideration is given as to whether operation is on the 'frontside' or 'backside' of the power-required curve. To attain the desired low approach speeds, the aircraft must, in fact, frequently be operated on the 'backside' of this curve with all the ensuing implications of potential stability problems.

The inclination of the thrust vector of STOL aircraft is generally more normal to the flight path than it is in conventional aircraft. Consequently, the inclination of the resultant aerodynamically generated force is often affected more significantly by variations in the magnitude of the thrust and this can lead to confusing and unexpected responses. As an example is quoted experience with the augmentor-wing, modified Buffalo being evaluated in a joint U.S.A.-Canadian programme, which decelerates when thrust is increased at constant pitch attitude in an approach configuration. Even when given control over both thrust magnitude and direction, the pilot will, in general, be required to coordinate thrust vector modulation with pitch to attain the desired longitudinal and vertical velocities.

Some aspects of trajectory control are related directly to flight speed. Speed disturbances which are quite acceptable at higher speeds have a proportionally greater and possibly unacceptable influence as trim-speeds decrease. This is true not only for perturbations induced by the pilot but also for those not directly under his control due to atmospheric turbulence, wind and wind shear.

An in-flight investigation, Ref. 1, has recently been completed with the aim of quantifying the influence of systematic variations in some of the above mentioned parameters on pilots' opinions.

The NRC, Flight Research Laboratory, Bell 47G-3B1 simulator, Ref. 2, was flown on an instrument approach task at 60 knots down an 8° glide slope with visual acquisition at 200 ft AGL of the touchdown point 200 ft upwind of the microwave guidance transmitter. The complete circuit is illustrated in Figure 1.

Investigated both for good augmented and typical unaugmented pitching characteristics were the effects on speed and flight path control of various levels of coupling between airspeed and normal acceleration. This coupling was achieved through independent variations in the derivatives Z_u and Z_w.

The evaluation pilots were required to complete a detailed questionnaire after each evaluation indicating which factors had most influenced their final assessments and ratings. Further details of both the experimental design and of the pilots' assessments may be found in Ref. 1.

2.0 FLIGHT PATH CONTROL IN THE PRESENCE OF EASILY CONTROLLED PITCHING CHARACTERISTICS

The analytical background required to bring into prominence the features pertinent to flight path control is summarized below and a description of the pilots' assessments of in-flight evaluations of these characteristics then follows.

2.1 Effect on Flight Path Dynamics of Modulating Pitch

If pitch attitude can be easily and precisely constrained to the desired levels by the pilot, the equations of motion for flight path control may be considerably simplified by using pitch attitude rather than elevator as the controlling function, as was originally indicated in Ref. 3 and subsequently reiterated in different forms in several recent publications.

Of interest to the present development is the ratio between height rate and speed fluctuations resulting from an attitude change. It is this coupling which establishes the effectiveness of changing attitude as a means of controlling flight path.

To illustrate more simply the concept, it is assumed that in the small-perturbation, longitudinal equations of motion, the following approximations may be made:

$$X_{\delta e} = Z_{\delta e} = W_o = \theta_o = 0 \quad \text{and} \quad g >> X_\alpha \ .$$

The above mentioned ratio then reduces to

$$\left.\frac{\dot{h}}{u}\right|_{\delta e \to \theta} = \frac{U_o Z_w}{g} \frac{(s + \lambda_h)}{s - Z_w} \quad , \tag{1}$$

where

$$\lambda_h = - \frac{g}{U} \frac{Z_u}{Z_w} - X_u \quad . \tag{2}$$

λ_h is the zero in the height rate to pitch attitude transfer function, which indicates where along the power-required curve the aircraft is being operated.

The trajectories that would be followed by the aircraft in response to a small step speed decrement (used only for illustrative purposes) through attitude changes for positive, zero and negative λ_h are shown in Figure 2.

Consider first the case where λ_h is zero, which corresponds to operation at the minimum power-required point. Equation (1) would then represent the expression for the exchange between kinetic and potential energy, at a constant dissipation rate, brought about by aircraft pitching motions. To be noted is that the height increment for a velocity decrement is given by

$$\left.\frac{h}{u}\right|_{\lambda_{h=0}} = - \frac{U_o}{g} \quad . \tag{3}$$

It is seen that, to obtain a given height increment relative to the flight path, the percentage speed change required is proportional to the square of the trim velocity. This factor has two consequences of increasing significance as trim speed is reduced, namely:

(i) Considerably greater speed decrements are demanded to attain a given increase in potential energy, and the ensuing fluctuations about the operating point thus also become greater.

(ii) The demanded speed perturbations may become such that they no longer remain negligible in comparison with the trim-speed. Thus, even if the rate of dissipation of energy were to remain unchanged (λ_h=0), the steady state change in speed would alter the flight path angle sufficiently to create the illusion of the aircraft being operated on the 'backside' of the power-required curve. The illusion would become more pronounced as trim-speed is reduced and as glide-path is steepened - two prerequisites for STOL operations.

If λ_h is positive, decreasing speed from the trim speed through attitude changes decreases the rate of dissipation of energy. The glide-path will thus become less steep than that obtained with λ_h=0, and conversely for negative values of λ_h corresponding to 'backside' operation.

The above developments have been concerned with the final flight path responses to attitude changes. The rate at which these values are achieved depends on the magnitude of the damping in heave derivative, Z_w. It would appear that to achieve a suitable compromise between the response to turbulence and the need to manoeuvre, designers will be restricted to the fairly narrow range of about $.25 < -Z_w < 1.0$ sec^{-1} for the landing approach phase. Limited freedom will thus be available for tuning initial responses to the pilot's desires, but the long term flight path response is established by the rate of dissipation of total energy and the only manner in which this can be adjusted if the inherent configuration characteristics do not provide suitable variations, is by modulating the thrust simultaneously with pitch. Reference 4 gives one approach to achieving the appropriate pitch and thrust modulation, whereas the following section is concerned more with investigating the limiting options available to a pilot in this control task.

2.2 Effect on Flight Path Dynamics of Modulating Thrust in Conjunction with Different Limiting Constraints obtained through Pitch Attitude Variations

The response to thrust inputs for the following three motion constraints is to be considered:

(i) Pitch attitude perturbations constrained to zero.

(ii) Longitudinal velocity perturbations constrained to zero through pitch attitude (STOL Technique).

(iii) Height rate perturbations constrained to zero through pitch attitude (CTOL Technique).

In all cases, for simplicity, the same assumptions as in section 2.1 will be made as regards quantities which may be neglected. It is also assumed that

$$\left|X_u + Z_w\right| >> \left|X_w \frac{Z_u}{Z_w}\right| \quad .$$

2.2.1 Pitch Attitude perturbations constrained to zero

$$\frac{u}{\delta T}(s) = \frac{1}{s - X_u + X_w \frac{Z_u}{Z_w}} \left[X_{\delta T} + \frac{X_w}{s - Z_w} Z_{\delta T} \right] . \tag{4}$$

$$\frac{\dot{h}}{\delta T}(s) = \frac{1}{\left(s - X_u + X_w \frac{Z_u}{Z_w} \right)(s - Z_w)} \left[-Z_u X_{\delta T} - (s - X_u) Z_{\delta T} \right] . \tag{5}$$

If, in addition, $\left| X_u \right| >> X_w \frac{Z_u}{Z_w}$,

$$\frac{\dot{h}}{\delta T}(s) = \frac{1}{s - Z_w} \left[\frac{-Z_u}{s - X_u} X_{\delta T} - Z_{\delta T} \right] . \tag{6}$$

It is seen that, not surprisingly, the most immediate response along any axis occurs when the thrust is inclined along that axis and that the response along the other axis is established by the magnitude of the crosscoupling derivative X_w or Z_u.

Moreover, unless

$$X_u - X_w \frac{Z_u}{Z_w} > 0 ,$$

this control mode remains stable.

The mode is indicative of the velocity vector variation that occurs for thrust inputs when the pilot does not attempt to use attitude to constrain either of the velocity components next considered.

2.2.2 Longitudinal Velocity perturbations constrained to zero through Pitch Attitude

$$\frac{\theta}{\delta T}(s) = \frac{1}{g} \left[X_{\delta T} + \frac{X_w}{s - Z_w} Z_{\delta T} \right] . \tag{7}$$

$$\frac{\dot{h}}{\delta T}(s) = - \frac{1}{s - Z_w} \left[\frac{U Z_w}{g} X_{\delta T} + Z_{\delta T} \right] . \tag{8}$$

To be noted is that the time constant governing the height rate response does not depend on the thrust inclination. Also, the requirement to change pitch attitude is reduced for a near normal thrust vector unless X_w becomes large compared to Z_w. Even then, less lead would be required for pitch compensation with a normal rather than a longitudinal thrust vector.

The mode is always stable unless Z_w becomes positive.

2.2.3 Height Rate perturbations constrained to zero through Pitch Attitude

$$\frac{\theta}{\delta T}(s) = \frac{1}{-U_o Z_w \left(s - \frac{g}{U_o} \frac{Z_u}{Z_w} - X_u \right)} \left[Z_u X_{\delta T} + (s - X_u) Z_{\delta T} \right] . \tag{9}$$

$$\frac{u}{\delta T}(s) = \frac{1}{s - \frac{g}{U_o} \frac{Z_u}{Z_w} - X_u} \left[X_{\delta T} + \frac{g}{U_o Z_w} Z_{\delta T} \right] . \tag{10}$$

Again, the time constant governing the velocity response is independent of thrust inclination. However, the pitch response demanded to constrain height rate to zero requires more lead on the part of the pilot as the thrust vector becomes more normal to the flight path. Furthermore, the solution becomes unstable for backside operation with

$$\left(\frac{g}{U_o} \frac{Z_u}{Z_w} + X_u \right) > 0 ,$$

whatever the thrust inclination.

The success of any of the modes of control delineated above depends upon the ease and precision with which pitch attitude can be modulated to constrain the appropriate velocity component to the desired level. Pilots, in general, favour minimum control interaction and one would thus expect a preference for the thrust inclination which demands the smallest pitch compensation to maintain constrained motion.

The STOL technique, for example, would encourage the use of a near normal thrust vector for height control. To attain zero steady state pitch perturbations, the following identity would need to be satisfied:

$$X_{\delta T}/Z_{\delta T} = X_w/Z_w \ .$$

The pilot would, however, in this case still be required to provide the transient attitude correction given by Eq (7) as

$$\frac{\theta}{\delta T}(s) = \frac{Z_{\delta T}}{g}\left|\frac{s \quad X_w}{s - Z_w}\right| \ .$$

A compromise between diminishing the initial and steady state compensations would probably be preferred for larger values of X_w/Z_w.

As control of pitch becomes more difficult, the need to coordinate it with thrust inputs places an increasing burden on the pilot and, for this reason, pitch stability augmentation needs to be one of the first stability modes provided.

2.3 Effect of the External Environment on Flight Path Control

2.3.1 Mean Winds and Wind Shears

The change in rate of descent required to maintain a constant ground-referenced glide-path angle in the presence of a wind of strength, U_W, which is approximately aligned with the longitudinal axis (Figure 3), is given by

$$\dot{h} = -\gamma_o U_W \quad \text{or} \quad \frac{\dot{h}}{\dot{H}_o} = -\frac{U_W}{U_o} \ . \tag{11}$$

The proportional change in rate of descent is dependent on the relative magnitude of the wind to airspeed and it is seen that when wind shear occurs with altitude, increasing demands may be placed on the pilot to maintain not only his airspeed but also the appropriate rate of descent, whenever the variation in wind along the trajectory of the aircraft becomes large relative to the trim speed.

A decrease in airspeed due, for example, to wind shear reduces the 'convertible' energy of the aircraft. If pitch attitude is held constant, operation on the 'frontside' of the power-required curve results in a decrease in the rate of dissipation of energy until the airspeed is restored and, as a result, some of the convertible energy is eventually regained. 'Backside' operation, however, results in an increase in the rate of dissipation of energy and in further depletion of the 'convertible' energy store. This behaviour is illustrated schematically in Figure 4. It is thus apparent that when the aircraft is being operated on the 'backside' of the power-required curve, it becomes necessary for the pilot to notice early any changes in airspeed due to wind shear in order to be able to reduce the thrust modulation necessary to maintain a ground referenced trajectory.

It was found during the investigation described in a subsequent section that, even though the majority of evaluations were deliberately carried out in light surface winds, the effects of wind shear were often cause for surprise and comment from the pilot when extreme 'backside' configurations were being evaluated. Not only did the pilot have to make appropriate adjustments to his rate of descent according to the time-varying kinematic relationship expressed in Eq (11) but, during 'backside' operation, his trajectory control problem was noticeably accentuated because of the need to observe early any deviations from trim-airspeed.

In a similar manner, the influence of lateral wind shears needs to be compensated for by the pilot. During the above experiment, localizer tracking often proved to be at least as demanding as glide-path tracking because of the effects of wind shear and caused a noticeable increase in the pilot's workload during this already demanding approach task.

It is suggested in Ref. 5 that the ground referenced trajectory be varied according to the predicted along-track wind during instrument approach tasks, much as is frequently done by pilots flying lower speed approaches under visual conditions. Although obvious physical limits to this concept would remain (such as ground obstacle clearance heights and guidance aid limits) even if the along-track wind could be accurately predicted, the range of configuration characteristics to which the pilot would be exposed by its application would be substantially reduced. This would be of benefit to the pilot who is already subjected to a high workload during this flight phase without his having to adapt to continuously varying configuration characteristics.

2.3.2 Turbulence

As speeds decrease, the wavelengths of some of the aircraft characteristic modes tend to coincide more with those of the turbulence components exhibiting high energy levels. The effects of turbulence on disturbing the aircraft from its trajectory can thereby become pronounced at low speeds, particularly if the derivatives, M_u, M_w, Z_u, Z_w, are relatively large.

2.4 Pilots' Assessments of Flight Path Control in the Presence of Good Pitch Control Characteristics

As very little documented in-flight data of the assessment of instrument approaches at typical STOL speeds in aircraft operating with various flight path control characteristics existed, the experiment described in detail in Reference 1 was carried out to provide pilots' evaluations of the influence of some of the parameters considered in the previous sections.

Simulator limitations only allowed a thrust vector inclination approximately normal to the flight path to be evaluated, but complete freedom did exist in the longitudinal plane to vary the normal force and the pitching moment characteristics.

For this phase of the investigation, the pertinent parameters were as follows:

(i) Short-Period Mode: $\omega_{SP} = 1.5$ r/s, $\zeta_{SP} = 0.7$.

These characteristics were obtained by augmenting the basic pitching characteristics of some of the configurations described in Section 3 with pitch rate and attitude feedback.

(ii) The following elevator command forms were used:

(a) Attitude Command

$$\frac{\delta e}{\delta e_p} = 1 \ .$$

(b) Rate Command

$$\frac{\delta e}{\delta e_p} = \frac{s^2 - (M_q + M_{\dot{\alpha}})s - M_\theta}{s[s - (M_q + M_{\dot{\alpha}})]} \ .$$

(iii) The non-zero closed-loop longitudinal force derivatives were well represented by

$$X_u = -.04, \quad X_w = -.03, \quad X_q = -.022 \ .$$

The steady state pitch attitude in straight and level flight was $\theta_o = -7°$.

(iv) Flight path control characteristics were changed through independent variations in the derivatives Z_u and Z_w. In cognizance of the ability of modern technology to allow some deviation from the traditional aerodynamic restraints, the ratio, Z_u/Z_w, was also allowed to deviate within sensible limits from the value expected for purely aerodynamically generated forces.

(v) The task was flown at 60 knots down an 8° glide slope. Only raw aircraft state data were presented to the pilot during the instrument portion of the task.

(vi) Artificial turbulence exhibiting a Von Karman spectral shape with a scale length of 400 ft, a normal distribution and an r.m.s. level of 2.5 ft/sec was used to represent the three turbulence components of the atmosphere, whereas the real wind and wind shear of the environment disturbed the trajectory of the simulator.

To be assessed were the maximum acceptable coupling between airspeed and normal force and, independently, the influence of the derivative, Z_w, when the pilot had control over a normal thrust vector. Also, the more suitable of the two above mentioned elevator command forms for this control task was to be established.

It was found that when the steady state velocity ratio, $\left.\frac{\dot{h}}{u}\right|_{ss}$, was negative, corresponding to 'frontside' operation, the easily controlled pitching characteristics allowed the pilot to control airspeed through pitch attitude modulation, and rate of descent through thrust modulation without significant control activity being required to compensate for undesired crosscoupled velocity responses.

Evaluation of three levels of Z_w, namely, -.25, -.5 and -1.0, in these circumstances, showed that the time constant associated with vertical velocity control, $-1/Z_w$,

was considered to be too long for $Z_w = -.25$, whereas the turbulence response in heave became too great for $Z_w = -1.0$. A value of $Z_w = -0.5$ appeared to result in a good compromise between controllability on the one hand and excessive turbulence response on the other.

The velocity coupling was next varied through increases in the magnitude of $-Z_u$ from zero to the maximum attainable aerodynamic value of about 0.6 for this airspeed. Typical plots of pilots' ratings are shown in Figure 5 for $Z_w = -0.5$ for both elevator command forms. It is seen that the rate command form was considered to be significantly worse than the attitude command form for extreme 'backside' operation but better for 'frontside' operation.

Pilots' comments indicated that the initial pitch response for the attitude command form could be so rapid that a propensity towards pilot induced oscillations existed whenever significant attitude changes were demanded in such manoeuvres as the flare. This accounts for the relative degradation in rating during 'frontside' operation. However, during extreme 'backside' operation, the need to control airspeed precisely to avoid speed coupling effects dominated to such an extent, that the added precision with which the attitude rather than the rate command forms could control the long term airspeed variations proved to be of considerable benefit to the pilot.

It may be noted from Figure 5 that a fairly extensive region of optimum ratings (say $|\dot{h}/u_{ss}| < 0.3 - 0.5$) existed, centred on zero steady-state velocity coupling. This trend was confirmed for the other levels of $-Z_w$.

The most objectionable feature for operation on the extreme 'backside' of the power-required curve was the coupling between airspeed and rate of change of height. This made the pilot much more aware of the effects of wind and turbulence and increased his general workload significantly. In his assessments of his workload and performance during various task phases, it was apparent that he felt that the former increased and the latter deteriorated in most phases, whenever the primary tasks of controlling either pitch attitude and airspeed or rate of change of height became difficult.

As the pitch control and hence airspeed control was degraded, the undesirable effects on handling qualities of operating on the 'backside' of the power-required curve became pronounced at lower levels of $-Z_u$. This behaviour, discussed further in Section 3.3, is illustrated quantitatively by the pilots' ratings plotted in Figure 6.

3.0 THE CONTROL OF THE PITCHING CHARACTERISTICS

Much of the foregoing has addressed the problem of flight path control in the presence of pitching characteristics which could be easily and precisely controlled. However, the inherent characteristics of STOL aircraft do not fall into this category and, although it may be argued that stability augmentation systems can always be incorporated to override the unaugmented characteristics, the control problems associated with system failure or inadequate augmentation remain. A considerable portion of the experiment was thus concerned with evaluating the influence of undesirable pitching characteristics on flight path control.

Consideration is given first to the configurations in which the short-period approximation represents well the roots characterizing the short term response, and this is followed by consideration of the effects on handling qualities of roots resulting from short and long term modes with small separation, where the classical assumptions regarding negligible quantities no longer remain adequate for determining the roots of the characteristic equation.

3.1 Classical Short-Period Approximation

It is assumed that longitudinal velocity perturbations have negligible influence on the pitch and heave degrees of freedom. In these circumstances, the pitch response to elevator inputs which describes the central control task facing the pilot, becomes

$$\frac{q}{M_{\delta e}\delta e}(s) = \frac{s - Z_w}{s^2 + 2\zeta\omega s + \omega^2} \qquad (12)$$

The unaugmented short-period characteristics of STOL aircraft in their landing approach configurations are often such that $-Z_w$ and ω^2 are of the same order of magnitude and less than 1.0. For these conditions, some insight into the initial (high frequency) response of concern to the pilot is given by expanding Eq (12) about the zero location to give

$$\frac{q}{M_{\delta e}\delta e}(s) = \frac{1}{s^2 + 2\zeta_A\omega_A s + \omega_A^2}\left[s - \frac{Z_w\omega_A^2}{s^2 + 2\zeta\omega s + \omega^2}\right], \qquad (13)$$

where

$$2\zeta_A\omega_A = 2\zeta\omega + Z_w$$

and

$$\omega_A^2 = \omega^2 + Z_w(2\zeta_A\omega_A) .$$

Providing that $|Z_w\omega_A^2|$ remains small in comparison with $|s(s^2 + 2\zeta\omega s + \omega^2)|$ in the frequency range of interest to the pilot in his short term control of pitch, one may

approximate the high frequency response by

$$\frac{q}{M_{\delta e}\delta e}(s) \approx \frac{s}{s^2 + 2\zeta_A\omega_A s + \omega_A^2} \quad . \tag{14}$$

To be noted is that when the usual short-period mode approximations are made,

$$2\zeta_A\omega_A = -(M_q + M_{\dot{\alpha}}) \tag{15}$$

and

$$\omega_A^2 = -(M_\alpha + M_{\dot{\alpha}}Z_w) \quad . \tag{16}$$

These are to be compared with the short-period mode values of

$$2\zeta\omega = -(M_q + M_{\dot{\alpha}} + Z_w) \tag{17}$$

and

$$\omega^2 = -(M_\alpha - M_q Z_w) \quad . \tag{18}$$

An idea of the adequacy of the approximation may be obtained from Figures 7 and 8 which show the responses obtained for variations in Z_w and M_w for a typical range of unaugmented STOL short-period characteristics. The response is exactly represented by Eq (14) for the case of pole-zero cancellation ($M_\alpha + M_{\dot{\alpha}}Z_w = 0$), but deviates ever more rapidly from the exact solution as $|Z_w(M_\alpha + M_{\dot{\alpha}}Z_w)|$ increases. Figure 9 illustrates the relationship between the roots of the approximation and those of the short-period mode for $Z_w = -.5$. The diagram is divided into four regions exhibiting the following characteristics:

(I) The apparent initial damping in this region is negative. It is unlikely that these characteristics will arise in practice as $-(M_q + M_{\dot{\alpha}})$ would normally be positive.

(II) In this region the apparent initial damping ratio is less than that expected from the short-period roots. Previous in-flight investigations have explored this region, particularly at the higher frequencies ($\omega^2 > 2$), and have reported PIO tendencies near the boundary between I and II even when favourable short-period characteristics existed (for example, Ref. 6).

(III) In this region, especially when the boundary between III and IV is approached, the apparent initial stiffness is reduced. However, providing that the origin of $2\zeta_A\omega_A$, ω_A^2 is not approached too closely, handling qualities remain satisfactory.

(IV) The apparent initial stiffness is negative in this region and the aircraft is characterized by a more sluggish pitch response to elevator inputs than would be expected from the short-period root locations.

Also illustrated in Figure 9, to give an indication of the region of present concern, is a range of typical unaugmented STOL short-period characteristics during the landing approach phase.

The influence of increasing $-Z_w$ on the apparent initial damping and stiffness is shown in Figure 10. In general, Regions I and IV, which correspond to negative initial damping and stiffness respectively, are expanded at the expense of Regions II and III. The higher the value of $-Z_w$ in relation to a given set of short-period roots, the more sluggish the initial response will appear to be. Expressed slightly differently, the increase in short-period damping and stiffness, obtained from Eqs (17) and (18), with increasing $-Z_w$ is not reflected in the initial response to elevator inputs - indeed, for the normally negative values of $M_{\dot{\alpha}}$, the apparent initial stiffness is reduced.

The marked change in initial response to control inputs resulting from different values of Z_w for the same short-period characteristics is illustrated in Figure 7 for $Z_w = 0, -.25, -.5, -1.0$ and the short-period characteristics, $2\zeta\omega = 1.75$, $\omega^2 = .625$.

3.2 Pilots' Assessments of Unaugmented Short-Period Characteristics

One of the advantages of the model following technique employed on the simulator utilized in the experiment was the accuracy with which low stiffness configurations could be simulated. This allowed exploration of a range of short-period characteristics which are representative of unaugmented STOL aircraft in this flight phase but which had not before been evaluated in flight in a systematic manner.

Decoupling from longitudinal velocity perturbations was ensured by setting M_u and Z_u to zero for this group of configurations. Various levels of total damping and stiffness were evaluated for different magnitudes of $-Z_w$.

The ease of controlling pitch dominated the pilot's concern but the effects of the magnitude of Z_w discussed in Section 2.4 again were apparent.

Dealing first with the configurations characterized by pole-zero cancellation, that is, those on the line between Regions III and IV in Figure 9, the ratings deteriorated rapidly when the basic time constant governing the pitch control mode $(1/-(M_q + M_{\dot{\alpha}}))$ became greater than about 1.0 sec. The trend in pilots' ratings for configurations with pole-zero cancellation is shown in Figure 11. Imprecise pitch control was blamed for the deterioration in handling qualities with increasing time constant and, once the latter had become too long, increasing the stiffness to move the short-period characteristics into Region III of Figure 9 did not improve the situation noticeably in the range investigated ($\omega \leq 1$ r/s). For example, all configurations with $Z_w = -1.0$ and $2\zeta\omega = 1.75$ and with $Z_w = -0.5$ and $2\zeta\omega = 1.0$ were deemed unacceptable. This indicates that a lower limit exists for the pitch damping, $-(M_q + M_{\dot{\alpha}})$, to attain acceptable pitching characteristics with these low stiffness configurations, even when the short-period damping, $-(M_q + M_{\dot{\alpha}} + Z_w)$, is at a favourable level.

When the basic time constant was classed as good, decreasing the stiffness so that ω_A^2 became negative led to a rapid deterioration in ratings. The complaint again became one of sluggish and imprecise pitch responses. It appears then that a lower limit, established by the pitching characteristics, also exists for the minimum acceptable short-period stiffness, and that this limit may be governed by the apparent initial pitch stiffness to elevator inputs. Increasing ω_A^2 from zero through changes in M_α accentuated the turbulence response but, in the range tested, did not degrade the overall ratings. The trends in pilots' ratings for varying stiffness, damping and Z_w are shown in Figure 12.

To be noted is that the pilots on several occasions had difficulty in assigning consistent ratings for these configurations which were often characterized by low total stiffnesses. This situation is not unusual when the pilot must concern himself with several mediocre to poor control characteristics rather than with one dominant characteristic.

3.3 Handling Qualities for Highly Coupled Degrees of Freedom

The short-term modes of unaugmented STOL aircraft in their landing approach configurations are often governed by two aperiodic roots, one of which may have a value close to zero. In these circumstances, the root locations may not be well approximated by those obtained using the classical assumptions for calculating separated short-period and phugoid modes of motion. When the constraints of zero values for M_u and Z_u applied in the previous group were relaxed, many of the configurations fell into this class.

As an example, root loci due to varying M_u are shown in Figure 13 both for well and poorly separated modes. It is seen that a noticeable redistribution of damping between the modes occurs as a result of small modal separation. In the example illustrated, a new complex pair with total damping considerably greater than that which would be expected using the classical phugoid assumptions, has resulted from the combination of one of the short-period roots with a phugoid root. This damping has been derived at the expense of an aperiodic instability arising from the remaining root near the origin. These root locations are, however, so sensitive to small variations in M_u that a redistribution of the roots to the locations expected from the normal short-period and phugoid approximations, can easily be achieved by the pilot closing a low-gain airspeed to elevator loop.

Pilots' evaluations of this situation confirmed that achieving this redistribution and hence stabilization of the aperiodic root (with time to double amplitude of 7 seconds) did not add significantly to the control task and that the instability was certainly not as detrimental to handling qualities as was one of similar time to double amplitude resulting from a reduction in the short-period stiffness through the derivative M_w, when decoupling was enforced through setting M_u and Z_u to zero.

It is thus seen that a single undesirable root location must be viewed in relationship to the other roots in the proximity before its effects on handling qualities can be ascertained.

Turning now to the general effects of non-zero M_u and Z_u on handling qualities, one finds that poor pitch characteristics accentuated the problems of flight path control considered in Section 2.4, as $-Z_u$ was increased. The reason lay with the difficulty in achieving precise long-term airspeed control. This is illustrated by the examples of variations in pilots' ratings for configurations without pitch stability augmentation with increasing $-Z_u$ shown in Figure 6, which should be compared with those of the augmented configurations shown in Figure 5.

The effect of M_u generally showed itself through the increased response of pitch to turbulence and, when M_u was positive, through the increased excitation of relatively high frequency phugoid oscillations.

4.0 CONCLUDING REMARKS

Consideration has been given to some of the factors which distinguish the handling qualities of STOL aircraft during the landing approach phase from those of conventional aircraft. It is shown that airspeed takes on an importance in its own right. At reduced speeds, control of flight path through pitch modulation becomes less effective as large speed perturbations may be demanded to attain a given height correction, and the long-term response may be undersirable because of operation on the

'backside' of the power-required curve. Wind and wind shear also have a more pronounced effect on trajectory control and may force the pilot to compensate for widely changing configuration characteristics during the course of an approach when a ground fixed trajectory is being followed.

Operation will often be on the 'backside' of the power-required curve. This makes it expedient for the pilot to control rate of change of height through thrust modulation and airspeed through pitch attitude to avoid speed instability problems.

In-flight evaluations of the landing approach phase of STOL configurations which were characterized by a normal thrust vector, indicated a preference on the part of the pilots for negligible long-term changes in flight-path angle with pitch attitude and hence airspeed, that is, operation near the aircraft's minimum power-required point.

The more easily and precisely the long-term pitch attitude could be controlled, the further along the 'backside' of the power-required curve the pilots were prepared to operate the aircraft. An attitude command form for elevator to pitch control proved advantageous in this respect as it allowed precise control of long-term speed variations.

When the pitching characteristics were not augmented and the resulting short-period stiffness became low, the pilots' principal concern lay with the control of pitch. This control problem was central to the flight-path control task and poor pitch characteristics accentuated poor flight-path control characteristics.

Finally, when the short-period and phugoid modes were not well separated, it was found that the difficulty associated with controlling an aperiodic instability was dependent not only on the location of the appropriate root taken in isolation, but also on the location of the neighbouring roots.

5.0 REFERENCES

1. K-H. Doetsch, Jr., D.W. Laurie-Lean, The Flight Investigation and Analysis of Longitudinal Handling Qualities of STOL Aircraft on Landing Approach. TR AFFDL-TR-74-18, March 1974. NRC/NAE Lab. Tech. Report LTR-FR-42, May 1974.

2. D.F. Daw, K. Lum, and D.M. McGregor, Description of a Four Degrees-of-Freedom V/STOL Aircraft, Airborne Simulator. NRC/NAE LR-499, Feb. 1968.

3. S. Neumark, Problems of Longitudinal Stability Below Minimum Drag Speed, and Theory of Stability under Constraint. R&M No. 2983, 1953.

4. J.G. Jones, Application of Energy Management Concepts to Flight-Path Control in Turbulence. In AGARD CP-140, May 1973.

5. W.S. Hindson, D.G. Gould, Modification of V/STOL Instrument Approach Geometry as a Means of Compensating for Along Track Wind Effects. NRC/NAE LR-573, Jan. 1974.

6. R.E. Smith, J.V. Lebacqz, and J.M. Schuler, Flight Investigation of Various Longitudinal Short-Term Dynamics for STOL Landing Approach Using the X-22A Variable Stability Aircraft. CAL Report No. TB 3011-F-2, Jan. 1973.

ACKNOWLEDGEMENTS

Part of the work reported here was carried out under Contract No. F33615-71-C-1722 to the United States Air Force and under Sub-Contract No. S-72-3 to CALSPAN. The assistance of Mr. D.W. Laurie-Lean during the acquisition of the experimental data of the programme under those contracts is acknowledged.

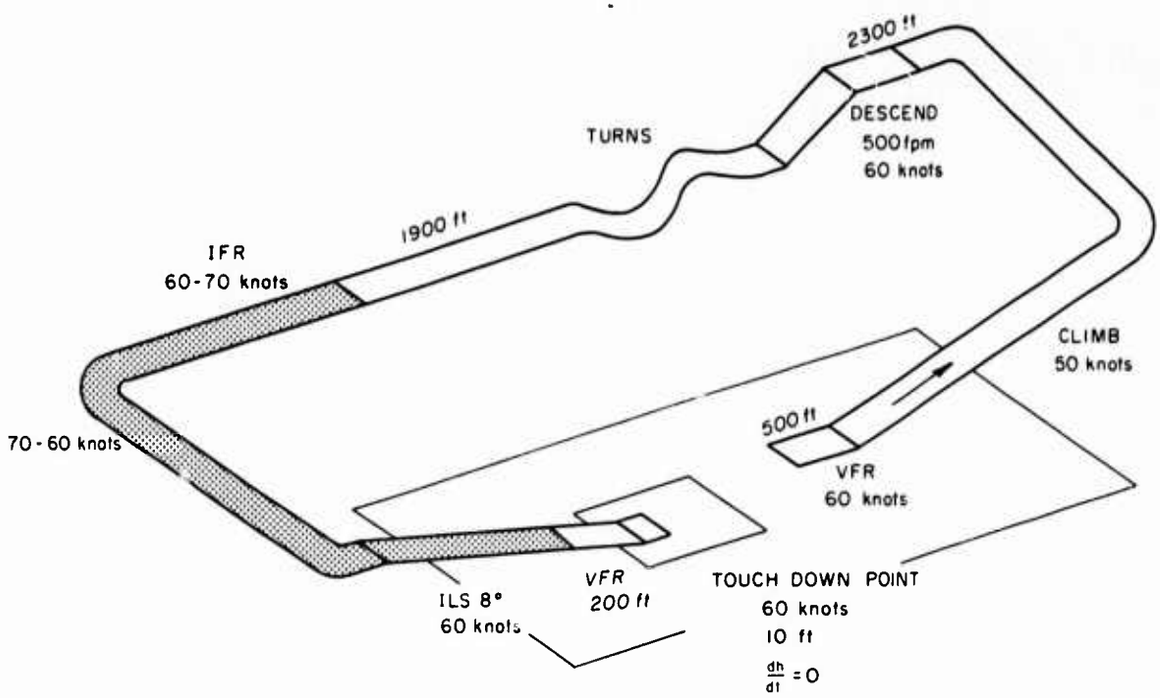

FIG 1 FLIGHT EVALUATION TASK

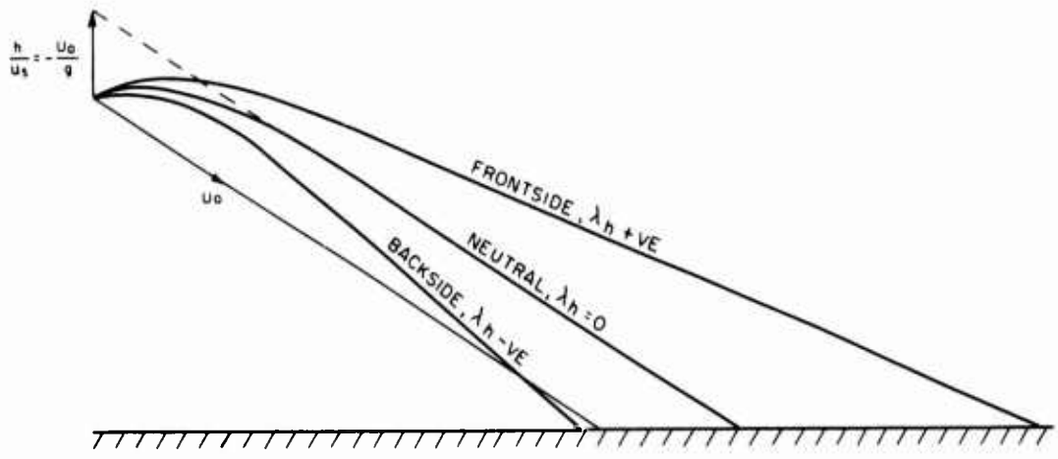

$$\frac{\dot{h}}{u}(s)\Big|_{\theta} = \frac{UZ_w}{q} \cdot \frac{s+\lambda_h}{s-Z_w}$$

$$U_o + u_s \simeq U_o$$

FIG 2 FLIGHT PATH TRAJECTORY FOR A SMALL STEP SPEED CHANGE, u_s, THROUGH PITCH ATTITUDE

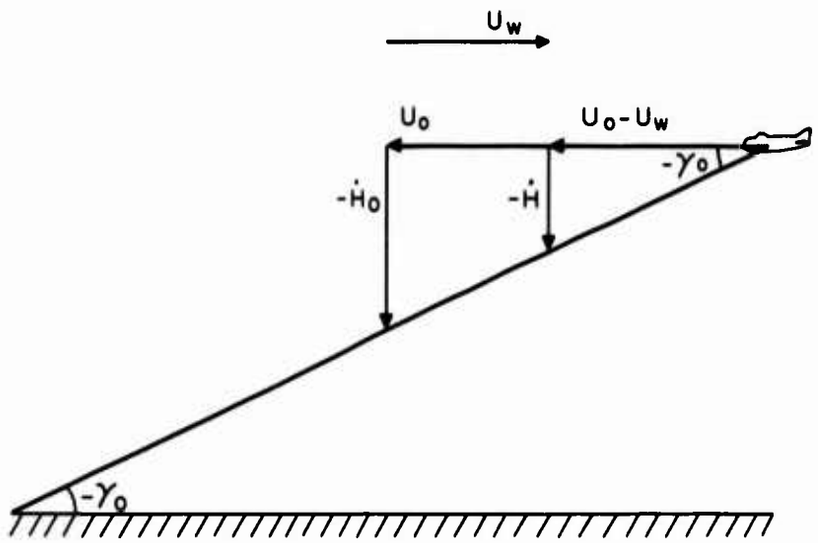

$$\frac{\dot{H}}{\dot{H}_o} = 1 - \frac{U_w}{U_o} \quad ; \quad \frac{\dot{h}}{\dot{H}_o} = -\frac{U_w}{U_o}$$

FIG 3 EFFECT OF WIND ON THE RATE OF DESCENT REQUIRED TO MAINTAIN γ_o

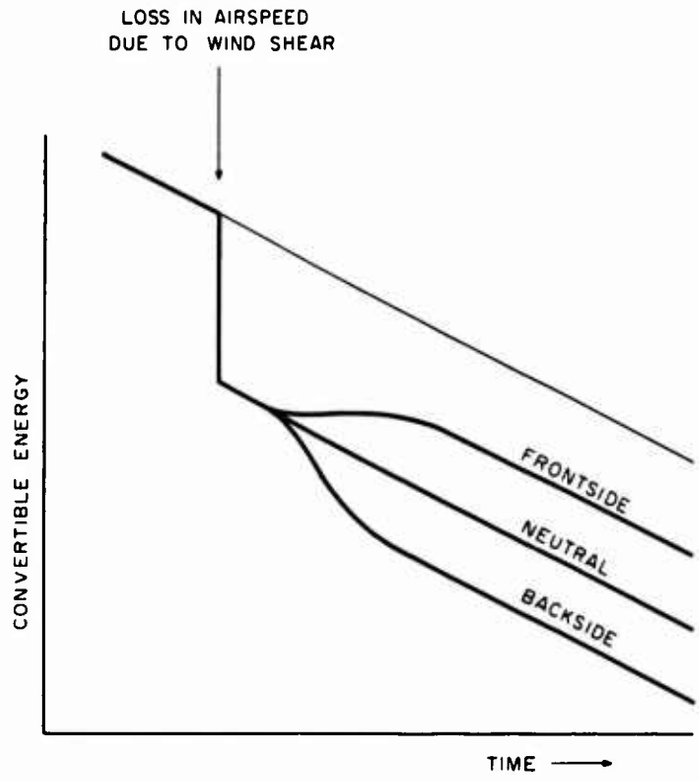

FIG 4 EFFECT OF LOSS IN AIRSPEED DUE TO WIND SHEAR ON 'CONVERTIBLE' ENERGY DISSIPATION RATE IF PITCH ATTITUDE REMAINS CONSTANT

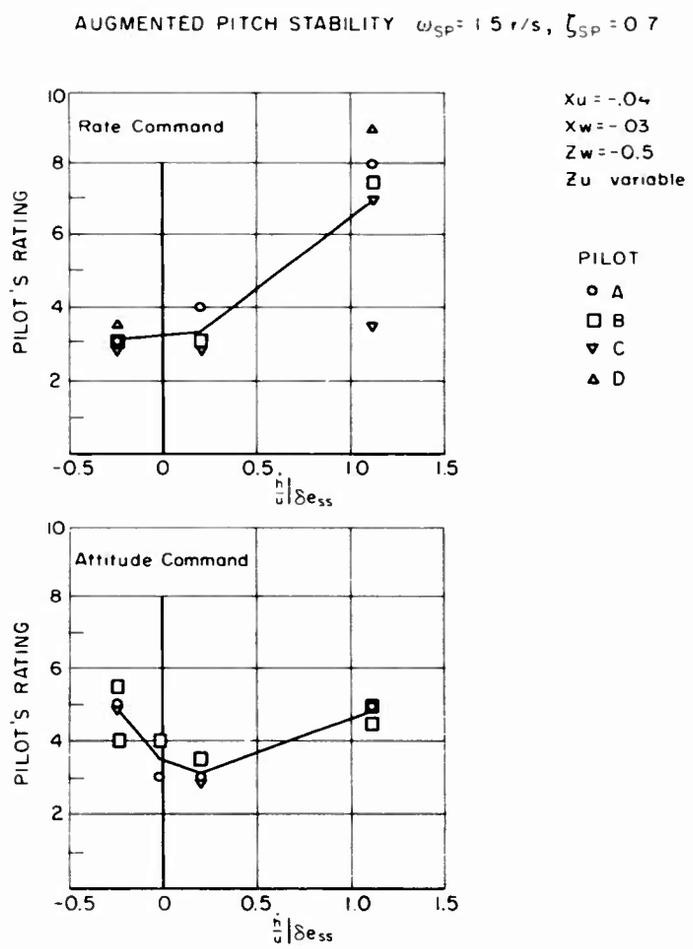

FIG 5 EFFECT OF STEADY STATE VELOCITY COUPLING ON PILOTS' RATINGS FOR TWO ELEVATOR-TO-PITCH COMMAND FORMS (REF 1)

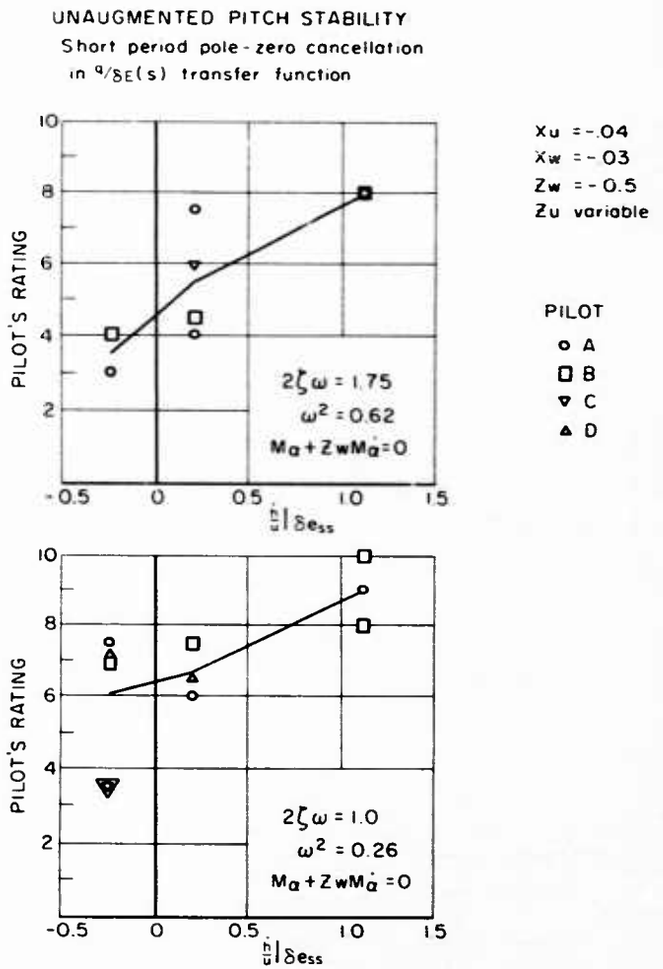

FIG 6 EFFECT OF STEADY-STATE VELOCITY COUPLING ON PILOTS' RATINGS FOR DIFFERENT SHORT PERIOD CHARACTERISTICS (REF 1)

Pitch rate response to unit $M_{\delta E} \cdot \delta E$ step $(2\zeta\omega = 1.75, \omega^2 = .625)$

——— $\dfrac{s - Z_w}{s^2 + 2\zeta\omega s + \omega^2}$ EXACT

– – – – $\dfrac{s}{s^2 + (2\zeta\omega + Z_w)s + (\omega^2 + Z_w(2\zeta\omega + Z_w))}$ APPROXIMATION

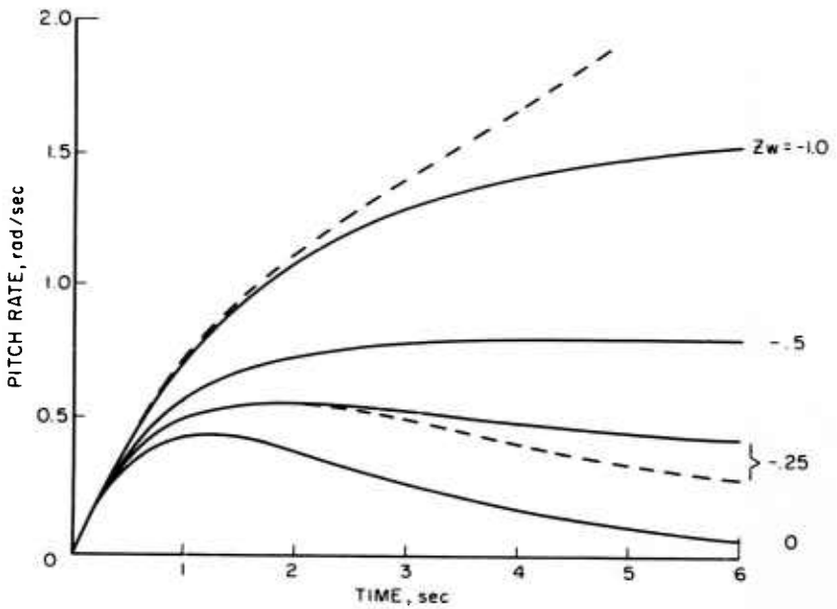

FIG 7 EFFECT ON PITCH RESPONSE OF MAINTAINING CONSTANT SHORT PERIOD CHARACTERISTICS FOR DIFFERENT VALUES OF Z_w

Pitch rate response to unit $M_{\delta E} \cdot \delta E$ step;

CASE	M_α	ω^2	MEAN PR
1	-.58	1.0	3.5 ± .5
2	-.21	0.625	3.5 ± .5
3	+.17	0.25	6.5 ± 1.5

$Z_w = -5$

$2\zeta\omega = 1.75$

——— EXACT

– – – EQUATION 14

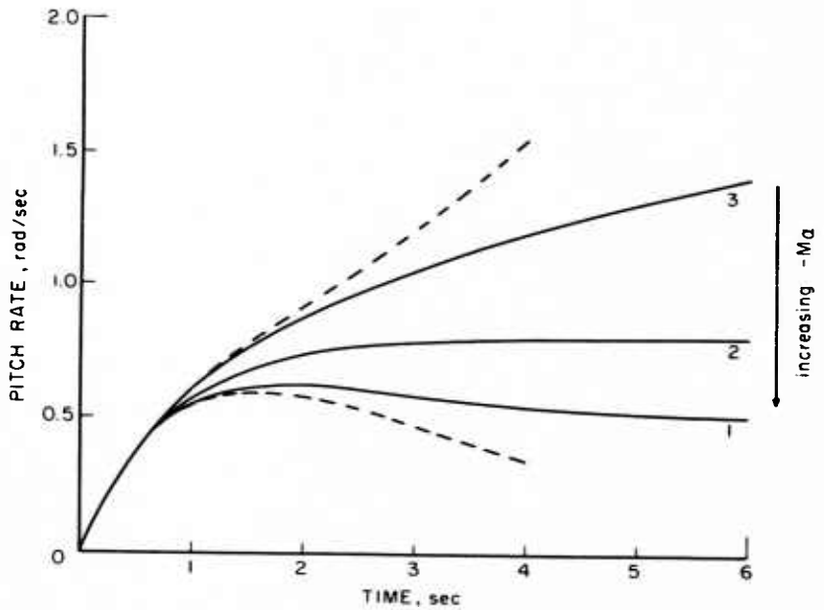

FIG 8 INFLUENCE OF M_α ON PITCH RESPONSE TO ELEVATOR INPUTS

$$F(s) = \frac{s+\lambda_N}{s^2+2\zeta\omega s+\omega^2}$$

$$F_A(s) = \frac{s}{s^2+2\zeta_A\omega_A s+\omega_A^2}$$

$$2\zeta_A\omega_A = 2\zeta\omega - \lambda_N$$

$$\omega_A^2 = \omega^2 - \lambda_N \cdot 2\zeta_A\omega_A$$

typical unaugmented STOL aircraft

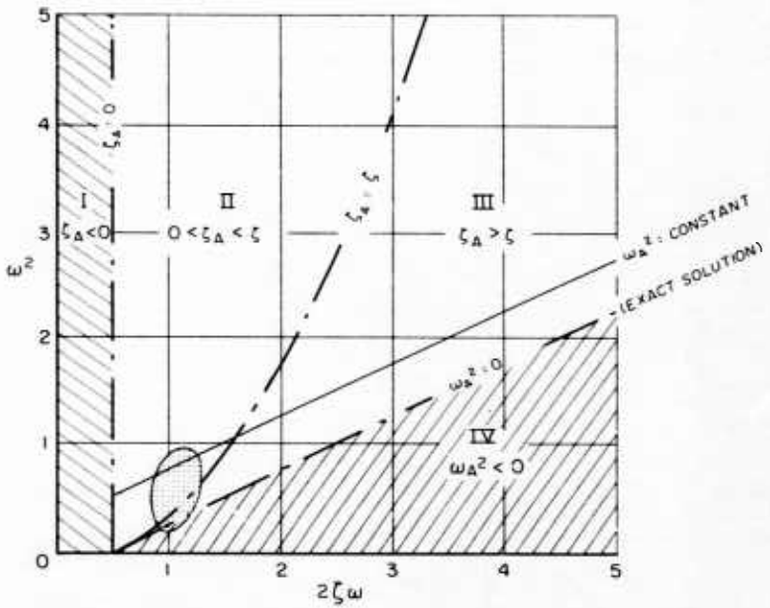

FIG 9 EFFECT OF FIRST ORDER LEAD ON APPARENT INITIAL DAMPING AND STIFFNESS OF A SECOND ORDER SYSTEM: $\lambda_N = 0.5$

$$F(s) = \frac{s+\lambda_N}{s^2+2\zeta\omega s+\omega^2}$$

– – – – – – – $\lambda_N = 1.0$

——— · ——— $\lambda_N = 0.5$

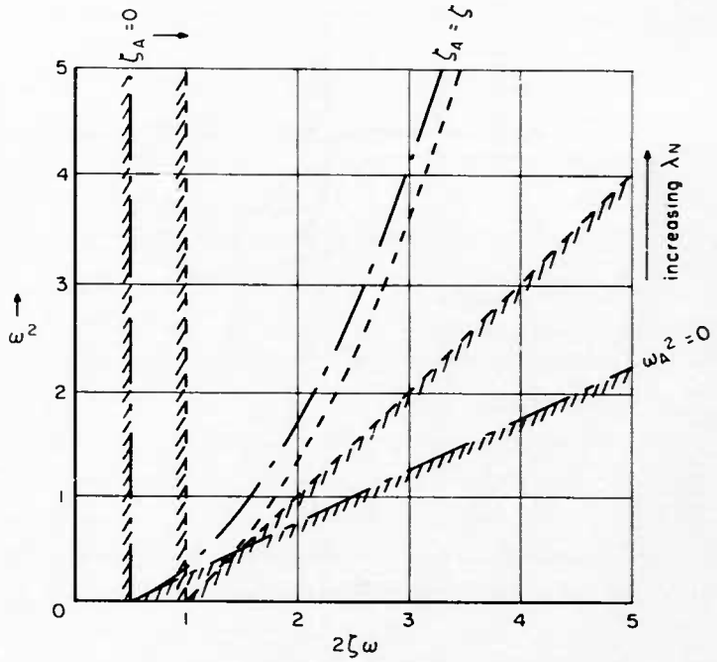

FIG 10 EFFECT OF MAGNITUDE OF FIRST ORDER LEAD ON APPARENT INITIAL DAMPING AND STIFFNESS OF A SECOND ORDER SYSTEM

MAJOR CONCERNS OF PILOT:

$Z_w = -.25$ Lack of precision in vertical velocity control

$Z_w = -0.5$, $Z_w = -1.0$ } Lack of precision in pitch control for $-(M_q + M_{\dot{\alpha}}) \leq 0.9$

$$\frac{q}{\delta E}(s) = \frac{1}{s-(M_q+M_{\dot{\alpha}})} \cdot \frac{(s-Z_w)}{(s-Z_w)} \cdot \frac{(s-X_u)}{(s-X_u)}$$

Z_w			PILOT
-.25	-.5	-1.0	
●	○	◔	A
■	□	◨	B
▼	▽		C
▲	△		D

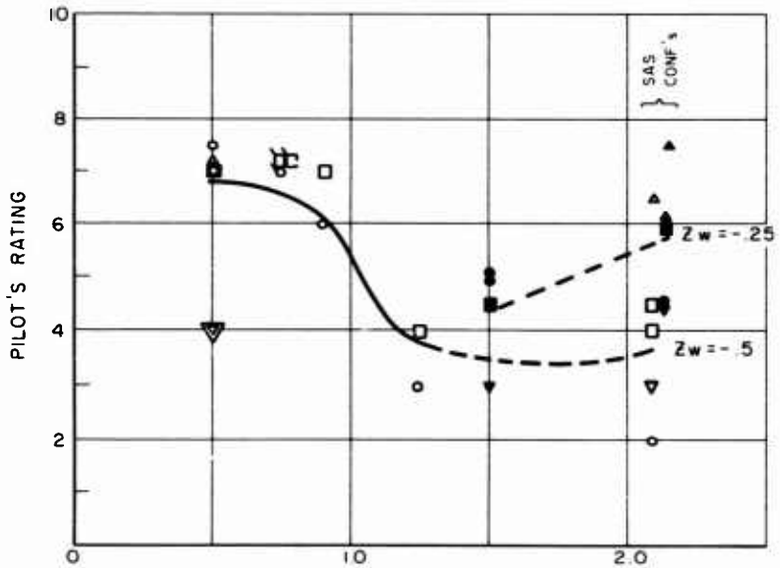

FIG 11 EFFECT OF PITCH CONTROL TIME CONSTANT ON PILOTS' RATINGS (REF 1)

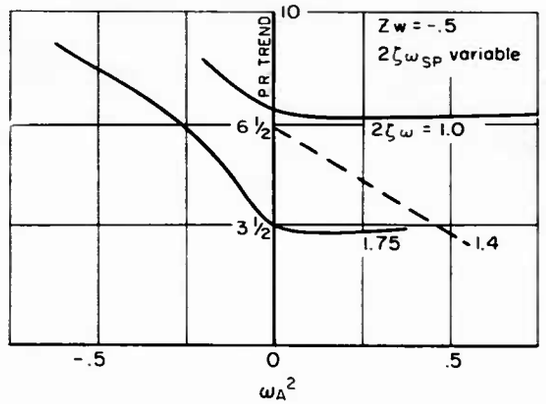

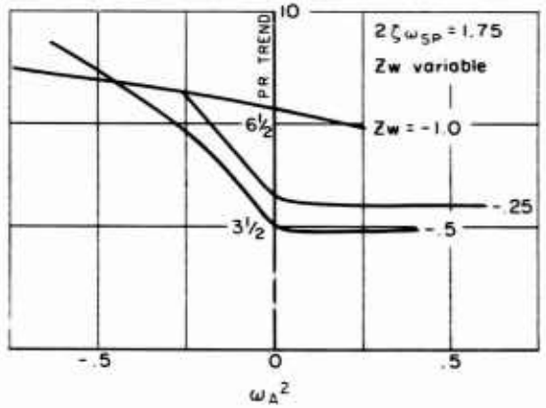

$$\omega_A^2 = \omega_{SP}^2 + Z_w(2\zeta\omega_{SP} + Z_w)$$

FIG 12 EFFECT ON PILOTS' RATINGS OF VARYING ω_A^2 THROUGH M_w FOR DIFFERENT LEVELS OF DAMPING AND Z_w. ($M_u = Z_u = 0$) (REF 1)

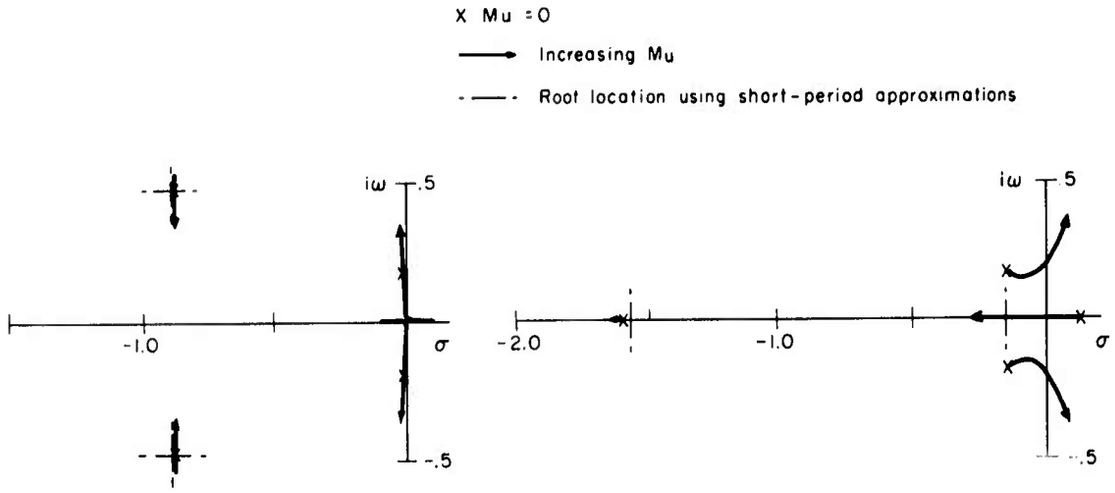

(a) LIGHTLY COUPLED DEGREES OF FREEDOM

(b) STRONGLY COUPLED DEGREES OF FREEDOM

FIG 13 EFFECT OF MODAL SEPARATION ON ROOT LOCI FOR Mu VARIATIONS

LOW-SPEED STABILITY AND CONTROL CHARACTERISTICS OF TRANSPORT AIRCRAFT WITH PARTICULAR REFERENCE TO TAILPLANE DESIGN

by

E. Obert
Aerodynamicist
FOKKER - VFW B.V.
P.O. Box 7600
Schiphol - Oost
The Netherlands

SUMMARY

For modern transport aircraft generally emphasis is put on operational flexibility. This means among other things that the ability is required to operate at low take-off and landing speeds under a wide range of loading conditions. Consequently the operational envelope of the aircraft covers a large range of lift coefficients and C.G. positions. The ensuing requirements for the design of horizontal tail surfaces and elevators are difficult to fulfil. In this paper some of the low-speed tailplane and elevator problems are considered. Particular reference is made to the possibility of tailplane stall. Some related experience obtained in the design and flight testing of the Fokker-VFW F-27 and F-28 is discussed.

LIST OF SYMBOLS

C_L	lift coefficient
$C_{L_{T-O}}$	lift coefficient for the aircraft less tail
C_T	thrust coefficient, $C_T = \frac{T}{qS}$
$C_{L_{\alpha h}}$	tailplane lift curve slope
$C_{L_{\delta_e}}$	elevator lift curve slope
$C_{m_{30}}$	pitching moment with the moment reference centre at 30% MAC
$C_{m_{T-O}}$	pitching moment for the aircraft less tail
$\bar{c}$	mean aerodynamic chord (MAC)
i_h	tailplane angle-of-incidence
l_h	tail moment arm
n	normal load factor
q	free stream dynamic pressure
q_s	dynamic pressure at the tailplane location
S	wing area
S_e	elevator area
S_h	tailplane area
V	airspeed
V_s	stalling speed as determined for certification purposes
$\bar{V}_h$	tailplane volume coefficient
α_h	tailplane effective angle-of-attack
α_R	aircraft angle-of-attack with respect to fuselage datum line
α_w	aircraft angle-of-attack with respect to wing root datum line
$\Delta\alpha_{(q)}$	change in tailplane angle-of-attack due to aircraft rate-of-pitch
δ_e	elevator angle
ε	downwash angle at the tailplane

1. INTRODUCTION

Operational flexibility is a key word in the design of modern transport aircraft. In particular short-haul transport aircraft must be able to operate with full payload from moderate to short runways. On the other hand when ample runway length is available high take-off weights for the longer range capability should be possible. Forthermore loading restrictions should in the operator's opinion be non-existent. The striving after of these goals has in the course of time led to two developments :

1. The maximum lift coefficient for take-off and landing and the number of take-off figurations that can be selected has increased considerably.
2. The centre-of-gravity range for which aircraft are certificated shows a tendency to increase.

Regarding the C.G. range it should be noted that at present there is a trend to include beforehand in a new design the loading flexibility needed upon developing the aircraft design further into a "family of aircraft". Stretching, a change of engines, a large variety of customer requirements, or the fitting of a large freight door may all affect the required C.G. range. It is often worthwhile to consider these points when sizing the tailplane and designing the control system.
Both developments are reflected in the heavy and often conflicting requirements put on the horizontal tailplane and elevator characteristics of present-day transport aircraft. Research into the quantification of desired handling qualities has also had its impact on the design of longitudinal control systems. The improved insight into the relation between a pilot's opinion on a aircraft's behaviour and measurable aircraft characteristics has led to a general increase in the level of what is considered as acceptable design standards.

The Fokker company was confronted with all these developments in the design and developments of the F-27 turboprop and F-28 turbofan transport aircraft. Both aircraft are now well-established in the air transport market. A three-view of both aircraft is presented in fig. 1.

2. LONGITUDINAL CONTROL DESIGN REQUIREMENTS

In table I a summary is presented of the various factors concerning low speed flight which influence the aerodynamic design of tailplane and elevator for a small to medium-sized transport aircraft. Both reversible and irreversible controls are considered. The inclusion of the former implicates that control forces and thus hinge moments also have to be taken into account.
In the table these factors have been grouped under five headings :

a. Static and dynamic stability
b. Control capacity
c. Trim capacity
d. Control forces
e. Out-of-trim control characteristics.

In this paper a closer view will be taken at the requirements concerning low-speed control and trim capacity. In particular the possibility of tailplane stall will be considered.

3. PITCHING MOMENTS AS AFFECTED BY $C_{L_{max}}$ AND C.G. RANGE

Fig. 2 shows in principle the pitching moment for a hypothetical transport aircraft, tail-off, as a function of flap setting and centre-of-gravity position. The total range of pitching moments that has to be balanced by the tail is quite large and lies between a high negative and a small position value. For equilibrium in pitch and under the assumption that $\bar{V}_h = 1$ the tailplane lift coefficient has to cover the same range of values.
It is also clear from fig. 2 that an increase in $C_{L_{max}}$ or C.G. range puts an increasing demand on the lifting capability of the tailplane. Furthermore it can be seen that the highest tail lift is required either at $C_{L_{max}}$ or at low C_L-values depending on the relative position of the most forward C.G. position and the aerodynamic centre of the aircraft-less-tail.

To find the trim changes when altering the aircraft configuration, airspeed or C.G. position pitching moment curves for the complete aircraft are required. Fig. 3 shows the tail-off and tail-on pitching moment curves for the F-28. The very small changes in trim due to flap extension at constant C_L are evident. However, when the required C.G. range is considered again a large range of pitching moments has to be coped with.

In fig. 4 the balancing pitching moment produced by the tail in order to maintain longitudinal equilibrium is described in a simplified equation form. (Tab effects are neglected.)

$$C_{m_{tail}} = -C_{L_{\alpha_h}} \left(\alpha_R - \varepsilon + i_h + \Delta\alpha_{(q)} + \frac{C_{L_{\delta_e}}}{C_{L_{\alpha_h}}} . \delta_e \right) \frac{q_s}{q} \bar{V}_h$$

In the preliminary design stage tailplane aspect ratio and volume coefficient are often selected on the following criteria :

1. Acceptable static stability at the most aft C.G. location

2. The ratio between maximum and minimum values for stickforce-vs.-speed gradient and stickforce/g over the required C.G. range.

3. A first estimate of the maximum usable tail lift coefficient to trim the aircraft on landing and to rotate the aircraft at take-off, both at the forward C.G. position.

If it is assumed for the moment that no appreciable power effects exists and that the tailplane is outside the wing wake, then $\frac{q_s}{q} = 1$.

The ratio between tailplane and elevator area is less directly obtained. It follows from the type of control system adopted (reversible or irreversible) and from a careful balance between the control capacity required and the resulting hinge moments. With regard to the latter both absolute values and the acceptable degree of non-linearity have to be taken into account.

The remaining factors are then :

1. average flow angle at the tailplane

2. tailplane incidence

3. elevator deflection.

From the foregoing three basic requirements emerge for the tailplane :

1. The tailplane must be able to produce both a large downward lift, either through a high negative tailplane angle-of-attack or through elevator deflection and a, generally smaller, amount of upward lift. The latter may be a significant point when asymmetric tailplane profile sections are used, including high-lift devices at the leading edge to cope with very large negative angles-of-attack.

2. Large trim ranges for tailplane and/or elevator are required.

3. The tailplane must be able to tolerate a large range of angles-of-attack, both positive and negative. This is in particular true for out-of-trim conditions where large tailplane angles-of-attack are not readily apparent because they are not necessarily coupled to high tailplane lift coefficients.

In the following some of the tailplane requirements and in particular the ability to cope with large negative angles-of-attack will be considered more in detail with examples drawn from F-28 and F-27 tests.

4. TAILPLANE CHARACTERISTICS OF THE F-28

The F-28 is equipped with a variable-incidence tailplane for trim and an aerodynamically balanced elevator for manoeuvring.
In fig. 5 the tailplane angle-of-attack is shown for two aircraft configurations as a function of lift coefficient, C.G. position and tailplane setting. For the landing case two sets of lines are drawn. The full lines indicate the tailplane angle-of-attack with the aircraft trimmed for zero stick-force. The broken lines show the change in α_h when the aircraft lift coefficient at n = 1 is varied by means of elevator deflection and the tailplane setting is held constant. This occurs when the speed is varied at a constant trim setting . Furthermore the figure shows the effect of a tailplane setting for maximum aircraft nose-up trim (i_h = -8.3 deg).

Also the tailplane angle-of-attack is shown for the condition where the aircraft is pushed over to n = 0.5 g at 1.3 V_S at the most forward C.G. position.
In the latter case the tailplane angle-of-attack shows an ample margin with respect to the tailplane stalling angle, however, this margin is largely lost when ice roughness at the leading edge is present. Although the F-28 aircraft is equipped with an anti-icing system and consequently normally should be completely free of any roughness at the leading edge it is practice at Fokker to consider the effect of ice roughness for cases of system malfunction or pilot neglect.

The F-28 tailplane is specifically designed for a high negative stall angle. A section was chosen with upward nose camber and a large nose radius.

Fig. 6 shows the lift curve slope as obtained from windtunnel tests both in the clean condition and with simulated ice accretion. The simulated disturbance corresponded to a 1½ inch thick mushroom shaped ice ridge over the complete leading edge.

In fig. 7 another adverse effect of ice accretion on tailplane characteristics at high angles-of-attack is shown. This figure shows the effect of ice on the elevator hinge moment. A lightening and eventually a reversal of control forces occurs at a much lower angle-of-attack when ice is present than when the leading edge is clean.

It is clear that the lifting capabilities of tailplanes, when consideration is given to the more severe flight conditions, are more limited than many publications, related to the subject of Control Configured Aircraft, suggest.

The critical flow conditions at the tail may occur with the flaps in the landing position and the C.G. at the most forward location under the following flight conditions :

1. When a push-over is made at a low airspeed.
   a) After the initial pull-up in a baulked landing in order to increase the speed.
   b) In a stall recovery manoeuvre during flight training.
2. During the initial stage of a pitch-down manoeuvre resulting from an autopilot failure.
3. When the aircraft is hit by a downward gust.

In the F-28 flight tests these conditions were simulated by flying at a speed near the placard speed for landing flaps and progressively varying the tailplane setting. The tail load was kept constant by applying elevator in the opposite sense. Also push-overs of varying abruptness were performed.

Various sizes and shapes of simulated ice accretion were tested. Stickforce irregularities and a lowering of the general stickforce level was experienced under these most extreme tailplane conditions.

5. POWER EFFECTS

Propulsive power may affect the tailplane angle-of-attack in various ways. One effect is the turning of the surrounding flow into an exhaust jet due to jet entrainment. On the F-28 this effect produces a slight nose-up pitching moment at constant speed when power is applied although the centre lines of the engine exhausts pass over the centre of gravity suggesting at first sight a nose-down moment.

Much larger changes in α_h occur when a coupling exists between propulsive and wing lift forces as is the case in the various blown-wing concepts. The oldest one is the wing completely or partly immersed in the slipstream of propellers in front of the wing. The phenomenae concerning the flow around the tail and the characteristics of tailplane and elevator have in principle remained the same, however,with the newer concepts like i.e. the externally blown flap.

In the late fifties the Fokker company (now Fokker-VFW) carried out a fairly extensive series of wind tunnel tests, and in a later stage also flight tests, on an F-27 STOL-variant, which did not go into production. During these tests particular emphasis was put on the investigation of the flow conditions at the tail. This aircraft was equipped with a double-slotted flap, the second slot opening after the flap was extended past 40 degrees. The maximum flap angle was 70 degrees.
The propellers of the wind tunnel-model could be operated at thrust coefficients corresponding to a full-scale engine power of up to 1950 shp. This value is slightly below the present take-off power of 2050 shp.
Some of the test results obtained on this model will be used to illustrate the effect of the interaction between lift and propulsion on tailplane and elevator characteristics.

Figure 8 shows the tail-off lift-curve for the model with fully deflected flaps and various thrust coefficients. Also the lift curve is presented for the case where the lift is varied at constant engine power and wing loading. The familiar increase in lift curve slope with increasing thrust coefficient is clearly demonstrated.

Figure 9 presents the pitching moment curves both tail-off and tail-on for the same flap setting and power conditions as the lift curves in the previous figure.
The dotted lines for constant T_c-values are estimated, based on linearized downwash data. The measured and calculated curves for i_h = 5 degrees are given as a check for the accuracy of the calculations.

Figure 9 shows some interesting features. The tail-off pitching moment coefficient becomes more negative with increasing thrust coefficient at constant C_L. Also the gradient of the pitching moment curves at constant T_c shows only a slight variation for different T_c-values. Consequently, although the slope of the moment curve for constant T_c has a positive sign, the moment curve for constant power and constant wing loading, i.e. the static stability for the aircraft-less-tail, has a negative sign. When the local slope of the pitching moment curves for constant power for the aircraft tail-off and tail-on are compared, figure 9 shows that near C_L = 3 the slopes of both curves are equal. This means that the tail contribution to stick-fixed static stability is zero and that the stick-fixed static stability is entirely determined by the aircraft-less-tail.

This result depends of course to a large extent on the relative vertical position of thrust centre line and vertical C.G. position, but the F-27 STOL-configuration is representative of what in general may be expected in this respect of blown wing aircraft.

Figure 9 shows thus in principle the effect of power on the longitudinal stability. Both the manoeuvre and the stick-fixed static stability are decreased. In fact for most propeller aircraft this decrease is so serious that neutral or even slightly negative stability exists at the most aft C.G. position in the low-speed climb. With high power and flaps retracted the strong downwash effects exist without the benefit of high negative pitching moments of the aircraft less tail.

The effect of power and lift-coefficient on the flow condition at the tail is further illustrated in the next two figures. Figure 10 shows the average downwash angle at the tailplane location as a function of tail-off lift coefficient and thrust coefficient The figure clearly shows the well-known fact that the downwash angle is primarily dependent on C_L with the thrust coefficient coming in as a second order effect. However, as the tailplane angle-of-attack can be written as

$$\alpha_h = \alpha_R - \varepsilon + i_h$$

the strong influence of T_c on C_L vs. α_R also causes the tailplane angle-of-attack to vary with T_c at constant C_L.

This is illustrated in figure 11 which presents ($\alpha_h - i_h$) versus C_L.

The following should be noted :

1. At low lift coefficients power and downwash have a small effect on ($\alpha_h - i_h$). The latter is almost entirely determined by the fuselage angle-of-attack which at such high flap settings can reach considerable negative values.

2. A push-over at a high power setting and at a low speed, for example in a baulked landing, produces a large negative angle-of-attack due to the high thrust coefficient and the negative pitching velocity.

3. With a high power setting the effect of C_L on tailplane angle-of-attack is much less than with power off. There is even a range of C_L-values where α_h is approximately constant. This means that $\left(1 - \frac{d\varepsilon}{d\alpha} \right) = 0$ and that stick-fixed static stability is entirely determined by the characteristics of the aircraft without tail as was shown in figure 9.

If the tailplane incidence is fixed at 0 deg. the tailplane must be able to cope with angles-of-attack as large as -20 to -23 deg. Even for steady flight at moderate power near the flap placard speed α_h is equal to about -20 deg.

The original tailplane of the F-27 had a symmetrical section of the NACA 6-digit series which at the low Re-numbers of the windtunnel tests had a stalling angle-of-attack of 14 deg. This means that if this tailplane would be installed on the model under the conditions mentioned (take-off power, $i_h = 0$, $\delta_f = 70$ deg.), the tailplane would be stalled over het complete α_R-range. Fig. 12 shows that this is indeed the case. The pitching moment contribution of the tailplane is less than half of what a non-stalled tailplane would have produced. (See also fig. 9). With power-off the tailplane stalls at $C_L = 1.4$ and comparison with fig. 11 will show that this corresponds to $\alpha_h = -14$ deg.

The risk of tailplane stall can of course be alleviated by increasing the tailplane incidence. This was already demonstrated in fig. 12. When the tailplane incidence was increased from $i_h = 0$ to $i_h = 5$ deg. the flow was fully attached.

A large drawback of this solution is that a considerable increase in elevator capacity for the stall is required. In particular when a reversible elevator control system is used the range over which the tailplane setting may be increased is therefore quite limited.

In the windtunnel tests it was also investigated what the effect was of placing the tailplane near the top of the fin. The effect on α_h is shown in fig. 13. It is evident that the static stability improves considerably. However the high negative angles-of-attack at low C_L -values have hardly decreased.

6. F-27 STOL FLIGHT TEST DEVELOPMENT

As the previously described windtunnel tests showed promises with respect to improved landing performance the double-slotted flaps were tested on the F-27 prototype in combination with a variable-incidence tailplane. The tailplane had upward camber forward of the front spar and the leading edge radius was increased by 50% compared to the tailplane on the windtunnel model. It was mechanically coupled to the flaps in such a way that the tailplane incidence ranged from -1.0 deg. with flaps retracted to + 3.6 deg. when the flaps were fully extended.

In order to counteract the effect of increased tailplane setting on elevator capacity in the stall the chord of the manually operated elevator was increased by 27 percent. Trimming was accomplished by a trim tab.

These flight tests produced the following results :

1. Investigations of push-over manoeuvres (n = 0.5 g) with the flaps fully deflected showed that the tailplane was close to stalling in this flight condition.

2. Although the elevator chord was considerably increased the aircraft could only be fully stalled at C.G. positions aft of 26% MAC with full flap deflection and the tailplane set at i_h = 3.6 deg.

3. Sufficient elevator power was available for wave-offs and push-overs in the most critical conditions although in the wave-off control forces could be high.

4. The coupled tailplane lowered the transient forces in extending or retracting the flaps.

5. Steep (9 degrees) slow approaches could be made without exceptional piloting skill.

7. SOME GENERAL REMARKS

1. In the previous chapters two concepts for a longitudinal control system were mentioned with which the control and trim requirements as listed in Table I may be tackled. The complexity of these requirements has led to the adoption of a range of widely different control configurations. A study of various aircraft leads to the list presented in table II.
This table shows solutions with an increasing capability to cope with widely different requirements coupled to an increasing hydraulic-mechanical complexity. In the final choice for a certain solution various factors should be considered, including such ones as the experience of the design office with a particular system. The choice between spring tabs or hydraulics may be influenced by this. A balance should also be struck between development time and cost versus production and maintenance costs . Also workshop capabilities of potential customers have sometimes te be considered as a design consideration.

2. Increasing complexity is not only due to the requirements for the normal functioning of the various components of the control system. A more elaborate failure analysis has to be performed which leads to many duplications and extras such as take-off warning systems for aircraft with non-coupled variable incidence tailplanes.

3. This paper deals with low-speed stability and control problems. However taiplane design is not governed by low-speed requirements alone. High-speed effects such as due to compressibility, aero-elastic deformation, both static and from flutter considerations, all play their part and can to a large degree determine the type of control chosen.

4. Design is always an iterative process. Therefore the choice of a certain control system may have its impact on the tail volume coefficient and aspect ratio chosen in an earlier design stage.

5. Although present windtunnels have a high degree of accuracy the test results should be regarded with some care in particular when control characteristics are considered. Hinge moments, local flow angles, ground effect have all occasionally been misjudged in particular when the tests had to be performed at low Reynolds numbers as is often the case when ground effector power effects are investigated. When regarding marginal characteristics for a chosen control lay-out this should be kept in mind.

8. CONCLUSIONS

The high degree of operational flexibility nowadays demanded of transport aircraft results in aircraft flight envelopes which cover a large range of lift coefficients and centre-of-gravity positions. As a consequence severe requirements have to be fulfilled by the horizontal tail with respect to longitudinal stability, control and trim.

In the foregoing some of the required characteristics have been dealt with. In particular the lifting capability of the tailplane and the hazard of tailplane stall was considered together with the required ability to cope with large negative angles-of-attack. It was also shown that in out-of-trim conditions the two requirements were not necessarily related, in particular when a variable-incidence tailplane was considered. Windtunnel and flight test results obtained with the F-27 and F-28 were used to illustrate some of the points made.

It seems that the problems around the tail contribution to longitudinal stability and the tailplane stall will stay with us and it may be expected that it's relative importance will increase with the present interest in blown-wing technology.

TABLE I

SURVEY OF LOW-SPEED LONGITUDINAL STABILITY, CONTROL AND TRIM REQUIREMENTS FOR CIVIL TRANSPORT AIRCRAFT

Requirement	Critical C.G. position	FAR 25
I Stability should be acceptable		
1. Stick-fixed static stability (May be a matter of concern in turbulence)	Aft	
2. Dynamic stability		
II Control capacity should be sufficient to perform the following manoeuvres:		
1. Rotation in the take-off	Forward	
2. Landing flare and touch-down	Forward	
3. Stall	Forward	
4. Prompt recovery prior to the stall $1.2\ V_s \leqslant V_{trim} \leqslant 1.4\ V_s$	Aft	§ 25.145 (a)
III Trim capacity should be sufficient to trim the aircraft for zero stick-force		
1. For all flap settings for speeds not less than $1.4\ V_s$	Forward	§ 25.161
2. For each flap setting up to its placard speed Preferably $V_{trim} \geqslant 1.2\ V_s$ for take-off flaps $\geqslant 1.3\ V_s$ for landing flaps	Aft	§ 25.161
IV Control forces must comply with the following requirements:		
1. When trimmed at $1.4\ V_s$ the stick-force curves shall have stable slopes over prescribed speed ranges.	Aft	§ 25.175
2. The stick-force gradient shall be $\geqslant$ 1 lb/6 kt.	Aft	§ 25.173 (c)
3. The stick-force gradient shall be sufficiently high to compensate the effect of the control friction band on the free return speed range. The latter shall lie within prescribed limits.	Aft	§ 25.173 (b)
4. With the flaps extended, power off and the aircraft trimmed at $1.4\ V_s$ stick-forces shall not exceed the following values.	Forward	
$V = 1.1\ V_s$ $F_e \leqslant$ 50 lb pull		§ 25.145 (b)
$V = 1.7\ V_s$ or V_{FE} (whichever is the lower) $F_e \leqslant$ 50 lb push		§ 25.145 (b)
$V = 1.8\ V_s$ $F_e \leqslant$ 80 lb push (landing flaps)		§ 25.175 (d)
5. Stick-force/g shall lie within acceptable limits	Forward and Aft	
6. Transient stick-force changes shall not be greater than 50 lb for various configuration changes such as flap extension and retraction or power application		§ 25.145 (b)
7. Stick-forces in the take-off shall be acceptable.		
8. Stick-forces in the landing shall be acceptable.		
V Out-of-trim control characteristics		
1. Tailplane and elevator shall be able to cope with the varying flow conditions at the tail when excursions from the trimmed conditions, as described above, are performed.	-	
2. At the extreme trim speeds sufficient control power shall be available to counteract gusts or apply corrections to the flight path.	Forward and Aft	
3. When a variable-incidence tailplane is used for trim sufficient elevator capacity shall be available for rotation in the take-off with the tailplane in a slight out-of-trim setting.	-	

TABLE II

LONGITUDINAL CONTROL AND TRIM SYSTEMS AS FOUND ON TRANSPORT AIRCRAFT

a) Fixed tailplane.
Manoeuvring by elevator.
Trim by trim tab.

b) Fixed tailplane.
Manoeuvring by elevator.
Trim by an element between tailplane and elevator
("double-hinged" elevator).

c) Fixed tailplane.
Manoeuvring by elevator.
Trim by trim tab.
Coupling between flap and separate trim tab on elevator.

d) Variable incidence tailplane coupled to flap.
Manoeuvring by elevator.
Trim by trim tab.

e) Variable incidence tailplane for trim.
Manoeuvring by elevator.

f) Variable incidence tailplane coupled to elevator for trim.
Manoeuvring by elevator.

g) Variable incidence tailplane coupled to flaps.
Elevator coupled to throttles.
Trim by variable incidence tailplane.
Manoeuvring by elevator.

h) "All-flying tail" with geared "elevator" for both manoeuvring and trim.

To prevent flow separation leading-edge slats and flaps are used and elevators have been fitted with fixed vanes.
On some experimental aircraft blowing at the tailplane leading-edge and at the elevator hinge line has been applied.

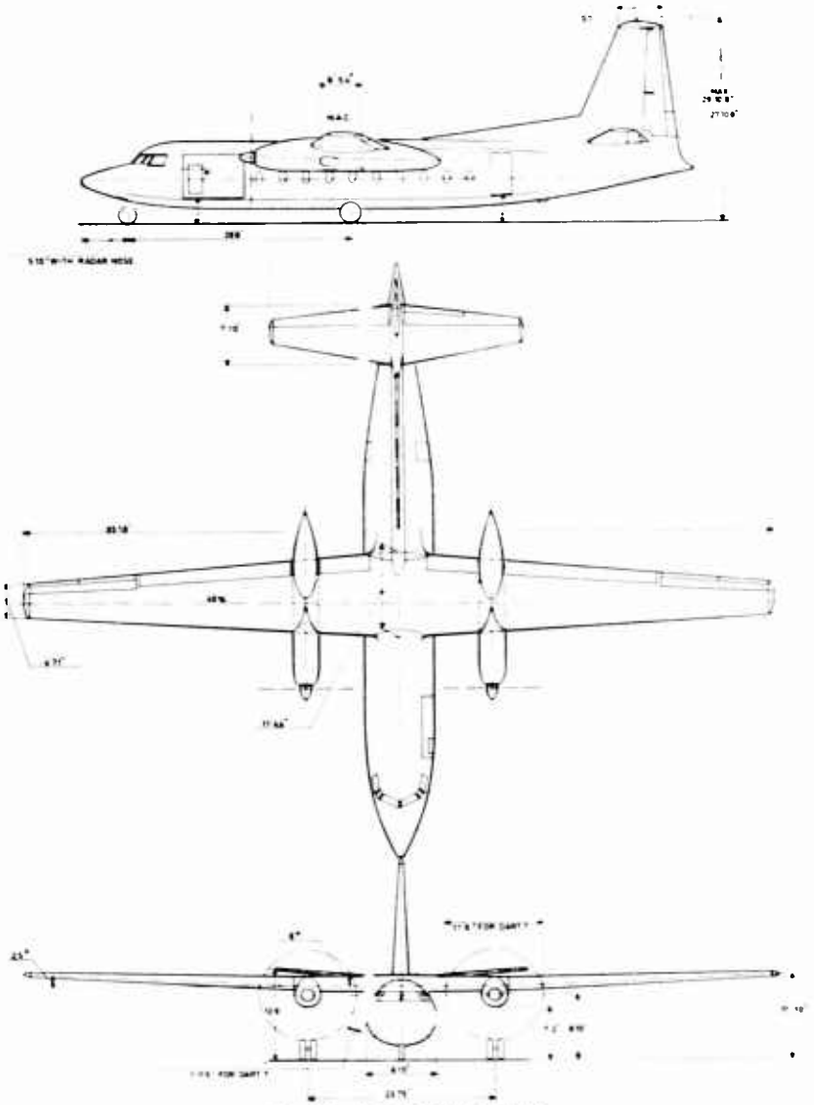

F-27 FRIENDSHIP

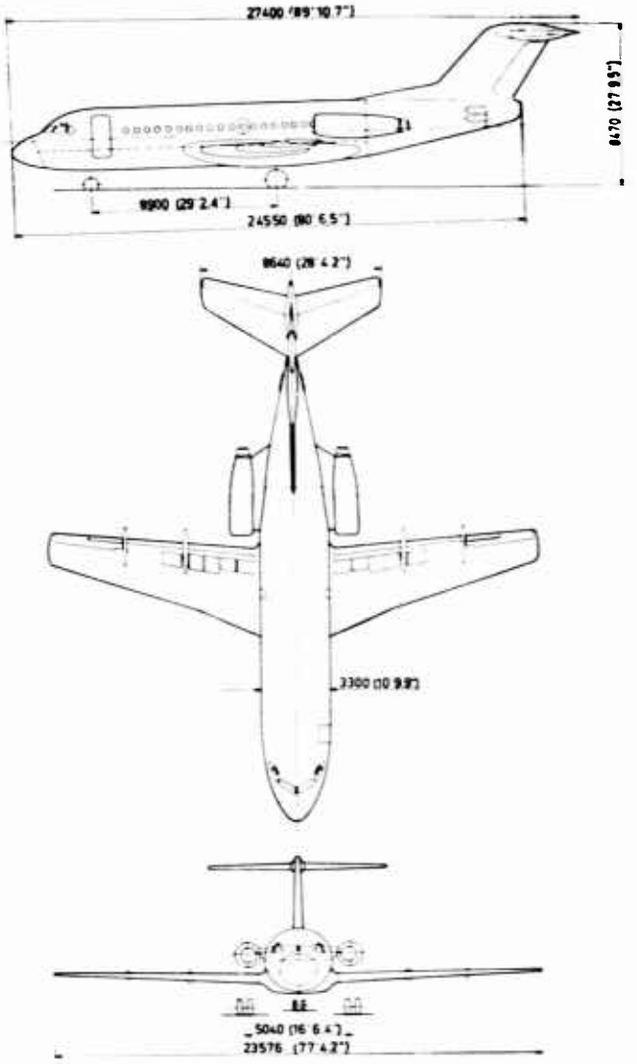

F-28 FELLOWSHIP

Fig. 1 Three views

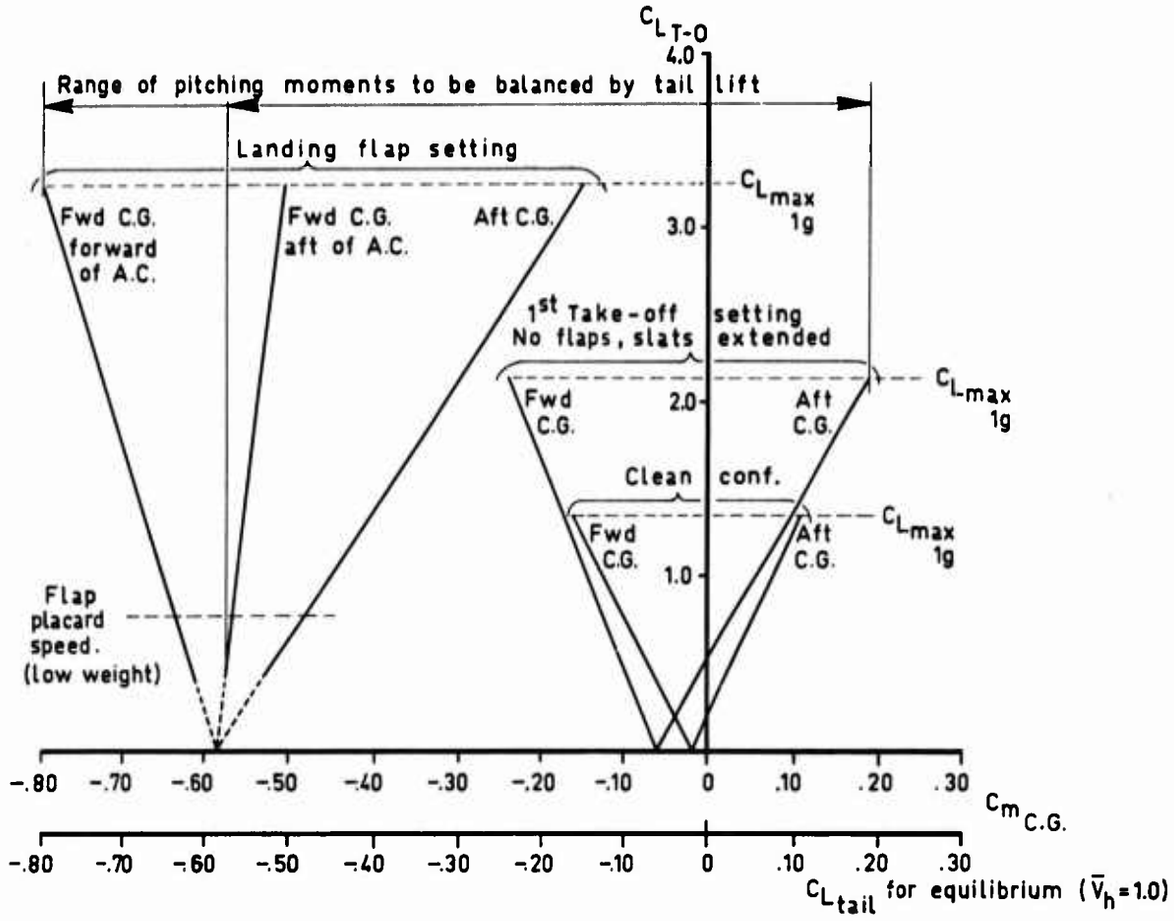

Fig.2 Pitching moment. Aircraft less tail

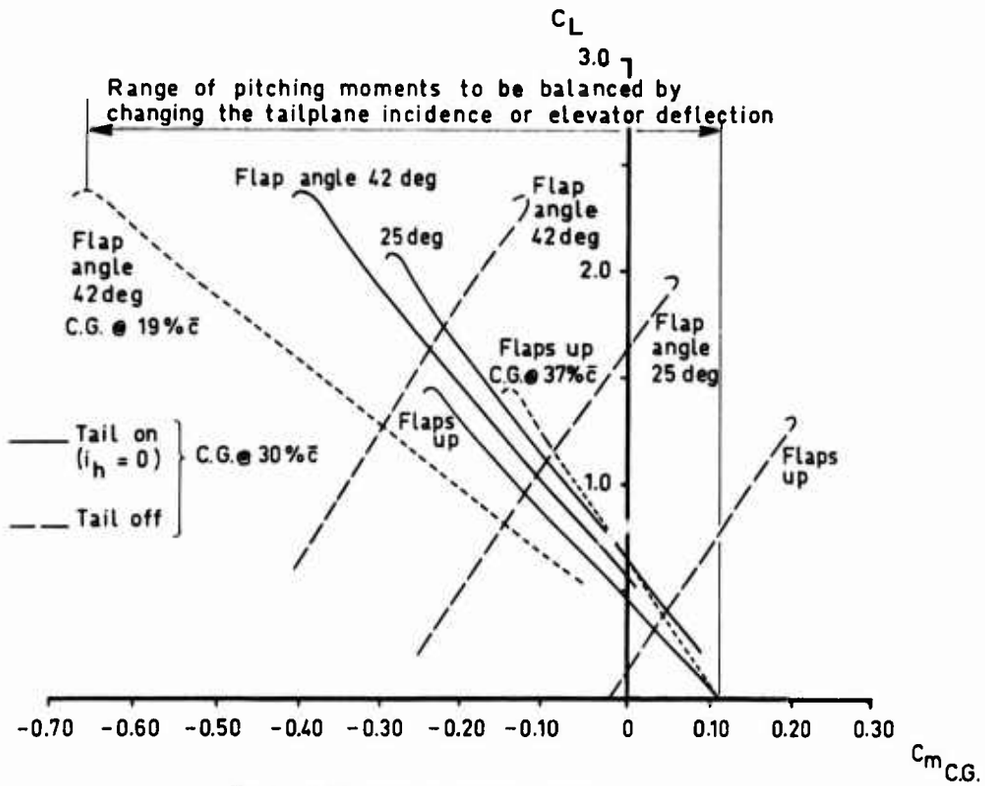

Fig.3 F-28 pitching moment curves

$$\textcircled{1} \quad C_{m_{tail}} = -C_{m_{T-0}} = -\left(C_{L_{\alpha_h}} \cdot \alpha_h + C_{L_{\delta_e}} \cdot \delta_e\right) \frac{q_s}{q} \bar{V}_h$$

$$\textcircled{2} \quad \alpha_h = \alpha_R - \varepsilon + i_h + \Delta\alpha_{(q)}$$

hence,

$$\textcircled{3} \quad C_{m_{tail}} = -C_{L_{\alpha_h}} \left(\alpha_R - \varepsilon + i_h + \Delta\alpha_{(q)} + \frac{C_{L_{\delta_e}}}{C_{L_{\alpha_h}}} \cdot \delta_e\right) \frac{q_s}{q} \bar{V}_h$$

Fig.4 Tail contribution to pitching moment equilibrium ($\ddot{\theta} = 0$)

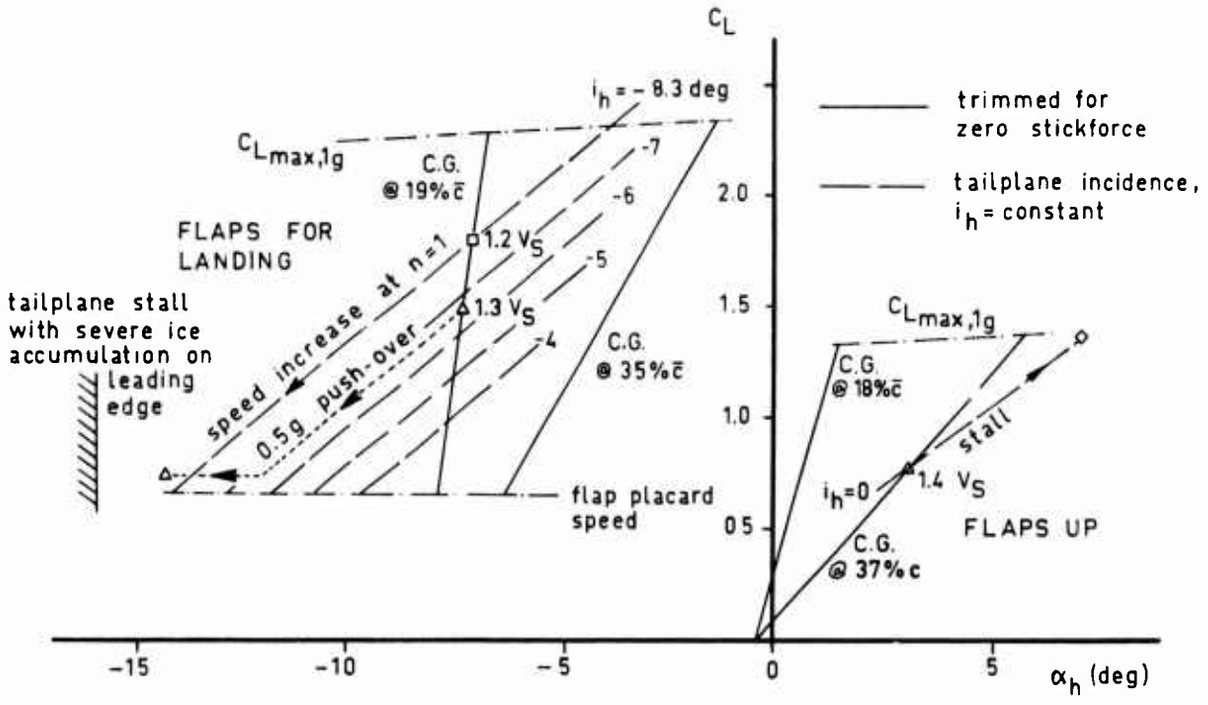

Fig.5 F-28 tailplane angle-of-attack

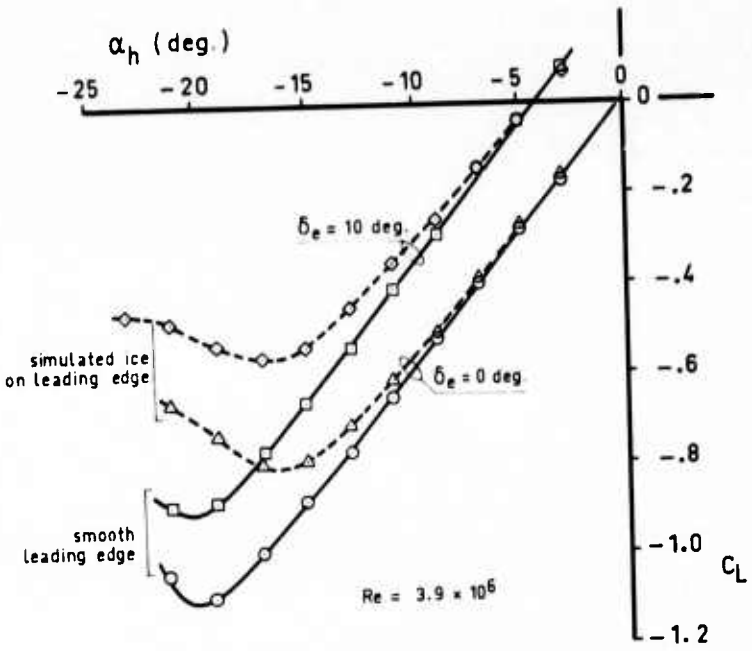

Fig.6 F-28 tailplane lift curves. Effect of simulated ice roughness

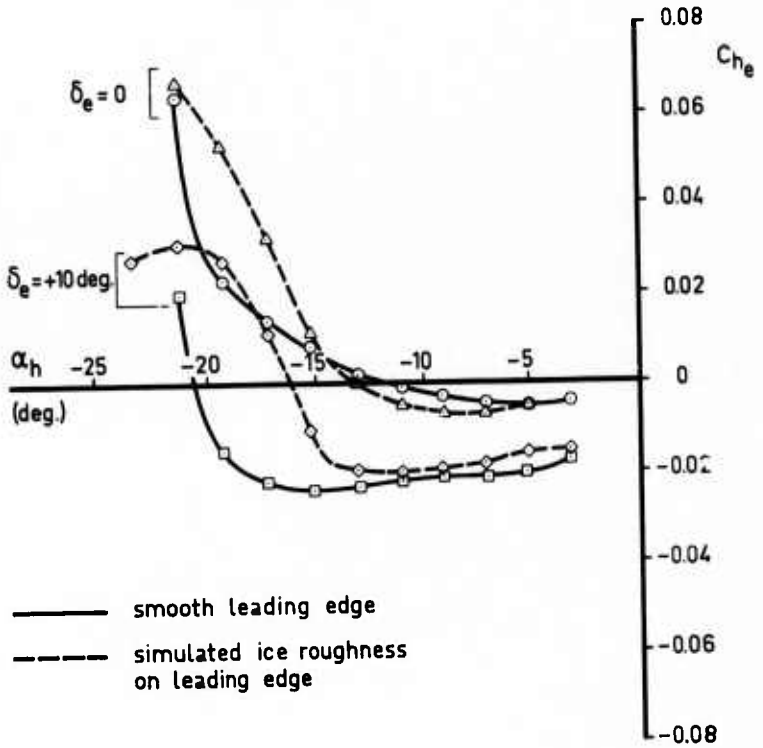

Fig.7 Effect of simulated ice roughness on elevator hinge moments

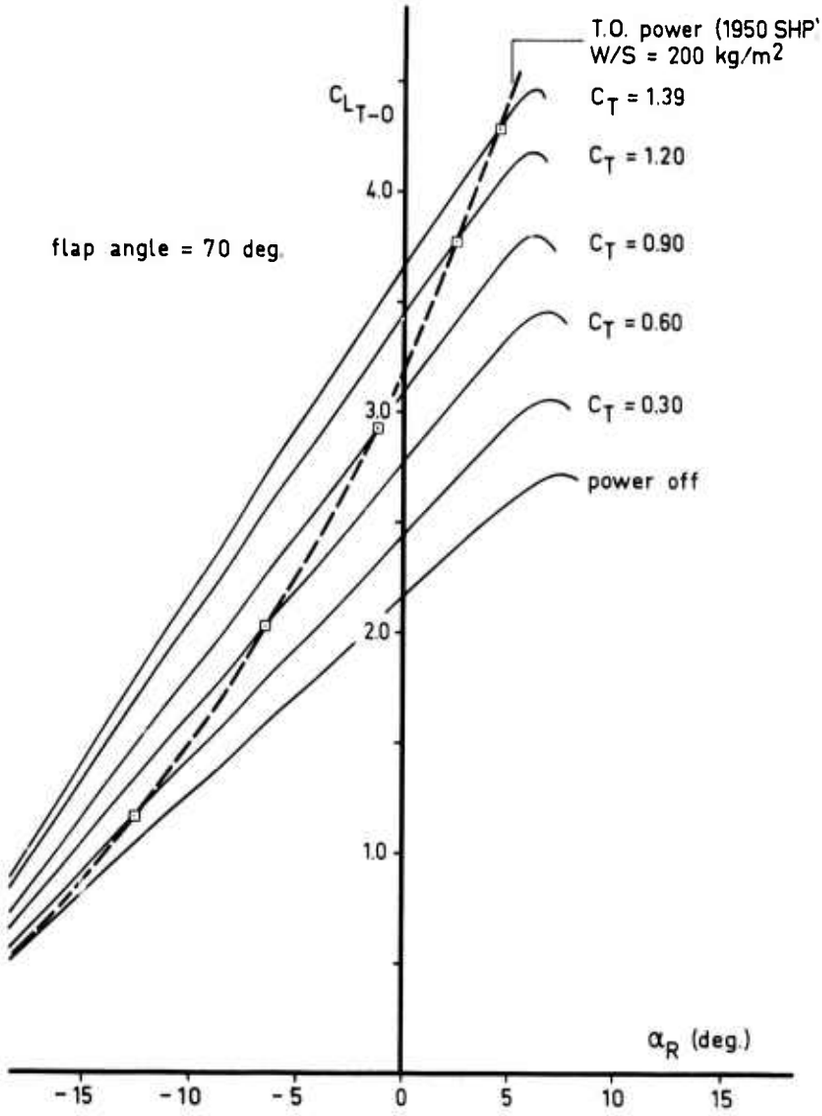

Fig.8 F-27 STOL. Tail-off lift curves

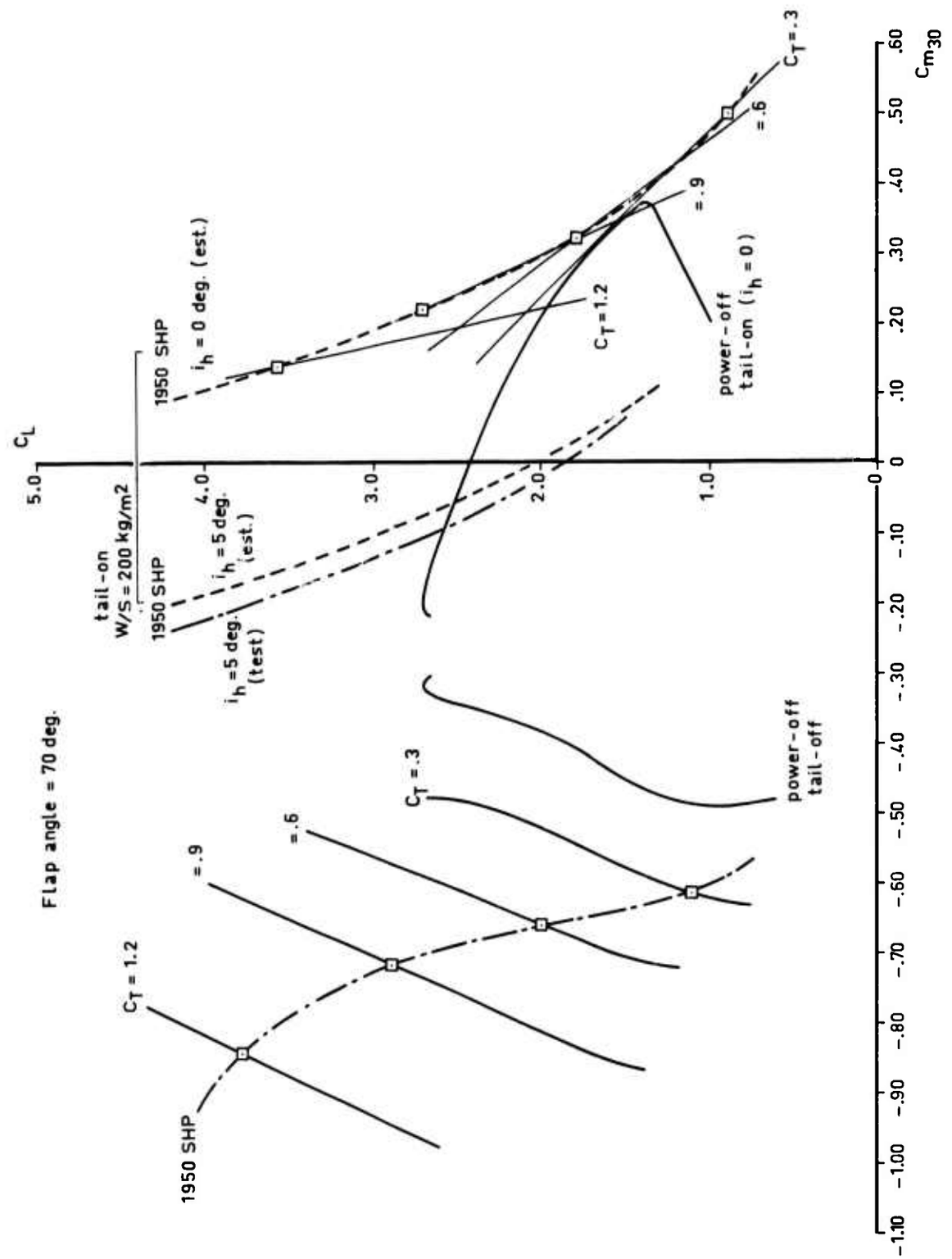

Fig.9 F-27 STOL. Effect of power on pitching moment curves

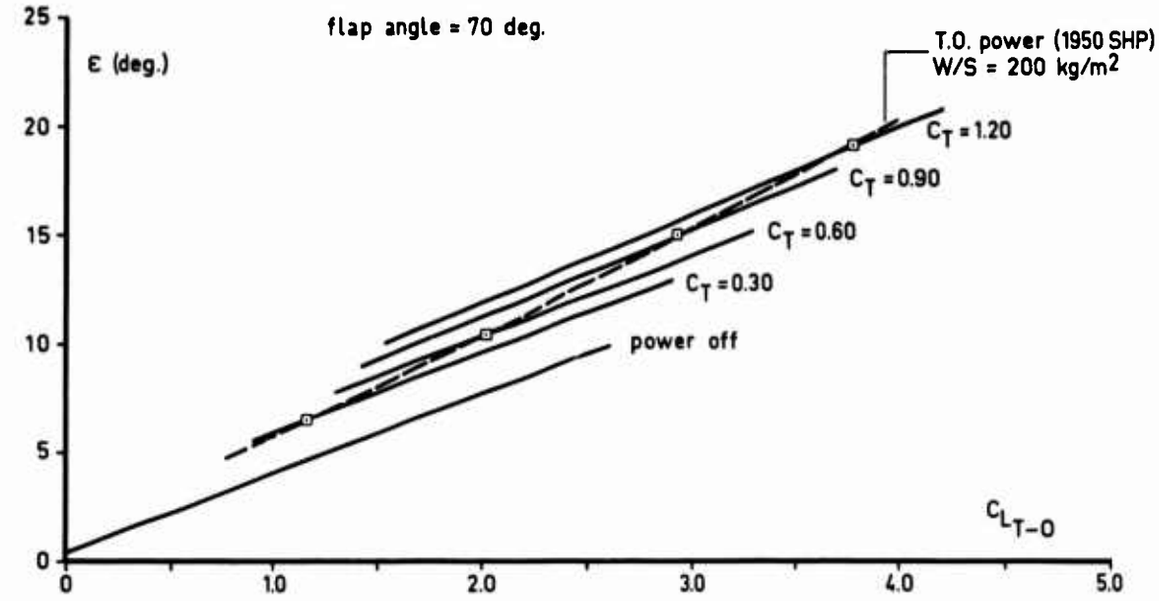

Fig.10 F-27 STOL. Downwash angles

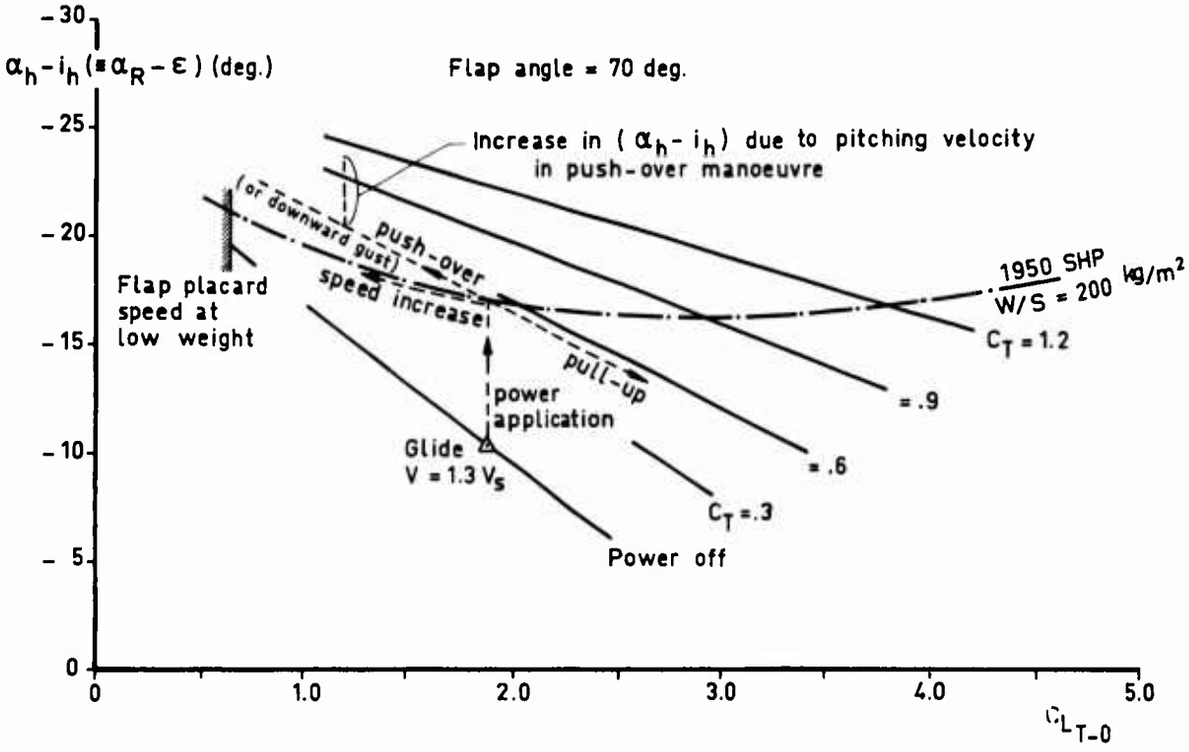

Fig.11 F-27 STOL. Effect of power, airspeed and load factor on tailplane angle-of-attack

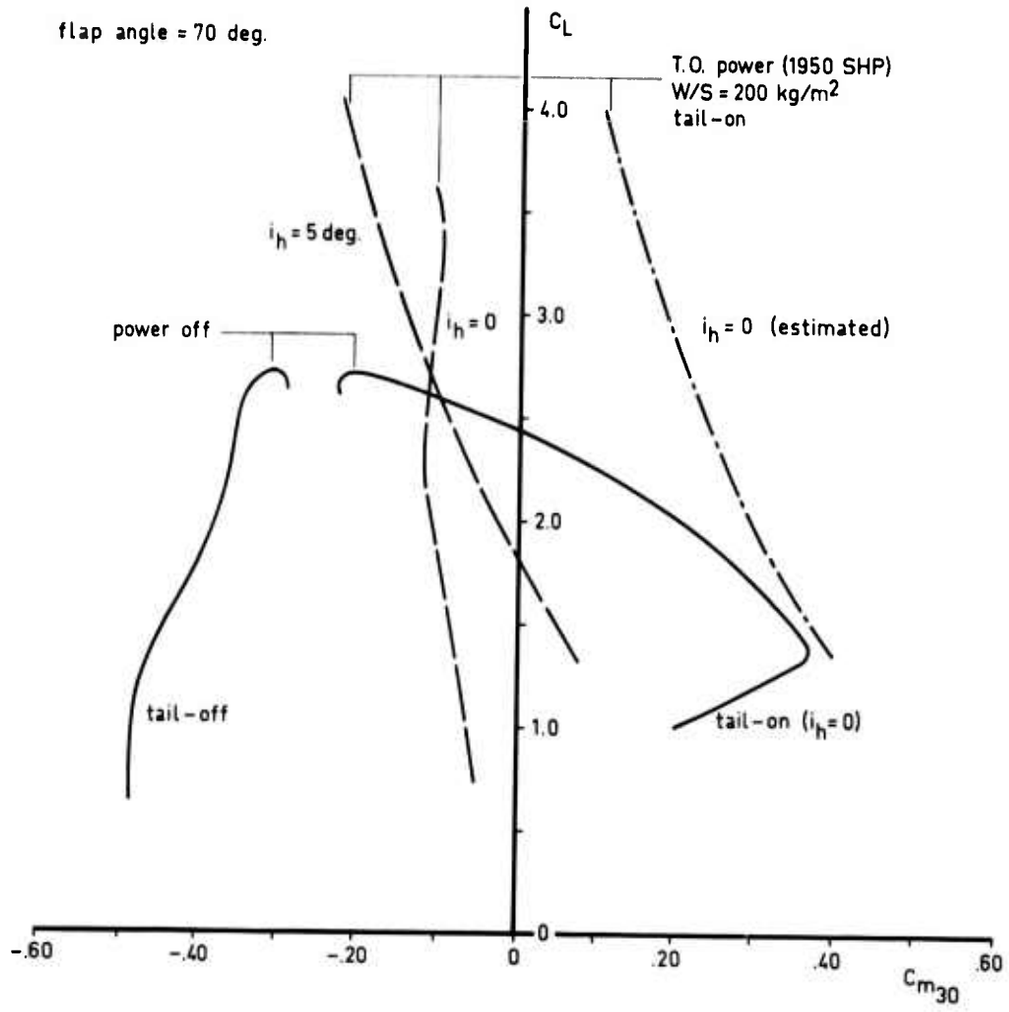

Fig.12 F-27 STOL. Pitching moment curves

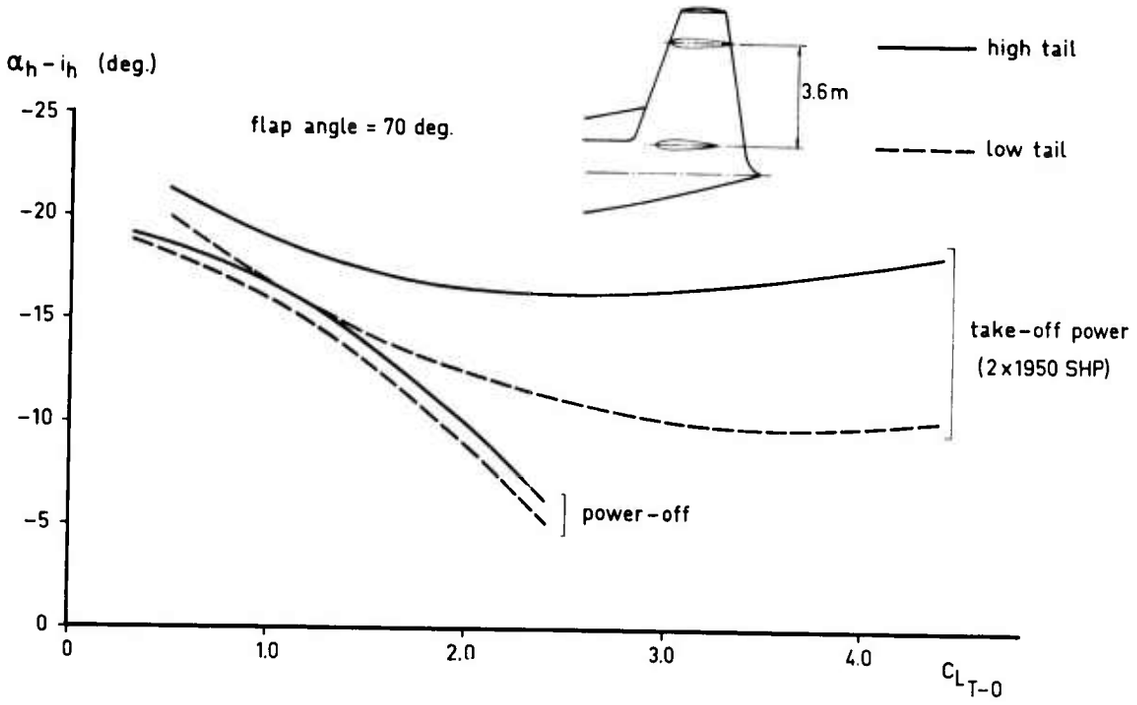

Fig.13 Effect of tailplane position on tailplane angle-of-attack

SOME LOW SPEED ASPECTS OF THE TWIN-ENGINE SHORT HAUL AIRCRAFT VFW 614

by

Hartmut Griem
aircraft sub-systems

Jürgen Barche
aerodynamics

Hans - J. Beisenherz
flight mechanics

Günther Krenz
aerodynamics

VFW-FOKKER GmbH, Bremen, Germany

SUMMARY

The paper gives a rough presentation of the twin engine short haul aircraft VFW 614 and discusses some selected low speed aspects of this aircraft as they came forward in design, realisation, and test. These aspects are: Wing stall aerodynamics, tail stall aerodynamics, longitudinal control, and lateral/directional.

1. INTRODUCTION

The paper discusses

Some low speed aspects of the twin engine short haul aircraft VFW 614

The aircraft - shown in fig. 1- is the world's first jet airliner with engines mounted on the upper side of a wing. Some low speed aspects are particularly connected with that engine position. A brief review of questions as

What was the VFW 614 design concept?

and

What was the technical approach?

seems therefore to be useful before discussing in more detail a selection of some low speed characteristics.

2. VFW 614 - DESIGN CONCEPT / TECHNICAL DATA

The design idea of the VFW 614 was to provide a jet airliner for short haul operation,

- to be operated from small provisional airfields
- with relatively low traffic density, and
- small growth rates

The aircraft therefore has

- to replace the partially obsolete propeller aircraft
- to offer higher cruise speeds, flexibility and comfort,

and

to be supplementary to any fleet of larger jet aircraft as - e.g. - DC 9, B 737 or BAC 111

These conditions led to specific DESIGN CRITERIA - see Fig. 2 - as

short airfield performance

multi-stage capability

rough airfield capability

minimum noise and pollution

independence from ground support

high dispatch and block to block reliability,

and finally to that OVER-THE-WING-MOUNTING OF ENGINES,

which is still unique among the world's aircraft.

There are some principal advantages for such a position (1, 2, 3) as

- unbroken long-span flaps
- short landing gear keeping the fuselage close to the ground for quick boarding and disembarking,
- no foreign body ingestion,
- a blanketing effect on engine noise, and
- a relativily wide c-g-flexibility

These advantages have been regarded to be of higher priority as all technological problems associated with any new engine position.

The principal technical data of the VFW 614 prototypes C 2 and C 3, as they are flight-tested now, are summarized in fig. 3 including

main dimensions as

- wing span	7o ft 6 in	(21,5 m)
- length	67 ft 6 in	(2o,6om)
- height	25 ft 8 in	(7,84 m)
- wing area	688 sqft	(64 m^2)
- aspect ratio	7.22	
- sweep angle (25%)	15^o	

and

weights as

- MTOW	44ooo lbs	(19 95o kp)
- MLW	44 ooo lbs	(19 95o kp)
- max. wing loading	64 lbs/sqft	(312 kp/m^2)

Both engines RR/SNECMA M 45 H with

2 x	(2 x 34oo kp)

thrust at sealevel and ISA conditions enable the aircraft to fly

M = o,65 at 2o ooo ft

over a range of 71oo NM (132o km)

and

to operate from fields down to 4 ooo ft lenght.

A typical diagram for short-haul service is shown in fig. 4.

3. VFW 614 - CONCEPT REALISATION

The realisation of a new aircraft concept is usually divided into classical and new technological realisation.

Here by CLASSICAL technology realisation is understood that work which has to be treated for any aircraft in order to meet the airworthiness regulations and performances predictions.

NEW technology realisation, however, defines that work to be done in order to get the full benefit of the new concept's potential within the frame of all regulations.

With the exception of its engine position the VFW 614 was designed conventionally in principle. New technology realisation problems at high speeds as well as at low speeds are therefore mainly connected with that engine mounting.

The paper is concentrated at low speed problems only. Due to the strong interactions between low and high speed design fig. 5 summarizes major problems in the development of that particular aircraft at both speed regimes. As it can be seen from that figure a concentrated theoretical and experimental work had to be done at

high speed

- to minimize additional pod/pylon drag and buffet,
- to optimize stability and control with simple systems,
- to minimize engine throttle effects, especially the effects of slam deceleration of both engines on longitudinal motion as well as single engine throttling on lateral directional motion

and at

low speed

- to minimize adverse pod/pylon effects on the stall characteristics
- to minimize wing stall effects on engine distortion,
- to optimize the aircraft STO potential on stability and control, especially under strong cross wind conditions, and with one engine inoperative
- to solve stick free stability problems associated with manual controls as well as the tail stall problems under icing conditions.

These particular low speed problems are broadly discussed in the following chapters.

4. DISCUSSION OF SOME LOW SPEED PROBLEMS

4.1 Wing stall aerodynamics

The predication quality of stall characteristics is still limited, since neither theoretical models on 3-D separation nor experimental facilities for high Reynolds number testing are sufficiently promoted. For the VFW 614 with its

by-pass engines mounted above the wing

STO-capability and

manual lateral controls

that lack of general knowledge led to an intensive special research work, however, some questions remained open until flight testing the aircraft.

The most important open question concerned the engine response to unsteady wing or intake lip separation effects, since the advantages of the engine position with respect to steady distortions were already verified (see (4)). With respect to the uncertain engine reaction the original design philosophy of the VFW 614 wing at stalling speeds had to take into account, that

- the steady distortion factor given by the engine manufacturer may not be exceeded during the stall
- a tolerated exceeding at angles of attack beyond that for maximum lift should be extremly time limites

- the intake flow schould not influence the stall flow pattern to avoid power setting interference

The combination of that requirements with classical characteristics and performance requirements such as

- high C_{lmax} at take-off and landing,
- low drag for take-off flap settings,
- increased nose down pitching moments at maximum lift

and

- no roll-off tendency and full lateral control

led to a wing design with separation starting at the trailing edge of the inner wing panel, extending forward and sideward but excluding the wing leading edge part in front of the engines.

In fig. 6a sketch of the recommended flow pattern is compared with 1:5 scale model results at $2{,}5 \cdot 10^6$ Reynolds number. The agreement between both patterns was satisfactory to start flight testing the aircraft without expending severe engine trouble.

In addition to the normal test equipment, tuft studies were recorded by a video-system as well as by a tail-camera during the stall tests. The evaluation of all information sources indicated that

- the flow separation started as predicated,
- but the separation boundary spreaded more intensive in spanwise rather than in chordwise direction, thus
- resulting in reduced longitudinal stability and
- increased rolling moments both due to flow break down and reduced aileron effectivness.

In addition power-on and power-off stalls demonstrated that

- the engines were less sensitive against unsteady wing separation effects, even at combinations of angles of attack well beyond maximum lift with side slip angles in the order of 30°.

This encouraging engine experience could be used to improve the stall propagation considerably by a modification of the outbord wing's leading edge together with a 6" stall promotor in the wing-body fairing. These short-time, low-cost changes resulted in favorable stall characteristics and high maximum lift for all flap settings.

In Fig. 7a typical stall history is illustrated. From on-line-data of this flight

angle of attack

indicated airspeed

elevator control forces

aileron control forces

were plotted against flight time T (sec) on the right hand side of the figure.

At three time steps, marked by dotted lines, wing flow development is taken by tuft photos, shown on the left side of the figure.

The propagation of flow break down can be followed from above to below. At flight time 2672 separation starts near the fuselage at an angle of incidence of about 14 degrees indicated. Some 0,5 degrees later the separation has spreaded over the wing panel between fuselage and engine position, and at an angle of 18° the wing is stalled up to about 0,4 semispan at the leading edge 0,6 at the trailing edge.

The complete stall was conducted with continuously increasing elevator pull force, and during the whole manoeuvre the bank angle was kept in limits of $\pm 5^\circ$ by about 15 kp aileron control force, at maximum.

To reach an overal understanding of the wing stall behaviour fig. 8 gives the propagation of flow break down for cruise, take-off amd landing configuration, which were plotted from tuft photos during flight test. For all flap settings a rather similar flow development was achieved, resulting as well in favourable stall characteristics as in favourable performances.

This can be checked from the lift data on the right hand side, obtained from flight performance test evalution for 3 flap settings and 1-g-stall. Applying FAA-stall procedure about six percent of minimum speed are saved thus gaining more than ten percent of C_{lmax} in comparison to the plotted C_L - Values.

Approaching the stall, the natural buffet warning is recognized by the pilots at about 6% before minimum speed. As this signal was not strong enough for all certification stalls an artificial optical/acoustical stall warning was incorporated.

g-break is well pronounced for all flap settings and neither gear nor spoilers have any noticeable influence on it.

4.2 Tail stall aerodynamics

A series of flight tests has been conducted, to check the full longitudinal trim capability of the aircraft. The flow angle at the horizontal tail increases to maximum values, when the aircraft is flown under the condition

forward c.g.

full flaps deflected

flap placard speed

To establish full trim capability, a sufficient margin against tail flow separation is required under these flight conditions. This margin must take into consideration adverse effects increasing the angle of attack at the stabilizer as by

gusts

pilot maneuver

icing conditions

c.g. shift forward beyond that certificated.

In order to check the tail performance, two types of pilot maneuver were conducted

- out of trim in six steps between 1.2 V_S and flap placard speed at constant speed with 3 deg of stabilizer movement aircraft nose up
- push over in the same trim steps up to $\Delta n = 0{,}5$

As the main criterium the pilot's feeling on the controls was considered and in addition this information was backed up by

stabilizer straingage measurements
tuft observations, which were related to
windtunnel studies

On the basis of these results full trim capability was confirmed with safe margin against tail separation.

Though a deicing system is installed in the stabilizer leading edge, full trim capability with ice at the tail is still required to cope with system or pilot failures.

A flight test with ice at the stabilizer leading edge was performed for the most critical configuration with respect to c.g., flap setting and speed. It was demonstrated that the pilot kept the aircraft fully controlled, however, higher stick forces due to increased hinge moments were observed.

4.3 Longitudinal Control

The basic aspects for longitudinal motion are

- Static longitudinal stability (stick-fixed and stick free)
- Dynamic longitudinal stability
- Trimchange with speed, centre of gravity shift, power and flap settings
- Control near the stall
- Change of stick force with speed, centre of gravity, power and flap settings
- Change of stick force in maneuvring flight

- High speed characteristics and speed recovery maneuvers
  (pitch upsets, c.o.g. shift, inadvertent control movement....)

On account of the direct controls (manual control system with booster support) the additional parameter of stick free stability has to be implied into control system lay out. This parameter depending on elevator hinge moment derivatives due to local angle of attack and due to elevator deflection has an influence on all aspects mentioned above. Since hingemoment determination during design stage entails uncertainties, means of adaptability have to be provided which in our case are

variable boost ratio

variable gear tab ratio

With the denominations of fig. 9 the connection of the basic controllability requirements and the aircraft characteristics is described in fig. 1o. For simplicity reasons this figure is based on linear hinge moments.

The lower part of the figure illustrates the loss of gain in "stick-free" stability depending largely on the ratio "b_1 / b_2", which can be influenced by the ratio of the gear tab. Actually it is used as an antibalance tab. The requirements, given in the upper part of the figure, must be met for the whole centre of gravity range (2o% M.A.C.) and different flap settings. The elevator control forces (K) can be adapted by the boost ratio. Looking at the chosen design curve it is obvious, that the whole range, admitted by the requirements is utilized by the large centre of gravity shift of 2o% M.A.C.

Designers usually have to expect rearward c.g. drift on their aeroplanes, so it happened with the VFW 614. For this reason, cruise configurstion with the most rearward c.g. position becomes marginally stable but is still acceptable.

As an example figure 11 shows some flight test results in terms of pilot's force at his controls versus speed and the corresponding elevator deflection. In this case-landing configuration and rearward c.g. position- the slope of stick force curve is more than twice of the required value.

4.4 Lateral and directional Control

4.4.1 Lateral and Directional Control Performances

The lateral and directional controls of the VFW 614 have been designed such that controllability requirements are fully met. These are

- roll performances
- engine failure balancing
- cross wind
- controllability under gust conditions
- short turns in final approach

If these requirements are fulfilled at low speeds controllability at high speeds will be guaranteed as well. Due to the lack of quantitive statements in FAR Part 25 the flight test results are compared with Mil F 8785 B and / or SAE recommendations (5.6).

Both roll rate and roll acceleration (bank after 1.8 sec) are in compliance with ambitious requirements, some small attention however has to be paid to reduction of roll control power effectiveness at extremely low speed due to flow separation and adverse tab positions (s. fig. 12 and 13).

Aileron deflection to balance engine failure is far below critical boundaries due to low rolling moments with side slip. Turns with one engine inoperative can easily be achieved to both sides ($\xi \quad 4^{\circ}$ at 1.4 V_S).

Directional control with on engine inoperative needs booster support in particular for engine failure during take off below V_2, which determines V_{mc}. Flight tests so far conducted indicate sufficient margin between V_2 and V_{mc} (fig. 14).

A series of take offs and landings was performed with heavy cross winds. A considerable wing lifting tendency has been observed during taxiing demanding up to 75% of full roll control power. In order to prove sufficient roll controllability during taxiing different pilots tested the aircraft at crosswind components up to 41 kts from both sides. The results are demonstrated in a statistic way in fig. 15 showing the time for which specified control throws were applied related to the total operating time. These results imply both the operation under gust conditions and turns during final approach for proper adjustment of the aircraft to runway.

4.4.2 Roll Control Forces

So far lateral and directional control performances have been considered as they resulted from flight tests without regarding control forces. Both roll and yaw controls are direct controls thus depending on hinge moments. While a quick approach to an optimal yaw control system was possible, some steps were necessary to find the optimal solution for the roll control system.

The basic roll control configuration is shown in fig. 16

- spring tab controlled ailerons
- geared trim tab at the left wing
- cross relation of both ailerons
- geared tabs at both wing sides (introduced in a later stage, making use of the trim tab)

with the most important system parameters described in fig. 17 (state of modification I). This lay out was the results of theoretical studies based on wind tunnel tested hinge moments, but it was not accepted by the pilots since the forces were too high. With the necessary modifications (fig. 18) the following problems had to be faced:

- precision of wind tunnel predicated hinge moments
- hinge moment nonlinearities
- parameter boundaries due to the flutter stability requirements
- control system stiffness
- loss of effectiveness due to adverse tab displacement and local flow separation
- limited tab authority

Inflight hinge moment measurements did not yield satisfactory results because of the difficulty to measure forces precisely and because the parameters could not be changed independently. So the control system had to be improved step by step. The following prescriptions had to be regarded during this optimisation:

- increase aerodynamic balance to obtain acceptable wheel forces, avoid overbalance in any condition
- keep parameters (particularly spring stiffness K and tab to swingrod ratio N) within the boundaries required for flutter reasons
- keep spring tab to aileron deflection below 1 to maintain full aileron authority
- define modifications of smallest cost and time impact.

The results of the different states of modification are compared in fig. 19. Due to the high spring stiffness in the first design, authority was reduced by high stick forces themselves and by elasticity effects as a consequence of the high stick forces. The reduction of spring stiffness (state of modification II) improved the forces but increased tab deflections to an undesired degree. So different means of stick force reduction had to be applied. To provide the best set of advantages in the shortest time four measures of precaution were carried out simultaneously (state of modification III):

- further reduction of spring stiffness
- reduction of aileron hinge moment slope by increased leading edge radius
- introduction of geared tabs (variable gear)
- enlarged authority of column deflection

The most outstanding results was an undue sensitivity of roll control and the tendency of overcontrol in combination with increased lateral gust sensitivity due to reduced stick free stability. However the total range of roll control characteristics was provided now and an effective means of adaptation was available by the variable gear of the geared tabs, which then permitted the optimal adjustment (state of modification V) as well as the investigation of the effectiveness of spring stiffness and leading edge changes by putting the gear to zero.

To maintain full control effectiveness at low speed and large aileron deflections a differential aileron was introduced the optimum of which was found by inflight tuft studies.

Although extensive flight test and modification work had to be done to find the final solution, the roll control system could be kept relatively simple with regard to cost, weight, maintenance and reliability of the operational aircraft.

5. CONCLUDING REMARKS

For the time being 7o% of certification flight testing has been conducted, for the rest no technical problems are expected, so final certification is scheduled for middle 1974. We hope to land the aircraft as smoothly and safely in a world wide market as in shown in fig. 2o.

6. LIST OF REFERENCES

(1) Stüssel, R.:
Jet bus VFW 614, Flugrevue Heft 5/6 1968

(2) Stüssel, R.:
VFW 614, the world expanding earth shrinker Friendship Bulletin, spring 1973 (published by VFW-FOKKER group)

(3) Stüssel, R.:
VFW 614, concept and market prospects, VFW-FOKKER Rep 1967, march 1973

(4) Barche, J.:
Beitrag zum Interferenzproblem von über den Tragflügeln angeordneten Triebwerken
DGLR Jahrestagung 1969

(5) SAE ARP 842 B 197o
Design objectives for flying qualities of civil transport aircraft

(6) MIL F - 8785 B
Flying Qualities of military aircraft

(7) VFW 614 flight test reports unpublished

Fig. 1 VFW 614 DURING TAKE OFF

- *SHORT AIRFIELD PERFORMANCE*
- *MULTI-STAGE CAPABILITY*
- *ROUGH AIRFIELD CAPABILITY*
- *MINIMUM NOISE and POLLUTION*
- *INDEPENDENCE from GROUND SUPPORT*
- *HIGH DISPATCH and BLOCK-TO-BLOCK RELIABILITY*

Fig. 2 VFW 614 DESIGN CRITERIA

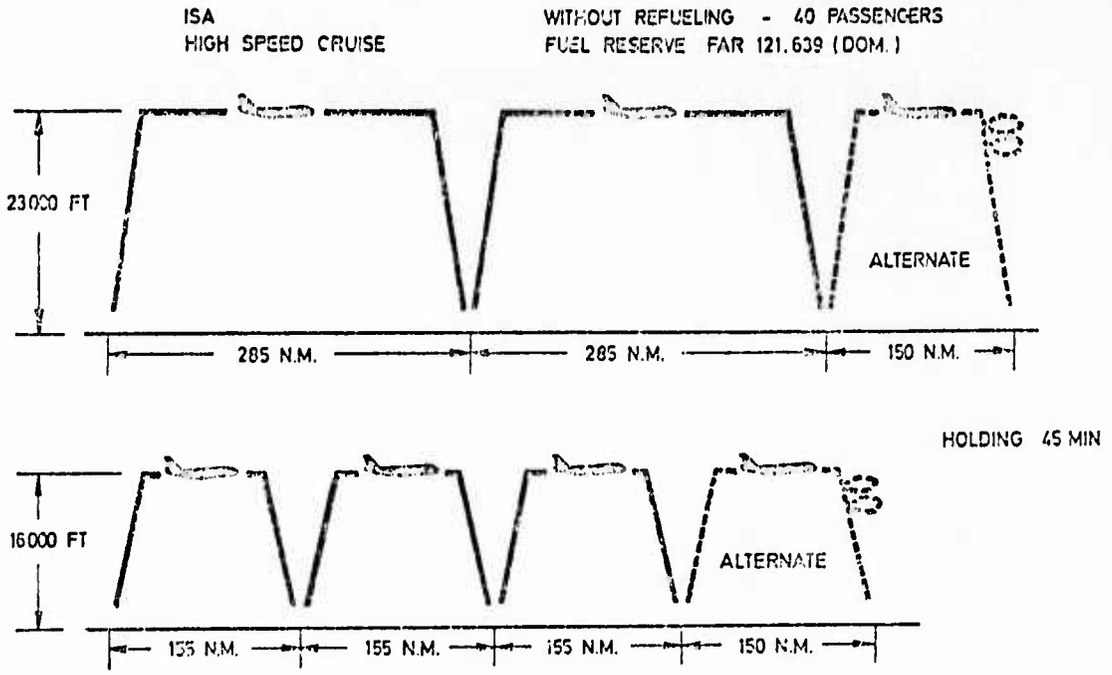

Fig. 3 MAIN DIMENSIONS OF VFW 614

DIMENSIONS	*WING SPAN* *LENGTH* *HEIGHT* *WING AREA* *ASPECT RATIO* *SWEEP ANGLE (25%)* *TAPER RATIO*	*21,5m / 70ft 6in* *20,6m / 67ft 6in* *7,8m / 25ft 8in* *64,0m² / 688 sqft* *7,22* *15°* *0,4*
WEIGHTS	*MTOW* *MLW* *WING LOADING, max.*	*19950 kp / 44000 lbs* *19950 kp / 44000 lbs* *312 kp/m² / 64 lbs/sqft*
ENGINES	*2 × RR/SNECMA M45H*	*2 × 3440 kp / 2 × 7570 lbs*
PERFORMANCE	*CRUISE MACH NUMBER* *at ALTITUDE* *RANGE* *T/O FIELD LENGTH (FAR)*	*0,65* *20000 ft* *1320 km / 710 n.m.* *4000 ft*

Fig. 4 TYPICAL SHORT HAUL OPERATION

Points of main development effort

High speed

- to minimize additional pod/pylon drag and buffet,
- to optimize stability and control with simple systems,
- to minimize engine throttle effects, especially the effects of slam deceleration of both engines on longitudinal motion as well as single engine throttling on lateral directional motion.

Low speed

- to minimize adverse pod/pylon effects on the stall characteristics
- to minimize wing stall effects on engine distortion,
- to optimize the aircraft STO potential on stability and control, expecially under strong cross wind conditions,
- to provide optimal controllability with respect to one engine inoperative, crosswind etc.
- to finish with stick free stability problems associated with manuel controls
- as well as the tail stall problems under icing conditions.

Fig. 5 POINTS OF MAIN DEVELOPMENT EFFORT

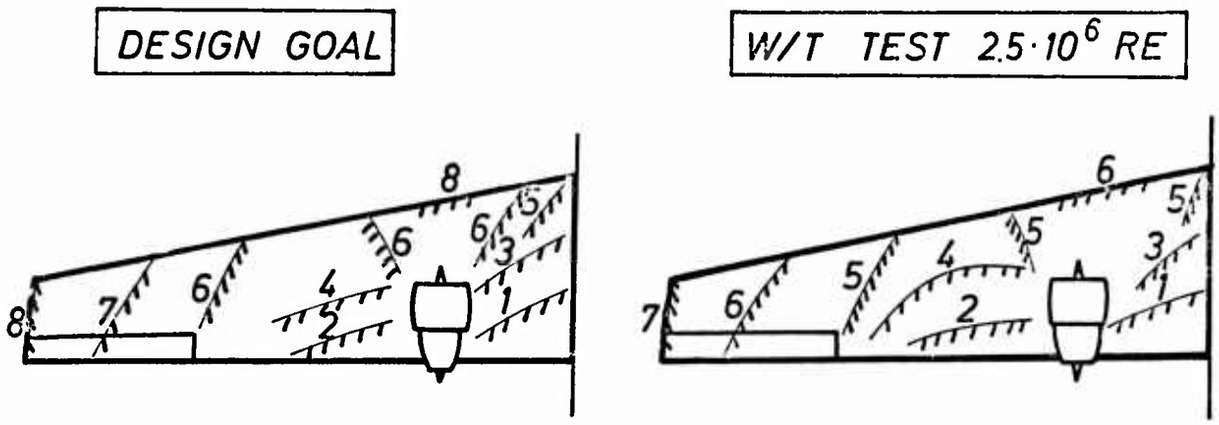

α-RANGE	1	3	5	6	7	8
	0°-12°	13°-14°	15°-16°	17°-18°	18°-20°	>20°

Fig. 6 STALL PROPAGATION / DESIGN / MODELL TEST

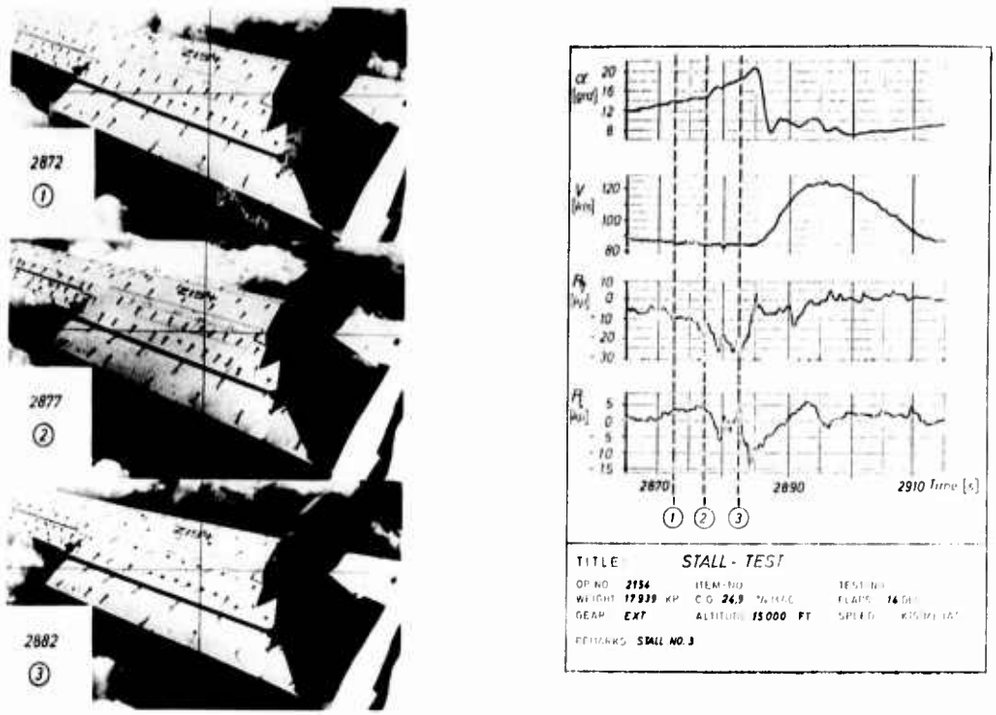

Fig. 7 STALL PROPAGATION / FLIGHT TEST

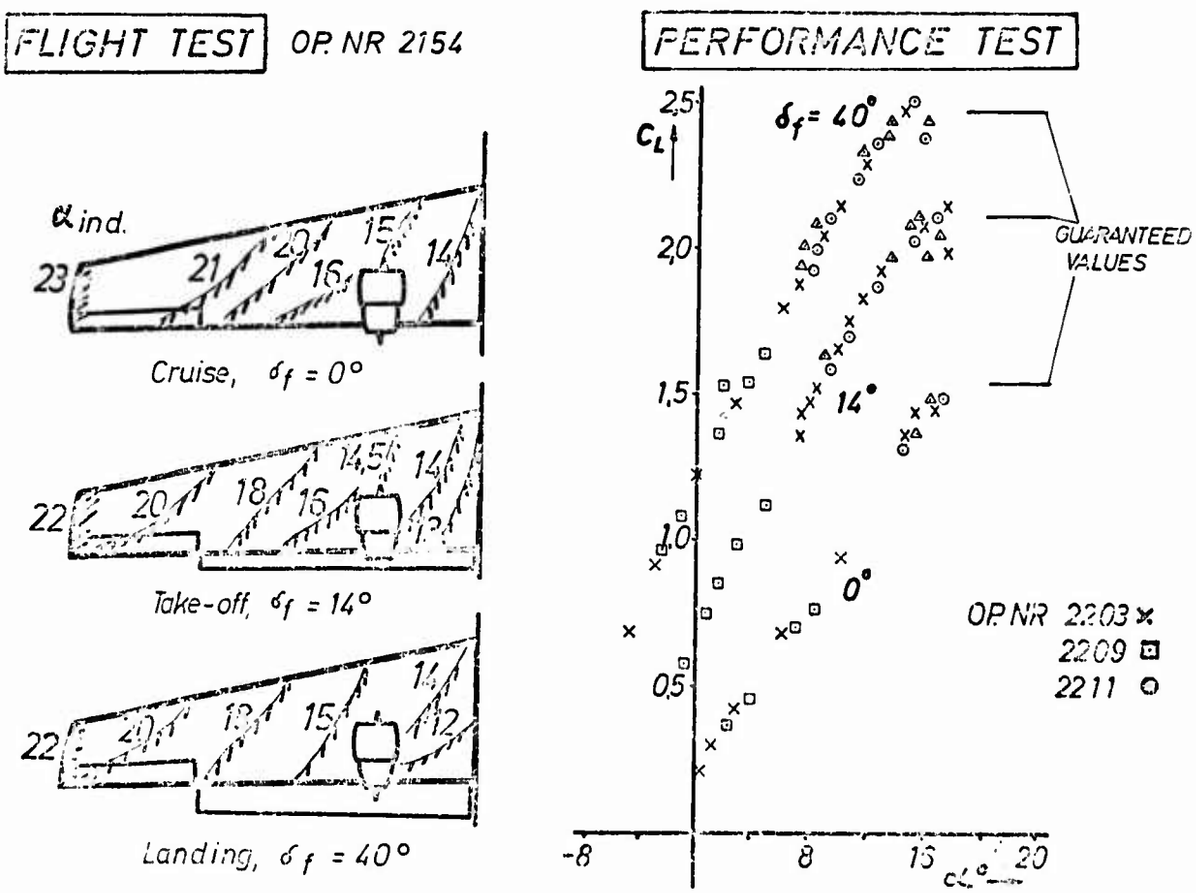

Fig. 8 STALL PROPAGATION / LIFT

Elevator Control (gear-tab)

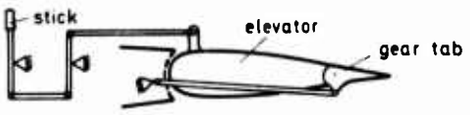

hinge moment coefficient : $C_H = b_0 + b_1 \cdot \alpha^* + b_2 \cdot \eta + b_3 \cdot \eta_T$ with

α^* the local aerofoil incidence

η, η_T the control and gear-tab angle

change in elevator hinge moment coefficient : $\Delta C_H = b_1^* \cdot \Delta\alpha + b_2^* \cdot \Delta\eta$ with

$b_2^* = b_2 + b_3 \cdot \frac{\eta_T}{\eta}$

and

stick force : $\Delta F = K \cdot q_0 \cdot \Delta C_H$ with

q_0 the dynamic pressure at trim point

K constant (stick gearing, boost ratio)

Fig. 9 ELEVATOR CONTROL PRINCIPLE

Layout of elevator control

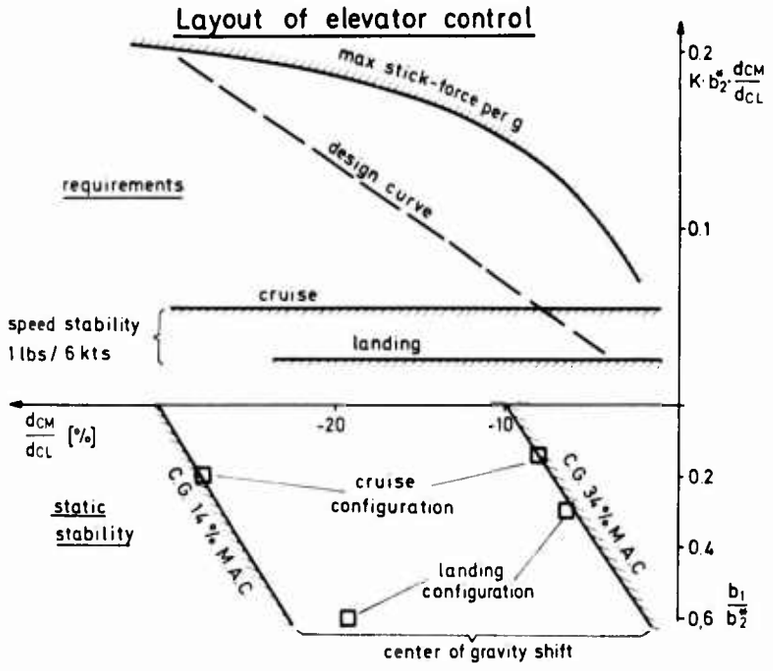

Fig. 10 ELEVATOR CONTROL LAY OUT

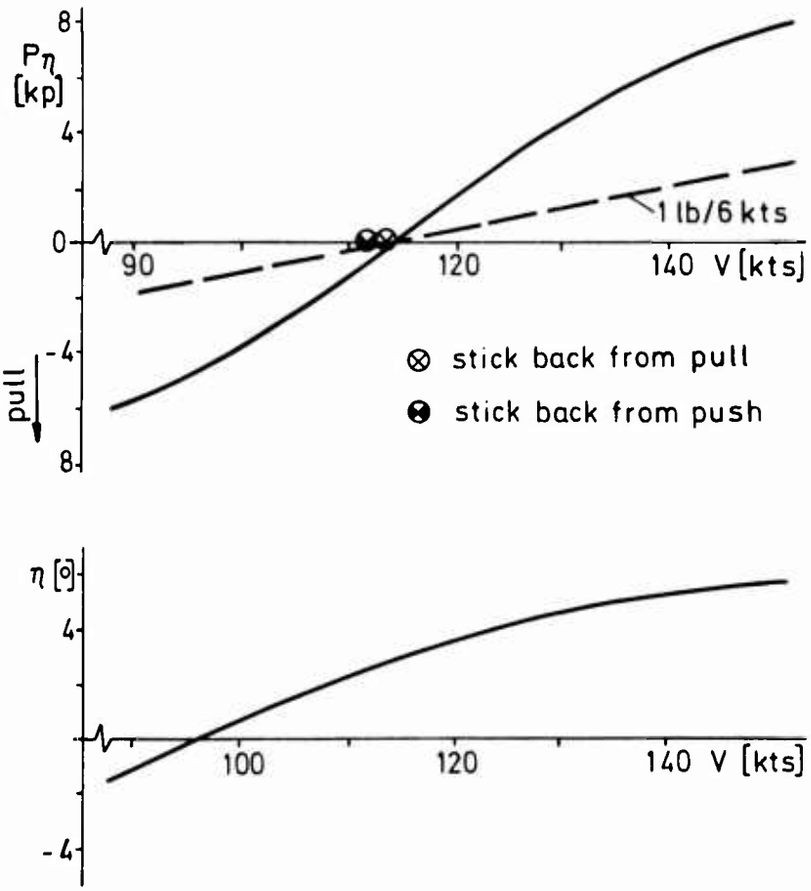

TITLE STATIC LONGITUDINAL STABILITY
OP. NO. 3286 ITEM-NO. 8.05.03.06.00 TEST-NO. 1
WEIGHT 18600 KP C.G. 32 % MAC FLAPS 35 DEG
GEAR EXT. ALTITUDE 13000 FT SPEED 114 KTS
REMARKS LANDING

Fig. 11 SPEED STABILITY (FLIGHT TEST)

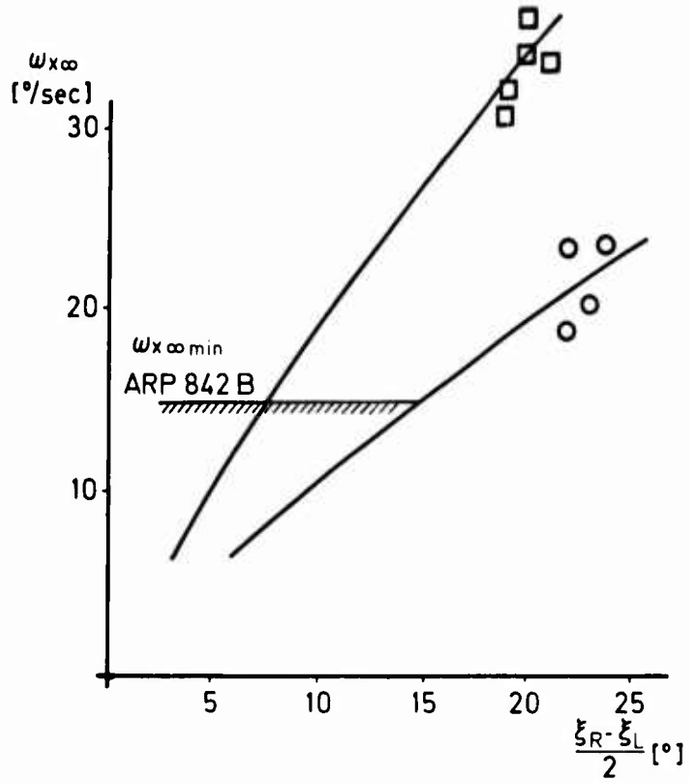

Fig. 12 ROLL RATE PERFORMANCE

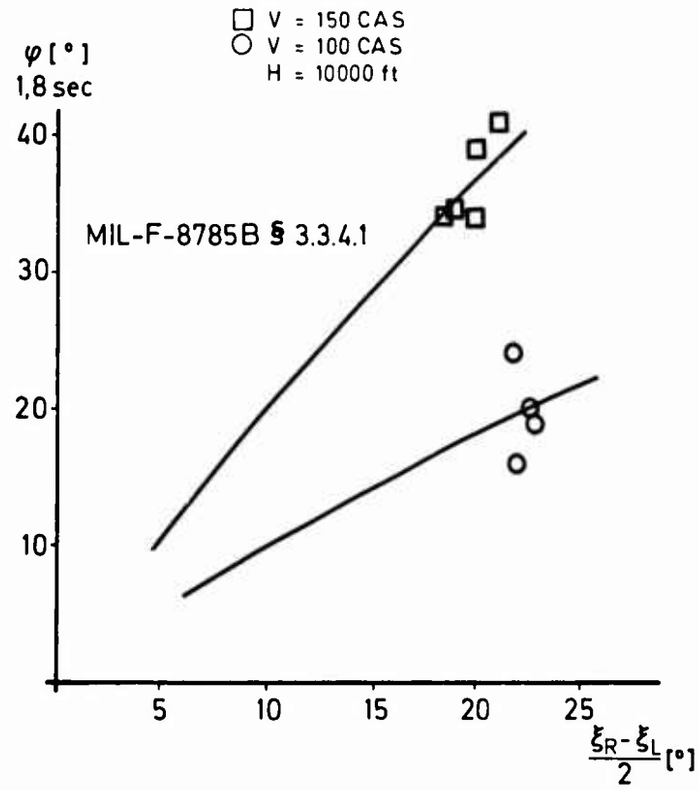

Fig. 13 ROLL ACCELERATION PERFORMANCE

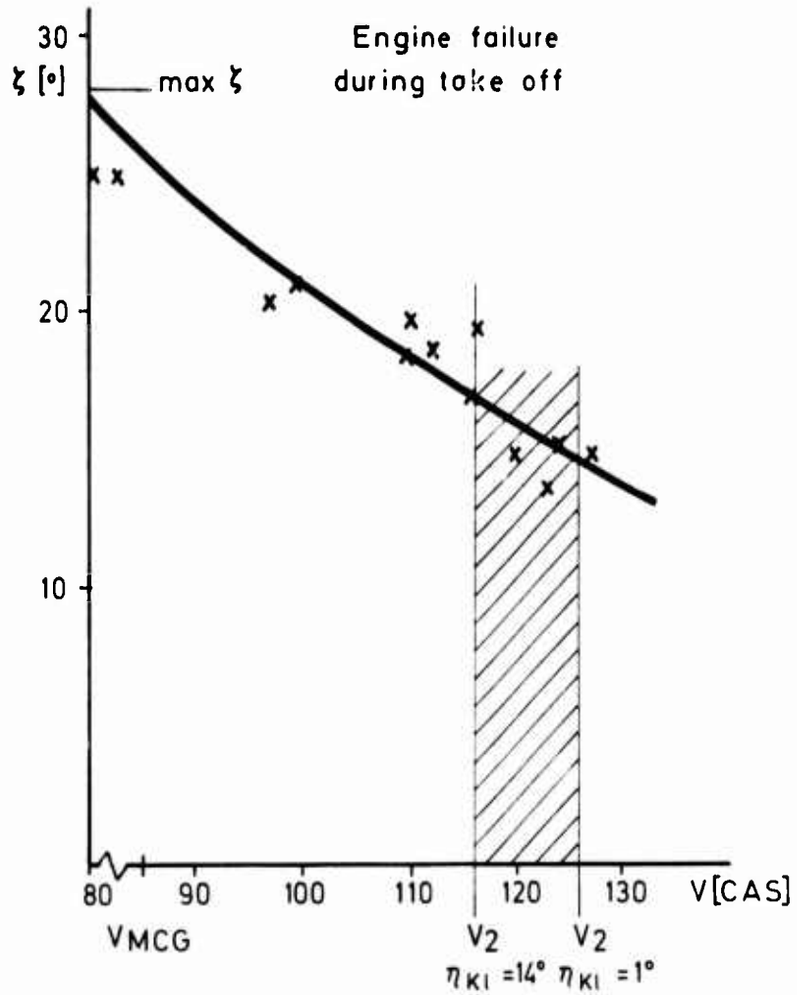

Fig. 14 MINIMUM CONTROL SPEED (FLIGHT TEST)

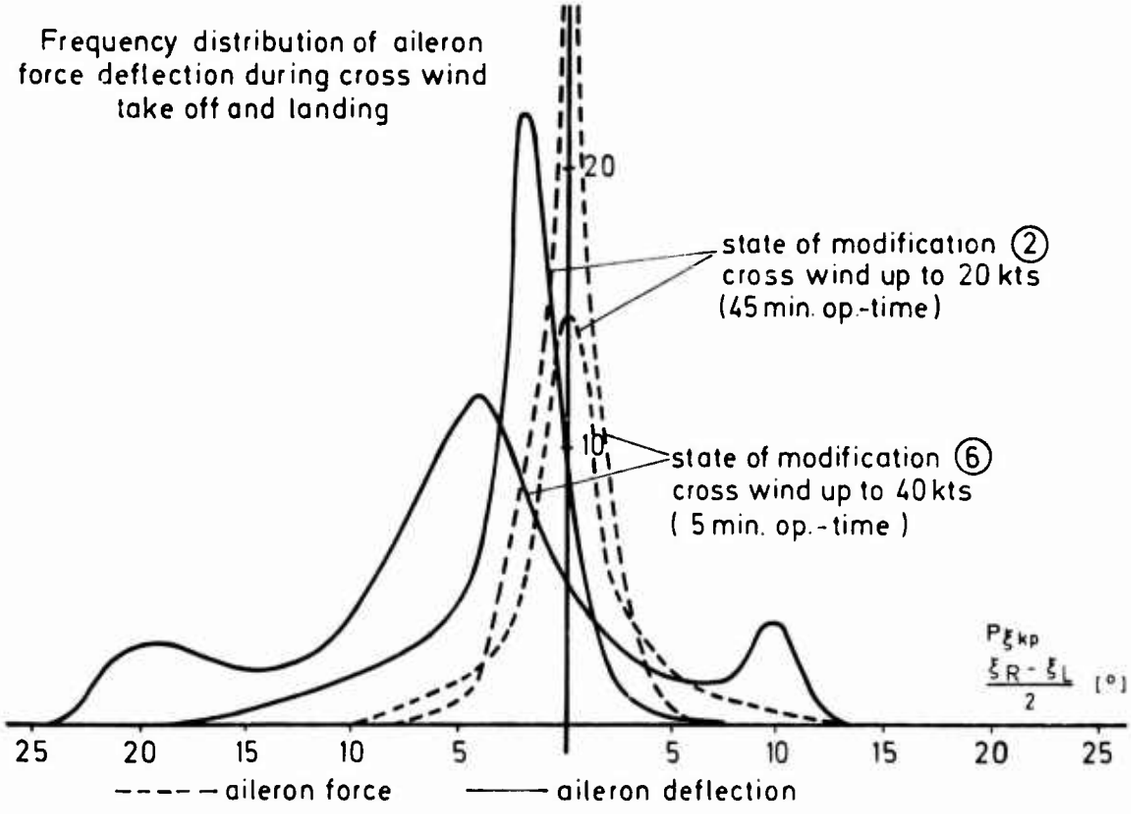

Fig. 15 FREQUENCY DISTRIBUTION OF ROLL CONTROL DEMAND AT CROSS WIND TAKE OFF AND LANDING

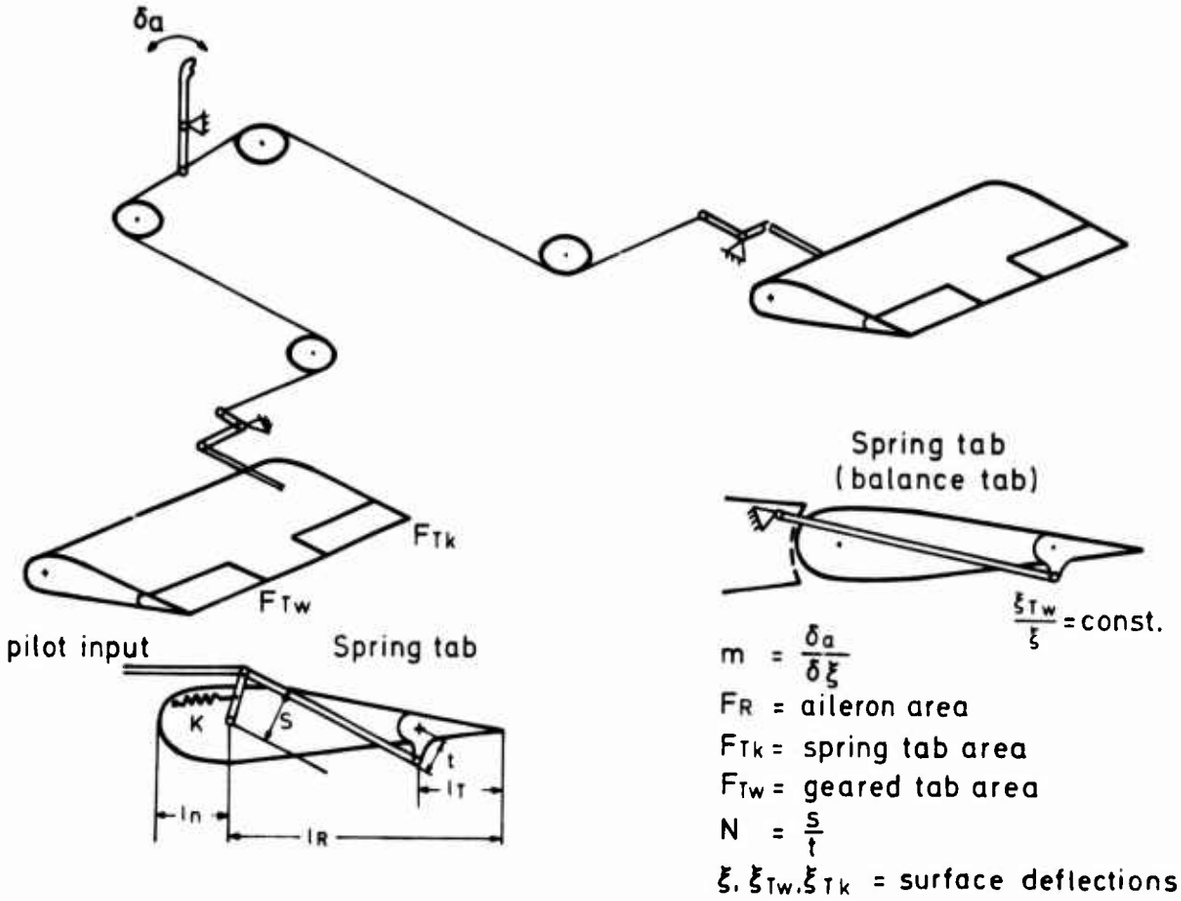

Fig. 16 BASIC ROLL CONTROL CONFIGURATION

LAYOUT DATA AILERON

	AILERON	SPRING TAB	TRIM TAB
AREA OF HINGE LINE [m^2]	2 x 1,62	2x0,194	0,153
SURFACE CHORD	0,25 lμ	0,0625lμ	0,0625 lμ
NOSE CHORD / SURFACE CHORD	0,30	0,13	0,13
POSITION [% SEMI SPAN] FROM TO	70% 98,5%	70% 82,3%	86,5% LEFT 98,5% SIDE
MAX. SURFACE DEFLECTION	±25°	±25°	±20°
MAX. CONTROL WHEEL DEFLECTION	±90°	-	-
GEAR BETWEEN WHEEL AND AILERON $\frac{\delta a}{\xi}$	2,58 $\frac{rad}{m}$	-	-
SPRING STIFFNES		14 kpm/rad	
LEADING EDGE SHAPE	ELLIPTICAL	ELLIPTICAL	ELLIPTICAL

Fig. 17 ROLL CONTROL SYSTEM PARAMETERS

STATE OF MODIFICATION

NR.	SPRING STIFFNES kpm/rad	LEADING EDGE SHAPE	MAX WHEEL DEFLECTION	AILERON DEFLECTION	GEAR TAB/ AILERON
①	16	ELLIPTICAL	±90°	±25°	-
②	8	ELLIPTICAL	±90°	±25°	-
③	4	CIRCULAR	±110°	±25°	-0,8
④	4	CIRCULAR	±110°	±25°	0
⑤	4	CIRCULAR	±110°	±25°	-0,56
⑥	4	CIRCULAR	±110°	+ 19° - 29°	-0,56

Fig. 18 MODIFICATION STEPS OF ROLL CONTROL SYSTEM

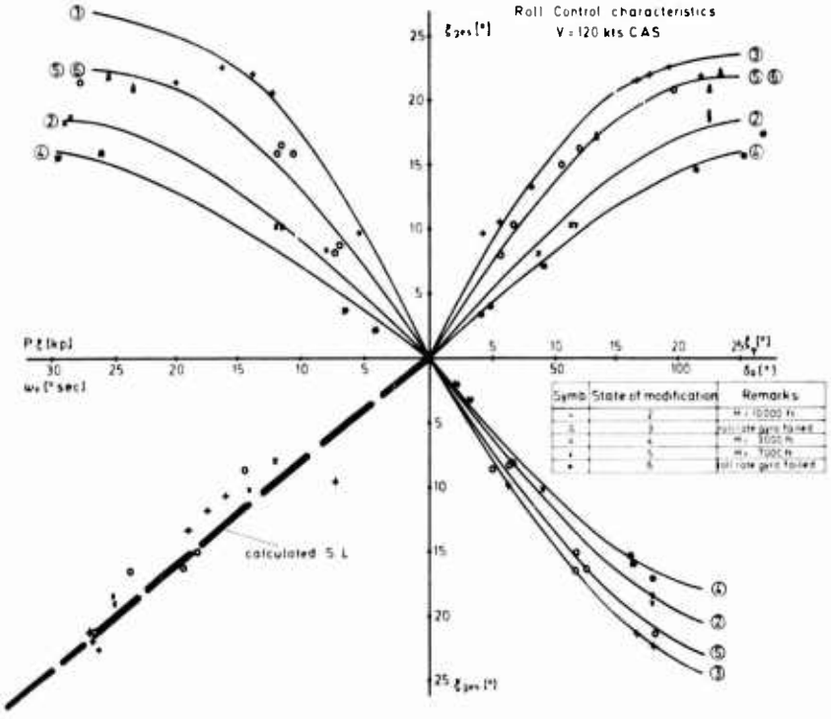

Fig. 19 ROLL CONTROL CHARACTERISTICS DEPENDING ON THE STATES OF MODIFICATION

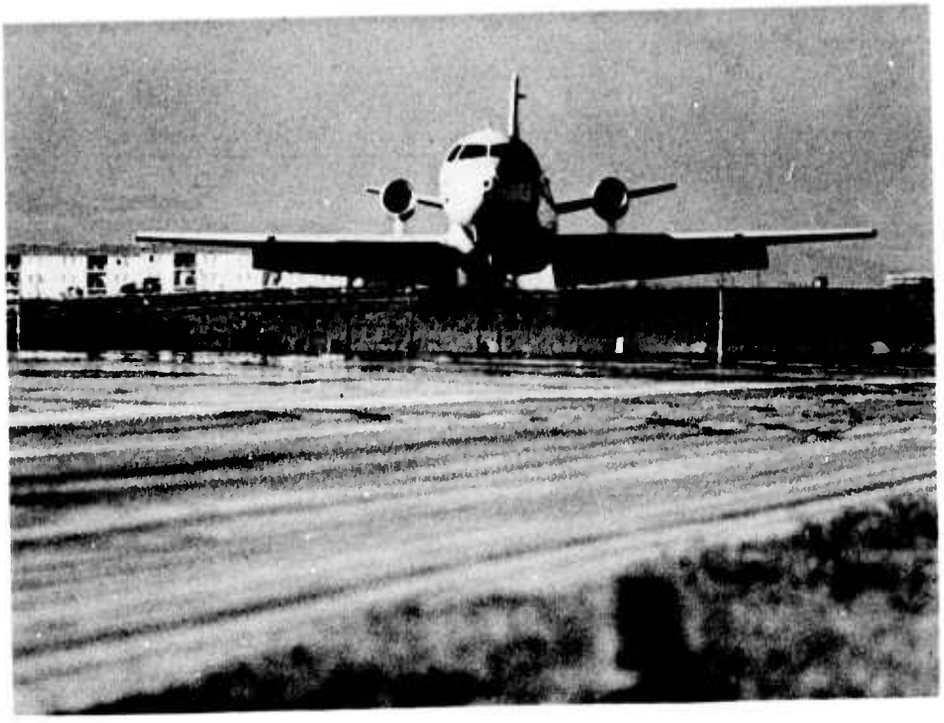

Fig. 2o VFW 614 DURING LANDING

DIRECT LIFT CONTROL APPLICATIONS TO TRANSPORT AIRCRAFT - A U.K. VIEWPOINT

M. R. Smith
Group Leader - Aerodynamics Dept.
Commercial Aircraft Division (Weybridge)
British Aircraft Corporation

SUMMARY

The longitudinal controllability of large conventional transport aircraft during the approach and landing flight phases, and of conventional high lift 'STOL' aircraft during short landings, is discussed.

The advantage of a direct lift control system (DLC) is indicated, and a practical design, using wing spoilers, is described, with its disadvantages.

Theoretical and flight simulator investigations on the VC.10 aircraft, and the BAC 1-11 aircraft are described, together with investigations of similar systems for improving the automatic landing of current British jet aircraft. Some recent investigations on a DLC application to a STOL aircraft are noted.

It is concluded that DLC applications can improve controllability and performance for most transport aircraft. A more detailed study is required for each application before its true value can be assessed, even for large transport aircraft. Application of DLC to conventional lift STOL aircraft looks attractive for achieving satisfactory flare performance.

1. INTRODUCTION

During the last few years, various studies and applications of direct lift control (DLC) have been reported on. Most of these applications of DLC have been on American aircraft. This paper discusses some of the studies and applications of DLC as carried out or to be carried out in the United Kingdom, particularly as regards application to jet transport aircraft, although it is fair to say that there has been less activity on DLC in the small aircraft military sphere.

2. INITIAL STUDIES OF CONTROLLABILITY

(a) Conventional aircraft (CTOL)

Initial consideration of DLC during the late 1960's was related to the apparent need to improve controllability, especially during the landing approach phase, of the larger transport aircraft being considered at that time. For example, BAC were working on a large twin design (BAC 3-11). The problem identified was of course the sluggish pitch response expected of the larger aircraft, especially during the critical landing approach flight phase. The situation was considered from experience on the BAC 1-11 (a small rear-engined aircraft) and the VC.10 (a large rear-engined aircraft). These aircraft have good handling qualities. Figure 1 shows the response to elevator during the landing approach for a range of aircraft including the above, the interest being in the initial response, so that the c.g. position is not too important. The more sluggish pitch response could be compensated for by using bigger elevator inputs, restoring most of the incidence (and 'g') response. The latter provides the lift to control the flight path. This argument was the basis for proposing manoeuvre boost, i.e. automatic augmentation of pilot-demanded elevator inputs, on at least one large aircraft. However, this could lead to an over-controlling tendency, especially on the aft c.g., with the longer response times and lower pitch stiffness.

(b) Short landing aircraft (STOL)

At the same time as the larger aircraft were being considered, design studies of various STOL aircraft were being carried out. BAC, for example, were looking at a conventional STOL aircraft with a powerful high lift system. Approach speed for this aircraft is 90 knots. Again, slow pitch response is to be expected at slow speeds, due to the lower elevator effectiveness, as illustrated in Figure 2. Again, larger control inputs would rectify that situation. But this means that with a conventional control system the pilot is having to pitch the aircraft through a larger attitude change for a required 'g' response, compared with a conventional aircraft. Now in addition to this, STOL performance is associated with steep approaches, to minimise the airborne segment of the landing distance. Calculations of a simplified (constant 'g') flare manoeuvre, Figure 3, indicate that, compared with a conventional flare, more 'g' must be applied, and there is less time to achieve it. Because of the limited time for the flare, and the lag in the elevator response as indicated in Figure 2, it will be difficult for the pilot, with a conventional control system, to achieve a consistently satisfactory landing performance. Significant variations of rate of descent at touchdown and of touchdown point will be probable, seriously affecting the expected landing performance.

3. CONTROLLABILITY WITH DLC SYSTEMS

The above discussions indicate the need to improve controllability for certain types of aircraft and for certain flight phases. The improvements are in the sense of giving quicker 'g' response, i.e. more direct control of lift, than is achieved with a conventional control system. Various devices can be used for this, such as quick acting flaps, drooped ailerons, airbrakes or even powered lift. For the aircraft considered in this paper, the requirement for DLC is for the landing approach phase only. This means that a conventional control system can be considered in the least complicated way, e.g. without extra cockpit controls.

Spoilers acting in front of the high lift flap system can provide adequate control of lift and are a good choice since most current or projected aircraft have them, they have quite rapid actuation rates, and often are arranged to be used as both airbrakes (symmetric operation) and spoilers (asymmetric operation). A DLC mode therefore involves little more than making the spoiler a primary rather than a secondary longitudinal control.

There are disadvantages with using spoilers. Obviously they must be set at some intermediate setting to provide both positive and negative lift control. They may still have the desired overall control of lift (equivalent to at least $\pm$ .1 'g') provided they cover sufficient span of the wing, say 30%, but are likely to have non-linear characteristics. Venting the base of the spoiler reduces the non-linearity at small angles. Care should be taken in relying on wind tunnel testing for this data, because of the unpredictability of scale effects. There can be significant effects on pitching moments due to spoiler deflection. These effects will depend on the position of the spoilers on the wing, and the position of the tail. For the BAC 1-11 aircraft, deflection of spoilers causes a nose-up pitching moment, almost entirely due to the effects on the wing lift, and this tends to reduce the effects of the spoilers as a DLC device, once the aircraft starts to respond.

This indicates that pitch compensation is required with DLC using spoilers, and a complete DLC system, along the lines indicated above, is shown diagrammatically in Figure 4. Movement of the main control circuit near the stick is sensed electrically, and the signal, modified by filters, used to drive the spoilers (pure DLC line) and to add to the pilot commanded elevator (pitch compensation line). The filter in the DLC line can compensate for spoiler non-linearity.

Investigation of a typical aircraft response to control inputs is shown on Figure 5, and it is indicated that since the elevator can ultimately provide satisfactory 'g' response, the DLC line can be washed out. The objective is to get the best compromise 'g' response for a step stick input, for

the extreme fore and aft c.g.'s. This indicates that the pitch compensation line must also be washed out, with a different time constant. A high gain between stick and spoilers is required, because of the lower 'g' capability of the spoilers, compared with elevator. The washout effect is advantageous here, for the otherwise direct connection between stick and spoilers would lead to complete saturation after small stick inputs, and any offset due to mis-rigging, or trim, or pulling 'g' in a steady manoeuvre, would give non-linear control.

4. U.K. RESEARCH

Having described a practical version of DLC, the question remained as to the handling benefits it brings. The provision of good handling qualities is a complex and difficult task, and theory is not always validated by practical experience. Original investigations were made at the Royal Aircraft Establishment (RAE) by Pinsker (Theoretical studies, Reference 1) and by Tomlinson (Flight simulation, Reference 2). Further investigations were as follows.

(a) VC.10 with a DLC system

This was a flight simulator investigation at BAC to determine what advantages there were in applying a DLC system to the largest jet transport yet built in the U.K. The emphasis in the program was to establish the relative merits of the basic aircraft handling, and the handling with DLC alone, and then with DLC and pitch compensation. The system was of the type described above, the gains and washouts being chosen after reviewing the step response data, and were as follows:-

DLC - Spoiler angle equals 9 times the demanded elevator angle, with a washout time constant of 3 seconds.

Pitch Compensation - Elevator angle equals and adds to the demanded elevator angle, with a washout time constant of 1 second.

The task performed was instrument approaches tracking the raw I.L.S., followed by a visual final approach and landing. Performance was assessed by pilot comments and ratings, and by a statistical measure of tracking performance, after sampling the glide slope (and localiser) deviation at 90 points during the latter stage of each approach.

The statistical data did not show a significant difference between the various configurations. This was considered to be due to the way the pilots flew the simulator, i.e. they were flying a normal type of instrument approach, which was only tight at the end of the approach. This view was supported by the measurements made of landing performance with the various configurations. Here data showed that the pilots achieved better landing performance (reduced touchdown point scatter and sink rate velocity at touchdown) with DLC, and further improvement with DLC and pitch compensation. For example*, at a given level of probability the sink rate at touchdown was about 15% less with DLC, and about 30% less with DLC and pitch compensation, despite the limitations of the simulator for measurements during this flight phase. Although the handling of the basic aircraft is worse on the aft c.g., and this was also found on the simulator, results indicated that if DLC and pitch compensation were incorporated, the differences between fore and aft c.g. configuration were reduced.

* See Fig 6

For the approach phase, pilots' comments indicated that, despite the performance results, the handling was improved if DLC was incorporated with pitch compensation. DLC alone was not generally liked, since although it did help flight path control (control of vertical speed on VSI), it was too sluggish in pitch. This reflects the fact that pilot opinion is based on both flight path control and attitude control. The combination of DLC and pitch compensation helps both these components. An overall conclusion was that the approach task was rated at 4 on the Cooper scale for the basic aircraft and 3 with DLC and pitch compensation. This investigation is reported in Reference 3.

(b) Conventional aircraft with DLC under automatic control

It was felt that perhaps automatic control might gain more from incorporation of a DLC mode, since it would not be constrained by pilot controllability requirements. A preliminary theoretical investigation was therefore carried out at the Avionics Department of the RAE on a range of transport aircraft with and without a representative DLC system. This work is about to be published (Reference 4) and will only be mentioned here. A parameter optimisation technique was used to determine autopilot control laws, and it was found that provided the DLC authority was high or had high gain, both pitch activity and deviations from the beam, in turbulence, could be reduced. (Typically $\frac{1}{2}$ x RMS pitch activity, $\frac{1}{2}$ x RMS vertical velocity). Also there was a reduction in scatter of touchdown velocity and touchdown point.

In parallel with the above investigations, Smiths Industries Limited investigated theoretically the application of a DLC system to the Hawker Siddeley Trident under control of an autopilot, (Reference 5). Under automatic control, ideally the elevator could maintain constant pitch attitude, with DLC to control vertical flight path. However, spoilers on the wing were considered as the DLC aerodynamic control, and again because of their limited control of lift were used to augment, rather than replace the incidence-induced lift due to elevator. The DLC was investigated for simulated automatic approaches and landing starting from 200 feet altitude on a $2\frac{1}{2}^{o}$ beam. The main purpose of the investigation was to determine improvements in flare performance due to DLC. Since the existing Trident system is satisfactory in normal conditions, investigations were made in high turbulence conditions, associated with a wind strength of 20 knots. It was found that performance was substantially improved. In general the scatters of all the significant touchdown variables had been reduced to about one half of their original values by suitable approaches, and it was possible to land the Trident from a 5 degree glideslope in the presence of shear

and turbulence with very good results.

(c) BAC 1-11 with a DLC system

From the above investigations it was evident that DLC had useful application, but required evaluation in flight conditions, particularly the manual application of DLC, but also the application to automatic control.

Accordingly, the Blind Landing Experimental Unit of RAE purchased a second-hand BAC 1-11, and this has been fitted out with a DLC system. The manual system is along the lines already indicated, and will be evaluated by RAE Aeroflight.

The aircraft is now in the flight line, but prior to this stage a further evaluation of DLC by flight simulation had been considered desirable. The simulation was carried out on the 5-axis motion Flight Simulator at BAC, since it was evident that motion was particularly important for a critical evluation of DLC. The previous investigations had indicated that the most benefit from DLC would be in the final landing approach and flare manoeuvre. Since the simulator did not have an adequate visual display, the task on the simulator was to track the raw I.L.S. with a fixed, high sensitivity, equivalent to that of an I.L.S. when passing through the 50 foot point on a 3^{o} approach. This could not be tracked with the conventional elevator control, but was sufficiently demanding to show up differences between various DLC systems. The purpose of the investigation was to indicate the best system for initial evaluation on the aircraft. The investigation is reported in Reference 6.

The DLC parameters varied were DLC washout, and overall gain. Evaluation was made by pilots' comments and by statistical analysis of measured performance and workload, by sampling glide slope error and stick movement a large number of times during each approach, and determining standard deviations, for the configuration of that approach.

Each run was set up starting on the beam with low I.L.S. sensitivity and slowly increasing the sensitivity to the required level, before evaluation started. Only light turbulence was simulated, to 'mask' slight roughness in the motion system. The levels of turbulence normally used would have affected the I.L.S. pointer too much at the high sensitivities required in the evaluation.

Figures 7 and 8 show examples of how performance varied as DLC parameters were varied, in turn. The datum values for each parameter was determined by theoretical investigation. The data generally substantiated the theoretical findings, except that the pitch compensation washout could be increased (to say 1 sec.), and correlated with pilots' qualitative assessment, except that they did not like the system without pitch compensation, since it appeared to them more difficult to fly because of the unconventional nature of the response.

With the above datum system, some conventional raw I.L.S. approaches were also carried out. Qualitatively, the pilots rated these only slightly better than with the basic aircraft, perhaps half better on the Cooper scale, from $3\frac{1}{2}$ to 3. A more significant improvement was obtained when using the flight director. This shows that DLC is one of perhaps several ways of improving the handling qualities of an aircraft for a specific task.

(d) BAC STOL aircraft with a DLC system

The BAC STOL aircraft, mentioned earlier, is the subject of a current theoretical and flight simulator handling assessment at BAC and RAE. This project aircraft uses a high lift system to make steep, slow approaches into short airstrips. Investigation of a DLC system for manual flying has not yet been carried out, but some of the investigations of the flare manoeuvre under automatic control have been completed. So far no satisfactory control laws have been found for elevator and throttle to achieve satisfactory flare performance, for all configurations, tolerances and certificable wind conditions and turbulence. However, a promising control law was found using a combination of step elevator and step DLC (spoiler) at flare initiation height, with closed loop control on the DLC for precise control of the flare.* The elevator step was to provide some of the lift required for flare by changing the aircraft incidence, as well as to compensate for the adverse pitching moments due to ground effect; the latter is significant for high lift STOL aircraft, even with a high wing and T-tail. The DLC step was also to provide lift for the flare, but since DLC authority was required for closed loop control after the initiation of flare, the initial step must be washed out, which can be compensated for by a larger elevator input, or the step must be backed off, which limits the effectiveness of the DLC. It is worth noting that speed loss in the flare is significant for high lift STOL aircraft, and can arise due to the large change in axial force, along the flight path, due to loss of the gravity component in the flare. Application of DLC in the way described reduces the drag in this critical phase, and helps to maintain the airspeed.

* See Fig 9

5. SAFETY ASPECTS OF DLC

It is not intended to cover the safety aspects of incorporating DLC fully, although they are obviously important. For the systems described, the DLC authorities are low, and the safety problems can be solved, For example, the RAE 1-11 has a simplex system. Hardovers were investigated on the simulator and during the clearance flying and found acceptable.

It is worth noting that incorporating DLC for both manual and automatic modes may require compromise; e.g. the pilot would not be aware of the elevator movement due to pitch compensation in the manual mode, whereas conventional autopilots are designed to move the control column proportional to their use of control surface.

An airworthiness aspect worth comment relates to the margins inherent in the allowable operating speeds. For the landing approach, compared with a conventional configuration, an aircraft with DLC using airbrakes will fly at a higher incidence for a given speed. Since the stalling incidence is not likely to change significantly with airbrakes deflected, then the incidence margin is less, unless the speed is increased. Typically this would be of the order of 4 knots. In fact, the approach speeds for a STOL aircraft may not need to be increased as much, since the target approach speed may well be determined by the need to demonstrate a satisfactory flare from an approach at target approach speed minus a margin (typically 5 knots). This could be dictated by the maximum lift available in ground effect, resulting in an increased margin of lift for a normal approach. This is illustrated in Figure 10. It can be argued that DLC would not affect the maximum lift in ground effect, since in the critical case, flare off a slow approach, it will certainly be providing significant lift augmentation, with the spoilers in.

6. CONCLUSIONS

1. Application of DLC can improve controllability and performance for most transport aircraft. A more detailed study is required for each application before its true value can be assessed, even for large aircraft.

2. Application of DLC to conventional high lift STOL aircraft looks attractive for achieving satisfactory flare performance.

3. DLC is only one of perhaps several ways of improving aircraft handling qualities, and is not necessarily the best.

4. DLC is at least as important for improving performance under automatic control as for manual control.

5. A practical DLC, if required, can be achieved relatively easily; it will probably augment the conventional elevator control and require a pitch compensation feature.

7. REFERENCES

1. W. J. G. Pinsker — The control characteristics of aircraft employing direct lift control. ARC R & M 3629 May 1968.

2. B. N. Tomlinson — Direct lift control in a large transport aircraft - a simulator study of proportional DLC. RAE TR 72154 November 1972.

3. A. G. Barnes, D. E. Houghton & C. Colclough — A simulator study of direct lift control. BAC (MAD) Report Ae 312. October 1970.

4. - — RAE TR 74013 (to be published)

5. P. H. Collins & K. J. Howes — Application of direct lift control to automatic landing. Smiths Industries Ltd. Rep. R & D. 1292 April 1972.

6. J. W. Gilbert & M. R. Smith — A theoretical and flight simulator investigation of a direct lift control system for a BAC One-Eleven aircraft. BAC (CAD) Report Aero/S&C/160 September 1972.

Fig.1

RESPONSE OF CTOL AIRCRAFT TO STEP STICK INPUTS

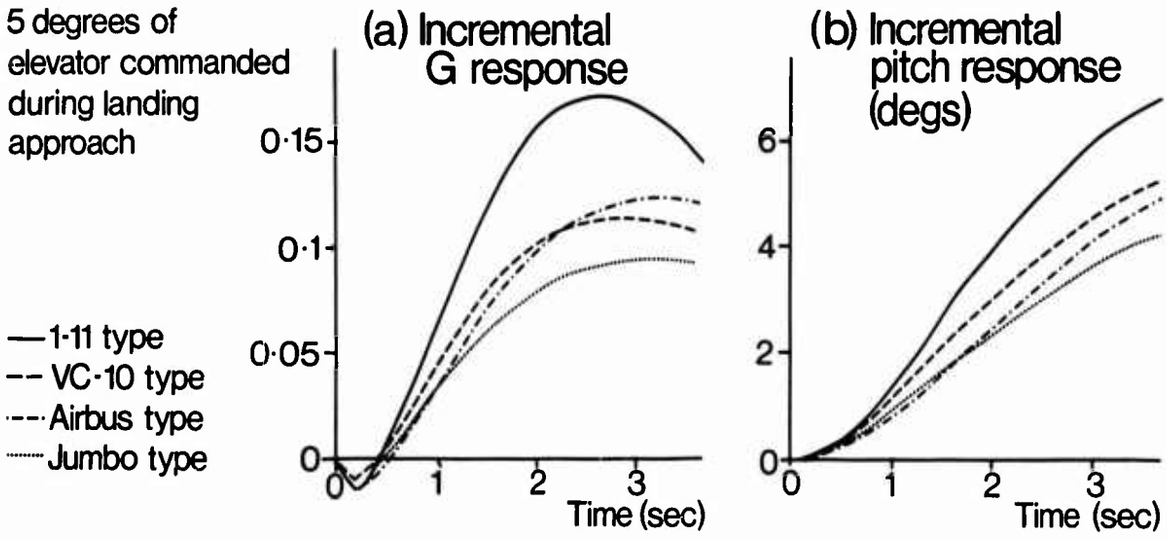

Fig.2

RESPONSE OF STOL AIRCRAFT TO STEP STICK INPUTS

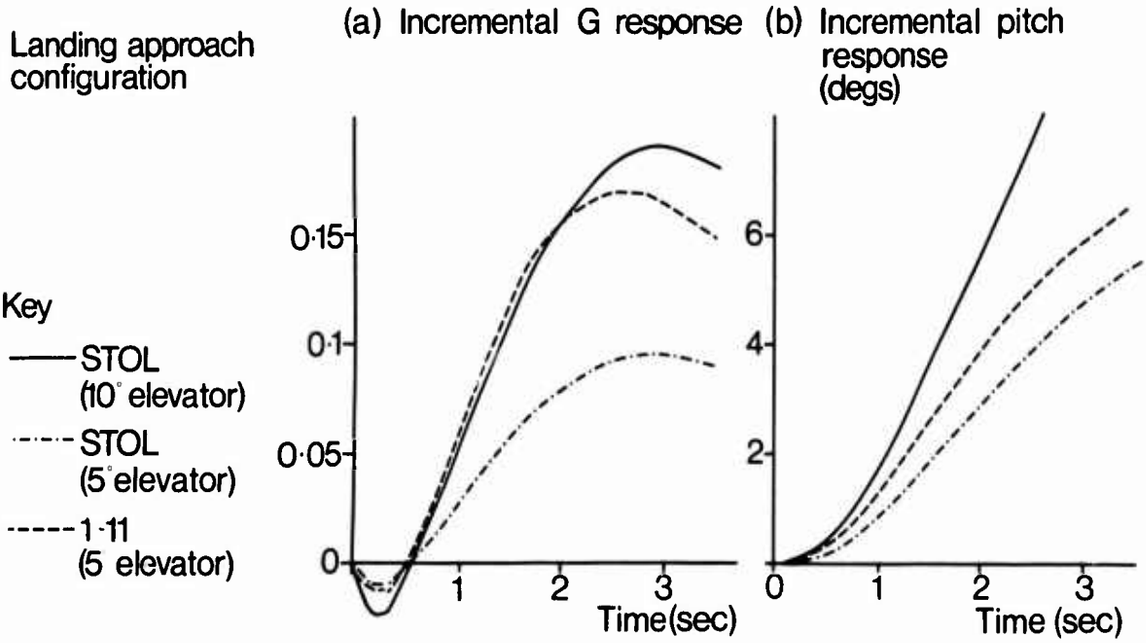

Fig.3

CHARACTERISTICS OF IDEALISED FLARE MANOEUVRE

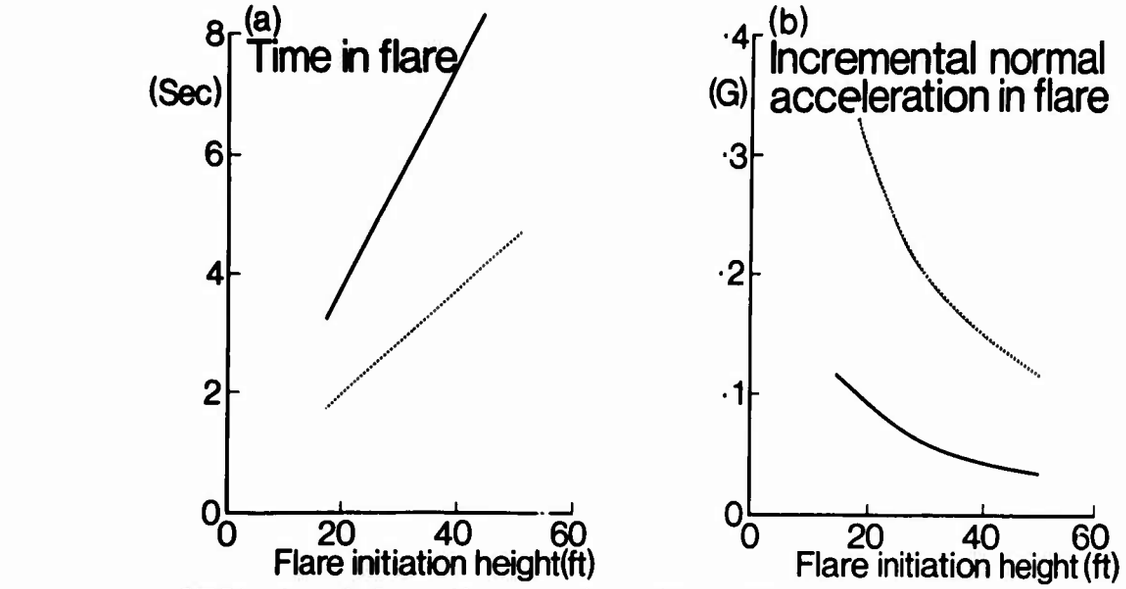

Fig.4

THE COMPLETE DIRECT LIFT CONTROL SYSTEM

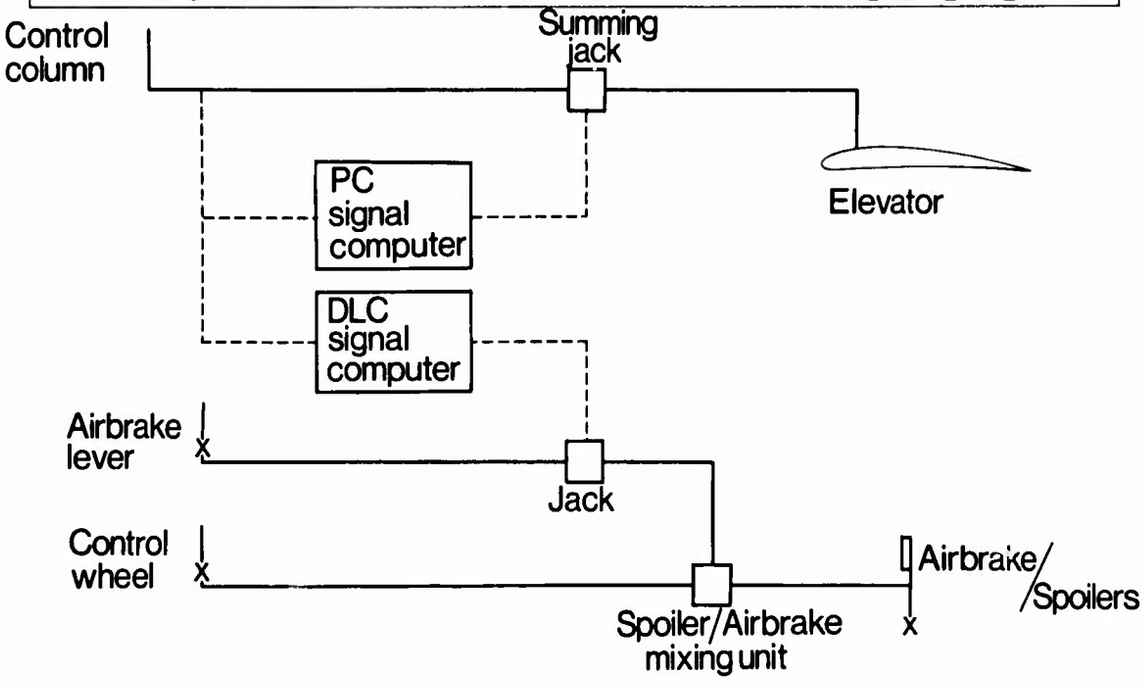

Fig. 5

RESPONSE TO A STEP STICK COMMAND INPUT WITH THE DIRECT LIFT CONTROL SYSTEM

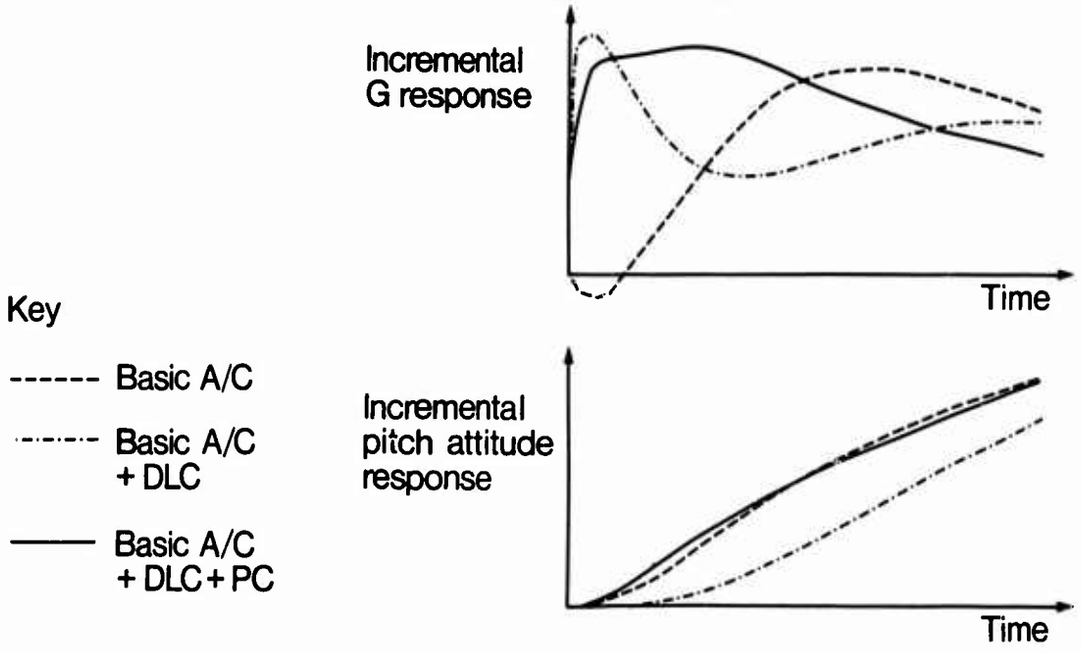

Fig 6

SINK RATE PROBABILITY CURVE

(From Fig 19 of Reference 3, for VC–10)

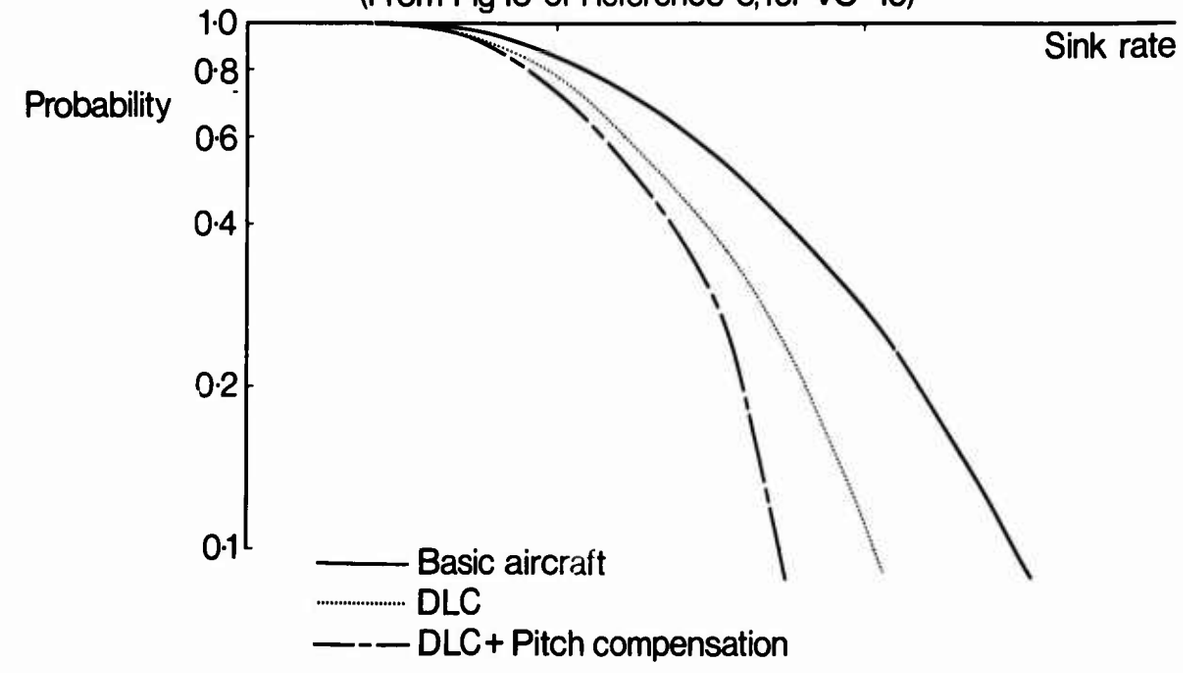

Fig. 7

PERFORMANCE ON THE GLIDESLOPE WITH VARIATION OF PITCH COMPENSATION CHARACTERISTICS

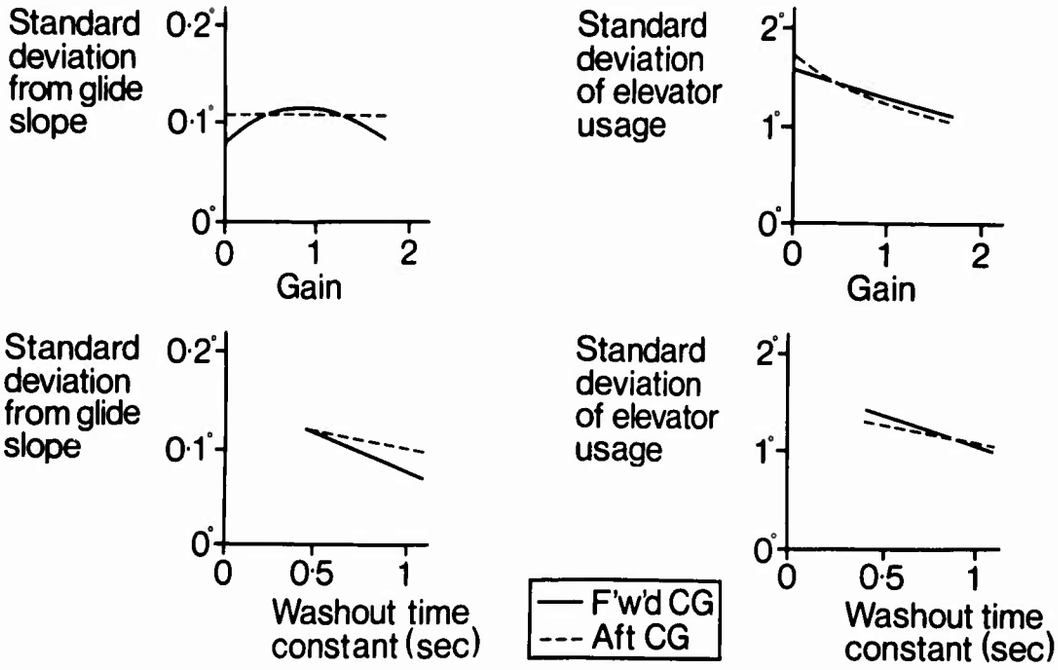

Fig. 8

PERFORMANCE ON THE GLIDESLOPE WITH VARIATION OF DIRECT LIFT CONTROL SYSTEM CHARACTERISTICS

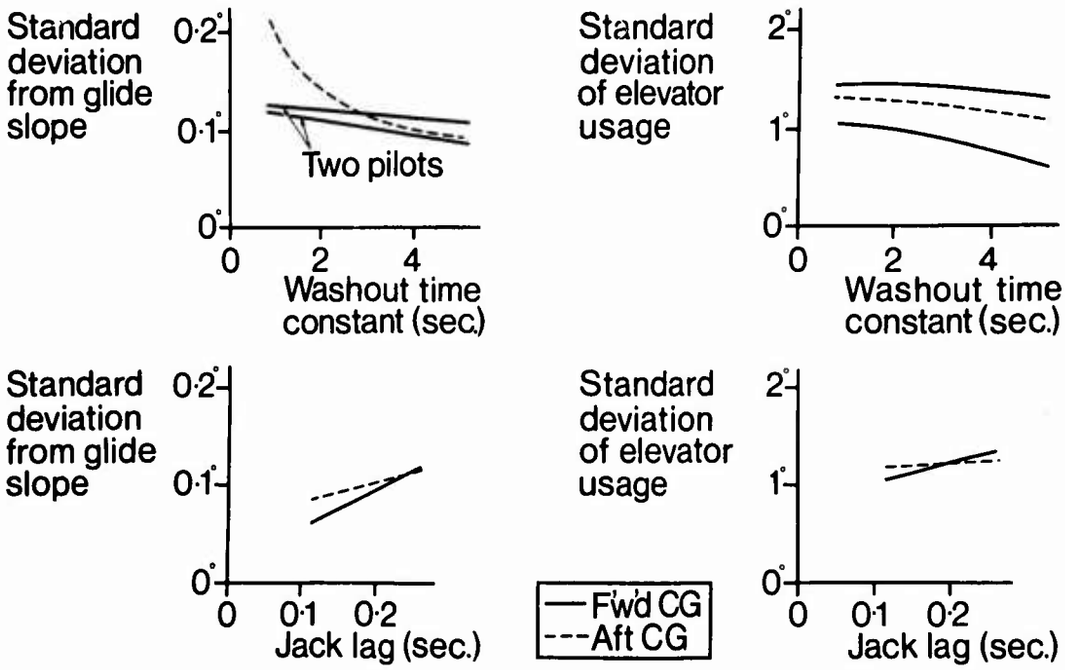

Fig. 9

LIFT CURVES FOR A REPRESENTATIVE STOL AIRCRAFT

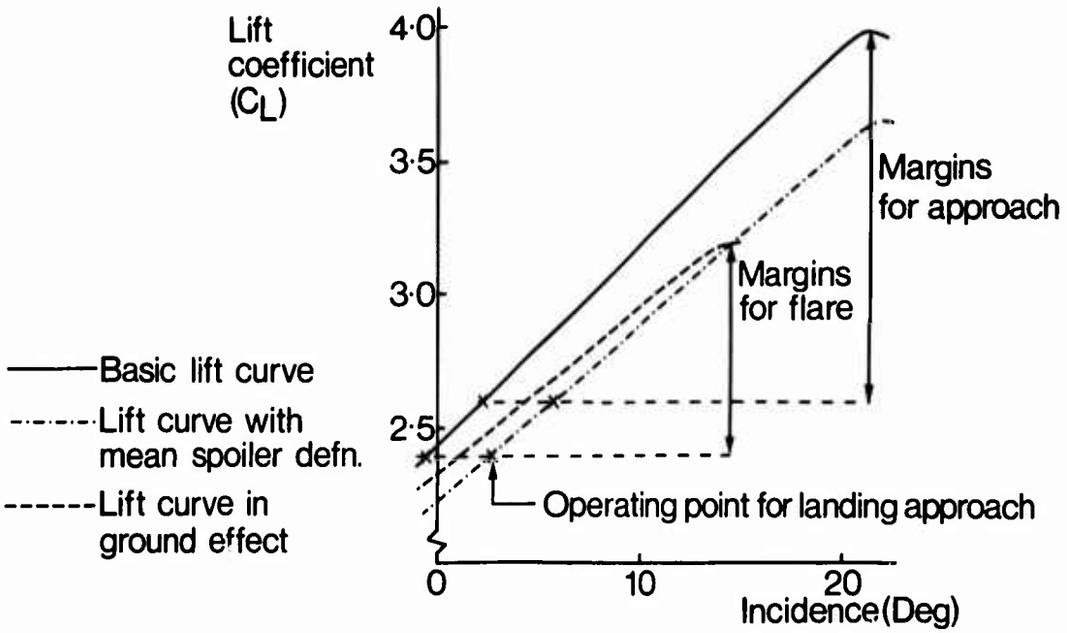

Fig 10

EXAMPLE OF USE OF SPOILERS FOR STOL FLARE

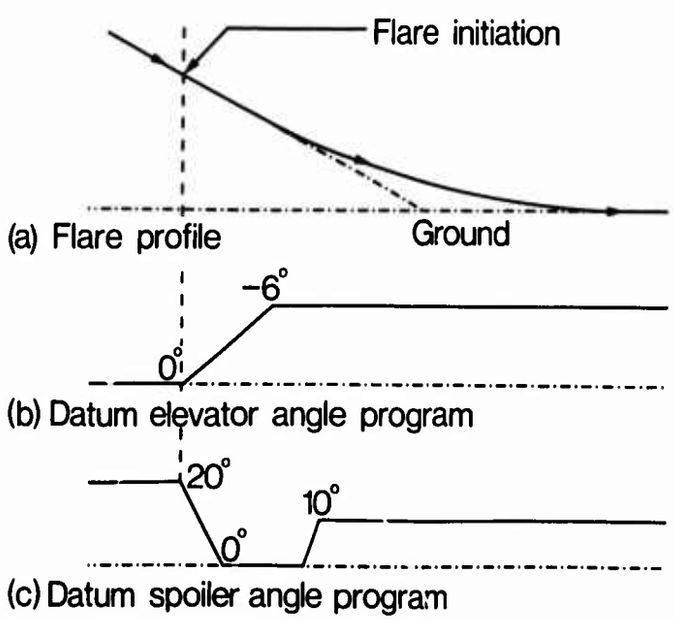

INVESTIGATIONS ON DIRECT FORCE CONTROL FOR CCV AIRCRAFT DURING APPROACH AND LANDING

by

Dr. Wolfgang J. Kubbat
Head of Guidance and Control Department
Messerschmitt, Bölkow, Blohm GmbH
Ottobrunn bei München
Federal Republic of Germany

1. INTRODUCTION

In recent years a number of investigations into the application of CCV methods in the designing of new aircraft have been carried out.

The main reasons behind this work can be defined as follows:

a. it has been shown that modern aircraft without feed-back control systems, on the whole, no longer serve their purpose, and that

b. in more complex aircraft designs, the control system is an important safety factor, and

c. it was also proved that

better performance could be achieved

weight reduced, and

life expectancy prolonged

by making use of the possibilities offered by the implementation of control techniques during the design phase.

The main activities involved in the CCV work are divided up as follows:

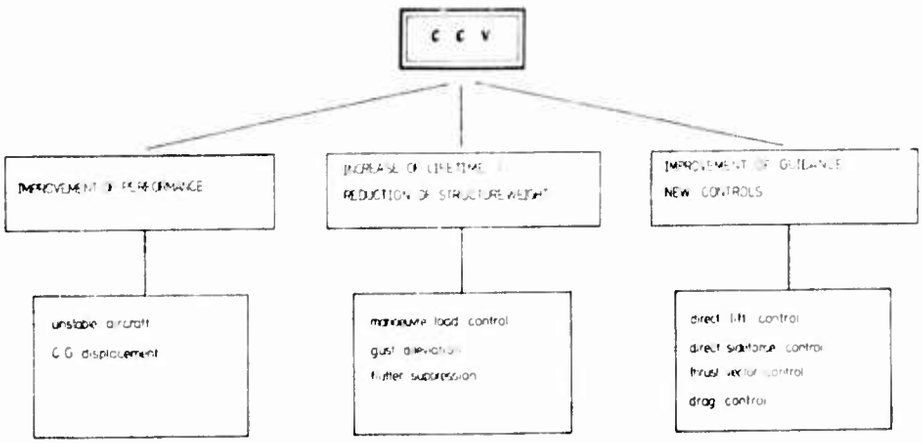

Fig. 1

2. DIRECT FORCE CONTROL

The "conventional" aircraft is controlled mainly by moments. In most cases, continuous use is no longer made of the thrust control.

For certain mission phases, especially during

weapon delivery and

landing

it would be advantageous to control the flight path without attitude changes. This can be achieved by using DFC.

Furthermore, under certain conditions, it is possible to increase the forces and moments which could still be introduced to the aircraft and thus shorten the response time of the aircraft.

In addition, there are further applications of DFC which have effect locally. The following gives a general picture:

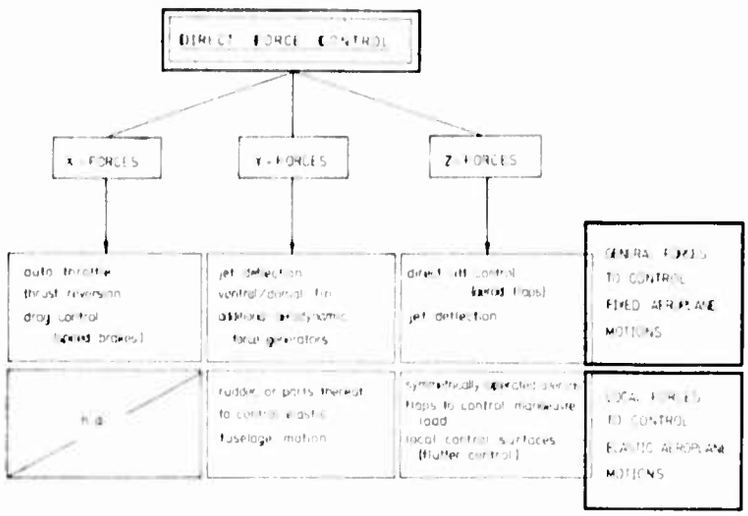

Fig. 2

The new control possibilities have, in fact, no exclusive effect in any one direction. For instance, there is normally an inseparable connexion between additional lift and additional drag, etc.

The previous figure shows, additionally, that certain controls can be used for various purposes. The ailerons, for example, can be operated for the control of the rigid aircraft motion, as well as for the control of the elastic wing motions (Manoeuvre Load Control). The figure demonstrates at least, that DFC is not an end in itself, but a means of following the basic CCV idea.

3. D F C DURING APPROACH AND LANDING

3.1. Definition of Objective

The previous comments have shown that a number of new possibilities exist. On the other hand, the introduction of new controls into the aircraft often necessitates a considerable amount of effort, and eventually, in this connexion, the safety question has to be mentioned.

It is the objective of this paper to make certain assertions on DFC in CCV aircraft, especially in connexion with the landing. From this the following points arise:

- The influence of the new controls on the natural stability
- The influence of DFC on the controllability of the aircraft
- The integration of DFC with the control system in CCV designs
- The behaviour of CCV aircraft with DFC during approach and landing
- The relationship of the results presented to the basic CCV idea.

3.2. Influence of DFC on the Stability of the Uncontrolled Aircraft

Essential feature of the CCV design is the need for a control system to form an indispensable component of the design, thus accepting the unstable behaviour of the free, uncontrolled aircraft. The question of stability in the free aircraft is nevertheless of importance, as it must be regarded in connexion with the question of safety. Depending on the behaviour of the uncontrolled aircraft, measures for the avoidance of unstable behaviour, in the case of the failure of the control system, must be undertaken. (Redundancy measures.)

To get a systematic answer the state variable form of the equation of motion of the aircraft was used.

The general form

$$\dot{x} = Fx + Gu$$

contains, in x, the variables describing the motions, and, in u, the controls.

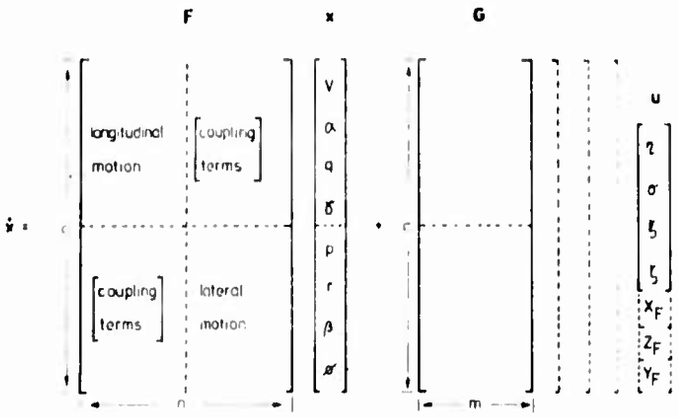

Fig. 3

The introduction of new controls obviously has an effect on the dimension and adds elements to the control matrix G.

Under certain circumstances this has, additionally, a considerable influence on the elements of the system matrix F.

The modification of the elements, and the alteration of the eigenvalues connected with it, lead to an undesirable change in the behaviour of the aircraft.

It is impossible to give a detailed derivation within the available framework, and on hand of certain examples it will be indicated that, in any case, it is necessary to calculate stability and controllability in their dependence on the new controls and the necessary configurative measures.

MEASURE	INFLUENCE ON NATURAL STABILITY
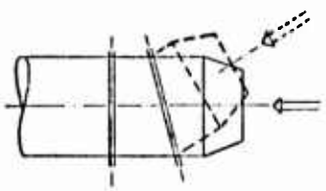 Thrust Vector Control	negligible
 Speed Brakes	positive, because $\frac{C_L}{C_D}$ -decrease increases phugoid-damping
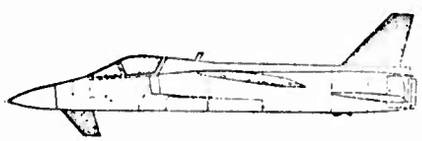 DSFC by means of Ventral/Dorsal Fins	negative, because of $C_{n\beta}$ -alteration until unstable

Fig. 4

Finally, it should be noted, that a possible de-stabilisation of the aircraft is not a serious problem, as it can be re-stabilised by means of control techniques; on the contrary, one of the main features of CCV design is to accept instability, in order to decrease weight and increase performance.

3.3. Influence of DFC on the Controllability of Aircraft

The introduction of new controls with regard to controllability can have several aspects:

- the achievement of complete controllability
- the increase in the degree of freedom of controllability
- the introduction of higher forces and moments for shortening the response time
- technical aspects, such as more favourable distribution of the forces to be introduced.

Further, a brief remark on system theory.

3.3.1. Controllability

is apparent if the matrix

$$\left[G,\ FG,\ F^2G,\ F^3G\ \ldots\ F^{n-1}G\right]$$

has the necessary rank n, where n is the dimension of the quadratic matrix F.

The condition for controllability, regarding the longitudinal motion of the aircraft, is generally not accomplished, if the aircraft control makes use only of the taileron. The joint use of the taileron and an x-force (i.e. thrust control or drag control) generally fulfills the condition.

In so far as controllability is already present (which is generally the case) the additional controls have two aspects, one mathematical and one technical.

An existing system may be increased with the addition of a new control.

If the rank of G were not to increase, from the point of view of the systems theory, then nothing has been gained. This is the case, for example, if thrust control is existent and an additional drag control is introduced. This example, however, also shows that a theoretical consideration has to be completed by technical considerations, as during landing a drag control would be more favourable, since it avoids fast changes in thrust. On the other hand, use is not normally made of drag control whilst cruising or manoeuvring at high speed.

If the rank of G has increased, there is also a theoretical gain, as the number of independently controllable variables increases also.

With the increase in the number of controls the energy appliable could be increased, thus shortening the response time.

3.4. Integration of DFC in CCV Aircraft Control Systems

As long as the aircraft is naturally stable, it may be justifiably asked, how these new controls are to be integrated into the pilot's control system. This is, however, not a point under discussion, as it has been assumed that CCV aircraft are not usually controllable manually. The only possibility considered, therefore, is to include the new controls in an automatic control system.

For safety reasons this would be a redundant (fly by wire) system, but this also is not a matter under discussion in this paper.

Since the method used is of great importance, a short summary follows.

We begin with the linearised equation of motion in state variable form

$$\dot{x} = Fx + Gu \qquad (1)$$

All following results have been achieved by the use of digital control. Therefore the subsequent statements have used the discrete form.

As is well known, for a constant sampling period T, in which the controls u are not altered, the results are:

$$x_{k+1} = Ax_k + Bu_k \qquad (2)$$

with

$$A = e^{FT} \qquad \text{(transition matrix)} \quad (3)$$

$$B = \int_0^T e^{F\tau}\, G\, d\tau \qquad \text{(control matrix)} \quad (4)$$

The given task

a. to stabilise the aircraft, and

b. to solve the guidance problem

can be solved by the introduction of the digital controller K.

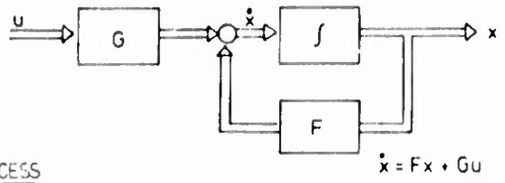

CONTINUOUS PROCESS

$\dot{x} = Fx + Gu$

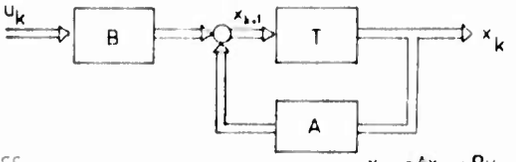

DISCRETE PROCESS

$x_{k+1} = Ax_k + Bu_k$

$t_{k+1} = t_k + T$

$A = e^{FT}$

$B = \int_0^T e^{F\tau} G d\tau$

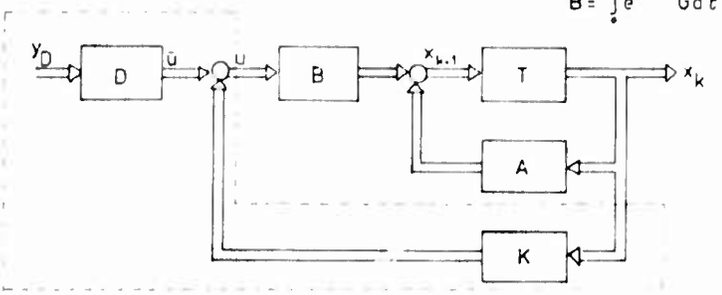

CONTROLLED DISCRETE PROCESS

$x_{k+1} = (A + BK)x_k + BDy_D$

Fig. 5

Here are two points of control theory (proof of which is not supplied here):

- if the complete state vector x is fed back, use is being made of the most complete information about the state of the flight. Every other combination of measurements is merely able to describe this state in a different form, but certainly not in a better one,
- only if each variable has influence on each control output, through the controller, can the best possible results be expected.

The controller K, introduced in the previous figure, is the result of a process of optimisation, the main steps being:

A) DISCRETE SYSTEM EQUATION

$$x_{k+1} = Ax_k + Bu_k$$

B) OPTIMISATION CRITERIA FOR THE CONTROLLED SYSTEM

$$I = \sum_{k=1}^{\infty} \left[(x - x_D)' Q (x - x_D) e^{2\alpha t_k} + \lambda (u - \bar{u})'_{k-1} H (u - \bar{u})_{k-1} e^{2\alpha t_{k-1}} \right]$$

$\bar{u}$ = control outputs for the demanded state $x = x_D$

Fig. 6

C) RESULT controler K

new system equation

$$x_{k+1} = (A + BK)x_k + BD\,y_D$$

independant controllable variables y where $y_k = Cx_k$

conditions rank(C) = rank(B), $\left[C(I-A)^{-1}B\right]^{-1}$ exists

$$D = \left[C(I-A-BK)^{-1}B\right]^{-1}$$

D) MINIMUM STABILITY IN THE Z-DOMAIN: ALL EIGENVALUES

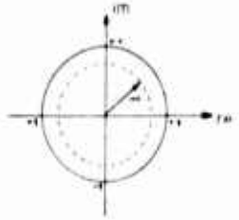

WITHIN A CIRCLE OF $e^{-\alpha T}$

T = sampling time

α = weighting factor (positiv)

Fig. 6 (contd.)

The purpose of the short summary showing the definition of the controller K is to clarify the following:

a. **as long as stability problems alone were apparent, and the condition of controllability achieved, the described method of optimal control with exponential time weighting would force stability without the aid of additional controls,**

b. **the obvious advantage of the new controls lies in the fact, that the number of variables which can be controlled increases.**

In addition, the following fact is also established:

if the aim is to achieve an optimal result, it is not possible to discriminate between stabilisation and guidance.

Furthermore, such a result could only be achieved with an integrated, multi-variable control system to take over the former tasks of stabilisation and autopilot.

3.5. Behaviour of CCV Aircraft with different DFC Possibilities during Approach

3.5.1. Aircraft Simulations

All the following results have been achieved using digital simulations. The basic aircraft was a fighter type, CCV designed a/c (see page 4).

Different configuration modifications were used for the DFC's shown in the following.

All results are shown for flight in turbulent air, since, as described in para 3.4., it is not difficult to achieve ideal behaviour in clear air. The turbulence model used was:

$$\Phi(\omega) = \left(\frac{L}{V}\right)\frac{2\sigma^2}{\pi}\,\frac{1}{1+\left(\frac{L}{V}\right)^2\omega^2}$$

with different scale lengths L and standard deviation σ for all three directions.

3.5.2. Direct x-Force Control

The following is a comparison between different x-force controls. The reason for this is to demonstrate, that almost the same good results can be achieved with either a speed brake control with no lag, or a thrust control with a time lag of second order with the dominant time constant T_1 = 0.3 sec.

The optimal control law is purely proportional; no integration was necessary.

Controls:	Taileron η Speed brakes ζ_{BK} } alternatives Thrust σ
Independent controllable variable:	2
Chosen:	Velocity and glide path deviation
Main result:	For this aircraft configuration almost the same result was achieved. There is no significant difference in the state variables.

Main differences: The aircraft configuration with thrust control shows a significant thrust change. In most cases this may be undesired.

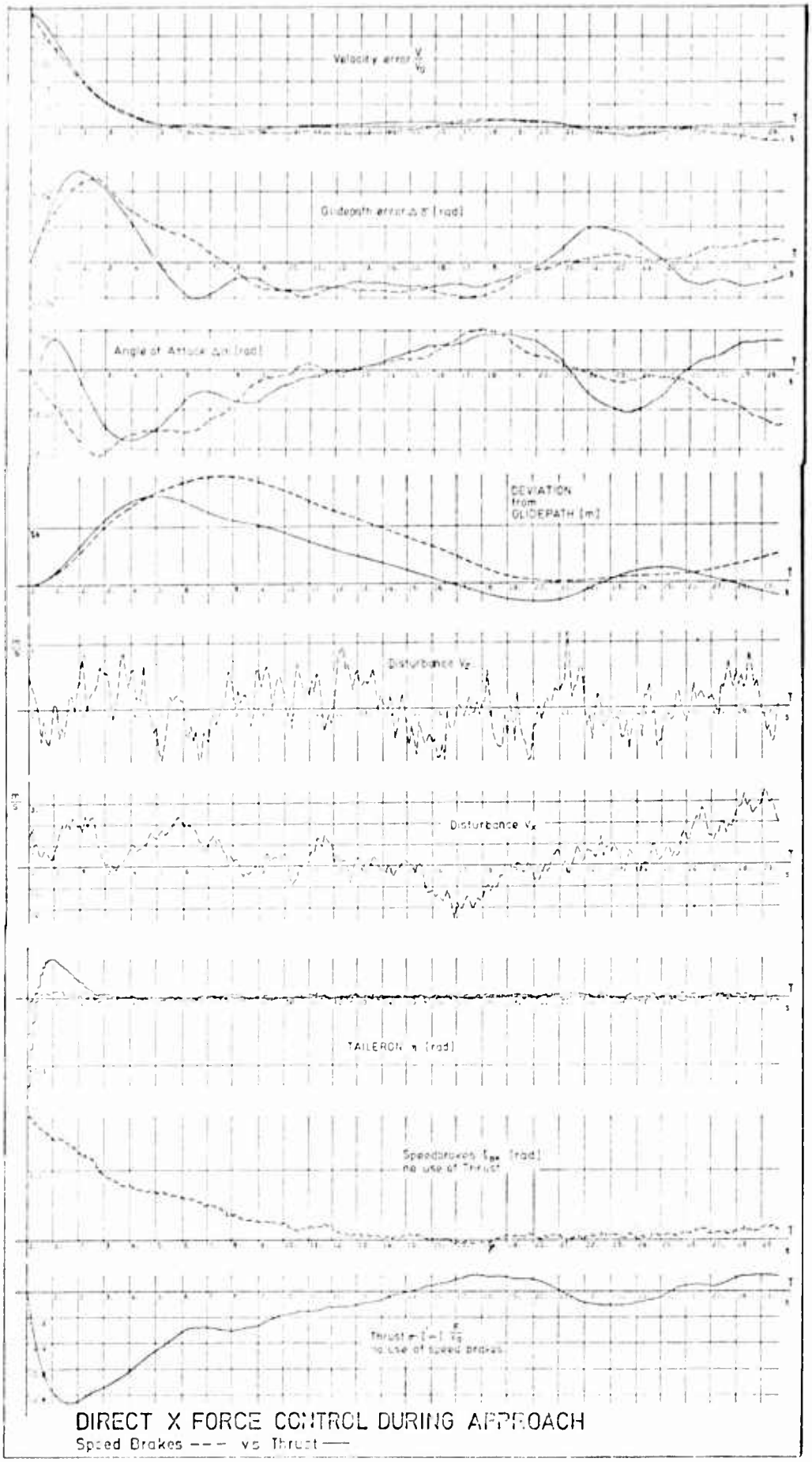

Fig. 7

3.5.3. Direct Lift Control

The next sequence of pictures presents results for the aircraft mentioned with and without DLC.

The glide path capture and hold is shown. These simulations were carried out with gusts, as in the previous example, 3.5.2. In this case, two possibilities exist for making use of the additional control, DLC: either to maintain the pitch attitude, or to improve the time behaviour. The latter was chosen.

Controls:	Taileron η } without Throttle σ } without Flaps η_k	} with DLC
Independent controllable variables:	2 without 3 with	} DLC
Chosen:	Velocity Glide path deviation } without Minimisation of time response	} with DLC
Main results:	The following time histories show improvements in the aircraft behaviour using DLC. But with regard to the magnitude of deviation in the state variables, it seems that for this specific aircraft during the approach DLC is not absolutely necessary.	
Main difference:	The approach is not the most favourable operation for demonstrating the superiority of DLC equipped aircraft. Another example, comparing DLC with conventional control during flare out will show remarkable improvements. DLC, in fact, can also be used to reduce attitude changes. This may be considered for different aircraft (passenger or larger aircraft) or for different missions (air refueling or weapon delivery).	

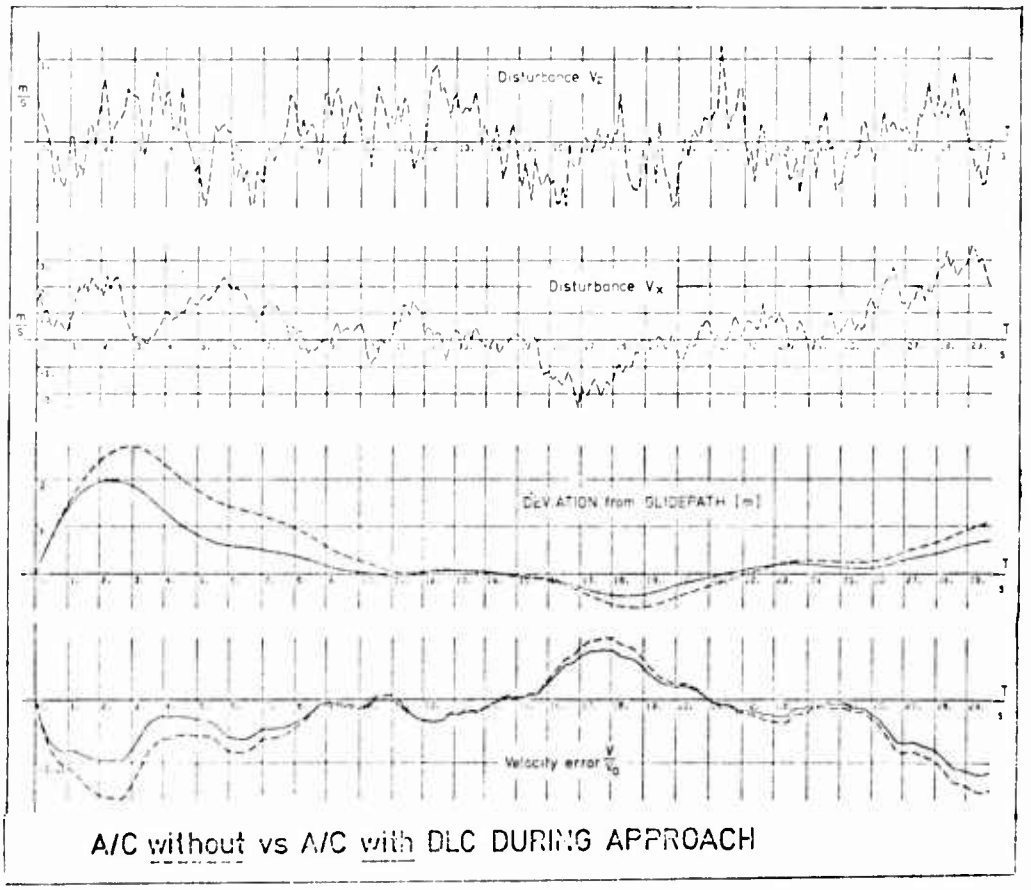

Fig. 8

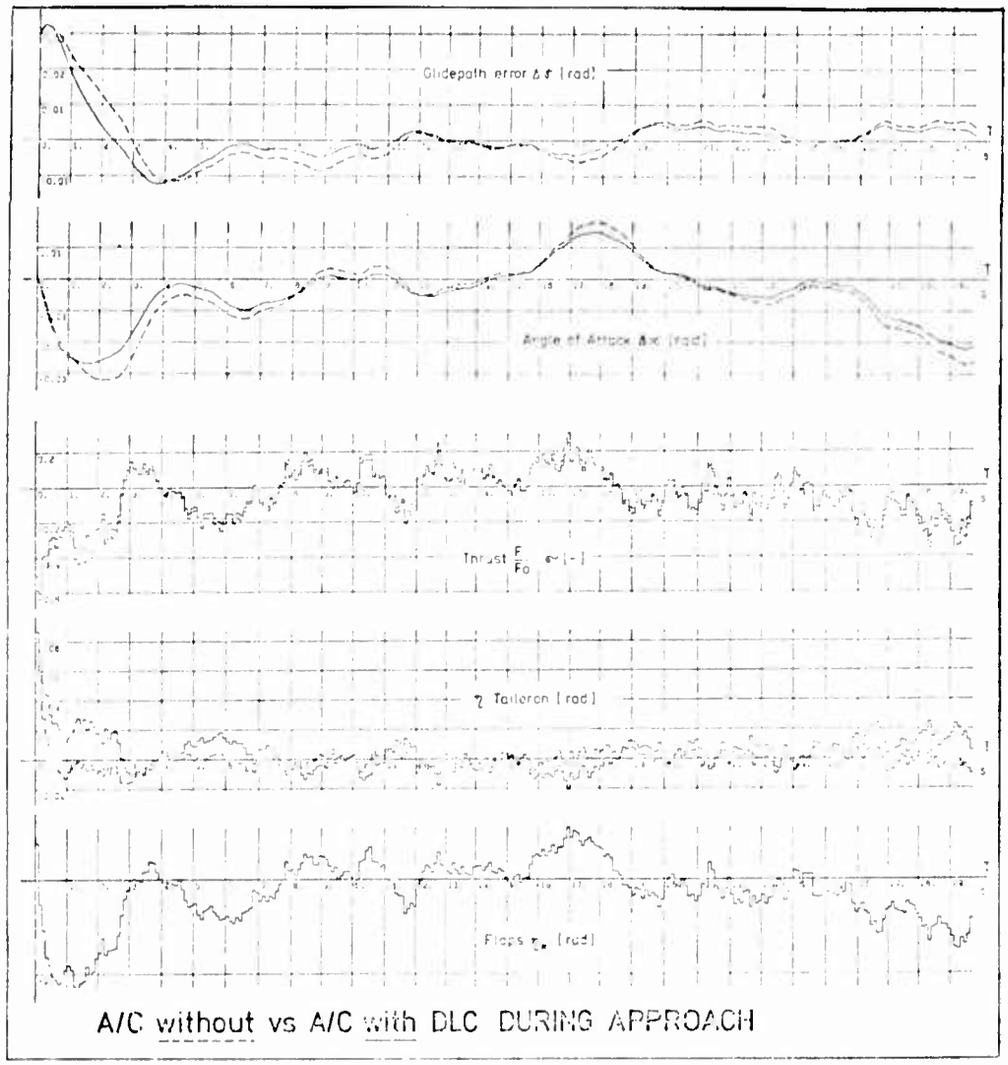

Fig. 8 (contd.)

3.5.4. Direct Side Force Control

Following is a comparison between an aircraft with DSFC and one without, by means of a ventral / dorsal fin combination. (For the configuration see page 4.)

It is shown, how the aircraft captures and maintains the localiser during turbulence.

Controls:	Rudder ζ	without
	Aileron ξ	without
	Moving Tail $\Delta\eta$	without
	Dorsal Fin	with DSFC
Independent controllable variables:	2 without	DSFC
	3 with	DSFC
Remark:	In this case one control can be presented as a linear combination of the others. Therefore, the number of independent controllable variables is not equal to the number of controls.	
Main result:	The results show a small improvement in the time history of the localiser deviation. They, additionally, demonstrate that in both cases the localiser can be maintained in a very good manner. The small effect of the gust is a result of the rapid aircraft reaction.	
Main difference:	The aircraft with DSFC compensates the disturbances almost by using the controls and maintains the roll attitude within small limits. The aircraft configuration without DSFC, therefore, shows a much higher activity in bank.	

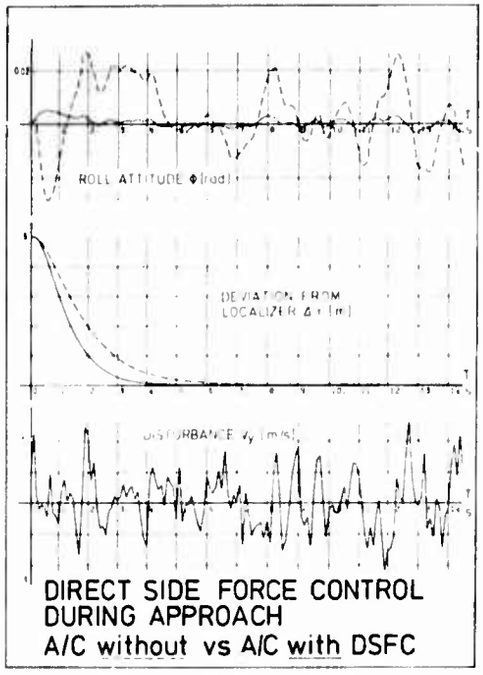

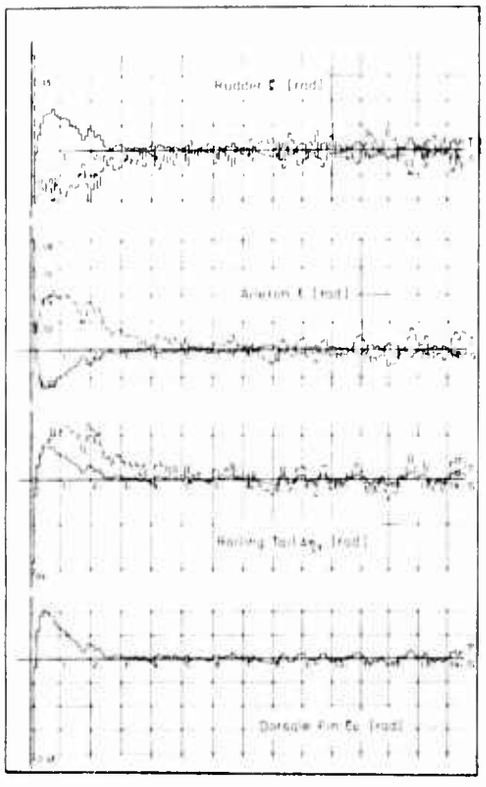

Fig. 9

3.6. Relevance of the Results to the Basic CCV Idea

By means of a CCV designed aircraft, three different DFC possibilities were shown together with simulation results of the flight of the aircraft on a glide path in turbulent air.

Even though the results with DFC show improvements, when compared with aircraft without DFC, their relevance to the basic CCV idea, i.e to save weight or increase life expectancy, has not yet been conclusively demonstrated.

3.6.1. D X F C

From a point of view of the control theory, it is essentially necessary to have an x force control, since the aircraft is not fully controllable without it.

The comparison between thrust control and speed brakes indicates a prolonged life expectancy for the engine because of the remarkable decrease in thrust changes.

In general, economic use can only be made of continuous speed brake control during the landing, and therefore its application instead of thrust control is limited.

3.6.2. D S F C

The following picture for three modifications on a basic configuration shows more than any comment.

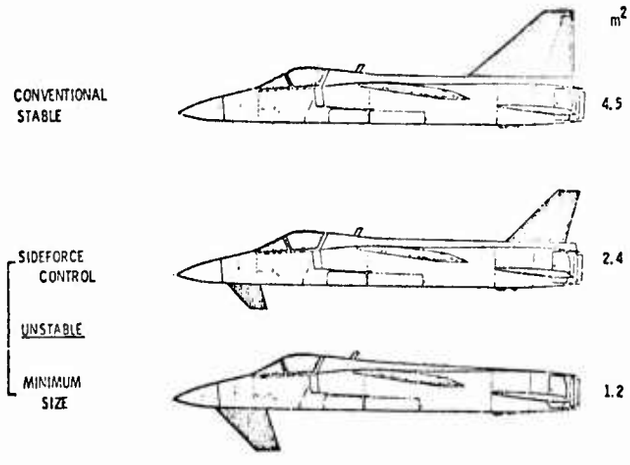

Fig. 10

The DSFC effort would be profitable only if the same time history results could be achieved as in the conventional design. The results in para 3.4.3. show an improvement and the necessary control surface decreases are remarkable.

3.6.3. D L C

Regarding the fact, that the entire landing takes only minutes, the results of para 3.5.3. would not be a reason to install DLC in a fighter type aircraft, because the improvement in maintaining the glide path, for instance, within one foot or within one inch is not of importance. However, the factor of 12 must be considered.

Nevertheless, there are good reasons for installing DLC anyway.

In conclusion some results of the flare with and without DLC in turbulent air follow.

They clearly demonstrate the superiority of the DLC configuration over the conventional one because of a significantly lower sink speed at the point of touch down for the DLC configuration.

However, these values are only comparable for these particular simulations and configuration These values are compared here:

V_z = -0.41 m/s without DLC

V_z = -0.137 m/s with DLC

Regarding the basic CCV idea, it ends with a difference in the impulses of $\times$ 2000 kgm/s which the landing gear has to absorb, and this could result in a prolonged lifetime.

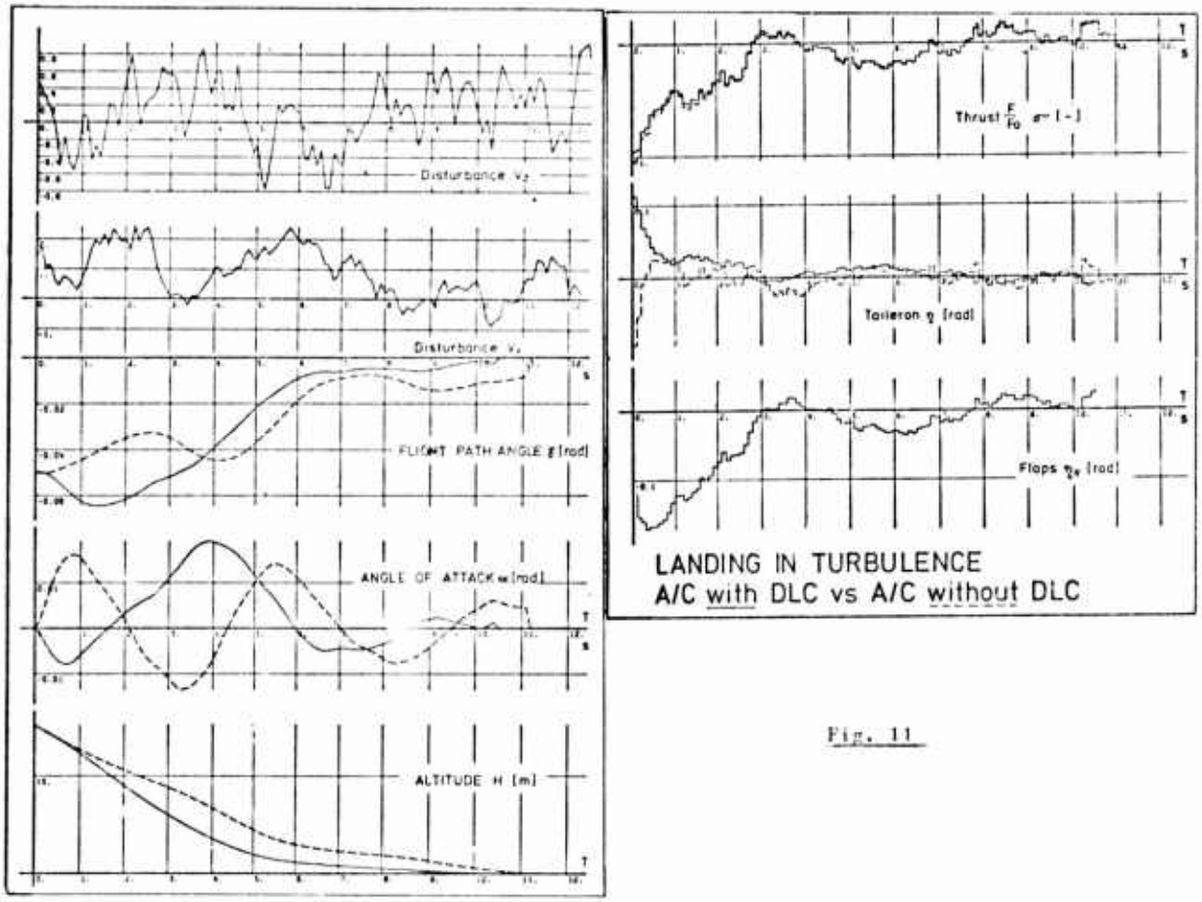

Fig. 11

3.6.4. Final Remark

As favourable as the results presented are, it must not be forgotten that they are achievable only with a total fly-by-wire system.

The solution to the safety problem will lead us to an answer which in certain modifications and variations will be named.

Redundancy.

The author's answer may be heard in Paris in October, 1974.

GUIDANCE PHILOSOPHY FOR MILITARY INSTRUMENT LANDING

by

George L. Yingling
Aviation Systems Consultant
399 Cheltenham Drive
Dayton, Ohio 45459, USA

SUMMARY

Instrument landing guidance philosophy for military aircraft is affected by the type of operation, the nature of the environment, the kind of aircraft involved and system dynamics considerations. Guidance philosophy and requirements are inseparable from control dynamics and tradeoffs exist between the two in arriving at an optimum solution for particular cases. In some countries, compatibility and interoperability with the civil system is considered important if not essential. The National Microwave Landing System program in the USA is of great interest internationally, and the USA Department of Defense is supporting, at present, the goal of a common civil/military system.

Representative unclassified operational requirements are reviewed as a lead to discussing the various factors having an impact on choice of guidance philosophy. The single most important consideration is the choice of technique to overcome landing guidance system multipath effects. The choice of technique must satisfy the many "system dynamic" considerations and present field test programs must provide clear and valid engineering data upon which to base a decision.

A system solution to a hypothetical but representative military situation is presented for discussion purposes. In addition a requirement for an all-airborne, self-contained landing system is discussed.

1. INTRODUCTION

It is fitting that in a meeting on "take-off and landing", concerned primarily with the flight mechanics aspects of the problem, guidance and control be treated. We are dealing with a problem where we must find "total system" solutions. In the past, aircraft have been designed with other than landing as a primary consideration. As we have progressed to lower minimums, the problems have become immensely more complex demanding a "total systems approach". The landing system involves a much broader scope of technological considerations than the "radio guidance" or "flight mechanics" functions alone. The system demands proper attention to aeronautics (in the broadest sense) electronics, human engineering, control theory, control-display, dynamic analysis, etc. However, we engineers have a long way to go to fully integrate the two most powerful aviation technologies, aeronautics and electronics, for the public use. Few aeronautical engineers really comprehend Air Traffic Control and Landing and its many electronic ramifications in the same depth they understand aircraft design or flight mechanics. Similarly, there are probably even fewer electronic engineers who really appreciate the impact of their electronic designs on the pilot, the aircraft and flight dynamics. The ultimate customer is the pilot/crew and the aircraft and it "all comes together" in the cockpit in controlling and maneuvering the aircraft precisely. Therefore, a pacing consideration in developing and implementing any landing system must be the flight physics/flight mechanics problem and associated airborne elements of the pilot, manual and automatic control and instrument displays. Fig. 1 is a "system" functional diagram.

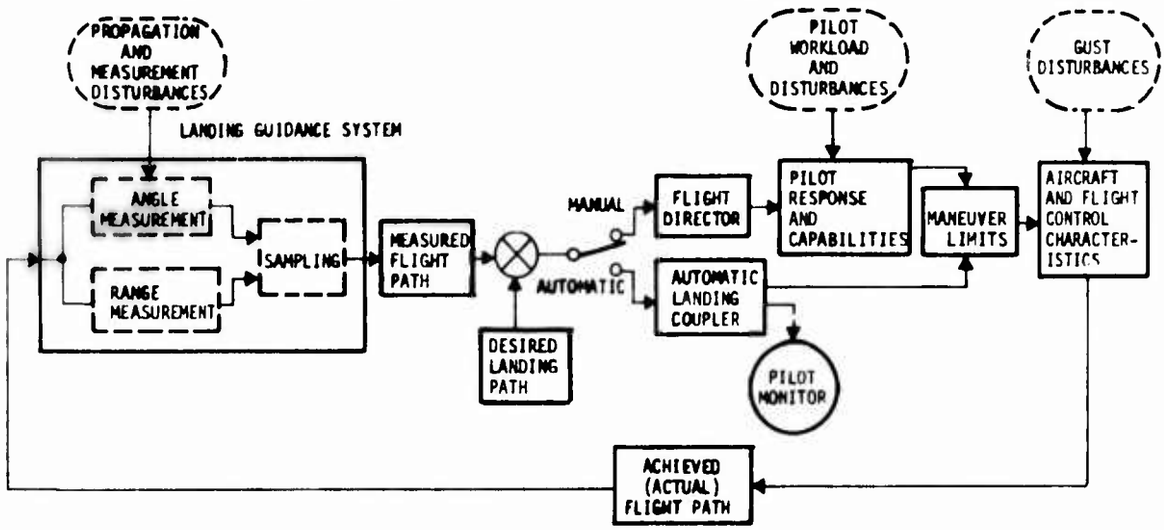

FIG. 1

Guidance philosophy for military instrument landing stems from several primary considerations: the type of operation, the nature of the environment and the kind of aircraft involved. Guidance philosophy and requirements are inseparable from control dynamics considerations and tradeoffs exist between the two in arriving at an optimum solution for particular cases. To meet satisfactorily all user needs

at all sites with a common ground guidance system may involve unacceptable compromises to airborne elements and operational capability. The National Microwave Landing System program (NMLS) has as its goal the establishment of a landing guidance concept (philosophy) and associated signal structure to assure satisfactory service to all potential users, hopefully without compromise. In the USA, the Department of Defense is supporting the goal of a common civil-military system and will continue to do so until there is good reason to depart from this objective. Interim military microwave landing systems are already in being and others may yet be forthcoming depending upon progress of the NMLS program and urgency of US military requirements. They are interim in the sense that they use established technology suitable for immediate relief of operational deficiencies, though not in their entirety, and will ultimately be supplanted by the more advanced NMLS. Other countries are pursuing similar activities in covering current deficiencies. The longer range approach to be taken by the various countries remains to be seen. Representative NMLS configurations are shown in Table 1-1.

Table 1-1. Capabilities Of Ground Station Configurations

SC-117 CONFIGURATION	B	D	F	I	G	I	K
	Straight Azimuth (Az) Basic DME	Straight Az Straight Elevation (El) Basic DME	Straight Az Select El Basic DME	Straight Az Straight El Basic DME	Straight Az Select El Precise DME	Curved Az Curved El Precise DME Missed Approach	Curved Az Curved El Precise DME Missed Approach
FACILITY PERFORMANCE*	CAT I	CAT I	CAT I	CAT II	CAT II	CAT III	CAT III
MINIMUM GUIDANCE ALTITUDE	150 Ft	150 Ft	150 Ft	50 Ft	50 Ft	Touchdown	Touchdown
COVERAGE							
ELEVATION	Not Applicable (NA)	8°	20°	8°	20°	20°	20°
AZIMUTH	±20°	±20°	±20°	±20°	±20°	±40°	±60°
MISSED APPROACH	.....	.....	.....	.....	.....	±40°	±40°
ACCURACY**							
ELEVATION (2σ)	NA	7 Ft	7 Ft	1.4 Ft	1.4 Ft	1.4 Ft	1.4 Ft
AZIMUTH (2σ)	26 Ft	26 Ft	26 Ft	11 Ft	11 Ft	9 Ft	9 Ft
RANGE (σ)	300 Ft	300 Ft	100 Ft	100 Ft	20 Ft	20 Ft	20 Ft
DATA RATE (Max)	2.5 Hertz (Hz)	5 Hz	5 Hz	5 Hz	5 Hz	10 Hz	10 Hz

*A CAT I facility provides guidance information from the limits of coverage to the point on the runway centerline extended on the glide path at a height of 200 feet or less above the horizontal plane containing the threshold.

A CAT II facility provides guidance information from the limits of coverage to the point on the runway centerline on the glide path at a height of 50 feet or less above the horizontal plane containing the threshold.

A CAT III facility provides guidance information from the limits of coverage to and along the surface of the runway.

2. MILITARY OPERATIONAL REQUIREMENTS

Let us review some of the military operational requirements and operational environments as published in unclassified documents. These are not all inclusive, internationally, but probably span most of the important features bearing on guidance philosophy. It should be understood that these requirements are provisional, subject to change and do not represent, yet, the official position of any of the military organizations treated.

2.1 USAF

2.1.1 GENERAL

The USAF is required to operate worldwide to accomplish its mission in support of the defense of the United States and free-world allies. The nature of the mission requires that USAF aircraft use not only organic US military air traffic control and navigation facilities but also those enroute and terminal facilities of the civilian aviation community in the USA, civil and military facilities of allies, and facilities that may be available from nonaligned nations.

While the USAF has traditionally depended upon Precision Approach Radar (PAR) to provide guidance during the approach and landing phase, there also is a need for the USAF to use the standard navigation and landing aids as defined by the International Civil Aeronautics Organization (ICAO). This interoperability is currently manifested in the additional implementation of ground and airborne ILS.

The USAF will continue to implement th approach and landing aids that are interoperable with standard national and international civilian a tion systems. It supported the work of the Radio Technical Commission for Aeronautics, Special Com ittee 117 (RTCA-SC-117) and actively supports the National Microwave Landing System Development program. Air Force requirements falling within the spectrum of those set forth by RTCA are outlined below along with unique USAF military requirements. Air Force requirements will be re-evaluated as cost/performance tradeoffs are identified during the NMLS development program.

2.1.2 GROUND SYSTEM REQUIREMENTS

A. General. The USAF will employ the ground portion of the Microwave Landing System at many locations for a wide range of missions. The USAF ground system requirements, along with examples of "typical" and "worst case" conditions, can be arranged in the following grouping:

1. Main Operating Bases (MOB): Main Operating Bases must support take-offs and landings by all types of fixed-wing, rotary-wing, and V/STOL aircraft. As a worst case, base configurations can include two parallel runways not less than 2500 feet apart supporting simultaneous IFR approaches. Large aircraft such as the C-5 will be present on runways, taxiways, and ramps. Helicopter operations will occur

on designated ramps, taxiways, and runways. Supplementary ground aids, lighting systems, and runway markings will be available. Runway acceptance rate should be the only traffic handling limitation. Runways will be from 4,000 to 12,000 feet long.

2. Forward Operating Bases (FOB): In their most austere form, Forward Operating Bases will be a Bare Base with minimum runway lighting and marking. Forward Operating Bases generally will not have parallel runways; however, they must support high recovery rates of tactical fighter and airlift aircraft. Runways will be from 4,000 to 12,000 feet long.

3. Combat Operating Base (COB):

a. Assault Landing Zones (ALZ). Terminal operations at an Assault Landing Zone may be conducted on a level field or clearing of sufficient size to permit landings by tactical airlift, forward air control, and rotary-wing aircraft. The area may be camouflaged and only primitive area markers or portable lights will be used to outline landing zones.

b. Extraction Zones (EZ). Terminal operations at an Extraction Zone consist of cargo aircraft executing flyovers at approximately six feet above ground level. The Extraction Zone may be nothing more than an open field or clearing with primitive area markers.

c. Drop Zones (DZ). Operations at a Drop Zone consist of cargo aircraft approaches at more than 200 feet above ground level in order to allow for parachute deployment. The terrain in the vicinity of a Drop Zone may be rough.

d. Helicopter Hover Points (HP). Terminal operations at a Helicopter Hover Point will be conducted at a designated point up to 100 feet above ground level. Due to helicopter operational requirements, flare-out and transition to hover will normally be conducted after descending below 100 feet Above Ground Level (AGL) under visual flight conditions.

B. Collocated Ground Navigation Aids: Complete area navigation coverage in the terminal area is required to provide the aircraft a positive position fix relative to the landing runway. However, it can be assumed that an appropriate fixed/transportable/airdroppable TACAN station can be collocated with the landing system equipment. Essentially all operational Air Force aircraft will be TACAN equipped.

C. Ground Landing System Characteristics: The following functional capabilities are required by various Air Force Microwave Landing System configurations:

1. Approach Zone Coverage:

a. Azimuth. Complete azimuth coverage in the terminal area is required (See II B). Precise position information from the Landing System should be available a minimum of $\pm 40^{0}$ on the final approach course; however, this requirement should not excessively compromise other characteristics of the system.

b. Elevation. The extent of the elevation coverage is dependent only on the glide slope limits of the aircraft to be served at specific bases of operation. For example, helicopter landing sites may use only high glide slope angles (5 to 15 degrees), aircraft with high approach speeds are capable of only low glide slope angles (2 to 5 degrees), and terminals serving a mix of CTOL, VTOL, and STOL aircraft will require the full range of elevation coverage. The modular nature of a Microwave Landing System should enable alternative elevation coverage units to be procured and utilized on a facility-need basis.

c. Range. The system must be capable of 20-nautical mile range with 30 miles preferred in the approach zone. The maximum range is required whenever size and weight permit; however, in tactical configurations a sacrifice in range may be acceptable to accommodate other system characteristics such as size, weight, or transportability. A range of ten nautical miles would be acceptable for airdroppable/tactical equipments.

2. Missed Approach and Departure Coverage: Missed approach and departure guidance away from the runway area is required for wake turbulence avoidance, noise abatement, terrain or obstacle clearance, hostile (ground fire) area avoidance, or parallel runway departures. The system should provide lateral position information $\pm 40^{0}$ from the runway centerline to a range of 5 NM. There must be a smooth transition between approach and missed approach and between takeoff and departure guidance.

3. Distance Measuring Equipment: It is anticipated that Air Force MLS ground stations will be collocated with a TACAN/DME ground station. The MLS will be required to provide more precise DME information in the approach and departure zones when it is required for curved/segmented approaches, multiple angle glide slopes, lower weather minimum approaches and landings (ICAO CAT II/III equivalent), hover point identification, and applications involving drop/extraction zones.

4. Weather Capability: Air Force MLS equipment should be capable of safely guiding combat aircraft anywhere within the approach zone through a standard rain cell model which is a cylinder of evenly distributed rain, five nautical miles in diameter, with a rainfall intensity of two inches per hour. Further definitions of the standard rain model is contained in Air Force Cambridge Research Laboratories Special Report No. 141, "The Detection Range of the AN/TPN-19 Radars in Heavy Rain (Baseline Scan Mode)," AFCRL-72-0368, 15 June 1972.

5. Anti-Jam Capability: In forward operating areas, Air Force MLS equipment should be designed to minimize the effect of intentional interference. Serious consideration must be given to providing a capability to detect the presence of interference in aircraft and at ground facilities.

6. Security: MLS equipment used at Forward or Combat Operating Bases should be designed to minimize the extent to which the system could furnish guidance or intelligence information to unauthorized users.

7. Mobility: There are no mobility requirements for ground systems used at Main Operating Bases. Systems for use at Forward Operating Bases must be air transportable by a C-130 or smaller aircraft. Systems serving tactical sites or drop zones are required to be airdroppable and to be capable of being moved short distances and set up by not more than two men without powered assistance. A precision approach capability equivalent to an ICAO CAT I should be available within 15 minutes.

8. Equipment Configurations: Elements (azimuth, elevation, DME) of tactical systems may be collocated. Landing systems for Main and Forward Operating Bases will employ split-site configurations to provide the higher accuracies required for lower weather minimums.

9. Reliability/Availability: To the maximum extent practical, Air Force MLS equipment used at Main and Forward Operating Bases must be redundant to assure uninterrupted service. Redundancy requirements will be relaxed in those ground systems intended for tactical use. Reliability must be the maximum available within the state-of-the-art and consistent with prudent cost considerations.

10. Integrity: The system must provide an output which automatically indicates a fault or out of tolerance condition to both the ground air traffic control facility and to user aircraft. External monitors may be used for ground units on main and forward operating bases; however, only internal monitoring should be considered for tactical units.

11. Data Link: RTCA SC-117 determined a number of functions which should be provided by a data link integral to the MLS. Data link functions should provide adequate data to allow Air Force aircraft to approach and land after experiencing a complete loss in other radio communications.

12. Flight Inspection: Except for initial commissioning of the facility, inflight calibrations and inspections of MLS ground stations should not be required. Tactical systems must be capable of providing service equivalent to ICAO CAT I without prior flight inspection and calibration.

Table 2-1 is a summary of Air Force MLS ground system requirements.

TABLE 2-1

SUMMARY OF AIR FORCE MLS GROUND SYSTEM REQUIREMENTS

FACILITY	NUMBER OF SYSTEMS	ICAO WEATHER CATEGORY	PARALLEL RUNWAYS	MISSED APPROACH DEPARTURE COVERAGE	MOBILITY	RANGE (NM)	NEAREST RTCA CONFIGURATION
MAIN OPERATING	12	IIIb	YES	YES	FIXED	20	I,K
BASE	110	II	YES	YES	FIXED	20	I*
FORWARD OPERATING BASE	40	II	NO	YES	TRANSPORT-ABLE	20	I*
COMBAT OPERATING BASE	40						
ASSULT LANDING ZONE		I	NO	NO	TRANSPORT-ABLE	10	E
DROP ZONE		I	NO	NO	AIRDROP	10	E
EXTRACT ZONE		I	NO	NO	AIRDROP	10	E
HOVER POINT		I	NO	NO	AIRDROP	5	E

* Less flare capability

2.1.3 AIRBORNE SYSTEMS REQUIREMENTS

A. Aircraft and Missions: For planning purposes, the Air Force inventory of aircraft in the 1980 time frame will consist of the following types: attack, bombers, cargo, fighters, trainers, and utility and miscellaneous.

B. Levels of MLS Avionics: Three modular categories of avionics equipment are provisionally required and reflected in Table 2.2.

AVIONICS CAPABILITY	ATTACK			BOMBERS		CARGO						FIGHTERS					TRAINERS				MISCELLANEOUS			
	A-7	A-10	A-37	B-1	B-52	C-5	C-9	C-130	KC-135	C-141	AMST	F-4	F-15	F-16A	F-111	LWF	T-37	T-38	T-39	T-43	UH-1	OV-10	HH-53	RPV
AUSTERE		Δ	Δ														Δ				Δ	Δ		
STANDARD	Δ			Δ	Δ		Δ	Δ	Δ		Δ	Δ	Δ		Δ	Δ		Δ	Δ	Δ			Δ	
ADVANCED						Δ				Δ				Δ										Δ

TABLE 2-2

1. Austere Avionics. Cost would be a primary consideration in this avionics configuration; however, the equipment must be capable of providing ICAO CAT I service. Cost considerations may dictate that range information be provided by the TACAN/DME system. The mission of aircraft in this category would primarily be conducted in VFR conditions. Some types of attack (A-10), trainers (T-37), and utility aircraft would use this category of equipment.

2. Standard Avionics. Capable of ICAO CAT II approaches in IFR conditions but not including an automatic landing capability. Classes of aircraft requiring avionics in this category would include some of the cargo aircraft (C-130), the heavy bombers (B-1 and B-52), tankers (KC-135), most fighters, and advance trainers (T-38).

3. Advanced Avionics. Capable of CAT IIIb approaches and landing. Aircraft requiring avionics in this category would include some of the cargo aircraft (C-5, C-141) and air defense interceptors.

C. Airborne System Capabilities:

1. Azimuth Guidance.

a. Selectable straight approach paths must be available to all USAF aircraft, thereby enabling the pilot to choose the optimum approach course.

b. Curved or segmented approach paths will be required on some aircraft to avoid no-fly zones for tactical or environmental reasons, such as wake turbulence, minimum time or fuel paths, noise abatement, adverse terrain or obstacle clearance, hostile area (ground fire), V/STOL optimized paths, and optimum approaches at terminals with parallel runways. However, not all aircraft types will be able to use this option because of their flight or maneuverability characteristics, or because of cost considerations.

c. Large transport aircraft will require decrab and rollout guidance to accomplish approaches and landings equivalent to ICAO CAT IIIb.

2. Elevation Guidance.

a. All USAF aircraft must have a minimum capability of a pilot selectable constant angle glide path that provides valid elevation guidance on the final approach course to a minimum height of 50 feet.

b. Aircraft with more sophisticated avionics capabilities will require multiple glide slope (segmented) angle approaches for terrain and noise abatement considerations.

c. Large transport aircraft will require automatic flare guidance to touchdown to accomplish approaches equivalent to ICAO CAT IIIb.

3. Integrity. The airborne system must provide a warning to the pilot in the event of receipt of inadequate, false, or ambiguous guidance information.

4. Integration. It is anticipated that guidance information from the MLS system will be displayed on new cockpit displays; however, the MLS must also integrate into inventory aircraft where no change of instrumentation is contemplated.

5. Continuity. The airborne equipment must permit execution of a complete approach, touchdown (if applicable) and initial phases of a missed approach without transition to other instrumentation.

6. Minimums. The pilot must be provided an automatic warning when the aircraft reaches the appropriate decision height for the class of ground facility and the airborne system.

2.1.4 ADDITIONAL CONSIDERATIONS

A. Cost of Ownership/Standardization. It is anticipated that the MLS will be universally adopted by the USAF and will replace all precision approach radars, Instrument Landing Systems (ILS), and the tactical TALAR system. Since implementation of MLS will affect virtually all USAF aircraft and bases, the procurement and supporting costs for MLS will be substantial. The USAF intends to reduce the cost of ownership by using avionics equipment developed for the competitive civil market. To the maximum extent

practical, the Air Force will procure equipment based upon the following standards and specifications in effect at the time of procurement:

FAA Technical Standard Orders (TSO)
RTCA Minimum Performance Standards
ARINC Characteristics

Ground systems designated for Main Operating Bases are expected to be identical with FAA systems used on major civil fields. Transportable and tactical systems are expected to be common to those of other Services.

B. Frequency Reservations. Military operations frequently dictate deployments on short notice. To permit the flexibility of operations required by the USAF, a portion of the frequency spectrum needs to be set aside for national use, similar to the arrangement presently in effect in the TACAN/DME band. This requirement would not be expected to exceed ten percent (20 channels) of the frequency spectrum presently identified. It is expected that the frequencies for landing systems at fixed bases would come from the frequencies allocated to the FAA for the National Airspace System.

C. Initial Operation Date. USAF implementation of the Microwave Landing System will commence after acceptance of the system as a standard national and international (ICAO) landing system. Target date for initial entry into the Air Force inventory is 1980; however, a significant MLS operational capability is not expected prior to 1985.

2.2 U. S. ARMY REQUIREMENTS

2.2.1 GENERAL

The configuration "G" system most nearly meets the Army landing system accuracy requirements. The following information supplements the functional requirements contained in the RTCA SC-117 documents. The Army requires a landing system which consists of a ground station capable of either split or collocated siting, and a compatible airborne set. The Army is required to operate aircraft from unimproved tactical landing areas and the system must provide reliable, positive guidance in this environment. Army landing areas are characterized by the presence of the following factors not normally present in civil aircraft operations: uneven, unprepared landing surface; proximity to obstacles such as trees, buildings, revetments and other structures, communications and other types of antennas; high velocity rotor wash and dust blown by rotor wash; and numbers of moving aircraft in close proximity to the radiating elements.

2.2.2 GROUND STATION REQUIREMENTS

A. Operational Requirements:

1. The azimuth and elevation guidance elements shall each have as a minimum, coverage sectors of plus and minus 30 degrees in azimuth and one to 20 degrees in elevation. Azimuth and elevation guidance shall be usable to a height of 50 feet along the inbound flight path.

2. The minimum operating range shall be 10 nautical miles in 50 mm/hour rainfall rate. While this requirement is recognized as being technically feasible, it should not prejudice the selection of a K_u frequency band which may offer significant advantages to the Army in terms of size, weight, and accuracy. Tradeoff determinations must be performed to identify the best overall system to fulfill Army requirements.

3. The azimuth and elevation guidance elements shall be designed for minimum setup time. Design goal for setup time is one hour using two men, clothed in apparel for worst climatic conditions. The azimuth and elevation elements shall be capable of being operated on terrain with slopes of as great as 10 degrees (any direction) with respect to the horizontal, and allow rapid establishment of the reference azimuth path to plus or minus 0.5 degrees. The requirement for boresighting the two guidance elements with respect to each other shall be reduced to a minimum and shall not require sophisticated survey equipment or skills.

4. DME coverage is required in the azimuth and elevation sectors. The operating range shall be the same as for the angle guidance. The DME will demonstrate an accuracy of plus or minus twenty feet.

B. Physical Characteristics:

1. The set shall be capable of split or collocated sighting of the azimuth and elevation guidance elements. The DME shall be sited optionally near either guidance element.

2. The size, weight and primary power requirements of all the ground station elements shall be minimized. The weight design goal for the total ground site (both angle guidance elements, DME elements, battery power for two to four hours' operation, transit case and setup equipment) is 120 pounds.

2.2.3 AIRBORNE SET

A. Operational Requirements:

1. Operationally compatible with civil MLS systems.

2. Selectable glide path angles in one-half degree increments over the range of 2.5 to 12 degrees.

3. Selectable azimuth guidance in one degree increments over the azimuth coverage area.

4. Range read-out to at least 12 nautical miles.

5. A warning that the aircraft had reached decision height for the approach. A light with the decision height selected and preset by the pilot is acceptable.

6. Warning to indicate the aircraft is below the safe minimum elevation angle for a centerline approach to the facility.

7. Course softening to provide acceptable indicator sensitivities as the azimuth and elevation courses converge near the ground facility.

8. Airborne antenna coverage volume shall be a minimum of plus 12 degrees and minus 25 degrees in elevation, and plus and minus 120 degrees in azimuth, relative to the nose of the aircraft. Omni-directional antennas are desired.

B. Physical Characteristics.

1. The airborne set shall be designed for minimum weight and size. The weight goal for the complete set (excluding aircraft displays) is 20 pounds.

2. Consideration should be given to packaging the airborne set into two parts, such that DME could be an optional item for use as required, instead of being installed in all aircraft.

3. The set shall operate from the aircraft central electrical system and power requirements shall be minimized.

2.3 COMMENT

The author takes exception to the Air Force requirement for RTCA configuration "I" without flare guidance for CAT II operation at Main and Forward Operating Bases. CAT II provides for see-to-land from a decision height of 100 feet. Definition of see-to-land in terms of minimum altitude beyond which a visual landing should not be attempted has not been adequately determined, particularly for a single-place aircraft. The author feels that, for safe operation to CAT II minimums, an automatic touchdown capability (with flare) should be provided not only in single-place military jet aircraft but in bomber/cargo/transport aircraft as well.

3. AIRCRAFT AND AIRBORNE EQUIPMENT DESIGN AND OPERATING INFLUENCES

Because of factors related to piloting techniques, passenger comfort, safety and military missions, normal operation of an aircraft is restrained to some performance region which is more restrictive than the basic airplane's performance envelope. Lift, drag, thrust and weight relationships clearly bound the speed and flight path angle capabilities of the aircraft. Control surface effectiveness imposes maneuvering limitations and in addition, attitude changes are not usually effected by full control surface deflections. Speeds close to stall, on the one hand, or near maximum permissible on the other, are avoided.

Most limitations on an aircraft maneuvering envelope could be classified as piloting technique or control considerations. Curved or segmented path requirements may call for deviation from current piloting techniques resulting in retraining and will most likely be met with resistance by the piloting community. Good piloting techniques have generally dictated a maximum bank angle of 30 degrees. The increasing difficulty in controlling the aircraft pitch axis at increasing bank angles because of misalignment between the aircraft lift vector and its weight vector, is a considerable influence, particularly under instrument flight conditions. Roll rates are typically constrained by piloting considerations. An aircraft's position in space is not changed appreciably by using roll rates at the limit of the aircraft's maneuvering capability. High roll rates tend to compound control and monitoring difficulties. We are, of course, speaking of near navigation, approach and landing circumstances, not military combat situations.

Specific aircraft characteristics are a concern in the design of autopilots and instrument displays and the control laws that drive them. In a general sense, computations optimized to drive a display for a given aircraft may not be expected to provide the same overall performance if used with a different aircraft. The problem becomes more pronounced as we design tighter tracking control laws (higher gains) for flying to lower minimums. We speak of inner and outer loop relationships, meaning a relationship between control and guidance functions. There are certain merits in being able to isolate guidance computations from control computations. Here, we are speaking of the guidance function as one of making use of position and velocity data to describe the progress of an aircraft along some desired path in space and to describe changes required to track that path. The control function, on the other hand pertains to basic aircraft stabilization and to the manipulation of the aircraft about and along its principal axes to satisfy the guidance requirements. The role of control is to establish a reasonably stable platform that can be expected to respond in a given manner to guidance commands. Besides dynamic characteristics peculiar to individual aircraft, we have environmental disturbances including wind, fog and rain. We also have noise and bias errors that occur in the basic signal transmitting and receiving process and other errors caused by propagation effects and radio frequency interference.

If we could design our inner attitude loops, either for flight director or autopilot, with very high bandwidths (fast response), the closed loop attitude response would not reflect the aircraft dynamics at all. The guidance loop could then be optimized for the tracking task and would be free from particular aircraft characteristics. However, loop tightness is normally constrained by vehicle inertias, control effectivity and servo response. Servo response is limited because high servo response

can mean the servo is capable of exciting bending modes. When used in combination with tight attitude loops, considerable power is consumed. All these quantities reflect on the weight and eventual total cost effectiveness of the vehicle.

Another consideration is that such high inner loop bandwidth would imply the transfer of high frequency display information by the pilot to his controls (in flight director operation) or the presence of very high control activity by the autopilot servos which in turn would be reflected to the control column (parallel servos). Since the pilot prefers to see the controls (which are repeating the autopilot-command, parallel-servo motion) move in a manner somewhat similar to the control actions he uses as he performs a given maneuver, he will not accept the rapid control actions, including a broader noise spectrum of a high bandwidth autopilot. In the case of flight director/pilot control, the pilot has definite bandwidth limitations. Any requirement for a pilot to close more than one attitude loop at a time at frequencies greater than 1 to 2 rad/sec can be expected to result in pilot ratings of too high workload. Stabilization systems used as a partner (limited-amplitude series servos) can help the pilot with these tasks.

The problems of inner and outer loop design, dynamics of airframes and effects of disturbances all become involved in choice of guidance philosophy. Feedback control can enclose all the unknowns in airframe dynamics and disturbances in an error correcting system that does not have to know all about these unknowns. It may be much more inefficient than a system designed with more knowledge of the unknowns. However, we have many aircraft already equipped with autopilots and flight director systems interfaced with ILS. If we expect to take advantage of non-straight-in paths which are made possible by certain configurations of the microwave landing system now under development, a retrofit program will be required. Hopefully, this can take place with only a change in the guidance data processing and computation.

As evident from an examination of Fig. 1, the flight control system engineer/designer has had to assume the "total system engineering" approach in integrating the various parts into an overall system which finally results in desired aircraft landing performance. He has had to accept aircraft design features selected to optimize other than landing characteristics. Many compromises have been necessary because of sensor or guidance system deficiencies, ILS being one major contributor. In more recent years, at least in commercial aviation, more attention has been given to aircraft stability and control design during landing than in the past. There is now the opportunity to influence the design of the new microwave landing guidance system to assure "total system capability" for CAT III operation without major compromises in flight control system design. This is not a matter of increasing the performance standards and complexity of the ground guidance system in order to ease the problem of the flight control system designer, as some have argued. Rather, it is a concern as to whether the system will work at all and whether all user needs can be met in a cost effective way.

As indicated elsewhere in this paper, the technique by which one eliminates or controls multipath effects can involve complex tradeoffs. In the case of scanning beam systems, the question of "scan rate" involves a complex tradeoff of economics, reliability, modulation-demodulation techniques, airborne vs. ground system complexity, and landing performance. The specification of high scan rates may result in a system that is so expensive that its use is very limited. On the other hand, if the system is to be effective, the scan rate must not be so low as to degrade approach and landing performance. The system should have a sufficient scan rate to accommodate future innovations in aircraft control systems such as direct lift. Thus, landing performance and safety are dominant factors in the determination of scan rate requirements.

One would like to determine position information and display it to the pilot with an accuracy of the order of 100-200 feet at 10 miles, better if practical. In addition, an accuracy of 5 to 10 feet at the runway threshold is desired. Granularity in the data sampling process of scanning beam systems is of concern to the flight control engineer. Improved beam data from which good quality beam-rate data can be derived for flight path damping purposes has been sought by the flight control engineer for many years. Pseudobeam rate techniques have been used, involving accelerometers and other sensors, but involve control law complexities. These compromises have been necessary with VHF ILS because of beam noise and beam inaccuracies. The sampling process inherent in scanning beam systems has an impact on the overall system stability and control and on control activity. For example, 1-foot granularity in position data can result in 2 to 4 feet/seconds of velocity noise at .5 to .25 second sample period. High frequency noise is relatively easy to filter (greater than 1 rad/sec). Bias errors with zero frequency content will be followed exactly. However, frequencies in the neighborhood of position loop frequencies can be troublesome. Proper design of filtering will be one of the major challenges that the airborne receiver designer must face and one which the flight control system engineer must influence. The filter designer must consider the tradeoffs between allowable signal phase shift, which impacts guidance loop and control loop gains and stability, and scan rate granularity. The filter design is also influenced by the noise characteristics of the sampled data. Filtering becomes particularly important in the case of microwave landing system analog signal outputs that are to be used with an existing aircraft autopilot to replace ILS signal outputs.

We can expect data rate to be most critical during the flare maneuver with high performance military aircraft. The path geometry and relative motion of parts of an aircraft may create a very serious need for very high data rates. With the antenna mounted in the nose, for example, during pitch rotation in flare, the nose travels up at a relatively high angular velocity as the wheels descend toward touchdown (Fig. 2). Altitude measurements at least as good as those from a radio/radar altimeter must be available (approximately ± 1 Foot). Deriving rate information (altitude) again becomes the hard task. Discrete changes of .5 to 1-foot at .1 second time interval (10 hertz per second) results, in raw form, in a 5 to 10 feet/sec altitude rate noise. "Sample and hold" techniques, sometimes proposed, are hardly satisfactory since the output is very granular. Radio altimeter high frequency noise is usually filtered and combined with body-mounted accelerometer information to provide altitude rate. Unless MLS flare guidance provides accuracy to .1 foot at 10 to 20 times per second, similar combination with accelerometer data will be necessary. This may be a tradeoff which is most cost effective if not altogether desired.

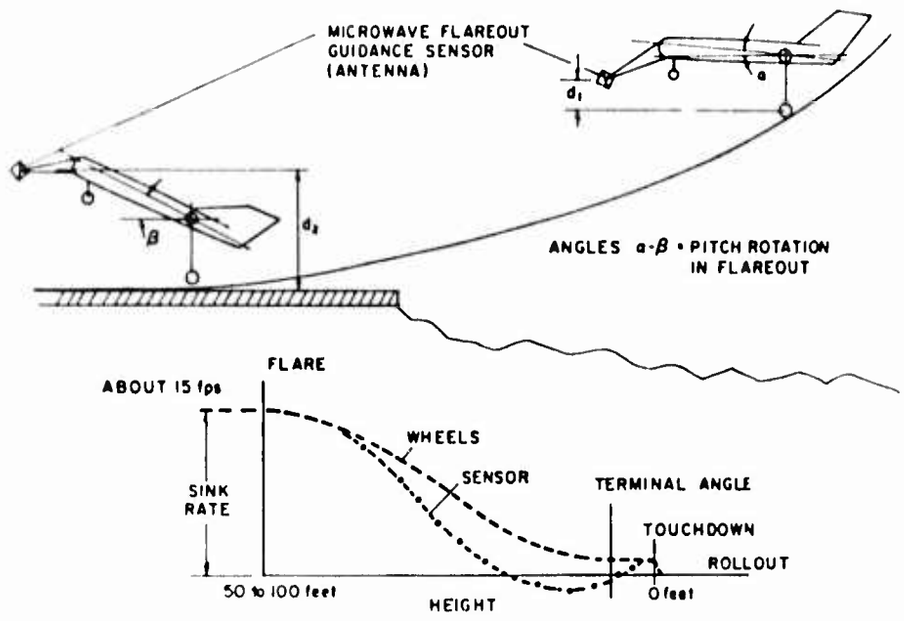

FIG. 2

An interesting mechanical analogy, explaining how guidance and flight control critical frequencies interact with one another, was developed by Collins Radio Company engineers in reference 2. Referring to Fig. 3 and quoting directly from the reference:

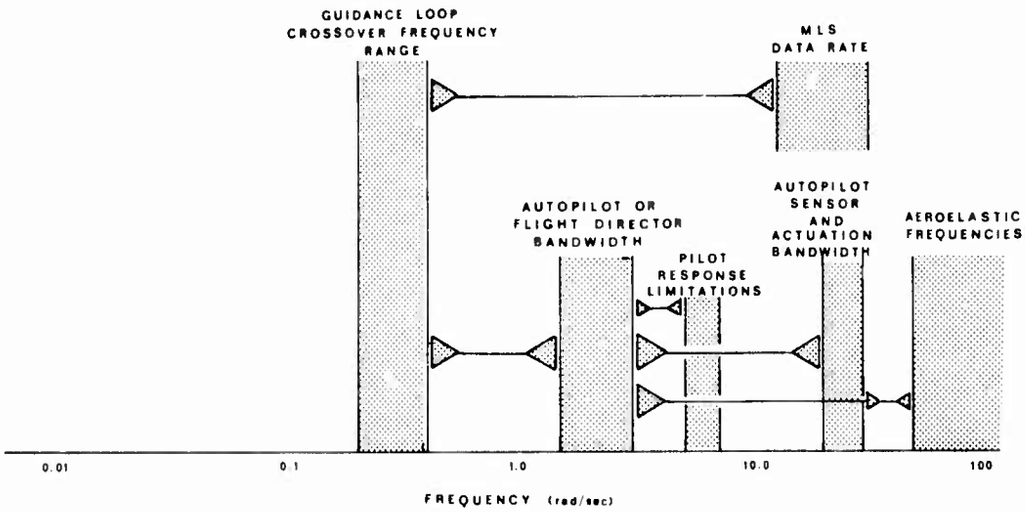

FIG. 3. Guidance/Control System Frequency Interaction Chart

"The horizontal [illegible] with triangles at either end should be thought of as being rigid members. That is, if we move a [illegible]l frequency along the frequency axis toward another frequency which is separated by a bar, then that critical frequency will also have to move in order to maintain either stability or performance. For example, the outer guidance loop stability is directly dependent upon MLS data rate and the autopilot or flight director attitude loop response characteristics. That is, if we significantly increase the bandwidth (position and rate gains) of the outer path tracking loop, we will need to speed up the response characteristics of either the autopilot or flight director attitude loops correspondingly. Herein lie the constraining factors. In the case of the pitch or bank autopilots, we typically set the closed loop bandwidths at a value slightly above the dutch roll (bank) and short period (pitch) frequencies. To broaden this bandwidth considerably will likely produce stability problems due to sensor or actuation lags. Even if these lags were overcome, the possibility of getting into a frequency region where aeroelastic bending or torsional modes could become a problem is something we

would like to avoid. Further, since the pilot prefers to see the controls (which are repeating the autopilot command parallel servo motion) move in a manner somewhat similar to the control actions which he uses as he performs a given maneuver, he will likely not accept the rapid control actions, including a broader noise spectrum, of a broad bandwidth autopilot. This last factor is a bit of an education and familiarity problem, and there is some evidence that pilots as a group are becoming more aware of the value of fast response autopilots, but it is an area of some controversy that should be entered with some caution and expectation of problems."

4. SITING INFLUENCES

As stated above, the nature of the environment has a decided influence on guidance philosophy. As can be seen from the military requirements just outlined, operations may be conducted from sites ranging from civil airports to the most primitive remote area, defying normal obstacle and terrain criteria. The necessity for maintaining guidance signal integrity to very low altitudes, and in some cases nearly to the ground, poses severe requirements on multipath control--a prime guidance philosophy influence. Civil/military interoperability being a requirement, any military guidance concept must show conceptually its ability to operate with VHF-ILS. The fact that some military tactical situations may result in the necessity for a specialized guidance system which is not interoperable with the forthcoming new civil/military microwave landing system, does not reduce the need for multipath control. Indeed, such special requirements may impose even more difficult multipath problems. However, it is not yet evident that all civil/military landing guidance requirements cannot be met by a common concept or philosophy.

Runways are not flat; airport standards permit grade changes resulting in humps as great as 10 feet. This means that an azimuth unit may have to be elevated as high as 20 feet in order to provide adequate signal coverage. Concepts using wide-azimuth, simultaneous signal coverage of a CW nature, such as Doppler, will experience vertical lobing problems and a host of reflections from objects near the runway (but within airport standards). Whether filtering processes can eliminate the adverse effects of these reflections is as yet unknown. Airport criteria permit hangers 80 to 100 feet high to be 700 to 1500 feet from the runway edge. In military situations one may find reflecting objects of significant height even closer to the runway. Applying standard airport criteria for clearance between buildings and runway/taxiway centerline, Figs. 4 and 5, we can see the devastating effect of such a valley of reflecting objects. Admittedly, worst cases are shown but such a situation is permitted by airport standards and large jumbo jet hangers are being built near runways. This is also true in military situations. Tactical sites are often nestled between hills and tree lines and protective structures can be found near runways. The landing guidance configurations outlined by RTCA SC-117 and being used in the US National Microwave Landing System development program as representative requirements, provide for, in some cases, 80 degrees of forward and 80 degrees of back-course azimuth coverage. These sectors include quantitative angular data to high accuracy throughout the 160 degrees involved. In other cases (such as configuration "K") the forward azimuth requirements are 120 degrees, and the rear azimuth requirements are 80 degrees for a total of 200 degrees of proportional, high-quality angular data.

If in a military tactical situation coverage is required at 20 to 30 miles at altitudes of 1,000 to 1,500 feet for terminal approach, this creates an elevation angle of only about ½-degree above the horizon. It is most difficult to maintain clear line-of-sight to 20 to 30 miles over a total sector 120 degrees wide in the presence of tree lines, hills, and large structures throughout the airport property. Depending upon altitude of the aircraft at the 20 to 30 mile point, the (area-navigational) coverage in azimuth will vary. At vertical angles to the main azimuth transmitter of, say, 6-degrees, the 120-degrees of azimuthal coverage may be ideal as compared to ½-degree elevation, assuming no obstructions would exist at 6-degrees elevation between the aircraft and azimuth transmitter. However, 6 degrees at 20 to 30 miles is an altitude of over 12,000 to 15,000 feet. Such terminal approaches are usually at much lower altitudes, between 1,000 and 5,000 feet.

Greatest accuracy will be needed for centerline control of widebodied jets on narrow runways (150-foot-wide runways). While some military bases have 300-foot-wide runways, many do not. Furthermore, low-visibility landing tests with "narrow-gauge" lights, centerline lights, runway edge lights and threshold lights, in various combinations, indicate that better visual cues are provided with a runway 150 feet wide. It is unlikely that there will be any significant widening of runways and precision requirements, based on 150-foot-wide runways for aircraft with large wheel base, must be considered.

In early phases (1965) of the Air Force's Tactical Instrument Landing Program (TACLAND), experiments were planned in which a microwave landing guidance system, TALAR III, with a relative narrow localizer course width (5 degrees), would be used as a localizer-only to define the centerline of the runway out to 3 to 5 miles from threshold. GCA was to be used to direct the aircraft into the beam and also provide guidance in the vertical. In other tests TALAR III was to be used at the threshold to provide lateral and vertical guidance with GCA being used to guide the aircraft into the beam. In this latter case, since in TALAR III the glide slope and localizer beams emanate from the same point, runway centerline is not defined beyond threshold. The purpose of these first phase tests was to show how low-visibility landing capability could be improved in the tactical environment by supplementing old GCAs with a compact microwave landing guidance unit. In other experiments, TALAR III, used as a localizer-only or at threshold as a glide slope and localizer transmitter, would be used with beacons for homing, portable TACAN, or airborne ground scanning radar for intercepting and aligning the aircraft with the tactical ground aid. Flight tests were conducted at a later date using TALAR IV at runway threshold, along with a portable Marine TACAN, with quite good results. The point to be made here is that a relatively narrow beam was to be used to define runway centerline in order to prevent multipath effects from objects near the runways. Acquisition of the beam would be provided by a variety of existing navigation aids.

More recently, Litchford, in reference number 1, has suggested a somewhat similar but more modern arrangement. He came by this suggestion as a result of studies of multipath problems as they impact operational situations. His concept, shown in Fig. 6 is included here to show how siting considerations

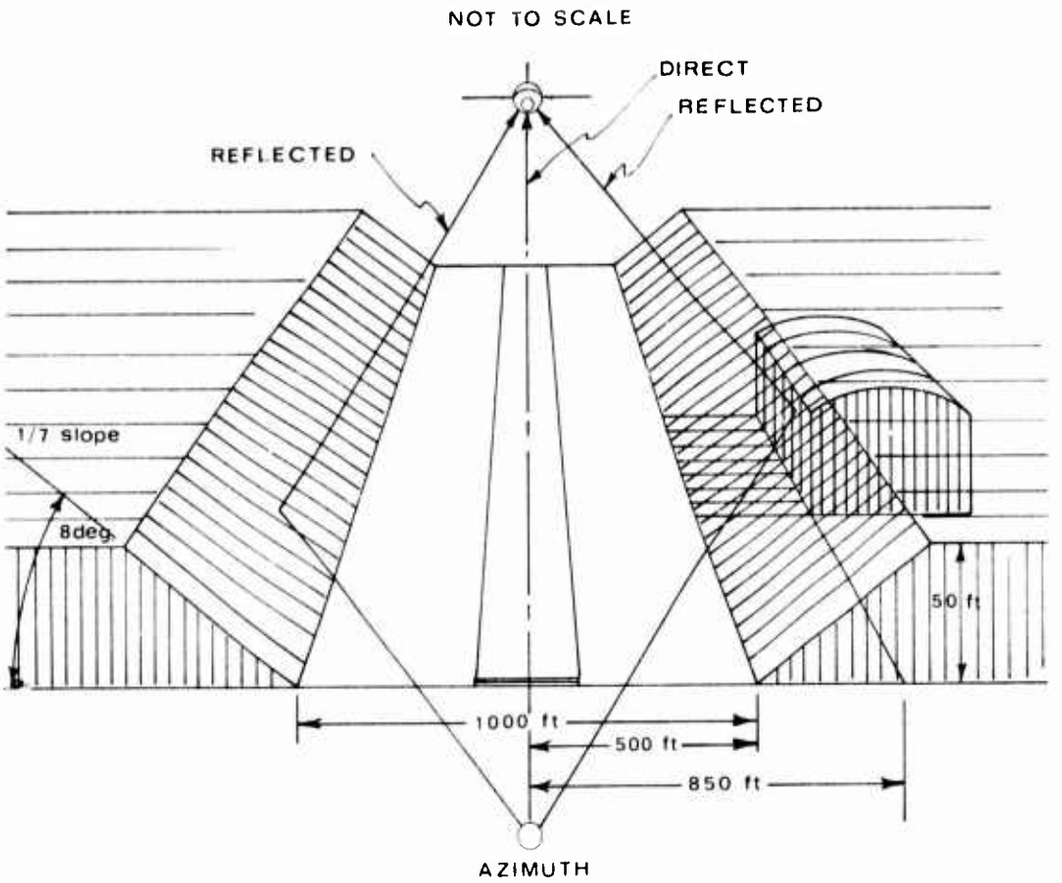

FIG. 4

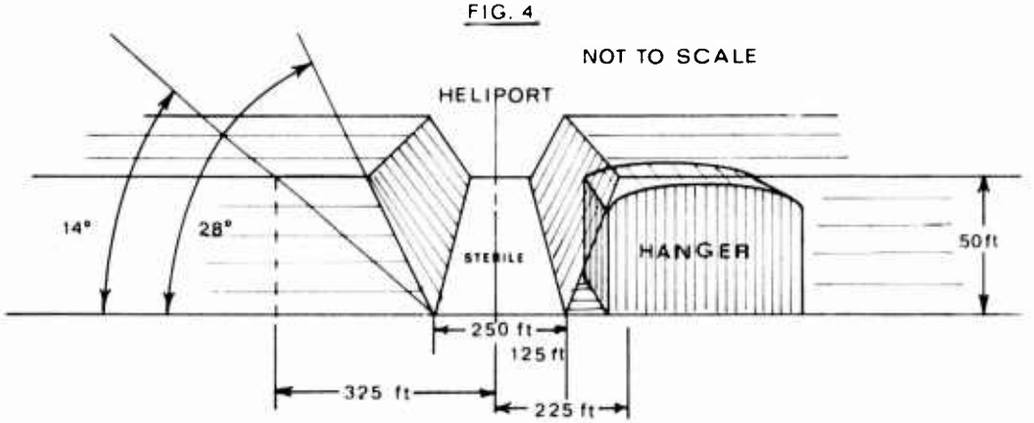

FIG. 5

can influence choice of guidance philosophy. A K_U-band azimuth scanner producing a ½-degree azimuth beam, or even a ¼-degree beam throughout ±5 degrees from runway centerline can be built reasonably and can produce guidance information with less granularity, less noise and with increased reduction in non-coherent multipath. By limiting scan angle, higher scan rates are possible with simple structures. Range out to 10 miles should be practical in heavy rain with reasonable power.

It may not be possible at many jetports to have an unobstructed line of sight at ½-degree elevation over an 80 to 120-degree sector from the end of the runway. Serving all aircraft to at least 10 to 20 miles and to altitudes as low as 1,500 feet is desirable. By locating the wide-azimuth scanner on top of a hanger or tower, the desired ½-degree vertical line of sight at all angles inside the scanned sector can be achieved. There might be some other open space on the airport which could provide desired unobstructed line-of-sight transmission and meet requirements of relative location of wide and narrow scan units.

Litchford chose a 4-degree beam using a 4-foot scanner for the wide-azimuth unit. Such an azimuth unit will be superior to VORTAC accuracy by at least ten times. At 3 to 5 times per second scan rate, less smoothing for guidance and flight control purposes will be required than for VORTAC (interface with R-Nav computers). A steady state, straight track distance, in instrument weather, of 5 miles before touchdown at 130 to 140 knots allows a pilot 2 to 2½ minutes to perform a host of functions. From about 5 to 30 miles beyond this straight-in approach sector we are dealing with terminal area navigation accu-

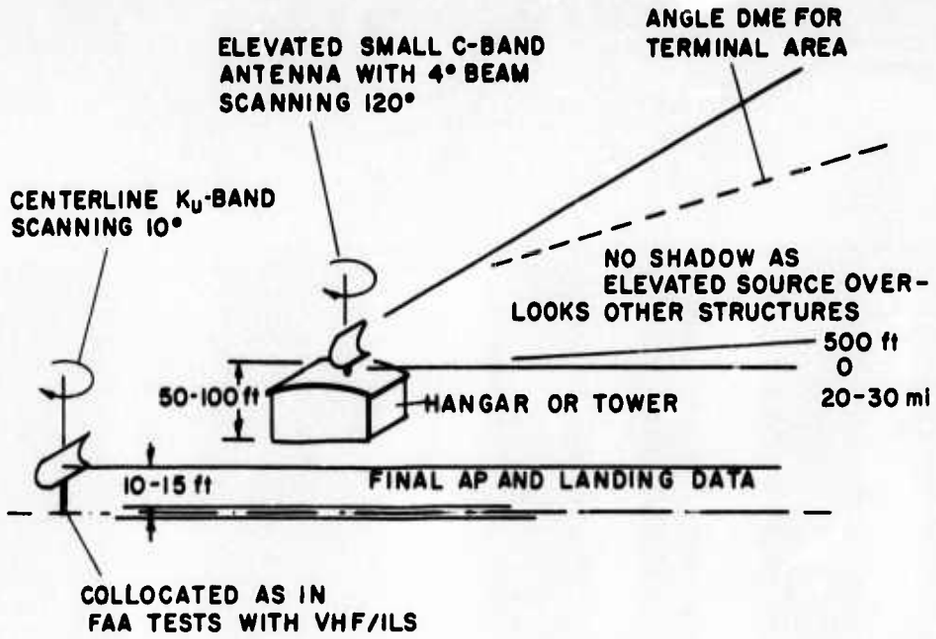

FIG. 6

racies. Depending upon the exact location of the wide-angle C-band unit, the fact that the origin can be elsewhere than on runway centerline is not a problem.

It is not the intent here nor was it Litchford's in his study to invent a new landing guidance system configuration. The example does illustrate practical "total-system considerations" and the influence of siting problems on choice of guidance philosophy. The technique chosen, whether it be conventional scanning beam, doppler scan or something else, must meet the test of all practical and possible operational situations if common civil/military objectives are to be met. It follows that the present field test program, being conducted under the National Microwave Landing Program, must yield "hard data" on multipath performance under representative difficult siting conditions or else a sound technical decision cannot be made. Many tradeoffs are possible not the least of which are those affecting "cost-effective" system dynamic performance.

5. ALL-AIRBORNE-SELF-CONTAINED

US Air Force Manual 100-11 states that an ultimate goal for zero visibility landing is by use of equipment wholly contained within the aircraft. The self-contained capability developed for low approach is an interim goal. The requirement implies a need for exploratory work to determine what techniques are needed to achieve a given capability, at what cost and at what risk. While zero-zero may not ever be a requirement for a self-contained system, a proper investigative program should identify the degree of sophistication required vs. risk and cost for all low-visibility conditions.

A multisensor arrangement may be foreseen using inertial and other navigation devices already on board. For the final approach and landing phase, high resolution radar which displays a perspective picture of the runway or a system of beacons producing a similar display, is the likely answer. Infrared, lasars, low-light level television, etc., can provide good perspective runway displays under certain environmental situations but are not satisfactory under critical fog and rain conditions. In addition, to be cost effective and most useful, a multipurpose radar is desirable which can also be used as a weather radar, detect hazards in the approach path and provide map-matching capability in the terminal area.

In addition to providing a self-contained capability, such a device may find a use as an independent-landing-monitor (ILM) for CAT III approaches. There are various thoughts on supplementing aircraft presently equipped with CAT I and CAT II systems with an ILM to achieve a lower minimum capability without retrofitting aircraft with an expensive CAT III autoland system. Whether such an approach is cost effective or not remains to be seen. The military situation is different from civil operations in that higher risks are often taken out of sheer necessity and whatever means at hand are used to accomplish a particular mission. If mission capability can be improved and risk reduced with an ILM radar or a multipurpose radar with an ILM modification, increased cost may not be very significant; failure to accomplish a mission could be catastrophic.

CONCLUSION

There are many tradeoffs that must be carefully considered in deciding upon a landing guidance philosophy for military operations. Interoperability with civil facilities is highly desirable and a goal of current USA programs. There is no reason, yet, to believe such a goal cannot be achieved. But all elements of the "total system" must be treated and there are differences in aircraft characteristics and operations between civil and military. Maintaining high quality, high integrity guidance information in the presence of a severe multipath environment is a key factor and present field test programs

must yield "hard data" in this respect before a guidance philosophy can be chosen for future use by the military.

REFERENCES

1. Litchford, G. B. "Study and Analysis of SC-117, National and USAF Plans For a New Landing System", Technical Report AFFDL-TR-72-76, Air Force Flight Dynamics Laboratory, Dayton, Ohio, July 1972, pages 148-164

2. Duning, K. E.
   Hemesath, N. B.
   Hickok, C. W.
   Lammers, D. G.
   Goemaat, M. L. "Curved Approach Path Study", Report DOT-FA72WA-2824, Department of Transportation, FAA, Washington, D. C., Final draft, Oct. 1972, pages 67-73 and Fig. 4-1

3. Litchford, G. B.
   Yingling, G. L. "Future Trends in Air Traffic Control and Landing", ICAS Paper No. 72-04, The Eighth Congress of the International Council of Aeronautical Sciences, Amsterdam, The Netherlands, Aug. 28 to Sept. 2, 1972

4. Anon. "Provisional Air Force Requirements for a Microwave Landing System", Draft, HqUSAF, Washington, D. C. April 1973

5. Parks, D. L.
   Fadden, D. M.
   Fries, J. R. "Control Display Testing Requirements Study", Technical Report AFFDL-TR-72-121, Vol. I, Air Force Flight Dynamics Laboratory, Jan. 1973

THE IMPROVEMENT OF VISUAL AIDS FOR APPROACH AND LANDING

A J Smith
D Johnson
BLEU
RAE BEDFORD
U.K.

SUMMARY

Very large vertical density gradients can occur in established fogs and these can produce large variations of visual range with height.

Consideration has been given to the effect that these gradients have on the operational performance of approach and runway lights. A new lighting design of improved performance is described.

The development of a precision approach path indicator is also reported.

1. INTRODUCTION

Although most aircraft are now fitted with some form of instrument approach aid, most landings are performed manually by the pilot by visual reference to the ground. Even in the case of fully automatic landing, the pilot visually monitors the procedure. In night-time or poor visibility conditions, therefore, lighting and marking patterns are required to provide the pilot with the necessary visual cues during the later stages of the approach and throughout the landing and roll-out along the runway. Ground based visual aids are adequate only if the pilot can obtain a clear indication of his position and quickly assess his relative velocities. To be able to do this he must see a meaningful pattern of lights for several seconds.

In a worldwide study of aircrew workload, carried out by the RAF Institute of Aviation Medicine with the co-operation of BOAC, it was reported[1] that fifty per cent of all letdowns were classified as placing a high workload on the pilot and that of these two-thirds involved limited and poor approach and runway lighting. In other words, one third of all landings are adversely affected by the standards of lighting aids that are currently provided. There is clearly a need for improvements and in this respect the results of recent work undertaken at the Blind Landing Experimental Unit (RAE) to identify the extent to which various factors, such as fog variability, are responsible for the present shortfall in the performance of approach and runway lighting is pertinent. This work has emphasized the extent to which the topics of lighting visual aids and visibility are inter-related.

The lighting for precision approaches, as presently specified, was originally developed for use in conditions where the visual range exceeded 800m. Subsequently, some additions were made to the patterns to support operations down to 400m visual range, but the beam characteristics of the lights were not redefined. Shortcomings are known to exist in this system and these are most marked in the lower visibilities. Consideration has therefore been given to improving the standard of lighting, even for use in the lowest visibilities, and the conclusions of the study have been verified by flight trials.

Research on steep gradient approaches has required the provision of precise glideslope information down to very low heights. A system using sharp-transition VASI units has been developed to meet this requirement and this work is also reported in this paper.

2. VARIABLE FOG DENSITY

When aircraft landings take place in low visibility conditions, operational planning and pilot training correctly place considerable emphasis on two potential sources of difficulty and danger: shallow fogs covering the whole airfield and dense fog patches on the runway. Our recent studies of the visual cues that can be acquired from approach and runway lighting in fog have clearly demonstrated how difficulties arise from the characteristics of the lights and the fog and re-emphasize the problems created by shallow fog or fog patches and the effects that these have on the safety of landing operations.

It is perhaps worth recalling that as an aircraft descends towards shallow fog the visual segment (the length of lighting pattern or ground seen by the pilot), which may initially be very large, will always reduce as the approach proceeds, becoming a minimum as the aircraft enters the fog top. The size and rapidity of the reduction may surprise the pilot who may find that he does not have a large enough visual segment to continue the approach safely. However, if runway visual range information determined on the ground is provided, the pilot is aware that he will see a much reduced visual segment during the later stages of the approach.

The variability of fog structure has recently been investigated in detail by BLEU and measurements have been taken in a wide variety of fog conditions. The data obtained has been examined along with information on fog variability from other sources. In the context of low visibility landings the most important information obtained from the analysis of the data is that a marked increase in fog density with height often occurs, particularly in well-established fogs. Such fog gradients adversely effect what the pilot can see during the approach and this can have a marked effect on the landing success rate to be associated with any particular fog. In the past experimental effort has been concentrated on measuring the effects of fog gradients, in terms of slant visual range and contact height, whereas the work now being reported has concentrated on measuring the fog gradients that cause the reduced visual ranges. As an illustration, Fig 1 shows the variation of visibility from a height 'h' to the ground that can be expected when the reported visibility at ground level is 800m. It can be seen that from a height of 60m (200ft) there is a 50 per cent probability that the meteorological visibility will be only

half of that at ground level and from a height of 30m (100ft) there is a 1 in 40 probability that the visibility will be only one quarter of that at ground level, if all fogs are treated collectively.

The influence that such fog gradients have on the visual range of a light is illustrated in Fig 2. In this diagram boundaries are shown which indicate, for a typical approach light, the maximum range at which that light would be seen in the visibility gradient conditions shown in Fig 1. An observer anywhere within the appropriate envelope will see the light, but if he is outside the boundary he will not see it. A curve for a fog of uniform density is also included for comparison purposes. This curve also illustrates how the polar diagram of the light beam affects the shape of the range boundary as all airfield lights have intensity distributions which are not uniform, but fall off from an on-axis peak value. A light of equal intensity in all directions would give, in a uniform fog, a curve having a constant range from the source. The marked effect that fog density gradients have on the visual range of lighting systems is clearly seen. For example, in the case considered above, an observer at ground level would see the light at a range of 1150m, no matter what the gradient. Most lighting designs and operational analyses assume that fog is uniform and on this basis it would be assumed that a pilot in an aircraft flying at a height of 50m would see the light at a range of 1270m. Our data indicates that on at least half the occasions he would only see it at a range of 880m and on one occasion in forty, he would see it at a range of 400m, or approximately one third of the distance indicated by observations made at ground level.

Fig 3 shows the geometry of a typical situation at the point on an approach where the pilot first makes contact with the approach lights. The range from the aircraft to the light is shown in the diagram to consist of two segments; the visual segment and the cockpit cut-off segment. Generally, as the approach continues the range to the furthest light increases and this, together with the steady reduction in the segment cut-off by the cockpit, results in an increased visual segment being seen.

To the pilot of an aircraft making an approach to land the overall effects of a fog gradient cause both the contact height and visual segments to be much lower than he expects from the information he is given about the ground level visibility. At decision or break-off height he may not have the expected and necessary position information to continue the approach. In Fig 4 examples are given of the range of contact heights and visual segment sequences that would result by day from the visibility conditions shown in Fig 1, if a standard set of airfield lighting were in use. The diagram clearly shows that if the visibility at ground level is 800m then vastly different amounts of information can be available to the pilot depending upon the fog gradient with height. The diagram shows that for a uniform fog, contact would be established with the lights at a height of 130m (430ft), the runway threshold would be visible at a height of 60m (200ft) and that the visual segment would always be in excess of 600m. On at least half the approaches the contact height would be of the order of 100m (330ft), the threshold would be seen at a height of 45m (150ft) and the visual segment would, in general, be in excess of 350m. In this situation if the associated decision height is 60m (200ft), a safe and regular operation can be performed and the lighting cues will be adequate, although the large reduction in visual segment that occurs between the heights of 57m and 45m, due to a mismatch of intensities of the approach and runway lights, does result in the threshold not being in view at the decision height. There is some experimental evidence that for this type of operation it is highly desirable that the threshold should be seen before a decision to land is taken.

Curve A ($2\frac{1}{2}$ per cent probability) highlights the strong influence that fog characteristics can have on the lighting visual aids. In this case the contact height is below 60m (200ft) and until the threshold is in sight the visual segment is small and not adequate to support manual flight. This situation is potentially dangerous since the only visibility evidence that is available as the pilot begins his descent is that the visual range at ground level is at least 800m. Based on this information the pilot is expecting to carry out an approach during which he can rely on visual aids to manually manoeuvre his aircraft during the 1.5km before touchdown. The data presented in Fig 4 shows how on a significant percentage of occasions pilots will begin an operation for which they actually need high quality automatic approach equipment if it is to be completed satisfactorily. The danger is that the pilot "will not believe his eyes" when at 60m, his decision height, he still cannot see the lights and that having seen them (at a height of 50m) in the subsequent overshoot he will be encouraged to make further attempts to land because he feels that "he almost got in last time" and that he must be able to land, because the visibility is reported as being 800m. In the interval between approaches the situation can worsen. The example given above refers particularly to a situation where the visibility at ground level is 800m, but similar conditions and variations can occur throughout the low visibility regime.

There are more extreme characteristics, for example when the fog lifts to a level that is a little above ground level. In such a situation, in the absence of a reliable cloud base measurement, the visibility at ground level will be a very misleading indication of the conditions at any other height, for example 60m. The most dangerous situation that can be imagined is a thin layer of fog just above the ground. In this case the reported visibility would be good and the pilot would make an early contact with the approach lights but the visual segment may reduce to an unacceptable extent below decision height. Any approach where the decision height is above the fog top is not as safe as one in similar conditions where it is below the fog top.

The run-back in the visual segment, mentioned above, occurs at the point on the approach where the lighting changes from the high intensity approach lights to the runway lights, which have a lower output. This discontinuity, which is caused by shortcomings in the lighting design, adds to the difficulties caused by fog variability and it should, as far as possible, be minimized in the lighting design.

3. THE MAINTENANCE OF AIRFIELD LIGHTING

For many years emphasis has been placed on the importance of specifying good visual aids, but it would appear that little effort has generally been made to maintain the high standards once the lighting equipment has been installed. At the present time airfield lighting is the only airfield navigational

aid that is not regularly checked to ensure that the full operational performance is being maintained. Lighting inspections are carried out, but at many airfields these are only of a cursory "is it alight" nature. No attempt is made to check that the intensity and beam shape criteria are being met.

It is important that adequate monitoring of the light output performance of lights takes place. This is best done by photographic means rather than by subjective visual assessment. A recent survey of runway centreline lights carried out by BLEU (Ref 2) produced the results shown in Fig 5. The fittings on Runway A had only been installed for a few months and some efforts had been made to clean them. This runway had been inspected from the ground and from the air and had been cleared for landing operations in visibilities as low as 400m, as had Runways B, C and D. Runway B was surveyed less than two weeks after being out of use for the annual maintenance period. The average intensity of the lights on Runway D was only 200 candela instead of the specified value of 5000 candela and even on Runway A the average intensity was only 2800 candela. On a day when the visibility is 800m, a 5000 candela light will be seen at a range of 1000m. If the output of the light is reduced to 2800 candela, the visual range is reduced to 900m. If the output of the lights is only 200 candela then the visual range is reduced to 500m, just half of the specified range. These large in-service performance variations are highly undesirable. In the future considerable operational benefits can be derived and the quality of the visual cues can be improved, by changing the design of light fittings to reduce the fall-off in performance and by monitoring the intensity and beam spread output of fittings in-service. The output intensity of lighting should never be allowed to fall below half the specified value and it should be the aim at all airfields to maintain outputs well above this level.

4. NEW APPROACH AND RUNWAY LIGHTING DESIGN

4.1 Design Study

There is a trend, particularly in civil aviation, towards extending landing operations in low visibility conditions. This fact, and the evidence that is available of the inadequacy of present lighting systems, some aspects of which have been considered in this paper, has led to a review of lighting standards. The objectives of this work were to effect overall improvements and in particular to allow operations to take place in lower visibility conditions, improve contact heights in fog gradient conditions and remove those discontinuities that exist in the visual segments seen by pilots which are due to mismatches between the light intensities of various elements of the lighting patterns.

It has been assumed that adequate approach and runway lighting cues should be provided in all visibilities down to a minimum visual range of approximately 100m. Below this range practical and economic considerations make the provision of position information by visual aids an unrealistic objective.

For the purposes of the study approach path envelopes, based on flight trials data, were calculated for each of the three ICAO all-weather operational categories - Fig 6. All aircraft approaching within these envelopes have a high probability of being able to land and lighting guidance is therefore required at all points within them up to a given height. This height will vary with the category of operation but it will be of the order of the decision height plus 15m.

As a result of the study it is now recognised that there is a requirement for increased beam spreads and increased setting angles. Table 1 compares a new specification to meet this requirement with existing standards. The most notable changes are the increased beam spreads of the runway centreline lights and the increased setting angles of all lights. In addition, to make the best use of the available light flux, it is necessary to grade the setting angles of the runway edge and centreline lights in the first 600m of the runway. To fully counteract the effects of fog gradients even greater beam spreads and setting angles would be required.

The extent to which existing lighting can be adapted to meet the new requirements given in Table 1 was also considered. With the exception of the runway centreline fittings, the beam spreads are similar and down to a limiting RVR of 150m most of the benefits of the new design can be obtained by simply re-aligning the setting angles of the lights. Re-alignment is not difficult, provided that the fittings are not of the inset type. The runway centreline poses particular problems because it is always inset and, therefore, re-alignment of the internal optics provides the only practical way of varying the setting angles. Some equipment is designed in such a way that these modifications cannot be carried out, but other equipment can be easily modified to meet the requirements. However, the problems posed by the large beam spreads probably cannot be solved in existing runway centreline lighting equipment and it would seem that new fittings need to be designed and manufactured to provide the required beam dimensions.

4.2 Flight Trials

To carry out flight trials within a reasonable timescale it was necessary to adapt existing equipment, as discussed above. The basis of the trials programme, which was carried out at RAE Bedford, was to make approaches in low visibility conditions and compare the performance of the two systems. To do this the fittings on the left-hand side of the approach and runway edge lighting patterns were set to the new, higher, angles whilst the right-hand side remained at the currently specified values. A comparison of the runway centreline lighting was made by carrying out some of the flight trials to the new standard and some with them at the currently specified settings. Modifications to a batch of centreline fittings to allow the lamp filament to be translated vertically with respect to the optics of the fitting enabled the centreline lights to have the varying elevation settings shown in the Table, but the beam dimensions could not be modified to the new standard.

All approaches were filmed to demonstrate the difference in visual segment between the two systems. The contact height of the lights using the new settings was noted for each approach, as was the reported value of runway visual range (RVR).

Analysis of the film records confirmed flight observations that the left-hand (improved) side of the runway lighting was always seen first and that at any height a bigger visual segment of lighting could be seen on this side. In some situations two bars of the 5-bar approach lighting were clearly seen on the left-hand side of the pattern whilst no contact was made with the complementary bars on the other side of the pattern. On the approaches where the elevated setting angles were being used in the runway centreline lights, it was very obvious that the "black-hole" that is normally apparent between the threshold and the nominal touchdown point had been eliminated so that the pilot was presented with a consistent visual segment of centreline lights throughout the approach and landing.

Plots of the contact heights and the associated RVR value observed on the approaches are shown in Fig 7. Also shown on this figure are the results obtained from similar trials using lighting set up to the present standards. It can be seen from this data that the contact height is significantly increased by the new setting angles.

The main conclusion that has been drawn from these flight trials is that worthwhile operational benefits have been demonstrated as being available from existing equipment, if it can be realigned.

5. GLIDESLOPE INDICATORS

Even in good visibility conditions, pilots experience difficulty in acquiring sufficient position information in the vertical plane whereas abundant alignment cues are available in the horizontal plane from the symmetry of the runway and the associated lighting patterns. Provided that the touchdown zone can be seen by the pilot there is great value in providing visual approach slope indicator (VASI) as a means of overcoming this shortcoming. The original VASI system developed at the RAE and now in use throughout the world, gives a long range indication of the correct approach path and therefore results in aircraft making more stable approaches. As a result, the aircraft are well placed for a safe landing, but, because the VASI is an approach and not a landing aid, the scatter of the touchdown point is still large.

Recent studies of steep and two-segment approach techniques at the RAE required the provision of precise visual glideslope information to heights as low as 30m (100ft) and with intercepts between the two glidepaths being defined to an accuracy of $\pm$ 3m.

The standard VASI light units project a light signal that consists of red and white sectors with a segment of pink light of rather ill-defined dimensions separating them. Such a unit is not suitable for use where accuracies of a few metres are required. A system based on two-colour light projectors that use a 17cm diameter lens and a sealed beam light source has been developed. The light units project a beam, the upper part of which is white and the lower red. There is no pink zone and the boundary between the two colours is clearly defined.

Early trials were carried out with these units in the normal VASI layout but closer spaced longitudinally and elevated at 6 degrees and with an additional unit placed midway between the two VASI bars to define the centre of the approach corridor - see Fig 8 (a). This arrangement gave a stable approach but it was considered that the addition of further units as shown in Fig 8 (b) was an improvement because it gave multi-position information to the pilot so that at all times he was able to assess the magnitude of any deviation from the glidepath. The performance of this system was very good by day. On 6 degree approaches it resulted in height errors as small as $\pm$ 2m at a height of 30m. However, at night the row of light units appeared to merge together due to refraction caused by contamination of the aircraft windscreen.

A system that overcomes this problem and uses fewer light units is the one that has been developed and used extensively in the RAE trials. This precision approach path indicator (PAPI) consists of a bar of four units located at the side of the runway, adjacent to the glideslope origin - Fig 8 (c). The beam setting angles (red/white interface) of the four units are graded, the differential angles being $\frac{1}{3}$ degree. The nominal glideslope angle is midway between the centre pair of units. Thus the "on course" signal is two red and two white lights. From a slightly lower position three red and one white light is seen and at the bottom of the corridor all four lights are seen red. The reverse coding is seen if the aircraft is above the glideslope.

The pilot task in following the visual indications has been found to be acceptable down to a range of 250m from the origin. At this range the height error is approximately 2m. Using this equipment pilots have made 3 degree approaches as well as steep approaches up to angles as great as 15 degrees. A large number of approaches have been made at 6 degrees with the flare being initiated at a height of 10-15m. The standard deviation of the touchdown scatter in these trials has been of the order of 35m.

Other trials have been carried out using two sets of this equipment to define a two-segment approach, as shown in Fig 8 (d). The intercept point has been as low as 40m on a large number of these approaches.

6. DISCUSSION

The main objectives of the recent work on lighting and visibility carried out by BLEU were to identify some of the important factors that determine the operational performance of lighting visual aids and to seek methods of improving the position information that lighting cues provide to pilots.

The experimental work has highlighted the significant extent to which vertical fog density gradients affect nearly all low visibility operations. From the data obtained, the large scatter observed in the past in contact height and visual segment values at decision height in conditions that were nominally identical is understandable.

If operations are to take place regularly and safely in very low visibilities it is essential that the operational performance of the approach and runway lighting should in no way add to the difficulties caused by variations in fog density. The measurements that have been made of light output from airfield lighting installations have shown that poor fitting design and poor maintenance are penalizing operations at the present time. Regular monitoring of lighting standards is essential if lighting standardization is to have any value.

As a result of the information discussed in this paper, the design of lighting to give adequate positional cues can be carried out with a much clearer understanding of the environment in which it has to work. It is now possible to compute the probable performance, in terms of contact height and visual segments, of any set of lighting. Alternatively, the lighting standards needed to provide reliable visual guidance can be specified for any new approach path envelope and fog gradient situation. For example, the intensities, beam spreads and length of approach lighting pattern needed to support steep gradient approaches can be evaluated.

The glideslope indicator described in section 5 provides more position information to the pilot of an approaching aircraft than is available from the standard VASI installation. In situations where precision is important during the latter stages of the approach and where touchdown scatter is required to be small, this system using sharp-transition units offers considerable benefits. Equipment of this type has been shown to be well suited for steep and two-segment approaches and it should be considered for conventional operations, particularly if the length of runway available is a critical parameter, since a small touchdown scatter can allow the nominal touchdown point to be moved closer to the runway threshold. Touchdowns closer to the runway threshold would have operational benefits, particularly for high performance aircraft with poor braking characteristics.

7. CONCLUSIONS

Very large vertical fog density gradients (with height) can occur in established fogs. These large variations are a major cause of the great variety of contact heights that are observed in low visibility operations. Lighting maintenance standards are poor and contribute to difficulties that exist in providing adequate visual references.

Significant improvements can be obtained in the visual guidance provided by approach and runway lighting by using lights having greater beam dimensions and set at higher elevation angles. Most of the improvements can be obtained in all but the very lowest visibilities by re-aligning existing lights to the new elevation angles.

A precision approach path indicator (PAPI) has been developed for steep gradient and two-segment approach trials. This equipment provides accurate multi-position information during the approach down to very low heights. Landings made using this equipment have been achieved with a touchdown scatter that is much smaller than is normally achieved.

REFERENCES

1 Sq Ldr A N Nicholson — Aircrew Workload during the Approach and Landing. Aeronautical Journal June 1973.

2 — The Degradation of Light Output from Runway Centreline Fittings. Unpublished RAE Paper.

Light	Average Intensity (Candela)	Beam Spread (deg)		Elevation Setting Angles (deg)
		Horizontal	Vertical	
Approach	20,000 *	± 11	± 5	4½ - 6
	20,000 ✖	± 13	± 5	6½ - 9
Runway edge	10,000 *	± 6½	± 3¾	2¾
	10,000 ✖	± 7½	± 4	3½ - 6½
Runway Centreline	5,000 *	± 5½	± 3½	3
	3,500 ✖	± 10	± 6	3 - 8

* Existing equipment
✖ New design

TABLE 1 Lighting Characteristics - Comparison of Design Study with existing equipment.

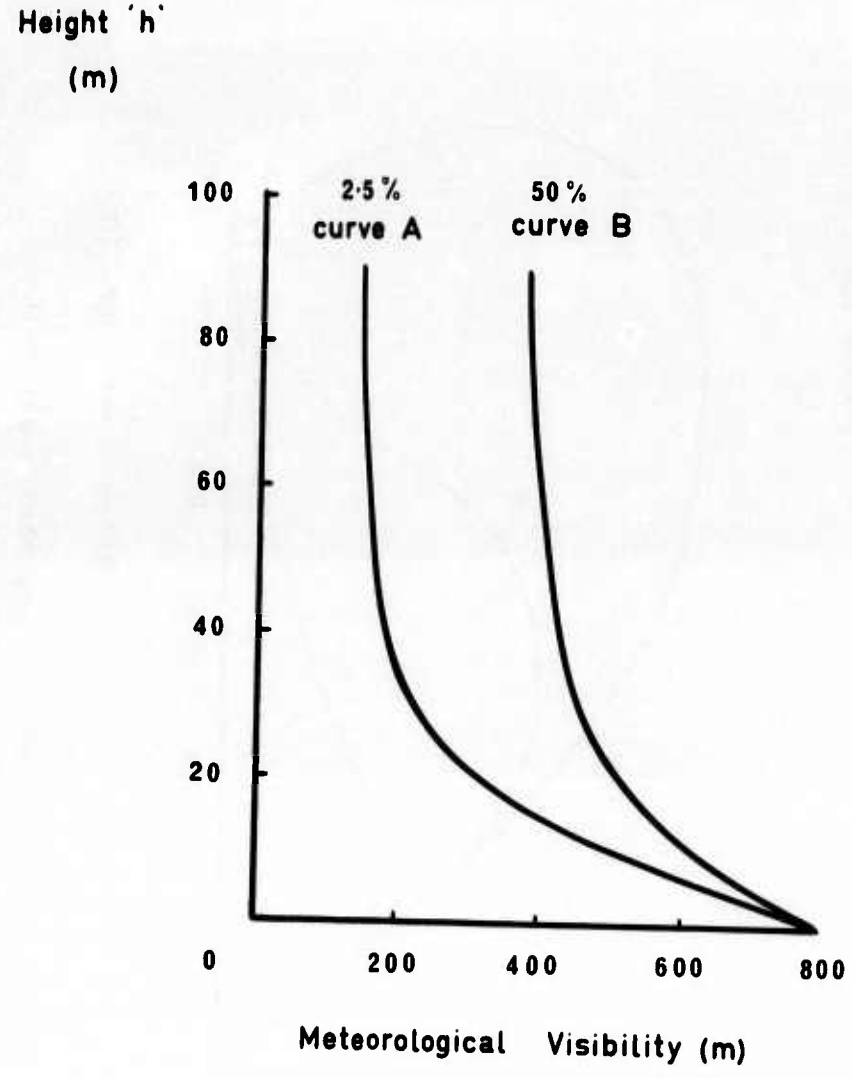

Fig.1 Variation of visual range to the ground, for two levels of frequency of occurence.

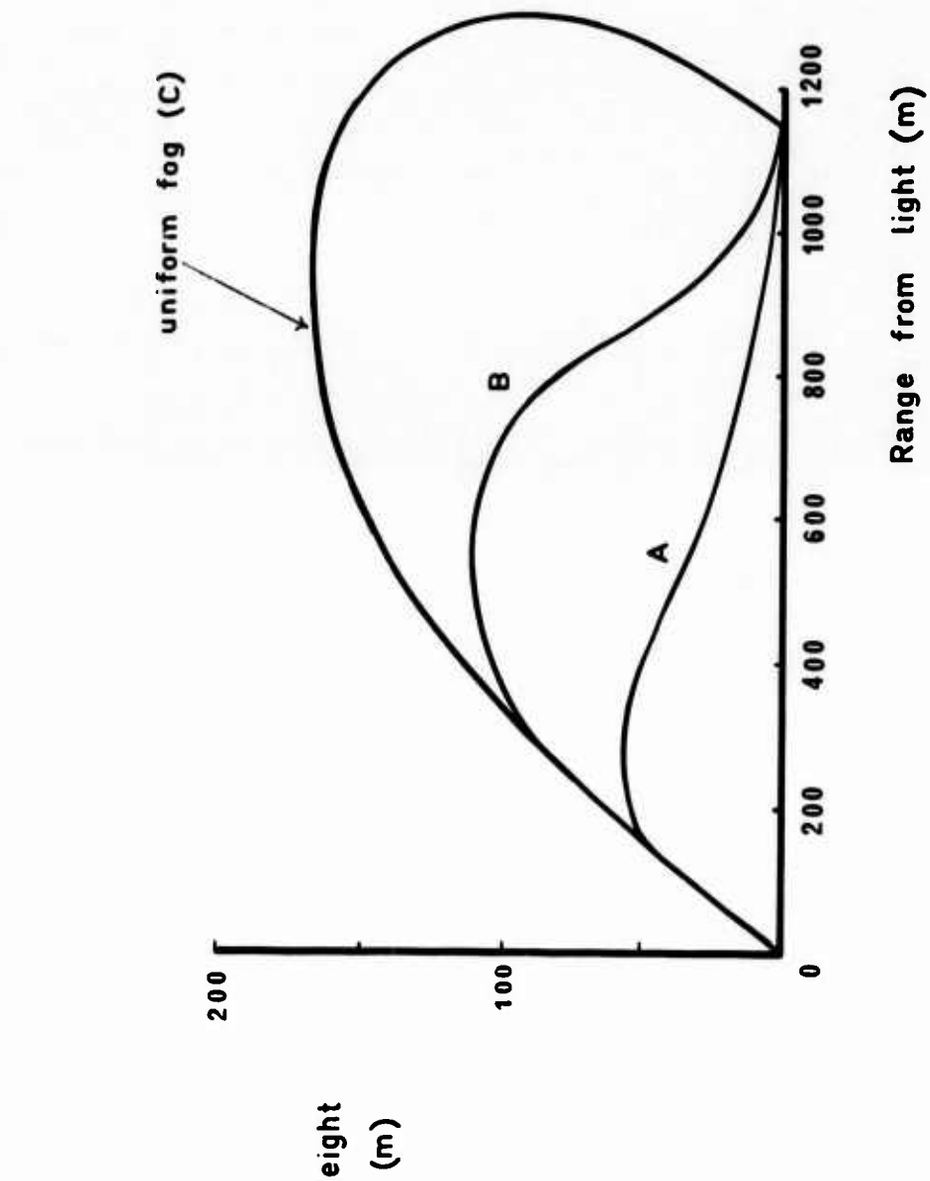

FIG. 2 Visual range boundaries for an approach light when the meteorological visibility is 800m. at ground level

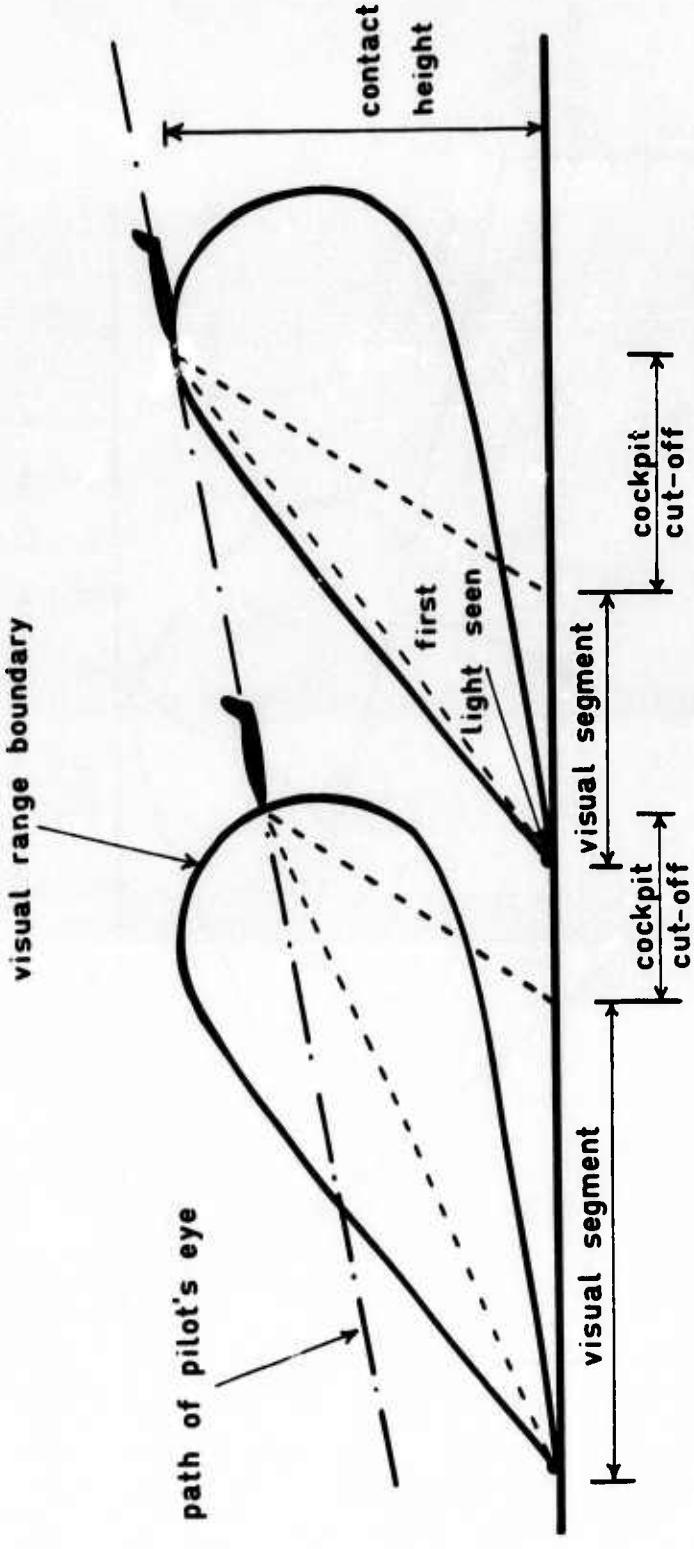

FIG. 3 The geometric relationship between the visual range of a light, the contact height and the visual segment

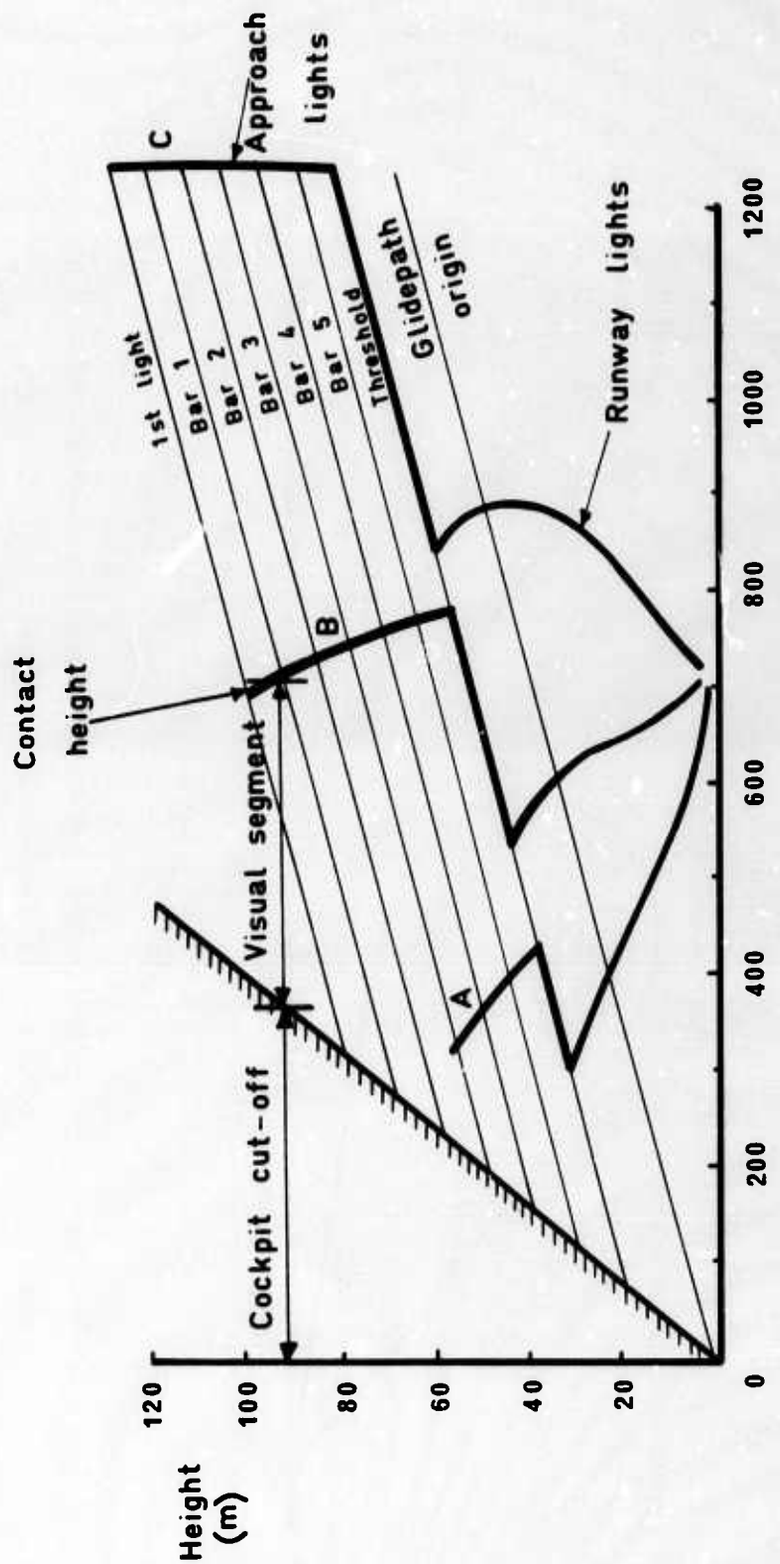

FIG. 4 Visual range to furthest light that can be seen by the pilot

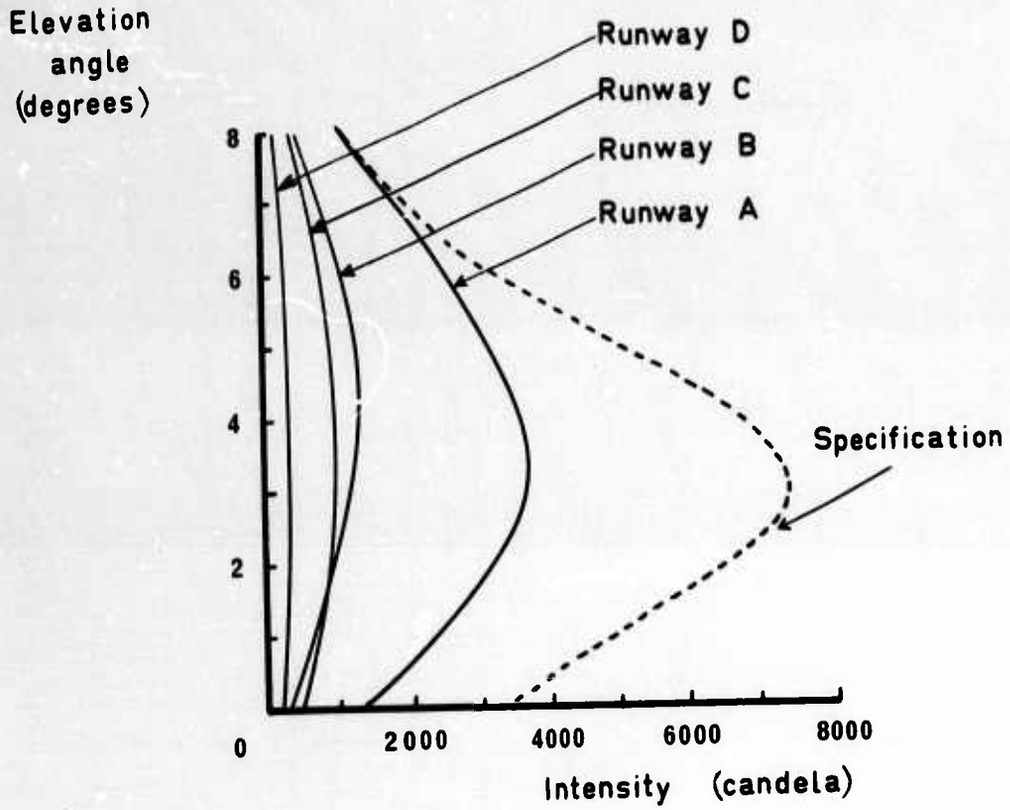

FIG. 5 Operational Intensities of a number of runway centreline lighting installations

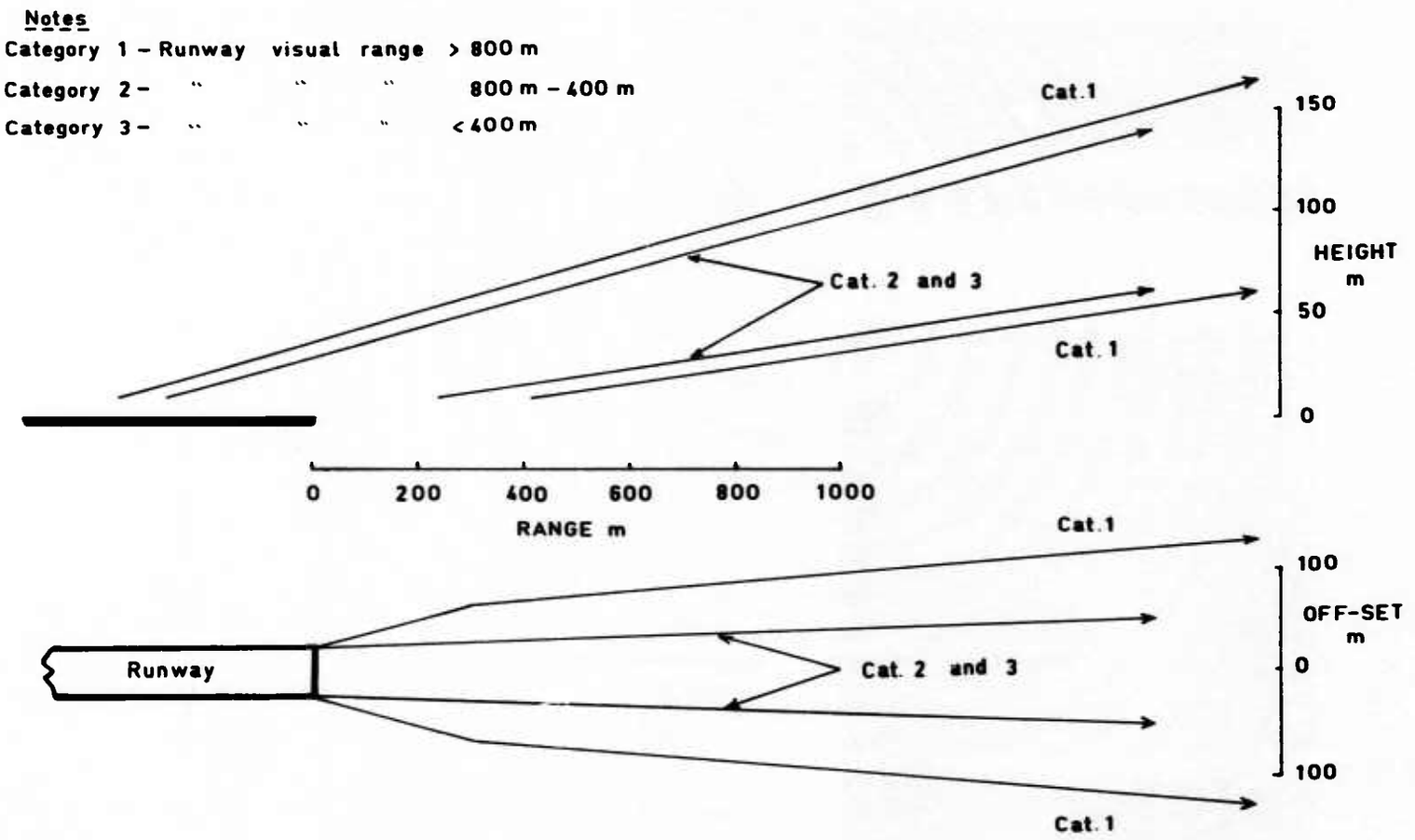

FIG. 6 APPROACH BOUNDARIES

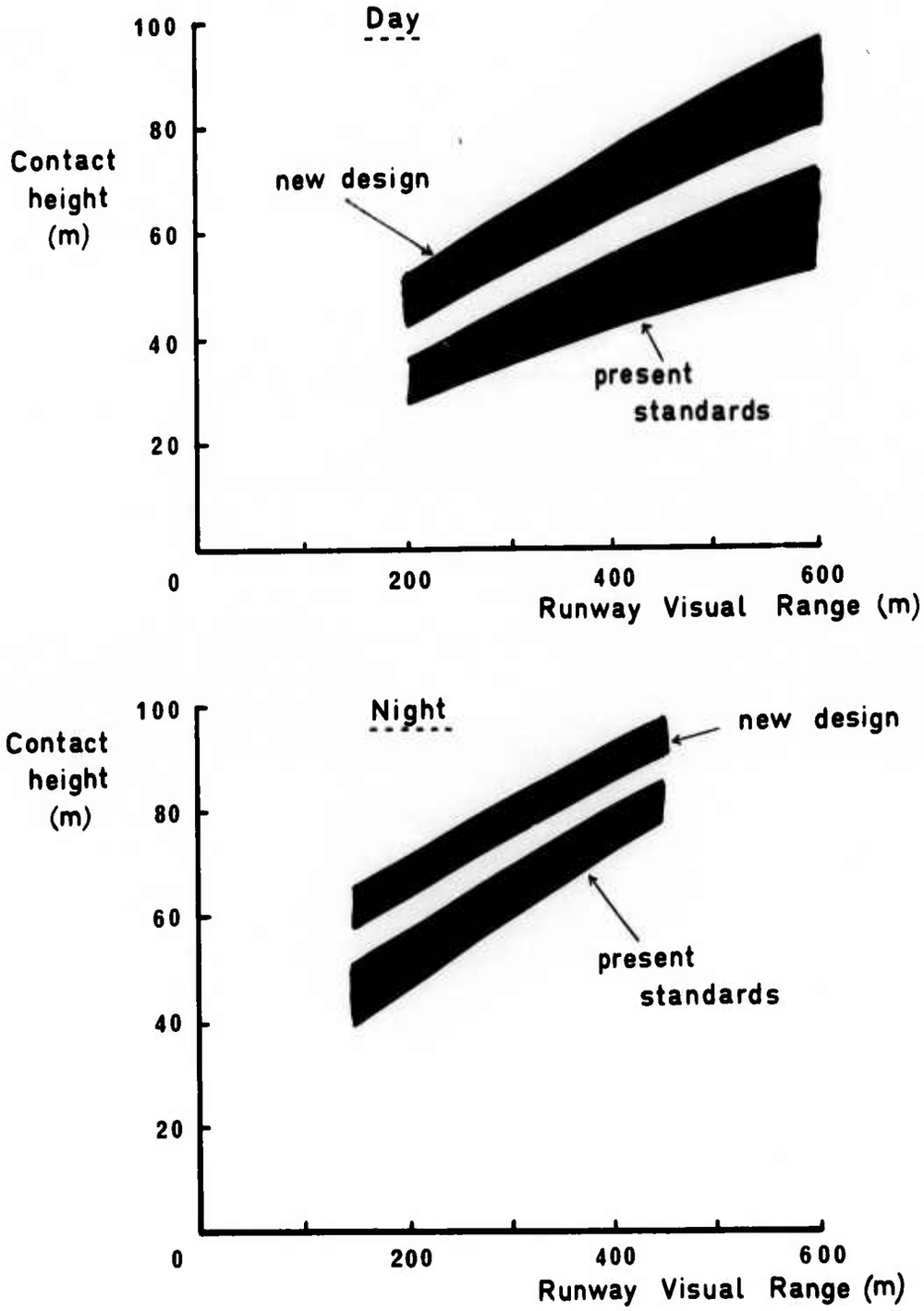

FIG. 7 CONTACT HEIGHT

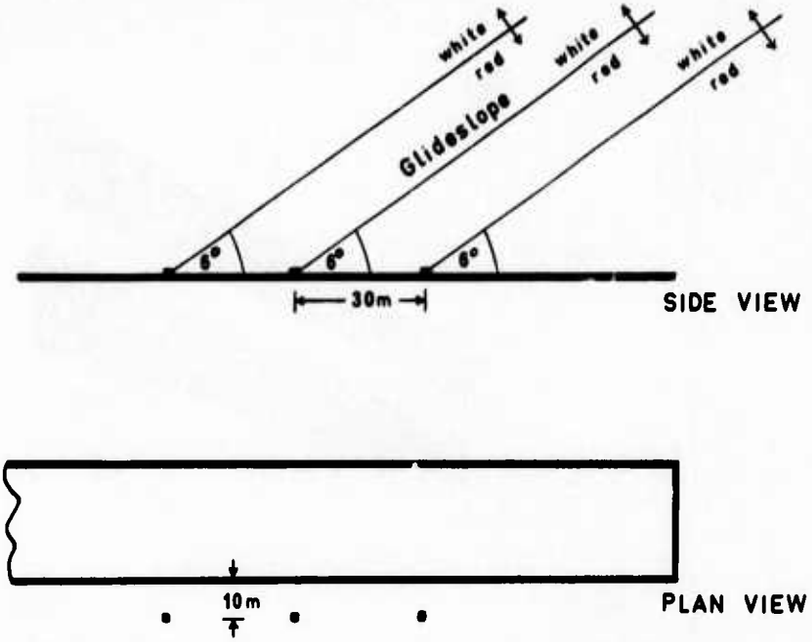

FIG. 8(a) Experimental Glideslope Indicator - centre of corridor defined

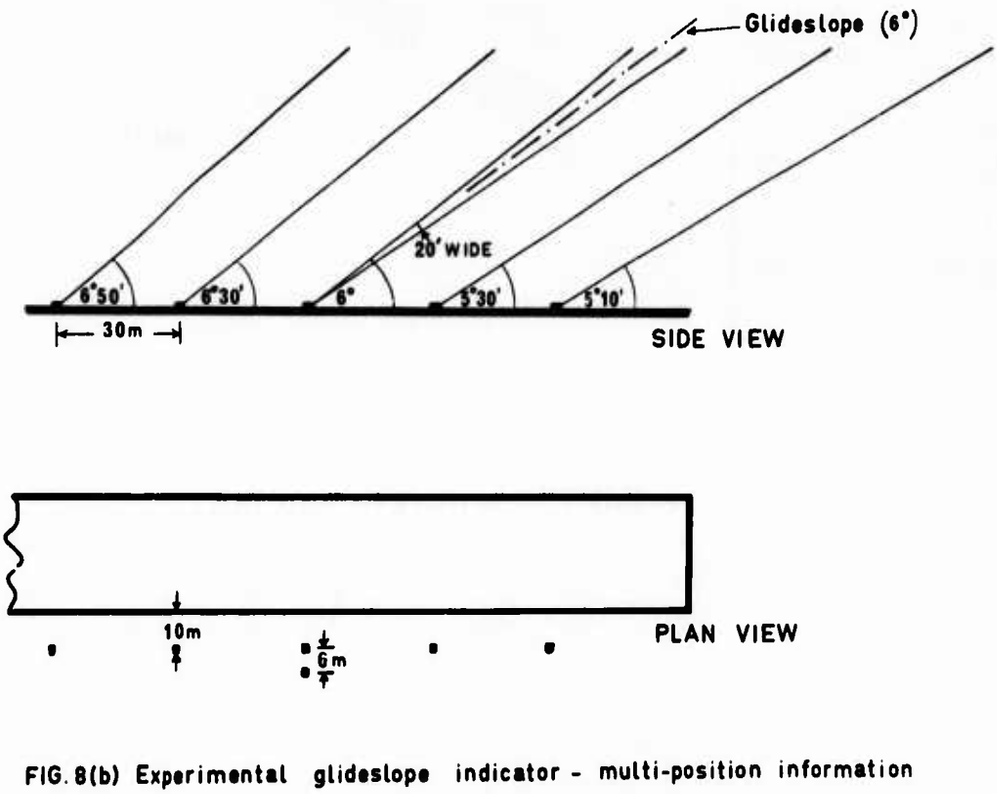

FIG. 8(b) Experimental glideslope indicator - multi-position information

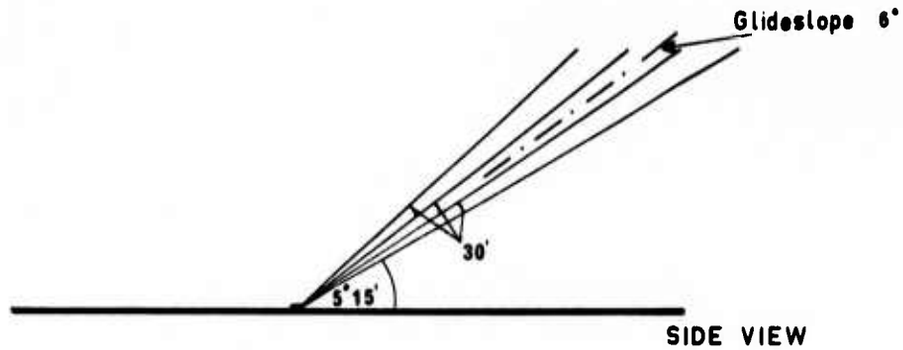

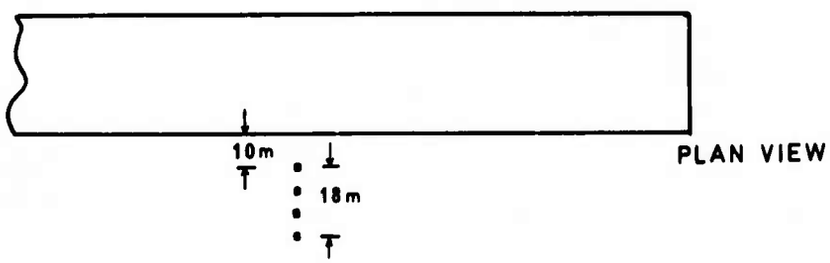

FIG.8(c) Experimental glideslope indicator - P.A.P.I.

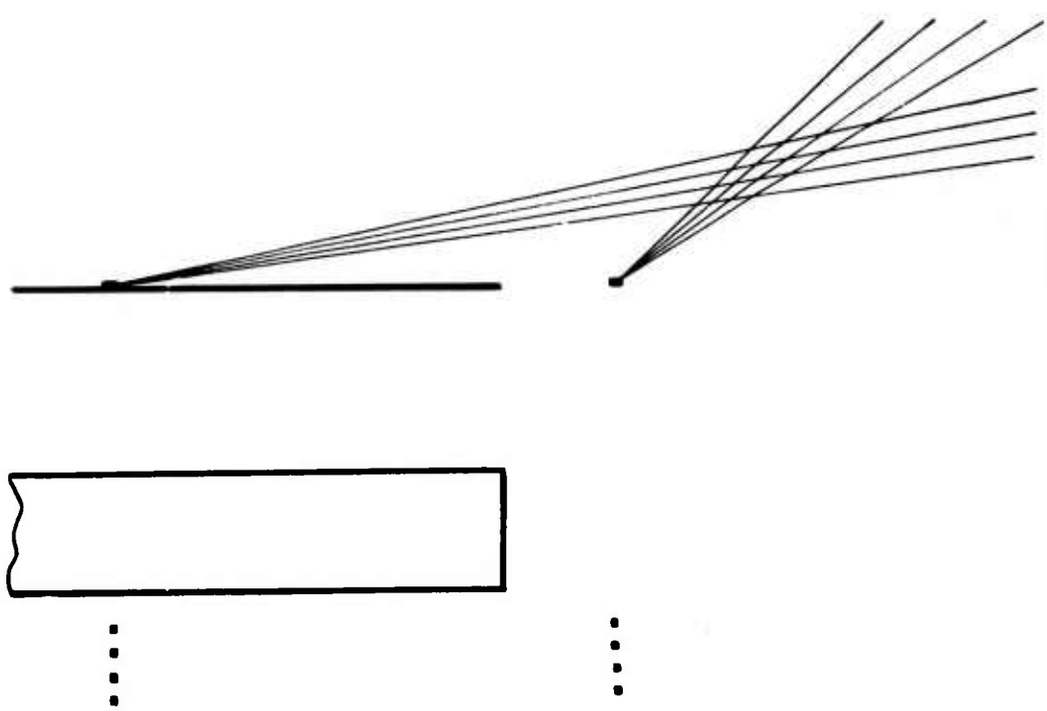

FIG.8(d) Experimental glideslope indicator - P.A.P I (two segment approaches)

FLIGHT TESTS WITH A SIMPLE HEAD-UP DISPLAY USED AS A VISUAL APPROACH AID

by

G.L. Lamers
National Aerospace Laboratory NLR
Anthony Fokkerweg 2
Amsterdam-1017
The Netherlands

SUMMARY

A simple head-up display (HUD), giving only glide path information with a depressed horizon bar, has been tested as an approach aid in visual flight conditions. An important improvement was observed in the accuracy of the glide path performance when approaches with the use of a HUD are compared with visual approaches without an approach aid. Using the HUD decreased the standard deviations of height by a factor of 2 to 4 depending on distance from the runway.

From this limited series of tests no significant differences in other flight parameters could be demonstrated.

The subject pilots indicated a preference for use of the HUD during visual approaches, especially in night conditions.

1. INTRODUCTION

In military aircraft head-up displays (HUD) are used to a large extent to increase the capabilities of the pilot/aircraft combination during different tasks. The displays used for these aircraft are very complex because they use quite a number of symbols to present information on a large variety of flight parameters. These HUD's also have several modes of operation, directed to the different phases of the mission, one of them being approach and/or landing.

For civil applications the use of a HUD as an approach aid was also suggested; reference 1. Flight and simulator tests have been conducted to study the use of a HUD as a primary instrument for manual control - or as a monitor of the auto-pilot - during bad weather approaches and as an aid for the transition from instrument to visual flight in cat. II approaches; references 2, 3 and 4.

Because of the relatively large number of approach accidents occurring in good weather conditions the HUD was also proposed as an approach aid - in particular for glide path information - in visual flight conditions. Such an approach aid may ease the pilot's task, especially under circumstances where very few visual cues are available to judge the position of the aircraft relative to the runway. Such an assessment of position is more difficult in the vertical plane; in the horizontal plane sufficient information is obtained from the runway centre line and/or edges, even at night when the edge lights are on.

To provide guidance in the vertical plane Visual Approach Slope Indicator Systems (VASIS) have come into use during the last decade. As these installations have only a limited range (maximum about 3 n.m.) especially in hazy conditions, and as not all runways are equipped with a VASIS, a better solution to the vertical guidance of aircraft can have a favourable effect on approach safety.

In the last few years several research and development programmes are reported in which simple HUD-symbology, giving only information on one or two carefully selected flight parameters, has been used; references 5, 6 and 7. The provision of glide path information is the main purpose of such HUD's. This information is derived from a so-called displaced horizon-bar, which is used either with or without a normal horizon-bar. The displaced bar is depressed approximately 3 degrees from the horizon. In order to ease the pilot's task in bringing the aircraft on the glide path, director information is sometimes also fed into the displaced horizon bar, references 6 and 7.

To obtain quantitative data on the accuracy of visual approaches with a HUD compared with approaches without HUD the National Aerospace Laboratory (NLR) has executed two series of flight tests with a Beechcraft Queen Air 80. The first series of tests is described in reference 8, the second series of tests is described in this paper.

In this series fifteen daylight and six night approaches were executed with the aid of a HUD-presentation consisting of a 3 degrees depressed horizon bar. An equal number of approaches were made without HUD.

In order to make the pilot's task more difficult, it was stated as a requirement for the tests, that no ground texture should be present under the approach path. The approaches were thus selected over water to simulated touch down points at the border of a lake. The direction of the simulated runway was indicated by dikes or canals behind the aiming points.

The results of the tests as obtained from measurements of some important flight parameters are discussed. Subjective opinions of the three evaluation pilots are also given.

The study was performed under contract with the Department of Civil Aviation in the Netherlands.

2. HEAD-UP DISPLAY

The HUD-system used for the approach tests was intended to study general use of a HUD - military as well as civil - and was therefore rather complicated, in particular with respect to sensors and interfaces. In this chapter only the part of the system will be described, that was necessary for the HUD-presentation used in the tests.

The operational use of the HUD-presentation will also be discussed.

2.1 System description

The Specto Aviation (now Smith Aviation) HUD used for the tests consists of a Wave Form Generator (WFG), Pilot's Display Unit (PDU), Extra High Tension Unit (EHT), solar cell and control panel, see figure 1. Symbology generated in the WFG is written on a cathode ray tube (CRT) in the PDU. The image of the CRT is viewed by the pilot via a folding mirror, a collimating lens (to set the CRT-image at infinity) and a combining glass. The maximum field of view of the display is 24 degrees in azimuth and elevation. The length of the horizon bar is 12 degrees.

The PDU was mounted on the right-hand side of the cockpit in front of the co-pilot's seat, see figure 2.

The roll stabilized horizon bar is driven by signals from the platform of a Litton LN-3 inertial system. The synchro outputs of roll and pitch attitude are conditioned in an interface unit to provide the d.c. signals for the WFG. A bias input selected on the control panel depresses the horizon bar 3 degrees below the true horizon.

2.2 Operation

From a pilot's point of view during an approach the ground features that are covered by the depressed horizon bar are 3° below the horizontal plane. So when an approach to a runway is made, the aircraft is on a 3° glide path when the depressed horizon bar is on the touch down point. The pilot's task is thus to maintain this bar over his aiming point on the runway.

When the horizon bar overlays the ground in front of the touch down point the aircraft is below a 3° glide path; on the other hand, the aircraft is above the glide path when the horizon bar is beyond the touch down point, see figure 3.

In cross-wind conditions with drift angles of more than 6 degrees, the full length of the horizon bar is on the left-hand or right-hand side of the runway. The pilot then has to mentally extrapolate the horizon bar to the runway to judge his position relative to the touch down point. For the test aircraft - approach speed 105 kts - this condition arises with a cross-wind component more than 11 kts.

It should be stressed that with this HUD presentation no lateral guidance information is given. This information can be drawn from the runway centre line and/or edges and therefore the requirement for lateral guidance on the HUD is much less than the requirement for vertical guidance. Aircraft height during the approach is very difficult to judge especially when little or no texture is visible on the surface below the approach path. The provision of glide path information only has an advantage that a very simple display system is needed. As a consequence the reliability of the HUD is increased, which will have a favourable effect on pilot's acceptance of such a system.

The head down instrumentation available to the subject pilot, consisted of airspeed indicator, altimeter, artificial horizon and directional gyro. The airspeed indicator was installed at the left-hand side of the instrument panel at the position occupied by the radio-altimeter indicator in figure 2. The artificial horizon was very difficult to read due to the obstruction formed by the PDU-mounting. The more complete instrument panel on the left-hand side of the cockpit was also available to the subject pilot, but this of course was difficult to read and the readings were influenced by large parallax errors.

3. TEST PROGRAMME

In the test programme 30 daylight and 12 night approaches were executed in four flights. Table 1 summarizes the approaches in terms of pilots and simulated touch down points (aiming points). In table 2 a detailed review of the test runs - including wind conditions - is given.

The approaches were flown with a Beechcraft Queen Air 80 by three subject pilots. In daylight all subject pilots flew one approach with HUD and one approach without HUD to five aiming points, see figure 4. The ten approaches of a subject pilot were equally divided over two flights. During a flight two pilots alternated as subject and safety pilot. During the night flight three approaches with HUD and an equal number of approaches without HUD were flown by both subject pilots. Only three of the five aiming points were used during the night flight.

Normally a subject pilot made two approaches and then pilots changed. Because of some unsuccessful approaches due to recording equipment or weather, three consecutive approaches had to be made by one pilot occasionally.

The approaches were started at an altitude of 1500 ft at 5 to 7 nm from the aiming point with the aircraft lined up on the "extended centre line" The subject pilot could only use visual cues - or the depressed horizon bar of the HUD - to decide at what position to start his descent.

The approaches were flown with an indicated approach speed of 105 kts, with gear down and 60 % flaps. Before reaching an altitude of about 100 ft an overshoot was initiated.

From table 2 it can be seen that the surface wind conditions during the tests were rather severe, up to 20 kts. Due to the orientation of the approaches variable conditions with respect to head/tail wind and cross-wind were experienced. Both the head wind and cross-wind components are quite normal, however, a tail wind of more than 5 kts is rather unusual.

From this chapter it can be seen that the tests were executed under rather difficult environmental conditions in particular with respect to:

- the absence of ground texture below the approach path
- the difference between the aiming points and the touch down point on a runway
- the severe wind conditions.

4. RESULTS

4.1 Approach parameters

The instrumentation system used to record approach parameters is described in the appendix.

The accurate reconstruction of the aircraft flight path during over water approaches is a difficult problem. In such cases no photographic methods can be used to determine aircraft position from ground features on photographs taken on board the aircraft. Also no optical means or radar were available to track the aircraft.

Distance from the aiming point had to be calculated from ground speed as recorded on the aircraft. The range calculation was started at the end of the approach and performed in the reverse direction.

From the calculated range and the recorded height the approach path in the vertical plane was drawn. Using these graphs the aircraft height at a number of fixed distances from the aiming point was determined. These heights are plotted for both the HUD- and the no-HUD-approaches, for example figures 5a to 5c. From these results mean heights and standard deviations are calculated as a function of range from the aiming point, figures 6a to 6d.

From the recordings the maximum and minimum value of approach speed (calibrated airspeed: V_c) were determined. These values are plotted in figure 7.

The maximum and minimum values of flight path angle (γ), pitch attitude (Θ) and heading (Ψ) were also determined from the recordings. The differences between maximum and minimum values of these parameters are given in figures 8, 9 and 10.

The roll stabilized horizon bar is driven by signals from the platform of a Litton LN-3 inertial system. The synchro outputs of roll and pitch attitude are conditioned in an interface unit to provide the d.c. signals for the WFU. A bias input selected on the control panel depresses the horizon bar 3 degrees below the true horizon.

2.2 Operation

From a pilot's point of view during an approach the ground features that are covered by the depressed horizon bar are 3^{o} below the horizontal plane. So when an approach to a runway is made, the aircraft is on a 3^{o} glide path when the depressed horizon bar is on the touch down point. The pilot's task is thus to maintain this bar over his aiming point on the runway.

When the horizon bar overlays the ground in front of the touch down point the aircraft is below a 3^{o} glide path; on the other hand, the aircraft is above the glide path when the horizon bar is beyond the touch down point, see figure 3.

In cross-wind conditions with drift angles of more than 6 degrees, the full length of the horizon bar is on the left-hand or right-hand side of the runway. The pilot then has to mentally extrapolate the horizon bar to the runway to judge his position relative to the touch down point. For the test aircraft - approach speed 105 kts - this condition arises with a cross-wind component more than 11 kts.

It should be stressed that with this HUD presentation no lateral guidance information is given. This information can be drawn from the runway centre line and/or edges and therefore the requirement for lateral guidance on the HUD is much less than the requirement for vertical guidance. Aircraft height during the approach is very difficult to judge especially when little or no texture is visible on the surface below the approach path. The provision of glide path information only has an advantage that a very simple display system is needed. As a consequence the reliability of the HUD is increased, which will have a favourable effect on pilot's acceptance of such a system.

The head down instrumentation available to the subject pilot, consisted of airspeed indicator, altimeter, artificial horizon and directional gyro. The airspeed indicator was installed at the left-hand side of the instrument panel at the position occupied by the radio-altimeter indicator in figure 2. The artificial horizon was very difficult to read due to the obstruction formed by the PDU-mounting. The more complete instrument panel on the left-hand side of the cockpit was also available to the subject pilot, but this of course was difficult to read and the readings were influenced by large parallax errors.

3. TEST PROGRAMME

In the test programme 30 daylight and 12 night approaches were executed in four flights. Table 1 summarizes the approaches in terms of pilots and simulated touch down points (aiming points). In table 2 a detailed review of the test runs - including wind conditions - is given.

The approaches were flown with a Beechcraft Queen Air 80 by three subject pilots. In daylight all subject pilots flew one approach with HUD and one approach without HUD to five aiming points, see figure 4. The ten approaches of a subject pilot were equally divided over two flights. During a flight two pilots alternated as subject and safety pilot. During the night flight three approaches with HUD and an equal number of approaches without HUD were flown by both subject pilots. Only three of the five aiming points were used during the night flight.

Normally a subject pilot made two approaches and then pilots changed. Because of some unsuccessful approaches due to recording equipment or weather, three consecutive approaches had to be made by one pilot occasionally.

The approaches were started at an altitude of 1500 ft at 5 to 7 nm from the aiming point with the aircraft lined up on the "extended centre line" The subject pilot could only use visual cues - or the depressed horizon bar of the HUD - to decide at what position to start his descent.

The approaches were flown with an indicated approach speed of 105 kts, with gear down and 60 % flaps. Before reaching an altitude of about 100 ft an overshoot was initiated.

From table 2 it can be seen that the surface wind conditions during the tests were rather severe, up to 20 kts. Due to the orientation of the approaches variable conditions with respect to head/tail wind and cross-wind were experienced. Both the head wind and cross-wind components are quite normal, however, a tail wind of more than 5 kts is rather unusual.

From this chapter it can be seen that the tests were executed under rather difficult environmental conditions in particular with respect to:

- the absence of ground texture below the approach path
- the difference between the aiming points and the touch down point on a runway
- the severe wind conditions.

4. RESULTS

4.1 Approach parameters

The instrumentation system used to record approach parameters is described in the appendix.

The accurate reconstruction of the aircraft flight path during over water approaches is a difficult problem. In such cases no photographic methods can be used to determine aircraft position from ground features on photographs taken on board the aircraft. Also no optical means or radar were available to track the aircraft.

Distance from the aiming point had to be calculated from ground speed as recorded on the aircraft. The range calculation was started at the end of the approach and performed in the reverse direction.

From the calculated range and the recorded height the approach path in the vertical plane was drawn. Using these graphs the aircraft height at a number of fixed distances from the aiming point was determined. These heights are plotted for both the HUD- and the no-HUD-approaches, for example figures 5a to 5c. From these results mean heights and standard deviations are calculated as a function of range from the aiming point, figures 6a to 6d.

From the recordings the maximum and minimum value of approach speed (calibrated airspeed: V_c) were determined. These values are plotted in figure 7.

The maximum and minimum values of flight path angle (γ), pitch attitude (θ) and heading (ψ) were also determined from the recordings. The differences between maximum and minimum values of these parameters are given in figures 8, 9 and 10.

4.2 Pilot's opinion

The subject pilots participating in the test programme were all of the opinion that their HUD-approaches were more stable than the no-HUD-approaches; moreover this better performance could be obtained with less effort.

It proved very natural to interpret the indication of the depressed horizon bar and thus to bring and maintain the aircraft on the glide path. Corrections could be made without any noticeable mental effort. Deviations of the depressed horizon bar from the aiming point were already observed when they were still very small.

The difference in approach stability was even more pronounced in night conditions. Visible features on the ground consisted only of some lights at or near the aiming point, so very few ground cues were available in the night approaches. In some approaches without HUD there was a strong tendency to remain far too high until quite close to the aiming point. The aircraft was then brought back to the glide path with a rather steep descent. This is essentially a dangerous situation because of the high rates of descent at low heights. This high rate of descent may be maintained too close to the ground, in particular as the pilot may still have difficulties in estimating his height. Besides large power corrections and attitude changes are needed to fly such a curved approach path.

It is known that several accidents, in good weather conditions, in which aircraft crashed a short distance in front of the runway, can be attributed to this type of approach instability.

In figure 11 recordings of night approaches with and without HUD to aiming point no. 1 - see figure 4 - are given. These approaches were flown by the same pilot. The tendency to remain high on the glide path in the no-HUD-approach, and the absence of this tendency in the HUD-approach, is clear from this comparison.

One of the drawbacks of the HUD is the obstruction of the "combining" glass. Apart from the physical obstruction, an optical obstruction is also present and small details at the limit of the visible range may become unnoticed or be less clear. The pilot therefore has a tendency to look for these details while viewing along the side of the combining glass. For normal viewing, to clear objects, the combining glass is hardly noticeable.

As indicated in paragraph 2.2 the horizon bar is rather short - 6 degrees either side of the centre -. It is to the side of the aiming point in moderate and severe cross-wind conditions (drift angles more than 6 degrees). Although this is an extra complication, the extrapolation of the horizon bar to the aiming point does not bring about large difficulties to the pilot. An enlarged horizon bar would also make this drawback less severe.

5 DISCUSSION

It can be seen clearly from figures 5a to 5c that deviations from a nominal or mean glide path are much less during HUD-approaches and that no striking differences exist between the performance of the three pilots, also the aiming point has no influence on approach accuracy.

In figures 6a to 6d the results of the height measurements are summarized. Statistical analysis has shown no significant difference between the mean height of the HUD- and no-HUD-approaches during daylight. Mean heights are quite close to the nominal height on a 3 degrees glide path; the mean approach angle of the daylight approaches is about 2.8 degrees.

The results of the HUD-approaches at night - figure 6d - compare very well with the daylight HUD-approaches - figure 6b - indicating a very stable approach under varying light conditions. However, the no-HUD-approaches made at night - figure 6c - have a mean height significantly greater than the mean height of the daylight approaches - figure 6a -. These quantitative results are supported by the subjective opinion of the pilots. When not using HUD they observed by themselves a tendency to remain high during the night approaches. The dangers of this line of conduct are already discussed in paragraph 4.2. In figure 11 an example of such an approach is compared with a HUD approach to the same aiming point and flown by the same pilot. Until $t \approx -60$ sec in the no-HUD-approach the aircraft is more than 400 ft above the nominal glide path, that was flown very accurately in the HUD-approach. At $t \approx -45$ sec the pilot starts a steep descent from a height of about 900 ft with a rate of descent of more than 1000 ft/min. This high rate of descent - about twice the value measured during the HUD-approach - is maintained down to about 150 ft. The much less accurate no-HUD-approach was executed after the HUD-approach; so even the effect of having made an approach to the same target only 40 minutes earlier, does not preclude the pilot from making an unstable approach.

The standard deviations of height of the no-HUD-approaches in both daylight and night conditions are significantly greater than those of the HUD-approaches. Without HUD the standard deviations of height are 2 to 4 times as great as the standard deviations of the HUD-approaches. They are about equal for day and night conditions when the HUD is used; however, the standard deviations of height during no-HUD-approaches are even larger at night, see figure 12.

The use of a HUD had no significant influence on other approach parameters. It may be argued that deviations from the reference indicated airspeed (105 kts) should be less during the more stable HUD-approaches. However, figure 7, does not show significant differences between HUD- and no-HUD-approaches. The same applies to flight path angle, pitch attitude and heading as shown in figures 8, 9 and 10.

From this series of tests no noticeable influence of the wind on glide path performance could be found, even though cross-wind components of more than 11 kts, with drift angles more than 6 degrees were experienced. As already explained in paragraph 4.2, in heavy cross-wind conditions the horizon bar is beside the aiming point. The pilot then had to mentally extrapolate the horizon bar to the aiming point to determine his position on the glide path.

At this point some additional remarks on the limitations of the tests are appropriate. Only a limited number of approaches has been made. A more elaborate series of tests is necessary to evaluate the HUD in more detail, especially with regard to the influence of the weather. The weather conditions were about the same in three of the four flights with surface winds of 15 to 20 kts; during the first flight the wind was much less, only 5 kts. These differences do not warrant definite conclusions with regard to wind influence - see table 2-.

In the present tests only roll angle and heading have been measured; as already mentioned before no differences between HUD and no-HUD-approaches could be determined from these parameters. However, lateral performance - e.g. deviations from the extended centre line - could not be measured in this test series.

The test results apply to the Beechcraft Queen Air 80 with the HUD-system as discussed in chapter 2 The application of these results to other aircraft and HUD-systems (symbology and sensors) should only be done with care.

6 CONCLUSIONS

In a series of flight tests with a Beechcraft Queen Air 80, approaches have been made to evaluate a simple HUD as an approach aid in good visibility conditions. From these tests the following conclusions can be drawn.

- In daylight conditions no significant difference in the mean height during HUD- and no-HUD-approaches was observed. Standard deviations of height, however, are decreased by a factor of 2 to 4 using a HUD.
- In night conditions there is a marked tendency to remain high above the glide path, resulting in a high rate of descent at low altitude when no HUD is used as an approach aid. With the HUD, approach accuracy is not deteriorated with regard to daylight conditions.
- The increased accuracy in height performance with the HUD was not reflected in a significantly increased stability of the other approach parameters such as indicated airspeed or flight path angle.
- The three subject pilots, who have flown the approaches agreed that the HUD was a valuable aid in good visibility conditions. As approach conditions became more difficult - because of a decrease in the texture visible on the ground - the subjective value of even this simple HUD increased. When using the HUD, the pilot's task was much easier than without HUD, especially at night.
- The results of these tests have been obtained from a relatively small number of approaches flown with one aircraft. The application of the tests to other circumstances should only be done with proper care.

7. REFERENCES

1 Report of Symposium: All weather operations / Head-up displays / Long range navigational aids. International Federation of Air Line Pilots Associations (IFALPA). Rotterdam, 13th - 16th October 1965.

2 Wieser, M.F. von — Operating a head-up display. Shell Aviation News, No.411 - 1972, pages 14-19.

3 Naish, J.M. — Application of the head-up display (HUD) to a commercial jet transport. Journal of Aircraft, August 1972, pages 530-536.

4 De Celles, J.L. Burke, E.J. Burroughs, K. — A real world situation display for all weather landing. AGARD - CP - 105. June 1972.

5 Harlow, R.A. — Flight assessment of head-up display as a clear weather approach aid. RAE TR 71141. July 1971.

6 Elson, Benjamin M. — Visual approach monitor being certified. Aviation Week and Space Technology, April 3, 1972, pages 37-39.

7 Koitsch, Paul A. — Visual approach monitor; a first step to head-up display. Shell Aviation News no.411-1972, pages 7-10.

8 Lamers, G.L. — Preliminary tests to evaluate a head-up display as an approach aid in good visibility conditions. NLR Memorandum VV-73-003, February 1973.

Table 1

Classification of approaches

	Aiming point / HUD *)	Flight 1					Flight 2					Flight 3					Flight 4		
		1	2	3	4	5	1	2	3	4	5	1	2	3	4	5	1	2	3
Pilot 1 (Δ) **)	1				X	X						X	X	X					
	2	X	X	X											X	X			
Pilot 2 (□)	1	X	X	X						X	X						X	X	X
	2				X	X	X	X	X								X	X	X
Pilot 3 (○)	1						X	X	X						X	X	X	X	X
	2									X	X	X	X	X			X	X	X

*) HUD 1: no HUD
HUD 2: displaced horizon bar

**) Symbols used in figures to indicate subject pilots

Table 2

Details of approaches

Flight	Run nr.	Pilot	Aiming point	HUD	Headwind (+) Tailwind (-) (kts)	Cross-wind L (-) R (+) (kts)
1	44	2	4	X	- 5	-
	45	2	2		-	+ 5
	46A	1	3	X	+ 5	-
	46B	1	4		- 5	-
	47	2	1		- 5	-
	48	2	5	X	-	- 5
	49	1	2	X	-	+ 5
	50	2	3		+ 5	-
	51	1	1	X	- 5	-
	52	1	5		-	- 5
2	53	3	5	X	+ 8	-15
	54	2	2	X	- 7	+15
	55	2	4		-12	-10
	56	3	3		+15	+ 7
	57	3	1		-15	- 8
	58	2	5		+ 8	-15
	59	2	1	X	-15	- 8
	60	2	3	X	+15	+ 7
	62	3	4	X	-12	-10
	63	3	2		- 7	+15
3	66	3	5		-19	-
	67	3	3	X	-	-19
	68	1	4	X	- 3	+19
	69	1	2		+19	+ 3
	70	1	1		-	+19
	71	3	2	X	+19	+ 3
	72	3	1	X	-	+19
	73	3	4		- 3	+19
	74	1	3		- 3	-19
	77	1	5	X	-19	-
4 nightfl.	78	3	2		+15	- 5
	79	3	3	X	- 5	-15
	80	2	2	X	+15	- 5
	81	2	1		+ 4	+15
	82	3	3		- 5	-15
	83	3	1	X	+ 4	+15
	84	2	2		+15	- 5
	85	2	3	X	- 5	-15
	86	3	2	X	+15	- 5
	87	3	1		+ 4	+15
	88	2	3		- 5	-15
	89	2	1	X	+ 4	+15

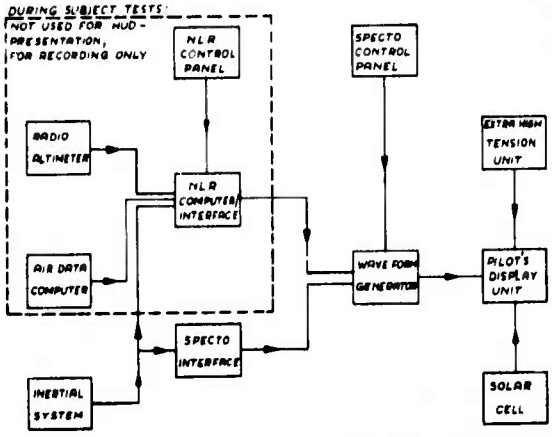

FIG. 1: BLOCK DIAGRAM OF THE HUD– SYSTEM.

FIG. 2: PILOT'S DISPLAY UNIT IN THE COCKPIT OF THE BEECHCRAFT QUEEN AIR 80.

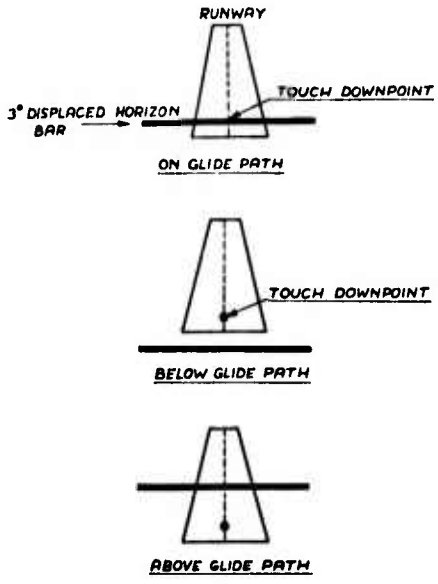

FIG. 3: THE POSITION OF A 3° DEPRESSED HORIZON DURING AN APPROACH.

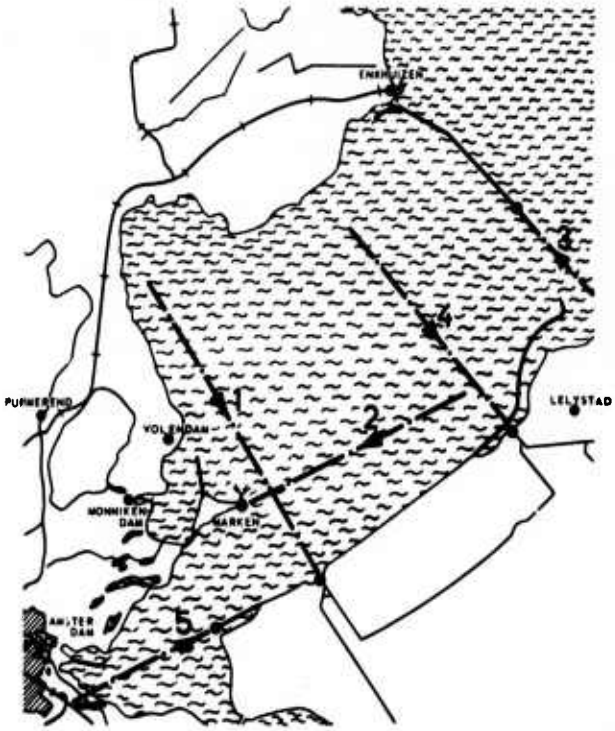

FIG. 4: OVER WATER APPROACHES FLOWN DURING TESTS.

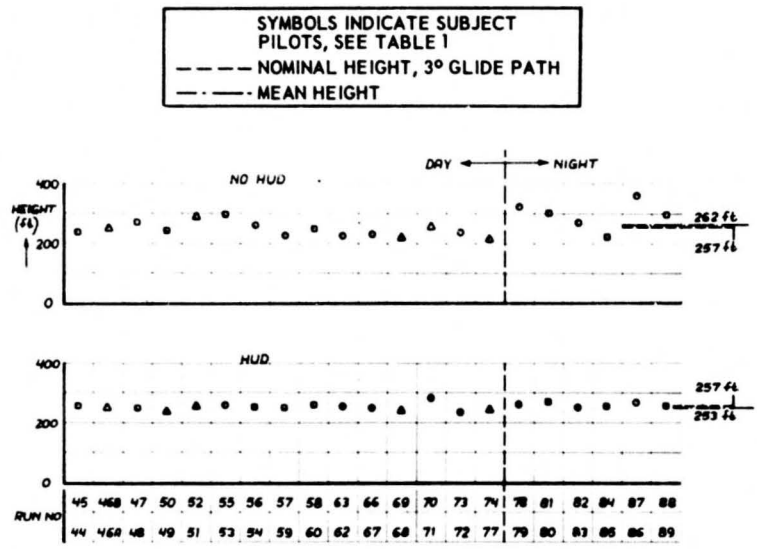

FIG. 5a: RANGE 1500 m.

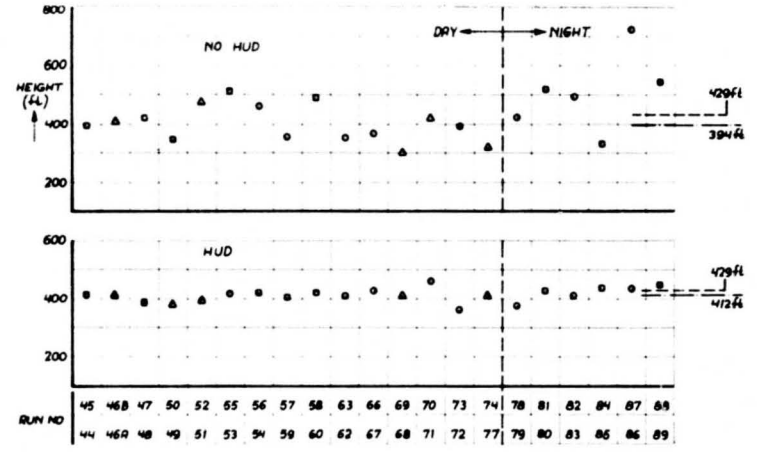

FIG. 5b: RANGE 2500 m.

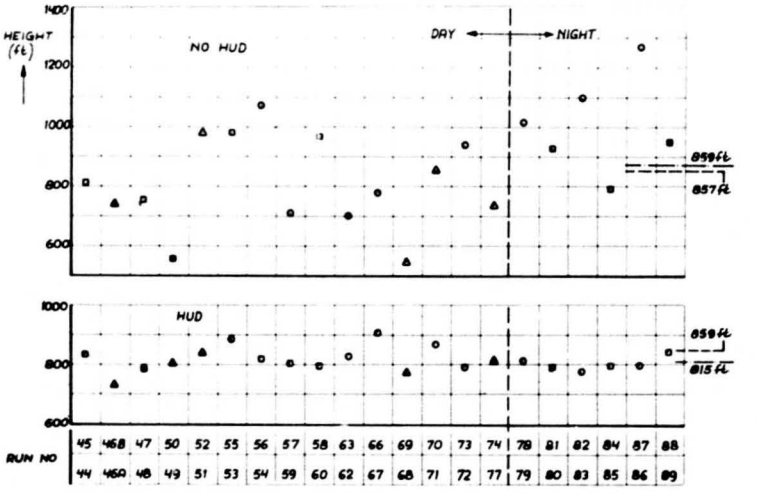

FIG. 5c. RANGE 5000 m.

FIG. 5: AIRCRAFT HEIGHT AT SPECIFIC RANGES FROM THE AIMING POINT DURING NO– HUD– AND HUD– APPROACHES.

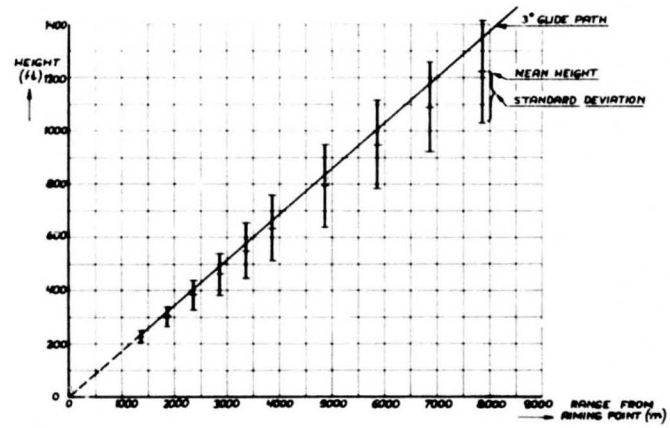

FIG. 6a: DAYLIGHT APPROACHE: NO – HUD.

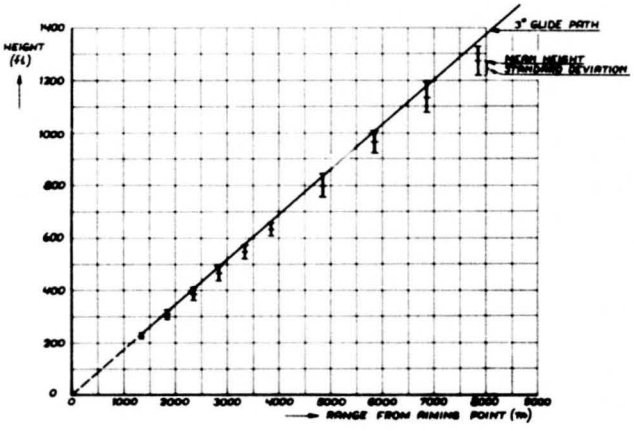

FIG. 6b: DAYLIGHT APPROACHES; HUD.

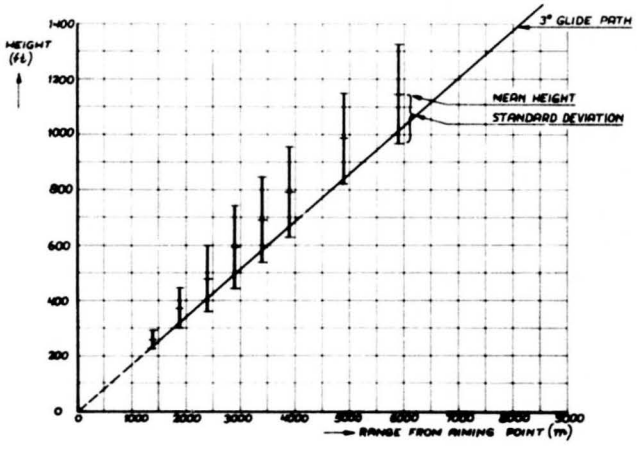

FIG. 6c: NIGHT APPROACHES; NO – HUD.

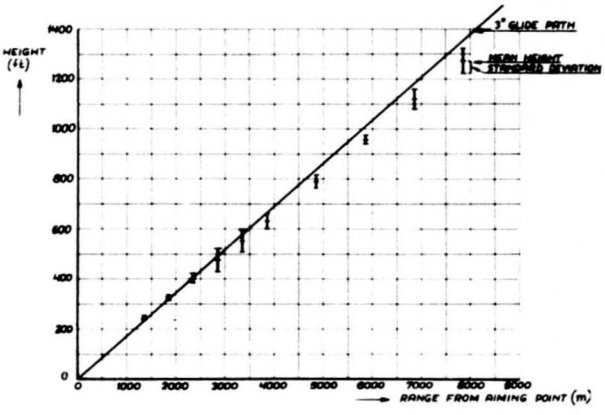

FIG. 6d: NIGHT APPROACHES; HUD.

FIG. 6: HEIGHT PERFORMANCE DURING APPROACHES.

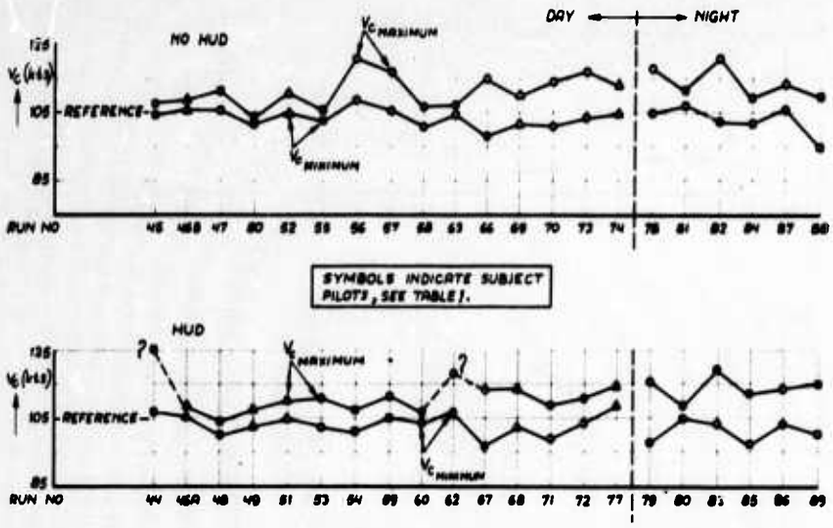

FIG. 7: MAXIMUM AND MINIUM CALIBRATED AIR SPEED (V_c) DURING NO– HUD– AND HUD– APPROACHES.

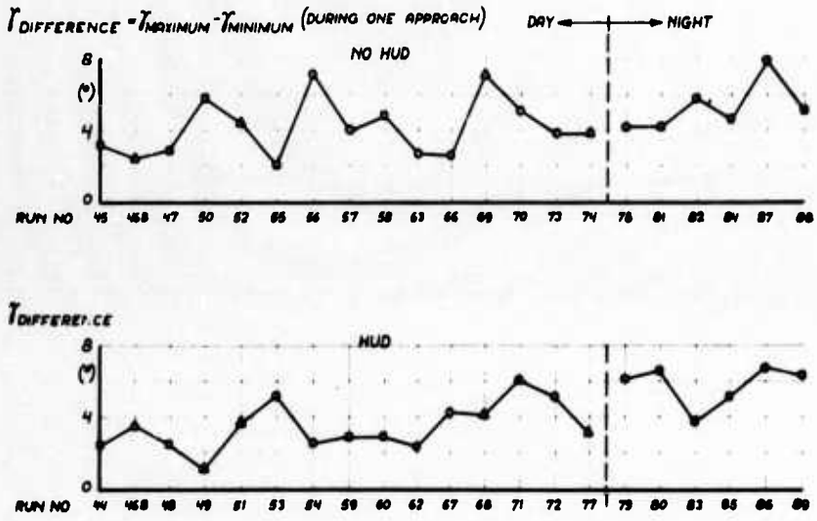

FIG. 8: "RANGES" OF FLIGHT PATH ANGLE (γ) DURING NO– HUD– AND HUD– APPROACHES.

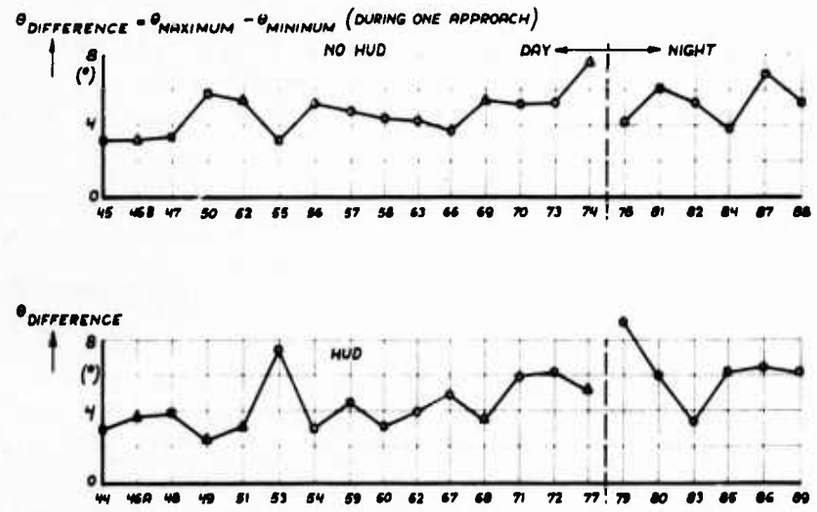

FIG. 9: "RANGES" OF PITCH ATTITUDE (θ) DURING NO– HUD– AND HUD– APPROACHES.

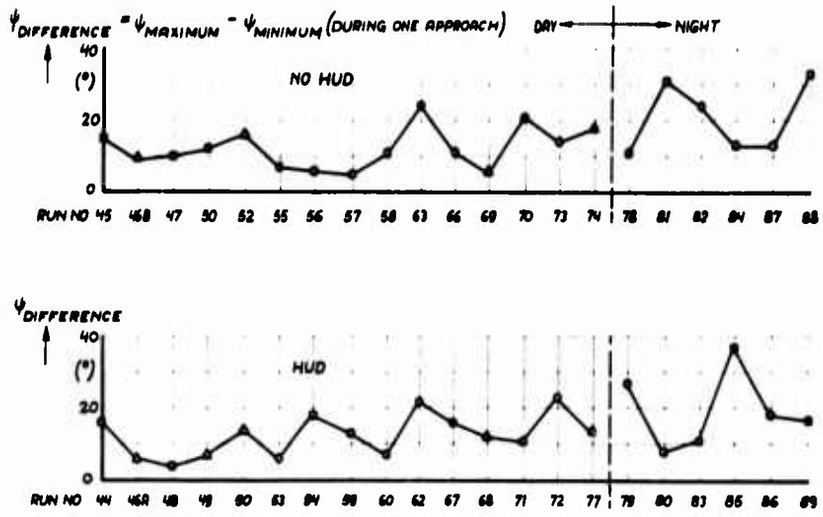

FIG. 10: "RANGES" OF HEADING (ψ) DURING NO-HUD- AND HUD- APPROACHES.

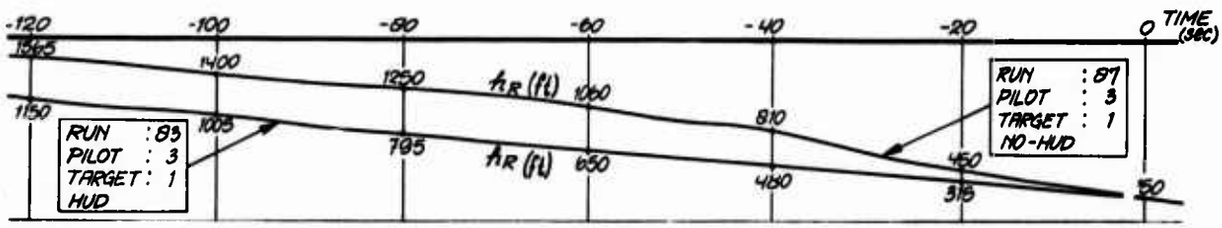

FIG. 11: NIGHT APPROACHES TO THE SAME AIMING POINT, FLOWN BY THE SAME PILOT WITH AND WITHOUT HUD.

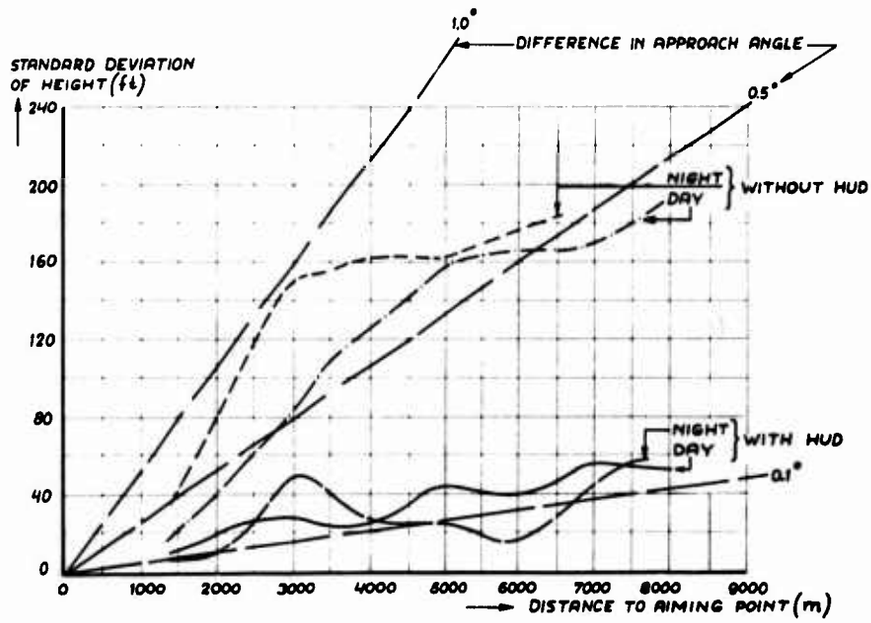

FIG. 12: COMPARISON OF STANDARD DEVIATIONS OF HEIGHT FROM APPROACHES WITH AND WITHOUT HUD.

Instrumentation

In order to obtain relevant data from the approaches the following parameters were recorded on an ACB-Schlumberger A 1322 trace recorder, running at 4 mm per sec:

Flight parameter		Sensor	Range
calibrated airspeed:	V_c	air data computer	90 - 120 kts
ground speed:	V_g	inertial system	70 - 135 kts
height:	h_R	radio-altimeter	0 - 1500 ft
flight path angle:	γ	inertial system and air data computer	-9° - $+3^\circ$
pitch attitude:	θ	inertial platform	-10° - $+10^\circ$
roll angle:	ϕ	inertial platform	-30° - $+30^\circ$
heading:	ψ	inertial platform	-45° - $+45^\circ$
event marking			

The calibrated airspeed was recorded as the difference from the reference speed during the approaches: 105 kts.

The aircraft height was measured with a radio-altimeter.

The flight path angle was calculated from vertical speed and ground speed. The ground speed was obtained from the inertial system, while vertical speed was obtained by integrating the vertical acceleration signal from the platform. In order to eliminate drift effects this signal was combined with the vertical speed from the air data computer.

The heading of the aircraft was recorded as the difference from the "runway" heading.

LE SYSTEME D'ATTERRISSAGE TOUS TEMPS DU MERCURE

par

Armand Pilé
Avions Marcel Dassault/Bréguet Aviation
78, quai Carnot
92210 - SAINT-CLOUD
FRANCE

RESUME

Les différentes versions du système d'atterrissage tous temps du MERCURE sont rappelées en introduction. Ce papier est ensuite consacré à la description des caractéristiques principales de l'une des versions du système, dans laquelle le commandant de bord dispose d'informations collimatées "tête haute" destinées à améliorer son appréciation à la hauteur de décision et à faciliter sa tâche dans le cas où un retour en pilotage manuel serait nécessaire.

INTRODUCTION

Le système d'atterrissage tous temps du MERCURE, conçu dès l'origine pour satisfaire aux exigences de la Catégorie III, se caractérise par une très grande facilité d'adaptation aux impératifs opérationnels propres à chaque exploitant. Plusieurs versions sont ainsi possibles, réalisées à partir d'éléments de base communs. Des ensembles BENDIX PB 75 M en constituent la partie centrale, et assurent les fonctions de Pilote Automatique (PA) et Directeur de Vol (DV). Une automanette et un calculateur de Décrabe séparés, fournitures A.M.D./B.A., complètent le système.

Une version opérationnelle après panne permet de satisfaire aux exigences de la Catégorie III A OACI. Elle comporte deux chaînes Pilote Automatique/Directeur de Vol (Fig. 1), entièrement séparées, fonctionnant en permanence durant l'approche et l'atterrissage automatique. Chaque chaîne est monitorée et détecte ses propres pannes. En cas de défaillance d'une chaîne, celle-ci est automatiquement déconnectée et le pilotage de l'avion est assuré jusqu'à l'impact par la chaîne intègre.

Une version opérationnelle après panne avec références visuelles permet de satisfaire aux exigences de la Catégorie III avec une hauteur de décision de 50 ft associée à une portée visuelle de piste de 150 m. Elle comporte une chaîne Pilote Automatique/Directeur de Vol, passive après panne, et une chaîne de présentation d'informations de pilotage sur un collimateur tête haute, ou "Head-Up Display" (Fig. 3). Chaque chaîne est monitorée et détecte ses propres pannes. Le système comprend également une chaîne Directeur de Vol copilote, distincte des deux précédentes. En cas de défaillance de la chaîne Pilote Automatique, celle-ci est automatiquement déconnectée et une alarme de reprise en mains est fournie à l'équipage. Si un contact visuel extérieur satisfaisant a été établi - c'est le cas au-dessous de la hauteur de décision - il est alors possible de poursuivre l'approche en pilotage manuel à l'aide des informations collimatées dans le champ des références visuelles du commandant de bord.

Une version passive après panne permet de satisfaire aux exigences de la Catégorie III avec hauteur de décision dans des conditions d'exploitation analogues à celles des CARAVELLE de la Compagnie AIR-INTER. Cette version est semblable à la précédente, mais ne comporte pas le collimateur tête haute (Fig. 2). En cas de défaillance de la chaîne Pilote Automatique, en conditions de visibilité de Catégorie III, l'apparition de l'alarme de reprise en mains doit être suivie d'une procédure d'approche interrompue.

Il existe enfin, mentionnée ici pour mémoire, une version sans calculateur d'arrondi, satisfaisant aux exigences de la Catégorie II.

L'objet du présent papier est de présenter le système d'atterrissage tous temps dans sa version avec collimateur, qui équipe les MERCURE destinés à la Compagnie AIR-INTER.

CONCEPTS OPERATIONNELS

Dans la version AIR-INTER du système d'atterrissage tous temps du MERCURE, une hauteur de décision de 50 ft, associée à une portée visuelle de piste de 150 m a été choisie en accord avec les autorités françaises de certification. L'adoption d'une hauteur de décision non nulle, qui n'est pas explicitement imposée dans la définition de la Catégorie III OACI, appelle les commentaires suivants :

- Si une autorisation d'emploi en Catégorie III A (portée visuelle de piste comprise entre 200 m et 400 m) a déjà été donnée, les Catégories III B et III C, qui n'imposent aucune référence visuelle dans la phase finale de l'atterrissage, semblent ne pas être envisageables dans l'état actuel des aéroports, dont l'installation de guidage standard est l'ILS. Dans ce cas, et quelles que soient les qualités des systèmes à bord des avions, il est en effet indispensable, avant l'atterrissage, de contrôler que la trajectoire radio-électrique suivie par l'avion aboutit correctement sur la piste.

- La nécessité d'un contrôle final étant admise, l'expérience acquise sur les CARAVELLE d'AIR-INTER montre qu'il est pratiquement toujours possible, au niveau des yeux du pilote, d'apercevoir la piste à une hauteur au moins égale au 1/8ème environ de la portée visuelle de piste annoncée. Pour un avion comme le MERCURE, et pour une portée visuelle de piste de 150 m, la hauteur des roues dans ce cas est supérieure à 50 ft. Dès lors, il est possible d'imposer une hauteur de décision limite de 50 ft sans introduire de contrainte opérationnelle. L'avantage est, par contre, important, puisque l'application d'une hauteur de décision de 50 ft donne l'assurance d'une trajectoire correcte, par un contrôle qui s'effectue au plus tard à une hauteur où, si nécessaire, la remise de gaz peut encore s'effectuer avec l'assurance de ne pas toucher le sol. Ce dernier point est fondamental puisque, si le contact visuel n'est pas établi à la hauteur de décision, il n'est pas possible d'être sûr que l'avion soit au-dessus de la piste.

STRUCTURE GENERALE DU SYSTEME

Nous ne reviendrons pas sur la définition de principe de la version AIR-INTER, déjà exposée. Dans tout ce qui suit, nous ne ferons mention que des éléments intervenant au cours de la partie finale de l'approche, au-dessous de 1000 ft, altitude à laquelle intervient la sélection du mode LAND par l'équipage. Les phases de capture Localiseur et Glide et d'acquisition de vitesse par l'automanette ne seront donc pas décrites. Les fonctions directeur de vol et amortisseur de lacet, dont l'utilisation est facultative, ne seront pas non plus abordées.

Nous considérons les sous-systèmes suivants :

- Sous-système pilote automatique :

Le pilote automatique contrôle les axes de profondeur et de gauchissement. En atterrissage automatique, il utilise les informations délivrées par le gyroscope de verticale n° 1, le radio-altimètre n° 1, le récepteur ILS n° 1, et l'accéléromètre normal n° 1.

Il comprend un calculateur de tangage, un calculateur de roulis et un adaptateur aux commandes de vol, auxquels il convient d'ajouter l'étage d'amplification et d'asservissement des servo-commandes auxiliaires électro-hydrauliques de profondeur et de gauchissement, qui transmettent à la timonerie les ordres du pilote automatique.

Un système de trim automatique, mentionné ici pour mémoire, asservit la position du plan horizontal au dispositif de restitution d'effort en profondeur.

- Sous-système automanette :

Une automanette assure, lorsqu'elle est utilisée, la commande automatique des manettes de gaz pour l'acquisition et le maintien d'une vitesse de l'avion préaffichée. Elle effectue également la réduction automatique des gaz au cours de la manoeuvre d'arrondi.

Le calculateur d'automanette utilise des informations élaborées par les centrales aérodynamiques, les accéléromètres longitudinaux, le gyroscope de verticale n° 1, le radio-altimètre n° 1. Il envoie des ordres électriques au vérin d'automanette, qui actionne les manettes de gaz par l'intermédiaire d'un embrayage.

- Sous-système décrabe :

Un dispositif de décrabe assure, lors de l'atterrissage automatique, la remise de l'avion dans l'axe de la piste par action sur la commande de lacet.

Le calculateur de décrabe fonctionne à partir des informations d'écarts QFU-Cap et d'altitude radio-altimétrique. Il envoie des ordres électriques au vérin de décrabe, qui agit sur les gouvernes de direction par l'intermédiaire de la commande de trim.

- Sous-système collimateur, ou "Head-Up Display" :

Le rôle du collimateur est de présenter dans le champ des références visuelles extérieures du commandant de bord les informations qui lui sont nécessaires dans le cas où, par suite d'une défaillance du système de pilotage automatique, il reçoit l'ordre de reprendre en mains l'appareil (apparition du voyant FLASH). En fonction de ses éléments d'appréciation, le commandant de bord peut alors décider de poursuivre l'atterrissage en pilotage manuel, à l'aide des informations collimatées suivantes (Fig.4) :

. assiette de roulis pour le maintien des ailes horizontales,
. assiette de tangage,
. barre d'incidence dont la présence au voisinage de la maquette fixe facilite la manoeuvre d'arrondi.

En cas de décision de remettre les gaz, les informations collimatées suivantes sont utilisées :

. assiette de tangage avec repère spécialisé pour la remise des gaz,
. assiette de roulis pour le maintien des ailes horizontales,
. écart de cap.

Pour réaliser ces fonctions, le collimateur reçoit des signaux en provenance du gyroscope de verticale n° 3, indépendant des chaînes pilote automatique et directeur de vol pilote et copilote, et reçoit également des informations d'incidence.

En complément, le collimateur fournit une indication de tendance latérale, qui assure les fonctions d'écart de cap, utilisée en cas de remise des gaz, et de roulage au sol ou tenue d'axe de piste, disponible à partir du début de la manoeuvre de décrabe. Les informations utilisées sont alors l'écart QFU-Cap et l'écart Localiseur. Enfin, le collimateur comprend deux voyants de hauteur de décision (DH), ainsi qu'un voyant de panne de la fonction décrabe.

PERFORMANCES ET LOIS DE PILOTAGE

Les performances du système satisfont aux exigences de l'Advisory Circular 20-57 A de la FAA, qui définit les critères de certification des systèmes d'atterrissage automatique pour les avions de transport civil.

Il a été choisi de tirer un maximum d'avantages des excellentes qualités de vol de l'avion en vue de parvenir à des lois de pilotage aussi simples que possible, afin de conférer au système une meilleure crédibilité et une fiabilité plus grande. Aussi, les lois de pilotage utilisées sont-elles généralement classiques, et nous n'en décrirons ci-après que quelques-uns des caractères principaux.

- Axe de tangage (Fig. 5) :

Durant la partie finale de l'approche et l'atterrissage, les seules informations utilisées sont l'écart Glide, l'accélération normale, l'altitude radio-altimétrique et l'assiette longitudinale. Il n'est pas fait appel aux informations anémométriques, qui ne sont utilisées qu'au-dessus de 1000 ft. On s'affranchit ainsi des pannes éventuelles de ces informations, et des perturbations possibles qu'elles peuvent apporter avant l'atterrissage lorsque se manifeste l'effet de sol.

Durant la phase de tenue de faisceau Glide, l'écart Glide est progressivement affaibli en fonction de l'altitude radio-altimétrique. Un signal dérivé peu bruité de cet écart est obtenu après filtrage complémentaire avec un terme d'accélération normale pseudo-intégré. Une partie du signal dérivé est à son tour utilisée pour le filtrage complémentaire de l'écart Glide.

A l'altitude de 60 ft, l'information de Glide n'est plus prise en compte dans le système, tandis qu'un programme de réduction de vitesse verticale assure, en fonction de l'altitude radio-altimétrique, la commande d'arrondi. Le retour d'asservissement en vitesse verticale est obtenu par dérivation de l'altitude radio-altimétrique et filtrage complémentaire avec l'accélération normale pseudo-intégrée. Le signal d'erreur est soumis à une limitation dissymétrique. La limite à cabrer est constante. Une faible autorité à piquer est également disponible et s'établit progressivement à partir d'une valeur nulle en début d'arrondi. Compte tenu des niveaux de la vitesse verticale programmée et de la limite sur le signal de vitesse verticale, tout à coup en début d'arrondi se trouve évité par le jeu de la limitation dissymétrique variable.

- Axe de roulis (Fig. 6) :

Durant la partie finale de l'approche et l'atterrissage, les seules informations utilisées sont l'écart Localiseur, l'altitude radio-altimétrique et l'assiette latérale. Pour les mêmes raisons que sur l'axe de tangage, aucune information anémométrique n'intervient dans le système au-dessous de 1000 ft. Il en est de même pour les informations de cap.

L'écart Localiseur est progressivement affaibli en fonction de l'altitude radio-altimétrique. Un signal dérivé peu bruité de cet écart est obtenu après filtrage complémentaire avec un terme d'assiette latérale pseudo-intégrée. Une partie du signal dérivé est à son tour utilisée pour le filtrage complémentaire de l'écart Localiseur. L'inclinaison commandée voit son autorité réduite en fonction de l'altitude radio-altimétrique. A 32 degrés durant la capture et jusqu'à 1000 ft, cette autorité décroît jusqu'à 5 degrés au voisinage du sol.

- Automanette (Fig. 7) :

Le calculateur d'automanette fait appel aux informations d'écart de vitesse indiquée, d'accélération et d'assiette longitudinale, d'altitude radio-altimétrique.

Les circuits de calcul sont particulièrement simples, l'avion étant très stable en vitesse.

L'accélération longitudinale est corrigée de l'assiette de l'avion de manière à donner une approximation satisfaisante de l'accélération selon la vitesse, qui vient amortir le terme d'écart de Vi. L'ensemble est traité par un filtre passe-bas tandis qu'une partie limitée de l'écart de Vi est intégrée. Un retour tachymétrique direct et intégré assure l'asservissement du moteur d'entrainement des manettes.

A l'altitude radio-altimétrique de 30 ft, un signal de commande des manettes à vitesse constante se substitue à l'erreur d'asservissement pour effectuer la réduction automatique des gaz.

- Décrabe (Fig. 8) :

Le calculateur de décrabe utilise les informations d'écart de cap par rapport au QFU de la piste, et l'altitude radio-altimétrique.

Les essais en vol de l'avion ayant montré qu'il était possible d'effectuer la manoeuvre de décrabe au moment de l'impact, à l'aide de la seule commande de direction, cet avantage a été mis à profit pour réaliser des circuits de calcul d'une extrême simplicité.

A l'altitude radio-altimétrique de 7 ft, l'écart de cap est mémorisé, et un déplacement de drapeau proportionnel à cet écart est commandé à vitesse constante. Lorsque l'avion se trouve ramené dans l'axe de la piste, le système de décrabe est automatiquement déconnecté.

SECURITE ET PRINCIPES DE SURVEILLANCE

Le très haut niveau de sécurité requis pour un système d'atterrissage tous temps ne doit pas être atteint au prix d'un important accroissement de complexité, qui tende à diminuer la crédibilité des démonstrations et à réduire la disponibilité en ligne. C'est pourquoi, là encore, la recherche d'un maximum de simplicité est apparue comme un souci constant lors de la conception et de la mise au point du système.

Les démonstrations de sécurité du système portent sur trois groupes essentiels de justifications :

- Influence des performances sur la sécurité. Il s'agit de démontrer que quelles que soient les causes perturbatrices possibles externes ou internes au système, le cas d'un impact en dehors du domaine admissible de sécurité est extrêmement rare.

- Etude des conséquences et des conditions de détection des pannes ou combinaisons de pannes des circuits de calcul. Il s'agit de démontrer que les situations correspondantes de l'avion ne peuvent être catastrophiques, à moins qu'elles ne soient extrêmement improbables, ni critiques, à moins qu'elles ne soient extrêmement rares.

- Justification des logiques de surveillance et d'alarmes. Il s'agit de démontrer que la conception et la réalisation des sécurités est telle que la non passivation du système ou la non apparition de l'alarme de reprise en mains après détection d'une panne est extrêmement improbable.

La figure 9 résume les principes d'élaboration des informations de pannes dans les chaînes de pilotage automatique roulis/tangage :

- pannes détectées par les comparateurs des chaînes de calcul,
- pannes au niveau de l'étage électro-hydraulique des commandes de vol,
- pannes au niveau des capteurs.

Les chaînes de calcul du pilote automatique sont surveillées selon la technique des points consolidés (Fig. 10). Le principe en est bien connu et permet d'adopter pour les comparateurs des seuils de détection efficaces sans risquer de compromettre le taux de réussite des approches. Une étude statistique faisant intervenir les tolérances des divers composants a permis d'approcher au mieux la définition des seuils optimaux.

L'étage électro-hydraulique des commandes de vol est surveillé de la façon suivante :

. Les circuits d'asservissement des servo-commandes auxiliaires électro-hydrauliques de profondeur et de gauchissement sont entièrement doublés, avec comparaison des étages d'amplification et des retours de position des servo-commandes. Sur chaque axe, les deux chaînes reçoivent, sur deux voies séparées, des ordres identiques de braquage des gouvernes en provenance du pilote automatique.

. Un verrou électrique contrôle en permanence que l'asservissement est correct, ce qui permet la détection d'une défaillance éventuelle de la partie mécanique de l'équipement.

Les informations analogiques délivrées par les capteurs au pilote automatique sont doublées.

La validité de la référence de verticale est obtenue grâce à une comparaison triple, avec lever de doute, entre les trois ensembles de verticale.

Le radio-altimètre et le récepteur ILS, dont l'auto-surveillance est très poussée, fournissent leurs propres signaux de validité.

L'accéléromètre normal est double. Un signal de validité est élaboré à partir d'une comparaison interne.

L'ensemble des signaux de validité est géré dans les logiques de panne du système et provoque, en cas de panne détectée, la déconnexion du pilote automatique et l'apparition de l'alarme de reprise en mains.

Automanette et décrabe sont surveillés selon des principes analogues, mais la détection d'une panne dans ces équipements déclenche la seule déconnexion du sous-système concerné et l'apparition d'une alarme spécifique.

Le collimateur est également autosurveillé, et toute panne détectée au niveau des capteurs dont il utilise les informations, ou au niveau de l'asservissement des réticules, provoque l'escamotage des figurations concernées.

Un dispositif de détection des écarts excessifs ILS, requis par les autorités françaises de certification, complète l'ensemble des surveillances. Indépendant du pilote automatique, ce dispositif est doublé et reçoit les écarts ILS en provenance des deux récepteurs. Il provoque, pour tout franchissement des seuils d'écarts Localiseur ou Glide, l'apparition d'une alarme située au-dessus de chaque ADI. En-dessous de 200 ft, cette alarme déclenche l'alarme de reprise en mains.

UTILISATION (Fig. 11)

Le collimateur est mis en position au cours de l'approche intermédiaire. Un test permet alors le contrôle du bon fonctionnement des asservissements des réticules et des sécurités qui leur sont associées.

La visualisation des phases successives de l'approche est assurée sur les tableaux de progression d'approche pilote et copilote situés à côté de chaque ADI : capture et tracking Localiseur (voyants V/L), capture et tracking Glide (voyants G.S.), armement et engagement de la fonction arrondi (voyants FLARE), armement et engagement de la fonction décrabe (voyants DECRAB), armement et engagement de la fonction remise des gaz automatique (voyants G.A.).

Au-dessus de chaque ADI figurent les alarmes pilote automatique (A/P), automanette (A/T), écarts excessifs ILS, flag généralisé. Les voyants "flag généralisé" constituent un répétiteur (ou master warning) des flags des principaux indicateurs.

A l'altitude de 1000 ft, les voyants FLARE des tableaux de progression d'approche clignotent ambre, invitant l'équipage à la sélection du mode d'atterrissage automatique. L'action sur le poussoir LAND du boîtier d'affichage de mode déclenche alors le "Preland Test", qui permet le contrôle de l'intégrité des sécurités du système. Le test s'achève vers 800 ft par l'allumage vert ou rouge des voyants d'intégrité Catégorie III aux tableaux de progression d'approche, cependant que les voyants FLARE et DECRAB signalent l'armement correct de ces fonctions.

A partir de 300 ft, le commandant de bord regarde exclusivement dehors, à travers le collimateur.

A l'altitude de 60 ft débute la manoeuvre d'arrondi ; les voyants FLARE passent verts. Le décrabe s'effectue à 7 ft, juste avant l'impact. Après le toucher des roues, le commandant de bord reprend le contrôle de l'avion pour la phase de roulage en s'aidant, en cas de visibilité réduite, de l'information de tendance latérale présentée dans le collimateur.

Durant la partie finale de l'approche et l'atterrissage, et une fois les tests effectués, toute défaillance de la chaîne de pilotage automatique se traduit par le débrayage de celle-ci et l'apparition de l'alarme de reprise en mains, ou FLASH, placée devant chaque pilote dans le bourrelet de l'auvent. Rouge clignotant, le FLASH a été conçu et réalisé pour être immanquablement perçu par l'équipage. Le commandant de bord doit alors reprendre en mains l'appareil. En l'absence de références visuelles extérieures, il effectuera une procédure d'approche interrompue au collimateur. Si les références visuelles sont acquises - ce qui est le cas si la panne survient au-dessous de la hauteur de décision - le commandant de bord aura la faculté d'achever l'atterrissage à la main, à l'aide du collimateur, qui enrichit ces références des informations d'assiettes et d'incidence.

En cas de panne de l'automanette, il a été démontré que l'approche pouvait se poursuivre dans des conditions satisfaisantes de sécurité, la charge de travail de l'équipage n'étant que très faiblement augmentée. Toutefois, si à 50 ft la panne n'est pas reconnue par l'équipage ou si, a fortiori, la panne survient au-dessous de 50 ft, l'alarme de reprise en mains est déclenchée.

En cas de panne du décrabe, il a été démontré que, sans nuire à la sécurité ni au confort des passagers, le nez de l'avion pouvait être aisément ramené dans l'axe de la piste, par une action au palonnier exercée juste après l'impact.

Enfin, en cas de disparition des informations collimatées d'assiettes, l'approche automatique peut être poursuivie mais la remise de gaz, si nécessaire, devra s'effectuer à l'horizon de secours. (Cas d'un contact visuel insuffisant à la hauteur de décision de 50 ft, ou cas très improbable d'une alarme de reprise en mains survenant au cours de la même approche).

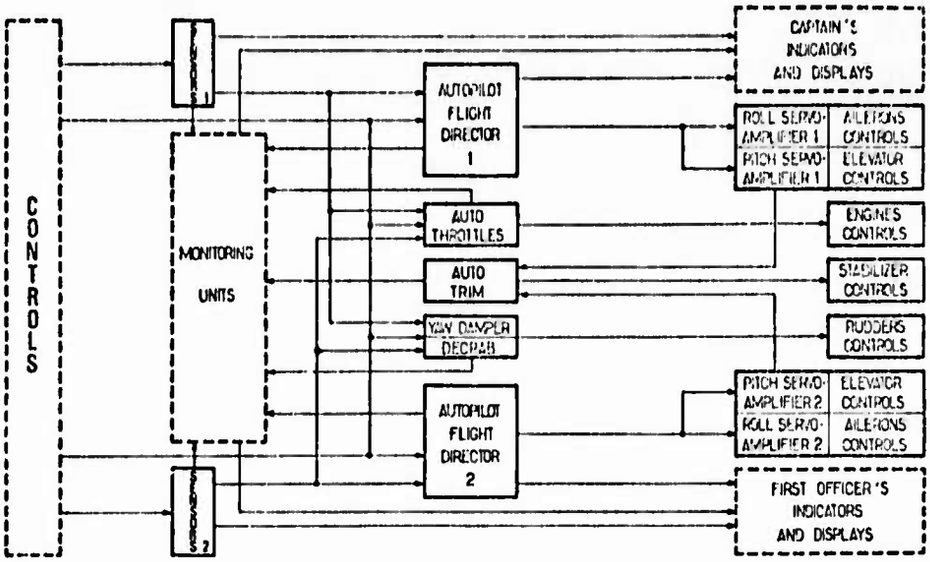

FIG. 1 - FAIL-OPERATIONAL CONFIGURATION

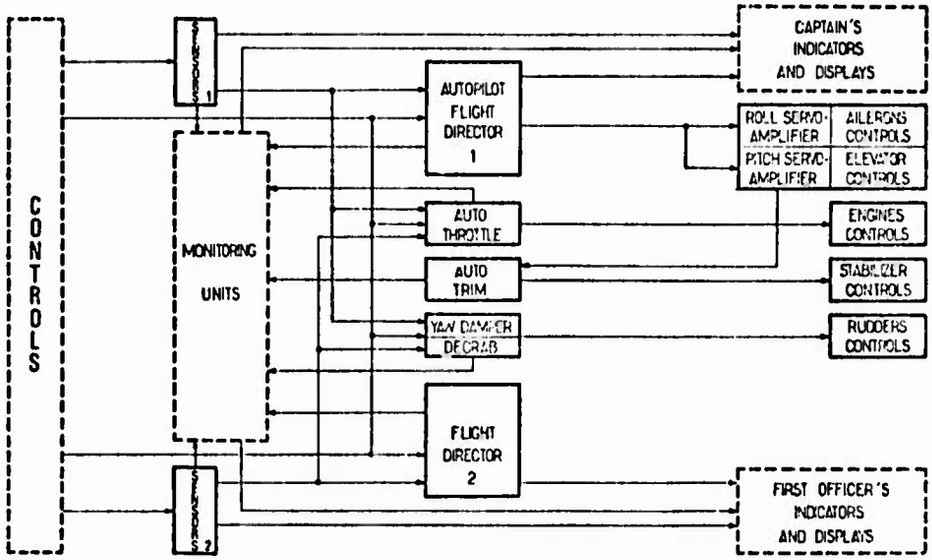

FIG. 2 - FAIL-PASSIVE CONFIGURATION

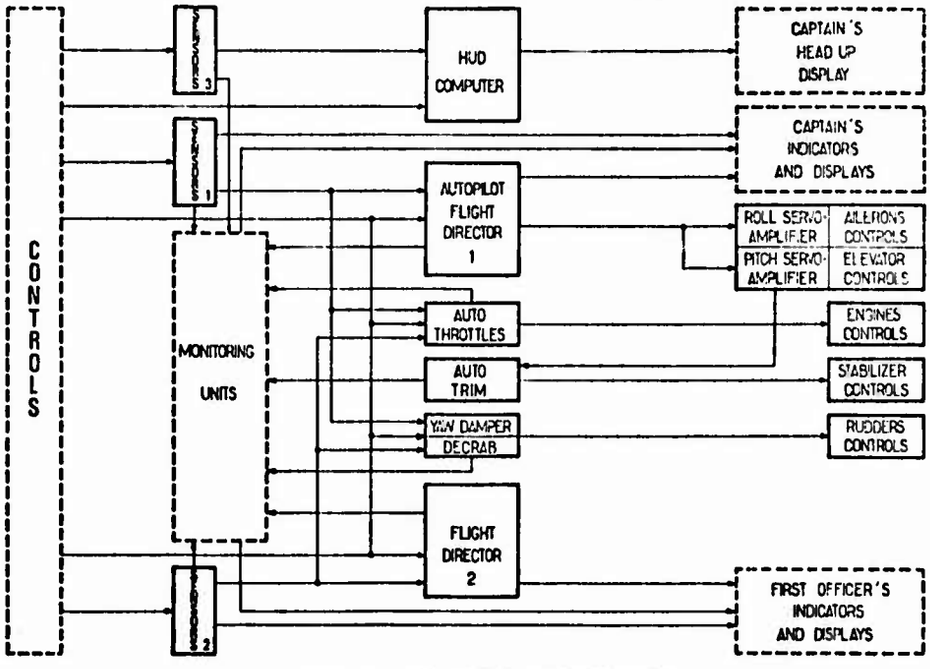

FIG. 3 - AIR INTER CONFIGURATION

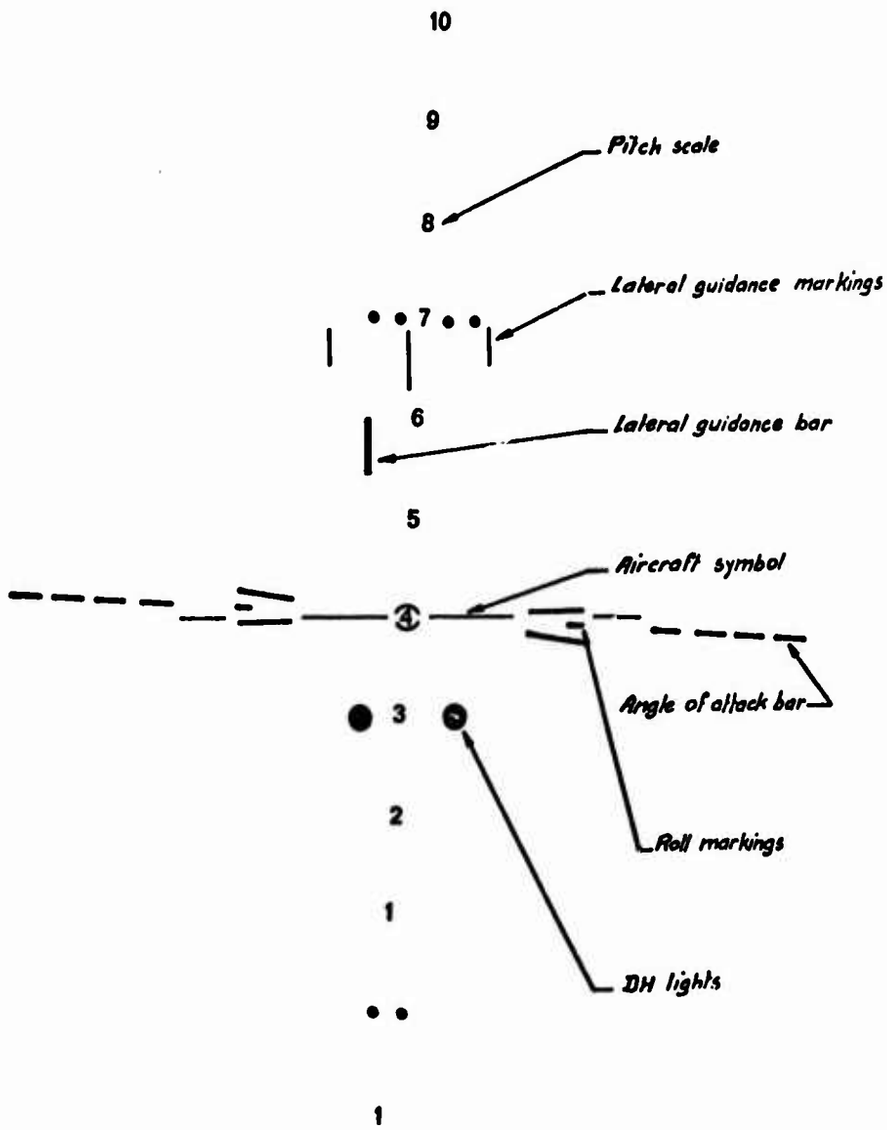

FIG. 4 - HEAD UP DISPLAY

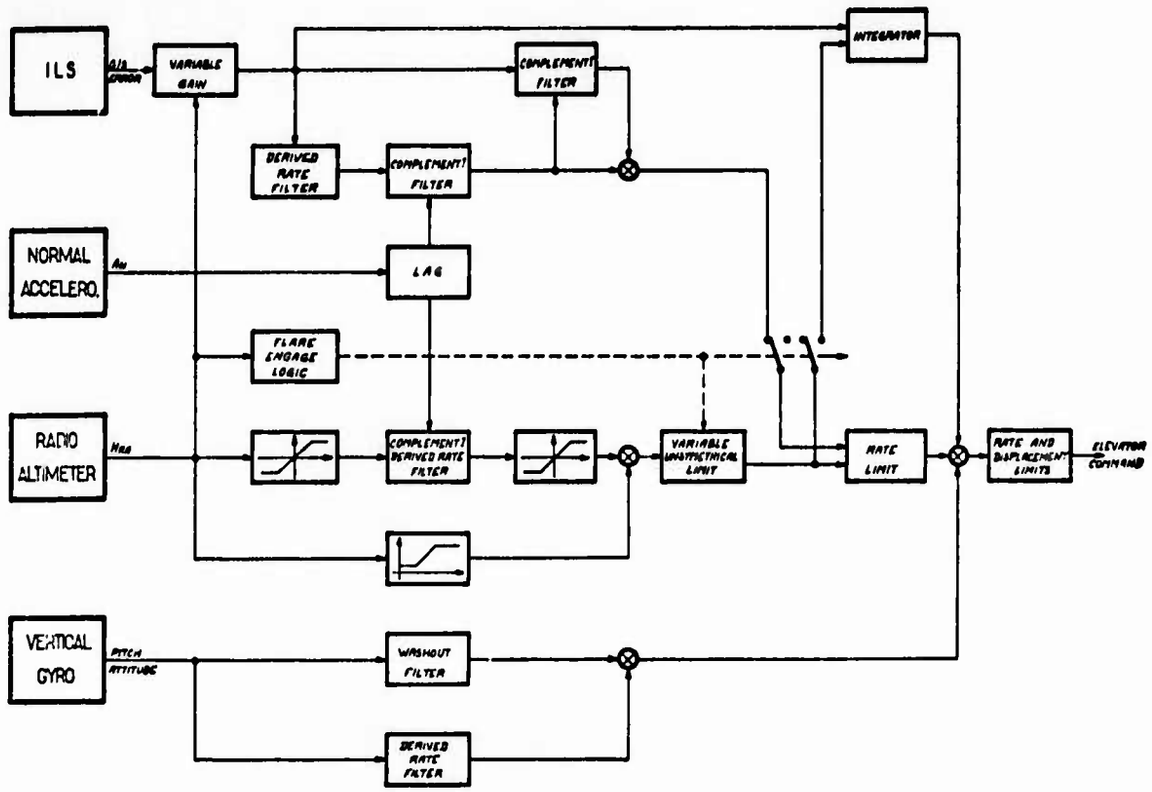

FIG. 5 - PITCH AXIS AUTOLAND (SIMPLIFIED BLOCK DIAGRAM)

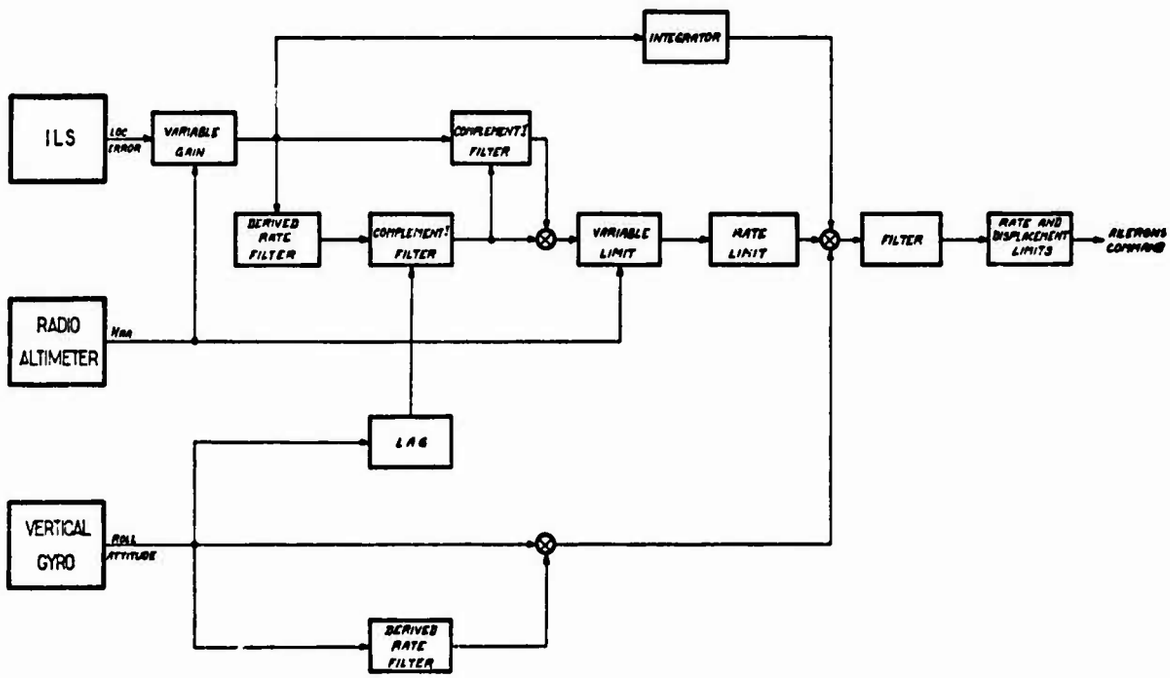

FIG. 6 - ROLL AXIS AUTOLAND (SIMPLIFIED BLOCK DIAGRAM)

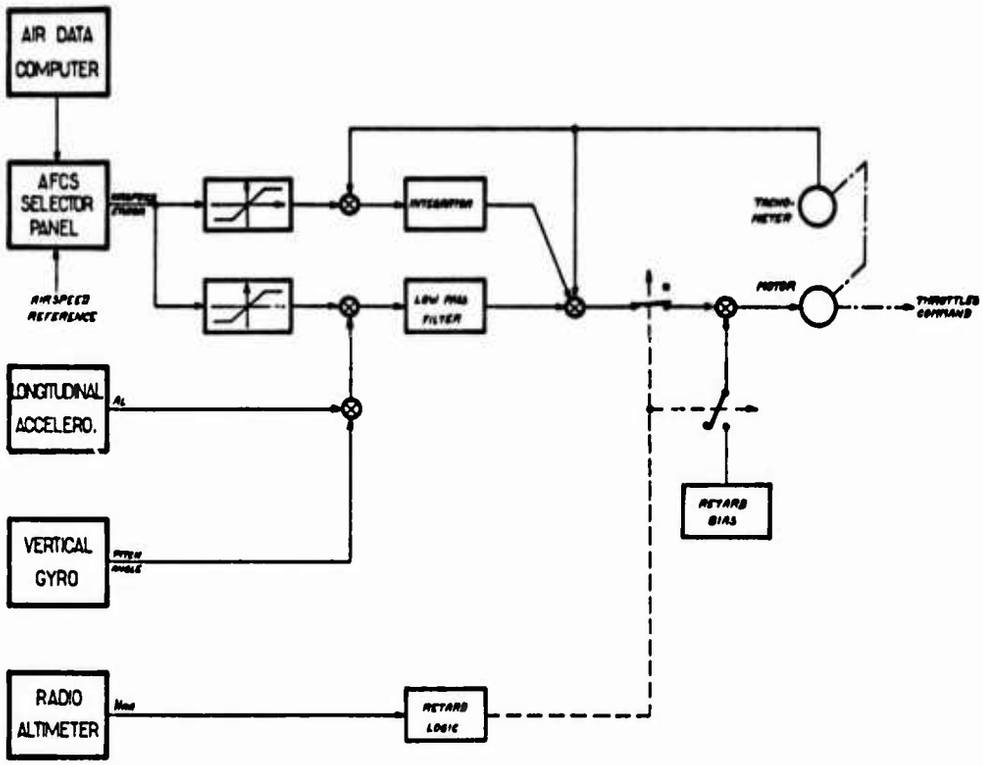

FIG. 7 - AUTOTHROTTLE (SIMPLIFIED BLOCK DIAGRAM)

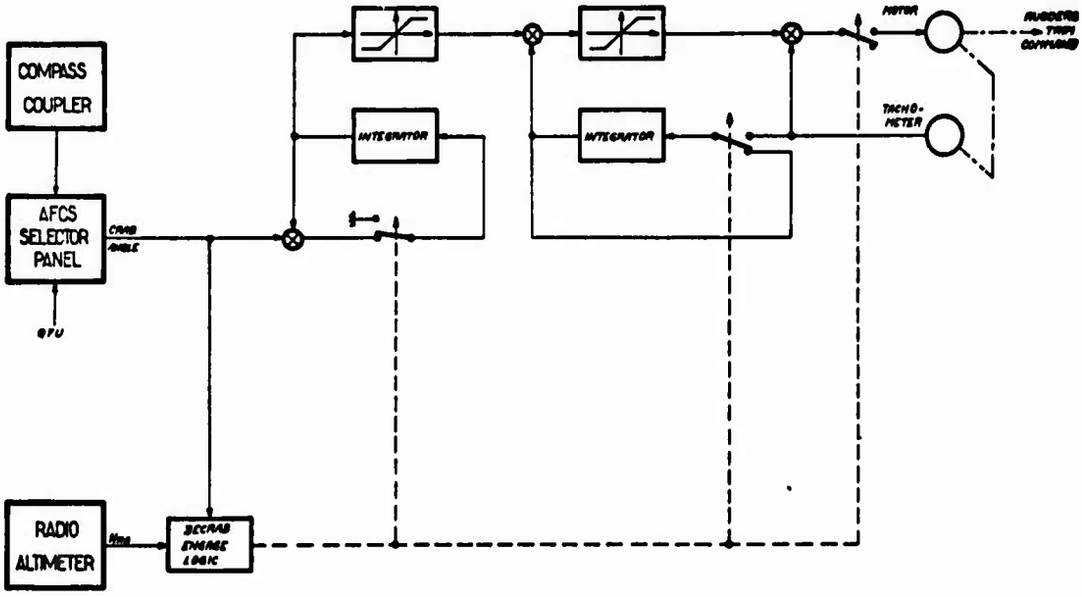

FIG. 8 - YAW AXIS DECRAB (SIMPLIFIED BLOCK DIAGRAM)

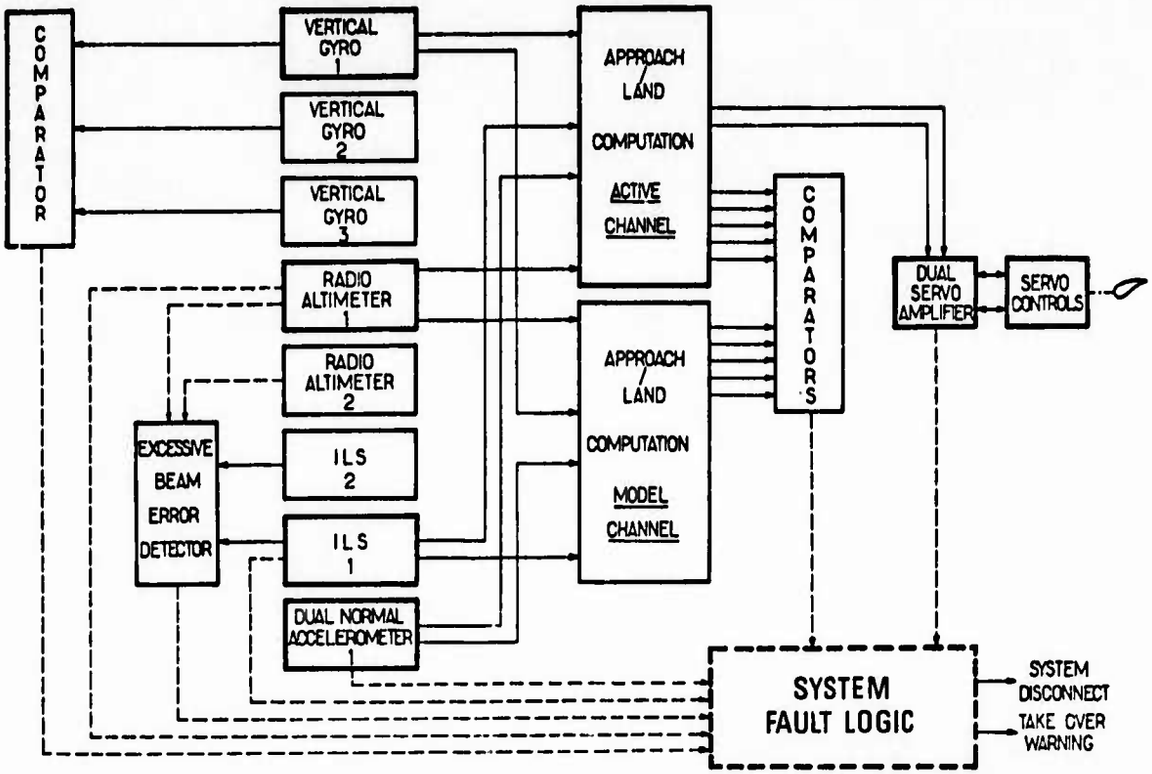

FIG. 9 - AUTOLAND PITCH/ROLL BASIC MONITORING CONFIGURATION

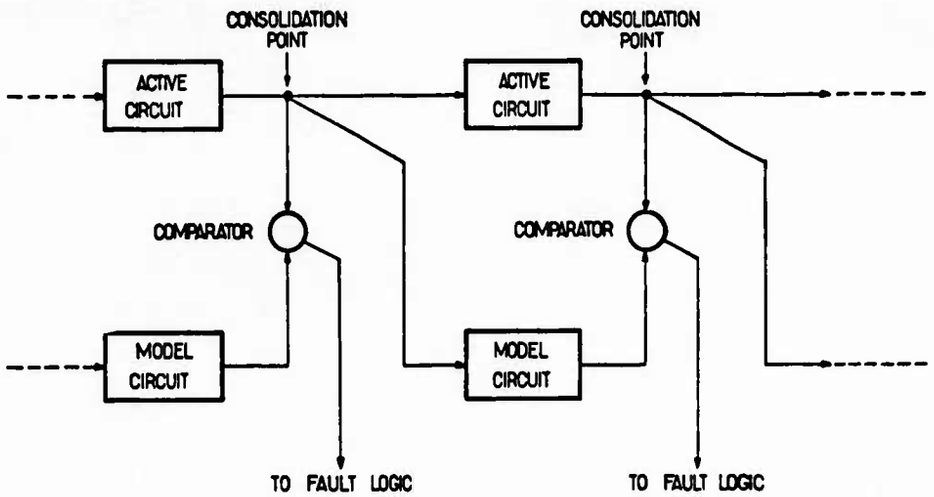

FIG. 10 - PRINCIPLE OF REDUNDANT SECTIONALIZATION

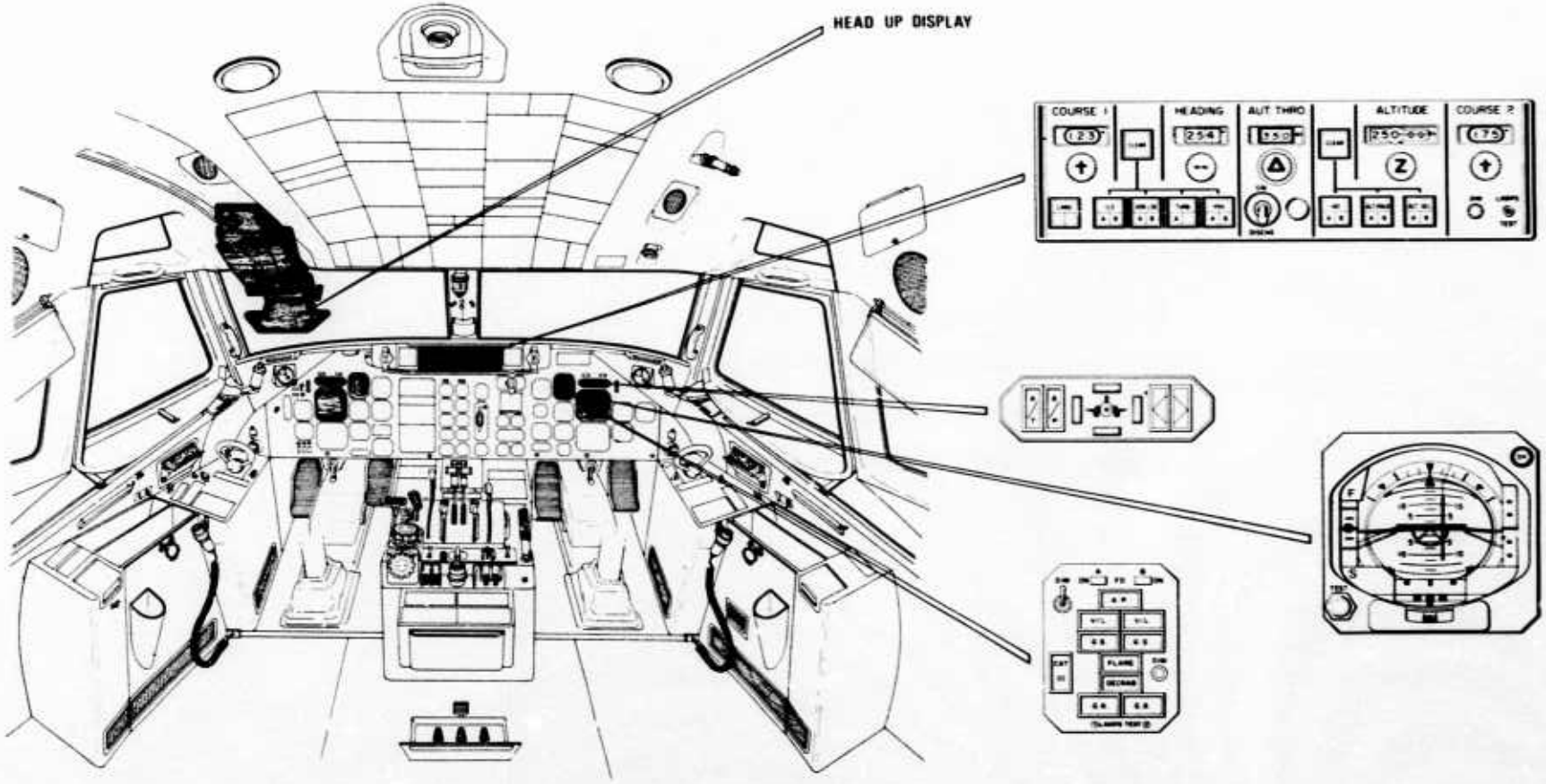

Fig.11 - **Cockpit layout**

PRÉSENTATION DES INFORMATIONS NÉCESSAIRES POUR LE DÉCOLLAGE ET L'ATTERRISSAGE

par Jean-Claude WANNER

Office National d'Etudes et de Recherches Aérospatiales (ONERA)
92320 Châtillon (France)

RESUME

L'étude du comportement du pilote au cours des phases de décollage et d'atterrissage, nous a conduit à bâtir un modèle de pilote. Ce modèle est utile pour déterminer quelles sont les informations nécessaires et en conséquence, quels paramètres doivent être présentés de façon à diminuer la charge de travail et augmenter la régularité et la sécurité du vol.

Cette étude nous a permis de préciser ce que pourrait être un futur tableau de bord. La partie principale de ce tableau de bord, conçue pour les phases décollage et atterrissage, est un viseur tête haute présentant la trace au sol du vecteur vitesse et la pente totale. A l'aide de ces deux informations le pilote peut directement agir sur la trajectoire, connaissant exactement le réglage moteur nécessaire, tout en respectant une marge de sécurité correcte sur l'incidence.

♦
♦ ♦
♦

REQUIRED PILOT CUES AND DISPLAYS FOR TAKE OFF AND LANDING.

SUMMARY

The investigation of the pilot behaviour during the take off and landing phases led us to build a model of the pilot. This model is useful to determine which are the necessary cues and consequently which parameters have to be displayed in order to minimize the pilot work load and increase the flight regularity and safety.

This study allowed us to determine what could be a future cockpit display. The main part of this display, designed for take-off and landing phases, is a head-up display presenting the ground track of the air velocity vector and the total climb angle. With these two parameters the pilot can directly handle the airpath, knowing exactly the necessary rating of the engines and observing a correct safety margin for the angle of attack.

◊

Nous vous proposons de chercher quelles sont les informations les mieux appropriées que l'on doit fournir au pilote afin de réduire sa charge de travail au cours des phases d'atterrissage et de décollage. A cet effet nous allons tout d'abord étudier le comportement du pilote durant ces phases de vol et préciser quelles sont les différentes boucles de pilotage utilisées compte tenu des informations fournies par les tableaux de bord classiques.

Les paramètres qui définissent la trajectoire de l'avion (position, vecteur vitesse et vecteur accélération) et ceux qui définissent la position angulaire du système de référence de l'avion par rapport au sol (assiette longitudinale, angle de gite et azimut ainsi que leur dérivée première et seconde) sont déterminés par l'équipage de différentes façons.

Certains de ces paramètres sont mesurés directement et indiqués sur le tableau de bord (le plus souvent sous forme analogique et quelquefois sous forme digitale). Parmi ces paramètres on rencontre la vitesse verticale, le cap, l'assiette longitudinale, l'angle de gite, le taux de variation de cap, le facteur de charge, l'incidence et le dérapage.

Certains paramètres ne sont pas mesurés directement comme par exemple la vitesse aérodynamique. Ils sont remplacés par des quantités plus facilement mesurables qui leur sont étroitement liées, par exemple, la vitesse indiquée et le nombre de Mach. Dans quelques cas, cependant, ces paramètres peuvent être déterminés par un calculateur embarqué à partir de données mesurées.

Les paramètres de position sont seulement déterminés à l'aide de système de navigation ou de système de guidage sol. Ces données peuvent être déterminées directement à partir des instruments du tableau de bord (aiguilles croisées de l'I.L.S.) ou indirectement par un système plus complexe dans lequel est indiqué la correction nécessaire pour annuler l'écart entre la trajectoire réelle et la trajectoire désirée (A l'aide d'un calculateur embarqué et d'un directeur de vol). Enfin, des indications sur la position de l'avion par rapport à la trajectoire désirée peuvent être transmises par radio par un contrôleur au sol suivant l'avion au radar (G.C.A.).

Certains paramètres ne sont pas mesurés parce qu'ils peuvent être déterminés directement par l'équipage (par exemple, la position de l'avion par rapport à la piste au cours d'un atterrissage à vue, l'assiette longitudinale en vol à vue, les accélérations normales et les accélérations angulaires).

Enfin, un certain nombre de paramètres caractérisant l'état de l'avion et le fonctionnement des moteurs sont fournis par le tableau d'instruments. Parmi ces paramètres on trouve, les indications des jauges et des débimètres (masse de l'avion), l'indicateur de centrage, l'indicateur de position des gouvernes, les paramètres de contrôle du moteur (vitesse de rotation du moteur, pression d'admission, EPR, etc ...).

Toutes ces données sont rassemblées par les différents capteurs humains : les yeux, les oreilles, les mains et les pieds (capteurs d'effort aux commandes), et la totalité du corps (capteur d'accélération linéaire). Comme nous l'avons déjà vu, ces données sont obtenues par lecture des instruments sur le tableau de bord, par perception visuelle, par l'écoute des informations transmises par radio et par la sensation directe des efforts aux commandes et des accélérations linéaires ou angulaires.

Notons que l'oeil peut être considéré comme un capteur double. La vision périphérique fournit une information imprécise sur le monde extérieur, mais il couvre un domaine relativement large. Les données rassemblées de cette manière peuvent servir principalement à avertir le pilote d'utiliser sa vision centrale pour examiner de plus près les phénomènes détectés par sa vision périphérique. La vision centrale est beaucoup plus précise et est en conséquence limitée à un champ étroit. Les instruments peuvent être seulement lus par la vision centrale. Une donnée particulière fournie par le tableau de bord ne serait pas transmise au cerveau si celui-ci n'avait pas "demandé" aux yeux "de lire" l'instrument en question. Etant donné son large champ d'action, la vision périphérique est capable de donner une image générale de la position angulaire de l'avion par rapport au sol. Ceci joue un rôle particulièrement important dans le contrôle des assiettes au cours des vols avec visibilité. Ce double rôle de l'oeil sera discuté un peu plus loin.

Contrairement à l'oeil, l'oreille est un capteur simple omnidirectionnel. La possibilité pour l'oreille de déterminer la direction ou l'origine d'un bruit est très limitée et peu précise ; en conséquence cette possibilité est très peu utilisée en vol. Si un son inusuel est entendu, indiquant un mauvais fonctionnement possible, cela constitue pour l'oeil un signal le conduisant à regarder sur le tableau de pannes si un système est tombé en panne (chacun sait combien il est difficile de trouver la source d'un "petit bruit" sur une automobile). Ainsi l'oreille est-elle essentiellement utilisée à détecter des signaux audibles (radio, alarme) dont la signification n'est pas fonction de leur direction d'origine.

L'oreille interne est un organe très complexe dont le principe n'est pas encore totalement compris. Une partie de l'oreille interne détecte la direction et l'intensité des accélérations linéaires au niveau de la tête. Ainsi cet organe donne une idée générale de la position de la tête par rapport à la verticale si l'observateur se déplace à une vitesse uniforme et par rapport à la verticale apparente si son mouvement est accéléré. Durant un mouvement accéléré (comme par exemple au cours d'un virage ou d'une manoeuvre de cabré au cours desquels les accélérations sont fortes), le fait de tourner la tête conduit à une perte d'équilibre parce que l'oreille détecte les accélérations dans un système de référence liée à la tête (modification de la verticale apparente due à l'accélération de Coriolis).

Une autre partie de l'oreille interne est constituée par les canaux semi circulaires. Le mouvement du liquide lymphatique à l'intérieur de ces canaux dû aux accélérations angulaires est détecté quand la tête tourne. Pour de nombreuses raisons, qu'il serait trop long de détailler ici, l'oreille interne est un détecteur imparfait des accélérations angulaires ; les sensations d'accélération angulaire ou de décélération continuent après que le phénomène ait cessé (ceci est en particulier le cas pour un danseur qui a l'impression de tourner encore une fois la valse terminée). Qui plus est, de petites accélérations angulaires ne sont pas perçues. Ce défaut est la base d'un phénomène qui n'est que trop familier au pilote volant sans visibilité : l'impression que l'avion est en virage permanent. Ceci provient probablement de l'impossibilité pour l'oreille interne de détecter un retour graduel en position ailes horizontales suivant un mouvement de roulis de grande vitesse angulaire.

Il est bon de noter que la sensation de virage, qu'elle soit réelle ou imaginaire, détectée par l'oreille interne, mais non confirmée par la vue, produit fréquemment des nausées. Il est bien connu qu'un observateur assis dans la cabine d'un avion de transport se sentira rapidement malade s'il regarde l'aile se déplaçant sur un ciel sans nuage pendant que l'avion effectue un virage à vitesse variable. Ceci est dû au fait que l'aile et l'avion apparaissent stationnaires à l'oeil alors que l'oreille interne détecte des accélérations angulaires (principalement en roulis).

Signalons, par ailleurs, que l'oeil est "piloté" en position par l'oreille interne ; autrement dit les informations de verticale apparente et les informations d'accélérations angulaires sont utilisées par le cerveau pour maintenir l'axe optique de l'oeil en position fixe par rapport au monde extérieur ; ce phénomène est confirmé par les deux expériences suivantes : les passagers situés à l'arrière de la cabine d'un avion de transport, sans vue de l'extérieur, "voient" nettement l'avant de la cabine monter au moment où le pilote lève la roulette au décollage : à cet instant, en effet, l'axe optique de l'oeil est maintenu horizontal, ce qui explique l'impression de voir monter l'avant de la cabine ; d'un autre côté, il est bien connu qu'au cours d'un atterrissage par temps turbulent il est plus facile de voir la piste que les instruments, encore une fois parce que l'oeil est maintenu sensiblement fixe par rapport au monde extérieur. Ces remarques auront une grande importance lorsque nous aurons à choisir les systèmes de présentation d'information.

La totalité du corps ressent les effets des accélérations linéaires par l'intermédiaire des variations des forces de réaction de contact du siège et de la ceinture. Les accélérations normales sont détectées par l'intermédiaire des variations de la tension des muscles maintenant le corps en position. Par ailleurs, le corps est plus sensible aux variations de facteur de charge qu'au facteur de charge lui-même, sauf dans le cas des facteurs de charge élevés.

Enfin, les mains et les pieds sont utilisés comme détecteurs des efforts aux commandes (par l'intermédiaire de la tension des muscles). Ce sont, par ailleurs, de mauvais détecteurs de position. A moins d'utiliser un contrôle par les yeux il est difficile de détecter des variations de l'ordre de un à deux centimètres par rapport à la position désirée d'un manche conventionnel.

En conséquence, les capteurs humains peuvent être divisés en deux grandes catégories :

a) les organes qui peuvent capter des données précises : les yeux (vision centrale), les mains et les pieds (pour les efforts aux commandes) ;

b) les capteurs qui transmettent des informations générales utilisées pour confirmer les données précises reçues par les organes de la première catégorie ou pour avertir le pilote d'une situation anormale (souvent les sensations transmises par ces capteurs sont en conflit avec les données fournies par les instruments). Parmi ces capteurs citons l'oreille interne, l'oeil (vision périphérique), le corps (qui capte les accélérations linéaires et dans une certaine mesure, l'oreille externe (qui détecte les sons).

Cette classification en deux catégories a quelque chose d'arbitraire. Il serait plus correct de classer les capteurs suivant le taux d'information qu'ils sont capables de transmettre et de leur attribuer un degré de noblesse en rapport avec le taux d'information reçu à chaque échantillonnage. En utilisant cette classification, l'oeil (vision centrale) est le plus noble et le corps (accélération linéaire) le moins noble.

D'une façon générale les informations détectées par un capteur ne sont transmises et en conséquence utilisées par le cerveau que si le cerveau a envoyé un ordre, autrement dit a appelé l'information.

Plus l'information collectée par un capteur est précise (c'est-à-dire plus le capteur est "noble") plus cette dernière remarque est valable.

En conséquence, les yeux (vision centrale) ne transmettent l'information que s'ils ont reçu un ordre venant du cerveau. Ceci est vrai non seulement parce que le cerveau doit diriger les muscles de l'oeil pour orienter celui-ci dans la direction de l'instrument ou du phénomène considéré, mais également parce qu'il doit émettre une demande d'information. On ne voit pas parce que l'on regarde ! La vision est un acte volontaire (par vision, nous voulons dire transmission au cerveau de données constituant une quantité d'informations ayant une grande valeur numérique, par exemple la valeur d'une altitude, d'un cap, d'un régime de rotation moteur etc ...).

D'un autre côté, plus une information est générale (capteur vulgaire) moins sa réception par le cerveau dépend d'un acte volontaire ; ainsi, l'acquisition de ce type d'information entre dans le domaine des réflexes conditionnés qui par exemple jouent une part importante dans le contrôle de l'attitude du corps durant la marche.

Les faits mentionnés ci-dessus ont des conséquences significatives.

Le cerveau est incapable de recevoir plusieurs données précises simultanément. Il demande à l'oeil de regarder un certain instrument, un certain phénomène, il demande qu'un certain signal soit écouté, il demande l'analyse de certaine force sur une commande donnée. Tout ceci est effectué successivement et non simultanément.

Cet acte volontaire consistant à percevoir un phénomène spécifique en utilisant un capteur et habituellement appelé mobilisation de l'attention, augmente les seuils de perception des autres capteurs et ceci d'autant plus que ces capteurs sont nobles. Le recueil d'information demande en effet la mise en service d'un nombre d'autant plus élevé de neurones que l'information est importante, ce qui en laisse d'autant moins de disponibles pour les autres informations.

Les pilotes savent bien que lorsqu'ils s'attachent à effectuer un virage serré ou une boucle avec une précision assez grande, ils ne ressentent pas les accélérations alors que les passagers en "sac de sable" les ressentent parfois douloureusement.

Lorsque l'oreille cherche à distinguer un signal faible au milieu d'un bruit de fond important, on a bien souvent "les yeux dans le vague".

Ceci montre en particulier que si l'on transmet au pilote des indications de position par un système auditif assez difficile à détecter (système du genre radio range qui transmettait un signal point trait d'un côté de l'axe, un signal trait point de l'autre côté et un signal continu sur l'axe), il ne faut pas espérer voir le pilote capter simultanément des informations visuelles et auditives.

Enfin dernier exemple, combien de pilotes portant toute leur attention sur le pilotage dans des conditions délicates (captation intensive de données visuelles) n'ont pas entendu l'avertisseur sonore signalant une panne ? Combien de pilotes se sont posés train rentré sans voir la lampe clignotante signalant le train non sorti parce que, la visibilité étant mauvaise par exemple, ils portaient toute leur attention sur la captation d'information de position par rapport à la piste.

En résumé les capteurs "nobles" ne fournissent des données précises que sur appel "volontaire du cerveau" ; les capteurs "non nobles" fournissent des indications complémentaires sur appel "du cerveau" ou bien fournissent des indications d'alarme lorsque les valeurs des paramètres détectés dépassent un seuil d'autant plus important que le cerveau est plus occupé par le recueil d'informations précises.

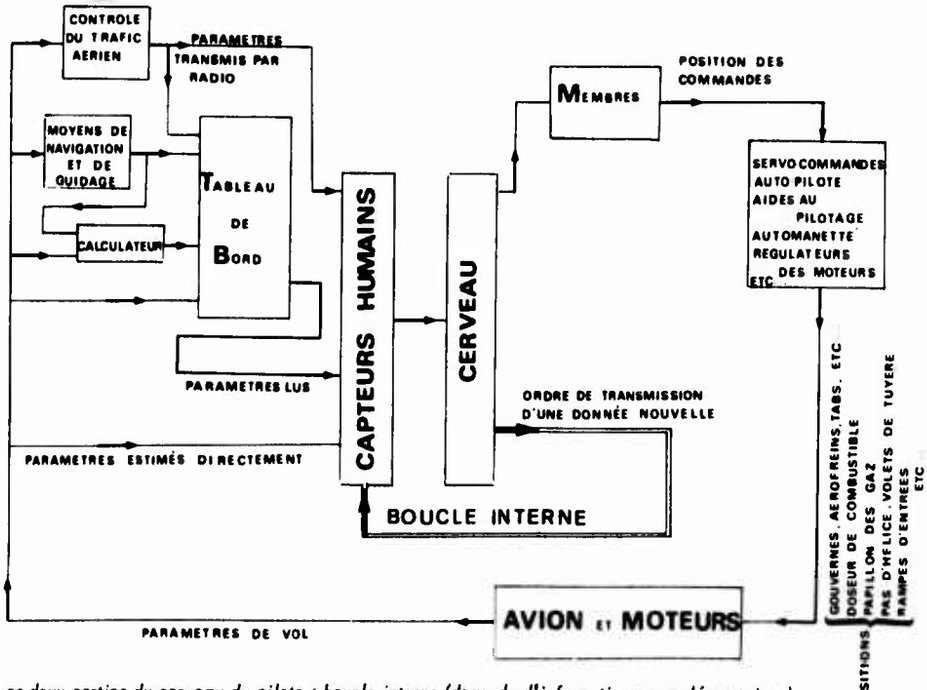

Fig. 1 - Les deux sorties du cerveau du pilote : boucle interne (demande d'informations complémentaires), boucle externe (action sur les commandes).

Les données une fois recueillies sont transmises au cerveau sous forme d'influx nerveux et traitées par celui-ci qui, soit par comparaison directe avec des données mises en mémoire, soit par calcul suivant des "programmes" stockés en mémoire en déduit deux types différents d'action (figure 1) :

a) une action par l'intermédiaire des mains et des pieds sur les commandes de pilotage

b) une sélection d'un capteur particulier en lui demandant de recueillir une donnée particulière.

Analysons de plus près ces deux sorties du cerveau en donnant un exemple.

Supposons le pilote amené à effectuer sans visibilité la Sous-Phase, descente finale de la Phase Approche I.L.S. Il dispose de l'indicateur d'I.L.S. à aiguilles croisées et de la planche de bord classique : horizon, altimètre, variomètre, anémomètre, conservateur de cap, bille et aiguille.

A un instant donné, le pilote a rassemblé l'information suivante :

- la vitesse est égale à la vitesse d'approche désirée,
- le cap est égal au cap "localizer",
- les ailes sont horizontales,
- l'assiette longitudinale est à la valeur recommandée (tenant compte de l'incidence et de la pente),
- l'indicateur I.L.S. montre que l'avion se trouve au-dessus et à droite de la trajectoire idéale,

En réalité, le cerveau du pilote n'a pas recueilli telles quelles ces informations. Par un balayage des yeux (nous reviendrons sur ce point) il a recueilli :

- une position de l'aiguille de l'anémomètre,
- une position de l'aiguille ou de l'alidade du conservateur de cap,
- une position angulaire de la barre de l'horizon artificiel et une position du centre de cette barre par rapport à la maquette,
- une position des deux aiguilles de l'I.L.S. par rapport au repère central de l'indicateur.

C'est donc à la suite d'une opération mentale assez complexe, comportant en particulier des comparaisons avec des données en mémoire (vitesse d'approche, cap localizer, assiette longitudinale et latérale), que le pilote parvient à l'analyse de cette situation.

Nous noterons que ces valeurs sont quelquefois mémorisées sous forme directe de position de l'aiguille (on sait par exemple qu'en approche, l'aiguille de l'anémomètre est horizontale à gauche ou verticale en haut) ; ce type de mémorisation dépend de la nature de la figuration.

Par une seconde opération mentale le pilote en déduit une tactique à suivre pour respecter la sécurité à court terme, c'est-à-dire passer par la fenêtre objectif à trois cents pieds (la loi de pilotage est là pour l'aider à trouver la bonne tactique).

Dans notre situation particulière, le pilote décide donc d'incliner l'avion à gauche et de diminuer l'assiette longitudinale. Sachant par expérience qu'une diminution d'assiette se traduit par une augmentation de vitesse sur trajectoire, il décide également de réduire la poussée (ou d'augmenter la trainée en utilisant les aérofreins). Suivant son entraînement c'est-à-dire suivant le nombre de données emmagasinées en mémoire, le pilote décidera, avec plus ou moins de précision, de l'ordre de grandeur des manoeuvres élémentaires à effectuer. Le pilote sait que pour corriger un écart de deux points d'indicateur I.L.S. en latéral, en début de descente, il suffit d'incliner l'avion à gauche de vingt degrés en cinq secondes, de l'incliner à droite de vingt degrés puis le ramener ailes horizontales avec le même taux pour corriger l'écart ; bien entendu les temps ne sont pas connus du pilote de façon aussi précise et les manoeuvres ne se font pas au chronomètre : le pilote utilise le taux d'inclinaison habituel et sait qu'un balancement vingt degrés à gauche, vingt degrés à droite et retour à l'horizontale donne la correction nécessaire. De même le pilote entraîné saura qu'une diminution d'assiette longitudinale de deux degrés pendant dix secondes suivie d'un retour à l'assiette initiale, corrigera l'écart d'altitude. Enfin, il saura qu'une diminution de cent tours/minute est nécessaire pour éviter une augmentation de vitesse hors tolérance au cours de la manoeuvre (si l'avion est au premier régime, le pilote pourra estimer qu'une variation de poussée n'est pas nécessaire pour une manoeuvre aussi courte).

Jusqu'ici le pilote n'a pas réagi ; il n'a effectué que les opérations mentales d'analyse de la situation et les décisions de tactique à suivre. Il lui reste encore une opération mentale à effectuer : déterminer les actions élémentaires sur les commandes pour réaliser les manoeuvres élémentaires, c'est-à-dire les actions sur la commande de gauchissement, sur la commande de profondeur et sur la manette des gaz ; là encore, s'il possède un entraînement suffisant, il saura qu'il faut fournir tel effort au gauchissement pendant tant de temps pour incliner l'avion à gauche de vingt degrés au taux normal, tel effort sur la profondeur, tel déplacement de la manette des gaz.

Nous noterons que la main n'étant pas un capteur de position mais un capteur d'effort, le pilote ne détermine pas une valeur de déplacement de manette, mais une réduction chiffrée en nombre de tours par exemple.

Une fois cette décision prise, le pilote agit, c'est-à-dire déplace les commandes. C'est alors qu'intervient le processus de contrôle des actions, sous forme d'ordres, aux divers capteurs, de recueil de données nouvelles.

Les actions sur les commandes vont être modifiées en fonction des résultats obtenus, c'est-à-dire en fonction des données recueillies : il y a donc une succession de boucles d'asservissement entre chaque action sur une commande et ceci jusqu'à ce que le résultat désiré soit acquis.

L'acquisition des données particulières d'évaluation du résultat nécessite l'appel par le cerveau de ces données, c'est-à-dire la mise en état de transmission du capteur adapté à la mesure. L'ordre de "mise en service" du capteur est transmis au capteur par ce que nous appellerons une boucle interne du cerveau pour la différencier nettement de la boucle externe d'asservissement décrites à l'alinéa précédent.

La première boucle interne à être mise en service est la boucle main cerveau (ou pieds cerveau) mettant en éveil le capteur d'effort constitué par la main (ou le pied).

Ainsi le cerveau va commander une action de déplacement du manche vers la gauche et commander la mise en service du capteur d'effort qui transmet une indication d'effort : le cerveau commandera le déplacement de la commande jusqu'à obtenir l'effort désiré ; le travail peut se schématiser ainsi :

- ordre de déplacement
- appel de donnée d'effort
- transmission de donnée d'effort
- comparaison de l'effort mesuré avec l'effort désiré

- action corrective de déplacement
- appel de donnée d'effort
- etc ...

L'action élémentaire ainsi réalisée : effort donné sur la commande de gauchissement, une deuxième boucle externe intervient pour contrôler la manoeuvre élémentaire. Le pilote sait que le taux de basculement en gauchissement doit être proche du taux désiré, mais il lui faut d'une part le vérifier et d'autre part stopper l'action lorsque l'angle de gite a atteint vingt degrés. Il met donc en service une deuxième boucle interne, la boucle oeil cerveau, pour recueillir les données nécessaires au contrôle de la boucle externe.

D'une façon analogue à ce qui a été décrit ci-dessus, le travail se schématise ainsi :

- ordre d'effort (ce qui suppose le contrôle d'effort décrit ci-dessus)
- appel de donnée d'angle de gîte
- transmission de la donnée d'angle de gîte
- comparaison avec l'angle de gîte désiré
- correction de l'ordre d'effort
- appel de donnée d'angle de gîte
- etc ...

Si le pilote veut contrôler le taux d'inclinaison en latéral, le travail sera plus complexe car l'acquisition de la donnée doit se faire par au moins deux prélèvements de données d'angle Φ séparés par l'intervalle de temps Δt pour estimer $d\Phi/dt$.

Le pilote ayant ainsi modifié l'angle de gîte doit cette fois contrôler l'effet de cette manoeuvre sur sa trajectoire : il lui faut recueillir des données sur la trajectoire ; il va donc appeler ces données nouvelles en dirigeant l'oeil, par la boucle interne oeil-cerveau, sur l'instrument le plus apte à le renseigner.

Cette fois, il ne va pas s'instaurer une boucle externe conduisant à une action immédiate du pilote. Il y a d'abord appel d'un certain nombre d'informations, cap et position d'aiguille d'indicateur I.L.S., analyse de la situation et par un processus analogue à celui décrit ci-dessus, mais moins complexe, décision de modification de la tactique.

Nous avons décrit, ici, le cas du contrôle des trajectoires par le système I.L.S. Si ce contrôle se fait grâce au système GCA, l'acquisition des données de trajectoire se fait par l'intermédiaire de l'oreille et c'est la boucle interne oreille-cerveau qui sera alors mobilisée à cet effet.

Il faut noter que dans ce dernier cas, une partie de l'analyse de la situation est faite par le contrôleur GCA au sol qui "prépare" la tactique à suivre en donnant non seulement des indications de position, mais des ordres d'action (ordre de cap à suivre et variation du taux de descente).

Cette remarque étant faite, on peut résumer le travail du pilote de la façon suivante :

- acquisitions de données générales portant sur la position de l'avion par rapport à la trajectoire désirée et sur les assiettes de l'avion, c'est-à-dire, paramètre intéressant la sécurité à court terme et paramètre intéressant la sécurité immédiate (il s'agit bien entendu non seulement des paramètres de position, mais également de leurs dérivées par rapport au temps),
- analyse de la situation et décision de tactique (basées sur la loi de pilotage),
- décomposition de la tactique en manoeuvres élémentaires et détermination de leurs "amplitudes",
- pour chaque manoeuvre élémentaire, détermination de l'amplitude de l'action élémentaire sur les commandes,
- action sur une commande,
- contrôle de l'effort, mise en service de la boucle interne main-cerveau,
- contrôle de la manoeuvre (modification de l'action élémentaire, c'est-à-dire de l'effort) (mise en service de la boucle interne oeil-cerveau recueillant les données relatives aux paramètres intéressant la sécurité immédiate),
- contrôle de la tactique par analyse des paramètres intéressant la sécurité à court terme (mise en service de la boucle interne oeil-cerveau ou oreille-cerveau).

Nous n'avons décrit, jusqu'ici, que le début de l'action générale du pilote tendant à "rejoindre" la loi de pilotage (heureusement, la manoeuvre est moins longue à exécuter qu'à décrire). Au moment où le pilote ayant achevé sa première manoeuvre élémentaire (inclinaison de 20° à gauche) déclenche la boucle interne oeil-cerveau pour l'acquisition de paramètres nécessaires à l'analyse de la situation, celle-ci peut avoir évolué d'une façon différente de celle prévue : chute de la vitesse par exemple sous l'effet d'une rafale. Le pilote peut donc être amené à abandonner la tactique initiale pour rétablir promptement la situation nouvelle qui peut se révéler dangereuse.

D'une façon générale, à chaque analyse de la situation, le pilote vérifie d'abord les paramètres intéressant la sécurité immédiate, c'est-à-dire les paramètres relatifs aux limitations avions, par exemple les paramètres intéressant la limitation d'incidence, c'est-à-dire le facteur de charge et la vitesse, ou bien l'assiette latérale etc ... Il vérifie ensuite les paramètres intéressant la sécurité à court terme, c'est-à-dire les paramètres liés à la réussite de la Sous-Phase en cours d'exécution (l'objectif de la sous phase est défini par quelques paramètres comme la position de l'avion, la grandeur et la direction du vecteur vitesse qu'il faut atteindre avec certaines tolérances en fin de sous-phase). La tactique du pilote a pour premier but de respecter la sécurité immédiate et pour second but, une fois la sécurité immédiate assurée, de respecter la sécurité à court terme. Notons que lorsque le pilote d'essais ne peut respecter la sécurité immédiate, en abandonnant la sécurité à court terme, il évalue les qualités de vol par une note de Cooper comprise entre 7 et 9 et que lorsqu'il ne peut même plus assurer la sécurité immédiate, il donne la note 10.

Ceci signifie qu'une fois les manoeuvres élémentaires effectuées (parfois même au cours de la manoeuvre), le pilote doit surveiller non seulement les paramètres utiles au contrôle de la manoeuvre, mais également tous les autres paramètres.

Cette opération est commandée par le cerveau qui centre la boucle interne oeil-cerveau successivement sur les différents instruments ; le passage d'un instrument à l'autre et l'ordre de balayage sont commandés soitpar un programme mis en mémoire et résultant de l'expérience du pilote, soit par une déduction logique résultant des lectures des instruments précédents et d'une analyse partielle de la situation : on peut "sauter" la lecture de l'altimètre si l'on a constaté que le variomètre est toujours au zéro (cas du vol en palier), ou la lecture du cap si l'angle de gîte est toujours nul.

Notons que cette opération de contrôle de la situation est très partiellement assurée par les capteurs non nobles qui peuvent intervenir pour avertir le pilote d'une situation anormale.

Nous avons décrit, en détail, le déroulement d'une manoeuvre avec sa boucle de contrôle externe nécessitant l'utilisation d'une boucle interne (oeil-cerveau en général). Dans certains cas, la manoeuvre peut être effectuée partiellement en boucle ouverte par le pilote ; il en profite alors pour contrer la boucle interne oeil-cerveau sur d'autres paramètres, afin de renouveler plus rapidement son analyse de la situation ; cela lui permet de diminuer les retards de la boucle externe de contrôle de la tactique.

Cette remarque met en lumière le fait suivant, très important : toutes les opérations mentales d'analyse de situation, de décision de tactique, d'élaboration des manoeuvres élémentaires et des actions sur les commandes, de recueil d'informations (commande des boucles internes) ne peuvent être effectuées que successivement, à de très rares exceptions près.

La technique de pilotage est constituée de l'ensemble de ces processus qui doivent être exécutés dans une période de temps déterminé par la Sous-Phase ; comme nous le définirons plus loin, la charge de travail du pilote est en relation directe avec ces processus. Aussi, le diagramme du pilote peut-il être résumé de la façon suivante (voir figure 2) :

Il y a trois types de boucles : la plus grande qui est la boucle de sécurité à court terme, la seconde qui est la boucle de sécurité immédiate et la plus petite qui est la boucle d'effort sur les commandes.

Il est très important de noter que le diagramme complet peut être rendu beaucoup plus complexe. En effet, il est possible de représenter tous les paramètres extérieurs venant de l'avion et tous les capteurs humains et obtenir ainsi un grand nombre de boucles des trois types donnés dans le diagramme.

Nous noterons aussi qu'à chaque moment il y a seulement une boucle en service, ce qui constitue la différence fondamentale entre un pilote et un pilote automatique.

Le choix de la boucle en service est fait par la partie centrale du cerveau qui est représentée sur le haut du diagramme, sous forme d'un ordre, au capteur choisi, de transmettre l'information nécessaire.

Le processus de pilotage, et par conséquent le nombre des opérations élémentaires d'acquisition de traitement des données, d'élaboration des manoeuvres et des actions sur les commandes, d'élaboration du processus d'acquisition et d'analyse des données, dépend de la Sous-Phase, de l'Etat de l'Avion (Configuration affichée, situation de panne, masse et centrage), de l'Etat de l'Atmosphère et bien entendu de la Loi de pilotage et du travail auxiliaire qui sont à la base du processus à suivre.

La charge du travail du pilote (ou en généralisant la charge de travail de l'équipage) durant une Sous-Phase est mesurée par le nombre des opérations élémentaires de traitement de l'information, nécessaires pour exécuter la Sous-Phase.

Ainsi, la charge de travail est déterminée par l'ensemble Sous-Phase, Etat de l'Avion, Etat de l'Atmosphère, Loi de pilotage et travail auxiliaire.

Et maintenant, comment concevoir le poste d'équipage et l'avion lui-même, afin de réduire la charge de travail ?

Un certain nombre de tentatives ont été faites dans ce sens, ces dernières années, avec plus ou moins de succès, et ces recherches ont montré qu'il est nécessaire d'être très prudent en modifiant le processus de pilotage.

Par exemple, il est facile de voir que la charge de travail n'est pas réduite en remplaçant tout le processus d'analyse mentale des deux premières boucles par un processus d'acquisition continu des données consistant à fournir des informations sur le tableau de bord sous la forme d'instructions directes de pilotage analogues à celles fournies par un directeur de vol.

Si l'on présente au pilote des ordres donnant directement le sens et la grandeur des actions sur les commandes, sans autre indication, le pilote doit mobiliser totalement la boucle interne oeil-cerveau sur cet unique instrument car il ne sait pas

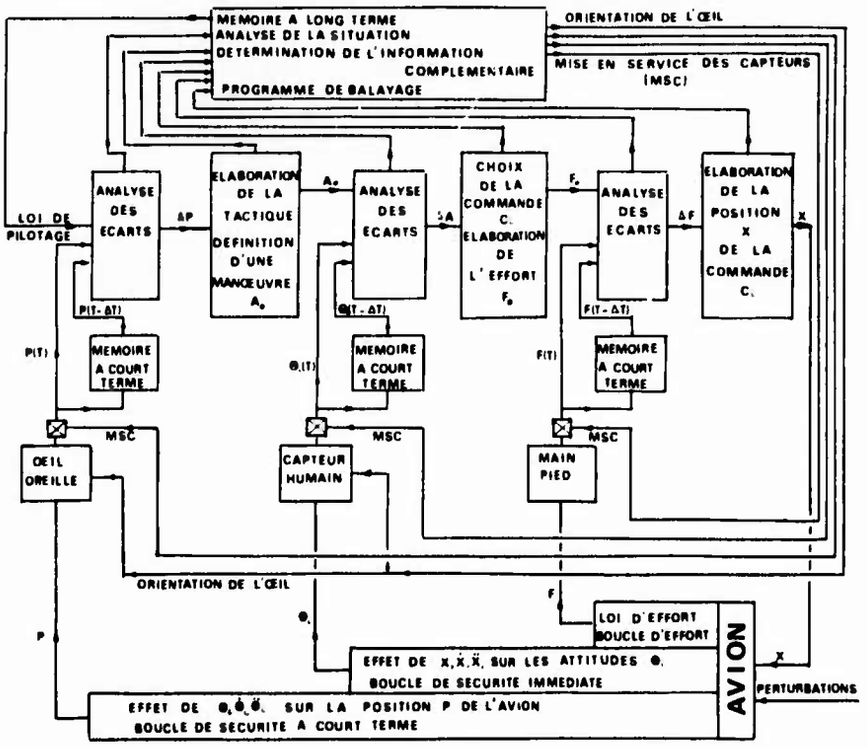

Fig. 2 - Schéma de fonctionnement du pilote. Les trois boucles de pilotage.

à priori quelle est la raison de son action : il ne peut plus lâcher des yeux l'instrument. Par exemple un ordre "manche à gauche" peut être donné au pilote dans les deux circonstances suivantes : l'avion est sur la trajectoire désirée mais une rafale l'a incliné à droite ou bien l'avion a les ailes horizontales, mais le vent l'a déplacé à droite de la trajectoire désirée.

Dans ce deuxième cas, l'ordre initial sera suivi d'un ordre d'inclinaison pour remettre les ailes horizontales, d'un deuxième ordre d'inclinaison à droite pour reprendre le cap initial puis un ordre d'inclinaison à gauche pour remettre les ailes horizontales ; dans le premier cas, il n'y aura pas d'ordre complémentaire et le pilote ne peut le savoir et ne peut détourner son attention de l'instrument dans l'attente de l'ordre suivant qu'il ne peut prévoir; autrement dit, un tel système annule totalement les processus d'analyse et d'élaboration des deux boucles de sécurité à court terme et de sécurité immédiate et le cerveau est entièrement mobilisé par l'acquisition des données.

Précisons que ces conclusions ne sont valables que dans le cas où l'indication transmise au pilote de façon analogique est une indication pure d'action sur la commande, par exemple manche à gauche ou à droite, à pousser, à tirer (avec ordre de grandeur des efforts). Les conclusions seraient très modifiées si les indications d'ordre étaient des ordres d'assiette à réaliser, doublés d'ordre de manoeuvre, par exemple incliner l'avion à gauche de 15° sur l'horizon pour une variation de cap de 30° à gauche, augmenter l'assiette longitudinale de 2°, car dans ces conditions, le pilote comprend ce qu'il fait et sait "où il en est".

Dans le même ordre d'idées, les indications de position transmises par le contrôleur GCA sont doublées d'ordres de manoeuvre (indication de cap par exemple ou de taux de descente). Le contrôleur GCA prend alors à son compte la boucle de sécurité à court terme, détermine les manoeuvres à réaliser et laisse au pilote les deux autres boucles pour effectuer les manoeuvres commandées. Autrement dit le contrôleur GCA assure la sécurité à court terme, laissant au pilote le soin d'assurer la sécurité immédiate.

En définitive, tout dispositif de présentation des données doit simplifier le processus d'élaboration et d'analyse de la boucle de sécurité à court terme (même les annuler) et laisser au pilote le contrôle de la boucle de sécurité immédiate tout en lui facilitant l'élaboration des efforts sur les commandes.

Voyons, maintenant, comment concevoir à la lumière de l'étude précédente, la présentation des informations pour les phases d'atterrissage et de décollage.

Cette conception est basée sur les remarques suivantes, concernant le pilotage avec le tableau de bord classique :

a) L'atterrissage à vue est plus facile à exécuter que l'atterrissage sans visibilité avec les instruments actuels.

b) Au cours de l'atterrissage à vue, il est facile d'aligner l'avion sur le plan vertical de symétrie de la piste, mais il est difficile de savoir si l'on fera un atterrissage long ou court ; en l'absence de tout moyen, la descente se fait par approximations successives, en réduisant ou augmentant les gaz (augmentation ou diminution de la pente de descente) à la suite d'observations de la perspective de la piste. Bien souvent le pilote utilise les indications de l'I.L.S. ou des préaffichages : éloignement vent arrière minuté après passage par le travers du seuil de piste pour se placer à une distance convenable de la piste (compte tenu du vent), affichage d'une poussée réacteur tenant compte du vent, de la masse avion et de la vitesse d'approche, etc ...

c) La poussée à afficher en approche pour maintenir un taux de descente donné à vitesse donnée est délicate à déterminer car le délai entre la variation de la position des manettes des gaz et l'établissement du nouveau taux de descente est très long (il dépend des caractéristiques de la phygoïde).

d) Au décollage, l'accélération réelle de l'avion n'est vérifiée que par le temps nécessaire pour atteindre une vitesse choisie, suffisamment grande pour que la mesure soit significative et suffisamment faible pour que le décollage puisse être interrompu sans risque, (en général 100 kt). Notons que même si la poussée nominale des moteurs est assurée par l'affichage d'un paramètre tel que l'EPR, l'accélération nécessaire peut être réduite par des traînées parasites (spoilers, trappes de train ouvertes), par un freinage hydrodynamique (slush, neige, flaques d'eau), par une panne du système de freinage, etc ...

e) Après le décollage, les manoeuvres antibruit amènent à faire une réduction a priori de la poussée avec risque d'affichage d'une poussée inférieure à la poussée nécessaire au vol à la vitesse et à la pente recommandée de montée.

f) En cas de panne de moteur ou de remise de gaz, le pilote est amené à effectuer des manoeuvres a priori basées sur des affichages de poussée et d'assiette longitudinale sans contrôle direct de sa trajectoire (le variomètre est un instrument dangereux en évolution, à cause de son retard dû à son principe même de fonctionnement),

g) Enfin, à vue, il est très difficile de savoir si l'avion passera ou non un obstacle donné (de même qu'il est difficile de prévoir le point d'impact sur la piste). Combien d'accidents sont dus au fait qu'en approche à vue (de nuit surtout) l'avion heurte une colline située dans l'axe de piste, alors que le pilote voyait parfaitement l'entrée de bande en début d'approche.

Pour corriger les défauts des tableaux de bord actuels nous proposons donc d'équiper le cockpit avec les dispositions suivantes :

- un dispositif de présentation tête haute (head up display) fournissant les paramètres suivants :

  . vecteur vitesse
  . horizon
  . piste synthétique
  . incidence
  . pente totale

Ces informations sont suffisantes pour piloter directement l'avion au cours des phases décollage, montée initiale, approche et atterrissage ou pour vérifier le fonctionnement du pilote automatique durant la phase atterrissage automatique.

- un dispositif de présentation des informations tête basse fournissant les paramètres utiles pour la navigation, le respect du domaine de vol, le contrôle des moteurs, le système d'alarme, etc ...

- un pilote automatique pour les Phases de vol stabilisées loin du sol ou pour la Phase d'atterrissage automatique

- un micromanipulateur pour piloter l'avion au cours des Phases voisines du sol.

Autrement dit la présentation tête haute et le micromanipulateur seront utilisés ensemble au cours des phases au voisinage du sol, là où il est nécessaire que le pilote ait une connaissance continue et parfaite de la situation de l'avion en position et

assiette. Néanmoins, afin de réduire le travail des pilotes des compagnies aériennes qui peuvent avoir à effectuer chaque jour un grand nombre d'atterrissages, il peut être judicieux d'utiliser le pilote automatique pour des atterrissages automatiques. La fiabilité de ces dispositifs n'est pas encore suffisante (même en multipliant les chaînes) pour assurer la sécurité. Aussi, est-il nécessaire que le pilote puisse vérifier le pilote automatique par un dispositif indépendant et qu'il puisse effectuer manuellement l'atterrissage en cas de panne. Nous pensons que la surveillance du pilote automatique et que le pilotage de l'avion par l'intermédiaire de la présentation tête haute est une solution aux problèmes de la fiabilité du pilote automatique.

D'un autre côté, la présentation tête basse et le pilote automatique seront utilisés au cours des Phases loin du sol où les problèmes de sécurité à long terme concernant la navigation sont plus importants que les problèmes de sécurité immédiate ou de sécurité à court terme.

L'idée fondamentale est de donner au pilote les mêmes informations pour le vol sans visibilité que pour le vol avec visibilité, mais en aucun cas de reproduire dans le dispositif de présentation tête haute les mêmes informations que celles fournies par un tableau de bord conventionnel. En effet, nos études ont montré que lorsque les informations classiques telles que : échelle d'altitude, échelle de vitesse, aiguilles d'I.L.S. sont fournies dans le dispositif tête haute, le pilote ne peut à la fois lire les données et regarder le sol, même quand les échelles sont collimatées à l'infini. Dans certains cas, au cours de nos essais, les pilotes n'ont pas cru que les échelles étaient collimatées à l'infini ; ils se plaignaient d'avoir à accommoder successivement sur les échelles puis sur le sol. Nous pensons que ceci provient peut-être du fait qu'il n'est pas naturel pour un pilote de voir une échelle altimétrique à l'infini ; aussi, le cerveau, par réflexe, demande-t-il à l'oeil d'accommoder à la distance normale pour un instrument, ce qui oblige alors le pilote à accommoder volontairement à l'infini.

Une autre raison importante pour présenter dans le dispositif tête haute des informations liées au monde extérieur, est fondée sur la remarque faite plus haut, que l'axe optique de l'oeil est maintenu sensiblement fixe par rapport au monde extérieur par un "asservissement" interne au cerveau mesurant les accélérations par l'oreille interne.

En conséquence, si des données relatives au monde extérieur, telles que l'horizon, la piste sont fournies dans le dispositif tête haute, le pilote n'éprouve aucune difficulté pour regarder ces symboles malgré les vibrations et les mouvements de l'avion dus à la turbulence. Ceci n'est exact que dans la mesure où les symboles sont fixes par rapport au monde extérieur. Si nous présentons dans le dispositif tête haute des symboles comme des échelles d'altitude ou des aiguilles croisées fixes par rapport à l'avion, le pilote aura, en turbulence, la même difficulté pour les regarder, même s'ils sont collimatés à l'infini, que dans le cas d'instruments classiques au tableau de bord.

D'un autre côté, si nous disposons des symboles tels que : horizon, piste, liés au monde extérieur, dans le dispositif tête basse, le pilote aura les mêmes difficultés de lecture en turbulence que pour les instruments classiques, même si les symboles sont à l'échelle un, parce qu'ils ne peuvent être collimatés à l'infini.

Aussi, donnerons-nous au pilote des informations aussi proches que possible des informations visuelles : horizon et piste synthétique. La piste synthétique peut être bâtie à partir d'informations provenant de l'ILS ou de tout autre système installé au sol ou à bord de l'avion. Théoriquement, ces informations devraient être suffisantes puisque durant un atterrissage visuel le pilote ne dispose d'aucune autre information (sauf la vitesse ; nous reviendrons sur ce point un peu plus tard). Mais l'expérience a montré qu'il n'est pas très facile d'effectuer l'approche avec l'angle de descente correct. Il est facile de piloter l'avion dans le plan vertical de symétrie de la piste, mais non pas le long du plan de descente. Ceci provient du fait que le vecteur vitesse est généralement dans le plan bien connu de symétrie de l'avion, mais que le pilote n'en connaît pas son orientation dans ce plan.

Aussi, allons-nous ajouter une nouvelle information dans le dispositif de présentation tête haute : la trace au sol du vecteur vitesse. Ce point est le point que l'avion atteindra si le pilote maintient les commandes en position fixe. Le mode d'utilisation de cette information est évident : quand le seuil de la piste est à 2°5 au-dessous de l'horizon, le pilote pousse sur le manche de façon à placer le vecteur vitesse sur le seuil et le maintient dans cette position.

C'est alors que se pose la question du choix entre les deux vecteurs vitesses possibles : le vecteur vitesse-air ou le vecteur vitesse-sol.

Au premier abord, il semble évident qu'il soit nécessaire d'utiliser le vecteur vitesse-sol puisque celui-ci tient compte de l'effet du vent sur la trajectoire. Néanmoins, un pilote sait aisément corriger la dérive due à un vent de travers ; pourquoi ne saurait-il pas en faire autant dans le plan vertical ? S'il voit par exemple que le vecteur vitesse air recule, ceci signifie qu'il y a un vent de face ; il est alors facile de viser un point à quelque cent pieds après le seuil. Nous devrons remarquer également que le vecteur vitesse au cours d'une approche est voisin de l'horizontale (environ 2,5 degrés). Ainsi l'angle entre la vitesse et la composante du vent le long de l'axe de la piste est seulement 2,5 degrés ce qui signifie que la dérive dans le plan vertical est très faible.

En conséquence, la dérive dans le plan horizontal et dans le plan vertical est facile à corriger et les avantages du vecteur vitesse-sol ne sont pas évidents (nous reviendrons, un peu plus loin, sur la façon pratique de tenir compte de ces deux dérives).

D'un autre côté, l'angle entre le vecteur vitesse air et l'axe de référence de l'avion est par définition l'angle d'incidence ; cette remarque a deux conséquences importantes :

a) La seule mesure de l'angle d'incidence peut fournir l'information nécessaire pour introduire le vecteur vitesse-air dans le dispositif de présentation tête haute. Cette information est fournie par des sondes ou des girouettes et est certainement plus facile à obtenir que les informations concernant le vecteur vitesse-sol qui exige au moins un radar doppler et une centrale de verticale.

b) La distance angulaire vue par le pilote, entre le vecteur vitesse et un point fixe dans le viseur représentant la trace de l'axe de référence de l'avion, est justement l'angle d'incidence mesuré à échelle unité. En conséquence, si le point est fixé dans une position telle que l'angle entre ce point et l'axe de référence est égale à l'angle d'incidence optimale pour la phase approche, il est facile pour le pilote de respecter la limitation d'angle d'incidence.

L'utilisation du vecteur vitesse donnée sur les figures 3 à 7 sera la suivante :

Le point fixe lié à l'axe longitudinal est un T inversé : la hauteur de ce T est de deux degrés

et quand le vecteur vitesse représenté par la croix atteint le sommet du T l'angle d'incidence est l'angle d'incidence optimal pour la phase approche ; on a supposé dans notre exemple que cet angle était de 14 degrés, correspondant à une vitesse d'approche de 160 kt. Si le vecteur vitesse atteint l'extrémité basse du T l'angle d'incidence est alors de 16 degrés, ce qui correspond au début de l'alarme d'incidence (klaxon, flash ou stick shaker).

Se déplaçant avec l'horizon, des graduations en degrés donnent les angles de montée ou les angles de descente. La ligne pointillée est à 2,5 degrés au-dessous de l'horizon.

Enfin, la piste représentée par un trapèze déformable est supposée avoir une longueur de 10 000 pieds et une largeur de 250 pieds.

Sur la figure 3 l'avion est supposé être en vol horizontal à l'angle d'incidence de dix degrés. Ainsi le vecteur vitesse est sur l'horizon et le sommet du T est à 4 degrés au-dessous du vecteur vitesse. L'altitude étant de 1 500 pieds et la distance au seuil de piste étant de 10 milles nautiques, la barre représentant le seuil est à 1°41 au-dessous de l'horizon.

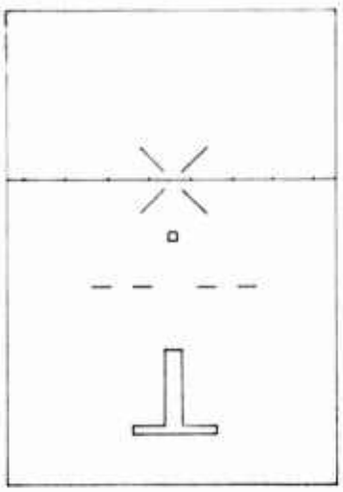

Fig. 3 - Collimateur de pilotage. L'avion est en vol en palier à 1500 ft à 10° d'incidence. La piste est à 10 miles nautiques.

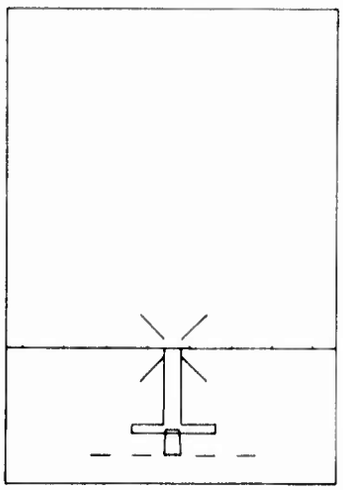

Fig. 4 - Collimateur de pilotage. L'avion est en vol en palier à 1500 ft à 14° d'incidence (incidence d'approche recommandée). Le seuil de piste à 5,7 miles nautiques est à 2,5° au-dessous de l'horizon. C'est l'instant de mise en descente.

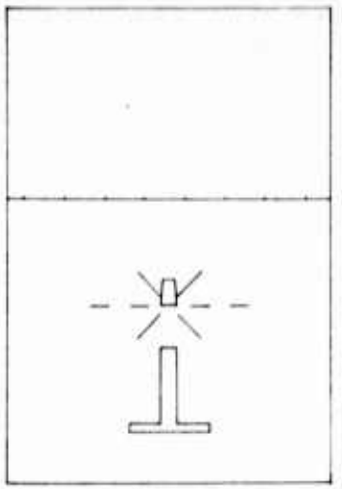

Fig. 5 - Collimateur de pilotage. L'avion est en descente sous une pente de 2,5°. Le pilote n'ayant pas suffisamment réduit la poussée, la vitesse a crû et l'incidence a diminué (13°).

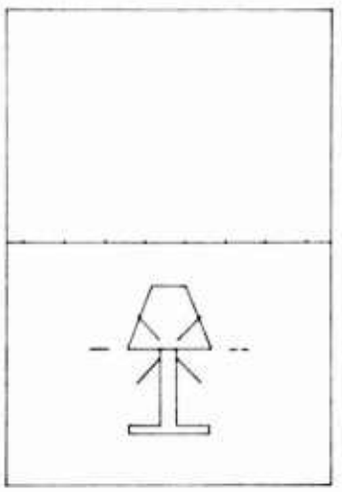

Fig. 6 - Collimateur de pilotage. L'avion est en descente sous une pente de 2,5° à l'altitude de 300 ft. L'incidence est de nouveau l'incidence d'approche recommandée (14°).

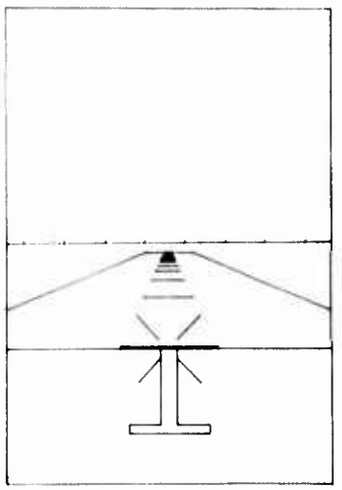

Fig. 7 - Collimateur de pilotage. L'avion est en descente sous une pente de 2,5° à l'altitude de 50 ft recommandée pour l'arrondi. Les bandes de 50 pieds de large sont espacées de 1000 pieds le long de l'axe.

Afin d'obtenir la vitesse optimale le pilote réduit la poussée en maintenant le vecteur vitesse sur l'horizon. La vitesse optimale est obtenue lorsque le sommet du T atteint le vecteur vitesse. En réalité le T ne se déplace pas dans le viseur et c'est le vecteur vitesse qui rejoint le T ; mais pour le pilote l'horizon est fixe, le vecteur vitesse est maintenu fixe sur l'horizon en tirant sur le manche, ce qui par conséquent, augmente l'assiette et déplace le T en direction de l'horizon et du vecteur vitesse.

Sur la figure 4 l'avion est supposé être encore en vol horizontal, mais à l'angle d'incidence de 14 degrés ; la distance au seuil étant maintenant de 5,7 milles nautiques, la barre représentant le seuil est près d'atteindre 2,5 degrés au-dessous de l'horizon : c'est le bon moment pour le pilote de commencer la manoeuvre de rendu de main de façon à placer le vecteur vitesse sur le seuil.

Sur la figure 5 le vecteur vitesse est sur le seuil, mais le pilote n'ayant pas réduit la poussée, la vitesse a augmenté et l'angle d'incidence est 13 degrés (ce qui représente une variation relative de vitesse de $\sqrt{\frac{14}{13}}$ c'est-à-dire de l'ordre de 4 % ou dans notre cas d'environ 6 noeuds). Ainsi, le sommet du T est à un degré au-dessous du vecteur vitesse ; l'action du pilote est évidente : réduire la poussée en maintenant avec le manche le vecteur vitesse sur sur le seuil en attendant que le sommet du T regagne le vecteur vitesse.

Sur la figure 6 le taux de descente et l'angle d'incidence sont corrects, l'altitude est de 300 pieds : l'avion est en bonne position pour l'atterrissage. On peut voir que la précision de visée du vecteur vitesse augmente lorsque la distance à la piste diminue puisque la taille de la piste augmente.

Enfin, sur la figure 7 l'altitude est de 50 pieds, l'avion est en bonne position pour commencer l'arrondi ; notant le signal donné par le radio altimètre à l'altitude de 50 pieds, le pilote réduit l'angle de descente en visant un point sur la piste à un degré par exemple au-dessous de l'horizon, c'est-à-dire à environ 1 700 pieds après le seuil de piste. (Pour mieux préciser la perspective sous laquelle est vue la piste, nous avons supposé que des bandes de 50 pieds de large étaient disposées tous les 1 000 pieds le long de l'axe). Dans ce cas, le taux de descente est 1,75 % de la vitesse ce qui donne pour notre avion une vitesse verticale de 4 pieds/seconde pour une vitesse d'atterrissage de 140 noeuds.

Revenons maintenant sur l'affichage des dérives verticales et horizontales. Le vecteur vitesse-Terre (*) du fait du vent, fait avec le vecteur vitesse-air un angle dont la projection sur le plan horizontal est la "dérive latérale" et la projection sur le plan vertical parallèle à la piste est la "dérive verticale". Si l'on veut maintenir la trace au sol du vecteur vitesse-terre en un point fixe de la piste (le milieu du seuil par exemple) il faut donc maintenir le vecteur vitesse-air non pas en un point fixe du sol, mais une distance angulaire fixe (repérée par les deux angles de dérive) du point visé. Pour fixer les ordres de grandeur, précisons que pour une vitesse d'approche de 130 kt et une pente de 2°5 l'angle de dérive verticale est de $0{,}02 \times V_{wa}$ où V_{wa} est la composante axiale du vecteur vent (exprimé en noeuds), soit 0°40 pour 20 kt (si le vent est de face, le vecteur vitesse-air doit être placé au-dessus du point visé). Pour la même vitesse d'approche, l'angle de dérive latérale est de $0{,}44 \times V_{wn}$ où V_{wn} est la composante normale à la piste du vecteur vent (exprimé en noeuds), soit 8°8 pour 20 kt de vent latéral. En pratique, la dérive verticale peut être affichée par le pilote en décalant vers le haut pour un vent de face le vecteur vitesse air à l'aide d'une commande graduée directement en vitesse de vent (une répétition digitale de cette valeur peut être fournie dans un coin du viseur). A condition que le repère fixe soit décalé du même angle, la distance vecteur vitesse, repère fixe fournit toujours l'indication de marge d'incidence disponible. Ce dispositif peut être simplifié pour les avions destinés à apponter sur porte-avion, puisque la vitesse du vent sur le pont est maintenue constante : un décalage constant (0°68 pour 30 kt de vent sur le pont et 110 kt de vitesse d'approche sous 2°5) peut être affiché pour l'appontage.

(*) Le terme vitesse-sol est réservé à la projection sur le plan horizontal du vecteur vitesse par rapport à la Terre ou vecteur vitesse-Terre.

En ce qui concerne la dérive latérale, il est plus commode de remplacer le vecteur vitesse ponctuel par une "barre" composée de points distants de un degré et asservie à rester parallèle à l'horizon (pour faciliter la lecture, les points gauche et droit à 5 et 10° peuvent être identifiés par un signe différent).

Ainsi pour un vent latéral gauche de 10 kt (à 130 kt de vitesse d'approche) le pilote placera le milieu du seuil de piste entre les points à 4° et 5° droit.

Le problème des dérives étant ainsi réglé, comment le pilote agit-il sur le vecteur vitesse? En ce qui concerne l'alignement latéral, le problème n'est pas changé par rapport au pilotage classique, il est même facilité du fait que l'angle de dérive latérale est directement visible. Pour l'alignement longitudinal, le vecteur vitesse est directement piloté par le manche ; si le vecteur vitesse est au-dessus du point visé, le pilote pousse sur le manche ; s'il est au-dessous du point visé, le pilote tire sur le manche. Remarquons que la fonction de transfert manche-vecteur vitesse est plus simple que la fonction de transfert manche assiette longitudinale; la réponse de l'assiette à un échelon de manche présente plus d'oscillations que la réponse du vecteur vitesse.

Néanmoins, si le mode d'utilisation du manche est évident, il n'en n'est pas de même pour la manette des gaz. Nous avons vu sur les figures 3 et 5 que lorsque le vecteur vitesse est au-dessus du haut du T l'angle d'incidence est trop petit, c'est-à-dire que la vitesse est trop grande. Autrement dit quand le vecteur vitesse est au-dessus du T le pilote doit réduire la poussée. Mais le pilote ne connaît pas exactement l'amplitude nécessaire de la réduction. Aussi, de façon à l'aider, nous adjoindrons dans le viseur un nouveau paramètre généralement appelé pente totale ou encore dérivée réduite de la hauteur totale.

Tout le monde sait que l'énergie d'un avion ayant une masse m, volant à la vitesse V, à l'altitude H est :

$$E = mgH + \frac{1}{2} m V^2$$

il est commode d'écrire :

$$E = mgH_T = mgH + \frac{1}{2} m V^2$$

ou

$$H_T = H + \frac{V^2}{2g}$$

où H_T est appelé hauteur totale.

Si w est la dérivée en fonction du temps de la hauteur totale :

$$w = \frac{dH_T}{dt} = \frac{dH}{dt} + \frac{V}{g}\frac{dV}{dt} .$$

Puisque

$$\frac{dH}{dt} = V \sin\gamma$$

nous avons

$$(1) \qquad \frac{w}{V} = \sin\gamma + \frac{1}{g}\frac{dV}{dt}$$

$\frac{w}{V}$ est la dérivée réduite de la hauteur totale.

D'un autre côté l'équation de propulsion où F_v est la composante de la poussée le long du vecteur vitesse s'écrit :

$$m\frac{dV}{dt} = F_v - \frac{1}{2}\rho S V^2 C_x - mg\sin\gamma.$$

Cette équation peut s'écrire encore :

$$(2) \qquad mg\frac{w}{V} = F_v - \frac{1}{2}\rho S V^2 C_x .$$

La signification des équations (1) et (2) est la suivante:

a) le paramètre w/V peut être piloté en agissant sur la poussée F : w/V augmente lorsque F augmente

b) pour une valeur donnée de w/V, il y a une valeur γ donnée par

$$\sin\gamma_p = w/V$$

pour laquelle l'accélération dV/dt le long de la trajectoire est nulle (cette valeur γ_p est appelée pente totale)

c) w/V peut être directement mesuré par un accéléromètre installé le long du vecteur vitesse.

Plaçons, en effet, à bord de l'avion, un accéléromètre schématisé par une masse μ maintenue par un ressort. La masse μ est soumise à son poids $\mu\vec{g}$, aux forces d'inertie $-\mu\vec{\Gamma}$ (où $\vec{\Gamma}$ est l'accélération de l'avion) et à la tension $\vec{T}$ du ressort. L'avion de masse m est soumis à son poids $m\vec{g}$, aux forces d'inertie $-m\vec{\Gamma}$ et aux forces extérieures (forces aérodynamiques et forces de propulsion) de résultante $\vec{R}$ Il en résulte que :

$$\vec{T} = \frac{\mu}{m}\vec{R} .$$

L'indication n fournie par l'accéléromètre est le rapport de la tension T à la tension de référence T_0 lorsque la masse μ n'est soumise qu'à son poids μg

Par suite

$$\vec{n} = \frac{\vec{R}}{mg} .$$

Si l'on oriente l'accéléromètre parallèlement au vecteur vitesse ($\vec{T}$ parallèle à $\vec{V}$), n ainsi mesuré est alors égal à $(F_v - \frac{1}{2}\rho S V^2 C_x)/mg$ c'est-à-dire w/V d'après (2).

Nous supposons que nous savons comment mesurer $\frac{w}{V}$ (nous verrons ceci plus loin); à chaque valeur de w/V correspond un angle γ_p pour lequel l'accélération dV/dt le long de la trajectoire est nulle. Ainsi pour chaque valeur mesurée de w/V, un index dans le viseur indiquera la valeur correspondante γ_p ; ceci signifie que la distance angulaire entre cet index et l'horizon est égale à γ_p . Si maintenant le vecteur vitesse est au niveau de cet index ceci signifie que l'angle de montée est juste égal à γ_p, autrement dit que l'accélération le long de la trajectoire est nulle et en conséquence, que la vitesse est constante. Si le vecteur vitesse est sous l'index, l'accélération est positive ; si le vecteur vitesse est au-dessus de l'index, l'accélération est négative.

D'un autre côté, si le pilote augmente ou réduit la poussée, il verra l'index monter ou descendre dans le viseur.

Ainsi, le pilote peut ajuster la poussée à chaque instant de façon à maintenir la vitesse constante, quel que soit l'angle de montée (ou l'angle de descente) dans la mesure où il peut augmenter ou réduire suffisamment la poussée, pourvu qu'il positionne l'index au même niveau que le vecteur vitesse.

Ainsi, revenant à l'exemple donné sur la figure 5, le pilote réduira la poussée en plaçant l'index par exemple 2 degrés au-dessous du vecteur vitesse ; sachant que 1 degré correspond à une accélération (ou à une décélération) de 1 noeud en 3 secondes, l'angle correct d'incidence (et la vitesse correcte) sera atteint en 9 secondes. A ce moment, le pilote réajustera la position de la manette de façon à placer l'index au même niveau que le vecteur vitesse, c'est-à-dire à 2,5 degrés au-dessous de l'horizon ; les figures 8 et 9 donnent les positions correctes de l'index correspondant au cas donné figures 5 et 6.

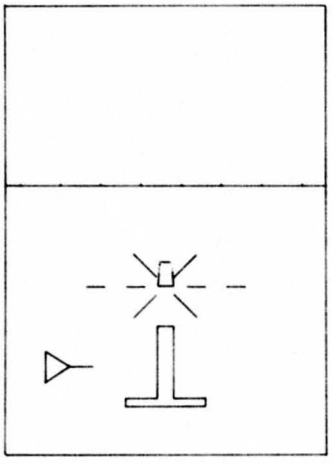

Fig. 8 - Collimateur de pilotage. Position du symbole de pente totale pour effectuer la correction d'incidence dans le cas décrit figure 5. L'incidence correcte sera atteinte en 9 secondes.

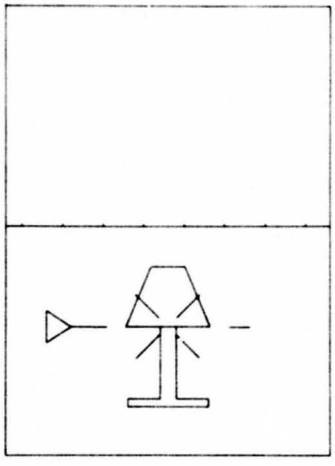

Fig. 9 - Collimateur de pilotage. Position du symbole de pente totale pour maintenir la vitesse (et l'incidence) constante au cours de l'approche (cas de la figure 6).

Et maintenant, comment mesurer l'angle d'incidence et la pente totale.

La plupart des sondes utilisées sur les avions commerciaux modernes pour la mesure de l'angle d'incidence, fournissent un signal électrique suffisamment précis pour piloter le spot du viseur tête haute. Il est nécessaire seulement de filtrer les hautes fréquences du signal électrique de façon à éviter d'avoir un point trop "secoué".

Pour mesurer la pente totale, deux solutions sont possibles :

1°) Calculer l'accélération le long du vecteur vitesse connaissant l'angle d'incidence et les accélérations jx et jz mesurées par deux accéléromètres fixés sur le système d'axe avion.

2°) Piloter par l'angle d'incidence l'axe de l'accéléromètre, lui-même, de façon à le maintenir parallèle au vecteur vitesse.

Regardons, maintenant, comment ce dispositif, ainsi défini pour répondre aux problèmes de l'approche finale et de l'atterrissage, peut être utilisé au décollage.

Au lâcher des freins, le pilote peut avoir immédiatement la valeur de l'accélération disponible, grâce à l'indication de pente totale. Or, c'est l'accélération disponible qui est en relation directe avec la longueur de décollage plus que la poussée du moteur indiquée par les instruments de bord. Ainsi, l'indicateur de pente totale est l'instrument le mieux adapté pour aider le pilote à décider la poursuite du décollage. Trois remarques doivent néanmoins compléter cette affirmation :

a) Au moment du lâcher des freins, la vitesse aérodynamique est trop faible pour que la mesure de l'incidence soit possible, que ce soit par une girouette ou par l'intermédiaire d'une mesure de pression différentielle. Or, pendant le roulement au sol, l'incidence est égale à l'assiette puisque la pente de la trajectoire est nulle ; ainsi tant que l'avion a les roues au sol (ou jusqu'à ce qu'il ait atteint une vitesse suffisante pour que la mesure d'incidence soit possible), le signal d'incidence envoyé au calculateur de pente totale doit être remplacé par un signal d'assiette longitudinale.

b) L'information de pente totale, durant l'accélération au sol, ne peut être fournie par la position de l'index dans le viseur tête haute, parce que la pente totale est trop grande. En effet, le rapport poussée sur poids varie de 0,2 (transports subsoniques) à 0,4 (transports supersoniques) et dépasse largement cette valeur pour les chasseurs. Or, à $F/mg = 0,2$ correspond un γ_v de 11°5 et à $F/mg = 0,4$ un γ_v de 23°5 ; le champ vertical du viseur n'est en général pas assez haut au-dessus de l'horizon pour pouvoir afficher une telle valeur.

L'information de pente totale au décollage doit donc être fournie au tableau de bord et non dans le viseur.

c) L'accélération disponible diminuant normalement avec la vitesse, le contrôle du décollage doit se faire en vérifiant que la pente totale est toujours supérieure à une valeur limite fonction décroissante de la vitesse. Cette fonction limite peut être calculée pour chaque distance de décollage disponible, et un calculateur, comparant la pente totale disponible à cette valeur limite, peut alors envoyer au pilote une indication "GO" "NO GO".

Par ailleurs, après le décollage, le pilote peut suivre une procédure anti bruit en respectant toutes les règles de sécurité, puisqu'il connaît l'angle de montée et exactement la poussée minimale nécessaire pour maintenir la vitesse constante dans ces conditions. En outre, en cas de panne moteur, le pilote peut ajuster l'angle minimum de montée de façon à éviter les obstacles connaissant exactement la véritable marge disponible de poussée.

Enfin, le système de viseur tête haute, tel que nous l'avons décrit, ci-dessus, est-il utilisable en cas d'approche automatique ?

Actuellement, la fiabilité des systèmes d'approche automatique est insuffisante, pour que l'on puisse accepter l'atterrissage sans surveillance du pilote et remise des gaz de la part de ce dernier en cas d'alarme signalant la panne. En effet, la fiabilité de ces systèmes est telle que la probabilité p de panne est de l'ordre de 10^{-6} par atterrissage. Or, un pilote effectue au cours de sa carrière environ 10 000 atterrissages. La probabilité P pour celui-ci de rencontrer au moins une fois la panne au cours de sa carrière est $P = 1 - (1 - p)^n$ où n est le nombre d'atterrissage soit pour $n = 10\,000$ $P = 0,00995$; statistiquement, un pilote sur cent, seulement, observera au moins une fois la panne au cours de toute sa carrière.* La probabilité pour qu'il rencontre la panne au cours de ses mille premiers atterrissages est de 0,001 ; statistiquement, un pilote sur mille rencontrera la panne au cours de ses mille premiers atterrissages.** Autrement dit, la probabilité de panne est suffisamment faible pour que les pilotes aient le sentiment que la panne est très rare et que "cela n'arrive qu'aux autres". Par contre, un avion effectue environ 10 000 atterrissages, ce qui représente une probabilité de 0,00995 de voir survenir la panne au cours de la vie totale de l'avion. S'il y a 1 000 avions équipés du système, on a une chance sur deux, de voir survenir la panne sur plus de 10 avions de la flotte et une chance sur cent, de voir survenir la panne sur plus de 17 avions. Ceci signifie, en pratique, que l'on verra sûrement survenir la panne sur une douzaine d'avions environ. On ne peut donc accepter de se reposer uniquement sur le système d'atterrissage automatique pour assurer la sécurité de la phase finale du vol et l'on est obligé de faire appel au pilote pour déceler "à temps" une panne du système et remettre les gaz. Or, le pilote n'est pas prêt psychologiquement à attendre la panne, puisqu'il n'y croit pas !

Si le pilote dispose des instruments classiques, dont l'interprétation demande un effort mental relativement important, et un système d'alarme détectant un mauvais fonctionnement du système d'approche, tout porte à croire que le pilote ne réagira que tardivement au signal d'alarme, parce que, seule l'analyse compliquée de la situation lui aurait permis de déceler, grâce à des incohérences entre divers paramètres, l'imminence du signal de panne. Or ne croyant plus à la panne, après tant d'atterrissages sans incidents, le pilote n'est pas préparé à faire un effort compliqué d'analyse, inutile à son avis.

Par contre, la présentation des informations que nous proposons dans le viseur tête haute, rend l'interprétation de la situation très aisée et permet de faire de la prévision à court terme, rendant inutile une attention soutenue de surveillance de l'alarme ; si, en effet, le vecteur vitesse est sur le point désiré du seuil de piste, si les ailes sont horizontales et si l'incidence est à la valeur recommandée pour l'approche, le pilote sait qu'il a plusieurs secondes devant lui pour réagir si la panne survient, car la situation ne peut se détériorer très rapidement.

Par ailleurs, les informations procurées par le viseur sont plus "intéressantes" que celles fournies par plusieurs instruments ne fournissant que des grandeurs numériques. Le pilote peut suivre la progression de son avion en approche en observant l'agrandissement de la piste synthétique et en guettant l'apparition de la piste réelle "derrière" cette piste synthétique, alors qu'il n'est guère "passionnant" de constater que les deux aiguilles de l'ILS sont constamment croisées au centre du cadran.

Bien entendu, cette surveillance du système d'approche automatique par le viseur tête haute néces-

---

* La probabilité pour qu'aucun pilote d'un groupe de 10 ne rencontre la panne est $(1 - p)^{10}$ soit 0,9. Par contre, la probabilité pour qu'aucun pilote d'un groupe de 100 ne rencontre la panne est $(1 - p)^{100}$ soit 0,37 et pour un groupe de 1 000 cette probabilité tombe à $4,5.10^{-5}$.

** La probabilité pour qu'aucun pilote sur 1 000 ne rencontre la panne est de 0,37.

site que les informations fournies par le viseur aient une origine différente de celles utilisées pour le guidage.

Il peut être également utile d'envoyer dans le viseur des informations de position de l'avion, indépendantes du système de guidage, permettant de bâtir une partie de la piste synthétique et des informations de position provenant du système de guidage, lui-même, pour bâtir le reste de la piste synthétique.* Par contre, les deux côtés et le seuil de sortie de piste sont fournis par le système de guidage, le seuil de piste et l'axe sont fournis par le système du viseur. Une discordance entre les deux systèmes ne peut pas passer inaperçue du pilote et doit inciter à mettre les gaz au maximum tout en plaçant prudemment le vecteur vitesse au-dessus de l'horizon, et au-dessous de la pente totale.

Par ailleurs, le pilote ayant volontiers l'oeil fixé sur le viseur pour surveiller l'horizon, la piste, le vecteur vitesse, toute alarme, due à la détection d'une panne du pilote automatique, peut être signalée par le clignotement de l'un de ces symboles (la suppression temporaire d'une indication utile est plus sûrement détectée que l'apparition d'un signal supplémentaire, visuel ou sonore, même très intense).

On voit donc que l'analyse du pilotage en approche automatique, permet de conclure aux avantages du viseur tête haute pour la surveillance active du système.

Avant de conclure, de quelle expérience de ce nouveau système de présentation des informations disposons-nous ?

Les essais de ces systèmes sont essentiellement de trois types différents :

1) des essais au simulateur portant sur le système le plus complet (vecteur vitesse, pente totale, horizon artificiel, piste synthétique, repère de pente à 6°, caps repérés sur l'horizon) type TC 123 permettant d'étudier les avantages et les inconvénients du dispositif dans le cas d'approche type STOL à forte pente.

Une centaine d'atterrissages ont été effectués dans ces conditions et ont abouti aux conclusions suivantes :

a) il est indispensable de disposer dans le viseur d'un champ latéral suffisamment grand pour ne pas perdre trop facilement la piste de vue lors d'évolutions face à celle-ci. L'idéal serait bien entendu de pouvoir apercevoir la piste aux gisements 90 et 270 c'est-à-dire latéralement comme en vol à vue. Seules des expériences complémentaires permettront de préciser le champ latéral minimal acceptable (sûrement supérieur à celui fourni par les dispositifs actuels qui sont surajoutés à une cabine existante alors que ces dispositifs devront être dessinés comme parties intégrantes des cabines au moment de leur conception).

b) le viseur tête haute avec vecteur vitesse et pente potentielle supprime les difficultés de pilotage au second régime. Cette conclusion nécessite une explication détaillée.

En pilotage aux instruments classiques le problème du pilotage au second régime est résolu par la règle suivante :

- la vitesse est maintenue constante à la valeur recommandée ($V_{App} = 1.3\, V_s$ en général) par action sur le manche ; si la vitesse est trop grande le pilote "tire" sur le manche.
- la pente est pilotée de façon à maintenir l'avion sur la trajectoire ILS par action sur la manette des gaz (une diminution de pente de descente s'obtient par augmentation de la poussée)

Un tel mode de pilotage à l'intérêt d'être "stable" même au second régime mais il a l'inconvénient de conduire à des corrections très lentes de trajectoires. La vitesse est très bien maintenue mais la recherche du bon régime moteur est lente et fastidieuse (surtout si les gradients de vent nécessitent des changements de régime au cours de la descente, principalement au voisinage du sol).

Le pilote a donc tendance à utiliser le mode de pilotage inverse à temps de réponse beaucoup plus court mais instable au second régime : piloter la pente au manche et maintenir la vitesse d'approche à la manette des gaz. On sait que ce mode de pilotage est instable si l'on cherche à suivre une trajectoire imposée ; une action à cabrer sur le manche conduit à une augmentation d'incidence ce qui instantanément diminue la pente de descente, mais conduit, si l'on ne touche pas aux gaz, à une pente de descente stabilisée plus forte (augmentation de traînée au second régime pour une diminution de vitesse).

Ce dernier mode de pilotage, très rapide (les variations de pente sont quasi instantanées) n'est instable que si l'on ne corrige pas l'augmentation de traînée, due à l'augmentation d'incidence, par une augmentation de poussée.

Avec les instruments classiques le pilote ne connait pas la poussée adéquate à afficher et toute erreur conduit à une accélération ou à une décélération qui ne cessent de croître avec l'écart de vitesse (d'où l'instabilité dite de propulsion).

Si le pilote dispose du viseur tête haute, il peut agir directement sur le vecteur vitesse pour modifier la trajectoire (action sur la pente par le manche) tout en affichant, grâce à la pente totale, la bonne poussée équilibrant à tout instant la traînée ; le problème d'instabilité de propulsion au second régime disparait donc.

2) des essais sur avions bancs d'essais comme le Nord 262 expérimental de l'Ecole Nationale Supérieure de l'Aéronautique et de l'Espace (équipé d'un collimateur TC 121 avec vecteur vitesse, horizon, piste synthétique, et pente potentielle et d'un collimateur CV 91 pour approche à vue avec un vecteur vitesse simple) ou comme un Nord 260 équipé de 2 collimateurs CV 91.

Le premier avion a permis de montrer la possibilité d'effectuer des atterrissages complets, avec roulement, en pilotage sous capote. C'est à notre connaissance, le seul dispositif ayant permis d'effectuer de façon sûre le pilotage aveugle de l'avion, en roulement après l'impact, jusqu'à l'arrêt sur la piste.

Les essais sur le Nord 260 (atterrissage à vue assistés par le collimateur) ont permis de vérifier que la présence de symboles en position tête haute ne "polarisaient" pas les pilotes au point de diminuer leur perception du monde extérieur. A cet effet des statistiques de position du point d'impact par rapport à une bande matérialisée sur la piste ont été relevées. Tant que la bande visée est loin du seuil réel de la piste la répartition des impacts est sensiblement gaussienne autour du point visé. Par contre lorsque la bande visée est très près du seuil, la répartition des impacts, toujours gaussienne est nettement décalée "long", ce qui prouve sans ambiguité que lorsque les pilotes sont "motivés" (ici pour éviter de "toucher avant la bande"), ils perçoivent nettement le monde extérieur "derrière" le collimateur.

---

* Par exemple, les deux côtés et le seuil de sortie de piste sont fournis par le système de guidage, le seuil de piste et l'axe sont fournis par le système du viseur.

3) des essais sur avions de ligne ou avions d'arme. Des collimateurs d'approche à vue du type CV 91 ont été montés sur les Mirages F1, sur quelques Etendard Marine, sur un DC 8 de l'UTA et sur un 747 d'Air France.

Il est plus difficile de faire part de résultats pour ce type d'expérience, qui avait pour rôle essentiel de faire connaitre le système plutôt que de fournir des conclusions.

On peut néanmoins retenir une très bonne acceptation du système, qui conduit, rappelons le, à une modification radicale du mode de pilotage. Cette acceptation est particulièrement large pour les catégories de pilotes les plus motivés c'est-à-dire les marins qui constatent une simplification non négligeable des manoeuvres d'apontage, et les pilotes de la compagnie UTA qui doivent se poser tous les jours sur des pistes courtes, mal dégagées et non équipées de système ILS.

Ainsi le collimateur tête haute, conçu initialement à la suite de considérations purement théoriques sur l'ergonomie des postes de pilotage, a déjà fait ses preuves expérimentales. Il ne remplacera toutefois une partie du tableau de bord classique, que dans la mesure où il sera intégré dans les cabines des avions futurs au stade même de la conception. Cette étape finale ne sera atteinte que si quelques avions expérimentaux dérivés d'avions modernes, sont "redessinés" avec ce système entre autre (en particulier tous les systèmes CCV) et essayés ainsi par les Services Officiels (certification), les Constructeurs, l'Armée de l'Air, la Marine et les Compagnies Aériennes.

Some DHC-6 Twin Otter Approach and Landing Experience in a STOL System.

by

Richard P. Bentham,
Engineering Test Pilot,
Ministry of Transport,
Ottawa, Ontario, KIA ON8,
Canada.

SUMMARY

The Canadian Government's decision to introduce a STOL demonstration service revealed a need for practical data and flight experience to assist in aircraft approval and development of safe operational procedures.

From 1971 to 1973, a series of flight tests concerned with the steep approach and landing task were carried out, initially in a DHC-6-100 Twin Otter and later in a DHC-6-300S. Approach angles of 6^{o}, 7^{o}, and 8^{o} were assessed in terms of pilot work load and aircraft touchdown and landing distances. Other relevant factors peculiar to the steep approach and landing task were investigated including transition from en-route guidance to approach guidance, crew co-ordination, night operation, missed approach and engine out missed approach, and approach turbulence and wind shear. Community noise sensitivity was closely monitored. The flight test programme resulted in some modifications to the production aircraft, the development of approach and landing operating procedures and the definition of some potential problem areas.

DESCRIPTION OF STOL SYSTEM

Aircraft

In the planned STOL system we will have six DHC-6-300S Twin Otters operated from STOLports at Ottawa and Montreal by Air Transit, an Air Canada subsidiary. The DHC-6-300S is a basic Series 300 Twin Otter with a number of modifications to enhance its performance and handling in the STOL system. Some of these modifications will be discussed later in this paper.

Electronic Systems

Litton 101M Area Navigation (R-NAV) equipment will be used for en-route 3 dimensional guidance, and the CO-SCAN scanning beam microwave landing system (MLS) will be used for precision steep approach guidance. Each aircraft will be equipped with an Airborne Data Acquisition System (ADAS) to gather operational data to aid in the development of future STOL regulations and standards.

The Litton 101M R-NAV equipment is programmed normally by a card reader but it also has a capability of reversion to manual inflight programming. Discrete STOL routings are stored on computer cards which are selected by the pilot prior to take-off. Information on the cards includes Standard Instrument Departure (SID), en-route airways, Standard Terminal Arrival Route (STAR), and missed approach. The Litton 101M uses DME/DME (rho/rho) as a primary operating mode, with DME/VOR (rho/theta) as a back-up mode. R-NAV approach guidance is programmed to coincide with the MLS approach path, so the pilot has the redundancy of two separate guidance systems on final approach. This R-NAV equipment provides the advantages of:

(a) direct routing
(b) minimum cockpit workload
(c) minimum Air Traffic Control (ATC) input.

Since the MLS localizer and glide path are co-located, the ground installation must be located at the side of the runway (for glide path considerations) with an offset approach course. At our STOLports, the MLS installation is located on the right side of the runway, 80 feet from the threshold, with the localizer on-course offset 3^{o} to the left. The Glide Path Intercept (GPI) is 125 feet from the threshold with a 6^{o} glide path angle.

The ADAS will record over 40 parameters on tape to be processed by a dedicated ground computer. This data will be used to assess items such as aircraft performance, pilot workload, R-NAV and MLS performance, effect of turbulence, etc. It is anticipated that it will provide a useful fund of knowledge for future STOL development.

STOLport

Figure 1 shows our STOLport lay-out. Two of these sites are now completed and are in operation at Victoria Park (about 5 minutes from downtown Montreal) and at Rockcliffe (near Ottawa).

Figure 2 shows the present STOLport runway lighting. The major differences from conventional airport lighting are:

(a) floodlighting of the touchdown zone.
(b) runway lights at 50 foot intervals for the first and the last 500 feet.
(c) white strobe lights to mark the threshold
(d) alternate red runway lights for the last 500 feet.
(e) no approach lights.

Figure 3 shows the layout, including target touchdown zones, of the STOL runway. The runway is 2000 feet long by 100 feet wide, with a stopway/clearway distance of 400 feet at each end.

FLIGHT TEST PROGRAMME

Instrumentation

In 1971 we initiated a flight test investigation of the various aspects of steep approaches into a STOLport. We concentrated on the approach and landing, as the take-off in the Twin Otter is the same for both STOLport and conventional airport operations. Prior to the start of this project, the Ministry of Transport was not equipped or organized to undertake flight research investigations of this nature. Accordingly we had a problem in acquiring adequate instrumentation and we had to make the best of the very limited resources which could be gathered together quickly.

For example, we manually recorded approach path deviation (in terms of dots) at the Decision Height, and airspeed and radio altimeter altitude at the runway threshold. We wanted to record the point on the runway at which the aircraft first touched down. This we did with a very simple system which worked very reliably and with surprising accuracy. A polaroid land camera was installed at a window on the right side of the aircraft, above the main wheel axle and at 90° to the fore and aft axis of the aircraft. Runway distances markers were surveyed in at 20 foot intervals along the right side of the runway. On the DHC-6-100 we used weight switches on the undercarriage to fire the camera on touchdown, and on the follow-up tests on the production 300S model we used the right wheel spin-up generator signal sent to the ground spoilers. Using a ground calibration, we were able to find the point on the polaroid print exactly abeam the main wheel axle, at 75 feet away (the distance from the runway centre-line to our distance markers). To allow for crosswind on touchdown, a correction of one foot per degree of crab angle was made.

This very simple installation was operated with great reliability by a single observer, who also read the polaroid print and recorded the data between landings. Thus we had instant re-play, and avoided the misery of undetected instrumentation failures spoiling a day's results. The only problems we had were one or two polaroid film jams. The system worked very well and gave good accurate data for our purposes.

The distance to the full stop was recorded visually by a sightline to the runway distance markers. We felt that the accuracy of a simple sightline was adequate.

We had no way to photographically record night touchdown distances, so these were estimated by two observers in the cabin using the runway distance markers for reference. Their observations of touchdown point were in close agreement and we believe that the maximum error was in the order of $\pm$ 5 feet.

Another problem area assessed with the instruments already available was that of the along track wind shear component on final approach. This was recognized through the appearance of sudden airspeed changes or approach path deviations. The pilots made an assessment of the degree of the wind shear effect using a simple scale of 1 to 4 based on the magnitude of the airspeed change.

We operated a small weather station which gave runway wind velocity at 30 feet. Weather balloons were used to measure winds aloft at 400 foot intervals up to 2000 feet above ground. We did not attempt to correct landing distances to zero wind conditions, but rather recorded the landing performance obtained with the existing known wind conditions.

I would like to add that this was a case of using very simple methods to obtain data, at minimum cost and in minimum time. Our intention was to gather data under known operational conditions, accepting the weather as it came, and to put together all these variable conditions of weather, pilots, braking conditions, etcetera. The net result would thus be representative of what might be achieved in the real world of aircraft operations.

Test Aircraft

In our initial series of tests conducted at Rockcliffe airport in 1971, we used a Series 100 Twin Otter. In 1973, when a production Series 300S Twin Otter became available we conducted a second test programme to compare results with our Series 100 tests.

Some of the pertinent data on the Series 100 and Series 300S Twin Otter are as follows:

	DHC-6-100	DHC-6-300S
Max Engine S.H.P.	550	620
Max Weight	11579 lbs	12,500 lbs
Power Loading	10.5 lbs/hp	10.1 lbs/hp
Wing Loading	27.6 psf	29.8 psf
Aspect Ratio	10.0	10.0
C_L Max	2.6	2.6

Pilots

For the DHC-6-100 tests, the subject pilots included 6 experienced operational pilots, (not on the DHC-6) and two test pilots. The second set of tests using the Series 300S Twin Otter were done with 3 Air Transit pilots (some DHC-6 experience) and one test pilot.

The pilot briefing for all of these flights was as follows:

i. Approach under simulated instrument conditions, command steering or raw data, as assigned.

ii. Intercept MLS glide path with landing flap down and airspeed set at 1.3 Vso (Vso, stall speed in the landing configuration).

iii. At Decision Height, go visual and land in the touchdown zone.

iv. Do not "duck under" for the landing.

v. Do not reduce power to idle until touchdown, if speed is below 1.3 Vso.

vi. Use moderate wheel braking to a full stop.

vii. Series 100
Do not use propeller discing (forward C.G. tests) Use propeller discing but not reverse (aft. C.G. tests)
Series 300S
Use propeller discing on all landings, but not reverse.

STEEP APPROACH TEST RESULTS

Vertical Speed and Time

The Series 300S Twin Otter at 1.3 Vso can achieve a rate of descent of 1400 fpm, or an equivalent glide path angle of 10.7°. The Series 100 at 1.3 Vso can achieve a rate of descent of 1300 fpm or an equivalent glide path angle of 10°. At maximum landing weight, 1.3 Vso on the DHC-6-100 is 73 knots Calibrated Airspeed (CAS), and 74 knots CAS on the DHC-6-300S.

The vertical speeds required at 1.3 Vso in still air and the approximate time remaining from the Decision Height at 200 feet to touchdown (T/D) are as follows:

Glide Path Angle	Vertical Speed	Time D.H. to T/D
6°	770 fpm	15 sec
7°	900 fpm	13 sec
8°	1030 fpm	12 sec

We found that there was no unusual landing problem associated with the vertical speed of an 8° glide path as long as the Decision Height was 200 feet or higher. With a D.H. lower than 200 feet, the pilots felt they were approaching a limit in the time available to carry out the landing task.

We found that the pilots could not tell easily what glide path angle they were flying when on instruments. Only after considerable experience and awareness of the effect of wind, could they guess whether it was a 6°, 7°, or 8° glide path. Although the margin of vertical speed available to correct down to the glide path was reduced as the glide path angle increased from 6° to 8°, the margin available for the 8° glide path was considered limiting but acceptable for the conditions encountered. The 300S has an increased flight idle engine speed and a reduced flight idle propellor blade angle. This combination produced only a slight increase in the vertical speed available, but it did produce an increased transient thrust/drag response to changes in the power levers. This increased thrust/drag response was considered to be a significant improvement. I should mention that the slight increase in vertical speed available in the Series 300S aircraft has been welcome, even on the 6° approach. The moral of all this seems to be that a pilot really appreciates having the ability to make prompt corrections during the approach.

Offset Approach

Figure 4 shows the approach path geometry for a 7° glide path. With the 3° offset approach, the aircraft just intercepts the extended runway centre line at a 200 foot Decision Height. The approach path geometry for an 8° glide path moves the 200 foot D.H. to the right of the extended runway centre line, and an "S" turn is required to line up for landing. For a 6° glide path, the 200 foot D.H. is to the left of the extended centre line and only a slight left turn is required to line up for landing. The "S" turn tended to make the 8° glide path 200 foot D.H. more difficult for the pilot. When a D.H. of 300 feet was used, there was no "S" turn required to line up, and no problem with time constraints and vertical speed effects in the landing task.

Landing Performance

Figure 5 shows landing performance results from one hundred 6°, 7° and 8° approaches combined. These results include the following operational conditions:

29 Runs - 6°	35 Runs Aft C.G.	82 Runs Day
43 Runs - 7°	65 Runs Fwd C.G.	18 Runs Night
28 Runs - 8°		

22 Runs 4 MPH Avg. Tailwind Component
78 Runs 5 MPH Avg. Headwind Component

Figure 6 shows a comparison of landing performance from 6°, 7° and 8° approaches. The average touchdown distance did not change in any consistent way, but the touchdown scatter decreased as the glide path angle increased. Landing roll distance was not affected by the glide path angle.

Night Landings

Figure 7 shows the landing results for night and day conditions. We found that our pilots liked the touchdown zone floodlighting because it gave good visual cues for the touchdown task. The fact that the average touchdown distance was almost exactly in the centre of the touchdown zone may be attributed to the pilots wanting very much to land in the floodlit area. The quality (vertical speed at touchdown) of the night landings was found to be as good as those under day conditions. All of the night landings were done at the foward C.G. limit, and propellor discing was not used for stopping.

We were concerned about the effect of floating past the floodlit touchdown zone into the unlit zone beyond it. However, this proved to be no problem. Since the aircraft was always very close to the ground by the time the touchdown zone was passed, the pilots found they were not concerned at all by the relative darkness beyond it.

Strobe lights were located at the threshold as we were concerned about positive identification of the runway in conditions of low visibility. Without the strobes, we have on record one case where on a clear night the pilot was unable to find the runway in time and had to overshoot. This was due to the 3° offset approach and a strong adverse crosswind which required a crab angle such that the runway was about 30° left, instead of straight ahead at the Decision Height.

Effect of Centre of Gravity

The effect of the position of the C.G. on touchdown distances and scatter was significant. Figure 8 shows the results of the DHC-6-100 with forward and aft C.G. loadings. The aft C.G. results include twelve landings each from 6° and 8° glide slope approaches and eleven landings from a 7° glide slope approach.

It should be noted that the aft. C.G. stopping distances included the use of propeller discing; hence the shorter stopping distances.

Due to reduced elevator nose up control power and increased stick forces at the forward C.G., landings tended to be harder, touchdown distances were shorter and touchdown scatter reduced when compared to results at the aft C.G. With the increased nose up elevator control power and reduced stick forces at the aft C.G., the pilot's attempts to make smooth landings resulted in increased touchdown distances and increased touchdown scatter.

Ground Control and Deceleration

In the ground deceleration phase, from touchdown to full stop, we found a wide variation in performance due to different pilot techniques and skill in the use of brakes and propellor discing. In this phase of the operation, pilot workload could be high under adverse conditions of wind and runway surface. Also, the individual pilot technique in using the means available to control and stop the aircraft was not always optimum. As will be seen later, modifications incorporated in the Series 300S aircraft made a very significant improvement in ground deceleration.

The quality of landings, in terms of bounce or vertical speed at touchdown were as good as in conventional operations. The pilots quickly adjusted to steep approach conditions and consistently made first class landings.

Approach Speeds

We looked at approach speeds of 1.4, 1.35, 1.3, 1.25 and 1.2 Vso, and found that 1.3 Vso, was the best compromise. At higher speeds the great tendency to float down the runway was unsatisfactory in that it produced long touchdown distances and increased touchdown scatter. At lower speeds, the limited ability to round out for landing at the forward C.G. was unsatisfactory. At 1.3 Vso the pilot could deviate from the target speed by $\pm$ 5 knots without creating any unusual problems, but at the other target approach speeds, high or low side airspeed deviations complicated pilot touchdown control.

Approach Path Guidance

The flight director was a modified Collins FD-109 using Distance Measuring Equipment (DME) for continuous gain scheduling. In the cockpit, full scale instrument deflection was $\pm$ 1.4° for the glide slope and $\pm$ 3° for the localizer.

We made twenty approaches not using the Flight Director command mode; that is the pilot had to assess the magnitude of corrections for localizer and glide path errors. Of these twenty approaches to 200 feet, two resulted in missed landings when the pilot did not correct an excessive vertical position error. In both cases, the aircraft was too high at the Decision Height to permit a landing.

Wind Shear

Wind shear was a cause for concern. Wind shear above about 400 feet was not a problem as the pilot had ample time to make adjustments. Lateral wind shear components and turbulence were not a problem anywhere in our tests. But along track wind shear effect did cause some concern. Our one missed approach due to wind shear occurred when transitioning from about a 20 knot tailwind into a calm condition at 200 feet above ground. The aircraft could not be slowed in time for a landing. In other cases of descending from a headwind into calm conditions at 100 to 200 feet above ground, we had several incidents of very low airspeed and accelerating sink rates close to the ground. The fact that the engines were at low power settings and in a slow acceleration response range (4 to 5 seconds to achieve maximum power) added to the pilot's problems. I should add that the Rockcliffe Airport is located in a natural bowl-like setting beside the Ottawa River and this is very conducive to a wind shear situation in the lower few hundred feet.

Missed Approach

The vertical velocity of 770 fpm (still air) on a 6^{o} glide path together with the 4 to 5 seconds required to accelerate the engines from low power settings to maximum power caused some concern about height losses to be expected in a missed approach. After reaching the Decision Height and not making visual contact, the aircraft must, of necessity, descend below the D.H. by some amount before a climb is established. The amount of the height loss before establishing this climb is determined primarily by the time delay of the crew in initiating the missed approach procedures by applying maximum power, checking the rate of descent, and raising the flaps.

In our tests, height losses were usually between 25 and 35 feet and were never more than 50 feet.

We feel confident that with good crew training and crew co-ordination a height loss of more than 50 feet would be highly improbable. A crew procedure has been established such that at Decision Height the Captain must decisively indicate that he has sufficient visual contact to land. The co-pilot is programmed to initiate the missed approach unless he hears and feels the captain taking over for the landing. Thus, there should be no uncertainty at the D.H. as to whether there are sufficient visual cues to make a landing. Unless the Captain takes the decisive action to call for the landing and take over control of the aircraft the missed approach is initiated by the co-pilot as soon as the D.H. is reached.

Engine-Out Missed Approach

A missed approach does not occur very frequently. Engine failure also occurs very infrequently and the two together, an engine failure at the critical moment in a missed approach, could be considered a very improbable event. However, because of the adverse conditions of the very high drag of the approach flap, the relatively high descent rate and the time required to bring an engine up to full power, we felt we should consider the case of an engine failure or hang-up at the critical moment of a missed approach.

The engine out go-around situation requires that the crew take the correct actions and carefully manage the energy available. At Decision Height, the flaps must be selected up and maximum power applied. If the engine failure occurs just before, or during this procedure, the pilot has a very high workload problem with asymmetric power, low speed and a high drag configuration.

The Twin Otter flaps operate very slowly - taking about 30 seconds for full extension or retraction. It takes approximately 10 seconds for the flaps to retract to a climbing configuration, and during this time the pilot must hold airspeed at 1.1 Vmca (about 73 knots CAS) and allow the aircraft to sink until the flaps retract sufficiently to permit a climb. Then airspeed is increased slowly to best climb speed as the flaps continue to retract. This demands some concentration, particularly when one is only 200 feet above the ground to begin with. If in addition one must, without delay, feather the dead engine, the workload in the cockpit becomes very high. Our initial experience using the DHC-6-100 was not very encouraging. In our initial procedure of selecting flaps fully up from the landing configuration, we noted that the final 10^{o} of flap retraction usually resulted in a pronounced aircraft sink as the pilot tried to accelerate from 76 knots at flaps 10^{o} to 87 knots at flaps 0^{o} to follow the best climb speed. With pilots experienced on other types, but not the Twin Otter, we observed height losses in excess of 200 feet, and large heading changes and lateral track excursions. These were due to various pilot techniques and the high cockpit workload compounded by the need for a manual feathering of the dead engine propellor.

Our efforts to improve the safety of our engine out missed approach were concentrated in reducing pilot workload and emphasizing pilot training. The autofeather system was modified to include a single torque arming capability. This provided autofeathering both in the event of power application following or during an engine failure, and autofeathering with an engine failure after power application.

A 10^{o} flap selector stop was introduced to hold the flaps on retraction at 10^{o} - the best single engine climb configuration. These changes in the autofeather and flap systems reduced pilot workload to the extent that the pilot of the Series 300S aircraft has only to manage speed control from a minimum of 73 knots CAS (1.1 Vmca) to 82 knots CAS during a single engine missed approach.

We found that line pilots often were reluctant to use full rudder in an asymmetric situation requiring full rudder. Without training emphasis on the use of rudder, they tended to use just enough rudder to keep the yaw rate low, but not enough to stop it. Thus the aircraft slowly turned, sometimes more than 90^{o} and made unacceptable lateral track excursions. In pilot training, emphasis was placed on the importance of using full rudder and 5^{o} of bank into the live engine in an asymmetric situation

at low airspeed. Emphasis was placed also on airspeed control.

These measures made a significant improvement in the engine out missed approach performance in the Series 300S Twin Otter. The pilot's workload was reduced to applying maximum engine power and controlling the aircraft. Heading and lateral track excursions were reduced to very small proportions. Height losses were reduced to between 50 feet and 90 feet. Because of this we have used a 100 foot height loss from an engine out missed approach as a guide in considering minimum Decision Height and zoning criteria.

It should be mentioned that in our initial tests on the engine out missed approach problem we tried making our approaches with 30^{o} flaps down to the Decision Height instead of the full 37^{o} landing flap, in an attempt to reduce the time required to raise the flaps to a climbing configuration. This had no significant effect on engine out missed approach performance. However, as it did significantly increase our touchdown distances and scatter we abandoned the idea of partial flap approaches.

THE DHC-6-300S

The flight tests on the DHC-6-100 just described contributed to the final modifications of the production Series 300S Twin Otter and to the operational procedures of the STOL service.

DHC-6-300S

Some of the modifications which are incorporated in the DHC-6-300 to produce the 300S model are as follows:

(a) Ground Spoilers - automatic on touchdown

(b) Hydro-Aire Mark III Anti-Skid Brakes

(c) Power Lever Detent
- for ease of selection of optimum propellor discing

(d) Auto-feather System
- available for missed approach case.

(e) Propellor and Ng Flight Idle Limits
- propellor angle reduced from 11^{o} to 10^{o}
- Ng idle increased from 50% to 55%

(f) Flap Selector Stop - 10^{o}

Ground control and deceleration were significantly improved by the addition of the spoilers, the power levers discing detent and the anti-skid brakes. It should be noted that we were very conscious of pilot workload and all of these modifications reduce pilot workload. The pilot has simple tasks to perform; none of them depend on recognizing annunciated visual or audio cues; none of them require precise careful judgement. The ground spoilers deploy automatically on touchdown and assist in ground control and deceleration capability by getting the weight on the wheels immediately after touchdown. The power lever discing detent allows the pilot to quickly and positively select maximum propellor discing. The anti-skid brakes eliminate the need to pick a braking path or pump the brakes on wet or icy runways. The ground spoilers and the propeller discing are largely drag complementary; the loss of one or the other has little effect on the total deceleration available.

As mentioned previously, flight characteristics and pilot workload have been improved by the changes in the auto-feather system, the propellor and Ng flight idle limits and the flap 10^{o} selector stop. The single torque arming of the auto-feather system provides auto-feathering in the event of an engine failure during a missed approach. Our tests indicated that this capability was essential to consideration of an engine failure during a missed approach. The change in engine idle speed from 50% to 55% was made to provide a better capability to handle high electrical loads. The resulting reduced propellor flight idle blade angle from 11^{o} to 10^{o} produces an increased available vertical speed of about 100 fpm, and more significant, an apparent increased thrust/drag response to power lever changes. The flap 10^{o} selector stop provides a reliable and simple selection of the best single engine climb configuration.

Figure 9 shows the results of 59 landings from 6^{o} glide slope approaches with the Series 300S. The average touchdown distance which is some 50 feet inside the touchdown zone is the target area that the pilots generally aim to hit. We feel that the great success in arriving there, and the significantly reduced touchdown scatter is due largely to the improved propellor blade angle and Ng flight idle combination. There was not an opportunity to see if the reduced touchdown scatter with increased glide path angle noted in the DHC-6-100 tests also held true with the DHC-6-300S. The reduction in ground deceleration distances due to incorporation of spoilers, power lever detent for maximum propeller discing and anti-skid brakes was impressive. It should be noted that 52 out of the 59 runs were made by Air Transit line pilots using their own version of moderate braking. The other 7 runs were made by a De Havilland Aircraft test pilot. Wind conditons, measured at 30 feet, were as follows:

-17 landings with an average tailwind component of 5 MPH.

-15 landings with calm conditions.

-27 landings with an average headwind component of 8 MPH.

Selection of Glide Path Angle

The glide path angles of 6°, 7° and 8° were all considered to be safely useable by the Twin Otter, with the 8° case being limiting due to the approach path geometry previously mentioned and due to the vertical speed available to correct down to the glide path. After all factors were taken into account, the 6° glide path was chosen over the 7° glide path. This choice was by no means unanimous.

DHC-6-300S Approach Procedures

Finally, a few words to describe the operational procedures that have been developed to date for the final approach into the STOLport.

Between the R-NAV initial approach waypoint and the R-NAV final approach waypoint at 1500 feet, the crew completes the final landing checks except for flaps and propellor pitch, decelerates to Vfe for full flaps, and transitions to the MLS for precision approach guidance. When the Flight Director is switched from R-NAV to MLS information, the R-NAV system continues to present its approach path information to the pilot on a separate indicator. A monitored approach method is used, in which the First Officer flies the aircraft and the Captains monitors the approach and uses the power levers to control airspeed. At Decision Height, the Captain takes control of the aircraft for landing.

The time of selection of full flaps is very important. It is desired to intercept the 6° glide path in the landing configuration at a speed of 1.3 Vso. The winds at 1,500 feet play a large part in the pilot's decision on when to select flap down. In the final DHC-6-300S tests, we had 3 incidents out of 59 approaches when the stall warning sounded during the run-in to glide path interception.

This happened because of unanticipated headwinds (low ground speed) with the result that the flaps were fully down before glide path interception. Because the interception looked so close (the glide path indicator showing just above interception) the pilots were badly misled. Glide path interception was close in terms of distance but not in terms of time. The high drag of the landing configuration required a substantial increase in power, but the pilots were reluctant to apply the power, expecting a glide path intercept at any moment. Without the required engine power, airspeed rapidly fell of to close to the stall. The opposite case, in which a tailwind produces a high groundspeed resulting in the aircraft flying through the glide path before flaps are extended fully also creates problems in getting down. The key to success is to be aware of ground speed (available from the R-NAV System) when approaching the glide path interception, and to select the flaps down at the appropriate DME distance from that point.

After glide path interception, and with airspeed at 1.3Vso, engine power is reduced and the propeller pitch is selected to full fine. This is left to the last for noise considerations.

At Decision Height, assuming the runway is in sight, the Captain takes control. His task is to land in the touchdown zone. On touchdown, the ground spoilers automatically deploy, the power levers are selected to the discing detent and wheel braking is applied as required.

At Decision Height, if the Captain has not decisively signalled that he has control and is going to land, the First Officer automatically, and without delay, applies maximum power and calls for flaps 10° for the missed approach.

PROBLEM AREAS

With respect to possible future problem there are two noteable ones; wind shear and STOLport lighting. Surprisingly noise does not appear to be a problem.

Noise

Although Rockcliffe airport is situated on the edge of a long established and affluent residential area, complaints about noise from the Twin Otter operation were rare. Noise measurements taken at critical area in the neighbourhood revealed that the noise levels from STOL operations were no worse than those from the normal local street traffic. The low number of noise complaints seemed to bear this out. Take-off power settings were confined to the airfield boundaries, with first power reduction being made at 400 feet above ground. On approach, the low power settings, 5 - 15 psi torque and low propellor speeds, (below 80% or 1760 RPM) resulted in very low noise levels. During one two day period in October 1973, we made 75 take-offs and landings at Rockcliffe without a single complaint of any kind being registered.

Wind Shear

The most interesting problem area is that of wind shear. We believe that the most effective thing we can do now in our Twin Otter operations is to ensure that the line pilots are thoroughly trained and are briefed daily on shear conditions expected at the STOLports. We are exploring means of predicting and reporting local shear conditions in a form useable to pilots.

STOLport Lighting

The night lighting of the STOLports is by no means final. At Victoria Park, the Bonaventure Expressway loops around the STOLport, and poses a problem of positive STOLport identification. As an adverse crosswind may place the STOLport 30° off to one side with the Expressway straight ahead, one can appreciate the problem. The solution here seems to lie in developing unmistakeable STOLport lighting.

CONCLUSION

This paper has described a very practical flight test exercise aimed at exploring a new operation field. The project was simple, inexpensive and results were applied quickly to aircraft development and operational procedures.

FIG. 1

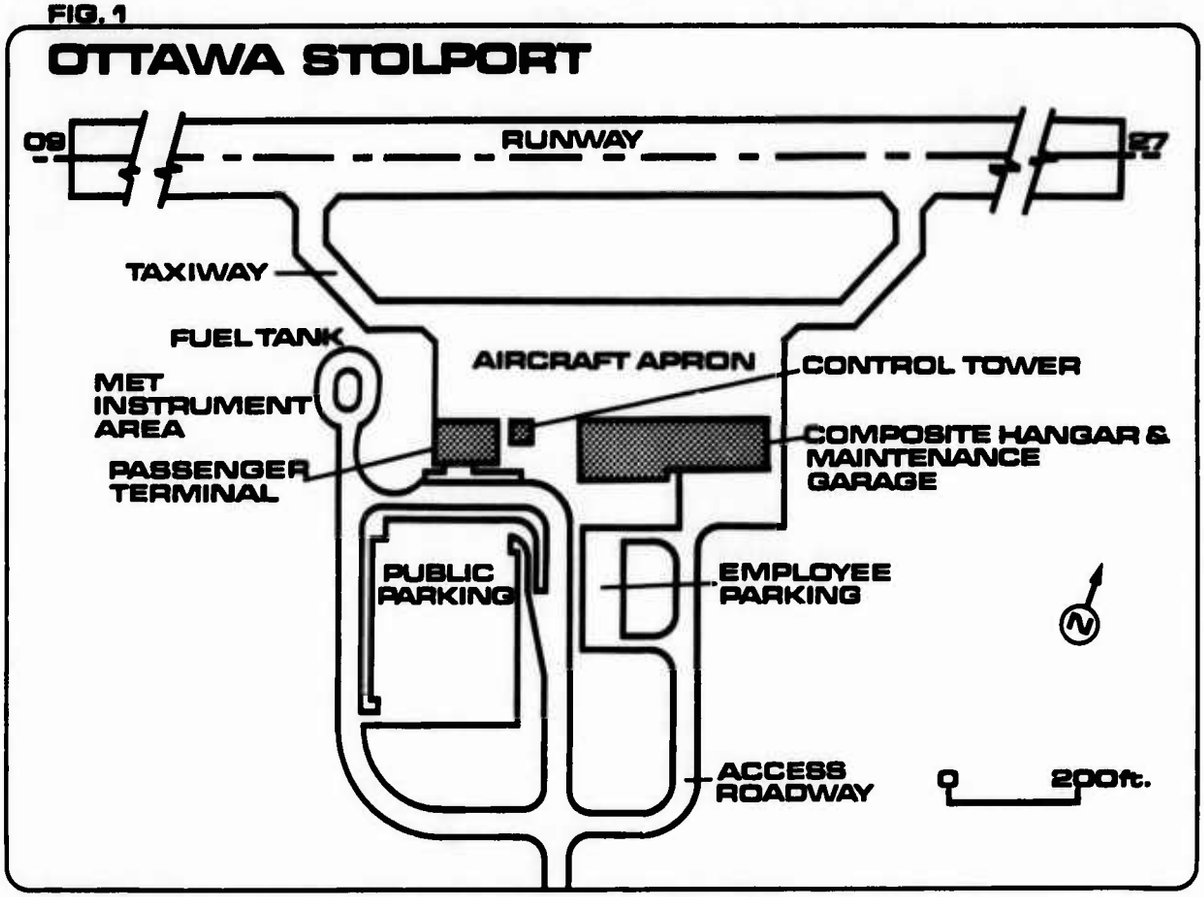
OTTAWA STOLPORT
09
RUNWAY
27
TAXIWAY
FUEL TANK
MET INSTRUMENT AREA
AIRCRAFT APRON
CONTROL TOWER
PASSENGER TERMINAL
COMPOSITE HANGAR & MAINTENANCE GARAGE
PUBLIC PARKING
EMPLOYEE PARKING
N
ACCESS ROADWAY
200ft.

FIG. 2

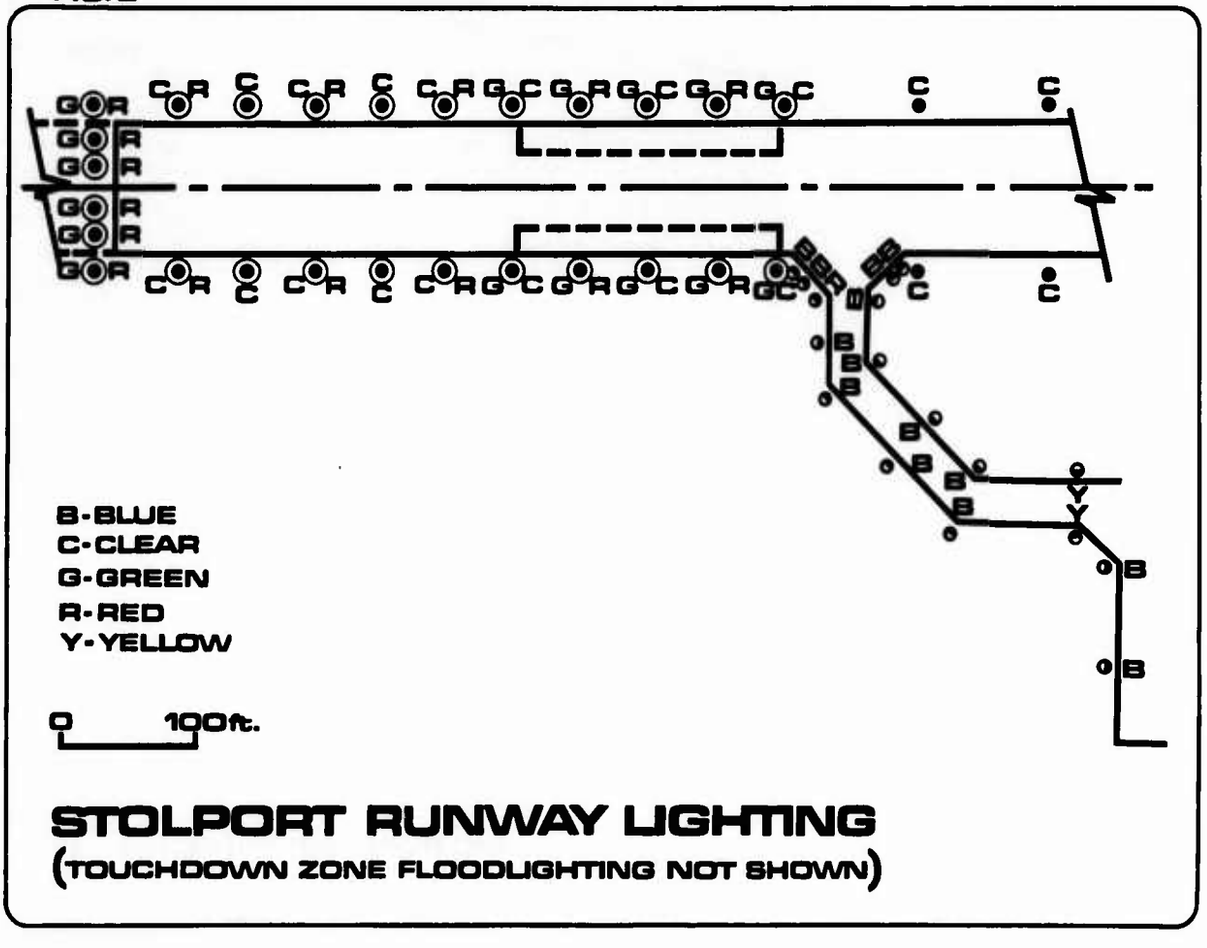
B-BLUE
C-CLEAR
G-GREEN
R-RED
Y-YELLOW
100ft.
STOLPORT RUNWAY LIGHTING
(TOUCHDOWN ZONE FLOODLIGHTING NOT SHOWN)

FIG. 3

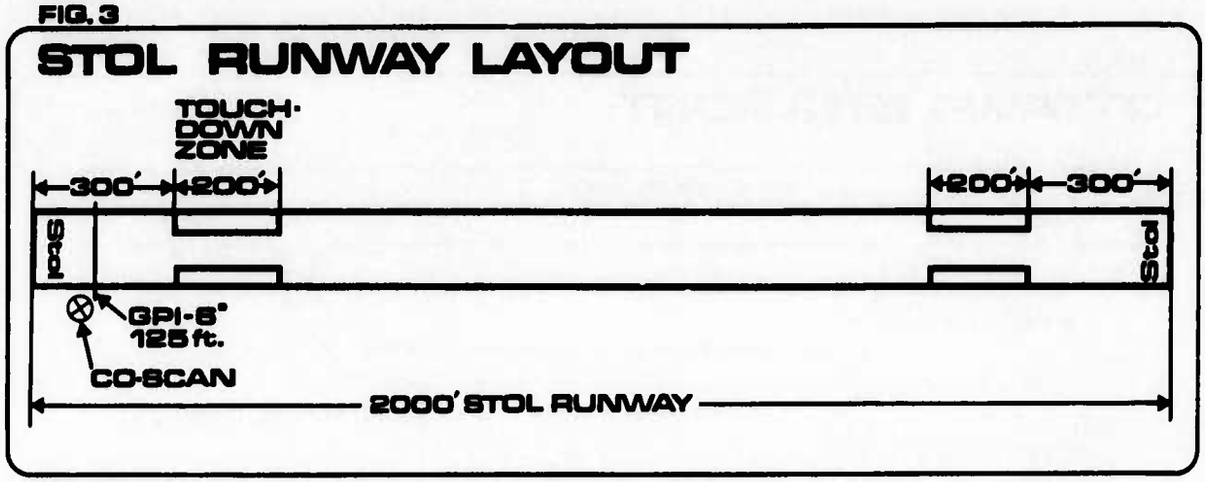

FIG. 4

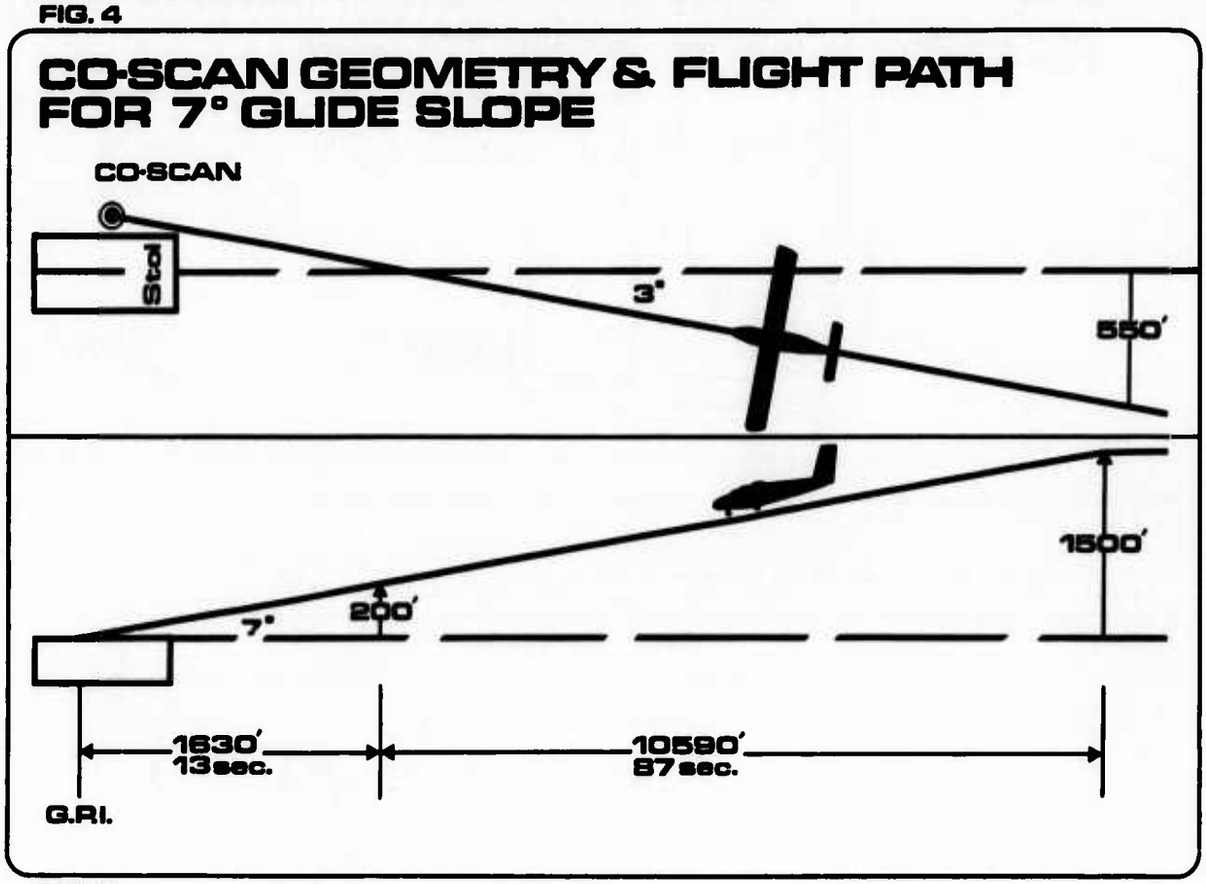

FIG. 5

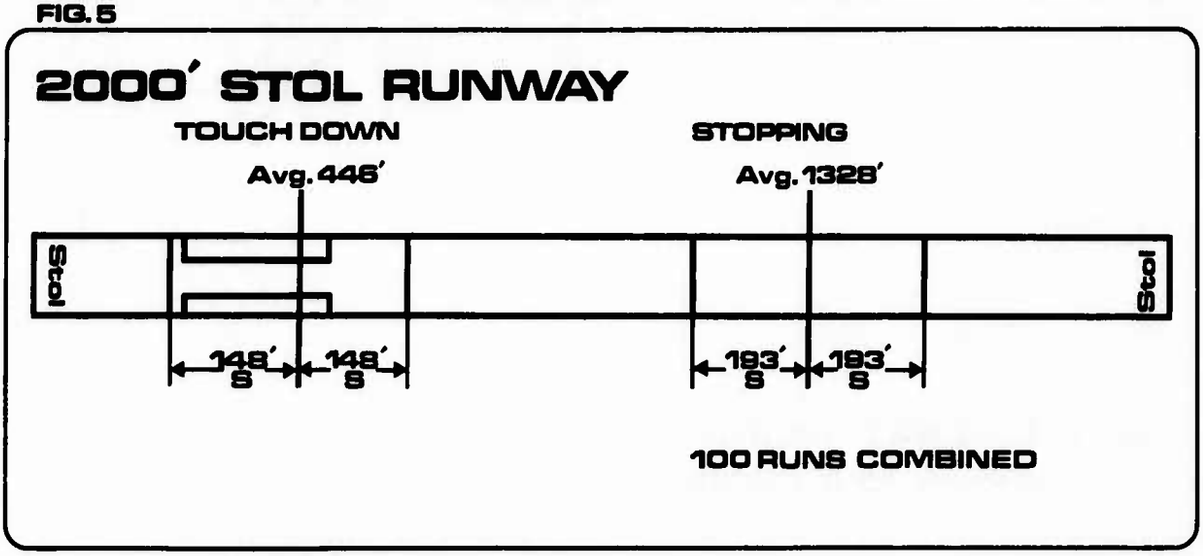

FIG. 6

DHC-6-100 LANDING PERFORMANCE 6°,7°,8° GLIDE PATHS

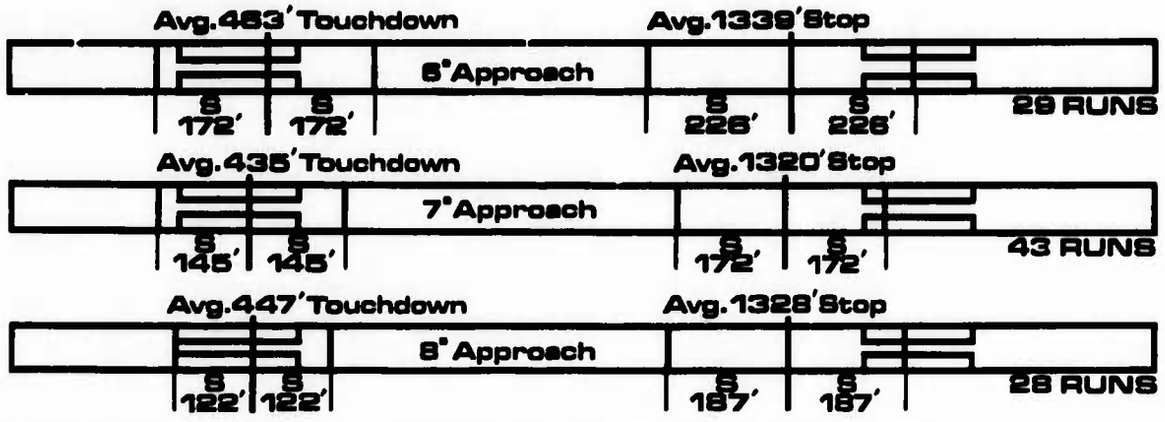

FIG. 7

DHC-6-100 LANDING PERFORMANCE NIGHT/DAY

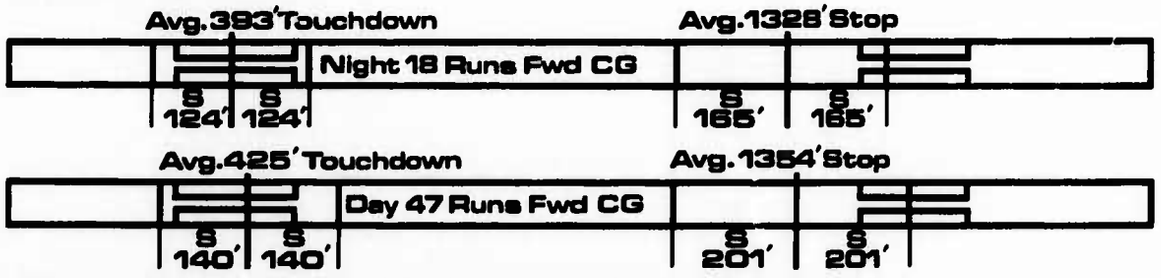

FIG. 8

DHC-6-100 LANDING PERFORMANCE AFT/FWD C.G.

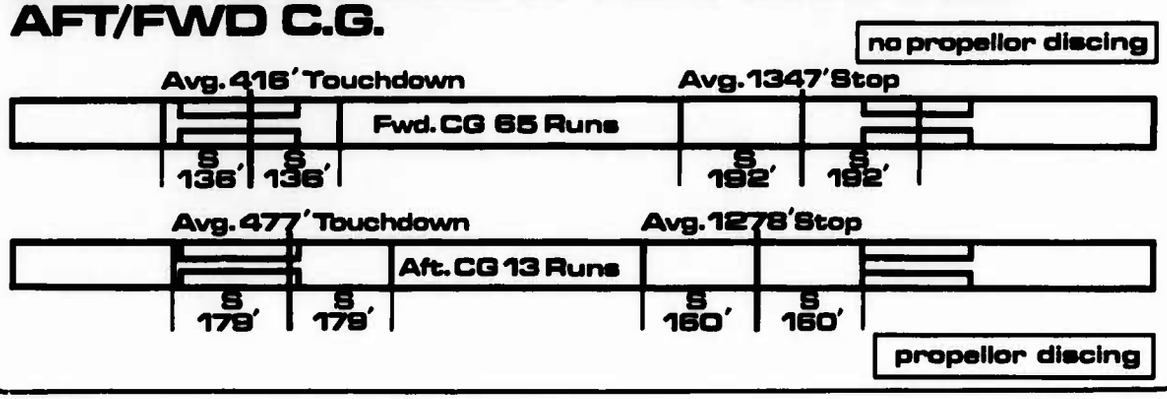

FIG. 9

DHC-6-300S LANDING PERFORMANCE

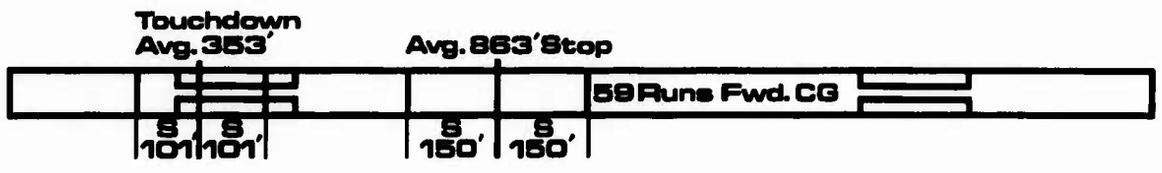

LOW POWER APPROACHES

by

B. Lyle Schofield
Chief, Flight Test Technology Branch
AFFTC/DOEST
Edwards AFB CA 93523

SUMMARY

Discussions are presented on current final approach-to-landing procedures along with the relationship of conventional approach speeds to the lift to drag (L/D) relationships of aircraft. The characteristics of L/D relationships are discussed in view the landing approach maneuver, identifying the potential advantages of operating on the "front side" of the L/D curve. Flight experience of low L/D, idle power approaches using the front side of the L/D curve are reviewed in light of the piloting task. The velocity convergence relationship for operating on the front side of the L/D curve are presented and the convergent characteristics for both transport and fighter aircraft are explored. Front side approach and landing performance for the KC-135A and T-38A aircraft are presented. Convair 990 touchdown dispersions from low L/D, idle approaches are presented. Other significant advantages of the low power, front side L/D landing approach are enumerated.

LIST OF SYMBOLS

SYMBOL	DEFINITION	UNIT
A_f	acceleration factor $(1 + \frac{V_t}{g}\frac{dV_t}{dh})$	- - -
C_L	lift coefficient	- - -
g	gravitational constant	32.2 ft/sec^2
h	altitude	feet (ft)
L/D	lift to drag ratio	- - -
n_z	normal load factor	g's
S	reference wing area	ft^2
V_c	calibrated airspeed	knots (kts)
V_e	equivalent airspeed	knots (kts)
V_t	true airspeed	ft/sec
Wt	weight	pounds
ρ	air density	$\frac{\text{pound sec}^2}{\text{ft}^4}$
σ	ratio of ambient air density to sea level air density	- - -
SUBSCRIPTS		
GS	glide slope	- - -

I. INTRODUCTION

Accident statistics bear out the fact the landing is a critical phase of flight. Some evidence of this is manifest in the U.S. air carrier statistic for 1972 where 87 percent of all airline fatalities occurred in landing accidents. U.S. Air Force statistics show that 15 percent of all major accidents occur during final approach and landing and 65 percent of these accidents result in fatal or major injuries.

These statistics are no surprise to pilots. They have always considered that setting up for final approach, maintaining the final approach glide slope, flare and touchdown are their most demanding piloting tasks and require constant proficiency training. In spite of our phenomenal technological advancements in the past two decades, this situation has seen no significant improvement and in many cases has worsened due to the increase in approach speeds, without increasing stall margins.

There must be a better way to perform this most difficult task. Considerable effort has been expended in providing improvements in high lift systems to lower speeds for approach and landing. These are steps in the right direction but maybe speed reduction, through better high lift devices, is not the only important payoff area for making the landing maneuver easier to fly and consequently safer.

II. CONVENTIONAL LANDING APPROACH

A brief review of the piloting task during final approach to landing will provide some insight into where improvements can be made. The pilot first must reduce his speed to effect the proper configuration changes for landing, i.e., flaps and gear down. Simultaneously he must maneuver to intercept a glide slope at which time further adjustment is required to obtain the proper speed and power setting to maintain the nominal three degree glide slope. Pitch attitude is used to correct to the glide slope and then power is required to compensate for resulting speed changes when approach speeds, to maintain the three degree glide slope, are at the top of the L/D curve. When making an approach on the back side of the L/D curve, airspeed must be maintained largely with attitude changes and power is used to control sink rate. (Figure 1) Handling qualities of the aircraft at these speeds are often sluggish at best. Communication tasks, about which little can be done, add an additional workload.

Cruise flight is performed well on the front side of the L/D curve where flight path control is performed with pitch control. Also, the aircraft is more responsive due to higher dynamic pressures.

Controlling flight path with attitude, operating on the front side of the L/D curve, is a natural technique to the pilot because most flight time is spent under these conditions. Is it possible, then, to perform landing approaches under these conditions and if so what are the benefits and drawbacks? The answer to these questions is the subject of this paper.

III. LOW L/D, IDLE POWER APPROACH EXPERIENCE

The potential of performing landing approaches on the front side of the L/D curve for conventional aircraft was an unexpected by-product of looking at the guidance problems associated with terminal area maneuvering of the planned space shuttle. Since the days of the X-1 research aircraft we, at Edwards Air Force Base, have been performing unpowered landings and consequently have been strong advocates of unpowered approaches for shuttle as a means of eliminating the requirement for airbreathing landing engines with a resultant weight savings. In support of this concept, a number of recent flight studies have been made of the navigational and landing requirements of the space shuttle.

It was during pilot debriefings for low L/D studies using an F-111 and B-52 aircraft (reference 1) that the potential benefit of unpowered approaches for conventional aircraft was identified. It was reported in the F-111 L/D studies, that the "... pilot's task of flying the low L/D approaches was considered by all participating pilots to be easier than flying a normal, powered three degree ILS approach." Quoting again from reference 1 concerning the NB-52 ground control approaches, "Here again, as in the case of the F-111A instrument approach, the piloting task was less demanding because the airplane was being flown in the speed stable region which required no throttling and the handling qualities were better at the higher (than normal) approach speeds." It should also be pointed out that these approaches were made at L/D ratios of 3.2 to 6.7 (figure 2). All L/D's but the F-111A 26 degree wing sweep, gear down configuration are significantly lower than would be the case for most transport aircraft landing configurations. The F-111A 50 and 72.5 degree wing sweep L/D characteristics are similar to those that can be expected from fighter aircraft at idle thrust.

IV. L/D CURVE CHARACTERISTICS

What are some of the characteristics of flying on the front side of the L/D curve which results in comments of "...easier than flying a normal, powered three degree ILS approach."? Let's examine some of the important characteristics of the L/D curve. (In this discussion, it should be kept in mind that flight path angles are inversely proportional to L/D, the higher the L/D, the shallower the flight path.) The L/D curve can be separated into basically three regions (figure 3); the front side, the top and the back side. The front side of the L/D curve is the stable operating area. When operating on the front side, lowering the aircraft nose will increase airspeed which lowers L/D thus producing a steeper flight path angle. Raising the nose will decrease airspeed which increases L/D thus producing a shallower flight path angle. The airplane will also be speed stable while flying along a particular flight path angle. That is, excess speed along a chosen flight path angle will produce excess drag, resulting in a deceleration toward the desired airspeed. The characteristic equations describing the speed stability will be discussed subsequently.

The back side of the L/D curve is unstable. Lowering the nose will increase speed but the L/D increases with increasing speed and consequently results in a shallower flight path. This says that in order to reduce flight path angle, without changing power, a pilot would have to pushover, which is completely opposite of normal pilot reactions. This is why power changes are so critical when flying on the back side of the L/D curve.

The speed is also unstable with respect to a particular flight path; i.e., excess speed along the flight path will result in the same lift but lower drag (higher L/D) and the airplane will accelerate away from the desired speed. Being slower on the glide slope will result in a continuing speed reduction, unless power is applied. Is it any wonder, then, that aircraft have experienced stall on final approach when the pilot is momentarily distracted and the airspeed slows divergently.

Flying on top of the L/D curve is a neutrally stable condition requiring techniques beside attitude and speed for flight path control (e.g. bank angle, speed brakes and thrust modulation).

V. FRONT SIDE L/D APPROACH

It is apparent from understanding the characteristics of the L/D curve that there are some very desirable features associated with making approaches on the front side of the L/D curve. First, corrections to the glide slope are natural. If you are below the glide slope you pull up and vice versa. Second, once on the glide slope, the speed will tend to stabilize at a given value. The speed to which the aircraft will stabilize is well above stall where it has responsive handling characteristics. Third, throttle or speed brake manipulations are significantly reduced or eliminated.

An approach based on these criteria would be as presented in figure 4. The initial approach glide slope would be from 6 to 12 degrees, depending on the aircraft's L/D characteristics for the landing approach configuration and power setting used. The point at which the initial approach slope intersects the plane of the runway is called the aim point and its location is selected on the basis of the aircraft's deceleration characteristics. The velocity at flare initiation is such that the airplane reaches touchdown speed beyond runway threshold.

VI. VELOCITY CONVERGENCE ALONG APPROACH GLIDE SLOPE

The post-flare deceleration distance is dependent upon the flare entry velocity. If the velocity is excessive, the airplane will float too far down the runway prior to touchdown. If the velocity is too low, it may land short of runway threshold. It is important, then, to be at the proper speed prior to the start of flare. This is possible, without the requirement for power changes, if the approach is made on the speed stable (front) side of the L/D curve.

The magnitude of this speed stability has been defined by an equation developed in a presently unpublished study by the author. This relationship was checked for validity using both flight test and simulator data. The equation is as follows:

$$\frac{\Delta V_e}{\Delta h} = \frac{1.128 \times 10^{4} \sigma \Lambda_{f_{GS}}}{V_e}\left[\frac{(L/D)_{GS}}{L/D} - 1\right]\left(\frac{kts}{1000\ ft}\right) \qquad (1)$$

$\frac{\Delta V_e}{\Delta h}$ = incremental change in airspeed due to incremental change in altitude

σ = atmospheric density ratio $\frac{\rho}{\rho_{SL}}$

$\Lambda_{f_{GS}}$ = acceleration factor for the glide slope velocity and altitude $(1 + \frac{V_t}{g}\frac{dV_t}{dh})$

V_e = equivalent airspeed (kts), $V_e \approx V_c$ for approach speeds

$(L/D)_{GS}$ = the L/D for the stabilized glide slope

L/D = instantaneous L/D

There are a couple of interesting characteristics of this equations. First, the velocity converges asymptotically to the glide slope stabilized airspeed. This is evident from the bracketed parameters:

$$\left[\frac{(L/D)_{GS}}{L/D} - 1\right]$$

As the instantaneous L/D approaches the glide slope L/D, the first factor in brackets approaches one and the value in brackets approaches zero. This is best illustrated by figure 5. The top graph in figure 5 illustrates the subsonic L/D performance of a representative aircraft. The glide slope L/D was selected to provide front side L/D variation of at least plus or minus one L/D. The bottom graph illustrates the glide slope stabilized airspeed as a function of altitude. The glide slope in this case was 11.9 degrees for a wing loading of 35 pounds per square foot (PSF). Also shown are velocity convergent characteristics for the case of being one L/D high

(slower than the glide slope airspeed) on the glide slope and one L/D low (high speed) on the glide slope. The start of descent for these conditions was 12,000 feet altitude. This, of course, would be an extreme case from an operational viewpoint and would be more representative of a space shuttle approach.

The second characteristic of the velocity convergence relationship is also associated with the bracketed parameters. The ratio of L/D for stabilized glide slope to the instantaneous L/D controls, to a great extent, the velocity convergent characteristics. This characteristic is dependent both on the magnitude of the glide slope L/D and on the local slope of L/D curve at the glide slope L/D. To better study these effects, typical L/D curves for both transport and fighter aircraft were defined. (Figure 6) The transport curves cover a range of idle power, landing configuration L/D characteristics for larger transport aircraft including the KC-135A with both 30 and 50 degrees flaps and the C-5. The fighter curves include the idle power, landing configuration characteristics of the T-38 aircraft. (The T-38 and F-5B are essentially equivalent in aerodynamic characteristics.)

A number of glide slope L/D's were selected on the front side of each curve and the local slope ($d(L/D)/dC_L$) were measured. From these data, velocity convergence characteristics were computed using equation (1) and the following relationships:

$$L/D = L/D_{GS} + \Delta C_L \frac{d(L/D)}{dC_L} \tag{2}$$

where

$$\Delta C_L = C_L - C_{L_{GS}}$$

and

$$C_L = \frac{295\, n_z\, (Wt/S)}{V_e^2} \tag{3}$$

The velocity convergence characteristics for transport and fighter aircraft are presented in figures 7 and 8 respectively, for a wing loading (Wt/S) of 60 pounds per square foot. Velocity convergence is for initial speeds of $V_{e_{GS}}$ plus 20 knots down to $V_{e_{GS}}$ plus five knots. Since the velocity convergence is also a weak function of altitude (σ and A_f) convergence was computed for altitudes of less than 7,000 feet.

Some interesting characteristics emerge from these data. The transport data shows that at the higher values of $d(L/D)/dC_L$ the lower L/D's result in a greater altitude loss to effect a given velocity convergence. At low values of $d(L/D)/dC_L$, the opposite is true. The crossover area occurs between slopes of eight (8) and twelve (12) and an associated altitude loss of around 4,000 feet altitude. Although the same crossover characteristic is not evident in the case of the fighter aircraft (figure 8), the minimum altitude loss is again about 4,000 feet and the $d(L/D)/dC_L$ slopes are between eight (8) and twelve (12).

Another interesting feature of these curves are that at very low slopes, the altitude loss for velocity convergence increases rapidly. This is to be expected since these slopes are representative of the top of the L/D curve where velocity convergence is weak or non-existent.

VII. IDLE POWER APPROACH CHARACTERISTIC OF REPRESENTATIVE AIRCRAFT

Idle power approach characteristics were investigated for three U.S. Air Force aircraft. These were the C-5A, KC-135A, and T-38A aircraft. Each aircraft was examined to determine if its idle power approach characteristics would permit an idle power approach. Then knowing the approach characteristics, the flare and landing were examined to determine the aim point and deceleration distance to touchdown. Deceleration distance due to weight, touchdown speed and L/D variations were also investigated. The KC-135A and the T-38A will be presented here in that they represent the extremes for the aircraft investigated.

Figure 9 presents the L/D characteristics of the KC-135A for the landing configuration (30 degree flaps). It will be noted that the effective lift to drag ratio (L/D_{cff}) characteristics change slightly with gross weight. This is due to the slight variation in idle thrust as a function of airspeed. Also noted are the flap limit speeds for the various gross weights. Allowable L/D variations are not significantly restricted by the flap limit speed except for the highest gross weight case. Also noted are the normal approach conditions.

The conditions associated with approach, flare and touchdown are shown in table I. The approach glide slope angle for this configuration was 5.8 degrees. Assuming that

WEIGHT (LBS)	APPROACH L/D	APPROACH SPEED V_e (KNOTS)	APPROACH ANGLE	ALTITUDE EXPENDED DURING FLARE (FEET)	END OF FLARE SPEED V_e (KNOTS)	DISTANCE FROM AIM POINT TO TOUCHDOWN (FEET)	TOUCHDOWN SPEED V_e (KNOTS)
211,450	9.41	191	5.8°	58	190	4023	159
177,300	9.41	181	5.8°	52	179	4169	146
121,100	9.41	156	5.8°	39	155	3438	121

Table I. L/D Front Side Approach and Landing Characteristics KC-135A Landing Configuration (30° Flaps)

the aim point would be located 3000 feet from runway threshold, this glide slope would place the airplane at 311 feet above ground level (AGL) one nautical mile off the approach end of the runway, at idle power. Using conventional approach techniques the airplane would be at height of 318 feet and would be carrying 40-45 percent of rated thrust.

Figure 10 presents touchdown dispersion from the aim points as a function of aircraft gross weight. Touchdown dispersion is presented for being both 5 knots fast and 5 knots slow at the start of flare, in addition to touchdown dispersion for an on speed condition. These dispersions are about the same as those encountered during normal landing operations.

The T-38A L/D curves for idle power approach are presented in figure 11. The approach speed were well within the flap limit speed of 220 knots. Touchdown dispersions, presented in figure 12, were less than 900 feet for the gross weight variations which were studied. In this case, the deceleration distances were about the same as for the KC-135A and would require selection of an aim point approximately 3,000 feet before runway threshold. The conditions associated with approach, flare and touchdown are shown in table II.

WEIGHT (LBS)	APPROACH L/D	APPROACH SPEED V_e (KNOTS)	APPROACH ANGLE	ALTITUDE EXPENDED DURING FLARE (FEET)	END OF FLARE SPEED V_e (KNOTS)	DISTANCE FROM AIM POINT TO TOUCHDOWN (FEET)	TOUCHDOWN SPEED V_e (KNOTS)
12,000	5.05	206	10.5°	222	195	4366	150
9,000	5.2	178	10.5°	167	170	3462	129

Table II. L/D Front Side Approach and Landing Characteristics T-38A Landing Configuration

Touchdown dispersion was investigated by Kock, Fulton and Drinkwater III (reference 2) using a CV-990, four jet engine, commercial aircraft. A ground command guidance system transmitted glide slope and localizer error to the aircraft for display to the pilot (ILS type presentation). Hooded approaches, on 11 or 12 degree glide slopes, were made down to 600 feet AGL where the pilot initiated a visual flare and touchdown. Touchdown dispersions for the 25 approaches made under these conditions are presented in figure 13. The variations experienced in these tests are shown to be about $\pm$800 feet, again within operational tolerance.

The handling characteristics of this aircraft were considered to be "...representative of this class of airplane, with the exception of lateral control forces, which are high." The Dutch roll characteristics were also poorer than would normally be encountered in present commercial aircraft, particularly since this aircraft did not incorporate any stability augmentation. In spite of these deficiencies it was reported that: "No unusual stability and control requirements were encountered during these tests, and the approach technique itself, in which high speeds were used, allowed

better airplane response than is possible at the constant, lower speeds of a conventional approach."

VIII. OTHER ADVANTAGES AND DISADVANTAGES

There are other significant advantages of this approach technique, in addition to the advantages already mentioned. These are:

1. Noise abatement which would acrue from both the steeper approach and lower power settings (probably idle) attendant with the front side approach.

2. Landings could be continued with minimal interruption and additional pilot workload in the event of power loss during landing approach.

3. If a missed approach is required, it may be initiated with the advantage that the approach speed is closer to best engine out or missed approach climb speed.

Implementation of front side L/D approach is not without its problems. The major drawback is that the present instrument landing systems could handle this type of approach only with a sophisticated onboard guidance system. Present instrument landing systems do not provide for multiple glide slope selection (reference 3), and more than one aim point may be required to handle all aircraft with acceptable touchdown dispersion.

The higher descent rates attendant with the higher approach speeds and steeper approach angles would seem to dictate a two segment glide slope approach in order to be compatible with the present Category Two IFR rules. This may best be done by a transition from the steeper glide slope to a 1-2 degree glide slope.

Another potential problem area is flap limit speeds because at the heavier gross weights investigated the front side L/D approach speed was close to the flap limit speeds. In some instances, aircraft design changes may be required to alleviate this area of concern, or approaches might have to be made at partial flap deflection.

IX. CONCLUSION

In summary it can be said that the advantages associated with performing the landing approach on the front side of the L/D curve are both numerous and significant. While there are some identified problem areas, this concept merits further consideration and study in an effort to improve safety for this most critical phase of flight.

X. REFERENCES

1 - Schofield, B. Lyle; Richardson, David F.; and Hoag, Peter C.: Terminal Area Energy Management, Approach and Landing Investigation for Maneuvering Reentry Vehicles Using F-111A and NB-52B Aircraft. FTC-TD-70-2, Air Force Flight Test Center, June 1970.

2 - Kock, Berwin M.; Fulton, Jr., Fitzhugh, and Drinkwater III, Fred J.: Low-Lift-to-Drag-Ratio Approach and Landing Studies Using a CV-990 Airplane, NASA TN D-6732.

3 - Raabe, Herbert P.: Instrument Systems for the Space Shuttle, IBM Corporation, NASA TM X-52876 Volume VI, July 1970.

4 - Schofield, B. Lyle: Gliding Flight Equations. FTC-TIM-70-1007, Air Force Flight Test Center, April 1970.

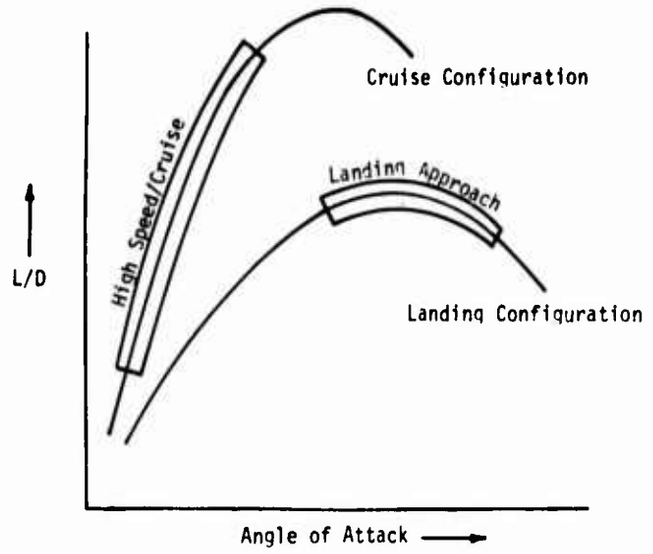

Figure 1. Conventional Flight Operations

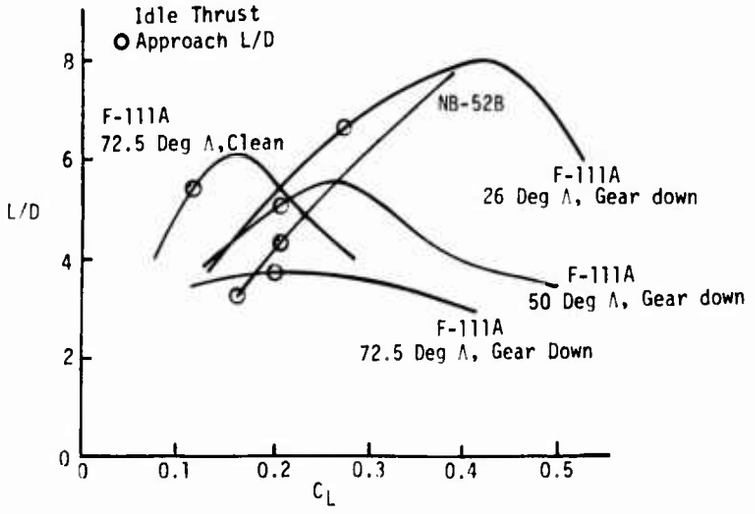

Figure 2. F-111A and NB-52 Low L/D Studies

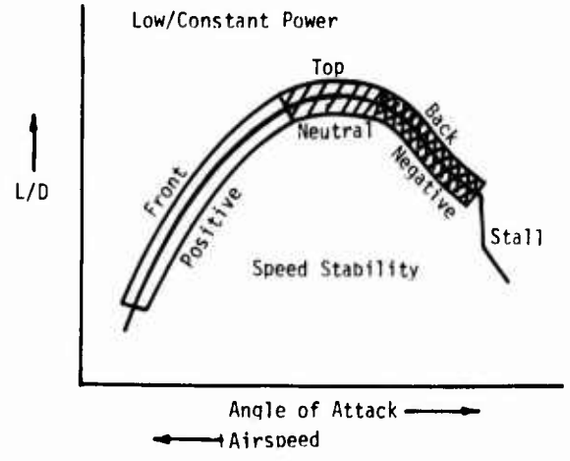

Figure 3. L/D Characteristics

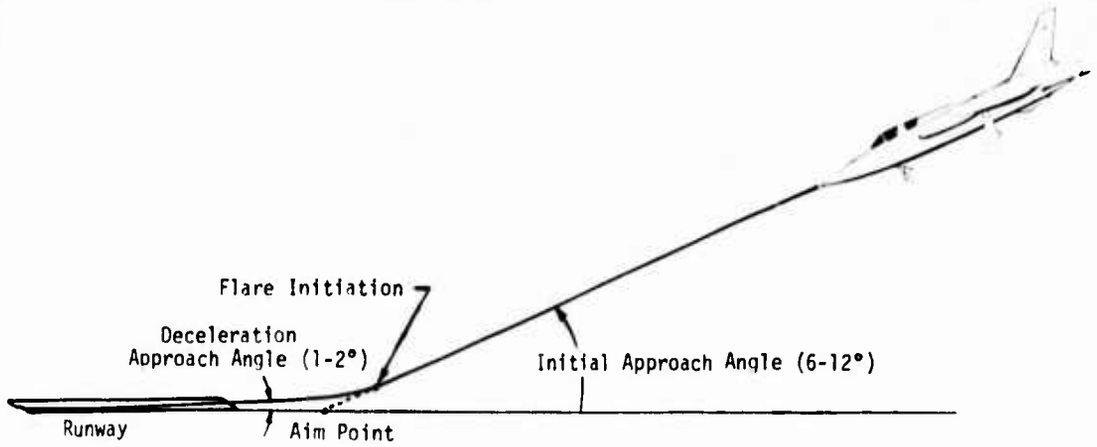

Figure 4. Low Power Approach Technique

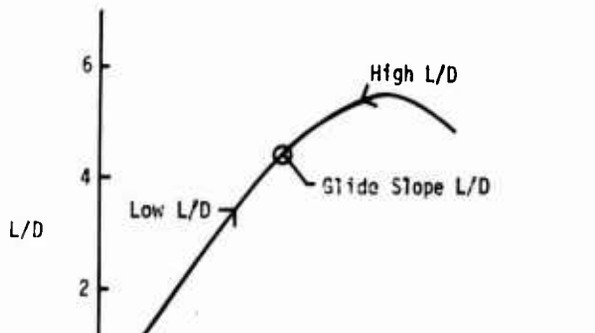

Representative Subsonic Performance of Shuttle Reentry Vehicle

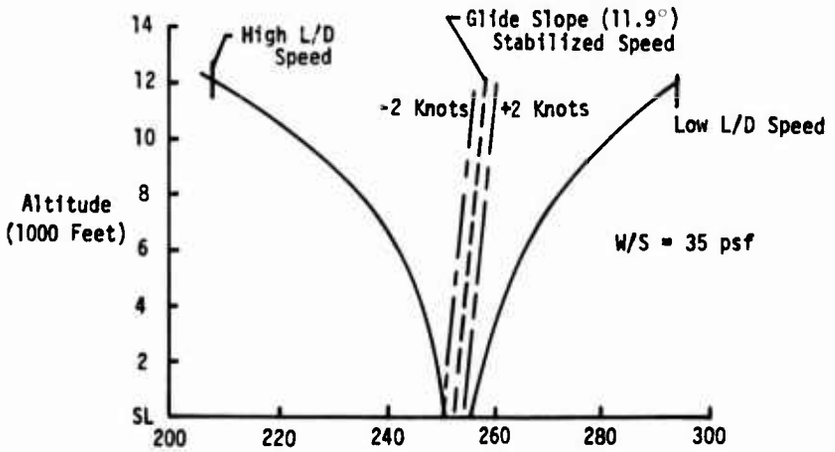

Figure 5. **Representative Velocity Convergence for Flight Along A Constant Glide Slope**

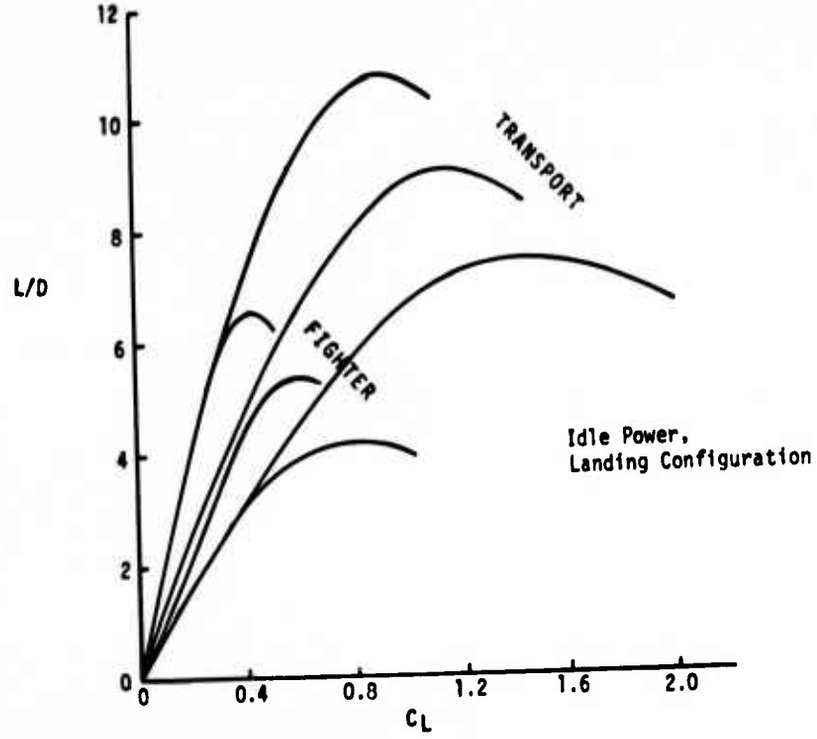

Figure 6. Typical L/D Characteristics

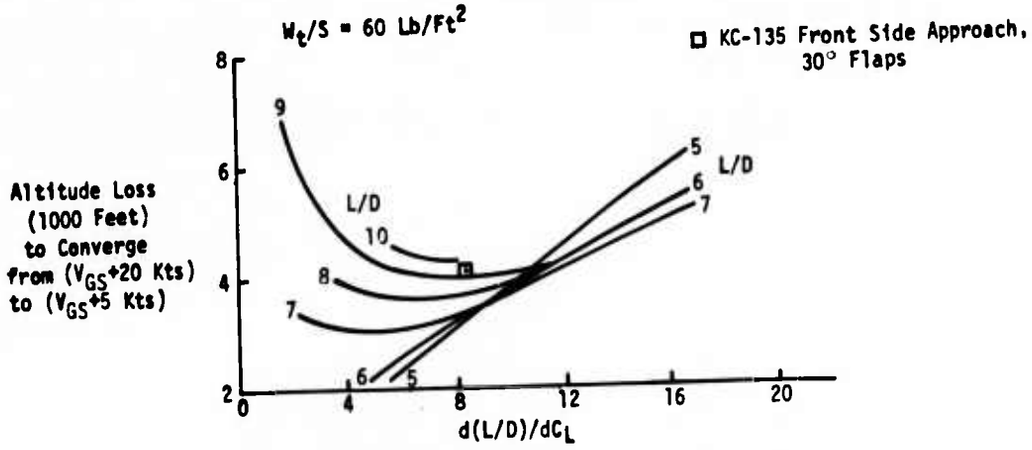

Figure 7. Typical Velocity Convergence Transport Aircraft

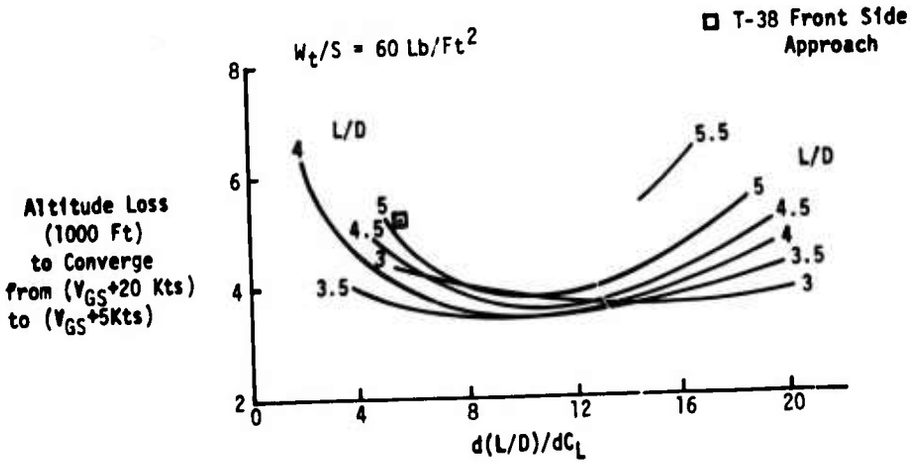

Figure 8. Typical Velocity Convergence Fighter Aircraft

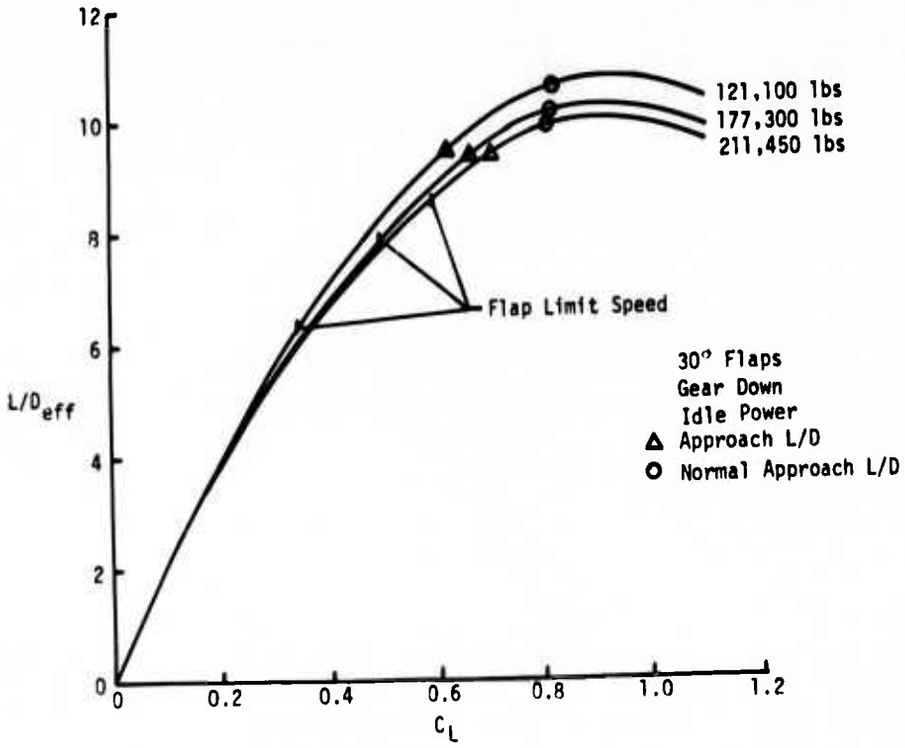

Figure 9. K-135A Landing Configuration

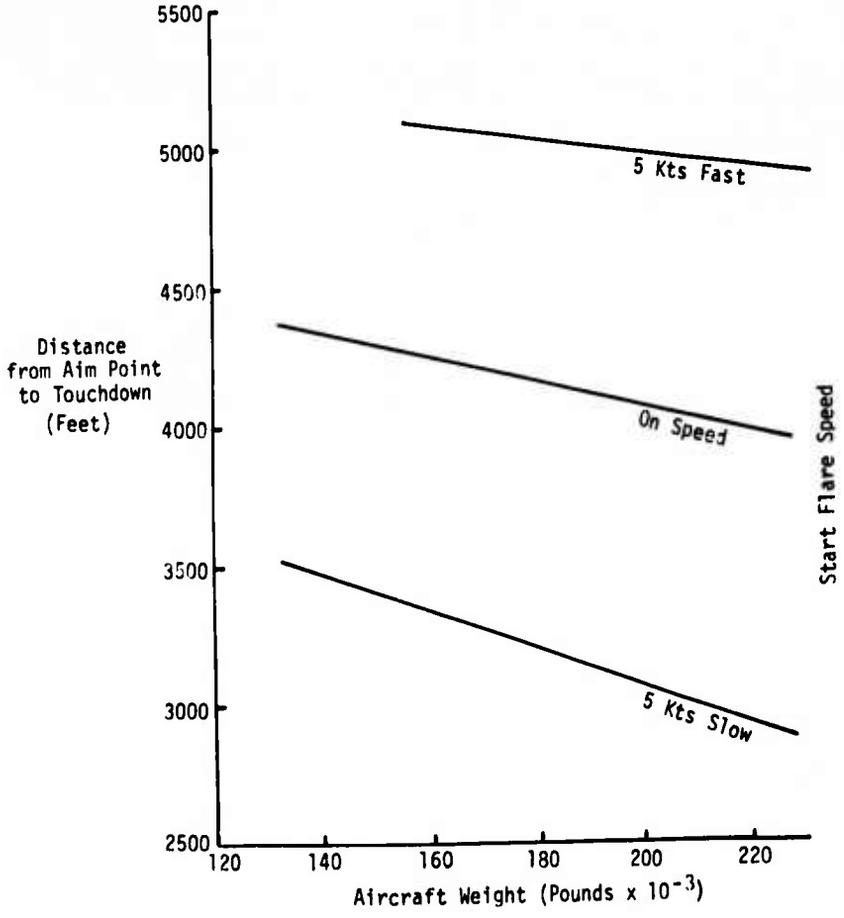

Figure 10. KC-135A Landing Configuration (30° Flaps)

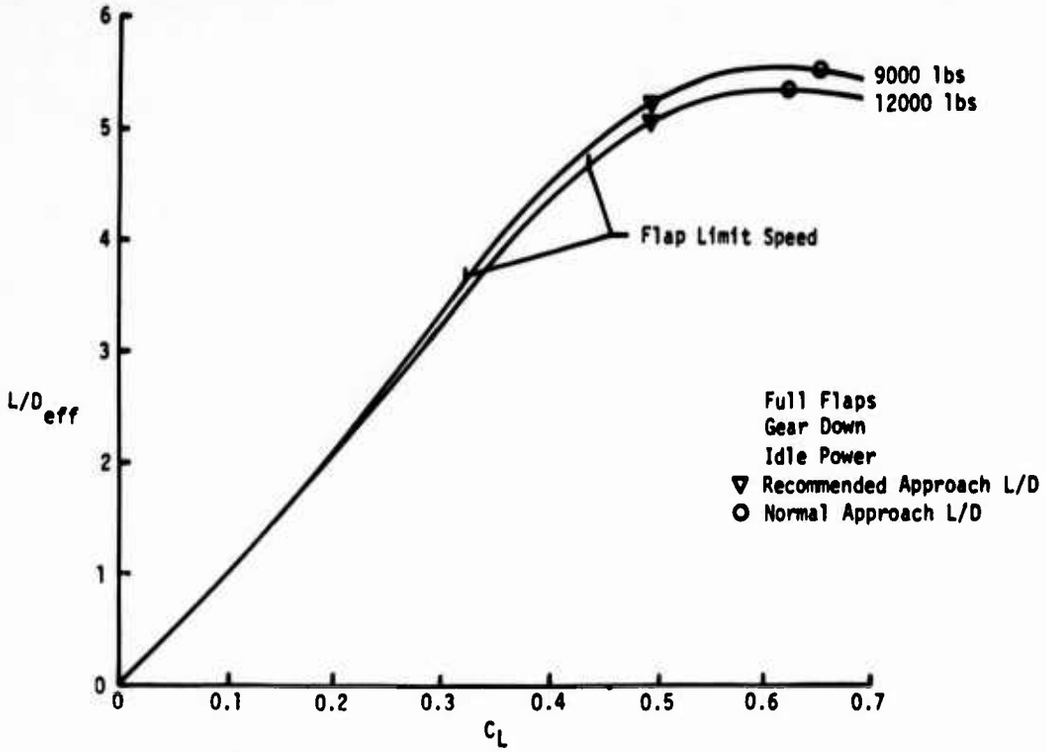

Figure 11. T-38A Landing Configuration

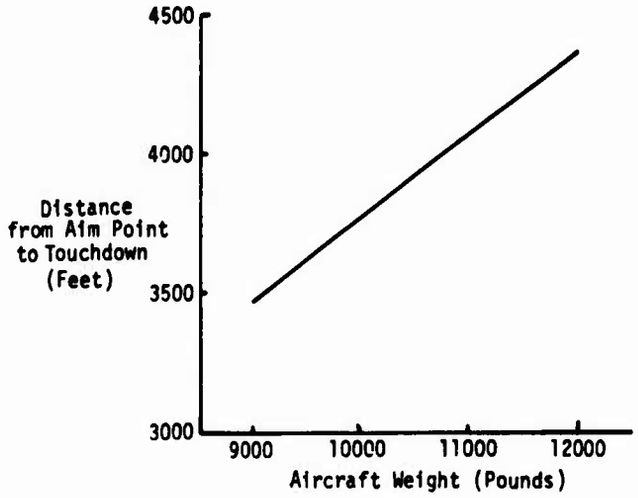

Figure 12. T-38A Landing Configuration

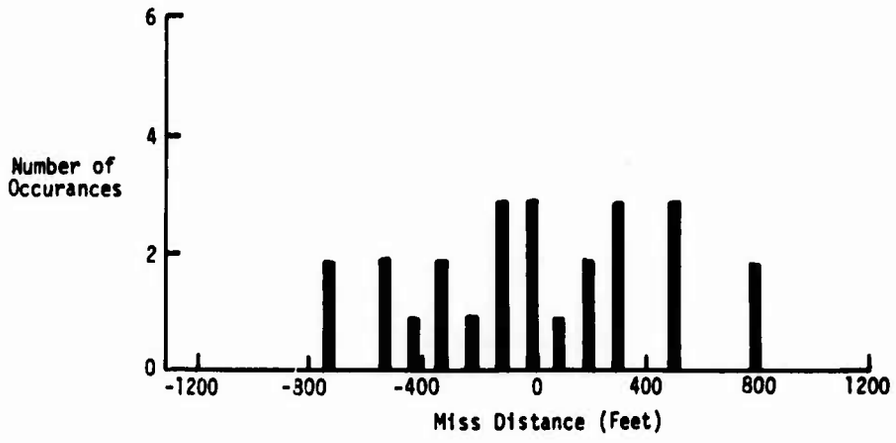

Figure 13. Touchdown Dispersion Data for CV-990 Ground Command Guidance Approaches

STEEP APPROACH FLIGHT TEST RESULTS OF A BUSINESS-TYPE AIRCRAFT WITH DIRECT LIFT CONTROL

P.G. Hamel
K.K. Wilhelm
D.H. Hanke
H.H. Lange

Institut für Flugmechanik

Deutsche Forschungs- und Versuchsanstalt
für Luft- und Raumfahrt e.V. (DFVLR)
Braunschweig-Flughafen

Summary

The trends in aircraft approach and landing procedures are such that increasingly noise abatement constraints impact on vehicle flying (handling) qualities.

A ground-based flight simulator program and concurrently a flight test program were conducted at the Institut für Flugmechanik of the DFVLR Research Center Braunschweig using a MBB-HFB-320 Hansa Jet airplane which was retrofitted with an analogue fly-by-wire flap and thrust control system. The direct-lift control system was used for alleviating handling qualities problems during steep noise-abatement landing approaches.

A variable direct lift control system was made feasible for optimization purposes by changing the gearing ratio of the electric flap-elevator interconnect. Facilitation in pilot's workload and improvements in flight path control were analyzed by statistical methods. Experiences gained by flight test results and noise measurements show that routine 2-segment noise-abatement approach paths can be introduced successfully when adequate path guidance, quick-response flight path corrections and minimum throttle activity are possible.

1. Introduction

Noise annoyance by aircraft during take-off and landing has become a serious environmental problem. Citizens affected by noise, form groups demanding restrictions to air traffic and airports. Approx. seventy-five percent of all complaints apply to landing aircraft which approach the airports at low altitudes and hight thrust levels (fig. 1).

Many of today's aircraft types still exceed the FAA noise limits when starting or landing. A certain number have been phased out already or will be replaced in the near future by aircraft of the "quiet generation", as, for instance, the widebodied DC-10, Tristar, B 747 B, the Citation, and many others. These aircraft represent the realization of the development of "quiet engines", which are one major accomplishment towards noise reduction.

Apart from technological progress, eliminating the noise at its source, the application of advanced approach and departure procedures can help to reduce disturbing aircraft noise.

Stimulated by the investigations of methods of reducing the noise of jet aircraft during take-off and landing at the NASA Ames and Langley Research Centers (ref. 1) and in view of severe noise problems in the Federal Republic of Germany, the DFVLR is currently conducting theoretical studies (ref. 2) and flight tests in the field of aircraft noise (ref. 3). An overall survey on problems associated with noise-abatement flight path profiles for CTOL and V/STOL aircraft can be found for example in reference 4.

Noise reducing departure procedures are achieved by a steeper climb angle which results in a faster increase of the distance between the observer on the ground and the source of the noise. Throttling the engines, i.e. by diminishing the intensity of the noise source is a further possibility to reduce at least the jet noise in limited areas. Finally, an increase of the flight speed in order to shorten the duration of the noise exposure reduces the subjective noise annoyance. Based on a number of theoretical

and experimental evaluations, such departure procedures are practiced world-wide by the airlines.

On the contrary, noise-abatement approach techniques do create problems. Flight tests have shown that a remarkable noise reduction would result from steeper angles of descent, ranging for CTOL aircraft from four to seven degrees. However, several problem areas like rate of descent near ground, flight-path control, pilot's workload,guidance and display information and engine response have to be taken carefully into account. Although two-segment steep approaches appear to be a feasible way of reducing airport noise and appropriate procedures are introduced into U.S. airline services, there is still the need to identify problem areas for further refinement before such procedures can be applied world-wide.

It is the purpose of this paper to define and discuss problem areas of steep noise-abatement landing procedures from a flight mechanics standpoint. Flight test results of the DFVLR research aircraft MBB-HFB-320 are presented. This aircraft (fig. 2) is equipped with a special analogue fly-by-wire direct-lift and throttle control system. Since an increased number of small executive jets are flying from private and regional airstrips, the aircraft noise problem has been spread out to additional thousands of residental areas. For this reason, the DFVLR-flight tests with a business-type aircraft are of special actual importance.

2. List of Symbols

CAP control anticipation parameter
DLC direct lift control
DOT cross-pointer scale
K flap-to-elevator gearing ratio
l_p distance CG-Pilot
M_w pitching acceleration due to velocity w
M_δ pitching acceleration due to control deflection δ
$\bar{M}_\delta$ frequency-dependent pitching acceleration due to control deflection δ
n_z vertical load factor
n_{zss} steady-state load factor
$n_{z\alpha}$ load factor angle of attack sensitivity
q pitch rate
s Laplace-variable
T_w time constant in γ/δ_e numerator
$T_{\theta 2}$ time constant in θ/δ_e numerator
U_o aircraft steady-state velocity
w vertical velocity perturbation
Z_w acceleration along Z axis due to velocity w
Z_δ acceleration along Z axis due to control deflection δ
α angle of attack
γ flight path angle
δ_e elevator deflection
δ_f flap deflection
δ_{th} throttle deflection
θ pitch attitude
$\ddot{\theta}_o$ instantaneous angular pitching acceleration
δ standard deviation
ω_{nsp} undamped natural frequency of short-period mode
ω_p pilot induced pumping frequency

3. Steep Approach Handling Qualities Problems

3.1 Control decoupling

Precise control response of the symmetrical motion of an aircraft along its flight path during the landing approach needs an accurate and easily interpretable guidance information. This will permit the pilot to determine his flight path error correctly. The reduction of the error requires that the flying qualities of the aircraft are satisfactory. Only the combination of satisfactory flight path information and flying qualities will result in satisfactory control characteristics.

During landing approach the pilot lays strong emphasis on his ability to control altitude. Decoupling of the two basic flight path response variables of the aircraft that, is altitude and speed, presents one aspect of a possible simplification of the pilot's control task. Looking at the conventional aircraft control inputs, elevator pitch control and throttle thrust control, it is necessary for the pilot to coordinate carefully the use of thrust and elevator if an altitude change is to be made without change of speed or vice versa. Thus, uncoupling of up-down and slow-fast control manually requires proper tuning and coordination of elevator and throttle. This usually results in an increase of pilot's workload.

On steep approaches the necessary throttling-back of engine power, sometimes down to idle, generates additional flight path tracking problems. The slow response of jet engines and especially fan-jet engines to throttle commands particularly at low thrust levels requires the pilot to generate some phase lead. This is very important in the flare phase or intercept phase of a two-segment noise-abatement approach. From this, it is evident that for precise flight path control the manual decoupling scheme up-down and slow-fast, using conventional pitch and throttle control inputs, is difficult to be applied for steep approaches.

3.2 Control anticipation parameter

It has been shown for manual flight path control that the pitch acceleration $\ddot{\theta}_o$ response of the fuselage is of concern to the pilot when he initiates a maneuver, and that the steady state response of concern is the normal load factor n_{zss} of the using experienced in a pull-up. The ratio of both values is defined by Bihrle as control anticipation parameter (ref. 5)

$$CAP = \frac{\ddot{\theta}_o}{n_{zss}} \tag{1}$$

or

$$CAP = \frac{M_\delta + M_{\dot{w}} Z_\delta}{(M_w/Z_w)Z_\delta - M_\delta} \frac{\omega_{nsp}^2}{Z_\alpha/g} \tag{2}$$

In the case of conventionally controlled aircraft (elevator control), the control forces Z_δ are usually neglected, thus,

$$CAP = \frac{\omega_{nsp}^2}{n_{z\alpha}} \tag{3}$$

On the basis of CAP, requirements of short-period frequency and acceleration sensitivity have been established (ref. 6). If an aircraft has a CAP value which is too small, (CAP < 0.16 rad/sec^{2}g), the pilot tends to overcontrol, rating response as sluggish. On the other hand, if the CAP is too large, (CAP > 3.6 rad/sec^{2}g), the pilot tends to undershoot his desired flight path, rating the response as abrupt and too sensitive. In both cases manual decoupled maneuvers become impossible.

The pilot of a low CAP-aircraft may apply for precision tasks a special control technique which involves a sinusoidal pumping of the pitch control surface in order to excite and sense an airframe response in angular acceleration see also (ref. 5). Figure 3 shows a time history of a typical control surface pumping incident of the HFB-320 during final approach. The pumping frequeny ω_p is about three times higher than the short period frequency ω_{nsp} of the aircraft, thus, a sufficiently high value for obtaining maximum angular acceleration with a minimum of phase-shift between control input and pitch acceleration. The CAP-value for the HFB-320 in the landing configuration is about 0.3 rad/sec^{2}g. For comparison, similar results for the F-84 E and F-105 aircraft are included from reference 5 in the pitch acceleration frequency response curves.

4. Direct Lift Control

4.1 General

The possibility of applying direct lift control (DLC) of vertical movements could enhance aircraft effectiveness for precise flight path control on steep two-segment noise-abatement approaches. An ideal DLC-system would permit an aircraft to translate without rotating as in conventional pitch control systems, thereby eliminating the troublesome transients, lags and overshoots resulting from coordinated maneuvers. An excellent review on the understanding of the possibilities and problems applying direct lift control was given by W.J.G. Pinsker (ref. 7). The possibilities, problems and pitfalls associated with the application of direct lift control are discussed in the following. Special applications will be given for the HFB-320 research aircraft.

Direct flight path control of conventional aircraft with pitch control systems (elevator) is difficult due to the aircraft's aforementioned response lags. Thus, the pilot is required to generate some lead for satisfactory aircraft flight path response. A flight director for example gives the pilot some lead information about necessary pitch changes. But the flight director cannot compensate the flight path lag if the elevator is the only control device. Direct lift control is a possibility to overcome the problem. Some insight can be obtained from the following manipulations with the flight path angle - pitch attitude transfer function (short period approximation)

$$\frac{\gamma}{\theta} = 1 - \frac{A_w\,(s + 1/T_w)\,s}{A_\theta\,U_o\,(s + 1/T_{\theta 2})} \tag{4}$$

where

$$A_w = Z_\delta\ , \tag{5}$$

$$A_\theta = M_\delta + Z_\delta\,M_{\dot{w}}\ , \tag{6}$$

$$1/T_w = M_\delta U_o/Z_\delta - M_q\ , \tag{7}$$

$$1/T_{\theta 2} = \frac{Z_\delta M_w - M_\delta Z_w}{M_\delta + Z_\delta\,M_{\dot{w}}} \tag{8}$$

For aircraft with elevator the γ/θ-transfer function is approximately given by

$$\frac{\gamma}{\theta} = \frac{1}{T_{\theta 2}\,s + 1} \tag{9}$$

where the time lag constant $T_{\theta 2}$ is directly related to the amount of aerodynamic heave damping Z_w

$$1/T_{\theta 2} = -\,Z_w \tag{10}$$

If direct lift control is applied, eq. (8) is valid. In this case a variation of the control derivatives M_δ and Z_δ alter the "high frequency" zeroes which influence the initial γ/θ response of the aircraft. Then, with proper tuning of the control margin M_δ/Z_δ the direct lift control system gives the pilot sufficient lead for a precision flight path control task.

A simple means of changing the control margin M_δ/Z_δ with DLC of the HFB 320 is the electric interconnect between elevator and flap (fig. 4). The influence of different flap-to-elevator gearings K on the flight path response is shown in figure 5.

4.2 Flap-elevator gearing

Note that flap deflection rate is about 10 degrees per second. For K = 0 the simple elevator controlled aircraft (pitch control) demonstrates the known lag between pitch attitude and flight path response. With increasing K the flight path response is quickened whereas in the pitch attitude reaction a time lag is developed. For the gearing ratio K = -6 is the flight path response similar to the pitch attitude response. In this case the pilot can read the direct information of the actual flight path from the pitch attitude changes indicated. Theoretically, one can show that for this condition the time constant T_w must be infinite, thus, from eq. (7) one yields the expression

$$\frac{M_\delta}{Z_\delta} = \frac{M_q}{U_o} \quad . \tag{11}$$

At a gearing ratio of K = -15 the flight path response in the initial phase is accomplished with practically no pitch changes.

The optimum gearing ratio for DLC is difficult to define. Thus far the limited experience with DLC up to date give no clear information about the way in which the DLC should be mechanized to improve the flying qualities. It can be stated from time histories and statistical analyses of flight mechanics variables that DLC can improve precise flight path control. But there are no handling qualities criteria which could be readily applied for DLC applications.

4.3 Modified Control anticipation parameter *)

The change of the control anticipation parameter CAP applicable for pitch control aircraft gives misleading results when applied for DLC-purposes. Figure 6 shows the computed CAP-variation for the HFB-320 as a function of the gearing ratio K. Since the CAP-value weighs the initial angular acceleration and not the initial vertical acceleration the values degrade with increasing K. Thus, it is suggested to discuss a modified parameter CAP^* which takes also the initial vertical acceleration of the aircraft at the CG into account. In contrary to eq. (1) the modified expression can then be written as

$$CAP^* = \frac{n_{zo}}{n_{zss}} \tag{12}$$

or with respect to eq. (2)

$$CAP^* = CAP\,\frac{l_p}{g} + \frac{\omega_{nsp}^2 / Z_\alpha}{M_\delta/Z_\delta - M_w/Z_w} \tag{13}$$

The change of CAP^* with the DLC-gearing ratio K is given in figure 6. The practical problem is now whether it is possible to establish for DLC control tasks corresponding upper and lower limits to the CAP^* value from a handling qualities standpoint such as they were found for the CAP-criterion relevant to pitch control.

The mutual connect between the initial pitch and initial vertical acceleration at the CG in the case of direct lift control can also be seen from the ratio

$$\frac{\ddot{\theta}_o}{n_{zCGo}} = -g\left[\frac{M_\delta}{Z_\delta} + M_{\dot{w}}\right] . \tag{14}$$

This relation is changed directly by the K-dependent DLC control margin M_δ/Z_δ and Mooij referred to it as

*) The authors wish to acknowledge the discussion contribution on this subject of A.G. Barnes, British Aircraft Corporation Limited, U.K.

a possible DLC handling qualities parameter (ref. 8).

4.4 Unsteady control aerodynamics

In the preliminary phase of flight tests with the HFB-320 research aircraft some important stability and control derivatives were extracted from in-flight measurements. These aircraft parameters were needed not only to determine the inherent stability and control characteristics but also as inputs for the ground simulator investigations. Some of the parameters extracted from flight measurements differed considerably from predicted values (ref. 9). Beyond constant aerodynamic derivatives, parameters were identified incorporating nonlinear and unsteady aerodynamic effects. The latter effects were mainly associated with the flap control derivatives which are of special importance for the DLC-control system. The physical background for these unsteady phenomena is not quite clear but it is assumed that unsteady local flap control lift lag effects (circulation lag) and time-delay effects (flap-tail downwash lag) yield the main contributions. These unsteady aerodynamic effects on the flap control derivatives were analytically taken into account by a lead-lag term. For example, the frequency-dependent unsteady flap control moment can be written in the form

$$\bar{M}_{\delta_f} = M_{\delta_f} \frac{1 + sT_1}{1 + sT_2} \tag{15}$$

where M_{δ_f} describes the steady flap control derivative for slow motions ($s = i\omega = 0$).

In figure 7 the computed overall control derivative

$$\bar{M}_{\delta} = M_{\delta_e} + K \bar{M}_{\delta_f} \tag{16}$$

for DLC-applications has been plotted as a function of the flap-to-elevator gearing ratio K. For K = 0 (pitch control) and low frequencies ($\omega = 0$) the value of the control derivative corresponds to the steady elevator control derivative M_{δ_e}, thus,

$$\bar{M}_{\delta} (K = 0, \omega = 0) = M_{\delta_e} = -3 \quad 1/\text{sec} .$$

For a control frequency of $\omega = 2$ rad/sec which is slightly above the short period mode frequency of about $\omega_{nsp} \approx 1.2$ to 1.4 rad/sec the effect of unsteady aerodynamics can be readily seen from the amplitude and phase plot of the unsteady control derivative $\bar{M}_{\delta}$. The phase-sensitivity of this derivative is especially strong in the DLC-region of the flap-to-elevator gearing ($K=K^*$). Thus, an optimum flap-elevator gearing for DLC-purposes may be influenced by unsteady control aerodynamics.

4.5 Long term effects on flight path control

It can be shown that the long term (steady state) flight path response due to a control input can be written as (velocity derivatives neglected)

$$\frac{d\gamma}{d\delta} = \frac{C_{L\delta}}{C_L} \left[\frac{C_D}{C_L} - \frac{C_{D\delta}}{C_{L\delta}} \right] - \frac{C_{M\delta}}{C_L} \frac{C_{L\alpha}}{C_{M\alpha}} \left[\frac{C_D}{C_L} - \frac{C_{D\alpha}}{C_{L\alpha}} \right] \tag{17}$$

The first term respresents the flight path change due to heaving, and the second term incorporates the pitching contribution. Thus, the effect of direct lift control (DLC) on the long term flight path response can be derived from the first (heave) term whereas the effect of conventional pitch control can be read from the second term. Since in most cases the aircraft lift and drag changes due to elevator control deflections, that is $C_{L\delta}$ and $C_{D\delta}$, are negligible there is a significant influence on these derivatives if DLC is used because of the relatively high lift and drag changes due to spoiler or flap deflections.

Figure 8 gives an impression of the influence of $C_{L\delta}$ and $C_{D\delta}$ on flight path control stability. Typical positions of a CTOL and a STOL aircraft are indicated, the latter aircraft operating on the

(unstable) "backside" of the drag-polar. Pitch control shifts the reference position parallelly to the pitch axis whereas direct lift control will generate a shift along the heave axis. Generating direct lift control through wing flaps will lead to a positive ratio $C_{D\delta}/C_{L\delta}$ leading to a deterioration of long term flight path control stability (upper arrows). On the other hand, using spoilers as direct lift control devices, the $C_{D\delta}/C_{L\delta}$ ratio is negative which increases the long term flight path stability (lower arrows).

As the high vertical load factor inducing wing flap systems are, in comparison to low load factor spoilers, preferable as direct lift controllers for quick and precise flight path corrections (short term response), attention must be given to the long term behaviour of DLC-flap systems. The possibility that the long term flight path response may become unstable, would demand for a drag compensation device like an autothrottle system. Since an autothrottle system will have to work with phase lags due to internal engine dynamics and varying, thus, disturbing noise characteristics, a drag-changing F-28-type airbrake control system could be a better alternative.

5. Aircraft and Test Equipment

A MBB-HFB-320 preproduction two engine jet aircraft, shown in figure 2, was used in the investigation. This aircraft is equipped with an analogue fly-by-wire flap and throttle control system. Figure 9 gives an overall view of the flight test equipment and system integration.

The direct lift flaps input were processed by an on-board analogue computer. The electric signal was put into a position feedback control system which was directly geared to both the torque-motors for the left and right hand landing flap. These torque motors were connected through a gear box to the rotating shafts for the control of the hydraulic basic flap system. By a hydraulic by-pass the basic hydraulic actuators were modified such that the rate of the flap deflection could be increased to 10 degrees/second.

This control system was switched and observed by two monitoring systems each of them being located in the cockpit and in the cabin, respectively. The flap control input signals were steered by means of an elevator position potentiometer. The measured flight test data were recorded via telemetry on the ground and parallel on an on-board magnetic tape. The DLC control schematic of the electric flap-to-elevator interconnect has already been shown in figure 4. The steady reference flap deflection for direct lift control purposes was adjusted to $\delta_f = 20^o$.

6. Flight Test Program

6.1 Conventional approaches

For selection of an optimal DLC gearing ratio K conventional 2,5°-ILS-approaches were undertaken at altitudes of 3800 ft GND. The evalulation pilots had the task to keep the aircraft velocity constant V = 150 kts. and to control the flight path precisely according to the cross-pointer-instrument information. The electric DLC-system was disconnected at a safety-altitude of 500 ft GND, the approach interrupted and a go-around procedure initiated (ref.10). The flight tests were done at the Hannover airport.

6.2 Steep two-segment approaches

In a second flight test phase steep two-segment approaches were carried through with and without DLC. The aim of these test flights was to investigate flyability problems of steep 6°- approaches using DLC. Since no ground-referenced 6°-glide slope was available, the flight path had to be computed on-board from the measured and filtered angle of attack and pitch attitude signals taking wind gradients into account. The steep segment approach was initiated on the localiser at 8.44 n.m. identified by radio cross-bearing and radarvectoring. The intercept maneuver on the conventional 2,5°-ILS-glide path was started for safety-reasons at an altitude of about 600 ft. After the flight path transition the aircraft configuration was changed to the procedure approach (V = 120 kts, $\delta_f = 50^o$).

7. Presentation of Results

7.1 Conventional approaches

Before steep two-segment approaches were investigated and analysed, several 2.5°-ILS-approaches were made to obtain an optimal flap-to-elevator gearing ratio K. Direct lift control with K = -10 significantly improved the flight path tracking capability as to be seen from figure 10. The standard deviations of the ILS-signal, the pitch attitude, angle of attack and flight path angle are plotted for conventional pitch control (K = 0) and direct lift control (K = -10). It can be seen that the ILS- and flight path deviations are remarkably reduced when DLC is applied. Further, decreased standard deviations of pitch attitude and angle of attack are apparent. The standard deviation of the DLC-flap activity, not shown in figure 10, did never exceed a value of 3°.

7.2 Steep two-segment approaches

Time histories of steep two-segment noise abatement approaches with and without DLC are shown in figure 11 and 12. The variables plotted are the ILS-signal, pitch attitude, flight path angle, pitch rate, flap, throttle and elevator deflection. Both approaches were made by the same pilot and during the same evaluation mission. The transition to the second 2.5°-segment is indicated by the flight path angle change on the right. Comparison of the time histories clearly show the smoother ride of the aircraft for the direct lift controlled steep approach.

Figure 13 compares the elevator, flap and throttle activity. It is evident that with DLC the elevator deflection amplitudes were reduced and that for both control systems no throttle activity was necessary due to the low DLC-flap amplitudes which have no essential influence on speed hold.

The main difference in handling qualities is shown by the comparison of pitch attitude and flight path angle variations (figure 14). In the case of elevator controlled approach the known lag between γ and Θ is evident especially for the transition maneuver. In the case of the direct lift controlled approach the γ-Θ lag disappears.

The pilots were of the opinion that by means of direct lift control glide path deviations could exactly be compensated, and that the reduced variations in the pitch attitude were perceived as pleasant. The same is especially true for flights in turbulence. In the case of large-scale maneuvers, however, leading to greater flap deflections, the flap induced drag had to be compensated by thrust changes for speed stability reasons (see also section 4.5).

7.3 Aircraft control and ground noise

The ground noise caused by the over-flying aircraft was measured by the DFVLR-Institut für Antriebssysteme at 8 sites underneath the approach path and as far as 15 n.m. away from the runway threshold. A precision ground radar of the DFVLR-Institut für Flugführung was used to measure the aircraft position. Communication existed between the aircraft, the Hannover tower, the ground radar and the central ground noise measuring station.

Figure 15 presents measured data of the engine thrust und the ground noise for a conventional approach (A) and a steep 2-segment approach (C). All flights were done with a 20°-flap setting until the conventional 2.5°-ILS-glide path was intercepted. During the final approach, the aircraft flap setting was increased to $\delta_f = 50°$. The associated drag rise was compensated by a specified thrust increase which, in turn, resulted in a noise increase of about 5 PNdB. This can be seen from the knees in the noise curves.

The noise reduction potential due to the steep two-segment approach procedure is noteworthy in aeras of a length of about 10 to 15 km (7 to 10 n.m.). But it must also be noted that inaccurate flight path guidance and high or changing thrust levels may deteriorate the noise-abating effect of a steep approach. From figure 15 it can be seen how strong inadequate guidance due to insufficient navigation aids in combination with a thrust increase for a climb maneuver and later for an intercept maneuver influences the noise reduction potential. This maneuver was flown with conventional pitch control.

A similar maneuver applying direct lift control is shown in figure 16. The throttle activity could be kept lower although the climb maneuver at the beginning is again from the noise-standpoint of disadvantage. Nevertheless, the intercept maneuver could smoothly be flown without additional noise spreading.

Thus, adequate flight path information and aircraft guidance and control are prerequisites for the excellent noise-reduction potential of steep two-segment approach flight paths.

8. Conclusions and Outlook

It was the purpose of this paper to give a survey over the first phase of a flight test program in the Federal Republik of Germany in the field of noise-abatement flight path profiles using a business-type aircraft equipped with electric-signalling direct lift and throttle control. Some of the main conclusions which emerge from this review are as follows:

1) Control decoupling of the in-plane motion is difficult to mechanize with conventional elevator and thrust control due to inherent aircraft and control dynamics.
2) Direct lift control through a combined and optimized flap-elevator control system shows promise for control decoupling.
3) Flight test experience has indicated that for short term precise flight path tracking with flap-type direct lift control no thrust compensation is necessary.
4) Optimum flap-elevator gearing for DLC-purposes may be influenced by unsteady control aerodynamics.
5) For long term flight path control and large-scale maneuvers some means of drag compensating device is necessary.
6) DLC-handling qualities criteria are not readily available.
7) A possibility for a modified CAP-criterion with respect to DLC-handling qualities is discussed.
8) Steep two-segment noise-abatement flight path profiles can be flown beneficially with DLC.
9) The noise reduction potential of steep two-segment approach paths is influenced by inadequate guidance.
10) Throttle activity during steep noise-abatement approaches must be kept to a minimum.

For summer 1974 a second flight test program is provided with improved instrumentation and limited variable stability characteristics. These flight tests will be carried through in a cooperative program with the U.S. Air Force. The tests will include investigations of both inner loop and outer loop problems during steep landing approach and define mechanization and response requirements for DLC and automatic throttle. A TALAR IV high angle guidance system will be available for accurate flight path information.

9. References

1. Quigley, H.C. et al. Flight and Simulation Investigation of Methods for Implementing Noise-Abatement Landing Approaches.
   NASA TN D-5781 (1970).

2. Henschel, F., Plaetschke, E., Schulze, H.-K. Minimum Noise Climbout Trajectories of a VTOL Aircraft.
   To be published in J. Aircraft, Vol. 11 (1974).

3. Hamel, P., Dahlen, H.W. Erprobung lärmmindernder Anflugverfahren mit dem DFVLR-Forschungsflugzeug HFB 320.
   DFVLR-Nachrichten, No. 10 (1973), pp. 413-416.

4. Hamel, P. Noise-Abatement Flight Profiles for CTOL and V/STOL Aircraft.
   DLR FB 71-10 (1971).

5. Bihrle, W., jr. A Handling Qualities Theory for Precise Flight Path Control.
   AFFDL-TR-65-198 (1966).

6. Chalk, C.R. et al. Background Information and User Guide for MIL-F-8785 B (ASG) "Military Specification - Flying Qualities of Piloted Airplanes".
   AFFDL-TR-69-72 (1969).

7. Pinsker, W.J.G. Direct Lift Control.
   The Aeron. Journal, Vol. 74 (1970), pp. 817-825.

8. Mooij, H.A. Flight Evaluation of Direct Lift Control and its Effect on Handling Qualities in Carrier Approach.
Princeton University Rept. No. 811 (1967).

9. Pietraß, A. Ermittlung von flugmechanischen Derivativen aus Flugmessungen durch manuelle Variation der Modellparameter am Analogrechner.
DLR FB 73-111 (1973).

10. Hanke, D., Lange, H.-H. Flugmechanische Probleme beim Landeanflug mit direkter Auftriebssteuerung am Beispiel der HFB 320 Hansa.
To be published in DLR-Mitt. 74-10 (1974).

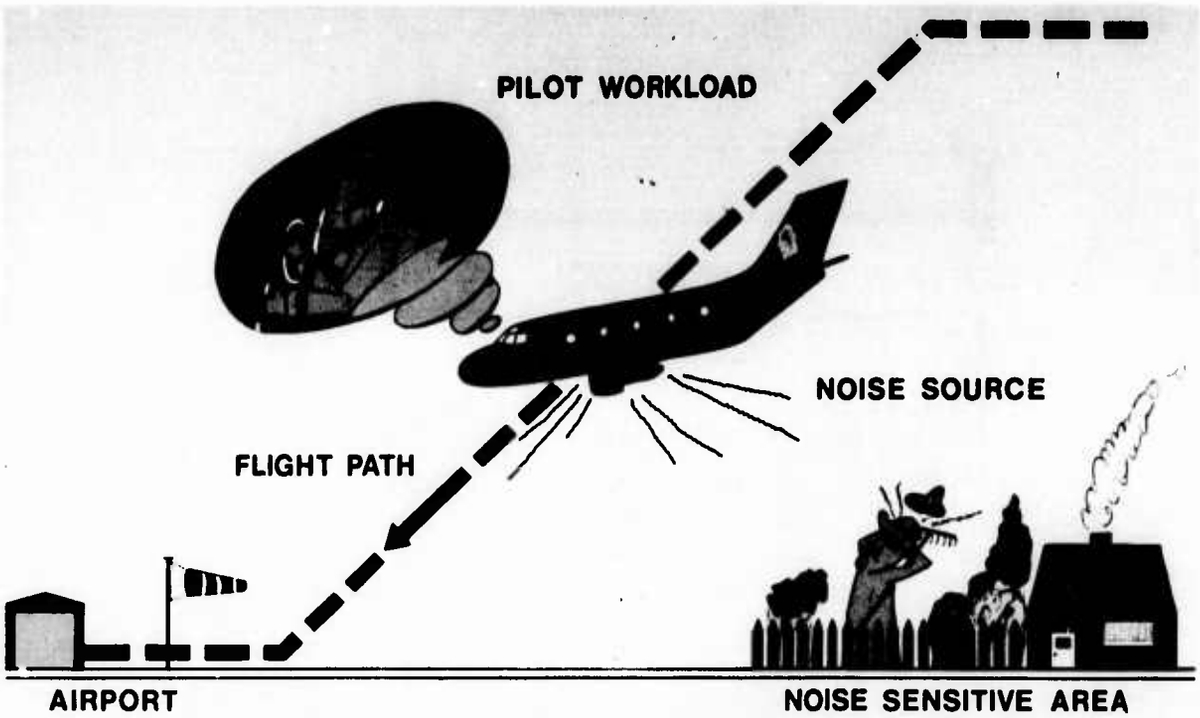

Fig. 1 Interacting problems of aircraft noise

Fig. 2 MBB-HFB 320 research aircraft

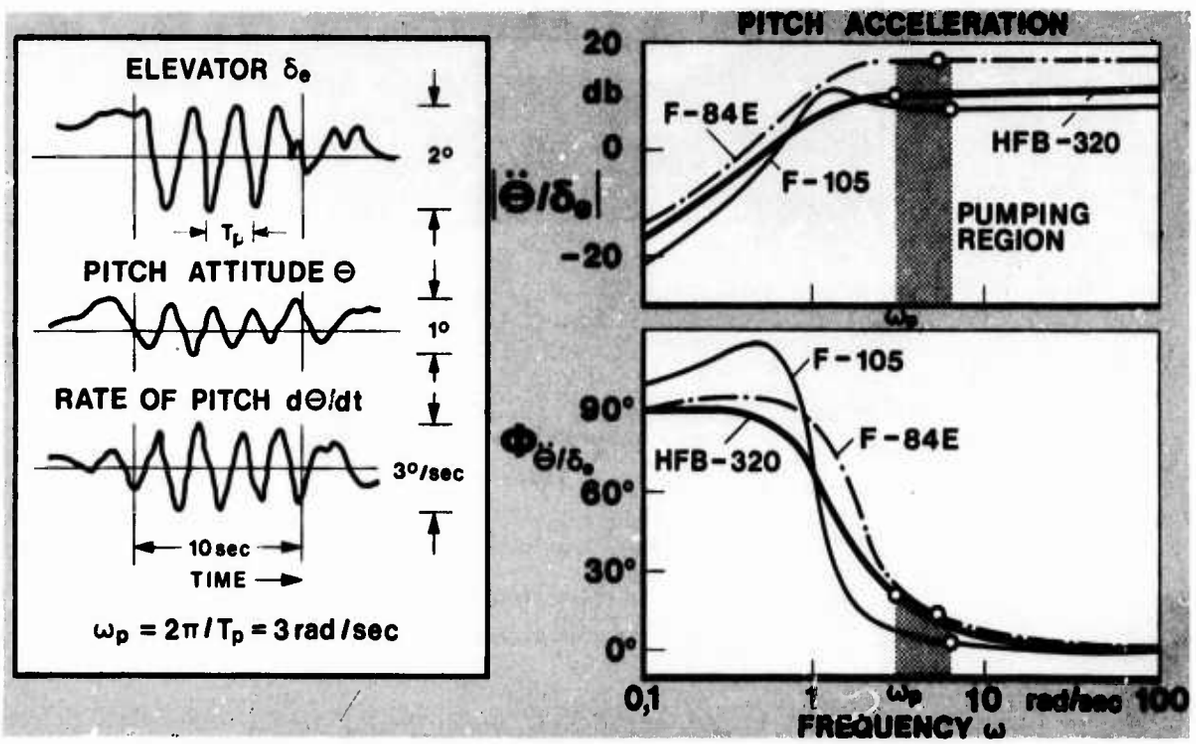

Fig. 3 Identification of control pumping

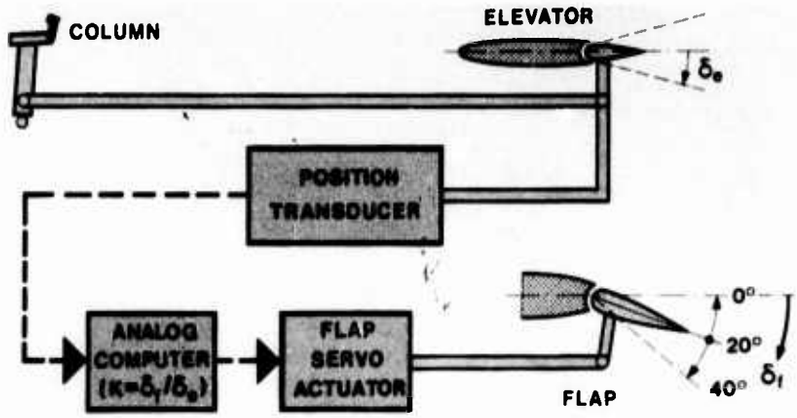

Fig. 4 Direct lift control system schematic

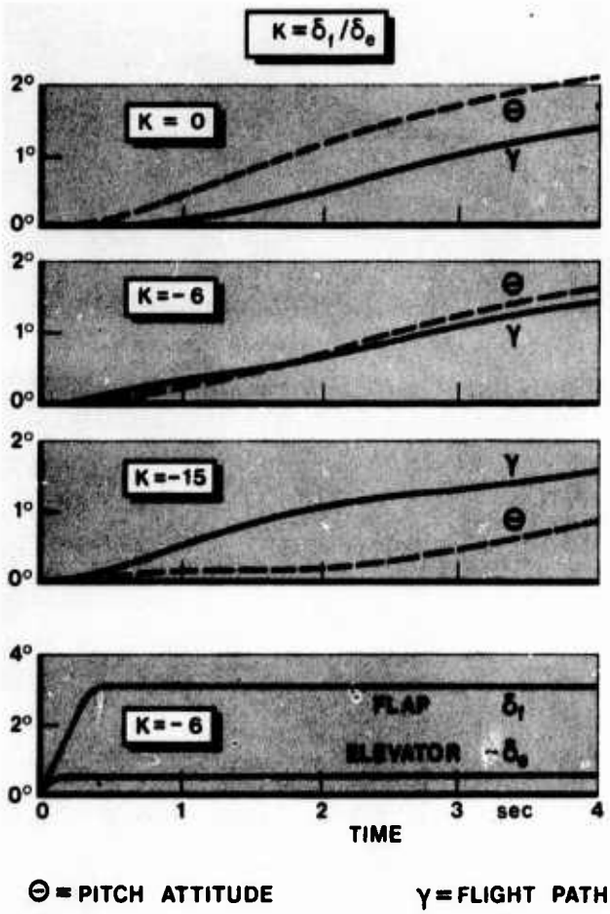

Fig. 5 Influence of flap-to-elevator gearing ratio K on aircraft response

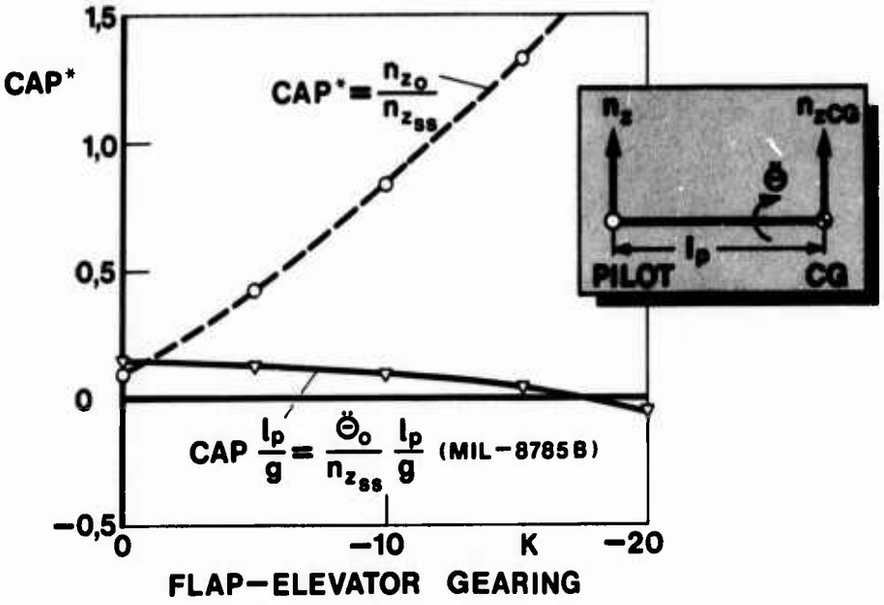

Fig. 6 Effect of DLC on CAP-rating

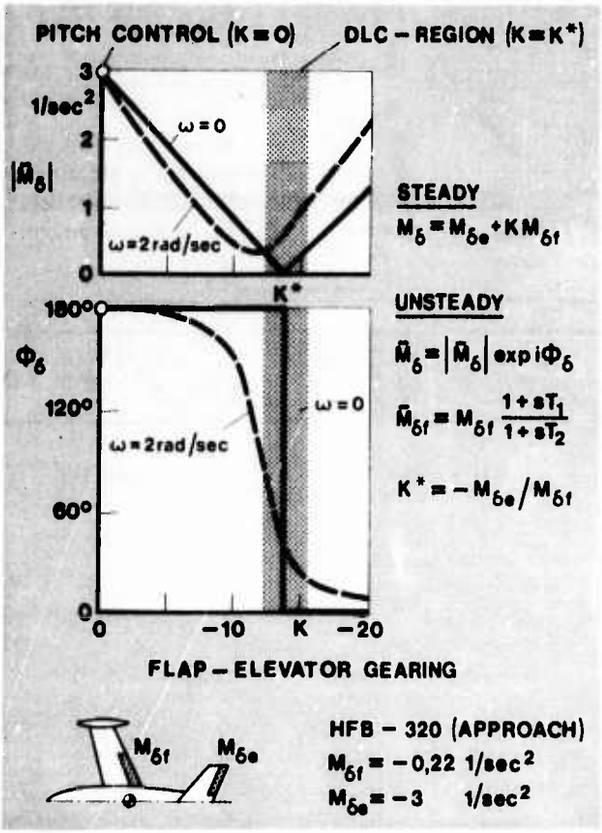

Fig. 7 Effect of unsteady aerodynamics on control derivative M_δ

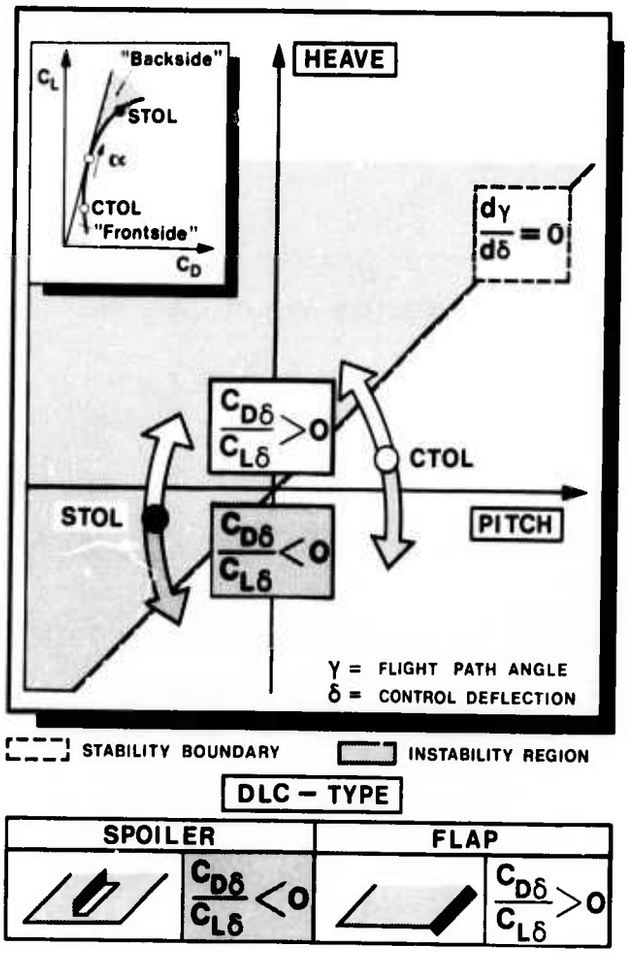

Fig. 8 Long term effect of DLC on flight path control

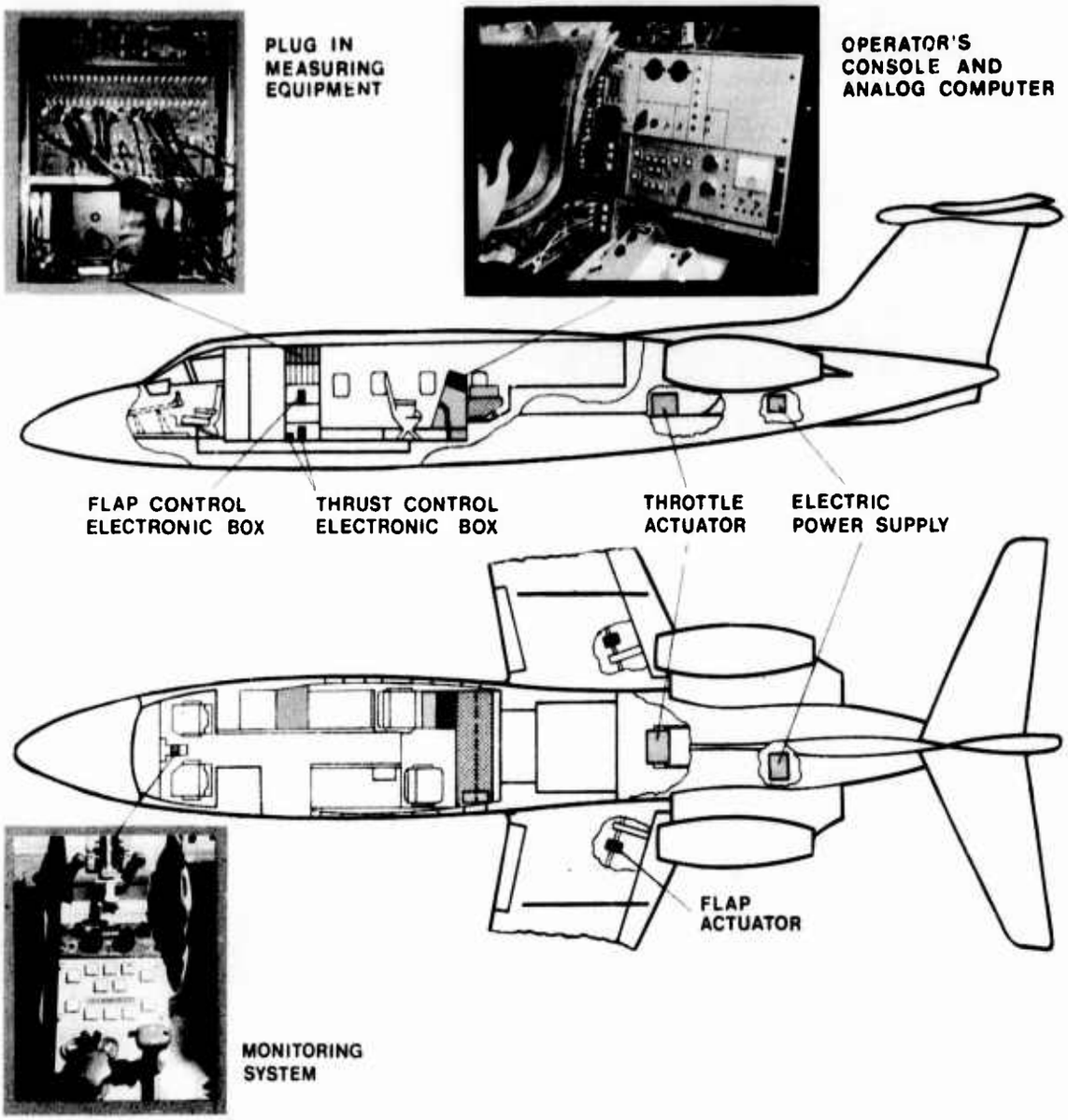

Fig. 9 HFB-320 System Integration

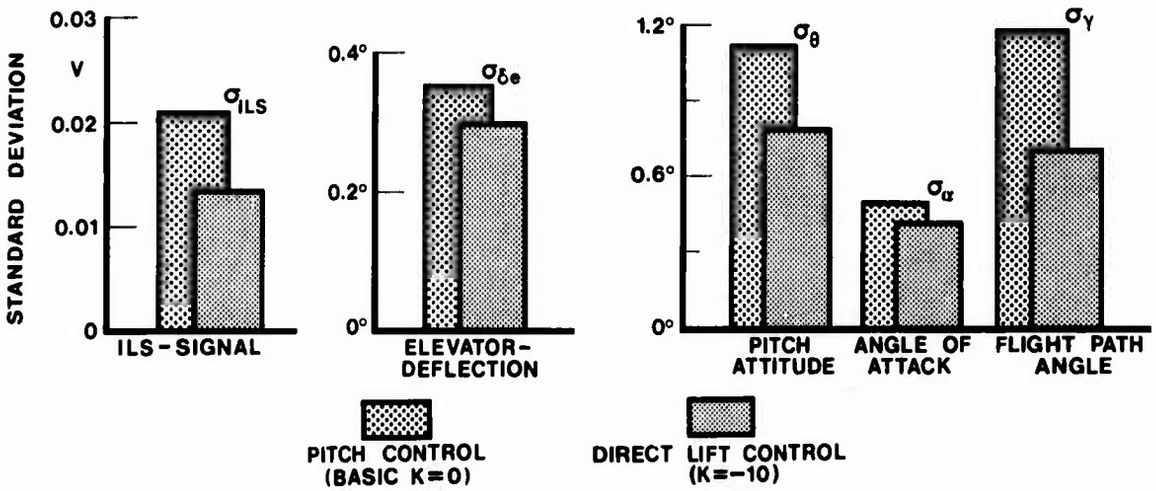

Fig. 10 Standard deviation of ILS-approaches with and without DLC

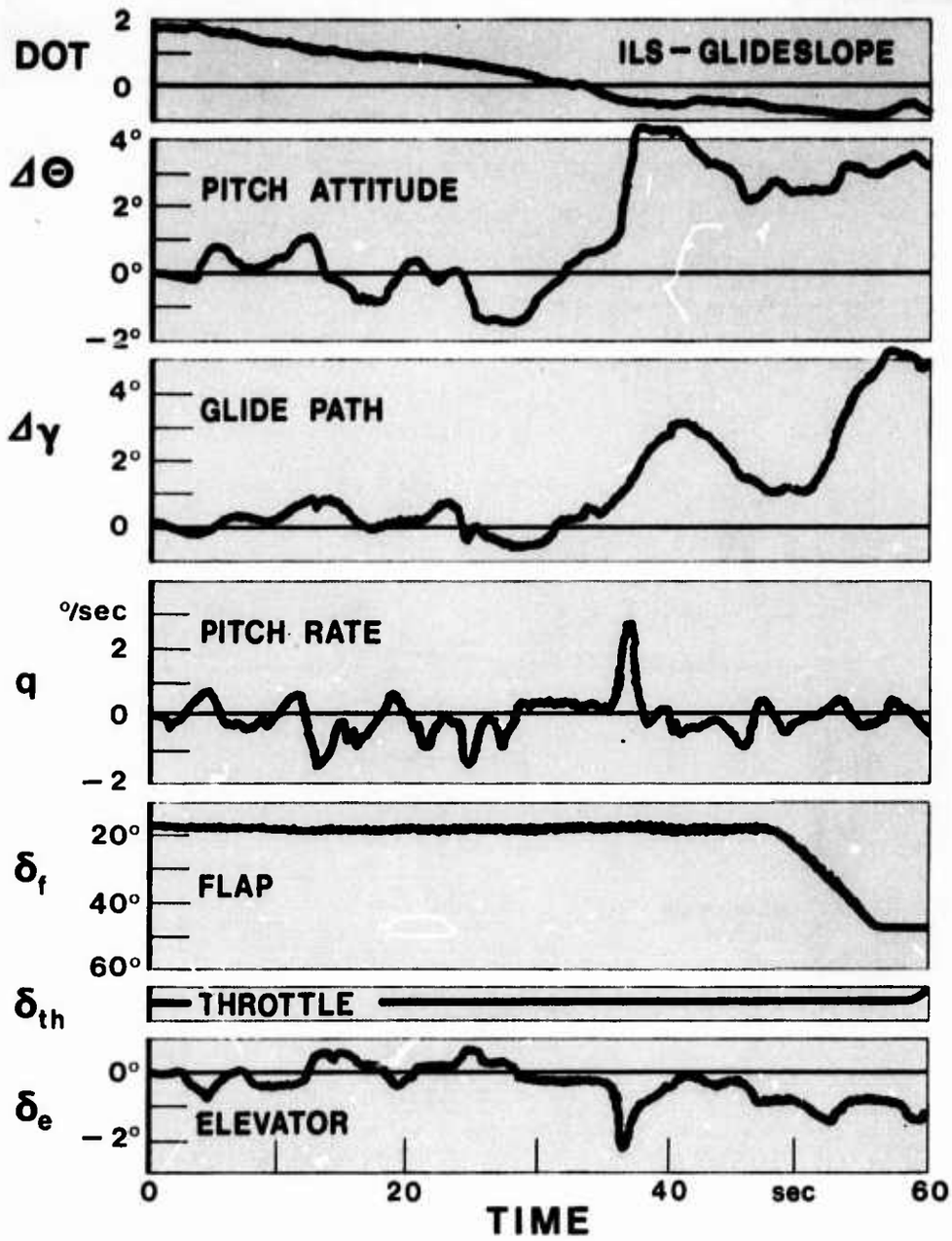

Fig. 11 Steep approach time histories (pitch control)

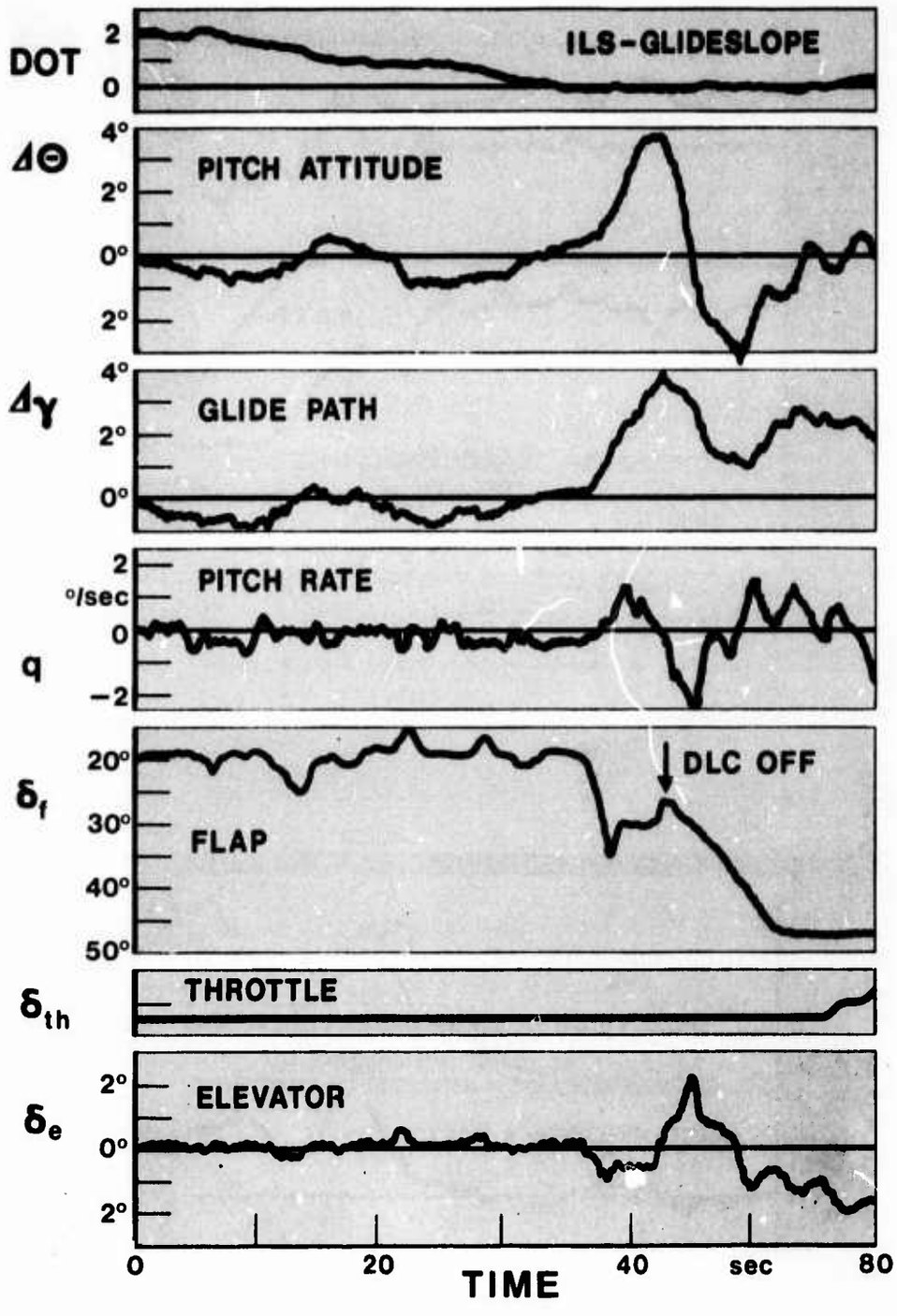

Fig. 12 Steep approach time histories (direct lift control)

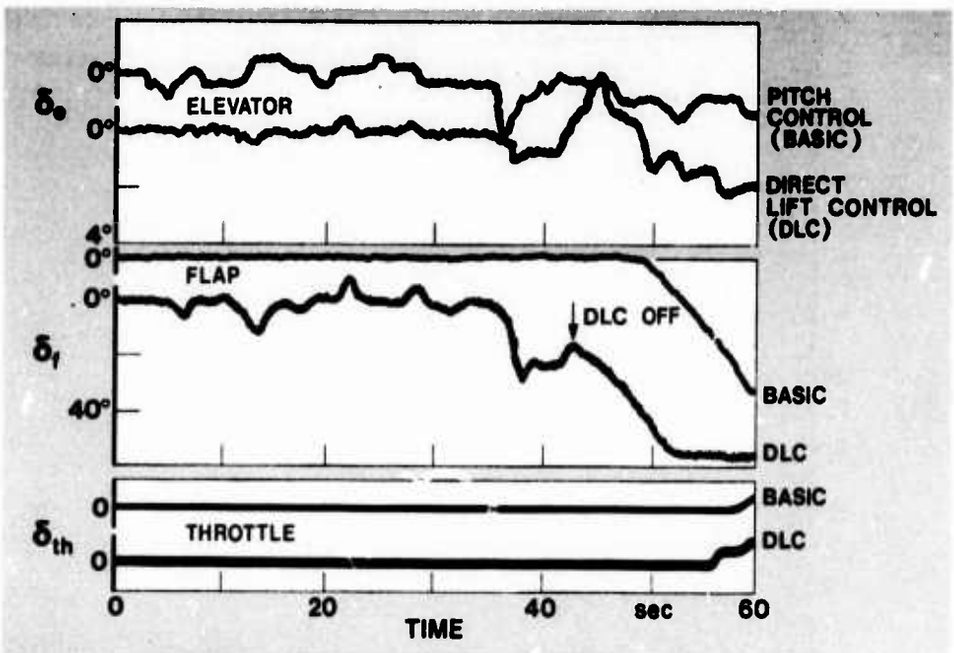

Fig. 13 Control activity during steep approach

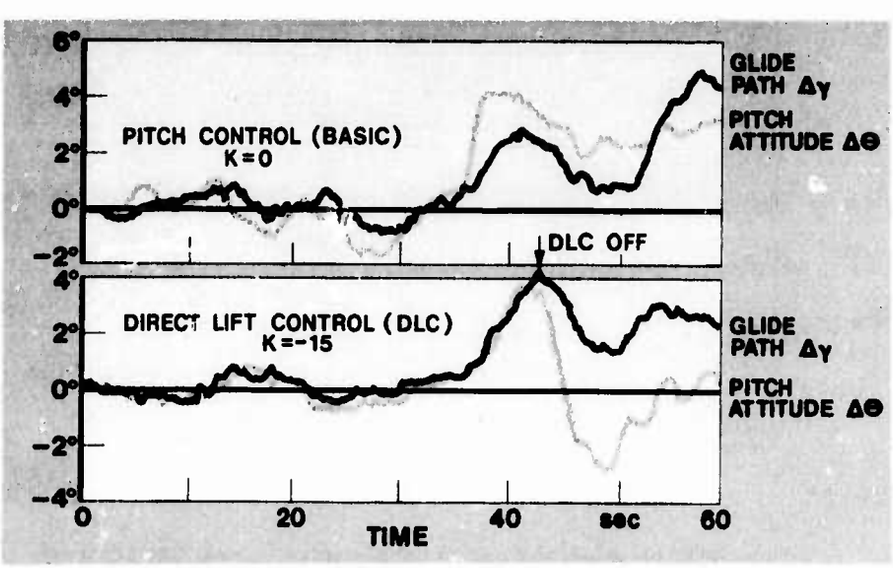

Fig. 14 Flight path and attitude phasing during steep approach

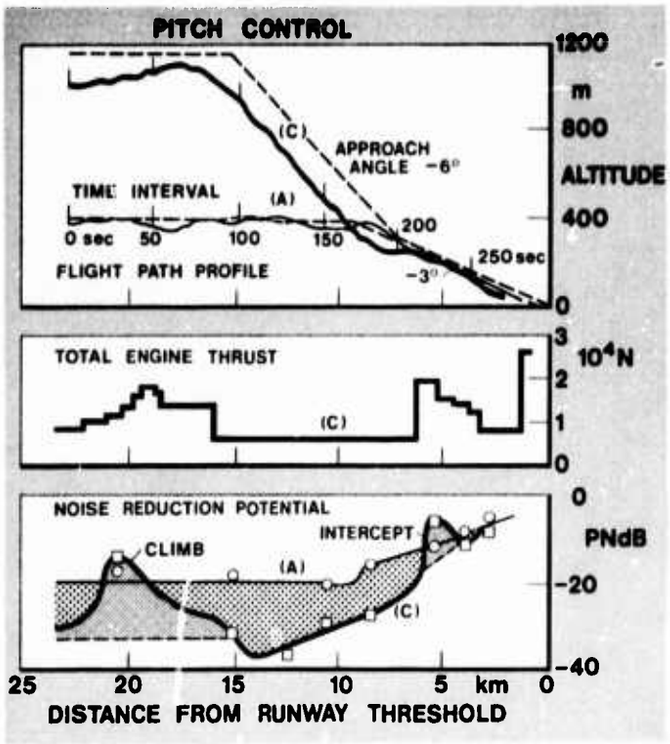

Fig. 15 Aircraft control and noise reduction (1)

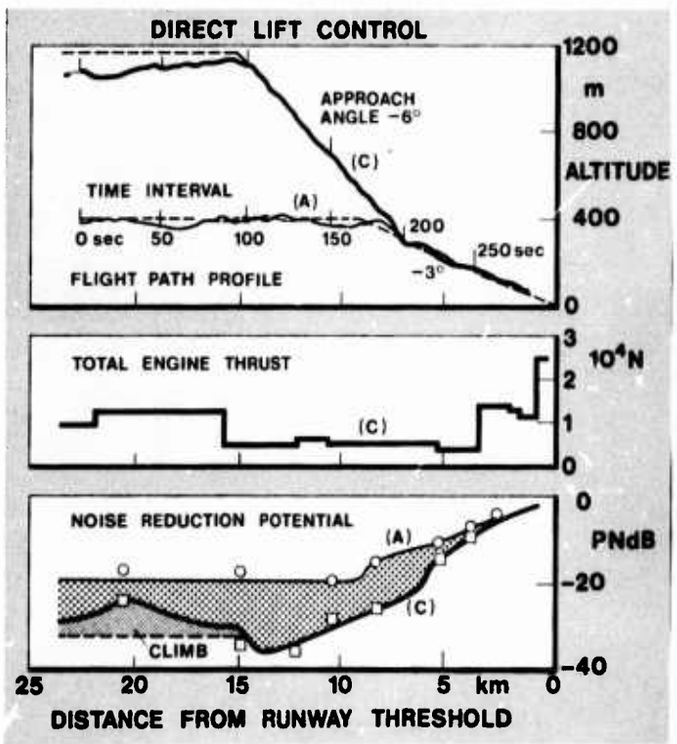

Fig. 16 Aircraft control and noise reduction (2)

MOYENS MODERNES DE TRAJECTOGRAPHIE

par

Alain TERT
Ingénieur de l'Armement
CENTRE D'ESSAIS EN VOL
91220 BRETIGNY-SUR-ORGE
FRANCE

L'évolution des avions et des équipements ainsi que celle des conditions des essais imposent l'utilisation de procédés nouveaux de trajectographie du décollage et de l'atterrissage.

Parmi les moyens implantés au sol le radar LASER par les possibilités d'intégration qu'il permet et par sa précision se révèle un moyen adapté pour les trajectographies précises requises, par exemple, dans les essais d'équipements d'atterrissage tout temps.

Les moyens embarqués utilisant les centrales à inertie pourront à condition que l'on use d'une procédure de correction, couvrir les besoins de trajectographie des performances tout en rendant l'avion indépendant de sa base d'essais.

* * * * * * *

Symboles utilisés

Trajectographie par radar LASER

S : Site du mobile par rapport à la station

G : Gisement du mobile par rapport à la station

ΔS : Ecart de poursuite en site

ΔG : Ecart de poursuite en gisement

D : Distance télémétrique.

Trajectographie par moyens internes :

x : position le long de l'axe de navigation

$\dot{x}$, $\ddot{x}$: dérivées successives de x par rapport au temps

g : accélération de la pesanteur

R : rayon terrestre

ω : pulsation de Schüller

b, Ka : biais et facteur d'échelle accélérométriques

ε, Kg : dérive instantanée et facteur d'échelle gyroscopiques

ϕ : erreur de verticale

Δx : erreur de position

ϕo, Δ xo, Δ $\dot{x}o$: valeurs initiales des erreurs

ωc : défilement commandé

Position du problème

Parmi les mesures importantes concernant les essais de décollage et d'atterrissage figurent celles traitant de la position et de la vitesse de l'avion au cours de ces essais, et présentant les données propres à permettre la mise au point et la certification.

En fait ces mesures sont la base principale qui permet de juger l'aéronef, tant en ce qui concerne les performances elles-mêmes que celles obtenues par utilisation des systèmes associés.

L'évolution des avions et des équipements, ainsi que celles des conditions d'essais a amené les responsables à orienter celle des systèmes de mesure en fonction d'un certain nombre d'impératifs parmi lesquels nous retiendrons les suivants :

- accroissement des précisions afin de couvrir les critères type catégorie III
- raccourcissement des délais d'obtention des résultats (temps réel ou formule "Quick look");
- autonomie du système.

Il est bien sur normal qu'un seul système, ne puisse couvrir tous ces impératifs; aussi, il a été choisi de mener - outre des études tendant à améliorer l'exploitation des systèmes existants - des études sur deux types de systèmes nouveaux :

- le radar LASER : l'utilisation d'une station LASER doit satisfaire les impératifs de précision, de raccourcissement des délais. Cette étude a abouti à la définition et la réalisation de la station STRADA, implantée au C.E.V. (Centre d'Essais en Vol) de BRETIGNY.

- les moyens inertiels, qui conduisent aux mesures par moyens internes, doivent satisfaire l'impératif délais et l'impératif autonomie. L'impératif précision doit au moins être, dans un premier temps satisfait en ce qui concerne la mesure des performances réglementaires. L'étude menée a conclu à la possibilité d'utiliser de tels moyens et a orienté les recherches vers l'utilisation conjointe d'un calculateur embarqué.

1 - TRAJECTOGRAPHIE PAR RADAR LASER

1.1 - Introduction

Avec le développement croissant des systèmes modernes d'approche et d'atterrissage des avions et hélicoptères civils militaires, il devenait de plus en plus nécessaire de disposer d'un moyen de trajectographie efficace répondant à certaines conditions:

sur - la précision des résultats
- la rapidité de dépouillement des mesures
- les équipements et modifications à apporter à l'avion

Le système STRADA a finalement été retenu et mis au point par le S.E.C.T.

C'est un système monostatique et autonome qui utilise un radar à LASER - L'écho infrarouge est renvoyé par un dispositif rétroréflecteur installé sur l'avion et est reçu par une optique collectrice coaxiale du faisceau d'émission LASER. Un récepteur d'écartométrie fournit les coordonnées angulaires de la cible - Un récepteur de télémètrie fournit la distance de la cible.

1.2 - Description d'ensemble (Figures 1.1 et 1.2)

La station est constituée d'un radar LASER ou LIDAR (Light Detection and Ranging) placé au sommet d'une petite tour d'une dizaine de mètres de haut et d'équipements de calcul, de visualisation des résultats, de commande et de contrôle rassemblés dans un bâtiment communiquant avec la tour.

L'émetteur LASER à impulsions et l'ensemble réception sont supportés par une tourelle de poursuite. L'orientation de son axe de visée est caractérisée par les angles de site (S) et gisement (G) mesurés sous forme digitale par l'intermédiaire de codeurs de position disposés sur la tourelle.

L'énergie lumineuse recueillie par le rétroréflecteur est alors distribuée - en partie dans un dispositif de mesure de distance (D) par calcul du retard entre impulsions émises et reçues
- en partie dans un dispositif d'écartomètrie mesurant les écarts angulaires en site (ΔS) et en gisement (ΔG) séparant l'axe de visée LASER de la direction émetteur LASER - rétroréflecteur. Ces dernières informations permettent la poursuite précise de l'avion par la tourelle.

Les valeurs angulaires S, G, ΔS, ΔG et la distance D sont transmises à un calculateur qui assure le calcul en temps réel des éléments de la trajectoire et l'édition de la position et de la vitesse du point de référence avion sous forme de courbes et de tableaux de chiffres.

1.3 - Description du LIDAR

La tourelle d'une masse de 880 kg, asservie en site et gisement supporte - la source LASER avec un système optique de réception
- les récepteurs d'écartomètrie et télémètrie
- une caméra de télévision et son optique associée.

1.3.1. Le LASER

Le LASER est un LASER YAG (Cristal de grenat d'Yttrium - aluminium dopé au néodyne) de structure de pompage à diffuseur circulaire; il est pompé par une source continue émettant à 1,06 μ . La sécurité d'emploi de l'émetteur est assurée par :

- un atténuateur optique faisant varier la puissance crête émise de 5 kw à 50 w de façon que le rapport signal sur bruit du récepteur reste constant.
- une butée mécanique actionnée par l'atténuateur renseigne le calculateur sur l'émission. Un programme de test autorise ou non le fonctionnement du LASER.

Avec ces précautions, les limites de sécurité sont :

- pour une exposition accidentelle de l'oeil : 10 m à 100 m
- pour une exposition prolongée de l'oeil : 100 m à 1000 m

1.3.2. Servo-mécanismes associés

Ils ont trois modes de fonctionnement :

- en commande manuelle de vitesse, permettant de pointer la tourelle par action sur un manche à ressort. On se sert alors pour la diriger, de l'écran de télévision.

- en désignation digitale issue du calculateur. Une séquence de balayage d'une portion de l'espace est alors programmée.

- en poursuite automatique.

1.3.3. Système optique de réception

Il a deux fonctions : - fournir une image de qualité sur la voie écartométrie
- collecter un maximum de flux par la voie télémétrie.

1.3.4. Récepteur d'écartométrie

Le système utilise un tube à balayage électronique, sensible à 1,06 μ . Les coordonnées du point image du rétroréflecteursont extraites du signal vidéo et mesurées par rapport à un réticule de référence. Elles représentent les écarts ΔS et ΔG qui sont transmis aux servo-mécanismes de la tourelle.

1.3.5. Récepteur de télémètrie

Il comprend :

- un récepteur sur la tourelle
- un chronomètre.

Le récepteur comporte 2 photodiodes à avalanche sensibles à 1,06 μ . L'une reçoit une faible partie de l'impulsion LASER émise l'autre reçoit une partie de l'impulsion réfléchie. On mesure l'intervalle de temps séparant l'impulsion "départ", et l'écho par un chronomètre comportant une horloge de 200 MHz, celui-ci délivre, à la fréquence de prélèvement de 50 Hz, la somme des distances comprises dans une fenêtre en distance (300m, 10 km) avec 64 mesures maximum.

Il délivre également le nombre de ces distances validées.

Les informations sont disponibles en digital dans 2 registres de 19 bits lus séquentiellement à 50 Hz par le calculateur. On contrôle l'émission LASER au moyen d'un bit caractérisant la position du disque d'atténuation.

1.3.6. Système de télévision

Il permet la visualisation de l'objectif poursuivi et facilite l'acquisition et la poursuite. Il comprend une caméra fixée sur la tourelle, un monteur TV, un générateur et mélangeur vidéo de symboles numériques, des commandes à distance du zoom et de la caméra.

1.3.7. Performances et conditions atmosphériques d'utilisation

La portée est de 7 km avec une surface utile de rétroréflecteur de 50 cm2 par une visibilité de 8 km.

Les vitesses et accélérations de la tourelle permettent la poursuite de l'avion dans toutes les phases. L'accélération atteint jusqu'à 2,5 rd/s^2 en site et en gisement.

Le LIDAR est protégé par une coupole climatisée. Il fonctionne de - 20° C à + 50° C avec une humidité de 100 %.

La portée est réduite par temps de brouillard et de pluie.

1.4 - Traitement de l'information

Les informations brutes en provenance du LIDAR sont prélevées séquentiellement par les signaux d'une horloge.

Elle sont ensuite traitées par le calculateur.

1.4.1. Le calculateur

Il comprend : - une unité centrale avec mémoire de 12 kmots de 20 bits (dont 1 de parité),
- un système de démultiplexage qui aiguille les informations sur les coupleurs,
- un ensemble de coupleurs qui assure l'adaptation des signaux et le contrôle du fonctionnement des périphériques.

1.4.2. Fonctions du calculateur

Le calculateur a essentiellement une mission temps réel. Ses principales fonctions sont :

1.4.2.1. Fonction désignation de l'objectif :

Les ordres sont élaborés :

- soit à partir des informations en provenance d'un radar d'acquisition
- soit à partir d'une séquence automatique permettant le balayage du LASER dans la zone d'attente de l'aéronef.

1.4.2.2. Fonction acquisition :

Tous les paramètres LIDAR sont lus séquentiellement à 50 Hz. En fonction de la présente de 2 bits correspondant aux seuils de détection et de poursuite de l'écartomètre, le calculateur envoie un ordre de poursuite aux servo-mécanismes de la tourelle . Il contrôle les commandes du pupitre à 10 Hz.

1.4.2.3. Contrôle de la puissance d'émission du LASER :

A 50 Hz, le calculateur teste la présence du bit signalant la butée du disque atténuateur à l'émission (puissance émise minimale), un bit de commande actionne ou non la fermeture d'un relais autorisant l'allumage du LASER.

1.4.2.4. Fonction calcul :

Des interruptions issues de l'horloge commandent 2 cycles de calcul :

Un cycle court de 20 ms (50 Hz) où les informations distances sont moyennées et transformées en mètres; les corrections d'écartomètre sont effectuées; les coordonnées cartésiennes sont calculées dans un trièdre lié à la piste, à partir des coordonnées sphériques.

Un filtrage efficace élimine les mesures aberrantes.

Un cycle long de 100 ms effectue :

- le lissage de la position,
- le calcul des composantes lissées de la vitesse.

1.4.2.5. Fonction visualisation :

Faite essentiellement sur le pupitre elle renseigne l'opérateur sur le fonctionnement des équipements de la station. Elle consiste en :

- des sorties numériques, pour affichage sur tubes "Nixie" : S, G, D, X, Y, Z.
- des comptes rendus de fonctionnement et des commandes (autorisation LASER, butée du disque atténuateur...).

1.4.2.6. Gestion des périphériques :

Les informations calculées sont envoyées séquentiellement dans des coupleurs qui les aiguillent :

- d'une part vers une unité de bande magnétique,
- d'autre part vers un traceur de courbe imprimante.

1.5 - Pupitre d'exploitation et de contrôle.

Il rassemble les fonctions permettant à un opérateur de mettre en oeuvre le LIDAR et d'en contrôler le fonctionnement, et à un ingénieur d'essai de diriger et surveiller le déroulement de l'essai.

Le site et le gisement de la tourelle sont affichés numériquement en degrés, dixièmes et centièmes de degrés; la distance de l'objectif est affichée en mètres. La puissance crête laser émise est affichée par dispositif analogique.

Les coordonnées de l'avion dans le référentiel lié à la piste sont affichées numériquement.

L'ingénieur d'essai a une visualisation instantanée de la position de l'avion.

Le pupitre permet :

- la commande de l'émetteur LASER, de mise en marche et arrêt des circuits
- la commande de la tourelle en poursuite automatique ou manuelle (manche à ressort)
- la commande de l'objectif zoom et de la caméra du système TV.

Les comptes rendus d'alimentations des équipements et des alarmes sont également visualisés.

1.6 - Coopération de l'avion

Elle est minimale et passive.

Un ensemble de trièdres rétroréflecteurs optiques, est monté sur la paroi extérieure et le plus près possible du centre de gravité.

Le pannoau comporte 20 trièdres de 4 cm d'arête

Les trièdres sont des coins de cubes à base équilatérale en verre et en silice.

1.7 - Performances obtenues; utilisations du système (figure 1.3)

Les performances de STRADA imposées par des exigences des essais des systèmes d'atterrissages automatiques de catégorie III lui confèrent, sur l'ensemble de son étendue de mesure, une précision supérieure à celle nécessitée par les essais des systèmes de catégorie I et II (voir tableau).

Cependant la propagation a une certaine influence sur la précision du système.

Le milieu de propagation étant un milieu stochastique, la température et par conséquent l'indice de l'air varient de façon aléatoire tout au long du trajet lumineux. Le phénomène se traduit par des fluctuations des grandeurs mesurées.

La fréquence élevée des mesures de distance permet de réduire dans une grande proportion les erreurs aléatoires dont sont affectées ces mesures.

Les mesures primaires effectuées par le LIDAR ont une précision de 40 cm en distance et de 10^{-4} rd en site et en azimut pour des prélèvements à 50 Hz. Ce système de haute précision possède de nombreux avantages par rapport aux moyens de trajectographie optique traditionnels utilisant les cinéthéodolites. Il délivre en temps réel la précision demandée et permet de s'affranchir des travaux de dépouillement généralement longs; de plus il possède une grande souplesse grâce à un calculateur programmable et ne nécessite sur l'avion qu'un équipement passif et minimal.

2 - UTILISATION DE MOYENS INTERNES EN TRAJECTOGRAPHIE.

2.1 - Objectifs.

Les moyens couramment utilisés font appel à la technique cinématographique et nécessitent un dépouillement long et difficilement automatisable. En outre, ces moyens nécessitent une implantation relativement importante au sol, une connaissance précise des emplacements géographiques des postes, qui compliquent la réalisation d'essais sur terrains non prévus à cet effet. Par ailleurs les moyens optiques nécessitent des conditions météorologiques minima que l'on ne rencontre pas facilement avec une probabilité suffisante sur tous les terrains.

Aussi l'emploi d'une centrale à inertie pour restituer la trajectoire dans le plan horizontal, associée à une radio sonde pour mesurer la hauteur, s'est avéré intéressant pour rendre l'avion autonome et pour obtenir rapidement les résultats.

Toutefois les erreurs propres aux systèmes inertiels rendent, en l'état actuel de leur technologie, nécessaire l'utilisation d'une méthode de correction, ainsi que nous allons le montrer.

L'évaluation qui a été faite de ces matériels, associés à cette méthode, a montré que l'utilisation de centrales à inertie est effectivement judicieux et permet d'effectuer les mesures avec la précision requise, tout en satisfaisant les critères opérationnels souhaités; notamment l'étude effectuée autorise l'utilisation de centrale à inertie couplée à un calculateur embarqué, doté de périphériques rapides, permettant la restitution, en temps réel, à bord, des éléments de trajectographie.

2.2 - Principes généraux de la navigation par inertie

Cette navigation exploite essentiellement des mesures internes que l'on utilise pour restituer la position et la vitesse du mobile. Il est nullement dans notre propos de développer ici la théorie complète des systèmes inertiels; il est toutefois utile de montrer comment ces systèmes sont constitués et quels principes ils utilisent.

Nous savons qu'un mobile soustrait à l'influence de toute action extérieure est animé d'un mouvement rectiligne et uniforme par rapport à un repère absolu. Il est alors impossible, sans référence extérieure, de connaître sa vitesse. Si un mobile est soumis à des forces extérieures, son mouvement est défini, à chaque instant par un vecteur accélération $\vec{\gamma}$, parallèle à la résultante $\vec{F}$ des forces appliquées, selon la loi bien connue de proportionnalité : $\vec{F} = m.\vec{\gamma}$

Le propos de la navigation par inertie est d'utiliser l'effet de cette loi sur des masses placées exclusivement à l'intérieur du mobile pour évaluer, dans un trièdre déterminé, la partie des forces extérieures non due aux forces de gravitation.

Nous allons examiner rapidement, comment peut-être réalisé, en s'inspirant de ces principes, un modèle simplifié de navigateur inertiel à un axe.(Figure 2.1).

L'ensemble est constitué d'une plateforme mobile, comportant un accéléromètre, un gyroscope et un système d'asservissement. Cet asservissement est conçu de telle manière qu'il maintienne la plate-forme à l'horizontale du lieu; pour parvenir à ce résultat si V est la vitesse du mobile, on voit qu'il faut commander un défilement ω_e égal à la vitesse divisée par le rayon terrestre R dans le cas où le modèle terrestre retenu est sphérique, tant en ce qui concerne sa géométrie, que son champ de gravitation. L'ensemble ainsi réalisé répond à un modèle du second ordre (Figure 2.2).

La propriété fondamentale de ce système est que sa période propre est égale à la période ω de Schüler (valeur : 84 minutes environ); c'est celle d'un pendule simple dont la longueur serait égale au rayon terrestre.

2.3 - Schématisation des erreurs en navigation inertielle

Le modèle décrit ci-dessus n'est qu'un cas très idéal. Tous les composants utilisés dans les systèmes réels sont imparfaits. Les accéléromètres ne donnent pas la composante vraie f de la force spécifique. Ils sont affectés d'un biais et d'un facteur d'échelle. L'ensemble d'asservissement, à cause des dérives des gyroscopes et des imperfections du modèle théorique ne réalise pas parfaitement le défilement attendu ω_e . On obtient ainsi un modèle d'erreurs élémentaires, auquel s'ajoutent des erreurs d'initialisation sur :

- la position Δx_o
- la vitesse $\Delta \dot{x}_o$
- la verticale ϕ_o

Le résultat est que le modèle décrit avant, ne s'applique plus et qu'il faut recourir à un nouveau modèle (figure 2.3).

Avec un tel système, au bout d'un temps t de navigation la verticale est fausse d'un angle ϕ, la position de Δx , la vitesse de $\Delta \dot{x}$. Sur l'accélération apparaît une composante de gravitation, due à l'erreur de verticale, et ce résultat lui même est affecté des erreurs de mesure de l'accéléromètre. Bien sur l'évolution de verticale est aussi erronée puisque la chaîne correspondante est imparfaite.

L'ensemble équivaut à un modèle d'erreur en position du second ordre dont la période propre est celle de Schüler. L'équation complète de ce modèle est :

$$\Delta \ddot{x} + \omega^2 \Delta x = b - g\phi_o + \omega^2 \Delta x_o - 2Kg(\dot{x} - \dot{x}_o) - g\int_o^t \varepsilon \, dt + Ka\ddot{x}$$

Un tel processus introduit des erreurs de navigation oscillatoire autour d'un modèle de base, du principalement à la dérive du système de verticale; la dérive en vitesse restant purement périodique. La période en question étant assez longue, pour des durées faibles il est possible de formuler un modèle linéaire par rapport au temps. Ce modèle comportera en terme constant l'erreur initiale de vitesse et en pente, le biais de l'accéléromètre et l'effet de l'erreur initiale de verticale; si on poussait plus loin l'évaluation de cette erreur on verrait que le terme du second ordre est du principalement à la dérive du gyroscope.

Dans le mouvement général, la partie du premier ordre observable au point fixe se conserve. On peut même dire que pendant une durée relativement faible et pour des mouvements tels que ceux, couramment rencontrés en aéronautique de transport, cette partie linéaire constitue la partie principale de l'erreur. L'exploitation de cette remarque a été développée systématiquement dans la méthode de trajectographie que nous allons décrire.

2.4 - Trajectographie inertielle avec recalages périodiques en vitesse

Si on dispose à bord de l'avion d'une centrale à inertie donnant les composantes Nord et Est de la vitesse sol, il est aisé, par changement d'axe et intégration, d'obtenir les vitesses selon l'axe de piste et perpendiculairement à celui-ci ainsi que les distances parcourues selon ces directions, depuis le début de l'intégration.

Pour obtenir des vitesses Nord et Est les plus exactes possibles on effectue, en une période voisine de l'utilisation, une observation de l'évolution des vitesses données par la centrale, pendant un point fixe. De cette observation on déduit la partie linéaire des dérives, en fonction du temps.

Pour effectuer la correction sur une période voisine on suppose que ce modèle de dérives se conserve (Figure 2.4).

On a ainsi pour tout instant suivant l'observation des dérives :

$$\begin{cases} \delta V_N(t) = \delta V_N(t_o+3o) + b_N^* \cdot [t - (t_o+3o)] \\ \delta V_E(t) = \delta V_E(t_o+3o) + b_E^* \cdot [t - (t_o+3o)] \end{cases}$$

et pour tout instant précédant l'observation des dérives :

$$\begin{cases} \delta V_N(t) = \delta V_N(t_o) + b_N^* \cdot (t - t_o) \\ \delta V_E(t) = \delta V_E(t_o) + b_E^* \cdot (t - t_o) \end{cases}$$

L'utilisation d'une correction de ce type, en remontant le temps, interdit la correction temps réel; ce n'est pas gênant pour des essais avec enregistrement; mais dans le cas d'une installation embarquée possédant la capacité temps réel, cela interdit la pratique du temps réel dans un tel cas.

Le profil d'utilisation retenu est :

- point fixe de 30", avec enregistrement des vitesses Nord et Est. Ces valeurs corrigeront les données du décollage.
- décollage avec enregistrement à 1 par seconde des vitesses Nord et Est, de la hauteur radio sonde et des paramètres anémométriques.
- approche et atterrissage, enregistrement des paramètres, comme pour le décollage
- point fixe de 30", les valeurs recueillies corrigeront les données atterrissage.

2,5 - Matériels utilisés

Nous ferons allusion ici essentiellement, aux matériels qui ont été utilisés à Brétigny pendant la phase probatoire où ont été vérifiées les précisions obtenues avec ce moyen d'essai.

La centrale à inertie était du type SAGEM S 111. Ce matériel, quoique ancien, nous a permis de mener tous les vols d'évaluation et donc de vérifier les principes énoncés précédemment.

Pour la mesure des hauteurs, l'avion était équipé d'une radio sonde TRT AH V6. Ce matériel à modulation de fréquence, s'est révélé être d'une excellente précision à basse altitude. Les données "bord" étaient enregistrées par le système d'acquisition EMMANUEL (EMD).

L'avion utilisé était un biturbopropulseur du type Nord 260. Les éléments caractéristiques, pour des conditions courantes sont : V1 = 90 kt
Vr = 95 kt
V2 ≃ 98 kt
1,3Vs = 90 kt

2.6 - Profil d'un vol d'évaluation

Le but des décollages et atterrissages d'évaluation était de vérifier les précisions obtenues par ce procédé de trajectographie. Pour cela ces phases de vol ont été couvertes également par cinéthéodolites. Les moyens de synchronisation courants ont permis de recaler l'une par rapport à l'autre les trajectoires obtenues d'une part à partir des enregistrements des données inertielles, d'autre part, à partir des photographies cinéthéodolites.

Le vol consiste en tours de piste : le décollage est considéré du lacher des freins jusqu'à une hauteur d'environ 400 pieds; l'atterrissage est considéré à partir de 400 pieds jusqu'à l'arrêt complet.

2.7 - Précisions obtenues

Les résultats utiles concernent 60 passes. Ils portent sur les écarts obtenus en vitesses et position entre les cinéthéodolites et l'inertie. Ils sont formulés en axes piste. La distance parcourue dans la partie utile des passes est d'environ 2 500 m.

Pour les décollages on obtient les courbes d'erreurs de la figure (2.5)

On peut retenir pour 66% des points :

$$t \leqslant 60\,s \quad (x \leqslant 3000\,m) : \begin{cases} \Delta V_x \leqslant 0{,}6\,kt \\ \Delta X \leqslant 10\,m \end{cases}$$

Le temps de passe est celui qui sépare du recalage.

En ce qui concerne les atterrissages on obtient les courbes de la figure (2.6)
et pour 66% des points on a :

$$\begin{cases} \Delta V_x \leqslant 0{,}5\,kt \\ \Delta X \leqslant 8\,m \end{cases}$$

Nous pouvons donc considérer que la méthode de correction utilisée permet la mesure des performances de décollage et atterrissage. Nous notons aussi qu'une correction d'ordre supérieur serait très certainement quelque peu illusoire. Elle pourrait peut être se révéler utile si la durée de mesure augmentait; mais il faudrait alors augmenter la durée d'observation au point fixe; la procédure deviendrait trop longue.

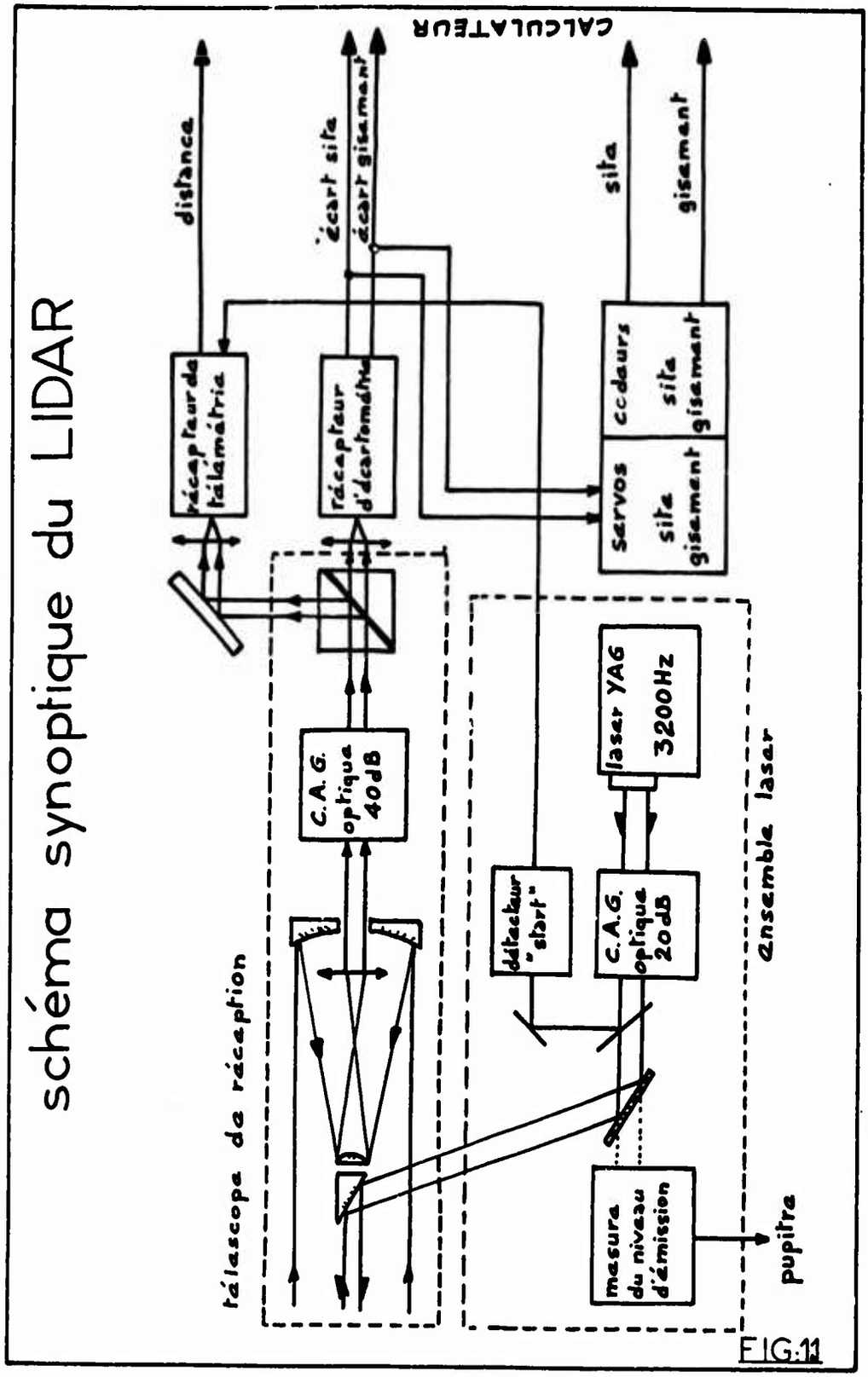
schéma synoptique du LIDAR
CALCULATEUR
distance
écart site
écart gisement
site
gisement
récepteur de télémétrie
récepteur d'écartométrie
servos
site
gisement
codeurs
site
gisement
C.A.G. optique 40dB
C.A.G. optique 20dB
détecteur "start"
laser YAG 3200Hz
télescope de réception
ensemble laser
mesure du niveau d'émission
pupitre

FIG.11

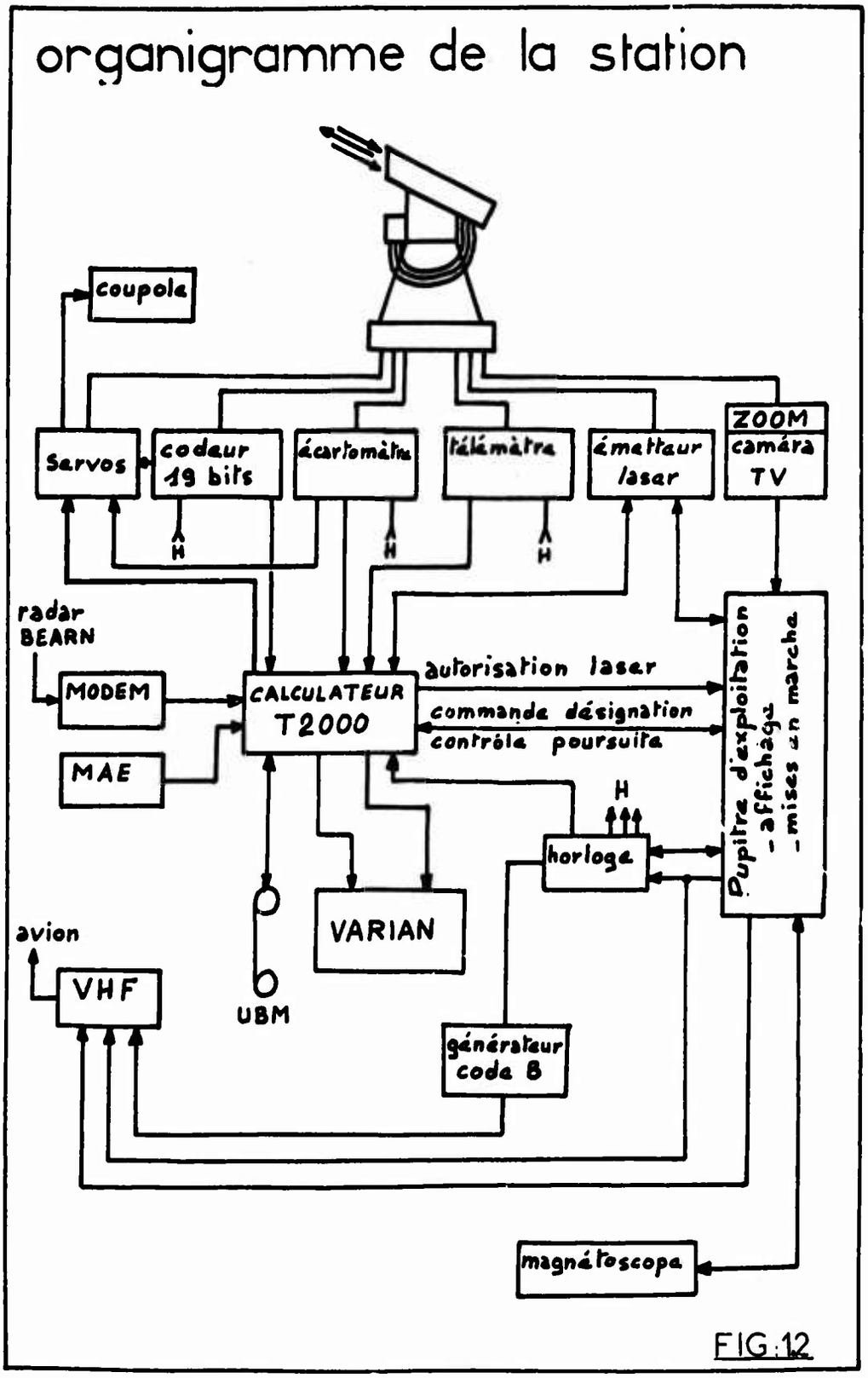
organigramme de la station
coupole
Servos
codeur 19 bits
écartomètre
télémètre
émetteur laser
ZOOM
caméra TV
H
H
H
radar BEARN
MODEM
MAE
CALCULATEUR T2000
autorisation laser
commande désignation
contrôle poursuite
Pupitre d'exploitation
- affichage
- mises en marche
H
horloge
VARIAN
avion
VHF
UBM
générateur code B
magnétoscope

FIG:12

précision du système STRADA

PARAMETRES	ERREURS POSSIBLES (2 σ)		
	Zône 1 $-5000m < X < -600m$ $Z > 250$ ft	Zône 2 $-600m < X < 0$ $75ft \leqslant Z \leqslant 250ft$	Zône 3 $0 < X < 1500m$ $Z < 75ft$
X	0,2 m	< 0,2 m	< 0,2 m
Y	⩽ 0,25 m	⩽ 0,1 m	< 0,2 m
Z	⩽ 0,25 m	⩽ 0,1 m	< 0,1 m
V_x	< 0,5 m/s	⩽ 0,5 m/s	< 0,5 m/s
V_Y	⩽ 0,5 m/s	⩽ 0,2 m/s	0,2 m/s
V_Z	⩽ 0,5 m/s	< 0,2 m/s	0,1 m/s

FIG.13

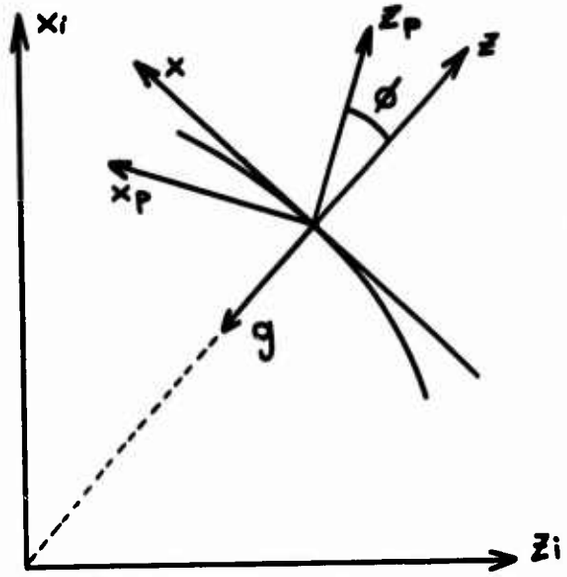

AXES NAVIGATION

SIMPLIFIEE

Figure 2.1

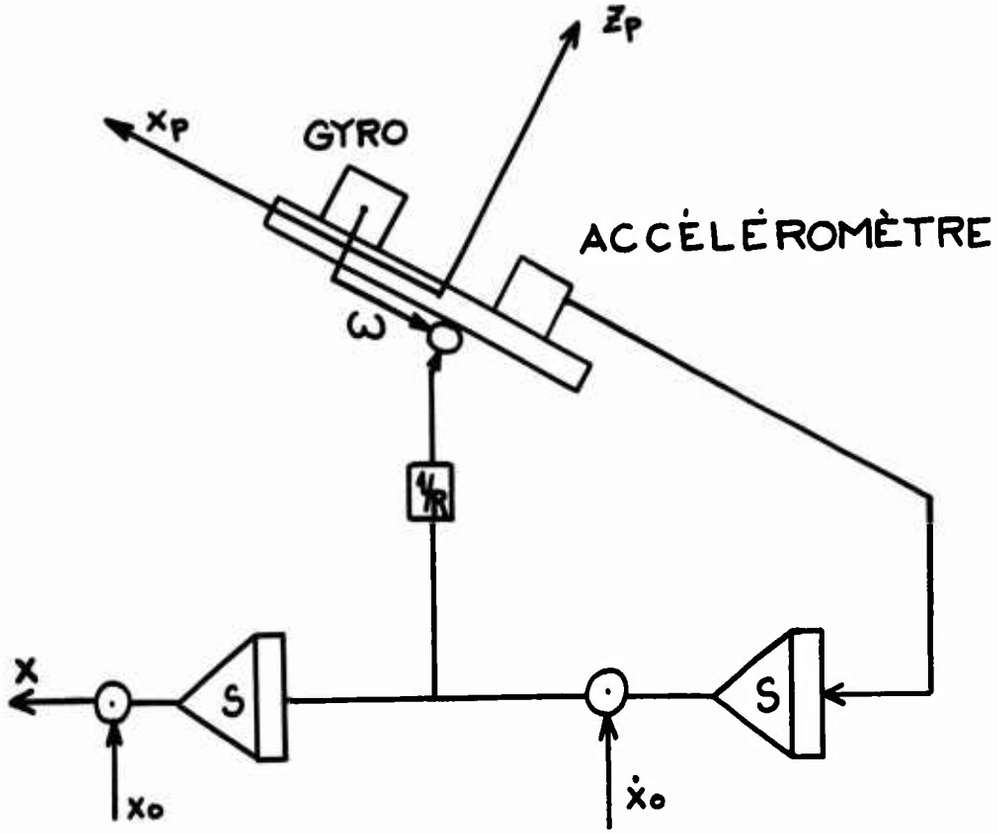

Figure 2.2

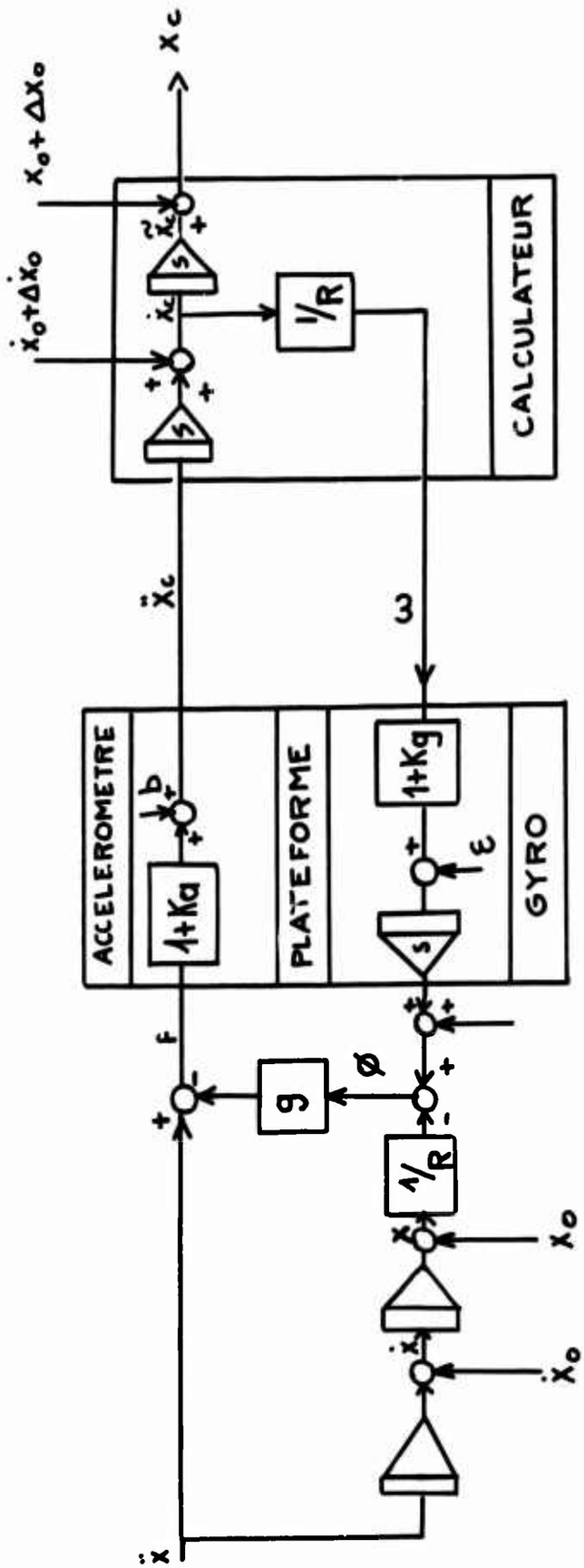

NAVIGATION SIMFLIFIEE

DIAGRAMME FONCTIONNEL

Figure 2-3

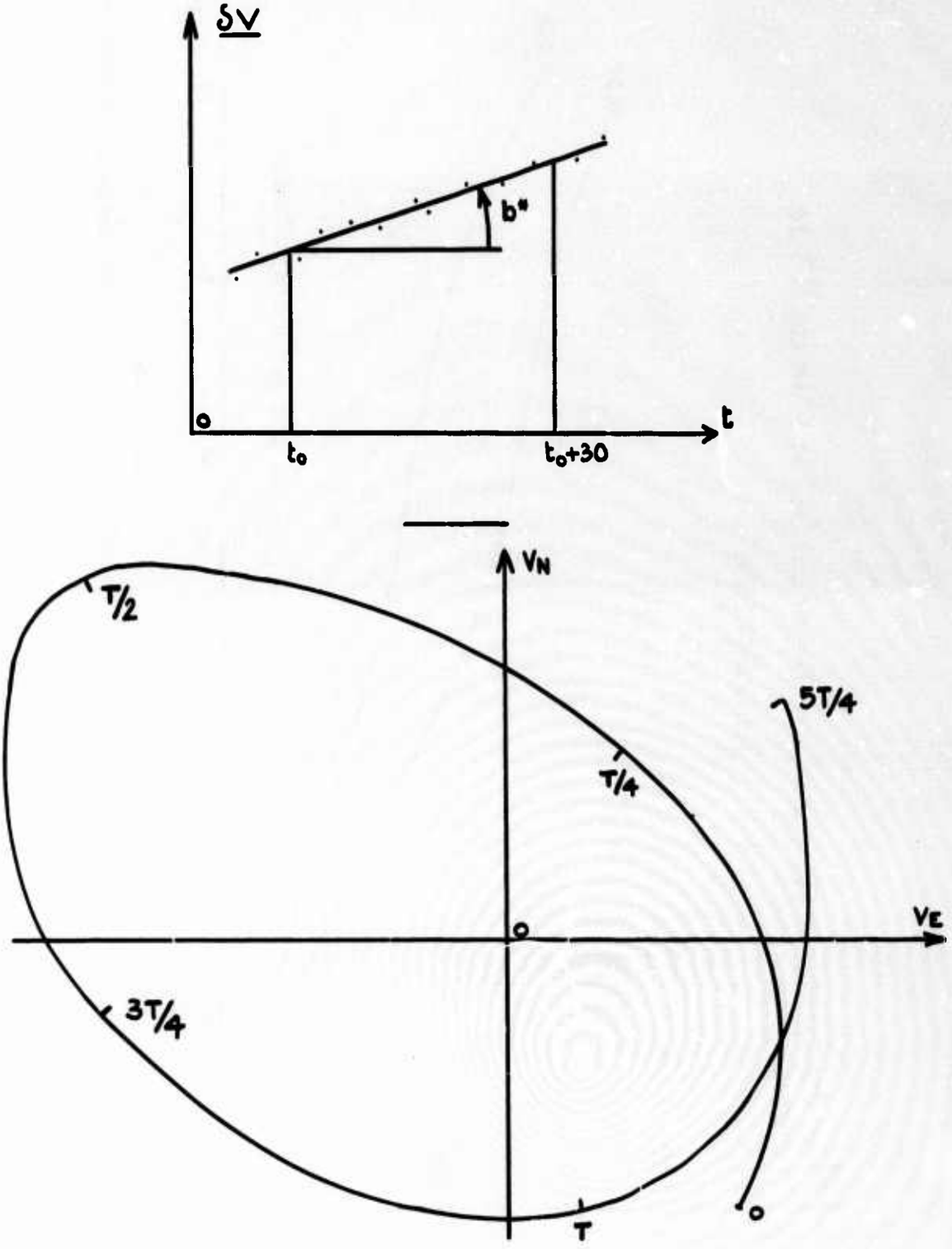

OBSERVATIONS des DERIVES

Figure 2.4

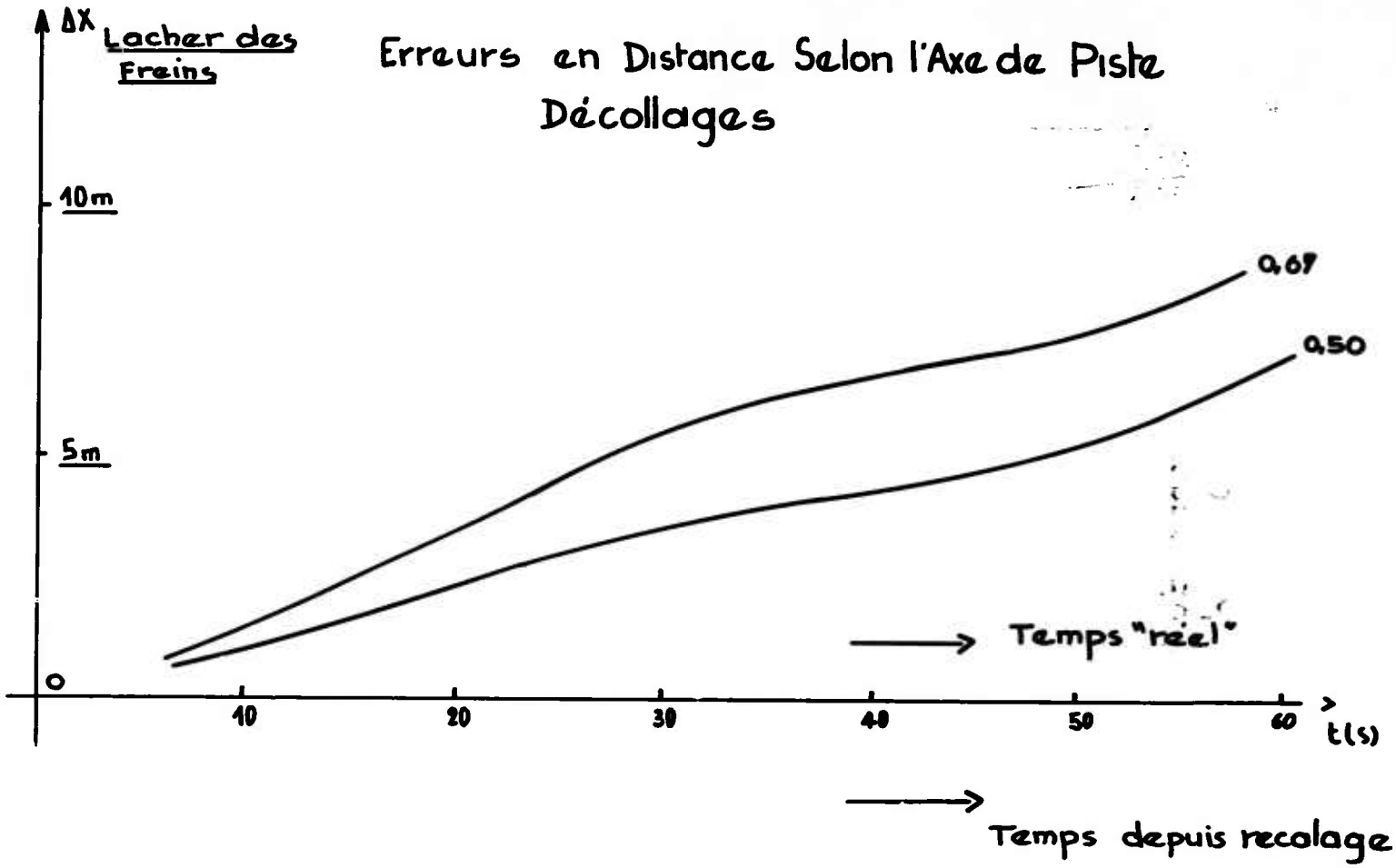
ΔX
Lacher des Freins
Erreurs en Distance Selon l'Axe de Piste
Décollages
10m
5m
0
0,69
0,50
Temps "réel"
10
20
30
40
50
60
t(s)
Temps depuis recalage

Figure 2·5

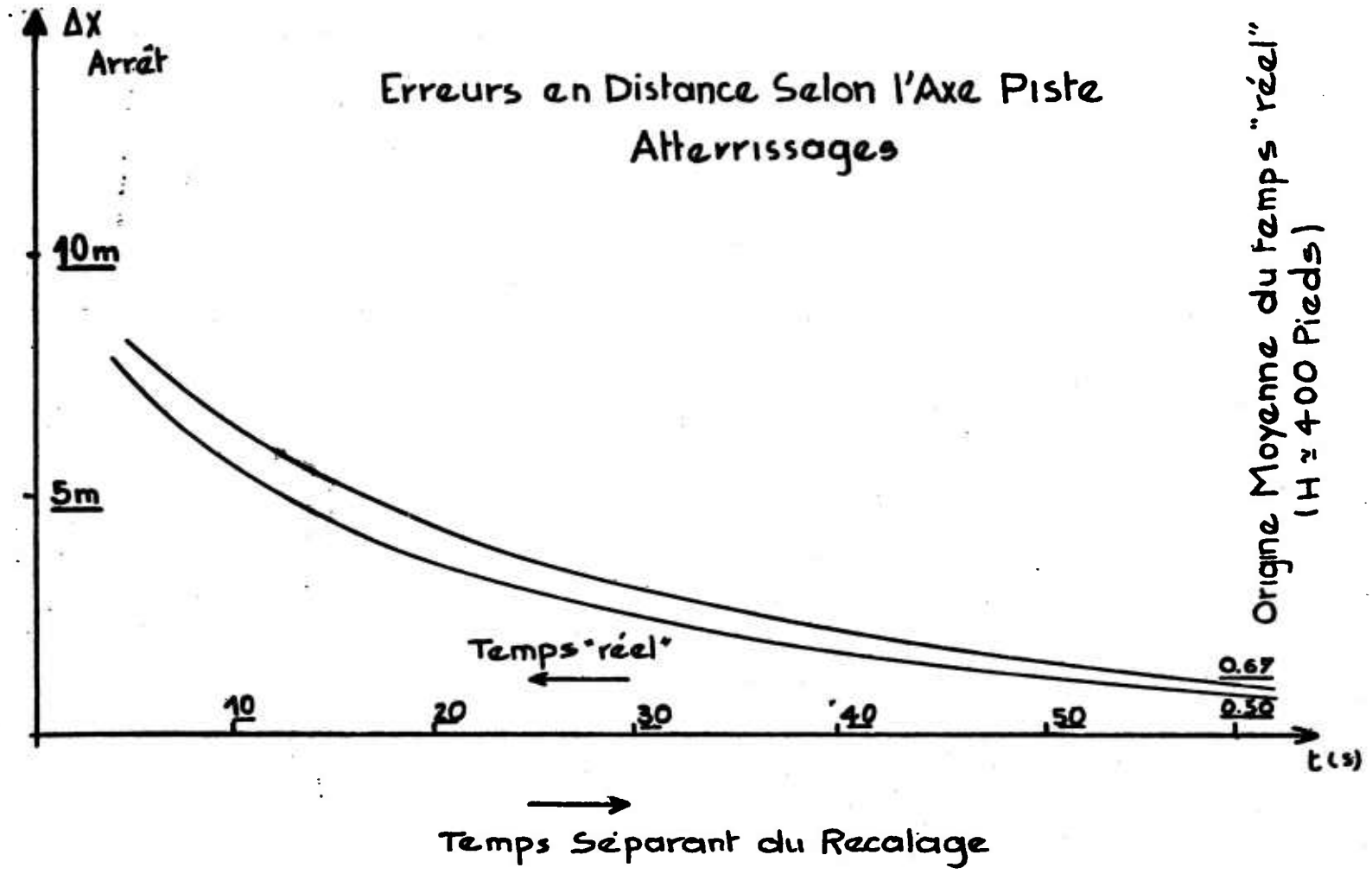
ΔX
Arrêt
Erreurs en Distance Selon l'Axe Piste
Atterrissages
10m
5m
Origine Moyenne du temps "réel"
(H ≈ 400 Pieds)
Temps "réel"
0.67
0.50
10
20
30
40
50
t(s)
Temps Séparant du Recalage

Figure 2·6